
Pacific Northwest National Laboratory

Operated by Battelle for the
U.S. Department of Energy

Characterization of Vadose Zone Sediment: Borehole 299-E33-46 Near B 110 in the B BX-BY Waste Management Area

R. J. Serne	C. W. Lindenmeier	S. R. Baum
B. N. Bjornstad	R. D. Orr	K. N. Geiszler
G. W. Gee	V. L. LeGore	M. M. Valenta
H. T. Schaefer	R. E. Clayton	T. S. Vickerman
D. C. Lanigan	M. J. Lindberg	L. J. Royack
R. G. McCain(a)	I. V. Kutnyakov	

(a) S. M. Stoller, Richland, Washington

December 2002



Prepared for CH2M HILL Hanford Group, Inc., and
the U.S. Department of Energy
under Contract DE-AC06-76RL01830

DISCLAIMER

This report was prepared as an account of work sponsored by an agency of the United States Government. Neither the United States Government nor any agency thereof, nor Battelle Memorial Institute, nor any of their employees, makes **any warranty, express or implied, or assumes any legal liability or responsibility for the accuracy, completeness, or usefulness of any information, apparatus, product, or process disclosed, or represents that its use would not infringe privately owned rights.** Reference herein to any specific commercial product, process, or service by trade name, trademark, manufacturer, or otherwise does not necessarily constitute or imply its endorsement, recommendation, or favoring by the United States Government or any agency thereof, or Battelle Memorial Institute. The views and opinions of authors expressed herein do not necessarily state or reflect those of the United States Government or any agency thereof.

PACIFIC NORTHWEST NATIONAL LABORATORY
operated by
BATTELLE
for the
UNITED STATES DEPARTMENT OF ENERGY
under Contract DE-AC06-76RL01830

Printed in the United States of America

Available to DOE and DOE contractors from the
Office of Scientific and Technical Information,
P.O. Box 62, Oak Ridge, TN 37831-0062;
ph: (865) 576-8401
fax: (865) 576-5728
email: reports@adonis.osti.gov

Available to the public from the National Technical Information Service,
U.S. Department of Commerce, 5285 Port Royal Rd., Springfield, VA 22161
ph: (800) 553-6847
fax: (703) 605-6900
email: orders@ntis.fedworld.gov
online ordering: <http://www.ntis.gov/ordering.htm>



This document was printed on recycled paper.

Characterization of Vadose Zone Sediment: Borehole 299-E33-46 Near B-110 in the B-BX-BY Waste Management Area

R. J. Serne	C. W. Lindenmeier	S. R. Baum
B. N. Bjornstad	R. D. Orr	K. N. Geiszler
G. W. Gee	V. L. LeGore	M. M. Valenta
H. T. Schaeff	R. E. Clayton	T. S. Vickerman
D. C. Lanigan	M. J. Lindberg	L. J. Royack
R. G. McCain ^(a)	I. V. Kutnyakov	

(a) S. M. Stoller, Richland, WA.

December 2002

Prepared for CH2M HILL Hanford Group, Inc., and
the U.S. Department of Energy
under Contract DE-AC06-76RL01830

Executive Summary

The overall goal of the of the Tank Farm Vadose Zone Project, led by CH2M HILL Hanford Group, Inc., is to define risks from past and future single-shell tank farm activities. To meet this goal, CH2M HILL Hanford Group, Inc., asked scientists from Pacific Northwest National Laboratory to perform detailed analyses on vadose zone sediment from within the B-BX-BY Waste Management Area. This report is the third in a series of three reports to present the results of these analyses. Specifically, this report contains all the geologic, geochemical, and selected physical characterization data collected on vadose zone sediment recovered from a borehole installed approximately 4.5 m (15 ft) northeast of tank B-110 (borehole 299-E33-46).

This report also presents our interpretation of the data in the context of the sediment lithologies, the vertical extent of contamination, the migration potential of the contaminants, and the likely source of the contamination in the vadose zone and groundwater east of the B Tank Farm. The information presented in this report supports the B-BX-BY field investigation report prepared by CH2M HILL Hanford Group, Inc.^(a)

Overall, our analyses identified common ion exchange and heterogeneous (solid phase-liquid solute) precipitation reactions as two mechanisms that influence the distribution of contaminants within that portion of the vadose zone affected by tank liquor. We did not observe significant indications of caustic alteration of the sediment mineralogy or porosity, but we did observe slightly elevated pH values between the depths of 15 and 25 m (52 and 83 ft) bgs. X-ray diffraction measurements indicate no evidence of mineral alteration or precipitation resulting from the interaction of the tank liquor with the sediment. However, no scans of samples by scanning electron microscopy were performed that might suggest that there is faint evidence of caustic attack.

Our analyses do not firmly suggest that the source of the contamination in the groundwater below and to the east of B Tank Farm is the 1971 transfer line leak at B-110. However, we are firmly convinced that the fluids from the transfer line leak event are present in the vadose zone sediments at borehole 299-E33-46 to a depth of 52 m (170 ft) bgs, within the Hanford H2 sand unit. Below this depth the concentration of nitrate still appears to be slightly elevated above natural background levels. There is also elevated technetium-99 between 68 and 69 m (222 and 226 ft) bgs in the Plio-pleistocene mud layer but we can't show that this contamination traveled through the entire vadose zone and in fact may have migrated horizontally from other sources.

The near horizontally bedded, northeasterly dipping sediment likely caused horizontal flow of the migrating contaminants. At borehole 299-E33-46, there are several fine-grained lens within the H2 unit at

(a) *Draft Field Investigation Report for Waste Management Area B-BX-BY*. RPP-10098, Draft, Volume 2, Appendix D, CH2M HILL Hanford Group, Inc., Richland, Washington.

26, 41, and 57 m (85, 168, and 186 ft) bgs that likely cause some horizontally spreading of percolating fluids. The 12.7-ft thick Plio-pleistocene fine-grained silt/clay unit is also an important horizontal flow conduit between 66 to 69.4 m (215 to 227.7 ft) bgs.

The porewater electrical shows a two-lobed elevated plume. The shallower but more concentrated lobe, between 15.42 and 25.91 m (50.6 and 85 ft) bgs, resides within the middle sand sequence in Hanford H2 unit. The shallow lobe appears to pond on top of the fine-grained lens at 85 ft bgs. The slightly less concentrated lobe resides between 27.61 and 42.67 m (90.6 to 140 ft) bgs within the Hanford H2 unit. Thus, the leading edge of the transfer line leak plume appears to reside well above the water table at 78.0 m (255.8 ft) bgs.

Elevated nitrate concentrations in 299-E33-46 borehole sediment start at 50.6 feet bgs but the more concentrated zone resides between 26.8 and 51 m (87.8 and 168 ft) bgs within the Hanford H2 unit. This more concentrated nitrate plume appears to stop at the fine-grained thin lens at 51 m (168 ft) bgs. The peak vadose zone porewater nitrate concentration is 1.5 g/L at 41 m (134 ft) bgs. The deeper units, H3 and PPlz, have porewaters that contain 100 to 200 and 130 mg/L nitrate, respectively. These values appear to be slightly elevated above natural background values. Even the coarse-grained PPlg unit that includes the water table has porewater nitrate concentrations that hover near 50 mg/L suggesting slightly elevated nitrate concentrations penetrate the entire vadose zone at this borehole. However, an alternate source of nitrate within and below the PPlz could be the nearby cribs and trenches with horizontal transport within the very moist fine-grained sediments.

Within the Hanford H2 unit the porewater fluoride and bicarbonate concentrations are also elevated above natural background levels down to a depth of about 37 m (120 ft) bgs. The porewater cation distributions show the ion exchange front wherein the sodium in the tank fluids pushes the naturally occurring divalent cations (calcium, magnesium and strontium) deeper into the sediments and out in front of the plume. The most concentrated portion of the vadose zone plume has a porewater chemical composition that is 0.15M sodium and 0.13 M bicarbonate, 0.01 M fluoride, 0.007 M sulfate, and 0.003 M nitrate. This composition is not as saline as contaminated porewaters below the BX-102 tank or under the S-SX tank farm.

The only detectable radionuclides in the vadose zone sediments from borehole 299-E33-46 are strontium-90, technetium-99 and a faint trace of water leachable uranium, which suggests non-natural uranium at very low concentrations. Strontium-90 is considered to be the primary radionuclide released from tank B-110 transfer line and is concentrated in the sediment between 19 and 28 m (62 and 83 ft) bgs at concentrations between 1,000 and 11,250 pCi/g. Strontium-90 in the sediments is not readily water leachable yielding an insitu desorption K_d value of >100 ml/g. All technetium-99 concentrations in the shallow depths is at or below the detection limit thus it is difficult to determine if the technetium profile at 299-E33-46 can be traced from below the tank all the way to the groundwater. The two more concentrated peaks of technetium-99 are found in the deep H3 unit and in the PPlz unit and it is more likely that the technetium found at the deeper depths is from some horizontal migration of fluids containing technetium-99

from other sources that was carried to depth by active disposal of large quantities of contaminated water or some other driving force such as domestic water line leaks, recharge from topographic lows for snow melt etc.

In summary, the moisture content, pH, electrical conductivity, sodium, and strontium-90 profiles do not suggest that the leading edge of the plume has penetrated below 52 m (170 ft) bgs. The profiles of two mobile constituents, technetium-99 and nitrate, suggest that the leading edge of the plume may have penetrated all the way to groundwater. But there may be other sources of these two mobile contaminants in the deep vadose zone. The very moist PPlz sediments, which contain a perched water table at several nearby wells, is a likely driving force to move fluids from other sources into the borehole environs.

Acknowledgments

This work was conducted as part of the Tank Farm Vadose Zone Project led by CH2M HILL Hanford Group, Inc., in support of the U.S. Department of Energy's Office of River Protection. The authors wish to thank Anthony J. Knepp, Fredrick M. Mann, David A. Myers, Thomas E. Jones, and Harold A. Sydnor with CH2M HILL Hanford Group, Inc., and Marc I. Wood with Fluor Hanford for their support of this work. We would also like to express our gratitude to Robert Yasek with DOE's Office of River Protection.

We would especially like to thank Kent D. Reynolds (Duratek Federal Services, Inc.) for his efforts in design and construction of the core extruder, and Victoria Johnston and Kevin A. Lindsey (Kennedy Jencks Consultants, Inc.) for their insights on the geologic nature of the materials penetrated by this borehole.

Dr. Karl Koizumi (MACTEC-ERS) was a co-author of Appendix C.

Finally, we would like to thank George Last, Bill Deustch, Ken Krupka, and Duane G. Horton for their technical review of this document, Karrol Lehman (Jacobs Engineering) for editorial and document production support and Shanna Muns (CH2M HILL Hanford Group, Inc.) for final word processing and formatting.

Acronyms and Abbreviations

ASA	American Society of Agronomy
ASTM	American Society for Testing and Materials
bgs	below ground surface
DFS	Duratek Federal Services, Inc.
EPA	U.S. Environmental Protection Agency
FIR	Field Investigation Report
g's	gravitational forces
GEA	gamma energy analysis
Hf/PPu(?)	Hanford formation/Plio-Pleistocene unit(?)
HPGe	high purity germanium
IC	ion chromatography
ICP	inductively coupled plasma
ICP-MS	inductively coupled plasma mass spectrometer
ICP-OES	inductively coupled plasma – optical emission spectroscopy
ID	inside diameter
NTA	nitrilo triacetic acid
OD	outside diameter
PNNL	Pacific Northwest National Laboratory
PPlc	Plio-Pleistocene calcic
PPlg	Plio-Pleistocene gravelly sand or sandy gravel
PPlz	Plio-Pleistocene mud
RCRA	Resource Conservation and Recovery Act
REDOX	Reduction Oxidation Plant
SEM	scanning electron microscope
TEM	transmission electron microscopy
UFA	unsaturated flow apparatus (ultracentrifuge for squeezing porewater out of sediment)
VZMS	vadose zone monitoring system
vol%	volumetric water content
XRD	x-ray diffraction
XRF	x-ray fluorescene
WMA	Waste Management Area
wt%	gravimetric moisture content

Contents

Executive Summary	iii
Acknowledgments	vii
Acronyms and Abbreviations	ix
1.0 Introduction	1.1
2.0 Geology	2.1
2.1 Geologic Setting of the 241-B Tank Farm	2.1
2.2 Drilling and Sampling Of Borehole 299-E33-46 (C3360).....	2.3
2.3 Geophysical Logging	2.12
2.4 Sample Handling	2.13
2.5 Sub-Sampling and Geologic Description.....	2.14
2.6 Geology of Borehole 299-E33-46	2.15
2.6.1 Backfill.....	2.15
2.6.2 Hanford Formation.....	2.15
2.6.3 Hanford Formation H3 Unit.....	2.17
2.6.4 Plio-Pleistocene Unit	2.17
2.7 Discussion On Increased-Moisture Zones	2.21
2.8 Historic Groundwater Levels.....	2.24
3.0 Geochemical Method and Materials	3.1
3.1 Sample Inventory.....	3.1
3.2 Tiered Approach.....	3.1
3.3 Materials and Methods.....	3.1
3.3.1 Moisture Content.....	3.2
3.3.2 1:1 Sediment-to-Water Extract	3.2
3.3.3 Porewater, Suction Candle, and Groundwater Composition	3.4
3.3.4 Radioanalytical Analysis	3.4
3.3.5 Carbon Content of Sediment.....	3.4
3.3.6 8 M Nitric Acid Extract.....	3.5
3.3.7 Elemental Analysis.....	3.5
3.3.8 Particle Size Distribution.....	3.6
3.3.9 Particle Density.....	3.6
3.3.10 Mineralogy.....	3.6
3.3.11 Water Potential (Suction) Measurements	3.8
4.0 Results and Discussion.....	4.1
4.1 Moisture Content	4.1
4.2 1:1 Sediment-to-Water Extracts	4.5

4.2.1	pH and Electrical Conductivity	4.6
4.2.2	Porewater Anion Composition	4.11
4.2.3	Porewater Cation Composition	4.12
4.2.4	Porewater Trace Constituent Composition	4.27
4.2.5	Porewater Solute Ratios	4.31
4.3	Radionuclide Content In Vadose Zone Sediment	4.46
4.3.1	Gamma Energy Analysis	4.46
4.3.2	Strontium-90 Content of Sediment from 299-E33-46.....	4.46
4.3.3	Uranium Content in Sediment	4.56
4.3.4	Technetium-99 Content in the Vadose Zone Sediments.....	4.63
4.3.5	Recharge Estimates Based on Technetium-99 Distribution in Sediments from Borehole 299-E33-46	4.65
4.3.6	Tritium Content in Vadose Zone Sediments.....	4.67
4.4	Total Carbon, Calcium Carbonate, and Organic Carbon Content of Vadose Zone Sediment	4.67
4.5	8 M Nitric Acid Extractable Amounts of Selected Elements.....	4.71
4.6	Sediment Total Oxide Composition	4.82
4.7	Particle Size Measurements On Vadose Zone Sediment	4.87
4.8	Particle Density of Bulk Sediment	4.87
4.9	Mineralogy	4.87
4.10	Matric Suction Potential Measurements.....	4.94
4.11	Vadose Zone Monitoring System.....	4.98
4.12	Groundwater Analyses	4.105
5.0	Summary and Conclusions	5.1
5.1	Conceptual Model of the Geology At 299-E33-46	5.1
5.2	Vertical Extent Of Contamination	5.3
5.3	Detailed Characterization To Elucidate Controlling Geochemical Processes	5.7
5.4	Estimates of Sorption-Desorption Values	5.8
5.5	Other Characterization Observations	5.9
6.0	References.....	6.1
Appendix A	– 299-E33-46 Geologic Descriptions of Split-Spoon And Grab Samples Performed During Core/Sample Opening In Pnnl Laboratory.....	A.1
Appendix B-1	– 299-E33-46 Splitspoon Core Sample Photographs	B.1
Appendix B-2	– 299-E33-46 Composite Grab and Splitspoon Shoe Sample Photographs	B.55
Appendix C	– Correlation of Spectral Gamma Log Response Through Borehole Casing With 90sr Concentration In Sediments.....	C.1
Appendix D	– X-Ray Diffractograms For Bulk And Clay Sized Sediments From Borehole 299-E33-46.....	D.1

Figures

2.1	Generalized, Composite Stratigraphy for the Late Cenozoic Sediments Overlying the Columbia River Basalt Group at the B Tank Farm.....	2.2
2.2	Location of Borehole 299-E33-46 Within the B Tank Farm.....	2.4
2.3	Summary Geologic Log for Borehole 299-E33-46.....	2.5
2.4	Sediment textural classification.....	2.14
2.5	Medium to coarse sand recovered from the Hanford Formation H2 Unit in Borehole 299-E33-46.....	2.16
2.6	Gravelly sand recovered from the Hanford formation H3 Unit in Borehole 299-E33-46.....	2.17
2.7	Calcareous, quartzo-feldspathic fine sand recovered from the upper portion of the PPlz unit in borehole 299-E33-46.....	2.20
2.8	Well-laminated silt to silty fine sand recovered from the lower portion of the PPlz unit in borehole 299-E33-46.....	2.20
2.9	Sandy gravel recovered from the PPlg subunit in borehole 299-E33-46.....	2.21
4.1	Moisture Content, Water Extract pH, Calculated Porewater, UFA and Suction Candle Porewater and Groundwater Electrical Conductivity for Borehole 299-E33-46.....	4.10
4.2	Major Anions Calculated (from sediment-to-water extracts), UFA and Suction Candle Porewaters and Groundwater from Borehole 299-E33-46.....	4.18
4.3	Cations Calculated (from sediment-to-water extracts), UFA, and Suction Candle Porewaters and Groundwater for Borehole 299-E33-46 Sediment.....	4.24
4.4	Pore Fluid Concentrations of Aluminum, Iron, Silicon, and Manganese (calculated from sediment-to-water extracts), UFA and Suction Candle Porewaters and Groundwater for 299-E33-46 Borehole Sediment.....	4.26
4.5	Radionuclide Pore Water (calculated from sediment-to-water extracts), UFA and Suction Candle Porewaters and Groundwater for 299-E33-46 Borehole Sediment.....	4.33
4.6	Porewater Ratios for Constituents versus Fluoride for 299-E33-46 Sediments.....	4.42

4.7	Porewater Ratios for Uranium and Sodium to Other Species.	4.43
4.8	Porewater Ratios for Key Constituents versus Each Other.....	4.44
4.9	Porewater Ratios for Key Constituents versus Chloride.....	4.45
4.10	Uranium-238 and Potassium-40 Content in Sediment from Borehole 299-E33-46.....	4.54
4.11	Strontium-90 Content of Borehole 299-E33-46 Vadose Zone Sediments.....	4.55
4.12	Correlation Between Bremsstrahlung Signal (count rate between 60 and 350 kev) and Actual Strontium-90 Concentration in Vadose Zone Sediments from Borehole 299-E33-46.....	4.56
4.13	Total Uranium in Sediment Based on Three Techniques	4.60
4.14	Technetium-99 and Uranium Concentrations in Acid and Water Extracts	4.64
4.15	Comparison Between Acid and Water Extractable Concentrations of Major Cations.....	4.80
4.16	Comparison Between Acid and Water Extractable Concentrations of Ba, Al, Si, and Fe	4.81
4.17	XRD Tracing of sample 110A along with the standard reference pattern for quartz.	4.90
4.18	XRD tracings of preferentially oriented clay slides taken from Borehole 299-E33-46 sample 110A.....	4.92
4.19	Matric Water Potential Measured by Filter Paper Technique on Core Samples from Borehole 299-E33-46	4.96
4.20	Matric Water Potential Measured by Filter Paper Technique on Core Samples from Borehole 299-E33-338 Located Outside the SE Perimeter of the B Tank Farm.	4.97
4.21	Vadose-Zone Monitoring System (without water-flux meter and temperature sensor) Before Deployment in B Tank Farm. Sensors from left to right are the Modified CSI Water Content Sensor, Advanced Tensiometer, Suction Candle, and Heat-Dissipation Unit.....	4.98

Tables

2.1	Stratigraphic Terminology Used in this Report for the Vadose Zone Beneath the B Tank Farm.....	2.2
2.2	Splitspoon Samples from 299-E33-46.....	2.6
2.3	Composite Grab and Split-Spoon Shoe Samples from 299-E33-46.....	2.7
2.4	Fine-Grained Beds in Borehole 299-E33-46.....	2.23
4.1	Moisture Content of Sediment from Borehole 299-E33-46. (4 pages).....	4.2
4.2	Water Extract pH and Electrical Conductivity Values.....	4.7
4.3	Anion Content of Water Extracts of Borehole 299-E33-46 (B-110 Sediment). (4 pages).....	4.14
4.4	Calculated Porewater Cation Composition from Water Extracts of Vadose Zone Sediment from 299-E33-46.....	4.19
4.5	Calculated and Actual Porewater Radionuclide Composition for Water Extracts of Sediment from 299-E33-46.....	4.28
4.6	Strontium-90 Recovery Waste Streams from Zirconium-Clad Fuel ^(a)	4.32
4.7	Ratio of Major Strontium Recovery Waste to Fluoride Found in Dilution Corrected 1:1 Water to Sediment Extracts.....	4.34
4.8	Ratio of Constituents in Dilution Corrected 1:1 Water Extracts Versus Each Other.....	4.38
4.9	Gamma Energy Analysis of Vadose Zone Sediment from Borehole 299-E33-46.....	4.47
4.10	Total Radionuclide Content of Vadose Zone Sediments from Borehole 299-E33-46.....	4.50
4.11	NTA Analyses for Selected 1:1 Sediment to Water Extracts From Strontium-90 Contaminated Sediments.....	4.52
4.12	Total Uranium Content in Vadose Zone Sediments Determined by Three Methods.....	4.57
4.13	Calculated In Situ Desorption K_d Values for Uranium in Vadose Sediments at 299-E33-46.....	4.61
4.14	Estimated recharge rates based on Tc-99 plume depth beneath B-110.....	4.66

4.15	Tritium Content in Vadose Zone Sediments Based on Water Extracts (pCi/g).....	4.68
4.16	Carbon Content in Vadose Sediment from 299-E33-46.....	4.69
4.17	Acid-Extractable Major Element Content of the Vadose Sediment from 299-E33-46 Borehole.....	4.73
4.18	Acid-Extractable RCRA Metal Content of the Vadose Sediment from 299-E33-46 Borehole.....	4.77
4.19	Total Composition of the Vadose Zone Sediment from 299-E33-46 Percent Weight as Oxides.....	4.83
4.20	Total Trace Constituents in Vadose Zone Sediment from 299-E33-46 in µg/g (ppm).....	4.85
4.21	Particle Size Distribution Percent Weight.....	4.88
4.22	Particle Density of Bulk Sediment from 299-E33-46	4.89
4.23	Semi-quantitative XRD Results of Minerals from the S01052 Borehole.....	4.91
4.24	Semi-quantitative XRD Results of Clay Minerals Separated from the Sediment Collected from Borehole 299-E33-46	4.93
4.25	Matric Potential Measurements on Core and Grab Samples from Borehole 299-E33-46.....	4.95
4.26	VZMS Sensor Placement in Borehole 299-E33-46 near Tank B110 in B Tank Farm	4.99
4.27	pH, Electrical Conductivity and Anion Composition of Suction Candle Derived Porewaters vs. Time.....	4.100
4.28	Major Cations and Selected Trace Metals Composition of Suction Candle Derived Porewaters vs. Time.....	4.101
4.29	Selected Trace Metals Composition of Suction Candle Derived Porewaters vs. Time	4.103
4.30	Composition of Groundwater Taken from Borehole 299-E33-46 at 255.8 ft bgs	4.106

1.0 Introduction

The overall goals of the of the Tank Farm Vadose Zone Project, led by CH2M HILL Hanford Group, Inc., are 1) to define risks from past and future single-shell tank farm activities, 2) to identify and evaluate the efficacy of interim measures, and 3) to aid via collection of geotechnical information and data, the future decisions that must be made by the Department of Energy (DOE) regarding the near-term operations, future waste retrieval, and final closure activities for the single-shell tank Waste Management Areas. For a more complete discussion of the goals of the Tank Farm Vadose Zone Project, see the overall work plan, *Phase 1 RCRA Facility Investigation/Corrective Measures Study Work Plan for the Single-Shell Tank Waste Management Areas* (DOE 1999). Specific details on the rationale for activities performed at the B-BX-BY Tank Farm waste management area (WMA) are found in CH2M HILL (2000).

To meet these goals, CH2M HILL Hanford Group, Inc., asked scientists from Pacific Northwest National Laboratory (PNNL) to perform detailed analyses of vadose zone sediment, both uncontaminated and contaminated, from within the B-BX-BY WMA.

Specifically, this report contains all the geologic, geochemical, and selected physical characterization data collected on vadose zone sediment recovered from borehole 299-E33-46 that is near tank B-110. We also provide our interpretation of the data in the context of determining the appropriate lithologic model, the vertical extent of contamination, the migration potential of the contaminants that still reside in the vadose zone, and the correspondence of the contaminant distribution in the borehole sediment to groundwater plumes in the aquifer proximate and down gradient from the B Tank Farm.

This report is one in a series of three reports to present recent data collected on vadose zone sediment, both uncontaminated and contaminated, from within the B-BX-BY WMA. Two other PNNL reports discuss the characterization of 1) uncontaminated sediment from a *Resource Conservation and Recovery Act* (RCRA) borehole [299-E33-338], to provide a baseline against information from contaminated sediment (see Lindenmeier et al. 2002); 2) contaminated sediment obtained from the 299-E33-45 northeast of tank BX-102 (see Serne et. al. 2002e), which has been decommissioned. This document describes all the characterization data collected and interpretations assembled by the Applied Geology and Geochemistry Group within PNNL's Environmental Technology Division. The main objective for placing the 299-E33-46 borehole at the location ~15 ft northeast from the B-110 tank wall was to investigate the vertical extent of strontium-90, uranium, technetium-99, and other mobile contaminants at a spot known to contain high strontium-90 contents based on bremsstrahlung signal in the spectral gamma logging. The borehole was extended to groundwater in order to track other mobile contaminants that can't be tracked with gamma logging such as technetium-99 and nitrate.

The documents contain preliminary interpretations to identify the distribution of key contaminants within the vadose zone and to determine what their future migration potential could be. The information will be incorporated in the B-BX-BY field investigation report.^(a)

This report is divided into sections that describe the geology, the geochemical characterization methods employed, the geochemical results that emphasize determination of the vertical extent of tank fluid migration and contaminant migration potential, as well as summary and conclusions, references cited, and four appendixes with additional details and sediment photographs.

^(a) *Draft Field Investigation Report for Waste Management Area B-BX-BY*. RPP-10098, Draft, Volume 2, Appendix D, CH2M HILL Hanford Group, Inc., Richland, Washington.

2.0 Geology

The geology of the vadose zone underlying the 241-B Tank Farm forms the framework through which the contaminants move, and provides the basis with which to interpret and extrapolate the physical and geochemical properties that control the migration and distribution of contaminants. Of particular interest are the interrelationships between the coarser and finer-grained facies, and the degree of contrast in their physical and geochemical properties.

This section presents a brief discussion on the geologic setting of the 241-B Tank Farm followed by a discussion on the drilling, sampling, and geophysical logging of borehole 299-E33-46 as well as a description and interpretation of the geologic materials penetrated by this borehole.

2.1 Geologic Setting of the 241-B Tank Farm

The 241-B Tank Farm was constructed in 1943 and 1944 to store high-level radioactive waste generated by chemical processing of irradiated uranium fuel at the chemical separation plants (DOE-GJPO 1999a). The tank farm was excavated into the Pleistocene-age Hanford formation and Holocene eolian deposits that mantle a portion of the northern flank of the Cold Creek flood bar (Wood et al. 2000). The geology beneath the B Tank Farm has been described in numerous reports (Price and Fecht 1976; Caggiano and Goodwin 1991; Caggiano 1996; Narbutovskih 1998; DOE-GJPO 1999a; Wood et al. 2000; and Lindsey et al. 2001). The major stratigraphic units beneath the tank farm include (in descending order); the Hanford formation, a unit described as Hanford formation/Plio-Pleistocene unit (?) [Hf/PPu(?)], and the Columbia River Basalt Group (Figure 2.1). The uppermost 10.7 m (35 ft) of the Hanford formation was removed during construction of the tank farm and the stockpiled sediments were later used as backfill, placed around and over the underground storage tanks.

The stratigraphic nomenclature used in this report is summarized in Table 2.1. Stratigraphic terminology used in this report is consistent with that presented in Wood et al. (2000) and Lindsey et al. (2001) for the Hanford formation. However, the interpretation of stratigraphic units underlying the Hanford formation differs for these two reports. Wood et al. (2000) interpret the gravel sequence under a thick (up to 10 m [33 ft]) Plio-Pleistocene age silt layer (PPlz) as a mainstream alluvial deposits of Plio-Pleistocene age, while Lindsey et al. (2001) interpret this gravel sequence as older Ringold Formation. The mafic content in these sandy gravels appears unlike that for the mostly quartzo-feldspathic Ringold Formation. Furthermore, numerous past studies (Tallman et al 1979; Last et al. 1989; Connelly et al. 1992; Williams et al. 2001) have never identified the Ringold Formation this far north within the 200 East Area. Therefore, we prefer the interpretation of Wood et al. (2000) that this gravel sequence is part of the Plio-Pleistocene unit, and thus it is designated as Plio-Pleistocene gravel (PPlg) in this report.

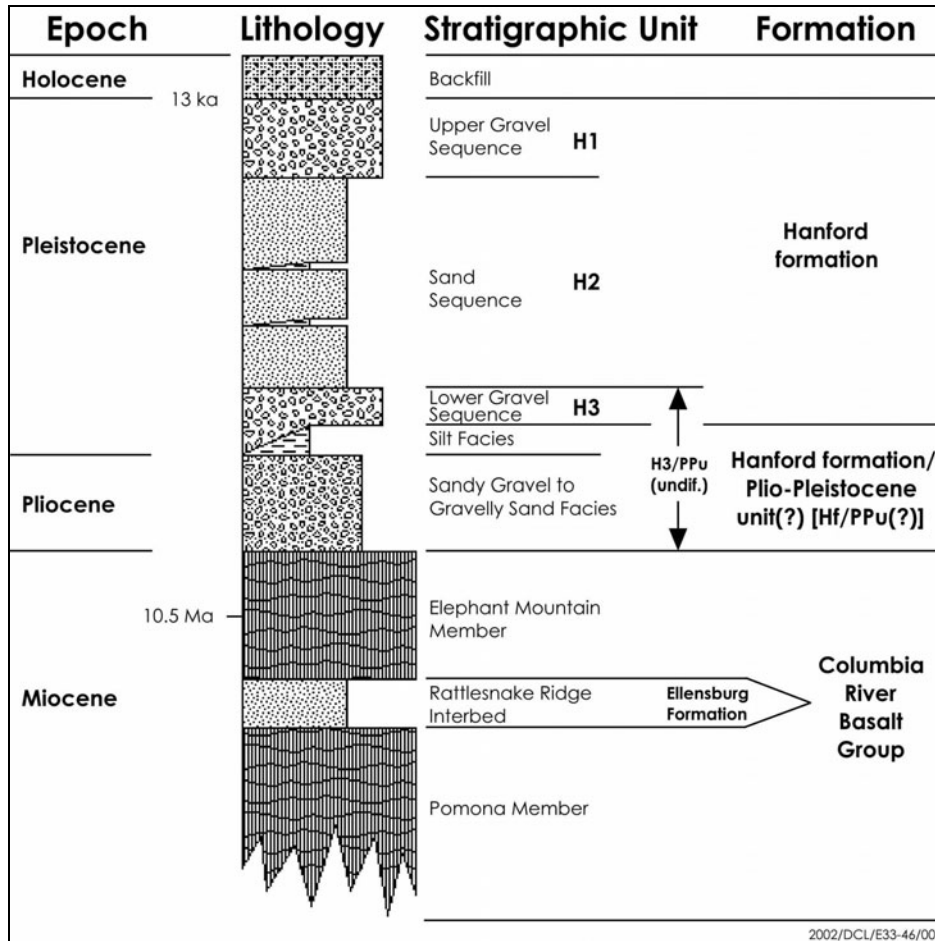


Figure 2.1. Generalized, Composite Stratigraphy for the Late Cenozoic Sediments Overlying the Columbia River Basalt Group at the B Tank Farm (Modified After Wood et al. 2000)

Table 2.1. Stratigraphic Terminology Used in this Report for the Vadose Zone Beneath the B Tank Farm. (2 Pages)

Stratigraphic Symbol	Formation	Facies / Subunit	Description	Genesis
Backfill	NA	Backfill	Poorly to moderately sorted cobbles, pebbles, and coarse to medium sand with some silt derived from coarse-grained Hanford formation (H1 Unit) excavated around tanks (Price and Fecht 1976)	Anthropogenic
H1	Hanford formation	Unit H1	Upper sandy gravel to gravelly sand sequence. Equivalent to the H1 unit discussed by Lindsey et al. (1994, 2001) the upper gravel sequence discussed by Last et al. (1989) and Lindsey et al. (1992), and the Qfg documented by Reidel and Fecht (1994). Excavated out and missing from most of B Tank Farm.	Cataclysmic Flood Deposits

Table 2.1. Stratigraphic Terminology Used in this Report for the Vadose Zone Beneath the B Tank Farm. (2 Pages)

Stratigraphic Symbol	Formation	Facies / Subunit	Description	Genesis
H2		Unit H2	Sand sequence consisting predominantly of sand-dominated facies, with multiple graded beds of horizontal to tabular cross-bedded sand to slightly gravelly sand. Graded beds sometimes capped with thin layers of silty sand to silt. Equivalent to H2 unit of Wood et al. (2000) and Lindsey et al. (1994, 2001), the sandy sequence of Last et al. (1989) and Lindsey et al. (1992), and to Qfs documented by Reidel and Fecht (1994).	
H3		Unit H3	Lower gravelly sand to slightly gravelly sand sequence. Equivalent to the H3 unit of Lindsey et al. (1994, 2001) lower gravel sequence discussed by Last et al. (1989) and Lindsey et al. (1992), and the Qfg documented by Reidel and Fecht (1994).	
Hf/PPu and/or PPlz	Hanford Formation/ Plio-Pleistocene Unit (?)	Silt-Dominated Facies	Silty sequence consisting of interstratified well sorted calcareous silt and fine sand. Equivalent to the Silt facies of the Hanford Formation/Plio-Pleistocene Unit(?) of Wood et al. (2000). Perhaps equivalent to the “early Palouse soil” originally described by Tallman et al. (1979) and DOE (1988). Also equivalent to the upper portion of the Hanford/Plio-Pleistocene/Ringold(?) of Lindsey et al. (2001)	Fluvial overbank and/or eolian deposits (with some weakly developed paleosols)
Hf/PPu and/or PPlg		Sandy Gravel to Gravelly Sand Dominated Facies	Sandy gravel to gravelly sand sequence consisting predominantly of unconsolidated basaltic sands and gravels. Actual origin of this unit is still uncertain. Without intervening silt facies (PPlz subunit) this unit cannot be differentiated from the Hanford formation H3 unit (Wood et al. 2000). Lindsey et al. (2001) suggested this unit may be part of the Ringold Formation.	Plio-Pleistocene age mainstream alluvium (Wood et al. 2000) or possibly Ringold Formation (Lindsey et al. 2001)

2.2 Drilling and Sampling of Borehole 299-E33-46 (C3360)

Borehole 299-E33-46 was drilled using the cable-tool technique between May 8 and June 26, 2001. The borehole is located approximately 5 m (15 ft) from the northeast edge of single-shell tank 241-B-110 (Figure 2.2), which was first recognized as a suspected leaker in 1973 later becoming an assumed leaker in 1984 (DOE-GJPO 1999b). Total depth of the borehole was 80.6 m (264.4 ft) below ground surface (bgs); the groundwater table was encountered at 78.0 m (255.8 ft) bgs. The borehole was later completed as a well for the installation of down-hole hydrologic sensors (Reynolds 2001). The surveyed well

elevation is 200.3 m (657.3 ft) above mean sea level; geographic coordinates are N13728.365 and E573792.553.

During drilling, a total of 33 two-ft long, 4-inch diameter split- spoon core samples were collected starting at a depth of about 3 m (10 ft) bgs (Table 2.2, Figure 2.3). Four 0.5 ft long stainless-steel core liners were used in each 2-ft split spoon. A geologic log was compiled in the field by a Duratek Federal Services, Inc. (DFS) subcontract geologist (KR Simpson), based on observations made on cuttings retrieved from the core barrel between core runs as well as the exposed ends of contained split-spoon samples (Reynolds 2001). Core extraction was performed later in a radiologically controlled PNNL laboratory between July 10th and 18th, 2001. At this time a second geologic log, which describes the character of the core interiors, was prepared by a PNNL geologist (BN Bjornstad). Geologic logging occurred after each core segment was emptied into an open plastic container, followed by photographing and sub-sampling for physical and chemical characterization. Material from each 0.5 ft liner was placed into a separate plastic container and after geologic logging, photographing and sub-sampling, the plastic containers were sealed shut and placed into cold storage. Selected composite grab samples were also examined in the laboratory.

Geologic description on the opened cores and composite grab samples was performed according to the procedure outlined in PNNL (1999). Both of the Duratek and PNNL geologic core logs from borehole 299-E33-46 are presented in Appendix B of Lindsey et al. (2001). A one-page summary log of borehole 299-E33-46, compiled from the geologic logs, is presented in Figure 2.3. Penetration resistance (i.e., blowcounts) and percent core recovered from each 2 ft core run are also plotted in Figure 2.3, based on data presented in Appendix D of Reynolds (2001).

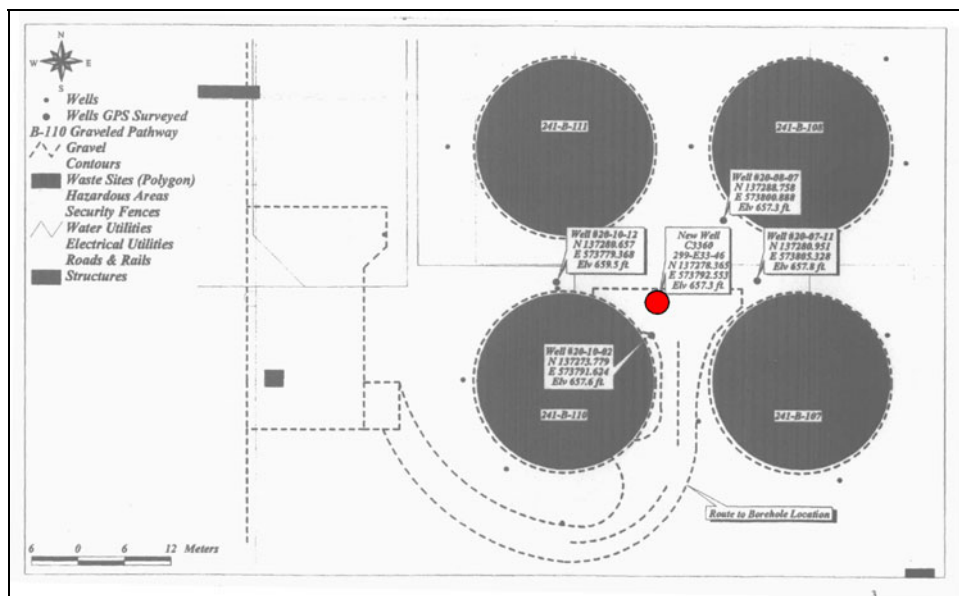


Figure 2.2. Location of Borehole 299-E33-46 Within the B Tank Farm. Modified after Reynolds (2001).

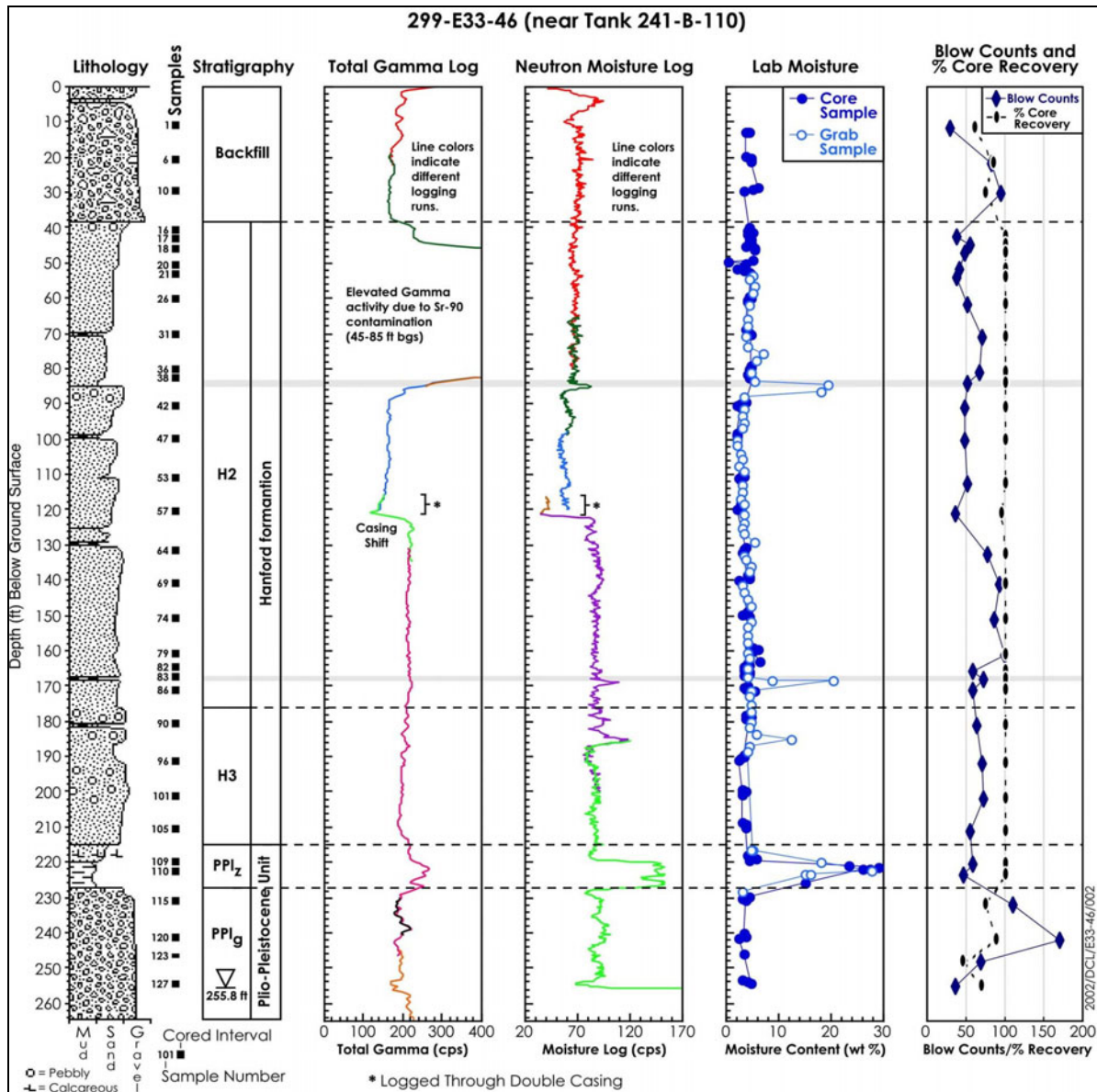


Figure 2.3. Summary Geologic Log for Borehole 299-E33-46.

Two sets of temporary casing were used to control the borehole during drilling and sampling (Reynolds 2001). Surface casing (13 3/8 in. outside diameter [OD]) was set to 37.0 m (121.3 ft) bgs; the second casing (10 3/4 in OD) was installed to just above total depth (80.5 m [264.2 ft] bgs). Anticipated perched-water conditions were not encountered atop a fine-grained silt layer at 67 m (220 ft) bgs, thus it was not necessary to telescope down to a smaller-diameter casing within this fine-grained zone. Eight vadose zone porewater sensor arrays were installed in the borehole prior to decommissioning and removal of temporary casing (Reynolds 2001).

Thirty-three split-spoon core samples were collected between 3 and 77 m (10 and 254 ft) bgs - an average of every 2.3 m (7.5 ft). Grab samples were collected between these core sample intervals to yield near continuous samples to a depth of 78.3 m (257 ft). The split-spoon samples were taken ahead of the

casing by driving a split-spoon sampler into the undisturbed formations below the casing. The complete list of split-spoon cores collected, depth interval, sediment description, and percent core recovery is listed in Table 2.2. The relative location of each 2-ft split-spoon core is shown graphically in Figure 2.3. Core recovery was excellent (95-100%) in the finer grained sediments, decreasing significantly in the coarser materials (Table 2.2, Figure 2.3).

Table 2.2. Splitspoon Samples from 299-E33-46. (2 pages)

Field Sample No.	Top Depth (ft)⁽¹⁾	Bottom Depth (ft)⁽¹⁾	Sampled Interval Thickness (ft)⁽¹⁾	Sediment Description	Stratigraphic Unit	% Core Recovery
S01052-1	9.5	11.7	2.0	Sandy gravel	Backfill	60
S01052-6	19.3	21.6	2.0	Sandy to pebbly gravel	Backfill	85
S01052-10	27.7	30.0	2.0	Sand and cobbles	Backfill	75
S01052-16	40.0	42.3	2.0	Sand	H2	100
S01052-17	42.3	44.6	2.0	Sand	H2	100
S01052-18	44.7	47.0	2.0	Sand	H2	100
S01052-20	48.9	51.2	2.0	Coarse sand	H2	100
S01052-21	51.3	53.6	2.0	Sand	H2	100
S01052-26	59.0	61.3	2.0	Sand	H2	100
S01052-31	68.7	71.0	2.0	Sand	H2	100
S01052-36	78.2	80.5	2.0	Sand	H2	100
S01052-38	81.3	83.6	2.0	Sand	H2	100
S01052-42	88.6	90.9	2.0	Sand	H2	100
S01052-47	97.9	100.2	2.0	Sand	H2	100
S01052-53	109.7	112.0	2.0	Sand	H2	100
S01052-57	118.2	120.5	2.0	Sand	H2	95
S01052-64	130.1	132.4	2.0	Sand, salt and pepper	H2	100
S01052-69	138.3	140.6	2.0	Sand	H2	100
S01052-74	148.4	150.7	2.0	Sand	H2	100
S01052-79	158.4	160.7	2.0	Sand	H2	100
S01052-82	162.8	165.1	2.0	Sand	H2	100
S01052-83	165.1	167.4	2.0	Sand	H2	100
S01052-86	169.4	171.7	2.0	Sand	H2	100
S01052-90	178.1	180.4	2.0	Sand	H3	100
S01052-96	189.1	191.4	2.0	Coarse sand	H3	100
S01052-101	199.2	201.5	2.0	Sand	H3	100
S01052-105	208.4	210.7	2.0	Sand	H3	100

Table 2.2. Splitspoon Samples from 299-E33-46. (2 pages)

Field Sample No.	Top Depth (ft) ⁽¹⁾	Bottom Depth (ft) ⁽¹⁾	Sampled Interval Thickness (ft) ⁽¹⁾	Sediment Description	Stratigraphic Unit	% Core Recovery
S01052-109	217.7	220.0	2.0	Sand/silt	PPlz	100
S01052-110	220.4	222.7	2.0	Silt/clay	PPlz	100
S01052-115	229.4	231.7	2.0	Gravel/sand	PPlg	75
S01052-120	239.4	241.7	2.0	Gravel/sand	PPlg	87.5
S01052-123	245.5	246.0	0.5	Gravel	PPlg	44
S01052-127	252.4	254.7	2.0	Gravel/sand	PPlg	69

⁽¹⁾ to convert to meters multiply by 0.3048

H2 = Hanford H2 Sand Sequence (see Table 2.1)

H3 = Hanford H3 Lower Sand Sequence (see Table 2.1)

PPlz = Plio-Pleistocene silt (see Table 2.1)

PPlg = Plio-Pleistocene gravel (see Table 2.1)

Table 2.3. Composite Grab and Split-Spoon Shoe Samples from 299-E33-46. (6 pages)

Sample No.	Top Depth (ft) ⁽¹⁾	Bottom Depth (ft) ⁽¹⁾	Sampled Interval Thickness (ft) ⁽¹⁾	Sample Type	Sample Description	Stratigraphic Unit
S01052-03	11.80	14.07	2.27	Composite Grab	*	*
S01052-04	14.07	15.90	1.83	Composite Grab	*	*
S01052-05	15.90	18.00	2.10	Composite Grab	*	*
S01052-06	21.37	21.60	0.23	Splitspoon Shoe	*	*
S01052-07	21.60	24.10	2.50	Composite Grab	*	*
S01052-08	24.10	26.00	1.90	Composite Grab	*	*
S01052-09	26.00	27.70	1.70	Composite Grab	*	*
S01052-10	29.67	30.00	0.33	Splitspoon Shoe	*	*
S01052-11	30.00	31.70	1.70	Composite Grab	*	*
S01052-12	31.70	33.30	1.60	Composite Grab	*	*
S01052-13	33.30	35.40	2.10	Composite Grab	*	*
S01052-14	35.40	37.80	2.40	Composite Grab	*	*
S01052-15	37.80	40.00	2.20	Composite Grab	*	*
S01052-16	41.97	42.30	0.33	Splitspoon Shoe	*	*
S01052-17	44.27	44.60	0.33	Splitspoon Shoe	*	*
S01052-18	46.67	47.00	0.33	Splitspoon Shoe	*	*
S01052-19	47.00	48.90	1.90	Composite Grab	*	*

Table 2.3. Composite Grab and Split-Spoon Shoe Samples from 299-E33-46. (6 pages)

Sample No.	Top Depth (ft) ⁽¹⁾	Bottom Depth (ft) ⁽¹⁾	Sampled Interval Thickness (ft) ⁽¹⁾	Sample Type	Sample Description	Stratigraphic Unit
S01052-20	50.87	51.20	0.33	Splitspoon Shoe	*	*
S01052-21	53.27	53.60	0.33	Splitspoon Shoe	*	*
S01052-22	53.60	55.60	2.00	Composite Grab	*	*
S01052-23	53.60	55.60	2.00	Composite Grab	*	*
S01052-24	55.60	57.80	2.20	Composite Grab	*	*
S01052-25	57.80	59.00	1.20	Composite Grab	*	*
S01052-26	60.97	61.30	0.33	Splitspoon Shoe	*	*
S01052-27	61.30	62.90	1.60	Composite Grab	*	*
S01052-28	62.90	64.90	2.00	Composite Grab	*	*
S01052-29	64.90	67.20	2.30	Composite Grab	*	*
S01052-30	67.20	68.70	1.50	Composite Grab	*	*
S01052-31	70.70	71.00	0.30	Splitspoon Shoe	*	*
S01052-32	71.00	72.70	1.70	Composite Grab	*	*
S01052-33	72.70	74.30	1.60	Composite Grab	*	*
S01052-34	74.30	76.50	2.20	Composite Grab	Medium sand	H2
S01052-35	76.50	78.20	1.70	Composite Grab	*	*
S01052-36	80.50	80.50	0.00	Splitspoon Shoe	*	*
S01052-37	80.50	81.30	0.80	Composite Grab	*	*
S01052-38	83.30	83.60	0.30	Splitspoon Shoe	Medium sand	H2
S01052-39	83.60	85.50	1.90	Composite Grab	Medium sand	H2
S01052-40	85.50	87.10	1.60	Composite Grab	*	*
S01052-41	87.10	88.60	1.50	Composite Grab	*	*
S01052-42	90.87	90.90	0.03	Splitspoon Shoe	*	*
S01052-43	90.90	92.00	1.10	Composite Grab	Slightly pebbly coarse sand	H2
S01052-44	92.00	94.30	2.30	Composite Grab	Medium sand	H2
S01052-45	94.30	96.00	1.70	Composite Grab	Medium sand	H2
S01052-46	96.00	97.90	1.90	Composite Grab	*	*
S01052-47	99.87	100.20	0.33	Splitspoon Shoe	Medium to coarse sand	H2
S01052-48	100.20	102.90	2.70	Composite Grab	Coarse sand	H2
S01052-49	102.90	104.80	1.90	Composite Grab	Medium to coarse sand	H2

Table 2.3. Composite Grab and Split-Spoon Shoe Samples from 299-E33-46. (6 pages)

Sample No.	Top Depth (ft) ⁽¹⁾	Bottom Depth (ft) ⁽¹⁾	Sampled Interval Thickness (ft) ⁽¹⁾	Sample Type	Sample Description	Stratigraphic Unit
S01052-50	104.80	106.60	1.80	Composite Grab	Medium to coarse sand	H2
S01052-51	106.60	108.30	1.70	Composite Grab	Medium to coarse sand	H2
S01052-52	108.30	109.70	1.40	Composite Grab	*	*
S01052-53	111.67	112.00	0.33	Splitspoon Shoe	*	*
S01052-54	112.00	114.00	2.00	Composite Grab	Coarse sand	H2
S01052-55	114.00	115.80	1.80	Composite Grab	Medium to coarse sand	H2
S01052-56	115.80	118.20	2.40	Composite Grab	Medium to coarse sand	H2
S01052-58	120.70	122.30	1.60	Composite Grab	Medium to coarse sand	H2
S01052-59	122.70	124.30	1.60	Composite Grab	Medium sand	H2
S01052-60	122.70	124.30	1.60	Composite Grab	Medium sand	H2
S01052-61	124.30	125.80	1.50	Composite Grab	Medium to coarse sand	H2
S01052-62	125.80	127.70	1.90	Composite Grab	Medium to coarse sand	H2
S01052-63	127.70	130.10	2.40	Composite Grab	Medium to coarse sand with silt lens	H2
S01052-64	132.10	132.40	0.30	Splitspoon Shoe	*	*
S01052-65	132.40	133.30	0.90	Composite Grab	Coarse sand	H2
S01052-66	133.30	135.10	1.80	Composite Grab	Coarse sand	H2
S01052-67	135.10	136.90	1.80	Composite Grab	Medium to coarse sand	H2
S01052-68	136.90	138.30	1.40	Composite Grab	Coarse sand	H2
S01052-69	140.30	140.60	0.30	Splitspoon Shoe		
S01052-70	140.60	142.20	1.60	Composite Grab	Medium to coarse sand	H2
S01052-71	142.20	144.50	2.30	Composite Grab	Medium to coarse sand	H2
S01052-72	144.50	146.50	2.00	Composite Grab	Medium to coarse sand	H2

Table 2.3. Composite Grab and Split-Spoon Shoe Samples from 299-E33-46. (6 pages)

Sample No.	Top Depth (ft) ⁽¹⁾	Bottom Depth (ft) ⁽¹⁾	Sampled Interval Thickness (ft) ⁽¹⁾	Sample Type	Sample Description	Stratigraphic Unit
S01052-73	146.50	148.40	1.90	Composite Grab	Medium to coarse sand	H2
S01052-74	150.40	150.70	0.30	Splitspoon Shoe	*	*
S01052-75	150.70	152.20	1.50	Composite Grab	Medium to coarse sand	H2
S01052-76	152.20	154.40	2.20	Composite Grab	Medium to coarse sand	H2
S01052-77	154.40	156.60	2.20	Composite Grab	Medium to coarse sand	H2
S01052-78	156.60	158.60	2.00	Composite Grab	Medium to coarse sand	H2
S01052-79	160.40	160.70	0.30	Composite Grab	Medium to coarse sand	H2
S01052-80	160.70	162.80	2.10	Composite Grab	Medium sand	H2
S01052-81	160.70	162.80	2.10	Composite Grab	Medium sand	H2
S01052-82	164.80	165.10	0.30	Composite Grab	Medium to coarse sand	H2
S01052-83	167.10	167.40	0.30	Composite Grab	Medium to coarse sand	H2
S01052-84	167.50	169.40	1.90	Composite Grab	*	*
S01052-85	168.10	168.40	0.30	Composite Grab	Fine sandy silt	H2
S01052-86	171.40	171.70	0.30	Composite Grab	Coarse sand	H2
S01052-87	171.70	174.10	2.40	Composite Grab	Medium to coarse sand	H2
S01052-88	174.10	176.10	2.00	Composite Grab	Medium to coarse sand	H2
S01052-89	176.10	178.10	2.00	Composite Grab	Pebbly sand	H3
S01052-90	180.10	180.40	0.30	Composite Grab	Pebbly sand	H3
S01052-91	180.40	183.10	2.70	Composite Grab	Fine to medium sand with silty fine sand lens	H3
S01052-92	183.10	184.30	1.20	Composite Grab	Pebbly sand	H3
S01052-93	184.30	185.90	1.60	Composite Grab	Pebbly sand	H3
S01052-94	185.90	187.80	1.90	Composite Grab	Medium sand	H3

Table 2.3. Composite Grab and Split-Spoon Shoe Samples from 299-E33-46. (6 pages)

Sample No.	Top Depth (ft) ⁽¹⁾	Bottom Depth (ft) ⁽¹⁾	Sampled Interval Thickness (ft) ⁽¹⁾	Sample Type	Sample Description	Stratigraphic Unit
S01052-95	187.80	189.10	1.30	Composite Grab	Medium sand	H3
S01052-97	191.40	193.50	2.10	Composite Grab	*	*
S01052-98	193.50	195.10	1.60	Composite Grab	*	*
S01052-99	195.10	197.50	2.40	Composite Grab	*	*
S01052-100	197.50	199.20	1.70	Composite Grab	*	*
S01052-102	201.50	203.30	1.80	Composite Grab	*	*
S01052-103	203.30	205.80	2.50	Composite Grab	*	*
S01052-104	201.50	203.30	1.80	Composite Grab	*	*
S01052-105	210.20	210.70	0.50	Composite Grab	*	*
S01052-106	210.70	213.70	3.00	Composite Grab	*	*
S01052-107	213.70	215.70	2.00	Composite Grab	*	*
S01052-108	215.70	217.70	2.00	Composite Grab	Fine sand	PPlz
S01052-109	219.90	220.00	0.10	Composite Grab	Fine sand over silt	PPlz
S01052-110	222.40	222.70	0.30	Composite Grab	Fine sandy silt	PPlz
S01052-111	222.70	224.30	1.60	Composite Grab	Silty fine sand	PPlz
S01052-112	222.70	224.30	1.60	Composite Grab	Silty fine sand	PPlz
S01052-113	224.30	227.50	3.20	Composite Grab	*	*
S01052-114	227.70	229.20	1.50	Composite Grab	Sandy gravel	PPlg
S01052-116	231.70	233.70	2.00	Composite Grab	*	*
S01052-117	233.70	235.70	2.00	Composite Grab	*	*

Table 2.3. Composite Grab and Split-Spoon Shoe Samples from 299-E33-46. (6 pages)

Sample No.	Top Depth (ft) ⁽¹⁾	Bottom Depth (ft) ⁽¹⁾	Sampled Interval Thickness (ft) ⁽¹⁾	Sample Type	Sample Description	Stratigraphic Unit
S01052-118	235.70	238.00	2.30	Composite Grab	*	*
S01052-119	238.00	239.40	1.40	Composite Grab	*	*
S01052-121	241.70	243.80	2.10	Composite Grab	*	*
S01052-122	243.80	245.20	1.40	Composite Grab	*	*
S01052-124	246.00	247.50	1.50	Composite Grab	*	*
S01052-125	247.50	249.50	2.00	Composite Grab	*	*
S01052-126	249.50	252.40	2.90	Composite Grab	*	*
S01052-128	254.70	255.10	0.40	Composite Grab	*	*
S01052-129	254.70	255.10	0.40	Composite Grab	*	*

⁽¹⁾to convert to meters multiply by 0.3048

H2 = Hanford H2 Sand Sequence (see Table 2.1)

H3 = Hanford H3 Lower Sand Sequence (see Table 2.1)

PPlz = Plio-Pleistocene silt (see Table 2.1)

PPlg = Plio-Pleistocene gravel (see Table 2.1)

* Not examined

Each of the 33 split-spoon core runs were disassembled in the field and the set of four, half-foot sample liners recovered. The lower most sample liner was labeled "A" and the upper most liner labeled "D". Each liner was individually capped and packaged for transport to the PNNL's radioactive sample handling laboratory at the 3720 Building, located within the 300 Area. All split-spoon liners and composite grab samples were surrounded by blue ice to maintain sample temperature between 2 to 4° C during transport. The shipping containers were sealed with custody tape and maintained under chain-of-custody protocols. Upon arriving at the 3720 Building, samples were placed into cold storage until such a time that liners could be opened and sub-sampled.

2.3 Geophysical Logging

Geophysical logging (total gamma, spectral gamma, and neutron moisture) in borehole 299-E33-46 was performed twice by Duratek Federal Services, Inc., once before downsizing to the smaller-diameter casing to a depth of 37.0 m (121.3 ft) bgs, and again upon reaching total depth (80.6 m [264.4 ft] bgs). Detailed descriptions of the logging tools and data analysis can be found in reports by Reynolds (2001)

and Lindsey et al. (2001). Composites of the neutron-moisture and total gamma logs are illustrated in Figure 2.3.

The neutron-moisture log is generally used to depict the relative moisture content within a 20 to 30 cm (8 to 12 in) radius around the borehole. However, the neutron-moisture logging tool was not calibrated for the casing conditions, therefore absolute moisture values cannot be obtained directly from the neutron-moisture log.

Two different high-purity germanium (HPGe) spectral-gamma logging events were conducted to identify the specific gamma-emitting radionuclides in the formation surrounding the borehole (Reynolds 2001). A different logging event was conducted at the end of each drilling phase, through a single thickness of casing (with the exception of short overlaps between successive events) (Lindsey et al. 2001).

A sharp prolonged increase in total gamma activity between 14 to 26 m (45 to 85 ft) bgs (Figure 2.3) is apparently associated with a zone of strontium-90 contamination in the subsurface (DOE-GJPO 1999b). The silt-dominated unit between 67 to 69.5 m (220 to 228 ft) bgs is also well defined on the total gamma log, coincident with a high-moisture zone on the neutron-moisture log (Figure 2.3).

2.4 Sample Handling

Once received by the laboratory the sample liners and grab samples were stored in a refrigerator to maintain the sample temperatures between 2 and 4° C. All the split-spoon sample liners were opened, sub-sampled, and geologically described. In addition, 54 out of a total of 120 composite grab samples listed in Table 2.3 were opened, sub-sampled, logged, and photographed.

Processing of the split-spoon cores (Table 2.2) was as follows. Each split-spoon sampler was taken to a fume hood, unpackaged and the lower two (i.e. deeper two designated A and B) of the four liners were opened. A small portion of the sample (approximately 1 cm) was scraped away and a sandwich of three filter papers (for matric potential measurements) was inserted into the sample. The scraped materials were then placed back over the filter paper sandwich such that the filter paper sandwich was surrounded by, and in intimate contact with, the soil matrix. The end cap was replaced, sealed with tape, and the sample returned to the refrigerated storage.

About three weeks later, all split-spoon liners were sequentially taken to a fume hood for sample processing. Initially, the liner end caps were removed and an estimate of the approximate amount of sample material retained in the liner (% recovery) was noted on the geologic log. Then all the material within a liner was placed in a plastic tray (one plastic tray per liner). Material within the plastic tray was then sub-sampled for physical and geochemical analysis, photographed, and described geologically.

Sediment within the sample liners was extracted using a hammer to tap on the stainless-steel liner to get the materials to fall out into the plastic sample tray. Efforts were made to keep the sample materials as intact as possible. However, the unconsolidated friable nature of these coarse-grained materials generally made it impossible to preserve the internal sedimentary structures in these materials.

2.5 Sub-sampling and Geologic Description

Immediately, upon extracting material from the core liner or grab sample container, moisture samples were collected. An attempt was made to sample the finer grained and/or wetter materials as well as distinct hydrogeologic units, while at the same time trying to avoid slough and/or other unrepresentative portions. The remaining portions of the samples were then used for a brief visual geologic evaluation.

The visual geologic evaluation was conducted in accordance with procedures American Society for Testing and Materials (ASTM) D2488 (ASTM 1993) and PNL-DO-1 (PNL 1990). Throughout the sub-sampling and geologic evaluation activities, the laboratory geologist made continual visual observations regarding the mineralogy, structure, grain-size distribution (and sorting), grain-shape (e.g. roundness), color, moisture, consolidation, and reaction to dilute hydrochloric acid (HCl) (used to test for the presence of calcium carbonate). Copies of the geologist's logs are found in Appendix A. Particular attention was given to visually estimate the percentage (by weight) of gravel, sand, and mud (silt + clay), and to visually classify the samples based on the modified Folk (1968) and/or Wentworth (1922) classification scheme historically used at the Hanford Site. This sediment classification scheme uses a ternary diagram to categorize the sediment into one of 19 textural classes based on the relative proportions of gravel, sand, and mud (silt + clay) (Figure 2.4). Geologic logs recording the visual observations made while opening, sub-sampling and characterizing and these materials, are presented in Lindsey et al. (2001, Appendix B). Photographs were also taken of each of over 100 core liners after extrusion into their respective plastic trays. A few of these photographs appear in subsequent sections of this report and most of them are in Appendix B. A portion of the grab samples (Table 2.3) were also examined and photographed in the laboratory. These photographs, along with core photos are available online to PNNL staff at [\\Wd26776\AGGPublic\B-110 Final Report\E33-46 Photos](http://Wd26776\AGGPublic\B-110 Final Report\E33-46 Photos).

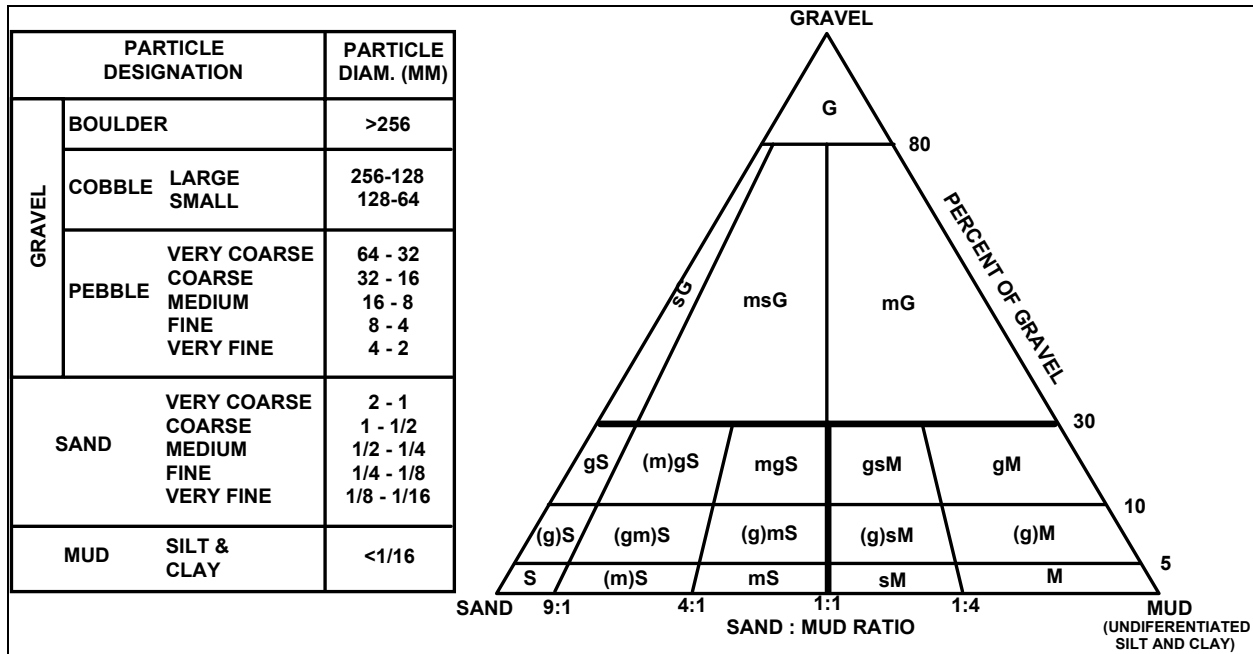


Figure 2.4. Sediment textural classification (modified after Folk 1968 and Wentworth 1922)

2.6 Geology of Borehole 299-E33-46

Figure 2.3 presents a summary log of borehole 299-E33-46 based on the field geologists logs, geologic descriptions of the split-spoon and composite grab sample materials, laboratory analyses, and geophysical logs. Three primary stratigraphic units were encountered by this borehole: 1) backfill materials, 2) the Hanford formation, and 3) the Plio-Pleistocene unit. A brief description of the sampled materials from each of these major stratigraphic units is presented below.

2.6.1 Backfill

The backfill extends from the ground surface to a depth of 11.7 m (38.5 ft) where it lies in contact with the Hanford formation (Figure 2.3). Three split-spoon samples were collected from the backfill. The backfill material consists of predominantly dark to olive gray, moderately sorted, silty sandy gravel to gravelly sand, which is unconsolidated and weakly to strongly calcareous. An unusual pink coating was noted on cobbles recovered from about 6.4 m (21 ft) bgs. The neutron-moisture log shows higher moisture just below the surface, probably associated with near-surface natural recharge. A greater penetration resistance (i.e., blowcounts) and poorer core recovery in the backfill are consistent with the relatively high percentage of gravel compared to the underlying sands of the Hanford formation.

2.6.2 Hanford Formation

Recent geologic reports (Wood et al. 2000, Lindsey et al. 2001), divide cataclysmic flood deposits of the Hanford formation beneath the 241-B Tank Farm into three informal units (H1, H2, and H3). However, it appears that the H1 unit was completely removed during excavation in the vicinity of borehole 299-E33-46, and then later used as backfill around the tanks. Based on the lithologies observed during drilling and in core samples, the Hanford formation beneath the backfill consists of mostly sand separated by several distinctly finer (fine sand to silt) strata. A total of three moisture spikes occur within the Hanford formation associated with these fine-grained intervals and/or other interfaces between strata with contrasting grain sizes (Figure 2.3).

The sands are associated with moderate to high energy deposition during flooding, while relatively thin fine sand to silt layers represent remnants of slack-water sedimentation deposited towards the end of ice-age flood episodes (Baker et al. 1991). According to Lindsey et al. (2001), the H2 unit, which consists of predominantly sand, occurs to a depth of 56.7 m (186 ft) bgs in 299-E33-46. However, the uppermost gravelly interval, used to define the boundary between H2 and H3, was observed 3 m (10 ft) higher in cores to a depth of 54 m (176 ft) bgs. Below this depth lies the H3 unit, a predominantly coarser-grained gravelly sand sequence that extends to base of the Hanford formation at 65.5 m (215 ft) bgs.

A significant zone, approximately 12 m (40 ft) thick, of radionuclide contamination (strontium-90) occurs at the top of the Hanford formation starting at the interface with the overlying coarse-grained backfill (Figure 2.3). The base of the strontium-90 contamination as defined by bremsstrahlung radiation in the spectral gamma log is well defined and occurs just above a 0.5 m (1.5 ft) thick very fine sand layer, which may have acted as a localized perched zone or capillary boundary.

2.6.2.1 Hanford Formation H2 Unit

The Hanford formation H2 unit is present between 12 to 54 m (38.5 to 176 ft) bgs. A total of 20 2-ft split- spoon cores were collected from this unit, which consists of mostly olive gray, moderately to well sorted, fine- to coarse-grained sand beds. These beds show occasional weak horizontal laminations and are generally noncalcareous to weakly calcareous. Within this sequence also lies several feet of loose, gravelly sand around 26 m (86 ft) bgs. Dispersed within the Hanford formation H2 unit are four separate, relatively thin (≤ 0.6 m [2 ft]), olive brown to grayish brown, compact, well-sorted fine sand to silt beds. These occur at depths of about 21.2, 30.0, 37.5, and 51.2 m (69.7, 98.5, 123.0, and 168.0 ft) bgs (Figure 2.3).

The most common sediment type within the H2 unit, a medium-to coarse grained sand, is represented in Figure 2.5. The term “salt and pepper” is often used to describe sands of the H2 unit on geologic logs due to the roughly equal amounts of dark- (basaltic) and light-colored (quartz and feldspar) grains. While this unit appears to be unconsolidated the penetration resistance (i.e., blow counts) increases slightly for the middle portion between 40 to 47 m (130 to 155 ft) bgs (Figure 2.3), which might reflect a greater degree of compaction within this interval. Core recovery was consistently 100% within the H2 unit.



Figure 2.5. Medium to coarse sand recovered from the Hanford Formation H2 Unit in Borehole 299-E33-46.

2.6.3 Hanford Formation H3 Unit

The top of the Hanford formation H3 unit is defined by a transition from predominantly sand to slightly gravelly sand at 53.6 m (176 ft) bgs (Figure 2.3). The Hanford formation H3 unit is about 11.9 m (39 ft) thick, the base of which is defined by the top of the Plio-Pleistocene unit silty facies (PPlz) at 65.5 m (215 ft) bgs. A total of four, two-foot split-spoon cores were collected from the Hanford formation H3 unit. Like the H2 unit, core recovery within the H3 unit was consistently 100%. This matrix-supported, gravelly sand sequence consists predominantly of gray to olive gray, “salt and pepper”, unconsolidated, moderately to well sorted, medium- to coarse-grained sand with pebbles up to 3 cm in intermediate diameter (Figure 2.6). The unit is unconsolidated and non-calcareous to weakly calcareous. The H3 unit in 299-E33-46 grades downward into medium to coarse sand with depth, identical to sands described for the overlying H2 unit (see section 2.6.2). Paleomagnetic results from a nearby borehole (299-E33-335) suggest ice-age flood deposits at roughly the same stratigraphic position as the H3 unit were deposited during the early Pleistocene Epoch, during very old flood events that occurred at least 780,000 years ago and perhaps as early as 2 million years ago (Bjornstad et al. 2001).



Figure 2.6. Gravelly sand recovered from the Hanford formation H3 Unit in borehole 299-E33-46.

2.6.4 Plio-Pleistocene Unit

The exact origin of the sedimentary deposits underlying the Hanford formation H3 unit is uncertain and still open to interpretation (Table 2.1). Recent reports have designated deposits beneath the Hanford formation H3 unit as the Hf/Ppu(?) (Wood et al. 2000) and Hanford/Plio-Pleistocene/Ringold(?) unit (Lindsey et al. 2001). Wood et al. (2000) recognized two facies of the Hf/PPu(?) beneath the 241-B, BX,

and BY Tank Farms; a fine-grained eolian/overbank silt (silt facies), up to 10 m (33 ft) thick, and a sandy gravel to gravelly sand facies. The thick silt-rich interval is believed to be a pre-ice-age flood deposit, since silty layers associated with ice-age flood deposits of the Hanford formation in this area are generally much thinner (few centimeters or less) (Wood et al. 2000). The texture, structure, and color of the thick silt layer are all identical to that of the early "Palouse" soil (Tallman et al., 1979; DOE 1988), more recently referred to as the PPlz or upper Plio-Pleistocene unit, which is widely distributed beneath the 200 West Area (Wood et al. 2000, Serne et al. 2002a).

Where the PPlz unit is absent beneath the B-BX-BY Tank Farms, the gravel sequence below the silt unit is indistinguishable from similar-appearing facies of the Hanford formation H3 unit, which overlies the PPlz unit (Wood et al. 2000). In fact, prior to the discovery of the thick silt layer, reported in Wood et al. (2000), gravels overlying basalt bedrock were always included in with the Hanford formation (Tallman et al. 1979; Last et al. 1989; Connelly et al. 1992; Lindsey et al. 1992). If the thick silt layer predates the Hanford formation, however, then the underlying gravels must also predate the Hanford formation. Thus, the gravel sequence beneath the silt layer must belong to either a mainstream alluvial facies of the Plio-Pleistocene unit or the Ringold Formation.

Lindsey et al. (2001) assigned the gravel sequence underlying the PPlz unit to the Ringold Formation based on:

- Iron oxide stains on clasts
- Brown, gray and olive colors
- Abundance of basalt clasts, but with numerous other lithologies
- Sand matrix ranging from basalt to quartz rich
- Reports of "hard" drilling on some borehole logs

However, none of the characteristics above are diagnostic of the Ringold Formation, exclusively, and in certain cases could be used to describe other stratigraphic units, including the Plio-Pleistocene alluvium and flood gravels. Lindsey et al. (2001) argued against a Plio-Pleistocene age for this gravel sequence, since Plio-Pleistocene-age gravels (informally named pre-Missoula gravels by PSPL [1982]) have previously been reported as "bleached" on the Hanford Site (Lindsey et al. 1994). However, unbleached alluvial gravels of Plio-Pleistocene age are reported for the 200 East Area (Williams et al. 2000) as well as south of the Hanford Site at Yakima Bluffs (Lindsey et al. 1994). Furthermore, gravelly deposits recovered from beneath the PPlz unit in 299-E33-46 did not display all the characteristics listed above. For example, iron oxide stains on clasts were not observed on either of the geologic logs prepared for borehole 299-E33-46 and the mafic content in these sandy gravels appears unlike that for the mostly quartzo-feldspathic Ringold Formation. Furthermore, this interval, described as "hard" to drill on the field-geologist's log, not because it consists of cemented Ringold Formation, but because drillers were trying to recover intact split-spoon cores, which is a very difficult thing to do in any clast-supported gravel unit. Finally, past studies (Tallman et al. 1979; Last et al. 1989; Lindsey et al. 1992; Connelly et al. 1992; Williams et al. 2001) have all shown the limit of the Ringold Formation as being much farther south than the B-BX-BY Tank Farms within the 200 East Area.

In summary, we believe insufficient evidence exists at this time to establish the presence of the Ringold Formation beneath B-BX-BY Tank Farms. Instead, we favor an interpretation that the gravel sequence beneath the PPlz unit belongs to a mainstream alluvial facies of the Plio-Pleistocene unit as previously defined by Wood et al. (2000). Thus, we designate this gravel-dominated facies as PPlg in this report (Table 2.1).

2.6.4.1 Silt-Dominated Facies (PPlz)

A fine-grained PPlz unit, 3.9 m (12.7 ft) thick, underlies the basalt-rich sands of the Hanford formation in borehole 299-E33-46 between 65.5 m (215 ft) and 69.4 m (227.7 ft) bgs. This unit can be subdivided into two facies types in borehole 299-E33-46. The upper part of the PPlz unit consists of a pale olive, loose, laminated, very well sorted, calcareous, fine- to medium-grained, quartzo-feldspathic sand (Figure 2.7). The lower part of the PPlz unit consists of a grayish brown, laminated to massive, compacted and very well sorted, moderately calcareous, silt to silty fine sand. One split-spoon core was collected from each of these facies types. The upper facies type, which begins at 65.5 m (215 ft) bgs was not recognized by the geologist in the field or by Lindsey et al. (2001), who picked the base of the Hanford formation 1.5 m (5 ft) deeper at 67 m (220 ft) at a sharp increase in the total gamma log. However, a distinct lithologic contrast exists between Hanford formation sands (above) and Plio-Pleistocene unit silt (below) in grab sample #108 (215.7 to 217.7 ft depth, Table 2.3) and the split-spoon core from the 217.7 to 220 ft depth. The characteristics of the sediment from this unit, including its relatively high calcium carbonate content, uniform texture, and predominantly quartzo-feldspathic mineralogy, suggest it is lithologically different from the Hanford formation. Thus, this subunit is interpreted as a slightly coarser-grained overbank and/or eolian facies of the Plio-Pleistocene unit.

Relatively high neutron moisture and gamma activity on geophysical logs (Figure 2.3), in addition to several core and grab samples corroborate that the lower part of the PPlz unit in this borehole is fine-grained (mostly silt). The contact between the silt and overlying fine sand exists within the 219.7 to 220.0 ft grab sample (#109, Table 2.3). The lower portion of the Plio-Pleistocene unit has characteristics similar to the PPlz unit which overlies an extensive Plio-Pleistocene calcic paleosol sequence (PPlc unit) beneath 200 West Area (Lindsey et al. 2000; Serne et al. 2002a).



Figure 2.7. Calcareous, quartzo-feldspathic fine sand recovered from the upper portion of the PPlz unit in borehole 299-E33-46.



Figure 2.8. Well-laminated silt to silty fine sand recovered from the lower portion of the PPlz unit in borehole 299-E33-46.

2.6.4.2 Sandy Gravel to Gravelly Sand Dominated Facies (PPlg)

A sequence of sandy gravel to gravelly sand was encountered starting at a depth of 69.4 m (227.7 ft) bgs. Four split-spoon cores were collected within this unit. It consists of mostly olive gray, loose, clast-supported, moderately to poorly sorted mixtures of gravel and sand (Figure 2.9). This unit contains a moderate amount (approximately 30-50%) of basalt and is noncalcareous. Poor core recovery (Figure 2.3) and considerable pulverization of the sample resulted from trying to drive a narrow-diameter (4 inch ID) split spoon through the clast-supported pebbles and cobbles. Surfaces of individual gravel clasts are relatively unweathered and lack surface staining.



Figure 2.9.. Sandy gravel recovered from the PPlg subunit in borehole 299-E33-46 .

2.7 Discussion on Increased-Moisture Zones

Absolute moisture values (in wt%) are available for a number of core and composite-grab samples analyzed in the laboratory; these data appear in Figure 2.3. There is general agreement between the neutron moisture log and moisture measured in the laboratory. In other words, spikes on the neutron moisture log coincide with zones of increased moisture measured in the laboratory. Increased moisture appears to be associated with the capillary boundary between sudden, large contrasts in grain size. Commonly, a lower-permeability fine-grained silty layer may be present along the boundary, but is not required for a high-moisture zone to develop. High-moisture zones may also develop along sharp lithologic boundaries where no silt is present.

Several notable increases in moisture content within the vadose zone occur in 299-E33-46. Only fine-grained beds about ≥ 0.3 ft thick show up as elevated-moisture zones on the neutron-moisture log and laboratory analysis (Table 2.4). Starting from the surface, a zone of increased moisture appears to

conform with a 0.5 m (1.5 ft) thick layer of fine sand sandwiched between layers of coarse sand at 25.6 to 26.1 m (84.0-85.5 ft) bgs (Table 2.4). A similar spike in neutron-moisture logs occurs in several nearby vadose zone boreholes (20-10-02, 20-07-11, and 20-08-07).

Another high-moisture zone is associated with a thin 9.1 cm (3.6 inch) silt layer at 51.2 to 51.3 m (168.1 to 168.4 ft) bgs; a core sample obtained from this zone yielded almost 20 wt% water in the laboratory. A zone of increased moisture occurs at about the same depth in two nearby coreholes (299-E33-45 and -338). A third increase in moisture lies near a sand-gravelly sand interface, perhaps associated with some fine and organic(?) -rich layers (between 56.4 to 57.9 m [185 to 190 ft] bgs). A final sharp increase in neutron moisture occurs at a depth between 67.1 to 69.5 m (220-228 ft) bgs associated with the silt-dominated facies (PPLz) of the Plio-Pleistocene unit.

A few other fine grained beds are present (i.e., 21.2, 30.0 and 39.3 m [69.7, 98.5, and 129 ft] depths), however these do not show up as increased-moisture zones on either the neutron-moisture log or in the laboratory analyses, probably because they are thin (0.5 to 1.0 cm [0.2 to 0.4 inch]). A critical thickness of at least 9 cm (3.5 inch) appears to be required for an elevated-moisture zone to appear on the neutron-moisture log for this borehole. These thin fine-grained beds also probably escaped sub-sampling for moisture in the laboratory, as suggested by Table 2.4.

Table 2.4. Fine-Grained Beds in Borehole 299-E33-46.

Depth	Sample #	Thickness of Fine-Grained Bed (ft [cm])	Stratigraphic Unit	Sample Type	Texture	Folk Classification (a)	Elevated Neutron Moisture?	Lab Moisture (wt%)
69.7	31C	0.016 (0.5)	H2	Core	Silty fine sand	mS	No	3.89
84.0-85.5	39-40	1.5 (46)	H2	Grab	Very fine sand	S	Yes	18.16-19.39
98.5	47C	0.03 (1.0)	H2	Core	Silty fine sand	mS	No	2.10
129.0	63	0.03 (1.0)	H2	Grab	Fine sandy silt	sM	No	5.49
168.1-168.4	85	0.3 (9)	H2	Grab	Fine sandy silt	sM	Yes	20.21
~181	91	0.1 to 2.6 (3 to 61)	H2	Grab	Silty fine sand	mS	?	4.37
219.8 - 227.7	109, 110 A-D	7.9 (241)	PP1z	Core and Grab	Interbedded silt and silty fine to medium sand	M, sM, mS	Yes	17.88 - 29.04
~ = approximate								
(a) – See Figure 2.4 for classification table								

2.8 Historic Groundwater Levels

Wood et al. (2000) reported that the discharge of large volumes of waste water in the early 1950s, raised the water table in the vicinity of the B Tank Farm to over 4.9 m (16 ft) above pre-Hanford conditions. They indicated that the groundwater reached a maximum elevation of approximate 124 m (407 ft) mean sea level in the 1967 to 1968 time frame, with a secondary maximum, just below this in the 1986 to 1989 time frame. Water levels have declined approximately 2.1 to 2.4 m (7 to 8 ft) since 1989 at a rate of approximately 20 cm/yr (0.7 ft/yr).

Given a surface elevation about 200 m (657.3 ft) mean sea level, the maximum water table is estimated to have reached a depth of about 76.2 m (250 ft) bgs. The geologists logs made during the drilling of 299-E33-46 indicate that the groundwater table was encountered at a depth of 77.9 m (255.8 ft) bgs. This suggests that the groundwater level has dropped almost 2 m (6 ft) in the vicinity of borehole 299-E33-46 since the late 1980s.

3.0 Geochemical Method and Materials

This chapter discusses the methods and philosophy used to determine which samples would be characterized and parameters that would be measured.

3.1 Sample Inventory

Samples were identified using a project-specific prefix, in this case S01052 followed by a specific sample identification suffix such as -01, for each split spoon. As noted in Section 2.0, the cores contained four sleeves identified by the letters A, B, C, and D, where the A sleeve was always in the position closest to the drive shoe (deepest in the formation at the time of sampling).

3.2 Tiered Approach

During the investigations at SX WMA, significant changes in sediment type and contaminant concentrations were noted within a distance of a few inches within a given sleeve. It was concluded that a more methodical scoping approach would be necessary to provide the technical justification for selecting samples for detailed characterization as defined in the data quality objectives process. Subsequently, a tiered method was developed that considered depth, geology (e.g., lithology, grain-size composition, carbonate content, etc.), individual sleeve contaminant concentration (e.g., radionuclides, nitrate, etc.), moisture content, and overall sample quality. Inexpensive analyses and certain key parameters (i.e., moisture content, gamma energy analysis) were performed on sediment from each sleeve.

The objective of the tier 1 characterization was to quantify the extent of penetration of mobile contaminants into the vadose zone sediment. We analyzed only the sediment from the A sleeve for most constituents except moisture and gamma energy. At borehole 299-E33-46 we did not notice measurable or significant drag-down effects for contaminants perhaps because the sediment was not highly contaminated with nuclides such as cesium-137 that are highly associated with fine-grained particles. Because drag down is dominated by highly contaminated sediment particles, the contaminants in this borehole had less chance of concentrating on particles.

Immediately following the geologic examination, the sleeve contents were sub-sampled for moisture content, gamma-emission radiocounting (for these samples, effectively natural potassium-40, uranium-238, and natural thorium-232 were found; although the strontium-90 bremsstrahlung emissions were evident over the depth interval (14 to 26 m [45 to 85 ft] bgs), one-to-one water extracts (which provide soil pH, electrical conductivity, cation, and anion data), total carbon and inorganic carbon content, and 8 M nitric acid extracts (which provide a measure of the total leachable sediment content of contaminants). The remaining sediment from each sleeve was then sealed and placed in cold storage. Later, additional aliquots of selected sleeves or grab samples were removed to measure particle size distribution and mineralogy and to squeeze porewater.

3.3 Materials and Methods

During sub-sampling of the selected core liner and grab samples, every effort was made to minimize moisture loss and prevent cross contamination between samples. Depending on the sample matrix, very

coarse pebble and larger material (>32 mm [1.26 inch]) was avoided during sub-sampling. Larger substrate was excluded to provide moisture contents representative of counting and 1:1 sediment-to-water extract samples. Results from sub-sample measurements should then take into consideration a possible bias toward higher concentrations for some analytes that would be considered associated with smaller sized sediment fractions. The sediment in the Plio-Pleistocene mud facies contained no large pebbles or cobbles.

Procedures ASTM D2488-93 (ASTM1993) and PNL-MA-567-DO-1 (PNL 1990a) were followed for visual descriptions and geologic description of all split-spoon and grab samples. The sediment classification scheme used for geologic identification of the sediment types is based on the modified Folk/Wentworth classification scheme described earlier (see Figure 2.4). However, the mineralogic and geochemical characterization relied on further separation of the mud into discrete silt and clay sizes.

At 299-E33-46 borehole, one groundwater sample was taken during the drilling process. This water sample along with the cores and grab samples and ultracentrifuged porewaters (from the sediments) constitute the scope of our characterization activity.

3.3.1 Moisture Content

Gravimetric water contents of the sediment samples from each sleeve and selected grab samples were determined using PNNL procedure PNL-MA-567-DO-1 (PNL 1990). This procedure is based on the ASTM procedure *Test Method for Laboratory Determination of Water (Moisture) Content of Soil and Rock* (ASTM D2216-98; ASTM 1998). One representative sub-sample of at least 15 to 70 grams was taken from each sleeve and selected grab samples. Sediment samples were placed in tared containers, weighed, and dried in an oven at 105°C until constant weight was achieved, which took at least 24 hours. The containers then were removed from the oven, sealed, cooled, and weighed. At least two weighings, after 24-hour heatings, were performed to ensure that all moisture was removed. All weighings were performed using a calibrated balance. A calibrated weight set was used to verify balance performance before weighing samples. The gravimetric water content was computed as percentage change in soil weight before and after oven drying.

3.3.2 1:1 Sediment-to-Water Extract

The water-soluble inorganic constituents were determined using a 1:1 sediment-to-deionized-water extract method. This method was chosen because most of the sediment was too dry to easily extract vadose zone porewater. The extracts were prepared by adding an exact weight of deionized water to approximately 60 to 80 grams of sediment sub-sampled from each sleeve and selected grab samples. The weight of deionized water needed was calculated based on the weight of the field-moist samples and their previously determined moisture contents. The sum of the existing moisture (porewater) and the deionized water was fixed at the mass of the dry sediment. The appropriate amount of deionized water was added to screw cap jars containing the sediment samples. The jars were sealed and briefly shaken by hand, then placed on a mechanical orbital shaker for 1 hour. The samples were allowed to settle until the supernatant liquid was fairly clear. The supernatant was carefully decanted and separated into unfiltered aliquots for conductivity and pH determinations, and filtered aliquots (passed through 0.45 µm membranes) for anion,

cation, carbon, and radionuclide analyses. More details can be found in Rhoades (1996) within *Methods of Soils Analysis Part 3* (ASA 1996).

3.3.2.1 pH and Conductivity

Two approximately 3-mm aliquots of the unfiltered 1:1 sediment-to-water extract supernatant were used for pH and conductivity measurements. The pHs for the extracts were measured with a solid-state pH electrode and a pH meter calibrated with buffers 4, 7, and 10. Conductivity was measured and compared to potassium chloride standards with a range of 0.001 M to 1.0 M.

3.3.2.2 Anions

The 1:1 sediment-to-water extracts were analyzed for anions using an ion chromatograph. Fluoride, acetate, formate, chloride, nitrite, bromide, nitrate, carbonate, phosphate, sulfate, and oxalate were separated on a Dionex[®] AS17 column with a gradient elution of 1 mM to 35 mM sodium hydroxide and measured using a conductivity detector. This methodology is based on U.S. Environmental Protection Agency (EPA) Method 300.0A (EPA 1984) with the exception of using the gradient elution of sodium hydroxide.

3.3.2.3 Cations and Trace Metals

Major cation analysis was performed using an inductively coupled plasma (ICP) unit using high-purity calibration standards to generate calibration curves and verify continuing calibration during the analysis run. Dilutions of 100x, 50x, 10x, and 5x were made of each sample for analysis to investigate and correct for matrix interferences. Details are found in EPA Method 6010B (EPA 2000b). The second instrument used to analyze trace metals, including technetium-99 and uranium-238, was an inductively coupled plasma mass spectrometer (ICP-MS) using the PNNL-AGG-415 method (PNNL 1998). This method is quite similar to EPA Method 6020 (EPA 2000c).

3.3.2.4 Alkalinity and Carbon

The alkalinity and inorganic/organic carbon content of several of the 1:1 sediment-to-water extracts were measured using standard titration with acid and a carbon analyzer respectively. The alkalinity procedure is equivalent to the U.S. Geological Survey Method Field Manual (USGS 2001) <http://water.usgs.gov/owq>. Inorganic and organic carbon in the water extracts were determined using a carbon analyzer and ASTM Method D4129-88 (1988) “Standard Test Method for Total and Organic Carbon in Water by High Temperature Oxidation and by Coulometric Detection.”

3.3.2.5 NTA

Analysis for NitriloTriacetic Acid (NTA) was performed using a 1 to 35 mM Gradient elution on a Dionex AS17 column for 20 minutes. The 1:1 extracts were spiked with 16 ppm NTA. The peak areas of the spiked extracts were then compared to the 1:1 extracts with no NTA added and the peak areas of a known 16 ppm NTA standard.

[®] Dionex is a registered trademark of Dionex Corporation, Sunnyvale, California.

3.3.3 Porewater, Suction Candle, and Groundwater Composition

Eleven samples (2B, 6B, 20B, 21A, 36A, 38A, 84, 105C, 110B, 110A, and 113) were packed in drainable cells that were inserted into an ultracentrifuge. The samples were centrifuged for up to 8 hours at several thousand gravitational forces (g 's) to squeeze the porewater out of the sediment. Further, sampling of suction candles that were emplaced in the borehole at strategic depths as the borehole was decommissioned was performed periodically for all the suction candles on the following dates: February 12, 2002, May 17, 2002, July 2, 2002, July 30, 2002, and September 24, 2002. Chemical composition results are compared with both the ultracentrifuged porewaters and the calculated porewaters from the 1:1 sediment to water extracts. The one groundwater sample was also characterized. All these solutions were for pH, electrical conductivity, cation, trace metals, and anions using the same techniques as used for the 1:1 sediment-to-water extracts.

3.3.4 Radioanalytical Analysis

3.3.4.1 Gamma Energy Analysis

Gamma energy analysis (GEA) was performed on sediment from all core "A" and selected "B, C, and D" sleeves and some of the grab samples. All samples for gamma energy analysis were analyzed using 60%-efficient intrinsic germanium gamma detectors. All germanium counters were efficiency calibrated for distinct geometries using mixed gamma standards traceable to the National Institute of Standards and Technology. In the first GEA counting campaign field moist samples were placed in 150-cm³ counting containers and analyzed for 100 minutes in a fixed geometry. All spectra were background subtracted. Spectral analysis was conducted using libraries containing most mixed fission products, activation products, and natural decay products. Control samples were run throughout the analysis to ensure correct operation of the detectors. The controls contained isotopes with photo peaks spanning the full detector range and were monitored for peak position, counting rate, and full-width half-maximum. Details are found in *Gamma Energy Analysis, Operation, and Instrument Verification using Genie2000 Support Software* (PNNL 1997).

3.3.4.2 Tritium Content in 1:1 Sediment to Water Extracts, Perched, and Groundwater

The tritium content of selected sediment samples was determined directly on the water extracts by liquid scintillation using PNNL-AGG-002 (PNNL 2000).

3.3.5 Carbon Content of Sediment

The carbon content of borehole sediment samples was determined using ASTM Method D4129-88, (ASTM 1988). Total carbon in all samples was determined using an UIC Coulometrics Inc. Model 5051 Carbon Dioxide Coulometer™ with combustion at approximately 980°C. Ultrapure oxygen was used to sweep the combustion products through a barium chromate catalyst tube for conversion to carbon dioxide. Evolved carbon dioxide was quantified through coulometric titration following absorption in a solution containing ethanolamine. Equipment output reported carbon content values in micrograms per sample. Soil samples for determining total carbon content were placed into pre-combusted, tared platinum

™ Model 5051 Carbon Dioxide Coulometer is a trademark of UIC Coulometrics, Inc., Joliet, Illinois.

combustion boats and weighed on a four-place analytical balance. After the combustion boats were placed into the furnace introduction tube, a 1-minute waiting period was allowed so that the ultrapure oxygen carrier gas could remove any carbon dioxide introduced to the system from the atmosphere during sample placement. After this system sparge, the sample was moved into the combustion furnace and titration begun. Sample titration readings were performed at 3 minutes after combustion began and again once stability was reached, usually within the next 2 minutes. The system background was determined by performing the entire process using an empty, pre-combusted platinum boat. Adequate system performance was confirmed by analyzing for known quantities of a calcium carbonate standard.

Inorganic carbon contents for borehole sediment samples were determined using a UIC Coulometrics, Inc. Model 5051 Carbon Dioxide Coulometer™. Soil samples were weighed on a four-place analytical balance, then placed into acid-treated glass tubes. Following placement of sample tubes into the system, a 1-minute waiting period allowed the ultrapure oxygen carrier gas to remove any carbon dioxide introduced to the system from the atmosphere. Inorganic carbon was released through acid-assisted evolution (50% hydrochloric acid) with heating to 200°C. Samples were completely covered by the acid to allow full reaction to occur. Ultrapure oxygen gas swept the resultant carbon dioxide through the equipment to determine inorganic carbon content by coulometric titration. Sample titration readings were performed 5 minutes following acid addition and again once stability was reached, usually within 10 minutes. Known quantities of calcium carbonate standards were analyzed to verify that the equipment was operating properly. Background values were determined. Inorganic carbon content was determined through calculations performed using the microgram-per-sample output data and sample weights. Organic carbon was calculated by subtracting inorganic carbon from total carbon and using the remainder.

3.3.6 8 M Nitric Acid Extract

Approximately 20 grams of oven-dried sediment was contacted with 8 M nitric acid at a ratio of approximately 5 parts acid to 1 part sediment. The slurries were heated to approximately 80°C for several hours and then the fluid was separated by centrifugation and filtration through 0.2 µm membranes. The acid extracts were analyzed for major cations and trace metals using ICP and ICP-MS techniques, respectively. The acid digestion procedure is based on EPA SW-846 Method 3050B (EPA 2000a) that can be accessed on-line at <http://www.epa.gov/epaoswer/hazwaste/test/sw846.htm>.

3.3.7 Elemental Analysis

The elemental composition of the bulk sediment and clay fractions was determined by a combination of energy and wavelength dispersive x-ray fluorescence using methods developed at PNNL. Samples analyzed by energy dispersive x-ray fluorescence method utilizing a KEVEX® 0810A commercial x-ray fluorescence excitation and detection subsystem. Sample preparation involved mixing the sample in a Coors high-density alumina (Al₂O₃) mortar and pestle. Six hundred milligrams of the mixed sample were removed and further ground to approximately 300 mesh size, placed between two sheets of stretched para-film, and loaded into the 0810A x-ray fluorescence unit. Acquisition times ranged between 600 and

© KEVEX is a copyright trademark of Thermo Kevex X-Ray, Scotts Valley, California.

3,000 seconds, depending on the targets (iron, gadolinium, silver, zirconium). Forty-one elements (aluminum, antimony, arsenic, barium, bromine, cadmium, calcium, cerium, cesium, chlorine, chromium, copper, gallium, indium, iodine, iron, lanthanum, lead, manganese, molybdenum, nickel, niobium, palladium, phosphorous, potassium, rhodium, rubidium, ruthenium, selenium, silicon, silver, strontium, sulfur, tellurium, thorium, tin, titanium, uranium, vanadium, yttrium, and zinc) were analyzed on each sample and the spectrum interpretation was by the backscatter fundamental parameter approach. Sample analysis by the wavelength method was accomplished using a Siemens Spectra 3000 instrument, equipped with both a flow counter detector to detect soft radiation of the low Z elements and a scintillation counter detector for the harder radiation of the higher Z elements. Bulk solid samples were prepared by taking 180 to 1,500 milligrams of approximately 300 mesh ground sample and pressing it into a 3.2-cm diameter pellet, using a 27,000-kilogram laboratory press. Standard addition and similar matrix methods were used to generate calibration curves for sodium and magnesium, which were then used to process the data. Additional discussion of x-ray fluorescence techniques for quantitative analysis of sediment are found in Chapter 7 “Elemental Analysis by X-Ray Fluorescence Spectroscopy” of ASA (1996), part 3, pages 161 to 223 and in the Siemens Spectra 3000™ Reference Manual.

3.3.8 Particle Size Distribution

The wet sieving/hydrometer method was used to determine the particle size distribution. The technique is described in (ASA [1986a], part 1; method 15-5 Hydrometer Method [pages 404 to 408]) and concentrated on quantifying the silt and clay distribution. The silt and clay separates were saved for mineralogical analyses. Samples from the borehole that were used for the hydrometer method were never air or oven dried to minimize the effects of particle aggregation that can affect the separation of clay grains from the coarser material.

3.3.9 Particle Density

The particle density of bulk grains was determined using pycnometers (see ASA 1986b, part 1; method 14-3 Pycnometer Method [pages 378 to 379]) and oven-dried material. The particle density is needed to determine the particle size when using the hydrometer method.

3.3.10 Mineralogy

The mineralogy of the whole rock and clay size fractions of the selected sediment samples was determined by x-ray diffraction (XRD) techniques. Each bulk sample was prepared for XRD analysis by placing two grams of sample into a tungsten carbide ball mill grinder for 10 minutes. The resultant powders were side packed into aluminum sample holders prior to being analyzed. Preparation of the clay fraction for XRD analysis began by dispersing the whole rock sediment using the following technique. Approximately 100 g of sediment was transferred into a 1.0 L bottle and mixed with 1.0 L of 0.001 M solution of sodium hexametaphosphate. The suspensions were allowed to shake over night to ensure complete dispersion. The sand and silt fractions were separated from the clay fractions by repetitively using Stoke’s settling law described in Jackson (1969). The lower limit of the silt fraction was taken at approximately 2 microns. The dispersed slurry was allowed to settle for approximately 24 hours and the

™ Spectra 3000 is a trademark of Siemens AG, Erlangen, Germany.

unsettled slurry decanted. The settled solids were then re-suspended in approximately 1 liter of the sodium hexametaphosphate solution and the settling repeated several more times. All batches of settled solution containing the suspended clays for each sample depth were composited. Once the supernatant solution appeared to be clear, the clay separation was complete.

Each composited clay suspension was concentrated to an approximate volume of 30 mls by adding a few drops of 10N magnesium chloride to the dispersing solution. Concentrations of clay in the concentrated suspensions were determined by drying known volumes of the suspension and weighing the dried sediment. The density of the slurry was calculated from the volume pipetted and the final weight of dried sediment. Volumes of slurry equaling 250 mg of clay were transferred into centrifuge tubes and saturated with either Mg^{2+} or K^+ cations. Clay samples were prepared using the Drever (1973) method and placed onto an aluminum slide for XRD analysis. Due to the tendency of the clay film to peel and curl, the Mg^{2+} saturated specimens were immediately solvated with a few drops of a 10% solution of ethylene glycol in ethanol and placed into a dessiccator containing excess ethylene glycol for a minimum of 24 hours. Potassium saturated slides were air dried and analyzed, then heated to 550°C for one hour and reanalyzed.

All bulk and clay-sized samples were analyzed on a Scintag XRD unit equipped with a Pelter thermoelectrically cooled detector and a copper x-ray tube. Randomly oriented whole sediment samples were scanned from 2 to 65° 2θ with a dwell time of 14 seconds. Slides of preferentially oriented clay were scanned from 2 to 45° 2θ with a dwell time of 2 seconds. Scans were collected electronically and processed using the JADE[®] XRD pattern processing software. Some patterns were corrected for minor angular deviation using the quartz reflection. Identification of the mineral phases was based on mineral powder diffraction files published by the JCPDS International Centre for Diffraction Data¹.

Semi quantification of mineral phases in the whole rock sediment samples were determined by the whole pattern fitting technique provided by JADE[®] XRD pattern processing software. The software allows the whole pattern fitting of the observed data and Reitveld refinement of crystal structures. A diffraction model is fit by non-linear least-square optimization in which certain parameters are varied to improve the fit between the two patterns. Success of the refinement process is measured by a ratio of the weighted and calculated errors. This value, referred to as “goodness of fit”, is expected to be close to one in an ideal refinement.

Clay mineral abundances in the less than 2 micron fraction were calculated using the method outlined by Brindley and Brown (1980), which relies on external standards. The relationship of intensity and mass absorption to the weight fraction of an unknown phase is expressed as:

$$I/I_p = \mu_p / \mu \text{ (wf)}$$

[®] JADE is a registered trademark of Rigaku Corporation, Tokyo, Japan.

¹ JCPDS International Centre for Diffraction Data, Newton Square, Pennsylvania.

Where:

I is the intensity of the unknown phase,

I_p is the intensity of the pure phase,

μ_p is the mass absorption of the pure phase,

μ is the average mass absorption of the unknown mixture, and

wf is the weight fraction of the unknown.

Pure mineral phases of illite, smectite, kaolinite, and chlorite were obtained from the Clay Mineral Society's source clays repository, (operated from the University of Missouri in Columbia, MO), and analyzed under the same conditions as the sediment samples. Quartz, feldspars, and calcite standards were purchased from the Excalibur Mineral Company (Peekskill, New York), ground and analyzed on the diffractometer to obtain intensities for pure non-clay phases. Based on previous data collected from Hanford sediments, an average mass absorption of $55 \text{ cm}^2 \text{ g}^{-1}$ was assumed for the clay samples. Mass absorption values for standard reference minerals were calculated from published chemical data. Furthermore, the copper x-ray tube used on the Scintag diffractometer generated a minor amount of tungsten $K\alpha$ radiation, which produced peaks in the XRD. These extra peaks were identified and did not compromise the quality of the XRD data.

3.3.11 Water Potential (Suction) Measurements

Suction measurements were made on the two lower core liners in each split-spoon sampler from the borehole using the filter paper method PNL-MA-567-SFA-2 (PNL 1990b). This method relies on the use of a sandwich of three filter papers that rapidly equilibrates with the sediment sample. The middle filter paper does not contact sediment that might stick to the paper and bias the mass measurements. At equilibrium, the matric suction in the filter paper is the same as the matric suction of the sediment sample. The dry filter paper sandwiches were placed in the airtight liners while still filled with the sediment for three weeks to allow sufficient time for the matric suction in the sediment to equilibrate with the matric suction in the filter paper. The mass of the wetted middle filter paper that has had no direct contact with the sediment is subsequently determined, and the suction of the sediment is determined from a calibration relationship between filter paper water content and matric suction.

The relationships used for converting the water content of filter paper to matric suction for Whatman #42 filter paper have been determined by Deka et al. (1995) and can be expressed as:

$$S_m = 10^{(5.144 - 6.699 w)}/10 \text{ for } w < 0.5$$

$$S_m = 10^{(2.383 - 1.309 w)}/10 \text{ for } w > 0.5$$

where: S_m = the matric suction (m) and

w = the gravimetric water content (g/g)

Two hundred forty-five core liner and grab samples from borehole 299-E33-46 were analyzed for water content and 60 of the core liners were analyzed for soil matric suction. The matric potential samples covered the entire borehole profile from 11.8 to 253.4 ft bgs (3.6 to 77.3 m).

4.0 Results and Discussion

This section presents the geochemical and physical characterization data collected on sediment from borehole 299-E33-46. The tier 1 phase emphasized tests that were inexpensive or that were key to determining the vertical distribution of contaminants. Information on the borehole sediment presented in sections 4.1 and 4.2 includes moisture content, pH and electrical conductivity of 1:1 sediment to water extracts, and measurements of major cations, anions, trace metals, and radionuclides in 1:1 sediment water extracts. A gamma energy analysis on the sediments was performed to look for gamma emitting isotopes and to define the extent of the strontium-90 bremsstrahlung penetration. In addition tritium, strontium-90, technetium-99, and uranium-238 concentrations in the sediment are discussed in Section 4.3. The particle size, mineralogy, and tritium content of selected sediment samples were measured in tier 2 phase to aid in selecting contacts between major geologic units and to attempt to better define the vertical extent of the tank B-110 loss event. We also were looking for geochemical and mineralogic changes caused by interaction with the caustic fluids leaking from piping infrastructure associated with tank B-110. Selected sediment samples were also placed in the UFA to squeeze out vadose zone porewater to check the accuracy of using the 1:1 sediment to water extracts to calculate porewater compositions. Finally, the results of sampling suction candles that were emplaced in the borehole at strategic depths as the borehole was decommissioned are compared with both the squeezed porewaters and the calculated porewaters from the 1:1 sediment to water extracts.

4.1 Moisture Content

The moisture content of the sediment from the sleeves and grab samples is listed in Table 4.1 and graphed in Figure 2.3. Figure 2.3 shows both the field volumetric moisture obtained via neutron logging and the gravimetric moisture content of small aliquots of sediment taken during the geologic description activities. The moisture content profiles correlate with the lithology described in Section 2.5 and shown in Figure 2.3. The first region with elevated moisture is the 0.5 m (1.5 ft) thick mud lens at 22.86 m (84 to 85.5 ft) bgs within the Hanford H2 sand unit. Near the bottom of the Hanford H2 unit at 51.21 m (168 ft) bgs is a moist approximate 9.1 cm (3.6 inch) thick lens of fine-grained material with moisture contents of 20.2% by weight. Within the Hanford H3 unit there is a slightly moist lens at 56.39 m (185 ft) bgs with a moisture content of 12.3 wt. % compared to values of 3 to 4 wt % nearby. The PPlz lithology between 67.06 and 68.88 m (220 and 226 ft) bgs is the wettest material in the borehole with moisture contents ranging from 15 to 29 wt %. The gravels below this PPlz silt are relatively dry down to the water table that currently is found at 77.97 m (255.8 ft) bgs.

The laboratory-generated data show gravimetric moisture content (wt%) and the field data are related to volumetric water content (vol%). If the field tool had been calibrated and the vadose zone bulk density profiles were known, one could convert the field data to gravimetric data by dividing by the bulk density. For our needs, we merely compare the two logs qualitatively to see if the moisture peaks correspond depthwise.

Table 4.1. Moisture Content of Sediment from Borehole 299-E33-46. (4 pages)

Lithologic Unit	Sample No.	Mid Depth (Vertical ft)⁽¹⁾	% Moisture	Lithologic Unit	Sample No.	Mid Depth (Vertical ft)⁽¹⁾	% Moisture
Bckfl	02C	12.94	3.89%	H2	64B	131.35	3.27%
Bckfl	02B	12.94	4.48%	H2	64A	131.85	3.11%
Bckfl	02A	12.94	3.60%	H2	65	132.85	3.36%
Bckfl	06D	19.62	3.71%	H2	66	134.2	3.66%
Bckfl	06C	20.12	4.66%	H2	67	136	4.56%
Bckfl	06B	20.62	4.78%	H2	68	137.6	4.29%
Bckfl	06A	21.12	4.84%	H2	69D	138.55	3.87%
Bckfl	10C	28.42	5.94%	H2	69C	139.05	4.32%
Bckfl	10B	28.92	4.94%	H2	69B	139.55	4.35%
Bckfl	10A	29.42	3.30%	H2	69A	140.05	2.52%
H2	16D	39.97	4.31%	H2	70	141.4	3.20%
H2	16C	40.72	4.15%	H2	71	143.35	3.44%
H2	16B	41.22	5.10%	H2	72	145.5	3.91%
H2	16A	41.72	3.97%	H2	73	147.45	4.66%
H2	17D	42.52	4.31%	H2	74D	148.65	4.16%
H2	17C	43.02	4.55%	H2	74C	149.15	3.83%
H2	17B	43.52	4.42%	H2	74B	149.65	3.03%
H2	17A	44.02	4.70%	H2	74A	150.15	4.27%
H2	18D	44.92	4.46%	H2	75	151.45	4.72%
H2	18C	45.42	3.72%	H2	76	153.3	3.87%
H2	18B	45.92	5.32%	H2	77	155.5	4.04%
H2	18A	46.42	5.33%	H2	78	157.6	4.05%
H2	20D	49.12	4.87%	H2	79D	158.65	4.43%
H2	20C	49.62	0.29%	H2	79C	159.15	5.03%
H2	20B	50.12	3.67%	H2	79B	159.65	6.14%
H2	20A	50.62	3.40%	H2	79A	160.15	5.12%
H2	21D	51.52	1.91%	H2	79	160.55	4.00%
H2	21C	52.02	3.29%	H2	80	161.75	4.36%
H2	21B	52.52	4.30%	H2	81	161.75	4.21%

Table 4.1. Moisture Content of Sediment from Borehole 299-E33-46. (4 pages)

Lithologic Unit	Sample No.	Mid Depth (Vertical ft)⁽¹⁾	% Moisture	Lithologic Unit	Sample No.	Mid Depth (Vertical ft)⁽¹⁾	% Moisture
H2	21A	53.02	4.82%	H2	82D	163.05	6.22%
H2	21(shoe)	53.44	5.15%	H2	82C	163.55	3.98%
H2	22	54.6	4.40%	H2	82B	164.05	4.32%
H2	24	56.7	5.25%	H2	82A	164.55	3.42%
H2	25	58.4	5.03%	H2	82	164.95	3.93%
H2	26D	59.22	4.24%	H2	82 Dup	164.95	4.14%
H2	26C	59.72	4.58%	H2	83D	165.35	3.29%
H2	26C-DUP	59.72	4.40%	H2	83C	165.85	4.33%
H2	26B	60.22	4.16%	H2	83B	166.35	4.23%
H2	26-A	60.72	4.08%	H2	83A	166.85	3.34%
H2	27	62.1	4.21%	H2	83	167.25	4.07%
H2	29	66.05	4.04%	**	84	168.45	8.77%
H2	30	67.95	4.18%	**	85	168.25	20.21% ^a
H2	31D	68.95	3.69%	H2	86D	169.65	3.87%
H2	31C	69.45	3.89%	H2	86C	170.15	3.43%
H2	31B	69.95	4.36%	H2	86B	170.65	3.82%
H2	31A	70.45	4.81%	H2	86A	171.15	5.31%
H2	31(shoe)	70.85	3.70%	H2	86	171.55	4.64%
H2	33	73.5	4.15%	H2	87	172.9	4.36%
H2	34	75.4	7.15%	H2	88	175.1	4.61%
H2	35	77.35	5.63%	H3	89	177.1	4.70%
H2	36D	78.95	4.78%	H3	90D	178.35	3.63%
H2	36C	79.45	4.79%	H3	90C	178.85	4.70%
H2	36B	79.95	4.36%	H3	90B	179.35	3.78%
H2	36A	80.35	4.38%	H3	90A	179.85	4.37%
H2	37	80.9	4.62%	H3	90	180.25	4.66%
H2	38D	81.55	3.98%	H3	91	181.75	4.37%
H2	38C	82.05	4.49%	H3	92	183.7	5.66%
H2	38B	82.55	4.35%	***	93	185.1	12.33% ^a
H2	38A	83.05	5.09%	H3	94	186.85	4.38%

Table 4.1. Moisture Content of Sediment from Borehole 299-E33-46. (4 pages)

Lithologic Unit	Sample No.	Mid Depth (Vertical ft)⁽¹⁾	% Moisture	Lithologic Unit	Sample No.	Mid Depth (Vertical ft)⁽¹⁾	% Moisture
H2	38(shoe)	83.45	5.23%	H3	95	188.45	4.07%
*	39	84.55	19.39%^a	H3	96D	189.35	3.37%
*	40	86.3	18.16%^a	H3	96C	189.85	3.41%
H2	41	87.85	3.49%	H3	96B	190.35	2.77%
H2	42D	89.12	3.74%	H3	96A	190.8	2.42%
H2	42C	89.62	2.67%	H3	101D	199.45	3.00%
H2	42B	90.12	2.12%	H3	101C	199.85	3.65%
H2	42A	90.62	2.83%	H3	101B	200.45	2.91%
H2	43	91.45	3.26%	H3	101A	200.95	2.94%
H2	44	93.15	3.00%	H3	105D	208.55	2.91%
H2	45	95.15	3.37%	H3	105C	208.95	3.83%
H2	46	96.8	3.16%	H3	105B	209.45	3.71%
H2	47D	98.12	2.03%	H3	105A	209.95	3.73%
H2	47C	98.62	2.10%	PPlz	108	216.7	5.06%
H2	47B	99.12	2.02%	PPlz	108 Dup	216.7	4.72%
H2	47A	98.62	2.18%	PPlz	109D	217.95	4.17%
H2	47(shoe)	100.04	2.09%	PPlz	109C	218.45	4.58%
H2	48	101.55	2.13%	PPlz	109B	218.95	5.75%
H2	49	103.85	2.75%	PPlz	109A	219.45	4.35%
H2	50	105.7	2.96%	PPlz	109	219.95	17.88% ^a
H2	51	107.45	2.53%	PPlz	110D	220.65	23.33% ^a
H2	52	109	3.52%	PPlz	110C	221.15	29.04% ^a
H2	53D	109.92	2.98%	PPlz	110B	221.65	27.24% ^a
H2	53C	110.42	3.21%	PPlz	110BDup	221.65	27.55% ^a
H2	53B	110.92	2.51%	PPlz	110A	222.05	25.94% ^a
H2	53A	111.42	2.58%	PPlz	111	223.5	14.98% ^a
H2	54	113	2.90%	PPlz	112	223.5	15.91% ^a
H2	55	114.9	2.97%	PPlz	113	225.9	14.99% ^a
H2	56	117	2.82%	PPlg	114	228.45	3.10%
H2	57D	118.42	2.80%	PPlg	115C	229.75	4.21%

Table 4.1. Moisture Content of Sediment from Borehole 299-E33-46. (4 pages)

Lithologic Unit	Sample No.	Mid Depth (Vertical ft) ⁽¹⁾	% Moisture	Lithologic Unit	Sample No.	Mid Depth (Vertical ft) ⁽¹⁾	% Moisture
H2	57C	118.92	2.98%	PPlg	115B	230.25	3.04%
H2	57B	119.42	2.72%	PPlg	115A	230.75	3.71%
H2	57A	119.92	2.09%	PPlg	120D	239.95	3.32%
H2	58	121.5	3.31%	PPlg	120C	240.45	3.46%
H2	59	123.5	3.21%	PPlg	120B	240.95	3.71%
H2	60	118.5	3.48%	PPlg	120A	241.45	2.50%
H2	61	125.05	3.17%	PPlg	123A	245.75	3.33%
H2	62	126.75	3.38%	PPlg	127C	254.15	4.57%
H2	63	128.9	5.49%	PPlg	127B	253.65	4.06%
H2	64D	130.35	3.63%	PPlg	127A	253.15	3.17%
H2	64C	130.85	3.21%				

⁽¹⁾ to convert to m multiply by 0.3048

H2 = Hanford H2 sand sequence

H3 = Hanford H3 unit-lower sand sequence

PPlz = Plio-pleistocene mud unit

PPlg = Plio-pleistocene gravelly unit

Bckfl = backfill

*, **, *** = various thin fine-grained lenses in the Hanford sand units.

^a denotes the wet zones described in the text.

No perched water was observed in the PPlz unit as was found between 69 to 71 m (227 to 233 ft) bgs during the drilling of borehole 299-E33-45 at the BX Tank Farm (see Serne et al. 2002e for details). A water sample was taken at the bottom of the 299-E33-46 borehole prior to its being decommissioned. The chemical composition for the groundwater is described along with the UFA porewaters, suction candle derived porewaters, and dilution corrected 1:1 sediment to water extracts in the sections that follow.

4.2 1:1 Sediment-to-Water Extracts

The main objective for placing the 299-E33-46 borehole at the location approximately 4.6 m (15 ft) from the tank wall was to investigate whether the field gamma log anomaly (bremsstrahlung radiation) truly could be correlated with strontium-90 in the vadose zone sediments and to investigate whether other non-gamma emitting radionuclides were present. Details on the drivers for installing this borehole are discussed in Section 3.2.2 in the B-BX-BY Field Investigation Report [FIR]. The borehole was extended to groundwater in order to track other mobile contaminants that can't be tracked with gamma logging such as technetium-99 and nitrate. The most economical method for determining the distribution of the mobile contaminants in the vadose zone sediment is to use water extracts of the sediments because most of the sediment is too dry to readily extract native porewater. The following sections discuss the results

of the analysis done on the water extracts and the few selected porewaters that were obtained by ultracentrifugation in the unsaturated flow apparatus (UFA).

4.2.1 pH and Electrical Conductivity

The pH and electrical conductivity for the water extracts and UFA squeezed porewaters are shown in Table 4.2 and Figure 4.1. The electrical conductivity for the 1:1 sediment-water extracts has been corrected for dilution with deionized water, but the pH is plotted as measured in the 1:1 sediment to water extracts. Note that Figures 4.1 through 4.5 also show data for porewaters obtained after the borehole was decommissioned through the use of suction candles. A discussion of the suction candles and data obtained over time from the candles will be discussed in Section 4.11.

The pH profile shows that between 30.48 and 45.72 m (52 and 83 ft) bgs (in the Hanford formation H2 middle sand sequence), there are elevated values (8.5 to 9.5) suggesting the presence of caustic waste interaction with the sediment. Below the fine-grained lens at approximately 25.6 to 25.9 m (84 to 85 ft) bgs is another lobe of slightly elevated pH with values between 8.8 and 9.1. This deeper zone with elevated pH extends from 29.3 to 36.6 m (96 to 120 ft) bgs and is also within the Hanford formation H2 unit. The thin fine-grained lens at approximately 25.9 m (85 ft) bgs does not show elevated pH or elevated electrical conductivity and thus appears to be acting as a partial barrier to tank related fluid migration. The electrical conductivity profile is similar to the elevated pH profile in that it shows two regions with high values. The shallower region starts at 15.4 m (50.6 ft) bgs, a bit shallower than the elevated pH zone, and extends down to the thin fine-grained lens at 25.6 to 25.9 m (84 to 85 ft) bgs. The dilution corrected (calculated) porewater electrical conductivity ranges from 6.5 to 15 mS/cm in this region. The deeper elevated EC zone extends from 27.6 to 42.7 m (90.6 to 140 ft) bgs with calculated porewater conductivities ranging from 5.7 to 12.75 mS/cm. This deeper zone of elevated electrical conductivity is less concentrated than the shallow zone and resides within the lower portion of the Hanford formation H2 unit. It is possible that small portions of tank related fluids have mixed with the natural sediment moisture all the way down to the thin fine-grained lens at approximately 51 m (168 ft) bgs but below 51 m (168 ft) bgs the electrical conductivity values are not significantly elevated compared to values calculated in this zone in an uncontaminated borehole, 299-E33-338 as discussed in Lindenmeier et al. 2002. The porewaters that were extracted from selected samples using the ultracentrifuge (UFA) show slightly lower pH values than the 1:1 sediment to water extracts and the actual porewater electrical conductivity values are often significantly lower than calculated porewater conductivities obtained by making dilution corrections on the 1:1 sediment to water extracts. This discrepancy was also found at borehole 299-E33-45 east of the BX-102 tank. Unlike the contaminated sediments around REDOX tanks in the SX tank farm, the more dilute wastes in the sediments that surround the two tanks studied in the B-BX-BY WMA appear to have more of the wastes in a form that is not present in the actual porewater but readily re-dissolves upon addition of de-ionized water. At the SX tank farm the actual porewater electrical conductivities and the calculated values from dilution correcting the 1:1 water extracts agreed reasonably well; however the absolute values at SX were much larger because of the very high sodium nitrate concentrations that were present.

Table 4.2. Water Extract pH and Electrical Conductivity Values

Sample ID	Mid Depth (ft) ⁽¹⁾	Dilution Factor	1:1 pH	1:1 EC (mS/cm)	Pore EC (mS/cm)
<i>Backfill</i>					
2B-UFA	12.94	1	7.89		6.35 ^a
02A	13.7	27.8	7.89	0.154	4.28 ^a
06B-UFA	20.62	1	7.90		7.54 ^a
06A	21.12	20.66	7.48	0.133	2.75 ^a
10A	29.42	30.33	7.83	0.139	4.22
<i>Hanford H2 Sand (upper sequence) Unit</i>					
16A	41.72	25.18	7.39	0.139	3.5
17A	44.02	21.29	7.78	0.137	2.92
18A	46.42	18.75	8.10	0.142	2.66
20B-UFA	50.12	1	8.23		0.85 ^a
20A	50.62	29.43	8.11	0.276	8.12 ^{ab}
21C	52.02	29.45	9.09 ^b	0.317	9.34 ^b
21A-UFA	53.02	1	8.69 ^b		NA ^b
21A	53.02	20.75	9.18 ^b	0.42	8.71 ^b
21A-dup	53.44	19.42	8.48	0.413	8.02 ^b
22	54.6	22.75	9.27 ^b	0.544	12.38 ^b
24	56.7	19.05	9.47^b	0.778	14.82^b
25	58.4	19.92	9.51^b	0.583	11.61 ^b
26C	59.72	19.45	9.49^b	0.549	10.68 ^b
26C-dup	59.72	22.74	9.54^b	0.567	12.89^b
26-A	60.72	24.5	9.49^b	0.615	15.07^b
27	62.1	23.78	9.52^b	0.586	13.94^b
29	66.05	24.84	9.18	0.367	9.12 ^b
31C	69.45	28.74	9.13	0.362	10.4 ^b
31B	69.95	23.92	8.89	0.367	8.78 ^b
31A	70.45	20.8	8.18	0.328	6.82 ^b
31A-dup	70.45	27.03	8.10	0.366	9.89 ^b
33	73.5	25.04	9.08 ^b	0.345	8.64 ^b
35	77.35	15.03	8.8	0.367	5.51 ^b
36C	79.45	21.67	8.84	0.346	7.5 ^b

Table 4.2. Water Extract pH and Electrical Conductivity Values

Sample ID	Mid Depth (ft) ⁽¹⁾	Dilution Factor	1:1 pH	1:1 EC (mS/cm)	Pore EC (mS/cm)
36A-UFA	79.95	1	8.39		1.03 ^{ab}
36A	79.95	22.85	8.44	0.354	8.09 ^{ab}
38C	82.05	24.7	9.00 ^b	0.345	8.52 ^b
38A-UFA	83.05	1	8.45		3.98 ^{ab}
38A	83.05	19.64	8.76	0.331	6.5 ^{ab}
Natural Background Sediments			7.1 to 7.5		1.4 to 4.0
<i>Thin Fine Grained Lens</i>					
39	84.55	5.17	8.26	0.345	1.78
39-dup	84.55	5.41	8.18	0.342	1.85
<i>Hanford H2 Sand (middle sequence) Unit</i>					
41	87.85	27.98	7.84	0.165	4.62
42A	90.62	35.28	7.74	0.163	5.75
46	96.8	31.85	8.90 ^b	0.276	8.79 ^b
47A	98.62	45.97	8.84 ^b	0.237	10.89 ^b
52	109	28.4	8.75 ^b	0.292	8.29 ^b
53A	111.42	38.76	9.09 ^b	0.329	12.75^b
57A	119.92	47.96	8.84 ^b	0.232	11.13 ^b
64A	131.85	32.15	8.19	0.257	8.26 ^b
69A	140.05	39.7	8.20	0.177	7.03
74A	150.15	23.41	7.67	0.189	4.42
79A	160.15	19.54	7.52	0.181	3.54
82A	164.55	29.22	8.28	0.178	5.2
83A	166.85	29.95	8.07	0.181	5.42
Natural Background Sediments			7.1 to 7.5		1.4 to 4.0
<i>Fine Grained Lens</i>					
84-UFA	168.45	1	8.02		1.52
84	168.45	11.44	7.64	0.217	2.48
<i>Hanford H2 Sand Unit</i>					
86A	171.15	18.85	7.90	0.204	3.84
<i>Hanford H3 Sand Unit</i>					
90A	179.85	22.89	7.60	0.154	3.52
96A	190.8	41.31	7.97	0.136	5.62

Table 4.2. Water Extract pH and Electrical Conductivity Values

Sample ID	Mid Depth (ft) ⁽¹⁾	Dilution Factor	1:1 pH	1:1 EC (mS/cm)	Pore EC (mS/cm)
101A	200.95	34.06	7.57	0.139	4.73
105C-UFA	208.95	1	7.16		1.70
105A	209.95	26.84	7.55	0.142	3.81
Natural Background Sediments			7.3 to 7.4		1.9 to 3.3
<i>Plio-plistocene Mud Unit</i>					
109A	219.45	23.01	7.30	0.169	3.89
110B-UFA	221.65	1	7.42		1.41
110A-UFA	222.05	1	7.49		0.71 ^a
110A	222.05	3.85	7.88	0.351	1.35 ^a
110A-dup	222.05	3.85	7.81	0.319	1.23
113-UFA	225.9	1	7.47		0.752 ^a
113	225.9	6.67	7.68	0.217	1.45 ^a
Natural Background Sediments			7.3 to 7.7		0.9 to 3.1
<i>Plio-plistocene Gravel Unit</i>					
115A	230.75	27.17	7.38	0.153	4.16
120B	240.95	28.68	7.61	0.159	4.56
120A	241.45	39.95	7.56	0.161	6.43
123A	245.75	30.01	7.57	0.156	4.68
127A	253.15	31.57	7.62	0.174	5.49
Natural Background Sediments			7.4 to 7.6		4.0 to 5.0

⁽¹⁾ to convert to meters multiply by 0.3048

^a allows easy comparison of true porewater EC with calculated porewater EC.

^b elevated values from caustic tank liquor.

Bold type = maximum values in profile.

EC = Electrical conductivity.

NA = not analyzed for lack of sample volume.

299-E33-46 (near Tank 241-B-110)

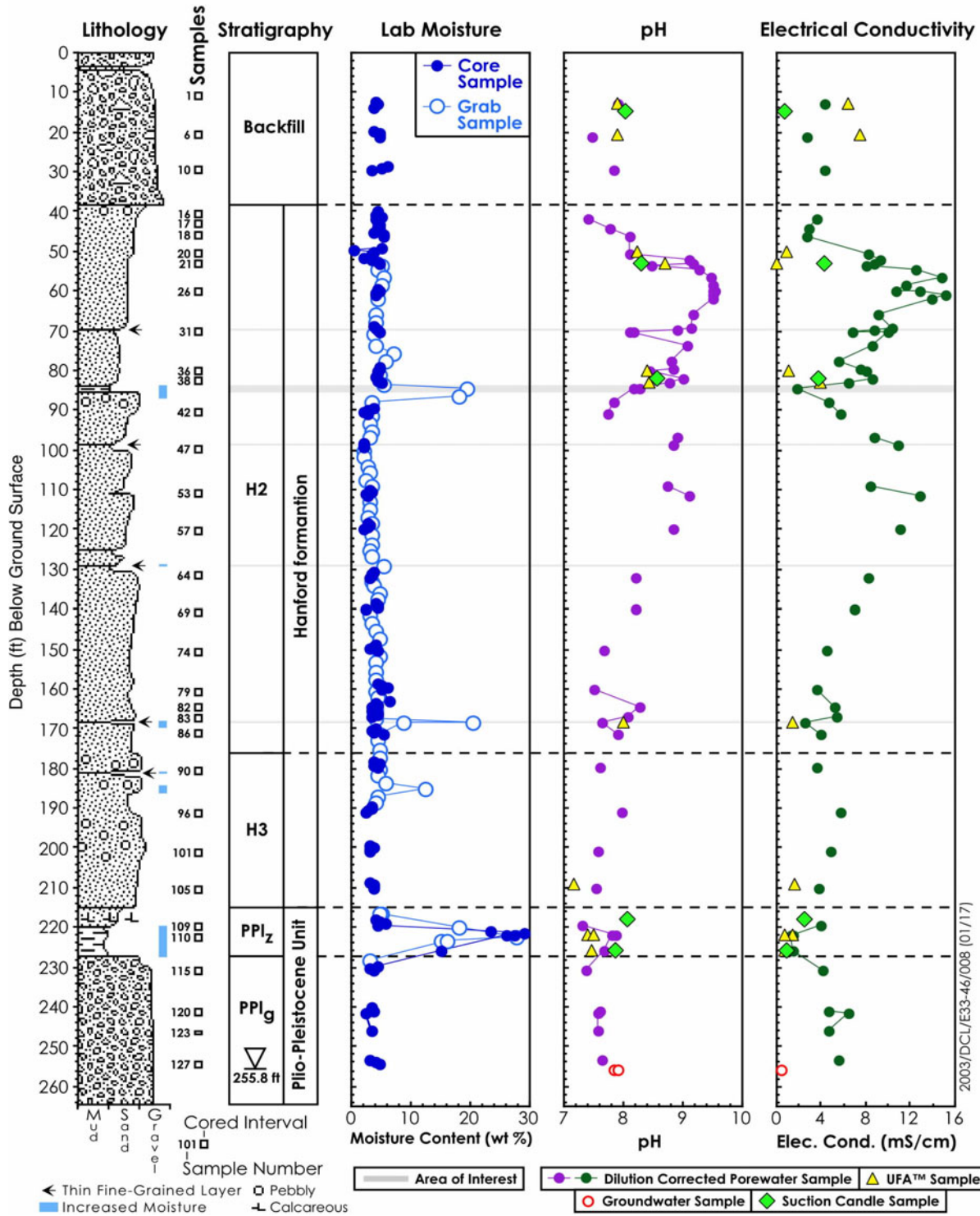


Figure 4.1 Moisture Content, Water Extract pH, Calculated Porewater, UFA and Suction Candle Porewater and Groundwater Electrical Conductivity for Borehole 299-E33-46

Because so many chemical reactions can affect the pH, it is not possible to determine whether the fluid lost from the B-110 piping traveled mainly in a vertical direction or spread horizontally resulting in a complicated vertical profile at this borehole.

4.2.2 Porewater Anion Composition

The 1:1 sediment-to-water extracts and the calculated porewater anion composition are shown in Table 4.3 and Figure 4.2, respectively. When compared to the uncontaminated “baseline” vadose zone sediments from borehole 299-E33-338 near the eastern fence line of the B tank farm, there are obvious signs of elevated porewater concentrations of nitrate, fluoride, and bicarbonate. There are some indications that phosphate and sulfate may be elevated in certain depth zones compared to the uncontaminated sediments nearby. There is shallow nitrate contamination starting at about 15.4 m (50.6 ft) bgs that extends to 23.6 m (77.4 ft) bgs, perhaps reaching the thin fine-grained lens at 25.8 m (84.5 ft) bgs. Still within the Hanford formation H2 unit between the depths of 26.8 and 51.2 m (87.8 and 168 ft) bgs is a more concentrated nitrate plume. At 40.2 m (132 ft) bgs the highest nitrate calculated porewater concentration is found (approximately 1500 mg/L). The H2 sediment porewater between 50.1 and 51.4 m (164.5 and 168.5 ft) bgs contains approximately 500 mg/L nitrate. The Hanford formation H3 sediment also appears to contain elevated nitrate porewater concentrations that vary between 100 to 200 mg/L compared to the uncontaminated H3 sediment porewater concentration of 4 to 17 mg/L. The PPlz unit also appears to contain slightly elevated nitrate porewater concentrations at approximately 130 mg/L compared to uncontaminated sediment porewater values that range from 2 to 14 mg/L. The 299-E33-46 borehole sediments in the PPlg coarse-grained unit may also contain elevated nitrate porewater concentrations of approximately 50 mg/L compared to a natural background value of 10 mg/L. Thus the sediment water extracts from this borehole appear to show elevated nitrate is present all the way to the groundwater; however the bulk of the nitrate is found in the sediment between the depth of 33.5 to 51.4 m (110 to 168.5 ft) bgs in the Hanford H2 sand sequence with values reaching as high as 1.5 g/L or approximately 0.025 M at 40.19 m (131.85 ft) bgs. The bulk of the water- extractable nitrate is bounded between two thin fine-grained lenses in the H2 middle sequence sand unit. The upper bound is the fine-grained lens at 37 m (120 ft) bgs and lower boundary is the fine-grained 2.5-ft thick lens that forms the bottom of the H2 unit at 51 to 52 m (167 to 170 ft) bgs.

The porewater fluoride concentrations are elevated above the uncontaminated sediment baseline range of 0.4 to 23 mg/L over a depth region from 15.4 to 33.9 m (50.6 to 111.4 ft) bgs. The highest fluoride porewater concentrations are found between 18.6 and 25.3 m (61 and 83 ft) bgs within the Hanford formation H2 unit at values that range from 110 to 210 mg/L.

The bicarbonate concentration in the porewaters also is elevated in the H2 middle sand sequence between 22.9 and 50.9 m (75 and 167 ft) bgs; both above and within in the same zone with the largest nitrate concentrations. Interestingly, the bicarbonate distribution in the sediment water extracts mimics the elevated pH profile suggesting that either dissolution of natural carbonate minerals or capture of vadose zone carbon dioxide during tank waste fluid neutralization might be the cause for the elevated bicarbonate. The largest calculated porewater bicarbonate concentration occurs in the suspected paleosol at 36.6 m (120 ft) bgs. However, based on the UFA squeezings the dilution-corrected 1:1 sediment to water extract bicarbonate values are biased high because of dissolution of carbonate bearing salts. The

porewater bicarbonate maximum concentration varies between 0.1 and 0.21 M between 33.5 to 39.6 m (110 to 130 ft) bgs around this potential paleosol at 36.6 m (120 ft) bgs.

The porewater sulfate concentrations appear to be slightly elevated in the deeper depths of the borehole, rather than within the Hanford H2 unit where tank related fluids are generally found. The most significant concentrations of sulfate in the shallow vadose zone are found in a narrow zone within the middle sand sequence of the H2 unit between 42.7 and 50.6 m (140 and 166 ft) bgs. No UFA squeezings were obtained from sediments from this narrow zone and the natural background sediments in the borehole to the east, 299-E33-338, are also elevated. More puzzling are the elevated sulfate concentrations in the PPlg lithology at the bottom of the borehole. The dilution corrected porewater concentrations reach values approximately 500 mg/L compared to natural background values of approximately 40 mg/L.

The porewater chloride concentrations do not appear to be significantly elevated compared to the nearby natural sediments from borehole 299-E33-338. Thus the observed chloride profile likely reflects natural conditions. The phosphate porewater distribution in the vadose zone sediment at borehole 299-E33-46 shows elevated concentrations between approximately 16.6 and 25 m (54.6 and 82 ft) bgs within the H2 upper sand sequence, the maximum concentrations are found in a thin zone at approximately 18 m (60 ft) bgs with a dilution corrected value of 108 mg/L (0.0011 M). Generally, soluble phosphate levels in natural sediments at Hanford are quite low because of precipitation of highly insoluble apatite minerals. Based on the measured 1:1 sediment to water extracts, the tank waste is not dominated by bismuth phosphate waste as was found at borehole 299-E33-45 northeast of tank BX-102. The nitrite porewater distribution in borehole 299-E33-46 shows no noteworthy elevated values throughout the profile.

The actual porewater concentrations (UFA squeezings) are plotted with the dilution corrected 1:1 water extracts in the tables and figures shown in this section. In the tables green shading is used to show the comparison. There are plausible explanations for the dilution-corrected water extracts (i.e., calculated porewaters) having larger concentrations, such as dissolution of material during the extraction process but we cannot offer a geochemical explanation for the observed opposite trend found for a few of the comparisons. The most likely explanation is analytical errors. In general, the comparison between actual porewater and calculated porewater concentrations for nitrate and chloride values is good. For bicarbonate, the dilution corrected extracts (calculated porewaters) show significantly larger values and for some of the fluoride comparisons the same trend is seen wherein actual porewater concentrations are lower than calculated concentrations.

4.2.3 Porewater Cation Composition

Table 4.4 shows the calculated concentrations of cations in the porewater from the vadose zone sediment at 299-E33-46 borehole obtained by dilution correction of the 1:1 sediment-to-water extracts and the selected actual porewaters obtained by ultracentrifugation. The distributions of several of the major cations and minor cations are shown in Figures 4.3 and 4.4. The depth profiles for the divalent alkaline earth cations calcium, magnesium, and strontium show remarkable similarities. All show depleted concentrations over the depth range from between 15.4 or 16 m (50.6 or 52 ft) bgs down to 37 m (120 ft) bgs where the concentrations return to values similar to those found in uncontaminated sediments.

Conversely, the porewater sodium concentration is elevated from 15.4 m (50.6 ft) bgs down to 37 m (201 ft) bgs in the H3 sand sequence. There is also elevated porewater potassium in the shallow vadose zone from 50.6 to approximately 24 m (80 ft) bgs. The cation profiles for the divalent cations (calcium, magnesium, and strontium) and the mono-valent cations (potassium and sodium) are related through ion exchange reactions wherein the divalent cations that dominate the exchange sites in the natural sediments are stripped off and replaced by the sodium and potassium (perhaps an impurity in the sodium hydroxide used at Hanford to neutralize acidic waste streams). Barium differs from the other divalent cations and is present at low concentrations perhaps reflecting only natural amounts are present that are not impacted by tank fluid losses. Apparently, the sodium concentration in the porewaters below 37 m (120 ft) bgs are not high enough to have stripped significant concentrations of the natural divalent cations from the sediments despite the sodium being elevated in comparison to uncontaminated sediment extracts.

There also appears to be elevated concentrations of soluble aluminum and iron in the shallow profile between 16 and 21 and 16 and 24 m (52 and 70 and 52 and 80 ft) bgs, respectively (see Figure 4.4). Soluble silicon also appears elevated in discontinuous zones between 16 and 37 m (52 and 120 ft) bgs and perhaps in a thin zone at 58 to 61 m (190 to 200 ft) bgs. These zones of high water soluble aluminum, iron, and silicon may represent reaction and the presence of amorphous (more soluble) weathering products from tank waste interactions with the vadose zone sediments.

Table 4.3. Anion Content of Water Extracts of Borehole 299-E33-46 (B-110 Sediment). (4 pages)

ID	Depth (ft bgs) ⁽¹⁾	Dil. Fac.	1:1 Extracts in mg/L							Dilution Corrected Porewater mg/L						
			NO3	F-	NO2	Cl	SO4	PO4	HCO3	NO3	F-	NO2	Cl	SO4	PO4	HCO3
<i>Backfill</i>																
02B-UFA	12.94	1								15.76 ^a	0.81 ^a	<0.08 ^a	13.28 ^a	71.9 ^a	0.24 ^a	178 ^a
02A	13.7	27.8	0.37	<0.5	<0.1	0.48	5.21	0.74	65.47	10.3 ^a	<13.9 ^a	<2.8 ^a	13.3 ^a	145 ^a	20.6 ^a	1820 ^a
06B-UFA	20.62	1								5.7 ^a	0.9 ^a	<0.08 ^a	19.7 ^a	94.6 ^a	<0.24 ^a	180 ^a
06A	21.12	20.66	<0.3	<0.5	<0.1	0.33	5	<0.5	55.18	6.2 ^a	<10.3 ^a	<2.1 ^a	6.8 ^a	103 ^a	10.33 ^a	1140 ^a
10A	29.42	30.33	0.4	0.69	<0.1	0.89	49.11	0.51	44.16	12.1	20.9	<3.0	27	1490	15.47	1339
<i>Hanford H2 Sand (upper sequence) Unit</i>																
16A	41.72	25.18	<0.3	<0.5	<0.1	0.29	7.21	<0.5	51.34	7.55	<12.6	<2.5	7.3	182	12.59	1293
17A	44.02	21.29	0.38	<0.5	<0.1	0.3	6.55	<0.5	50.65	8.1	<10.6	<2.1	6.4	139	10.64	1078
18A	46.42	18.75	0.46	1.31	<0.1	0.2	5.06	<0.5	55.27	8.6	24.6	<1.9	3.8	95	9.38	1037
20B-UFA	50.12	1								8 ^a	12 ^a	<0.08 ^a	7.25 ^a	31.1 ^a	1.8 ^a	216 ^a
20A	50.62	29.43	0.36	2.77	<0.1	0.15	5.21	<0.5	142.45	10.6 ^a	81.5 ^b	<2.9 ^a	4.4 ^a	153 ^a	14.71 ^a	4192 ^b
21C	52.02	29.45	0.55	2.389	<0.7	0.26	3.407	0.446	199.041	16.2	70.4 ^b	<20.6	7.7	100	13.1	5862 ^b
21A-UFA	53.02	1								17.2 ^a	14.4 ^a	<0.08 ^a	13 ^a	93 ^a	2.2 ^a	468 ^a
21A	53.02	20.75	0.34	3.63	<0.1	0.15	7.82	0.99	214.3	7.1 ^a	75.3 ^b	<2.1 ^a	3.1 ^a	162 ^a	20.5 ^a	4446 ^b
21A-dup	53.44	19.42	0.38	3.68	<0.1	0.19	6.9	0.9	199.72	7.4	71.5 ^b	<1.9	3.7	134	17.5	3879 ^b
22	54.6	22.75	5.03	7.008	<0.7	0.45	5.033	1.937	317.638	114.3 ^b	159.4 ^b	<15.9	10.2	115	44.1 ^b	7227 ^b
24	56.7	19.05	8.13	10.79	<0.7	0.8	13.409	1.902	387.411	154.8 ^b	205.5 ^b	<13.3	15.2	255	36.2 ^b	7380 ^b
25	58.4	19.92	5.8	6.807	<0.7	0.53	5.804	1.111	348.533	115.6 ^b	135.6 ^b	<13.9	10.6	116	22.1 ^b	6941 ^b
26C	59.72	19.45	1.72	5.943	<0.7	0.41	5.552	1.29	319.593	33.5	115.6 ^b	<13.6	8	108	25.1 ^b	6215 ^b
26C-dup	59.72	22.74	1.87	5.927	<0.7	0.41	5.165	1.48	348.568	42.5	134.8 ^b	<15.9	9.3	118	33.7 ^b	7926 ^b
26-A	60.72	24.5	0.69	6.82	<0.1	0.4	6.68	4.39	307.13	16.9	167.1 ^b	<2.4	9.8	164	107.6 ^b	7525 ^b
27	62.1	23.78	3.71	6.909	<0.7	0.34	5.597	1.676	351.331	88.2 ^b	164.3 ^b	<16.6	8.1	133	39.9 ^b	8355 ^b

Table 4.3. Anion Content of Water Extracts of Borehole 299-E33-46 (B-110 Sediment). (4 pages)

ID	Depth (ft bgs) ⁽¹⁾	Dil. Fac.	1:1 Extracts in mg/L							Dilution Corrected Porewater mg/L						
			NO3	F-	NO2	Cl	SO4	PO4	HCO3	NO3	F-	NO2	Cl	SO4	PO4	HCO3
29	66.05	24.84	4	5.84	<0.7	0.38	9.117	0.351	211.701	99.4 ^b	145.1 ^b	<17.4	9.4	226 ^b	8.7	5258 ^b
31C	69.45	28.74	8.63	5.727	<0.7	0.47	7.946	0.561	207.478	248 ^b	164.6 ^b	<20.1	13.5	228 ^b	16.1 ^b	5962 ^b
31B	69.95	23.92	2.95	7.917	<0.7	0.38	9.048	0.811	202.361	70.6 ^b	189.4 ^b	<16.7	9.1	217 ^b	19.4 ^b	4841 ^b
31A	70.45	20.8	3.02	7.72	<0.1	0.37	8.77	0.9	162.7	62.8 ^b	160.6 ^b	<2.1	7.7	182 ^b	18.7 ^b	3385 ^b
31A-dup	70.45	27.03	2.45	7.79	<0.1	0.37	8.24	0.98	171.26	66.2 ^b	210.6 ^b	<2.7	10	223 ^b	26.5 ^b	4629 ^b
33	73.5	25.04	3.26	6.839	<0.7	0.35	6.803	0.389	213.114	81.5 ^b	171.2 ^b	<17.5	8.8	170	9.7	5336 ^b
35	77.35	15.03	4.91	7.115	<0.7	0.43	9.183	0.516	218.09	73.8 ^b	106.9 ^b	<10.5	6.5	138	7.8	3277 ^b
36C	79.45	21.67	0.89	7.288	<0.7	0.45	8.696	0.704	217.218	19.2	157.9 ^b	<15.2	9.8	188	15.3	4707 ^b
36A-UFA	80.35	1								5 ^a	24.7 ^b	<0.08 ^a	7.2 ^a	60.4 ^a	<0.24 ^a	385 ^a
36A	79.95	22.85	0.55	7.45	<0.1	0.37	9.12	0.87	175.64	12.6 ^a	170.3 ^b	<2.3 ^a	8.5 ^a	208 ^a	19.9 ^b	4014 ^b
38C	82.05	24.7	0.5	8.609	<0.7	0.41	6.943	0.586	209.791	12.4	212.7 ^b	<17.3	10.1	172	14.5 ^b	5182 ^b
38A-UFA	83.05	1								13.3 ^a	28.2 ^b	<0.24 ^a	17.8 ^a	114 ^a	<0.72 ^a	421 ^b
38A	83.05	19.64	0.46	8.75	<0.1	0.3	7.84	0.69	155.19	9 ^a	171.8 ^b	<2.0 ^a	5.9 ^a	154 ^a	13.5 ^a	3047 ^b
Natural Sediments in Upper H2 Sand										18 to 41	4 to 6	<5	10 to 21	73 to 92	<8	1020 to 1650
<i>Thin Fine Grained Lens</i>																
39	84.55	5.17	33.866	6.29	<0.7	1.45	18.469	0.585	160.454	174.9	32.5	<3.6	7.5	95.4	3	828.8
39-dup	84.55	5.41	34.405	6.196	<0.7	1.44	18.68	0.567	162.164	186	33.5	<3.8	7.8	101	3.1	876.5
<i>Hanford H2 Sand (middle sequence) Unit</i>																
41	87.85	27.98	14.004	1.056	<0.7	0.41	5.029	0.141	66.075	391.9 ^b	29.6	<19.6	11.5	141	3.9	1849
42A	90.62	35.28	5.68	1.41	<0.1	0.29	6.27	<0.5	79.66	200.4 ^b	49.7 ^b	<3.5	10.2	221	<17.6	2810 ^b
46	96.8	31.85	4.113	1.814	<0.7	0.25	3.636	0.326	182.588	131 ^b	57.8 ^b	<22.3	8	116	10.4	5815 ^b
47A	98.62	45.97	0.32	1.31	<0.1	0.13	5.45	<0.5	106.87	14.7	60.2 ^b	<4.6	6	251	<23.0	4913 ^b

Table 4.3. Anion Content of Water Extracts of Borehole 299-E33-46 (B-110 Sediment). (4 pages)

ID	Depth (ft bgs) ⁽¹⁾	Dil. Fac.	1:1 Extracts in mg/L							Dilution Corrected Porewater mg/L						
			NO3	F-	NO2	Cl	SO4	PO4	HCO3	NO3	F-	NO2	Cl	SO4	PO4	HCO3
52	109	28.4	16.711	1.031	<0.7	0.59	7.912	0.321	142.045	474.6 ^b	29.3	<19.9	16.8	225	9.1	4034 ^b
53A	111.42	38.76	5.51	1.02	<0.1	0.33	6.9	<0.5	139.76	213.6 ^b	39.5	<3.9	12.8	267	<19.4	5417 ^b
57A	119.92	47.96	5.05	0.51	<0.1	0.2	6.1	<0.5	87.42	242.2 ^b	24.5	<4.8	9.6	293	<24.0	4192 ^b
64A	131.85	32.15	45.32	<0.5	<0.1	0.98	12.62	<0.5	51.59	1457.2 ^b	16.08	<3.2	31.5	406	<16.1	1659
69A	140.05	39.7	8.85	<0.5	<0.1	1.01	8.2	<0.5	62.89	351.3 ^b	19.85	<4.0	40.1	326	<19.8	2496
74A	150.15	23.41	11.65	<0.5	<0.1	0.98	8.56	<0.5	63.29	272.7 ^b	11.71	<2.3	22.9	200	<11.7	1482
79A	160.15	19.54	15.19	<0.5	<0.1	1.1	10.12	<0.5	59.06	296.8 ^b	9.77	<2.0	21.5	198	<9.8	1154
82A	164.55	29.22	17.42	<0.5	<0.1	0.92	8.56	<0.5	58.4	509.1 ^b	14.61	<2.9	26.9	250	<14.6	1707
83A	166.85	29.95	16.03	0.5	<0.1	0.85	8.2	<0.5	53.26	480.1 ^b	15	<3.0	25.5	246	<15.0	1595
Natural Sediments in Middle H2 Sand										1 to 48	0.4 to 23	<5	2 to 130	6 to 390	<9	1200 to 1900
<i>Fine Grained Lens</i>																
84-UFA	168.45	1								482 ^b	0.47 ^a	<0.08 ^a	21.3 ^a	95.32 ^a	<0.24 ^a	63.31 ^a
84	168.45	11.44	35.383	0.401	<0.7	1.5	12.246	0.076	52.048	404.9 ^b	4.6 ^a	<8.0 ^a	17.2 ^a	140 ^a	0.9 ^a	595.5 ^a
Natural Sediments in Fine Grained Lens										3 to 8	4 to 5	<2	7 to 11	83 to 140	<3	500 to 750
<i>Hanford H2 Sand Unit</i>																
86A	171.15	18.85	6.99	<0.5	<0.1	1	9.17	<0.5	81.24	131.7 ^b	<9.4	<1.9	18.8	173	<9.4	1531
<i>Hanford H3 Sand Unit</i>																
90A	179.85	22.89	1.29	<0.5	<0.1	0.89	8.51	<0.5	58	29.5	<11.4	<2.3	20.4	195 ^b	<11.4	1327
96A	190.8	41.31	5.03	0.62	<0.1	0.73	7.52	<0.5	42.5	207.8 ^b	25.6	<4.1	30.2	311 ^b	<20.7	1756
101A	200.95	34.06	5.73	<0.5	<0.1	0.58	6.66	<0.5	44.59	195.2 ^b	<17.0	<3.4	19.8	227 ^b	<17.0	1519
105C-UFA	208.95	1								201.4 ^b	1.8	2.76	65.2	281.6 ^b	<0.48 ^a	287 ^a

Table 4.3. Anion Content of Water Extracts of Borehole 299-E33-46 (B-110 Sediment). (4 pages)

ID	Depth (ft bgs) ⁽¹⁾	Dil. Fac.	1:1 Extracts in mg/L							Dilution Corrected Porewater mg/L						
			NO3	F-	NO2	Cl	SO4	PO4	HCO3	NO3	F-	NO2	Cl	SO4	PO4	HCO3
105A	209.95	26.84	3.14	0.82	<0.1	0.8	8.04	<0.5	48.8	84.3 ^b	22	<2.7	21.5	216 ^b	<13.4 ^a	1310 ^a
Natural Sediments in Hanford H3 Sand Unit									4 to 17	4 to 7	<5	12 to 15	90 to 96	<4 to 10	800 to 1880	
<i>Plio-pliostocene Mud Unit</i>																
109A	219.45	23.01	2.27	0.71	<0.1	1.02	8.95	<0.5	62.99	52.2 ^b	16.3	<2.3	23.5	206	<11.5	1449
110B-UFA	221.65	1								270.8 ^b	<0.028 ^a	<0.08 ^a	32.9 ^a	174 ^a	<0.24 ^a	61 ^a
110A	222.05	3.85	33.29	0.66	<0.1	3.77	38.22	0.5	101.3	128.3 ^b	2.5 ^a	<0.4 ^a	14.5 ^a	147 ^a	1.93 ^a	390.5 ^a
110A-dup	222.05	3.85	33.51	0.69	<0.1	3.32	34.84	<0.5	95.86	129.2 ^b	2.7 ^a	<0.4 ^a	12.8 ^a	134 ^a	1.93 ^a	369.5 ^a
113-UFA	225.9	1								105.5 ^b	<0.03	2.52	16	79.5	<0.24	59
113	225.9	6.67	19.431	0.57	<0.7	2.85	27.718	0.105	74.466	129.6 ^b	3.8	<4.7	19	185	0.7	496.8
Natural Sediments in Plio-pliostocene Mud Unit									2 to 14	2.6 to 9.5	<1 to <5	18 to 33	80 to 180	1.4 to <6	300 to 1430	
<i>Plio-pliostocene Gravel Unit</i>																
115A	230.75	27.17	0.48	0.94	<0.1	1.02	9.87	<0.5	60.12	13	25.5	<2.7	27.7	268 ^b	<13.6	1633
120B	240.95	28.68	<0.012	0.548	<0.7	0.82	17.333	<0.014	60.752		15.7	<20.1	23.5	497 ^b	0.4	1743
120A	241.45	39.95	0.44	1.05	<0.1	1.29	13.83	<0.5	54.52	17.6	42	<4.0	51.5	553 ^b	<20.0	2178
123A	245.75	30.01	1.57	<0.5	<0.1	0.67	13.93	<0.5	47	47.1 ^b	<15.0	<3.0	20.1	418 ^b	<15.0	1410
127A	253.15	31.57	1.52	<0.5	<0.1	0.7	7.87	<0.5	57.29	48 ^b	<15.8	<3.2	22.1	248 ^b	<15.8	1809
Natural Sediments in Plio-pliostocene Gravel Unit									9	15	<4	21	39	<7	1200	

⁽¹⁾ to convert to meters multiply by 0.3048

^a UFA squeezing vs. calculated porewater comparisons

^b Zones with elevated concentrations in comparison with the nearby uncontaminated sediment (ranges shown in **Bold**)

NA = not analyzed

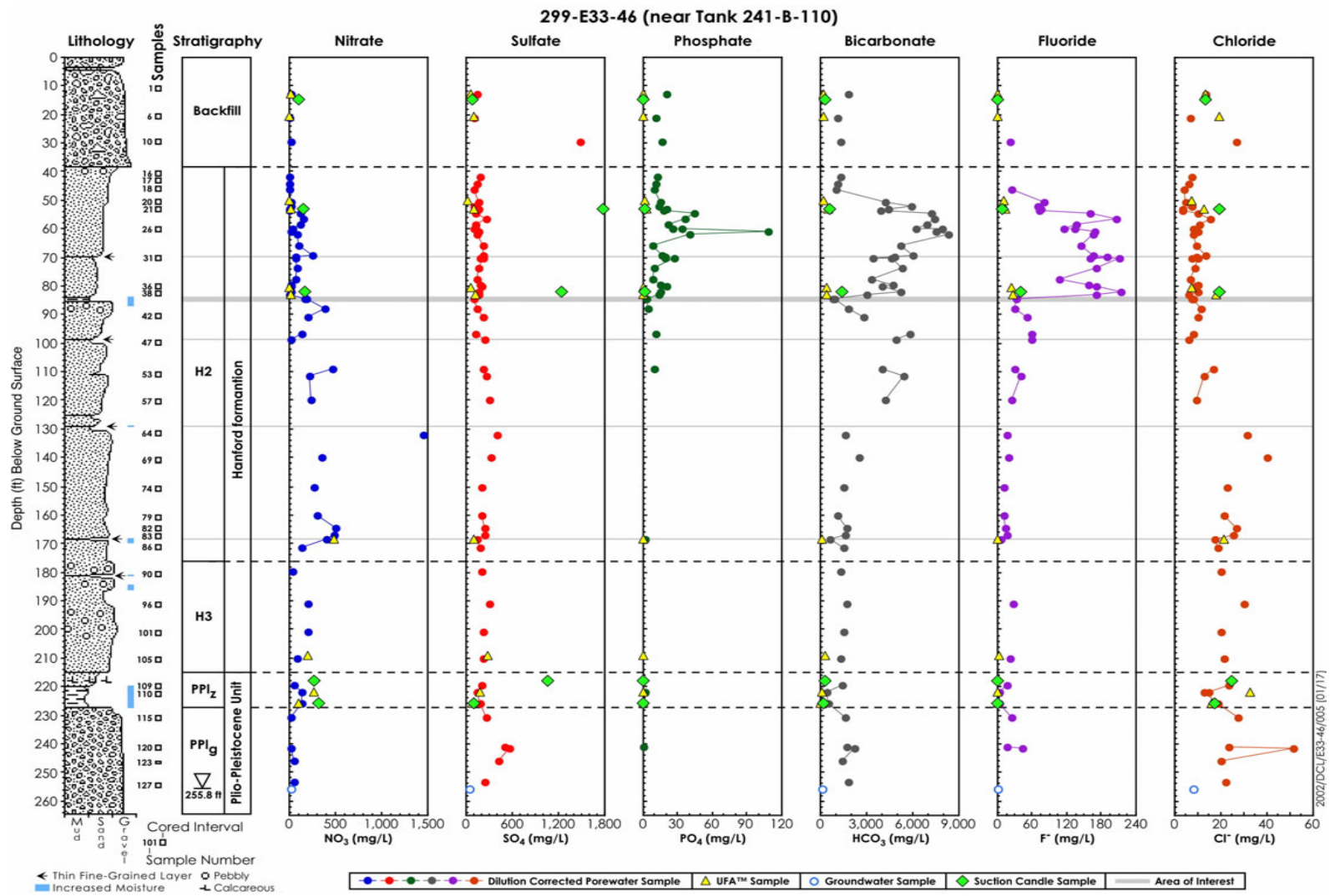


Figure 4.2. Major Anions Calculated (from sediment-to-water extracts), UFA and Suction Candle Porewaters and Groundwater from Borehole 299-E33-46

Table 4.4. Calculated Porewater Cation Composition from Water Extracts of Vadose Zone Sediment from 299-E33-46

ID	Depth (ft bgs) ⁽¹⁾	Dil. Fac.	Dilution Corrected Porewater Concentration of Cations								
			Aluminum	Barium	Calcium	Iron	Potassium	Magnesium	Sodium	Silicon	Strontium
			mg/L	mg/L	mg/L	mg/L	mg/L	mg/L	mg/L	mg/L	mg/L
<i>Backfill</i>											
02B-UFA	12.94	1	0.15 ^a	0.07 ^a	28.7 ^a	0.2 ^a	10.2 ^a	6.6 ^a	69 ^a	23.5 ^a	0.15 ^a
02A	13.7	27.8	0.78 ^a	0.37 ^a	161 ^a	2.4 ^a	124.2 ^a	36.02 ^a	545 ^a	305 ^a	0.78 ^a
06B-UFA	20.62	1	0.15 ^a	0.11 ^a	41.2 ^a	0.21 ^a	8.61 ^a	9.3 ^a	55.6 ^a	19.2 ^a	0.23 ^a
06A	21.12	20.66	0.58 ^a	0.19 ^a	147.5 ^a	0.4 ^a	69.4 ^a	29.73 ^a	250 ^a	237 ^a	0.66 ^a
10A	29.42	30.33	1.45	0.83	480.4	0.4	179.9	99.29	674	309	2.63
<i>Hanford H2 Sand (upper sequence) Unit</i>											
16A	41.72	25.18	1.39	0.22	111	1.3	96.9	21.62	444	263	0.54
17A	44.02	21.29	0.94	0.44	86.7	2.2	74.7	21.42	358	227	0.43
18A	46.42	18.75	0.72	0.2	84.6	1.2	96.8	22.84	344	197	0.43
20B-UFA	50.12	1	0.42 ^a	0.02 ^a	6.7 ^a	0.38 ^a	27.3 ^a	1.7 ^a	188 ^a	15.5 ^a	0.04 ^a
20A	50.62	29.43	7.76 ^a	0.21 ^a	16.7 ^a	11.9 ^a	185.3 ^a	4.55 ^a	1737 ^a	350 ^a	0.1 ^a
21C	52.02	29.45	17.51 ^b	0.53	16.4 ^c	33.1 ^b	138	7.5 ^c	1986 ^b	355 ^b	0.1 ^c
21A-UFA	53.02	1	0.24 ^a	0.08 ^a	7.35 ^a	0.39 ^a	16.2 ^a	1.8 ^a	284	13.7 ^a	0.04 ^a
21A	53.02	20.75	3.39 ^a	0.19 ^a	11.4 ^a	3.8 ^a	111.5 ^a	2.01	2047 ^a	279 ^a	0.06 ^a
21A-dup	53.44	19.42	3.25 ^a	0.13 ^a	9.1 ^a	4.3 ^a	100.8	1.77 ^a	1853	284 ^a	0.05 ^a
22	54.6	22.75	15.2 ^b	0.75	9.4 ^c	23.9 ^b	154.7 ^b	4.29 ^c	2677 ^b	25 ^b	0.05 ^c
24	56.7	19.05	3.57	0.22	9.1 ^c	5.9 ^b	156 ^b	1.22 ^c	3193 ^b	249 ^b	0.04 ^c
25	58.4	19.92	9.67 ^b	0.18	7.2 ^c	16.4 ^b	127.7 ^b	2.94 ^c	2454 ^b	211	0.03 ^c
26C	59.72	19.45	10.94 ^b	0.16	7.3 ^c	17.9 ^b	118.1 ^b	3.1 ^c	2318 ^b	203	0.03 ^c

4.19

Table 4.4. Calculated Porewater Cation Composition from Water Extracts of Vadose Zone Sediment from 299-E33-46

ID	Depth (ft bgs) ⁽¹⁾	Dil. Fac.	Dilution Corrected Porewater Concentration of Cations								
			Aluminum	Barium	Calcium	Iron	Potassium	Magnesium	Sodium	Silicon	Strontium
			mg/L	mg/L	mg/L	mg/L	mg/L	mg/L	mg/L	mg/L	mg/L
26C-dup	59.72	22.74	9.65 ^b	0.3	9.3 ^c	12.8 ^b	147.2 ^b	2.35 ^c	2767 ^b	248 ^b	0.04 ^c
26-A	60.72	24.5	9.28 ^b	0.2	10.2 ^c	10.3 ^b	146.3 ^b	1.97 ^c	3504 ^b	294 ^b	0.05 ^c
27	62.1	23.78	10.78 ^b	0.55	9.3 ^c	15.4 ^b	109.2 ^b	3.07 ^c	2865 ^b	242 ^b	0.05 ^c
29	66.05	24.84	7.14 ^b	0.3	10.9 ^c	10 ^b	113.6 ^b	2.96 ^c	1874 ^b	252 ^b	0.05 ^c
31C	69.45	28.74	7.35 ^b	0.38	12.9 ^c	9.7 ^b	117.6 ^b	3.18 ^c	2220 ^b	301 ^b	0.06 ^c
31B	69.95	23.92	8.03 ^b	0.28	14.2 ^c	9.2 ^b	118.7 ^b	3.68 ^c	1851 ^b	236 ^b	0.07 ^c
31A	70.45	20.8	3.61	0.11	12.2 ^c	3.4 ^b	107.9 ^b	2.66 ^c	1839 ^b	198	0.06 ^c
31A-dup	70.45	27.03	4.57 ^b	0.12	15.3 ^c	2.7 ^b	134.5 ^b	3.26 ^c	2362 ^b	265 ^b	0.08 ^c
33	73.5	25.04	6 ^b	0.33	11.5 ^c	5.8 ^b	121.7 ^b	2.39 ^c	1754 ^b	205	0.07 ^c
35	77.35	15.03	2.69	0.17	7.2 ^c	2.5 ^b	83.5	1.35 ^c	1111 ^b	126	0.04 ^c
36C	79.45	21.67	4.18	0.22	10.2 ^c	5.7 ^b	110.6 ^b	2.06 ^c	1629 ^b	213	0.07 ^c
36A-UFA	79.95	1	1.16 ^a	0.03 ^a	7.28 ^a	0.94 ^a	21.1 ^a	2.1 ^a	244 ^a	13.7 ^a	0.04 ^a
36A	79.95	22.85	3.89 ^a	0.09 ^a	12.9 ^a	2 ^a	120.3 ^a	2.42 ^a	1866 ^a	211 ^a	0.07 ^a
38C	82.05	24.7	4.04	0.15	12.3 ^c	4.1 ^b	42.4	2.53 ^c	1841 ^b	218	0.08 ^c
38A-UFA	83.05	1	0.19 ^a	0.03 ^a	5.54 ^a	0.28 ^a	10.7 ^a	1.38 ^a	315 ^a	15.4 ^a	0.03 ^a
38A	83.05	19.64	2.57 ^a	0.13 ^a	10.5 ^a	1.4 ^a	26.9 ^a	2.18 ^a	1645 ^a	180 ^a	0.06 ^a
Background Upper H2 Sand			0.7 to 1.8	0.5 to 1.1	130 to 170	0.5 to 1.2	58 to 70	36 to 44	120 to 150	130 to 150	0.7 to 0.9
<i>Thin Fine Grained Lens</i>											
39	84.55	5.17	0.16	0.04	10.8 ^c	1.6	10.9	3.32	360	51	0.07
39-dup	84.55	5.41	0.14	0.05	10.7 ^c	1.7	11.6	3.27	376	52	0.07

Table 4.4. Calculated Porewater Cation Composition from Water Extracts of Vadose Zone Sediment from 299-E33-46

ID	Depth (ft bgs) ⁽¹⁾	Dil. Fac.	Dilution Corrected Porewater Concentration of Cations								
			Aluminum	Barium	Calcium	Iron	Potassium	Magnesium	Sodium	Silicon	Strontium
			mg/L	mg/L	mg/L	mg/L	mg/L	mg/L	mg/L	mg/L	mg/L
<i>Hanford H2 Sand (middle sequence) Unit</i>											
41	87.85	27.98	2.27	0.42	46.1 ^c	15.1 ^b	48.5	9.88 ^c	815 ^b	221	0.21 ^c
42A	90.62	35.28	3.2	0.19	64 ^c	2	67.9	15.18 ^c	1346 ^b	330	0.3 ^c
46	96.8	31.85	8.84 ^b	0.21	16.2 ^c	10.4 ^b	40.3	3.88 ^c	1864 ^b	310	0.09 ^c
47A	98.62	45.97	8.19 ^b	0.16	32.7 ^c	3.3	80.9	6.98 ^c	2392 ^b	455 ^b	0.18 ^c
52	109	28.4	6.62	0.4	15.5 ^c	9	45.3	4.05 ^c	1764 ^b	290	0.1 ^c
53A	111.42	38.76	5.49	0.18	20.2 ^c	2.2	63.8	3.8 ^c	2916 ^b	481 ^b	0.11 ^c
57A	119.92	47.96	7.76	0.45	31.3 ^c	4.2	90	8.15 ^c	2263 ^b	483 ^b	0.18 ^c
64A	131.85	32.15	1.77	0.31	250.5	2.3	159.2	54.18	1211 ^b	272	1.09
69A	140.05	39.7	2.39	0.41	190.2	2.6	166.7	51.5	981 ^b	344	0.96
74A	150.15	23.41	1.91	1.42	86.9	1.3	90.4	24.14	698 ^b	207	0.49
79A	160.15	19.54	1.25	0.51	81.1	0.9	71.7	23.81	567 ^b	175	0.43
82A	164.55	29.22	1.4	0.29	160.8	0.8	135.2	47.31	777 ^b	250	0.84
83A	166.85	29.95	2.06	0.74	146.3	1	111.1	43.8	716 ^b	261	0.79
Background Middle H2 Sand			1 to 5	0.4 to 1.3	180 to 225	1 to 6	60 to 140	40 to 60	120 to 390	140 to 300	0.7 to 1.4
<i>Fine Grained Lens</i>											
84-UFA	168.45	1	0.01 ^a	0.09 ^a	86.7 ^a	0.18 ^a	21.1 ^a	28.9 ^a	171 ^a	14.5 ^a	0.51 ^a
84	168.45	11.44	2.84 ^a	0.23 ^a	74.7 ^a	2.9 ^a	41.4 ^a	22.76 ^a	325 ^a	102 ^a	0.41 ^a
Background Fine Grained Lens			0.2 to 0.5	0.3 to 0.6	75 to 92	0.2 to 0.7	40 to 50	20 to 26	120 to 125	70 to 130	0.4 to 0.6
<i>Hanford H2 Sand Unit</i>											
86A	171.15	18.85	0.69	0.19	74.2	0.5	64	23.99	658	207	0.42

Table 4.4. Calculated Porewater Cation Composition from Water Extracts of Vadose Zone Sediment from 299-E33-46

ID	Depth (ft bgs) ⁽¹⁾	Dil. Fac.	Dilution Corrected Porewater Concentration of Cations								
			Aluminum	Barium	Calcium	Iron	Potassium	Magnesium	Sodium	Silicon	Strontium
			mg/L	mg/L	mg/L	mg/L	mg/L	mg/L	mg/L	mg/L	mg/L
<i>Hanford H3 Sand Unit</i>											
90A	179.85	22.89	0.77	0.3	117	0.6	75.9	32.53	435 ^b	244	0.62
96A	190.8	41.31	1.48	0.91	307.4 ^b	6.1	156.4 ^b	81.73 ^b	401 ^b	411 ^b	1.68 ^b
101A	200.95	34.06	1.35	0.48	214.4	0.7	134.6	55.48	483 ^b	343 ^b	1.16
105C-UFA	208.95	1	0.025 ^a	0.11 ^a	45.8 ^a	0.05 ^a	11.9 ^a	12.9 ^a	88.8 ^a	20.4 ^a	0.25 ^a
105A	209.95	26.84	1.53 ^a	0.66 ^a	153.1 ^a	1.1 ^a	107.8 ^a	38.09 ^a	422 ^a	262 ^a	0.83 ^a
Background H3 Sand			0.5 to 1.8	0.4 to 0.7	100 to 170	0.3 to 1.1	60 to 100	30 to 45	150 to 250	100 to 220	0.6 to 1.0
<i>Plio-plistocene Mud Unit</i>											
109A	219.45	23.01	1.24	0.79	205.3	1	97	54.31	369	191	1.18
110B-UFA	221.65	1	ND ^a	0.13 ^a	113 ^a	(0.02) ^a	14.6 ^a	31.9 ^a	119 ^a	15.3 ^a	0.65 ^a
110A	222.05	3.85	0.19 ^a	0.29 ^a	93.9 ^a	1.1 ^a	16.5 ^a	24.4 ^a	136 ^a	50 ^a	0.54 ^a
110A-dup	222.05	3.85	0.1	0.16	85.7	0	16.1	22.28	127	48	0.48
113-UFA	225.9	1	ND ^a	0.05 ^a	53.2 ^a	(0.02) ^a	13.0 ^a	14.7 ^a	68.2 ^a	12.5 ^a	0.31 ^a
113	225.9	6.67	1.42 ^a	0.3 ^a	101.5 ^a	1 ^a	32.1 ^a	25.16 ^a	137 ^a	59 ^a	0.61 ^a
Background PPlz			0.04 to 2.5	0.2 to 1.1	60 to 185	0.1 to 4	10 to 90	10 to 45	70 to 290	45 to 235	0.3 to 1.1
<i>Plio-plistocene Gravel Unit</i>											
115A	230.75	27.17	0.8	0.59	265.8	0.5	98.2	59.68	341	257	1.44
120B	240.95	28.68	4.66	0.73	206.8	8 ^b	132.6	62.46	512	270	1.26
120A	241.45	39.95	2.07	0.82	310.8	2	226.5 ^b	92.57 ^b	778 ^b	376	1.84
123A	245.75	30.01	1.48	0.84	217.3	1.5	128.1	62.56	401	294	1.35

Table 4.4. Calculated Porewater Cation Composition from Water Extracts of Vadose Zone Sediment from 299-E33-46

ID	Depth (ft bgs) ⁽¹⁾	Dil. Fac.	Dilution Corrected Porewater Concentration of Cations								
			Aluminum	Barium	Calcium	Iron	Potassium	Magnesium	Sodium	Silicon	Strontium
			mg/L	mg/L	mg/L	mg/L	mg/L	mg/L	mg/L	mg/L	mg/L
127A	253.15	31.57	2.03	0.62	242.9	1.7	158.7	69.19	530	268	1.44
Background PPIg			0.8	1.2	240	0.7	110	65	350	350	1.3

⁽¹⁾ to convert to meters multiply by 0.3048

^a UFA squeezing vs. calculated porewater comparisons

^b Zones with elevated concentrations in comparison with the nearby uncontaminated sediment (ranges shown in **BOLD**)

^c Zones with depleted divalent cation concentrations because of sodium ion exchange.

NA = not analyzed

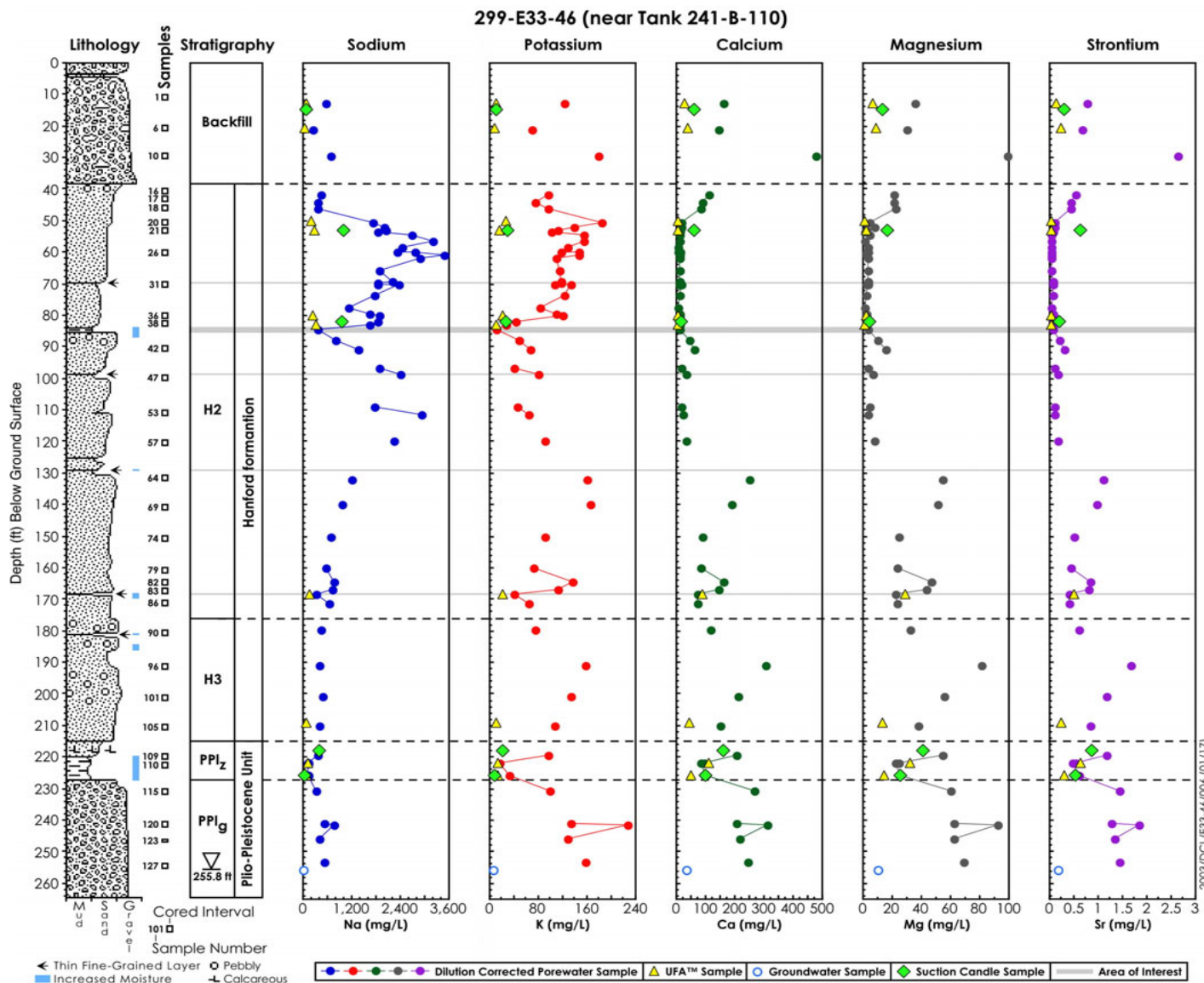


Figure 4.3. Cations Calculated (from sediment-to-water extracts), UFA, and Suction Candle Porewaters and Groundwater for Borehole 299-E33-46 Sediment

The maximum sodium porewater concentration is about 0.122 M in the zone from 16.6 to 18.9 m (54.6 to 62.1 ft) bgs and 0.101 M between 30 and 37 m (98 and 120 ft) bgs. The three highest porewaters based on electrical conductivity have a chemical composition that is essentially 0.15 M sodium and 0.13 M bicarbonate, 0.01 M fluoride, 0.007 M sulfate and 0.003 M nitrate.

The actual porewater cation concentrations are in general always lower than the calculated porewater concentrations derived from dilution correcting the 1:1 sediment to water extracts. The actual cation concentrations vary from about one-half as large to one-seventh as large as the calculated porewater concentrations as shown in Table 4.4 in the green shading for samples from the same depth intervals. This suggests that there is readily dissolvable material in the vadose zone sediments that is not in the dissolved state prior to the sediment extraction process.

The divalent cation distributions right below 37 m (120 ft) bgs do not show significant increases above natural concentrations as would be expected at the very leading edge of the sodium ion exchange pulse. However, the vadose zone sediment at 58 m (190 ft) bgs does appear to show excess divalent cations, but because the sampling frequency near this depth is one sample every 3 m (10 ft) it is difficult to delineate whether there is in fact a zone of excess divalent cations at the very leading edge of the sodium plume. The sodium calculated porewater distribution does not show a distinct drop that could be a sign of the maximum vertical extent of the tank related fluid lost to the ground.

This differs from the cation profile from borehole 299-W23-19 that shows very distinct separation of the divalent cations from the sodium plume (see Figure 4.4 in Serne et al. 2002b) or the less pronounced but still discernable separation from the sodium profile at the two more saline plumes between SX-108 and SX-109 tanks (see Figures 4.3 in both Serne et al. 2002c and 2002d). Based on personal communication with Dr. Carl Steefel at Lawrence Livermore National Laboratory, the ion exchange separation of the divalent cations, which are naturally the dominant cations on Hanford sediment exchange sites, from the invading high sodium fluids is maximized when the invading sodium concentrations are not large and when the ion exchange capacity of the sediments is moderate. This was the case at 299-W23-19. The sodium concentrations observed at 299-E33-46 is about the same as at 299-W23-19 and fifty to one hundred thirty times less concentrated than the pore fluids around SX-108/SX-109. The cation exchange capacity of the sediments near the tank B-110 is smaller than the cation exchange capacity for the sediments below the SX tank farm. Both of these facts would make the separation of divalent cations from the sodium porewater plume at 299-E33-46 the same or slightly less than that observed at 299-W23-19. Thus, it seems strange that some separation is not observable at 299-E33-46. Perhaps the fact that sample frequency was only one sample per every 3 m (10 ft) in the deeper vadose zone at 299-E33-46 as compared to near continuous coring at 299-W23-19 is the problem. Because the chemical composition of the tank fluid lost near tank B-110 is not understood we can not evaluate whether the calculated porewater composition is consistent with the fluids that were lost from tank B-110. See the B-BX-BY FIR section 3.2.2.4 for more details.

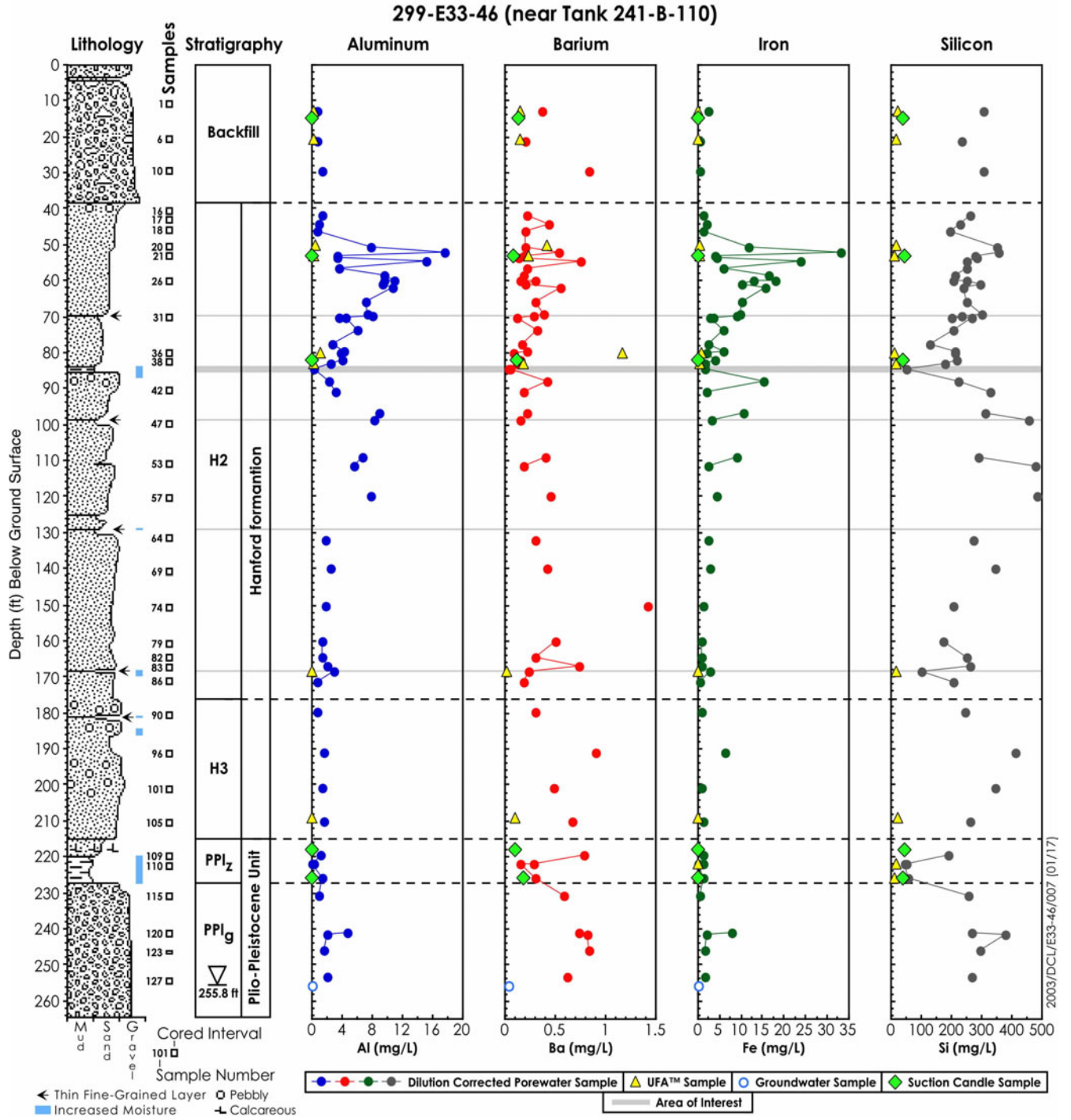


Figure 4.4. Pore Fluid Concentrations of Aluminum, Iron, Silicon, and Manganese (calculated from sediment-to-water extracts), UFA and Suction Candle Porewaters and Groundwater for 299-E33-46 Borehole Sediment

4.2.4 Porewater Trace Constituent Composition

The last group of analyzed constituents included radionuclides and trace metals. Calculated porewater concentrations that were derived from dilution correction of the water extract values are listed in Table 4.5 and shown in Figure 4.5. No strontium-90 above a detection limit of 9000 pCi/L was found in water extracts.

Because the sediments are very dry in the Hanford formation (i.e., dilution factors are large), the porewater technetium-99 concentrations appear to be between 39,800 and 89,800 pCi/L in places within the Hanford formation and as large as 230,000 pCi/L in the Plio-Pleistocene mud unit. The analytical data are difficult to interpret because of the low acid extractable and water extractable amount of technetium per gram of sediment (generally <20 and <10 pCi/g, respectively). Technetium-99 water extract and porewater data that are unequivocally above the quantitation limit are shown in Table 4.5. All the data in the shallow depths is suspect thus it is difficult to determine if the technetium profile at 299-E33-46 from the tank B-110 transfer line leak can be traced from below the tank all the way to the groundwater and whether B-110 is the source of technetium-99 in the deep sediments and groundwater. Other sources could be nearby crib discharges.

Table 4.5 and Figure 4.5 show that there are elevated concentrations of uranium in the vadose zone pore water between 15.4 and 37 m (50.6 and 120 ft) bgs (within the upper sand sequence of H2). There is no indication of elevated uranium in the H3 unit, PPlz or PPlg units. There is no indication that uranium has penetrated below 37 m (120 ft) bgs or into the fine-grained PPlz strata at this borehole. Thus the source of the uranium in the groundwater near the B-BX tank farms is also not definitively explained from the data generated from this borehole. The tank overflow at BX-102 or other sources are much more probable sources for uranium in the groundwater below the B-BX-BY WMA. The pore water data for chromium, arsenic and selenium are not consistent or of sufficient quality, because of low concentrations, to evaluate their vertical distributions and to determine whether Tank B-110 fluids are present in the borehole sediments.

There is very good agreement between the technetium-99 and uranium-238 concentrations found in the actual porewater obtained using the UFA and the dilution corrected sediment-water extracts in all regions and lithologies.

Table 4.5. Calculated and Actual Porewater Radionuclide Composition for Water Extracts of Sediment from 299-E33-46. (3 Pages)

ID	Depth (ft bgs) ⁽¹⁾	Dilution Corrected Porewater Concentrations			
		Dil. Fac.	Technetium-99	Uranium-238	Strontium-90
			pCi/L	µg/L	pCi/L
<i>Backfill</i>					
02B-UFA	12.94	1	<1000 ^a	32.2 ^a	NA
02A	13.7	27.8	<10000 ^a	27 ^a	<9000
06B-UFA	20.62	1	<1000 ^a	25.4 ^a	NA
06A	21.12	20.66	<10000 ^a	24 ^a	<9000
10A	29.42	30.33	<10000	15	<9000
<i>Hanford H2 Sand (upper sequence) Unit</i>					
16A	41.72	25.18	<10000	22	<9000
17A	44.02	21.29	<10000	21	<9000
18A	46.42	18.75	<10000	35	<9000
20B-UFA	50.12	1	(1.35E+03)	39.7	NA
20A	50.62	29.43	<10000	70 ^b	<9000
21C	52.02	29.45	(3496)	63 ^b	<9000
21A-UFA	53.02	1	(1.12E+04) ^c	93.6 ^{ab}	NA
21A	53.02	20.75	<10000 ^a	69 ^{ab}	<9000
21A-dup	53.44	19.42	<10000 ^a	66 ^{ab}	<9000
22	54.6	22.75	(3859)	597 ^b	<9000
24	56.7	19.05	(3231)	632 ^b	<9000
25	58.4	19.92	(3040)	175 ^b	<9000
26C	59.72	19.45	(2968)	148 ^b	<9000
26C-dup	59.72	22.74	(3085)	180 ^b	<9000
26-A	60.72	24.5	(2493)	560 ^b	<9000
27	62.1	23.78	(2823)	842 ^b	<9000
29	66.05	24.84	(3370)	2056 ^b	<9000
31C	69.45	28.74	(5849)	9714 ^b	<9000
31B	69.95	23.92	(5275)	9731 ^b	<9000
31A	70.45	20.8	<10000	8510 ^b	<9000
31A-dup	70.45	27.03	<10000	10946 ^b	<9000
33	73.5	25.04	(2972)	2703 ^b	<9000

Table 4.5. Calculated and Actual Porewater Radionuclide Composition for Water Extracts of Sediment from 299-E33-46. (3 Pages)

ID	Depth (ft bgs) ⁽¹⁾	Dilution Corrected Porewater Concentrations			
		Dil. Fac.	Technetium-99	Uranium-238	Strontium-90
			pCi/L	µg/L	pCi/L
35	77.35	15.03	(2039)	1351 ^b	<9000
36C	79.45	21.67	(2940)	1847 ^b	<9000
36A-UFA	79.95	1	(2.03E+03) ^a	638 ^{ab}	NA
36A	79.95	22.85	(11627) ^a	2161 ^{ab}	<9000
38C	82.05	24.7	(2933)	3547	<9000
38A-UFA	83.05	1	(3.55E+03) ^a	1215 ^{ab}	NA
38A	83.05	19.64	(19315) ^a	3425 ^{ab}	<9000
Background Upper H2 Sand			<10000	6 to 9	
<i>Thin Fine Grained Lens</i>					
39	84.55	5.17	(1314)	312 ^b	<9000
39-dup	84.55	5.41	(1467)	270 ^b	<9000
<i>Hanford H2 Sand (middle sequence) Unit</i>					
41	87.85	27.98	(4271)	40	<9000
42A	90.62	35.28	<10000	160 ^b	<9000
46	96.8	31.85	(3781)	836 ^b	<9000
47A	98.62	45.97	<10000	580 ^b	<9000
52	109	28.4	(8669)	98 ^b	<9000
53A	111.42	38.76	(657)	150 ^b	<9000
57A	119.92	47.96	<10000	141 ^b	<9000
64A	131.85	32.15	(91071)	31	<9000
69A	140.05	39.7	(30970)	33	<9000
74A	150.15	23.41	(15088)	32	<9000
79A	160.15	19.54	(15576)	26	<9000
82A	164.55	29.22	(36181)	43	<9000
83A	166.85	29.95	(40382)	34	<9000
Background Middle H2 Sand			<10000	7 to 24	
<i>Fine Grained Lens</i>					
84-UFA	168.45	1	3.90E+04 ^{ab}	32.3 ^a	NA
84	168.45	11.44	31438 ^{ab}	18 ^a	<9000
Background Fine Grained Lens			<10000	7 to 10	

Table 4.5. Calculated and Actual Porewater Radionuclide Composition for Water Extracts of Sediment from 299-E33-46. (3 Pages)

ID	Depth (ft bgs) ⁽¹⁾	Dilution Corrected Porewater Concentrations			
		Dil. Fac.	Technetium-99	Uranium-238	Strontium-90
			pCi/L	µg/L	pCi/L
<i>Hanford H2 Sand Unit</i>					
86A	171.15	18.85	(23013)	33	<9000
<i>Hanford H3 Sand Unit</i>					
90A	179.85	22.89	(24454)	27	<9000
96A	190.8	41.31	(129618)	24	<9000
101A	200.95	34.06	(164075)	19	<9000
105C-UFA	208.95	1	1.25E+05 ^{ab}	11.5 ^a	NA
105A	209.95	26.84	(55542) ^{ab}	17 ^a	<9000
Background H3 Sand			<10000	8 to 13	
<i>Plio-pliostocene Mud Unit</i>					
109A	219.45	23.01	(89756)	17	<9000
110B-UFA	221.65	1	3.09E+04	22.4	NA
110A	222.05	3.85	89755	5	<9000
110A-dup	222.05	3.85	84523	4	<9000
113-UFA	225.9	1	2.30E+05 ^{ab}	9.0 ^a	NA
113	225.9	6.67	39832 ^{ab}	5 ^a	<9000
Background PPlz			<10000	2 to 10	
<i>Plio-pliostocene Gravel Unit</i>					
115A	230.75	27.17	(21656)	12	<9000
120B	240.95	28.68	(11189)	13	<9000
120A	241.45	39.95	<10000	20	<9000
123A	245.75	30.01	(20867)	10	<9000
127A	253.15	31.57	<10000	12	<9000
Background PPlg			<10000	15	

⁽¹⁾ to convert to meters multiply by 0.3048

^a UFA squeezing vs. calculated porewater comparisons

^b Zones with elevated concentrations in comparison with the nearby uncontaminated sediment

(uncontaminated ranges shown in **BOLD**)

NA = not analyzed

() = values in parentheses are below quantitation limit but above the detection limit and thus considered useful

4.2.5 Porewater Solute Ratios

Besides plotting individual constituent porewater profiles versus depth, we calculated ratios of some of the major constituents in strontium recovery waste, which as discussed in the B-BX-BY FIR section 3.2.2.4 is the best guess as to the type of waste that was lost from piping associated with tank B-110. The best, yet incomplete, estimate of the chemical composition of strontium recovery waste is shown in Table 4.6, which is taken from Table 3.8 in the B-BX-BY FIR and originally from Larson 1967. The ratios for several key parameters in Larson's estimate are shown in Tables 4.7 and 4.8. These ratios have the units of pCi/mg for the technetium-99 to fluoride or other chemicals and mg/mg for the ratios of various chemicals to each other, excepting ratios with uranium that has units of μg .

The dilution corrected porewaters in general do not appear to be of the same composition as this estimate for strontium recovery waste. The technetium-99 concentrations found in the porewaters are generally much lower than those that should be found in strontium recovery waste. Compared to the fluoride found in the porewater, both the technetium-99 and nitrate are too low based on Larson's estimates of the chemical composition of strontium recovery waste. Based on the sodium to fluoride ratios in the porewater, there is too little sodium by a factor of 2 to 4 in the zone where both chemicals are at their highest concentrations (from 15 to 25 m [50 to 83 ft] bgs). Two explanations are that the sodium is reacting with the sediments (adsorbing onto cation exchange sites) while fluoride does not interact as much or the Larson estimate may overestimate the sodium concentration in the waste stream. The sodium to fluoride ratio does approach Larson's ratio over the depth of 90 to near the bottom of the H2 sand unit at 51 m (168 ft) bgs, above the fine-grained thin lens of silt. The bicarbonate to fluoride ratio in the porewater is much higher than Larson's estimate for strontium recovery waste excepting between 21 and 26m (70 and 85 ft) bgs where the ratio agrees with the estimate. The sediment and the vadose air are large sources of inorganic carbon besides the waste stream so that one might expect the environment to dominate the ratio more so than the waste stream. In Tables 4.7 and 4.8, the porewater ratios that are reasonably close to the Larson estimate for strontium recovery waste are shown in red type. Most of the porewater samples do not have ratios that are very close to the strontium recovery waste. However, as discussed in the B-BX-BY FIR the other waste streams considered are even further out of sync with the measured porewaters from borehole 299-E33-46. We agree with the summary statement made in the FIR:

“Neither the volume nor the waste type is well understood for the borehole placed near B-110. Soils analysis data from borehole 299-E33-46 indicate a waste stream rich in strontium-90, fluoride, and bicarbonate. Historical records suggest a plausible waste stream derived from strontium recovery waste from dissolved PUREX fuel as opposed to an initial conclusion (Jones et al. 2001) that the waste was a cesium recovery waste similar to that released by the tank BX-101 pump pit leak.”

One method to evaluate vertical migration of mobile contaminants from the B-110 release would be to plot ratios of the key contaminants versus nitrate or some other conservative (non-sorbing) constituent in the leaked fluid. If tank liquor dilution with extant porewater, potable water line leaks, or recharge water were the only reasons for the decrease in concentrations for all the mobile constituents, then the ratios of one to another should remain constant from the source to the furthest extent of migration as long as the diluting water did not contain the mobile constituents.

Table 4.6. Strontium-90 Recovery Waste Streams from Zirconium-Clad Fuel ^(a)

Chemical / Radionuclide (M)	Concentration	Chemical / Radionuclide	Concentration
Sodium	3.3	Phosphate (M)	<0.003
Aluminum	0.0305	Total Carbonate (M)	0.8 ^(c)
Iron	<0.1	Fluoride (M)	0.10
Chromium	0.00545	HEDTA (M)	0.52
Hydrogen	^(b)	Hydroxyacetic acid (M)	0.25
Hydroxide	^(b)	Cs-137 (Ci/gal)	Assumed ~2
Nitrate	3.1 – 4.0	Sr-90 (Ci/gal)	0.43
Nitrite	NR	Tc-99	0.00042 M
Sulfate	<1.8	pH ^(b)	~10 (assumed)

^(a) Data in this includes the 1AW data from Table 11 of Larson 1967

^(b) Assumed waste stream neutralized to pH ~10 with sodium carbonate.

^(c) Assumed sodium carbonate used to neutralize HEDTA, AcOH, and initial acid.

Reference: Larson 1967, "B Plant Phase III Flowsheets", ISO-986.

299-E33-46 (near Tank 241-B-110)

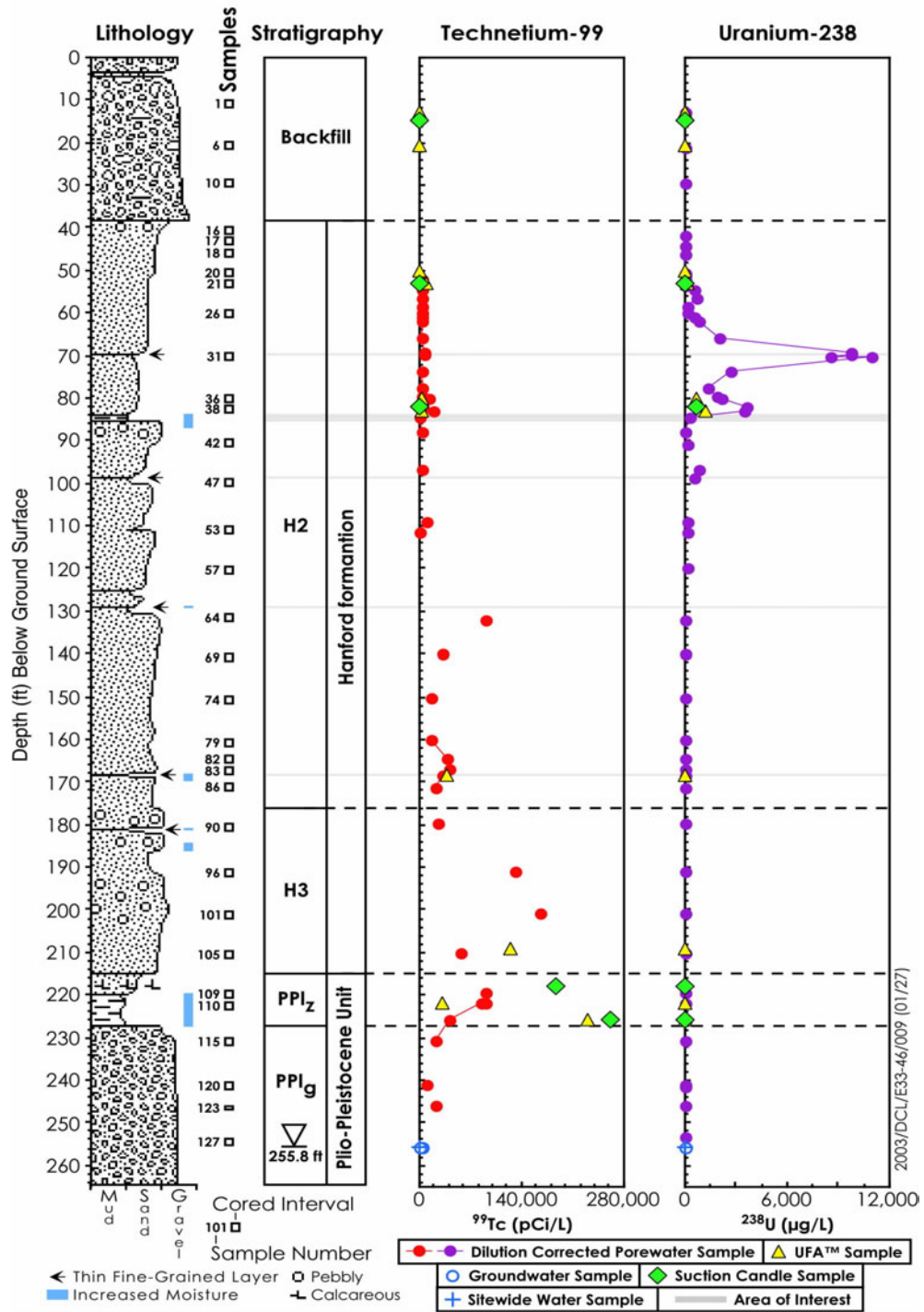


Figure 4.5 Radionuclide Pore Water (calculated from sediment-to-water extracts), UFA and Suction Candle Porewaters and Groundwater for 299-E33-46 Borehole Sediment

Table 4.7. Ratio of Major Strontium Recovery Waste to Fluoride Found in Dilution Corrected 1:1 Water to Sediment Extracts

ID	Depth (ft bgs)⁽¹⁾	NO₃/F (mg/mg)	⁹⁹Tc/F (pCi/mg)	Na/F (mg/mg)	SO₄/F (mg/mg)	HCO₃/F (mg/mg)
Strontium Recovery Waste Stream		114	3.71E+05	39.9	75.8	25.68
<i>Backfill</i>						
02A	13.70	0.74	0	39.2 ^a	10.4	130.95
06A	21.12	0.6	0	24.2	10.0	110.35
10A	29.42	0.58	0	32.2 ^a	71.2 ^a	64.00
<i>Hanford H2 Sand (upper sequence) Unit</i>						
16A	41.72	0.6	0.0	35.3	14.4	102.69
17A	44.02	0.76	0.0	33.6	13.1	101.29
18A	46.42	0.35	0.0	14.0	3.9	42.19
20A	50.62	0.13	0.0	21.3	1.9	51.43
21C	52.02	0.23	49.7	28.2	1.4	83.32
21A	53.02	0.09	0.0	27.2	2.2	59.03
21A-dup	53.44	0.10	0.0	25.9	1.9	54.27
22	54.60	0.72	24.2	16.8	0.7	45.33
24	56.70	0.75	15.7	15.5	1.2	35.90
25	58.40	0.85	22.4	18.1	0.9	51.20
26C	59.72	0.29	25.7	20.1	0.9	53.78
26C-dup	59.72	0.31	22.9	20.5	0.9	58.81
26-A	60.72	0.10	14.9	21.0	1.0	45.03
27	62.10	0.54	17.2	17.4	0.8	50.85
29	66.05	0.69	23.2	12.9	1.6	36.25
31C	69.45	1.51	35.5	13.5	1.4	36.23
31B	69.95	0.37	27.9	9.8	1.1	25.56 ^a
31A	70.45	0.39	0.0	11.5	1.1	21.08 ^a
31A-dup	70.45	0.31	0.0	11.2	1.1	21.98 ^a
33	73.50	0.48	17.4	10.2	1.0	31.16 ^a
35	77.35	0.69	19.1	10.4	1.3	30.65 ^a
36C	79.45	0.12	18.6	10.3	1.2	29.80 ^a
36A	79.95	0.07	68.3	11.0	1.2	23.58 ^a
38C	82.05	0.06	13.8	8.7	0.8	24.37 ^a

Table 4.7. Ratio of Major Strontium Recovery Waste to Fluoride Found in Dilution Corrected 1:1 Water to Sediment Extracts

ID	Depth (ft bgs) ⁽¹⁾	NO ₃ /F (mg/mg)	⁹⁹ Tc/F (pCi/mg)	Na/F (mg/mg)	SO ₄ /F (mg/mg)	HCO ₃ /F (mg/mg)
38A	83.05	0.05	112.42	9.6	0.9	17.74
<i>Thin Fine Grained Lens</i>						
39	84.55	5.38	40.44	11.1	2.9	25.51 ^a
39-dup	84.55	5.55	43.80	11.2	3.0	26.17 ^a
<i>Hanford H2 Sand (middle sequence) Unit</i>						
41	87.85	13.26	144.5	27.6	4.8	62.57
42A	90.62	4.03	0.0	27.1	4.4	56.49
46	96.80	2.27	65.4	32.3 ^a	2.0	100.65
47A	98.62	0.24	0.0	39.7 ^a	4.2	81.58
52	109.00	16.21	296.1	60.3 ^a	7.7	137.77
53A	111.42	5.40	16.6	73.8 ^a	6.8	137.02
57A	119.92	9.90	0.0	92.5 ^a	12.0	171.41
64A	131.85	90.64 ^a	5664.7	75.3 ^a	25.2	103.19
69A	140.05	17.70	1560.3	49.4 ^a	16.4	125.77
74A	150.15	23.30	1288.9	59.6 ^a	17.1	126.58
79A	160.15	30.38	1594.2	58.0 ^a	20.2	118.11
82A	164.55	34.84	2476.2	53.2 ^a	17.1	116.80
83A	166.85	32.06	2696.7	47.8 ^a	16.4	106.52
<i>Fine Grained Lens</i>						
84	168.45	88.24 ^a	6851.7	70.8 ^a	30.5	129.80
<i>Hanford H2 Sand Unit</i>						
86A	171.15	13.98	2442.3	69.9 ^a	18.3	162.47
<i>Hanford H3 Sand Unit</i>						
90A	179.85	2.58	2137	38.0 ^a	17.0	116.00
96A	190.80	8.11	5061	15.6	12.1	68.55
101A	200.95	11.46	9633	28.3	13.3	89.17
105A	209.95	3.83	2523	19.2	9.8	59.51
<i>Plio-pliestocene Mud Unit</i>						
109A	219.45	3.20	5494	22.6	12.6	88.72
110A	222.05	50.44	35282	53.5 ^a	57.9	153.48
110A-dup	222.05	48.57	31782	47.8 ^a	50.5	138.92
113	225.90	34.09	10474	36.1 ^a	48.6	130.64

Table 4.7. Ratio of Major Strontium Recovery Waste to Fluoride Found in Dilution Corrected 1:1 Water to Sediment Extracts

ID	Depth (ft bgs) ⁽¹⁾	NO ₃ /F (mg/mg)	⁹⁹ Tc/F (pCi/mg)	Na/F (mg/mg)	SO ₄ /F (mg/mg)	HCO ₃ /F (mg/mg)
<i>Plio-pliestocene Gravel Unit</i>						
115A	230.75	0.51	848.0	13.3	10.5	63.95
120B	240.95	0.00	711.8	32.6 ^a	31.6	110.86
120A	241.45	0.42	0	18.5	13.2	51.92
123A	245.75	3.14	1390.74	26.7	27.9	93.99
127A	253.15	3.04	0	33.6 ^a	15.7	114.58

⁽¹⁾ to convert to meters multiply by 0.3048

^a Samples whose ratios are consistent with being Strontium Recovery Waste

The porewater ratios of the key waste constituents versus each other are shown in Table 4.8 and Figures 4.6 through 4.9. These ratios have the units of pCi/mg for the technetium-99 to any stable chemical and µg/mg for the uranium to other stable constituents, and mg/mg for chemicals versus each other. For the ratios where technetium or uranium are in the denominator the units are the reciprocal of those just stated. We also show the ratios for the strontium recovery waste stream (where available) that are plausible sources of the vadose zone contamination. The data for the waste streams are taken from Table 4.6 that is taken from Larson 1967.

None of the porewater ratios listed in Table 4.8 are close to the values for strontium recovery waste and more importantly none of the ratios for suspected mobile contaminants such as technetium-99, nitrate, and to lesser extents sodium, uranium, and sulfate to each other show a constant ratio over the depth ranges in the profile where elevated concentrations are found. About the only useful observation is that the porewater ratio of sodium to technetium (sodium/technetium) is significantly lower below 37 m (120 ft) than in the shallower sediments. Because the bulk of the tank related fluid seems to still reside in the zone between the tank bottom and 37 m (120 ft) bgs, and the fact that sodium does react with the sediments to a limited extent, the ratio should drop deeper in the profile where the small amount of technetium seems to reside either carried down deeper or brought in from another leak source.

Thus unlike the ratios for porewaters from the SX borehole, we do not see definitive signs that wastes are migrating vertically in unison with each other. It is likely that the low absolute concentrations of constituents such as technetium-99 and relatively low concentrations of nitrate and uranium found in the borehole 299-E33-46 porewater cause the ratio approach to be compromised by analytical error. This makes it difficult to show that several contaminants are traveling essentially in concert with each other through the vadose zone sediments even though we suspect that technetium-99 and nitrate do migrate essentially un-retarded through the vadose zone sediments. The waste that was lost in the vicinity of tank B-110 did not contain significant amounts of either technetium-99 or nitrate or for that matter uranium, sulfate, or sodium compared to other tank leaks or overfills studied to date.

There is also a zone below 55 m (180 ft) bgs to the water table where the technetium-99-to nitrate ratio ranges about 10 times higher than the ratios for porewaters above 55 m (180 ft) bgs. This change in technetium-99 to nitrate ratio might be explained by two different sources for the water that carries the contaminants. As stated previously the technetium to nitrate ratios for the strontium recovery waste do not correspond to the values found in the calculated porewaters. The observed values for the technetium/NO₃ ratio are significantly lower than the Larson estimate. The ratios for technetium-99-to-nitrate, uranium-to-nitrate, uranium-to-technetium are plotted in Figure 4.7 and 4.8 for the dilution corrected porewaters, ultracentrifuged porewaters, and groundwater as a function of depth.

The technetium-99 to nitrate ratio for the groundwater at 78 m (255.8 ft) bgs is 111 pCi/mg; a value considerably lower than for the porewater in the deep vadose zone of borehole 299-E33-46. This suggests that there may be a source of water that contains nitrate but not technetium in the groundwater. Overall, the ratio approach, where the main contaminants from the leaking tank are ratioed against each other, does not give a clear picture on the geochemistry of the vadose zone or the type of waste stream that leaked from the piping infrastructure associated with B-110. Part of the problem is that the porewaters at borehole 299-E33-46 are not very concentrated in chemicals in general, and the natural porewaters have most of the same chemicals at concentrations only 10 to 50 times less concentrated. These facts limit the usefulness in the ratio approach that was of much more value in interpreting the porewater data at the SX tank farm (see Serne et al. 2002b, c, and d.)

Table 4.8. Ratio of Constituents in Dilution Corrected 1:1 Water Extracts Versus Each Other

ID	Depth (ft) ⁽¹⁾	⁹⁹ Tc/NO ₃ pCi/mg	U/NO ₃ µg/mg	Na/NO ₃ mg/mg	U/ ⁹⁹ Tc µg/pCi	Na/ ⁹⁹ Tc mg/pCi	U/Na µg/mg	U/SO ₄ µg/mg	⁹⁹ Tc/SO ₄ pCi/mg	Na/SO ₄ mg/mg
B-110 Waste		3.25E+03	Unk	0.35	Unk	1.08E-04	Unk	Unk	4.90E+03	0.527
Backfill										
02A	13.70	0	2.61	52.9	InDet	InDet	0.05	0.19	0	3.76
06A	21.12	0	3.89	40.3	InDet	InDet	0.1	0.23	0	2.42
10A	29.42	0	1.28	55.6	InDet	InDet	0.02	0.01	0	0.45 ^a
Hanford H2 Sand (upper sequence) Unit										
16A	41.72	0	2.93	58.8	InDet	InDet	0.05	0.12	0	2.45
17A	44.02	0	2.56	44.2	InDet	InDet	0.06	0.15	0	2.56
18A	46.42	0	4.04	39.9	InDet	InDet	0.1	0.37	0	3.63
20A	50.62	0	6.58	164	InDet	InDet	0.04	0.45	0	11.3
21C	52.02	215	3.88	122	0.018	0.568	0.03	0.63	34.9	19.8
21A	53.02	0	9.83	290	InDet	InDet	0.03	0.43	0	12.6
21A-dup	53.44	0	8.94	251	InDet	InDet	0.04	0.49	0	13.8
22	54.60	33.7	5.22	23.4	0.155	0.694	0.22	5.21	33.7	23.4
24	56.70	20.9	4.08	20.6	0.195	0.988	0.2	2.47	12.7	12.5
25	58.40	26.3	1.51	21.2	0.057	0.807	0.07	1.51	26.3	21.2
26C	59.72	88.6	4.42	69.2	0.050	0.781	0.06	1.37	27.5	21.5
26C-dup	59.72	72.7	4.24	65.2	0.058	0.896	0.07	1.53	26.3	23.6
26-A	60.72	147	33.1	207	0.225	1.406	0.16	3.42	15.2	21.4
27	62.10	32	9.6	32.5	0.298	1.015	0.29	6.33	21.2	21.5
29	66.05	33.9	20.7	18.9	0.610	0.556	1.1	9.08	14.9	8.28
31C	69.45	23.6	39.2	8.95	1.660	0.380	4.37	42.54	25.6	9.72
31B	69.95	74.7	138	26.2	1.845	0.351	5.26	44.96	24.4	8.55

Table 4.8. Ratio of Constituents in Dilution Corrected 1:1 Water Extracts Versus Each Other

ID	Depth (ft)⁽¹⁾	⁹⁹Tc/NO₃ pCi/mg	U/NO₃ µg/mg	Na/NO₃ mg/mg	U/⁹⁹Tc µg/pCi	Na/⁹⁹Tc mg/pCi	U/Na µg/mg	U/SO₄ µg/mg	⁹⁹Tc/SO₄ pCi/mg	Na/SO₄ mg/mg
31A	70.45	0	135	29.3	InDet	InDet	4.63	46.65	0	10.1
31A-dup	70.45	0	165	35.7	InDet	InDet	4.63	49.15	0	10.6
33	73.50	36.5	33.2	21.5	0.910	0.590	1.54	15.87	17.5	10.3
35	77.35	27.6	18.3	15.1	0.663	0.545	1.22	9.79	14.8	8.05
36C	79.45	153	96	85.0	0.628	0.554	1.13	9.8	15.6	8.65
36A	79.95	925	172	148	0.186	0.160	1.16	10.37	55.8	8.95
38C	82.05	237	287	149	1.209	0.628	1.93	20.68	17.1	10.7
38A	83.05	2138 ^(a)	379	182	0.177	0.085	2.08	22.25	125.5	10.7
<i>Thin Fine Grained Lens</i>										
39	84.55	7.51	1.78	2.06	0.237	0.274	0.87	3.27	13.8	3.77
39-dup	84.55	7.89	1.45	2.02	0.184	0.257	0.72	2.68	14.5	3.73
<i>Hanford H2 Sand (middle sequence) Unit</i>										
41	87.85	10.9	0.1	2.08	0.009	0.191	0.05	0.28	30.4	5.79
42A	90.62	0	0.8	6.72	InDet	InDet	0.12	0.72	0.0	6.08
46	96.80	28.9	6.4	14.2	0.221	0.493	0.45	7.22	32.7	16.1
47A	98.62	0	39	163	InDet	InDet	0.24	2.32	0.0	9.55
52	109.00	18.3	0.21	3.72	0.011	0.203	0.06	0.44	38.6	7.85
53A	111.42	3.1	0.7	13.7	0.227	4.431	0.05	0.56	2.46	10.9
57A	119.92	0	0.58	9.35	InDet	InDet	0.06	0.48	0	7.74
64A	131.85	62.5	0.02	0.83	0.000	0.013	0.03	0.08	224	2.98
69A	140.05	88.2	0.09	2.79	0.001	0.032	0.03	0.1	95.1	3.01
74A	150.15	55.3	0.12	2.56	0.002	0.046	0.05	0.16	75.3	3.48
79A	160.15	52.5	0.09	1.91	0.002	0.036	0.05	0.13	78.8	2.87

Table 4.8. Ratio of Constituents in Dilution Corrected 1:1 Water Extracts Versus Each Other

ID	Depth (ft)⁽¹⁾	⁹⁹Tc/NO₃ pCi/mg	U/NO₃ µg/mg	Na/NO₃ mg/mg	U/⁹⁹Tc µg/pCi	Na/⁹⁹Tc mg/pCi	U/Na µg/mg	U/SO₄ µg/mg	⁹⁹Tc/SO₄ pCi/mg	Na/SO₄ mg/mg
82A	164.55	71.1	0.08	1.53	0.001	0.022	0.06	0.17	145	3.11
83A	166.85	84.1	0.07	1.49	0.001	0.018	0.05	0.14	164	2.91
<i>Fine Grained Lens</i>										
84	168.45	77.7	0.04	0.8	0.0005	0.010	0.05	0.13	224	2.32
<i>Hanford H2 Sand Unit</i>										
86A	171.15	175	0.25	5	0.0014	0.029	0.05	0.19	133	3.81
<i>Hanford H3 Sand Unit</i>										
90A	179.85	828	0.92	14.7	0.0011	0.018	0.06	0.14	126	2.23
96A	190.80	624	0.12	1.93	0.0002	0.003	0.06	0.08	417	1.29
101A	200.95	841	0.1	2.47	0.0001	0.003	0.04	0.08	723	2.13
105A	209.95	659	0.2	5	0.0003	0.008	0.04	0.08	257	1.95
<i>Plio-pliostocene Mud Unit</i>										
109A	219.45	1718	0.32	7.06	0.0002	0.004	0.05	0.08	436	1.79
110A	222.05	699	0.04	1.06	5.72E-05	0.002	0.03	0.03	609	0.92
110A-dup	222.05	654	0.03	0.98	4.58E-05	0.002	0.04	0.03	629	0.95
113	225.90	307	0.04	1.06	0.0001	0.003	0.04	0.03	215	0.74
<i>Plio-pliostocene Gravel Unit</i>										
115A	230.75	1661	0.93	26.1	0.0006	0.016	0.04	0.05	80.8	1.27
120B	240.95	InDet	InDet	InDet	InDet	0.046	0.03	0.03	22.5	1.03
120A	241.45	InDet	1.14	44.2	InDet	InDet	0.03	0.04	0.0	1.41
123A	245.75	443	0.21	8.51	0.0005	0.019	0.02	0.02	49.9	0.96
127A	253.15	InDet	0.25	11.1	InDet	InDet	0.02	0.05	0.0	2.14

Table 4.8. Ratio of Constituents in Dilution Corrected 1:1 Water Extracts Versus Each Other

ID	Depth (ft)⁽¹⁾	⁹⁹Tc/NO₃ pCi/mg	U/NO₃ µg/mg	Na/NO₃ mg/mg	U/⁹⁹Tc µg/pCi	Na/⁹⁹Tc mg/pCi	U/Na µg/mg	U/SO₄ µg/mg	⁹⁹Tc/SO₄ pCi/mg	Na/SO₄ mg/mg
-----------	-------------------------------------	--	-----------------------------------	------------------------------------	-------------------------------------	--------------------------------------	-----------------------	-----------------------------------	--	------------------------------------

⁽¹⁾ to convert to meters multiply by 0.3048

^a Ratio is consistent with water extracts being Strontium Recovery Waste

InDet = one or both of the constituents are present below its detection limit so values are indeterminate.

Unk = the strontium recovery waste stream estimate did not have values for uranium so no ratio could be estimated.

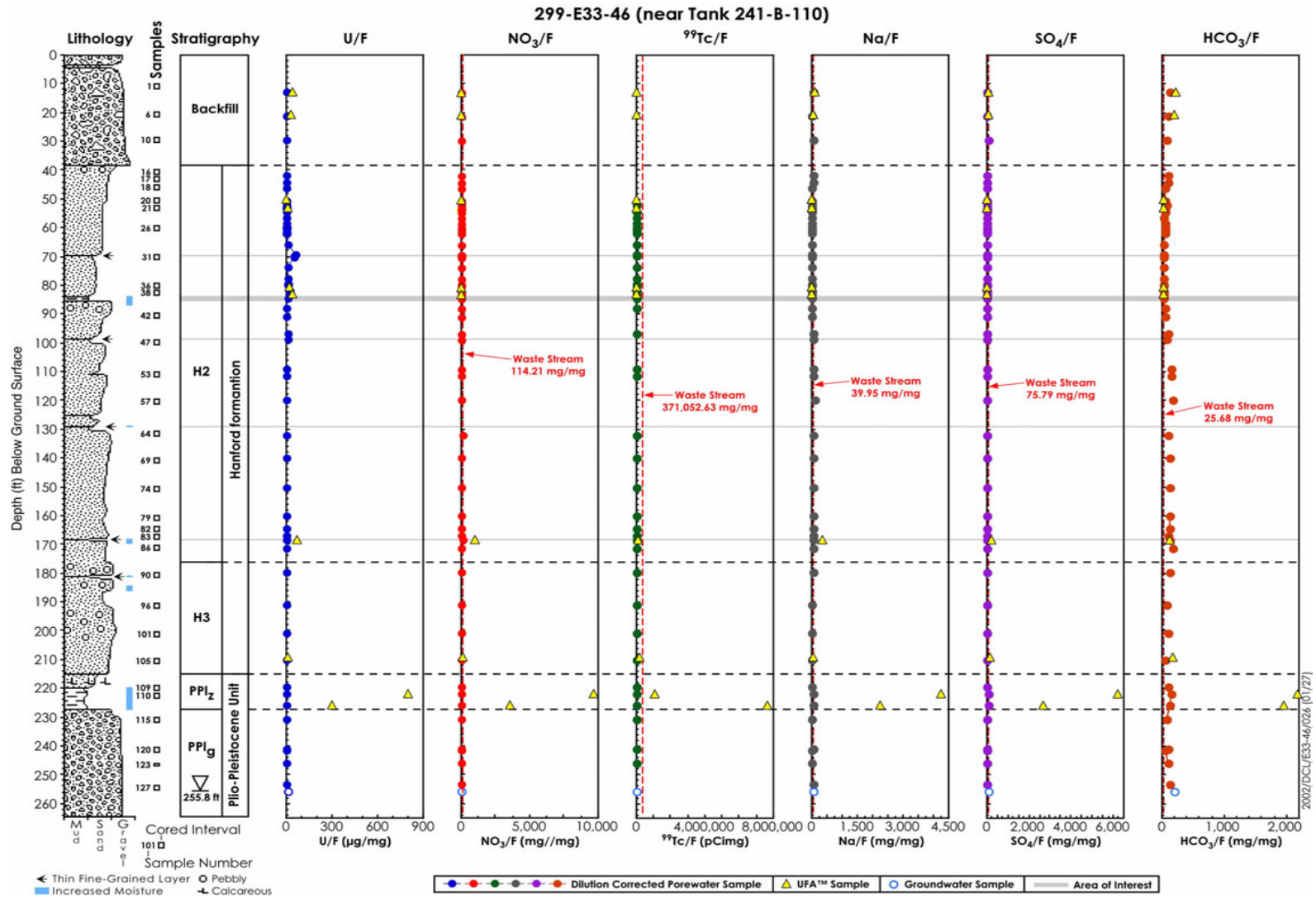


Figure 4.6. Porewater Ratios for Constituents versus Fluoride for 299-E33-46 Sediments.

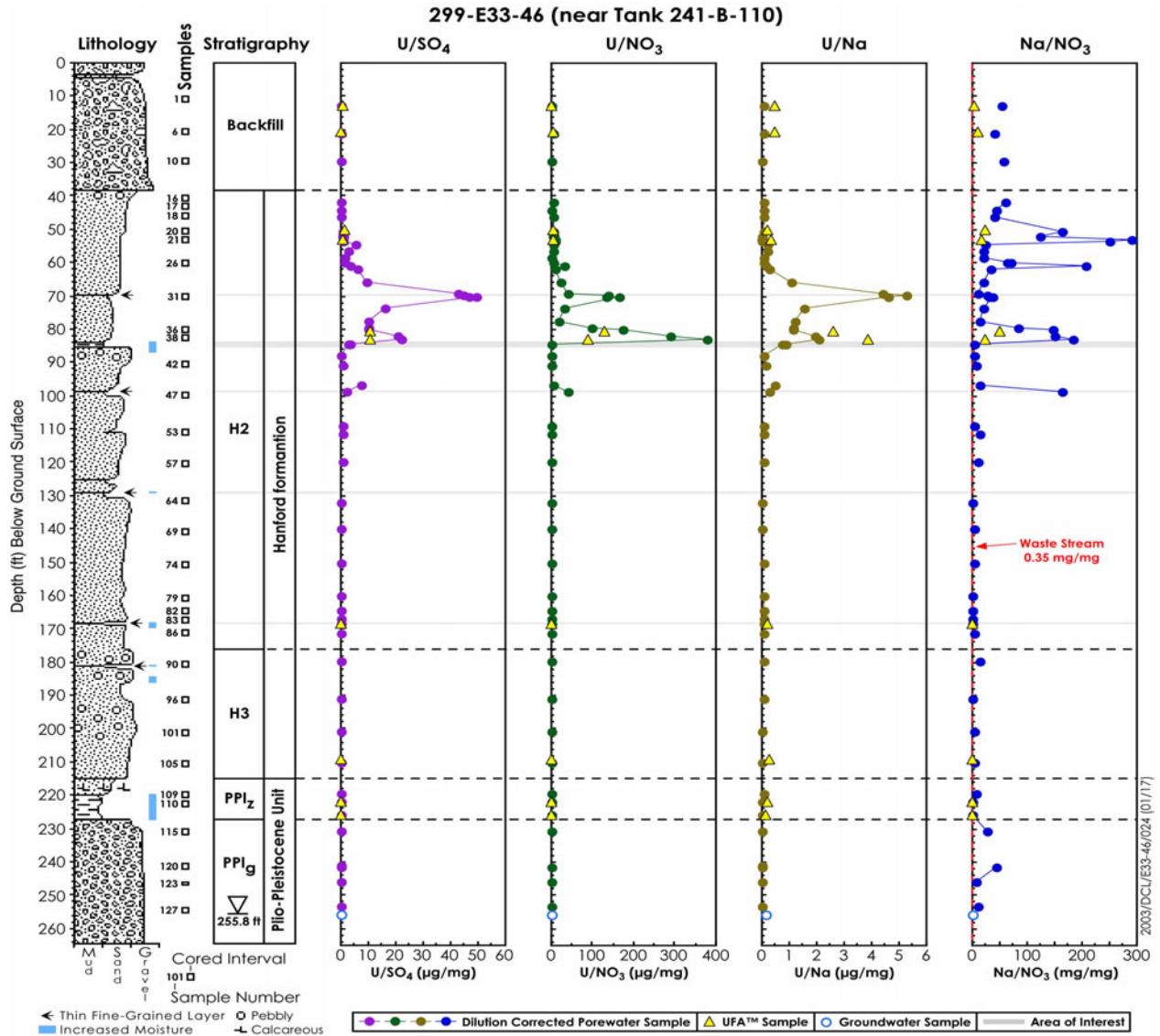


Figure 4.7. Porewater Ratios for Uranium and Sodium to Other Species.

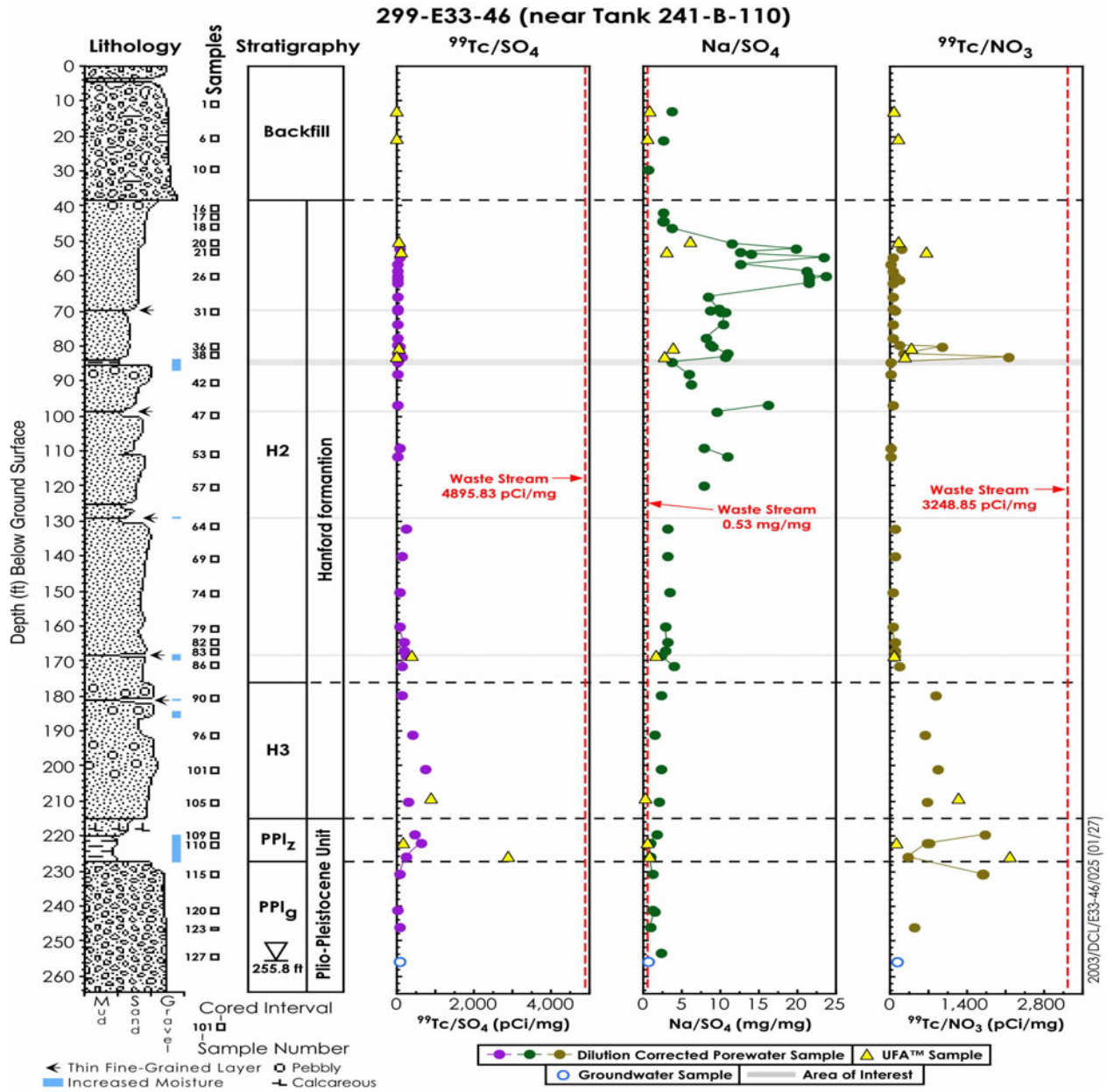
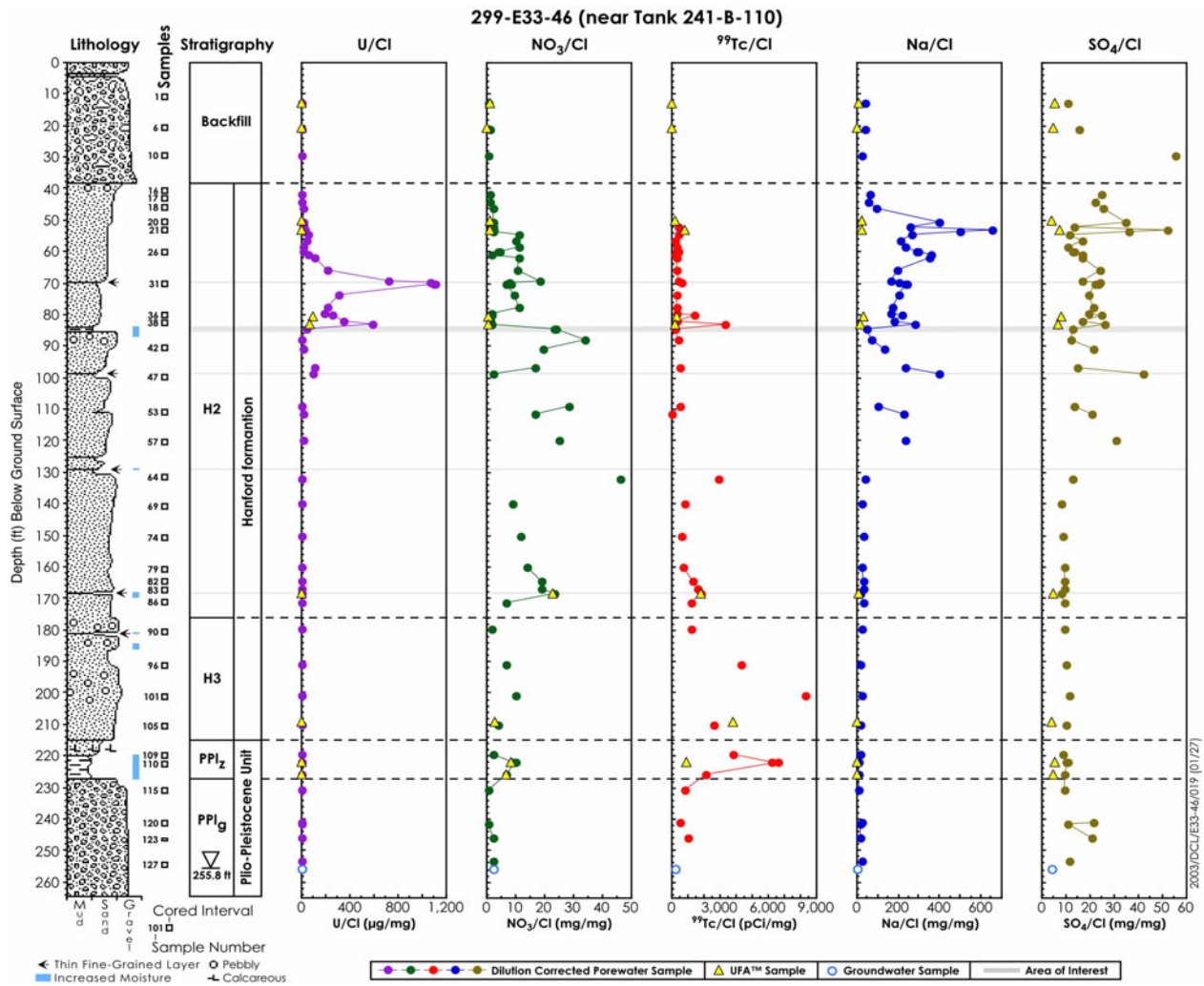


Figure 4.8. Porewater Ratios for Key Constituents versus Each Other



4.3 Radionuclide Content in Vadose Zone Sediment

The sediment cores from 299-E33-46 posed no worker dose challenges (did not contain much gamma radioactivity aside from bremsstrahlung radiation between 14 and 27 m [46 and 89 ft] bgs). The radioanalytical analyses performed on the sediment included direct gamma energy analysis and tritium analysis of the one to one sediment to water extracts (assumed to be equivalent to the standard distillation of tritium out of the sediment and condensation on special targets). The technetium-99 and uranium-238 contents of the strong acid extracts were analyzed by ICP-MS to represent the total Hanford contribution to the sediments. The strontium-90 content of the sediments was determined by strong acid extraction followed by liquid scintillation counting. The strontium-90 content of the sediment to water extracts was determined by liquid scintillation with any further wet chemical separation because there was no other beta emitters present that could have interfered. The only Hanford derived radionuclides found in the sediments from 299-E33-46 were uranium, strontium-90, technetium-99 and tritium.

4.3.1 Gamma Energy Analysis

The GEA radionuclide content of the sediment is shown in Table 4.9. Potassium-40 was the only isotope quantitated in the profile, but the bremsstrahlung radiation was observed between the depths of 14 and 27 m (46 and 89 ft) bgs as evidenced by the higher detection limit for uranium-238 shown in Table 4.9. The uranium-238 activity was below the GEA detection limit for the entire vadose zone profile suggesting low concentrations are present. No detectable gamma emitting fission products such as cesium-137, europium-152, europium-154, antimony-125, or the activation product Cobalt-60, that are often observed in the field logging of the dry boreholes around Hanford's single shell tanks were observed in the sediments. Detection limits for these commonly found isotopes in the laboratory measurements varied from 0.2 to 0.6 pCi/g dependent on isotope. The vertical distributions of uranium and potassium-40 in the vadose zone sediment are plotted in Figure 4.10. Neither profile is noteworthy for delineating any zones of contamination excepting the zone with bremsstrahlung radiation that interferes with measuring the uranium-238, which is based on measuring its daughter thorium-234.

The potassium-40 distribution is somewhat featureless. There are no signs of elevated potassium-40 in the fine-grained lens within the Hanford formation sediments. At most we note a slightly increased concentration of potassium-40 in the Plio-Pleistocene silts, PPLz unit, in comparison to the shallower H3 unit and deeper Plio-Pleistocene gravelly sands (PPLg).

4.3.2 Strontium-90 Content of Sediment from 299-E33-46

Table 4.10 and Figure 4.11 show the distribution of strontium-90 in the vadose zone sediments from borehole 299-E33-46. Strontium-90 is considered to be the primary radionuclide released from tank B-110 transfer line and is concentrated in the sediment between 19 and 28 m (62 and 83 ft) bgs at concentrations between 1,000 and 11,250 pCi/g. There is some strontium-90 as shallow as 14.2 m (46.5 ft) bgs with 600 pCi/g concentration and the bottom of the plume lies between 27 and 33 m (89 and 111 ft) bgs where the concentrations range between 20 and 70 pCi/g. As shown in Table 4.5, the strontium-90 in the sediments is not readily water leachable with distilled water after several hours contact. In general, the water leach and total acid leachable strontium in the vadose zone sediments suggest that the in-situ desorption K_d value is >100 ml/g for the diluted 1:1 sediment to water extract

solution. More detailed studies on the leachability of the strontium-90 in these sediments is found in Appendix D2.4 of the B-BX-BY Field Investigation Report, where it is shown that the desorption of strontium-90 is highly dependent on solution composition and contact time. Simply stated, the strontium-90 present in the vadose zone sediments between 14.2 m and 33 m (45.6 and 111 ft) bgs is not currently mobilized by dilute vadose zone recharge waters.

Table 4.9. Gamma Energy Analysis of Vadose Zone Sediment from Borehole 299-E33-46.

Sample ID	Depth (ft) ⁽¹⁾	Uranium-238 (GEA) (µg/g)	Potassium-40	± Uncertainty
			(pCi/g)	
<i>Backfill</i>				
02C	12.18	<11.6	1.454E+01	7.568E-01
02B	12.94	<11.6	1.426E+01	1.522E+00
02A	13.7	<10.8	1.417E+01	1.338E+00
06D	19.62	<12.1	1.484E+01	1.512E+00
06B	20.62	<11.0	1.024E+01	6.651E-01
06A	21.12	<11.4	1.248E+01	7.098E-01
10C	28.42	<11.5	1.083E+01	1.457E+00
10B	28.92	<11.8	1.224E+01	1.400E+00
10A	29.42	<14.1	1.596E+01	2.076E+00
<i>Hanford H2 Sand (upper sequence) Unit</i>				
16D	39.97	<14.3	2.039E+01	1.074E+00
16C	40.72	<13.9	1.789E+01	1.892E+00
16B	41.22	<12.6	1.689E+01	8.790E-01
16A	41.72	<15.9	2.241E+01	2.681E+00
17D	42.52	<12.4	1.346E+01	1.569E+00
17C	43.02	<12.9	1.993E+01	1.728E+00
17B	43.52	<18.0	2.763E+01	3.180E+00
17A	44.02	<16.2	1.801E+01	2.069E+00
18D	44.92	<13.6	1.934E+01	1.763E+00
18C	45.42	<22.2	2.041E+01	1.166E+00
18B	45.92	<22.3	1.879E+01	1.939E+00
18A	46.42	<33.5	1.797E+01	1.605E+00
20D	49.12	<93.4	2.170E+01	1.353E+00
20C	49.62	<45.7	1.745E+01	1.856E+00
20B	50.12	<88.9	2.100E+01	1.019E+00

Table 4.9. Gamma Energy Analysis of Vadose Zone Sediment from Borehole 299-E33-46.

Sample ID	Depth (ft) ⁽¹⁾	Uranium-238 (GEA) (µg/g)	Potassium-40	± Uncertainty
			(pCi/g)	
20A	50.62	<81.6	1.786E+01	2.229E+00
21D	51.52	<50.1	1.867E+01	1.797E+00
21C	52.02	<72.1	1.940E+01	1.452E+00
21B	52.52	<63.2	1.766E+01	2.373E+00
21A	53.02	<88.4	1.996E+01	9.725E-01
26D	59.22	<95.1	1.876E+01	2.529E+00
26C	59.72	<79.6	1.636E+01	1.698E+00
26B	60.22	<83.1	1.986E+01	9.383E-01
26-A	60.72	<101.2	1.642E+01	2.655E+00
31D	68.95	<38.6	2.015E+01	2.036E+00
31C	69.45	<34.6	2.084E+01	1.734E+00
31B	69.95	<46.3	1.929E+01	2.547E+00
31A	70.45	<39.0	1.786E+01	1.704E+00
36D	78.95	<64.1	1.782E+01	2.330E+00
36C	79.45	<48.7	1.645E+01	9.125E-01
36B	79.95	<40.1	1.713E+01	1.547E+00
36A	80.35	<48.5	1.526E+01	2.281E+00
38D	81.55	<32.4	1.697E+01	9.172E-01
38C	82.05	<33.5	1.952E+01	1.850E+00
38B	82.55	<36.3	1.979E+01	2.307E+00
38A	83.05	<34.7	1.913E+01	2.678E+00
<i>Thin Fine Grained Lens</i>				
No sample was analyzed				
<i>Hanford H2 Sand (middle sequence) Unit</i>				
42C	89.62	<15.5	1.665E+01	2.359E+00
42B	90.12	<13.0	1.728E+01	1.782E+00
42A	90.62	<11.4	1.650E+01	1.235E+00
47C	98.62	<13.0	1.749E+01	1.790E+00
47B	99.12	<10.7	1.719E+01	1.227E+00
47A	98.62	<14.8	1.669E+01	1.092E+00
53D	109.92	<12.7	1.672E+01	8.839E-01
53C	110.42	<12.4	1.754E+01	1.534E+00

Table 4.9. Gamma Energy Analysis of Vadose Zone Sediment from Borehole 299-E33-46.

Sample ID	Depth (ft) ⁽¹⁾	Uranium-238 (GEA) (µg/g)	Potassium-40	± Uncertainty
			(pCi/g)	
53B	110.92	<15.3	1.847E+01	2.157E+00
53A	111.42	<11.8	1.918E+01	1.435E+00
57A	119.92	<15.6	1.468E+01	2.465E+00
62	126.75	<15.0	Not Reported	
64A	131.85	<12.5	1.681E+01	1.754E+00
69A	140.05	<11.6	1.665E+01	8.341E-01
74A	150.15	<15.1	1.701E+01	1.973E+00
79A	160.15	<14.8	1.713E+01	1.819E+00
82A	164.55	<12.9	1.863E+01	9.431E-01
83A	166.85	<13.7	1.634E+01	1.907E+00
<i>Fine Grained Lens</i>				
86A	171.15	<12.3	1.655E+01	8.635E-01
<i>Hanford H3 Sand Unit</i>				
90A	179.85	<14.8	1.574E+01	1.086E+00
96A	190.8	<12.8	1.424E+01	1.646E+00
101A	200.95	<10.5	1.475E+01	7.331E-01
105A	209.95	<15.2	1.425E+01	1.042E+00
<i>Plio-pliestocene Mud Unit</i>				
109A	219.45	<13.3	1.515E+01	8.835E-01
110A	222.05	<14.9	1.869E+01	1.763E+00
<i>Plio-pliestocene Gravel Unit</i>				
115A	230.75	<13.5	1.671E+01	1.960E+00
120A	241.45	<10.9	1.122E+01	6.808E-01
123A	245.75	<09.8	1.507E+01	6.876E-01
127A	253.15	<14.9	1.305E+01	1.839E+00

⁽¹⁾ to convert to meters multiply by 0.3048

**Table 4.10. Total Radionuclide Content of Vadose Zone Sediments from
Borehole 299-E33-46**

ID	Depth (ft bgs)⁽¹⁾	Technetium-99 (pCi/g)	Uranium-238 (µg/g)	Strontium-90 (pCi/g)
<i>Backfill</i>				
02A	13.70	(1.45E+00)	<10.8	1.07E+01
06A	21.12	NA	<11.4	NA
10A	29.42	(1.46E+00)	<14.1	6.57E+00
<i>Hanford H2 Sand (upper sequence) Unit</i>				
16A	41.72	(3.73E+00)	33	2.72E+00
17A	44.02	NA	<16.2	2.13E+01
20A	50.62	(1.57E+00)	NA	6.34E+03
21C	52.02	(3.76E+00)	NA	7.857E+03
21A	53.02	(8.09E+00)	NA	5.93E+03
21A-dup	53.44	(2.57E+00)	NA	7.80E+03
22	54.60	(3.77E+00)	NA	6.533E+03
24	56.70	(5.18E+00)	NA	1.096E+04
25	58.40	(4.62E+00)	NA	8.559E+03
26C	59.72	(4.99E+00)	NA	9.517E+03
26C-dup	59.72	(4.56E+00)	NA	8.341E+03
26-A	60.72	(3.58E+00)	12.9	1.05E+04
27	62.10	(4.97E+00)	NA	1.125E+04
29	66.05	(4.58E+00)	NA	7.760E+03
31C	69.45	(4.74E+00)	NA	1.603E+03
31B	69.95	(5.43E+00)	13.5	NA
31A	70.45	(2.64E+01)	NA	1.57E+03
31A-dup	70.45	(2.58E+01)	NA	NA
33	73.50	(5.75E+00)	NA	5.467E+03
35	77.35	(4.52E+00)	NA	5.053E+03
36C	79.45	(4.70E+00)	NA	3.399E+03
36A	79.95	(1.42E+01)	NA	2.21E+03
38C	82.05	(4.61E+00)	NA	1.811E+03
38A	83.05	(2.19E+01)	NA	6.89E+02

Table 4.10. Total Radionuclide Content of Vadose Zone Sediments from Borehole 299-E33-46

ID	Depth (ft bgs)⁽¹⁾	Technetium-99 (pCi/g)	Uranium-238 (µg/g)	Strontium-90 (pCi/g)
<i>Thin Fine Grained Lens</i>				
39	84.55	(4.98E+00)	NA	9.563E+02
39-dup	84.55	NA	NA	NA
<i>Hanford H2 Sand (middle sequence) Unit</i>				
41	87.85	(3.63E+00)	NA	5.281E+01
42A	90.62	(4.41E+00)	17.1	4.44E+00
46	96.80	(4.60E+00)	NA	7.122E+01
47A	98.62	(4.74E+00)	<14.8	1.54E+01
52	109.00	(3.75E+00)	NA	NA
53A	111.42	(1.40E+00)	<11.8	2.58E+01
57A	119.92	(2.12E+00)	<15.6	3.84E-01
64A	131.85	(3.04E+00)	<12.5	5.96E+00
69A	140.05	(7.65E-01)	<11.6	2.94E+00
74A	150.15	(3.12E+00)	<15.1	5.39E+00
79A	160.15	(3.11E+00)	<8.5	8.53E+00
82A	164.55	(1.52E+00)	<12.9	1.99E+00
83A	166.85	(1.53E+00)	<13.7	3.17E-01
<i>Fine Grained Lens</i>				
84	168.45	(7.18E+00)	NA	NA
<i>Hanford H2 Sand Unit</i>				
86A	171.15	(3.02E+00)	<8.8	3.35E+00
<i>Hanford H3 Sand Unit</i>				
90A	179.85	(1.45E+00)	<14.8	2.57E+00
96A	190.80	(7.72E+00)	<12.8	3.99E+00
101A	200.95	(7.72E+00)	<8.4	1.66E+00
105A	209.95	(8.43E+00)	<15.2	1.70E+00
<i>Plio-pliestocene Mud Unit</i>				
109A	219.45	(9.93E+00)	<13.3	1.35E+00
110A	222.05	5.22E+01	<7.8	2.50E+00
110A-dup	222.05	4.52E+01	NA	6.11E+00
113	225.90	(2.36E+01)	27.3	NA

Table 4.10. Total Radionuclide Content of Vadose Zone Sediments from Borehole 299-E33-46

ID	Depth (ft bgs) ⁽¹⁾	Technetium-99 (pCi/g)	Uranium-238 (µg/g)	Strontium-90 (pCi/g)
<i>Plio-pliestocene Gravel Unit</i>				
115A	230.75	(3.48E+00)	<9	2.58E+00
120B	240.95	(4.69E+00)	NA	NA
120A	241.45	(7.26E-01)	<10.9	8.37E+00
123A	245.75	(7.43E-01)	<7.7	1.29E+01
127A	253.15	(2.40E+01)	<14.9	3.96E-02

⁽¹⁾ to convert to meters multiply by 0.3048

(Values) are below quantification level but thought to be useful

NA = not analyzed; for U used XRF when available and GEA when XRF not available; High strontium-90 interfered with uranium analysis.

As discussed in the B-BX-BY FIR section 3.2.2.4 and Appendix D2.2.3.1.3 it was originally thought that the fluid that leaked from the transfer line contained a complexing agent NTA (nitrilo-triacetic acid or trimethylaminetricarboxylic acid; C₆H₉NO₆). Data presented in Appendix D2.2.3.1.3 show that the presence of NTA at 15 mmol/L in 0.015 mol/L NaHCO₃ background electrolyte, the approximate vadose zone pore fluid in contact with the strontium-90 contaminated sediments, reduced the Sr²⁺-K_d in B tank farm composite sediment from approximately 56 ml/g to 3.16 ml/g. But when the NTA concentration was lowered to 1.5 mmol/L, NTA had no effect on Sr²⁺ ion exchange adsorption in HCO₃ electrolyte. We analyzed 1:1 sediment to water extracts from the zone of strontium-90 contamination for NTA using ion chromatography. Results are shown in Table 4.11. We did not find any traces of water extractable NTA in the water extracts but could readily measure, with 100% recovery, 16 ppm of NTA that was spiked into the water extracts. The sensitivity of the ion chromatograph (IC) for determining NTA was very good. The 16 ppm spike equals 8.4 X 10⁻³ mM about 2000 times below the concentration that was found to impact the strontium adsorption-desorption K_d values. This suggests that there is no indication that water soluble NTA is present today in the vadose zone where the strontium-90 contamination currently resides. It has since been determined that the strontium recovery waste stream did not contain NTA as originally thought so the results in Table 4.11 confirm the absence. As mentioned, using the water extract and acid extract data we find the current in-situ desorption K_d for strontium-90 is greater than 100 mL/g.

Table 4.11. NTA Analyses for Selected 1:1 Sediment to Water Extracts From Strontium-90 Contaminated Sediments. (2 Pages)

Sample Name	Area (arbitrary units)
NTA 16 PPM	1.332
21A--53.02 ft bgs	0.00
26A--60.72 ft bgs	0.00

Table 4.11. NTA Analyses for Selected 1:1 Sediment to Water Extracts From Strontium-90 Contaminated Sediments. (2 Pages)

Sample Name	Area (arbitrary units)
31A--70.45 ft bgs	0.00
36A--80.35 ft bgs	0.00
21A SPK 16 PPM NTA	1.326
26A SPK 16 PPM NTA	1.350
31A SPK 16 PPM NTA	1.339
36A SPK 16 PPM NTA	1.339
NTA 16 PPM II	1.269

Instrument was not Calibrated for NTA so results are area under curve where NTA eluted

Dr. Rick McCain, currently at S. M. Stoller, did a detailed analysis of the field gamma ray logging of borehole 299-E33-46 through the zone where bremsstrahlung radiation was present with the laboratory derived strontium-90 measurements on the sediments obtained by split spoon sampling. The details are found in Appendix C. The goal was to determine if a simple empirical calibration factor between bremsstrahlung signal (as quantified as counts in specified energy channels in the gamma log) and the direct lab measurements of strontium-90 could be derived. As described in Appendix C, there is some theory that can be used defend the concept. The results of the analyses were that a fairly strong correlation was found between the bremsstrahlung signal and lab measured strontium-90 concentration for borehole 299-E33-46 as shown in Figure 4.12 but the correlation value was not the same as theory. The fact that the casing used to drive borehole 299-E33-46 was significantly thicker than the casings used in the 1970s to install other dry well monitoring boreholes around the single-shell tanks was thought to be key to the disagreement. The correlation between observed bremsstrahlung and actual strontium-90 concentrations in surrounding sediments is dependent on casing thickness and the distribution of strontium-90 in the vadose zone sediments. The dependence of the gamma signal to these two factors, casing thickness and contaminant distribution, is not well understood. Therefore the hope that some general correlation between measured bremsstrahlung signal and actual vadose zone strontium-90 concentration has not been successfully demonstrated. Thus although there are other wells, especially in the B Tank Farm that show characteristic bremsstrahlung signal it is not possible to determine accurately the strontium-90 concentration because of the differences in casing thickness and unknown effect of differing contaminant distributions. Several recommendations of additional activities that could be pursued to further attempt to derive more general correlations between bremsstrahlung radiation and quantifying strontium-90 are discussed in Appendix C.

299-E33-46 (near Tank 241-B-110)

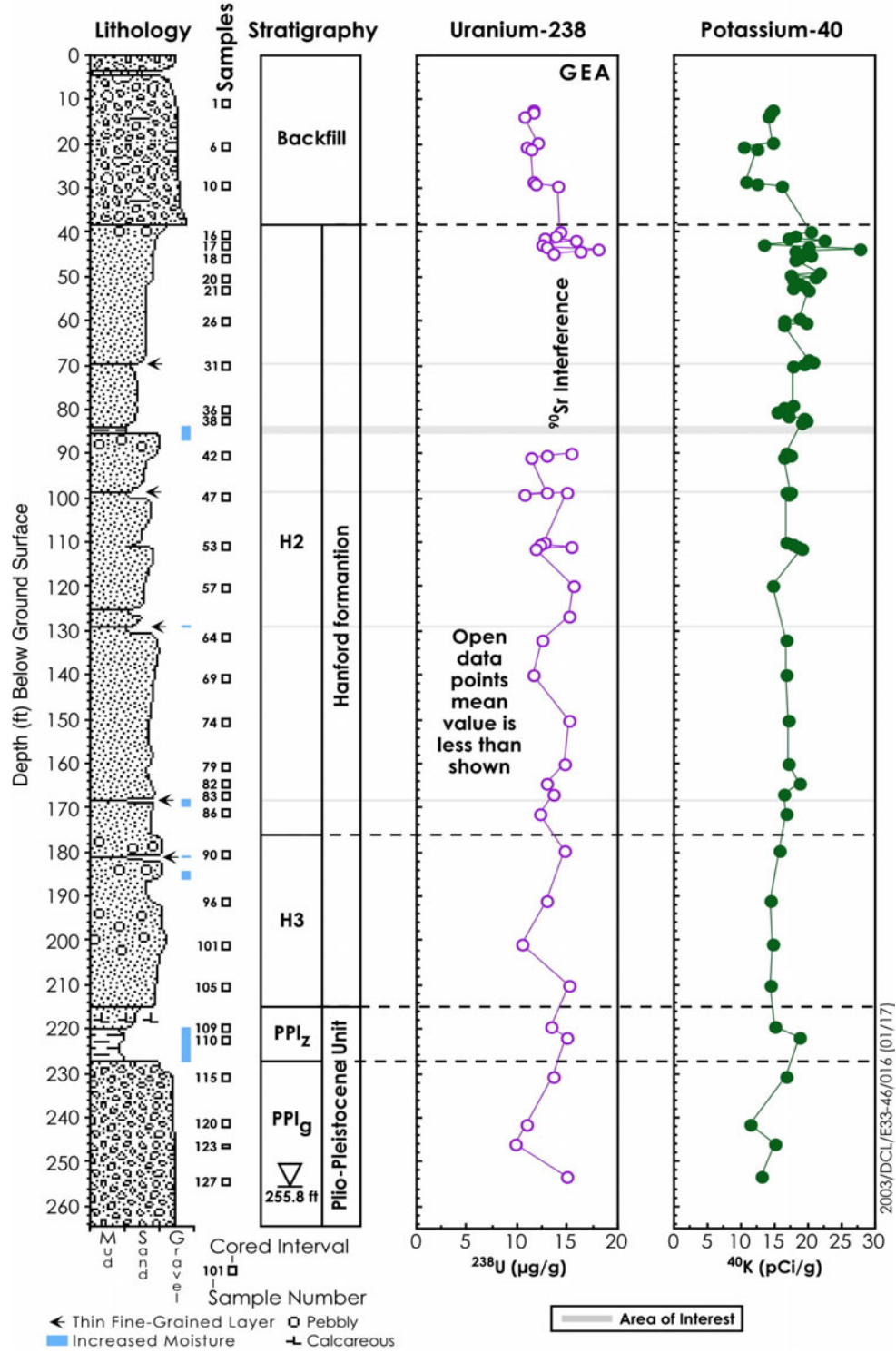


Figure 4.10. Uranium-238 and Potassium-40 Content in Sediment from Borehole 299-E33-46.

299-E33-46 (near Tank 241-B-110)

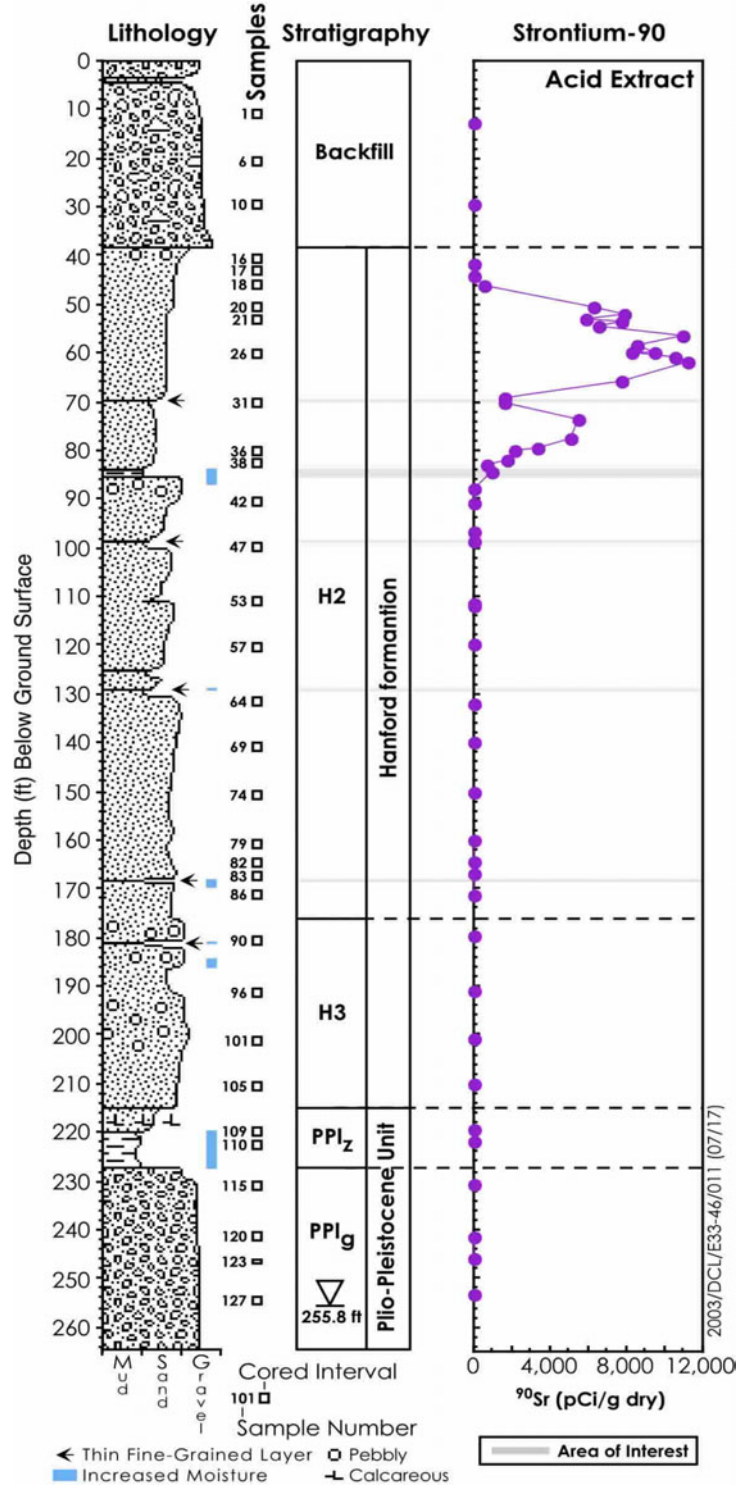


Figure 4.11. Strontium-90 Content of Borehole 299-E33-46 Vadose Zone Sediments.

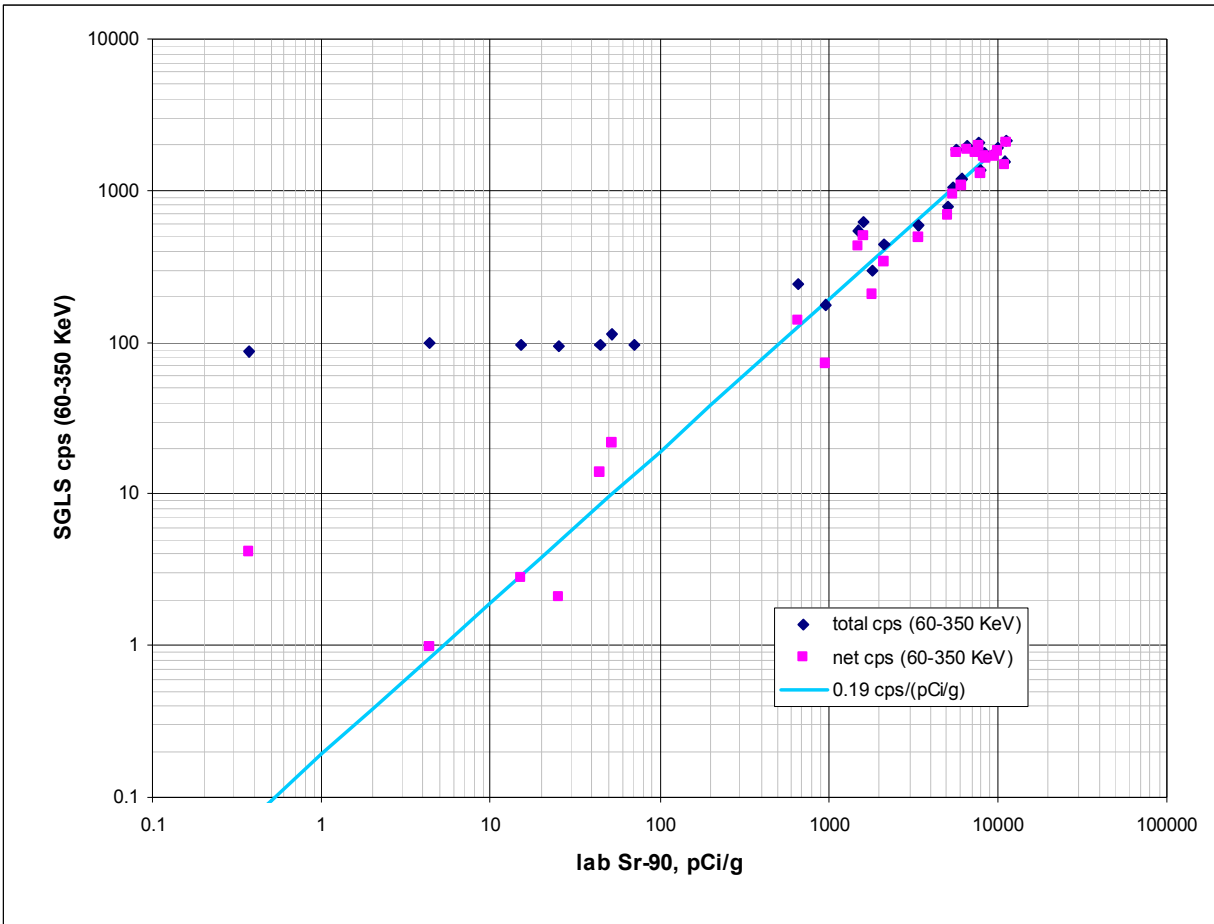


Figure 4.12. Correlation Between Bremsstrahlung Signal (count rate between 60 and 350 keV) and Actual Strontium-90 Concentration in Vadose Zone Sediments from Borehole 299-E33-46

4.3.3 Uranium Content in Sediment

Figure 4.10 shows the uranium content of the sediment using spectral gamma measurements. Uranium concentrations in the sediment are not distinguishable from natural background but the zone immediately below the bottom of the tank was not adequately measured because gamma energy analysis was affected by the bremsstrahlung signal from the strontium-90 present in the sediments.

A second characterization that combined the results from measuring the total uranium content in the sediments by three different methods is shown in Table 4.12 and Figure 4.13. The three methods are 1) measuring uranium-238 by the gamma emission from the short-lived thorium-234 daughter and converting activity to mass; 2) directly measuring total uranium mass by x-ray fluorescence (XRF); 3) and performing the strong nitric acid extract and measuring the uranium-238 mass by ICP-MS. In general, the agreement between the three methods was shown to be good at the BX-102 tank overflow borehole (299-E33-45) where there was elevated uranium concentrations (see Serne et al. 2002e). However, at borehole 299-E33-46 where there is very little uranium, aside from natural background levels, the acid extract data show much lower concentrations than the total uranium concentrations

measured by GEA and XRF. This shows that the natural uranium is bound tightly in crystal lattice sites in minerals that are only partially dissolved in the 8 M nitric acid extraction. Throughout the sediment, acid extraction did not remove more than 3 µg/g of uranium. Such values are similar to the total concentrations of uranium in uncontaminated sediments. The XRF data does suggest that two samples have elevated uranium but the first one at 12.72 m (41.72 ft) bgs seems too shallow compared to the depths where other chemicals suggest tank fluid resides. The second high value is at 68 m (222 ft) bgs in the Plio-Pliocene mud and could reflect natural uranium accumulation in the mud. Neither of these two higher XRF values is supported by the less sensitive GEA analyses, therefore it is difficult to assess whether there is any uranium in the sediments at borehole 299-E33-46 from Hanford activities.

However, the water extractable uranium values shown in Table 4.5 and Figure 4.5 suggest that there is uranium from Hanford fuel reprocessing activities at low concentrations between the depths of 15.4 and 37 m (50.6 and 120 ft) bgs. The deepest penetration of Hanford-related uranium is down to the thin fine-grained bed in the Hanford H2 unit at approximately 37 m (120 ft) bgs.

An indication of the present uranium mobility is calculated based on the ease of water extraction of the uranium compared to the total uranium in the sediment. If one assumes that the dilution corrected 1:1 water extract is equivalent to the uranium content in the porewater, then an in-situ K_d value can be calculated. Table 4.13 shows in-situ K_d values based on taking the best data for the total U in the dry sediment and the calculated porewater concentrations from Table 4.5. In all cases the total uranium measured also includes the uranium that was in the porewater such that a small correction should be made for those samples where appreciable uranium is water leachable. Such corrections only affect a few of the values in Table 4.13 and because most of the measured total uranium concentrations in the solid were less than values, the K_d values shown represent the lowest values one should expect if only natural recharge water was the mobilizing fluid in the future.

Table 4.12. Total Uranium Content in Vadose Zone Sediments Determined by Three Methods. (3 Pages)

ID	Depth (ft bgs) ⁽¹⁾	GEA (µg/g)	XRF (µg/g)	Acid (µg/g)	ID	Depth (ft bgs) ⁽¹⁾	GEA (µg/g)	XRF (µg/g)	Acid (µg/g)
<i>Backfill</i>					36D	78.95	<64.1	NA	0.88
02C	12.18	<11.6	NA	NA	36C	79.45	<48.7	NA	0.78
02B	12.94	<11.6	NA	0.47	36B	79.95	<40.1	NA	NA
02A	13.7	<10.8	NA	NA	36A	80.35	<48.5	NA	NA
06D	19.62	<12.1	NA	NA	38D	81.55	<32.4	NA	1.08
06B	20.62	<11.0	NA	NA	38C	82.05	<33.5	NA	1.20
06A	21.12	<11.4	NA	NA	38B	82.55	<36.3	NA	1.09
10C	28.42	<11.5	NA	NA	38A	83.05	<34.7	NA	1.21
10B	28.92	<11.8	NA	NA	<i>Thin Fine Grained Lens</i>				

**Table 4.12. Total Uranium Content in Vadose Zone Sediments Determined by Three Methods.
(3 Pages)**

ID	Depth (ft bgs) ⁽¹⁾	GEA (µg/g)	XRF (µg/g)	Acid (µg/g)	ID	Depth (ft bgs) ⁽¹⁾	GEA (µg/g)	XRF (µg/g)	Acid (µg/g)
10A	29.42	<14.1	NA	0.56	NO SAMPLES ANALYZED				
<i>Hanford H2 Sand (upper sequence) Unit</i>					<i>Hanford H2 Sand (middle sequence) Unit</i>				
16D	39.97	<14.3	NA	NA	42C	89.62	<15.5	NA	0.52
16C	40.72	<13.9	NA	NA	42B	90.12	<13.0	NA	0.59
16B	41.22	<12.6	NA	0.68	42A	90.62	<11.4	17.1 ^a	0.58
16A	41.72	<15.9	33.2 ^b	NA	47C	98.62	<13.0	NA	NA
17D	42.52	<12.4	NA	NA	47B	99.12	<10.7	NA	NA
17C	43.02	<12.9	NA	NA	47A	98.62	<14.8	NA	0.46
17B	43.52	<18.0	NA	0.55	53D	109.92	<12.7	NA	NA
17A	44.02	<16.2	NA	NA	53C	110.42	<12.4	NA	NA
18D	44.92	<13.6	NA	NA	53B	110.92	<15.3	NA	0.46
18C	45.42	<22.2	NA	NA	53A	111.42	<11.8	NA	0.47
18B	45.92	<22.3	NA	0.53	57A	119.92	<15.6	NA	NA
18A	46.42	<33.5	NA	NA	62	126.75	<15.0	NA	0.50
20D	49.12	<93.4	NA	NA	64A	131.85	<12.5	NA	0.43
20C	49.62	<45.7	NA	NA	69A	140.05	<11.6	NA	0.49
20B	50.12	<88.9	NA	0.53	74A	150.15	<15.1	<8.5	0.45
20A	50.62	<81.6	NA	NA	79A	160.15	<14.8	NA	0.34
21D	51.52	<50.1	NA	0.47	82A	164.55	<12.9	NA	0.42
21C	52.02	<72.1	NA	NA	83A	166.85	<13.7	<8.8	0.45
21B	52.52	<63.2	NA	0.79	<i>Fine Grained Lens</i>				
21A	53.02	<88.4	NA	0.63	NO SAMPLES ANALYZED				
21A-DUP	53.02	NA	NA	0.71	<i>Hanford H2 Sand Unit</i>				
22	54.6	NA	NA	0.75	86A	171.15	<12.3	NA	0.43
22-DUP	54.6	NA	NA	0.59	<i>Hanford H3 Sand Unit</i>				
24	56.7	NA	NA	0.72	90A	179.85	<14.8	NA	0.62
25	58.4	NA	NA	0.54	96A	190.8	<12.8	<8.4	0.42
26D	59.22	<95.1	NA	0.58	101A	200.95	<10.5	NA	0.44
26C	59.72	<79.6	NA	NA	105A	209.95	<15.2	NA	0.47
26B	60.22	<83.1	NA	0.56	<i>Plio-plistocene Mud Unit</i>				
26A	60.72	<101.2	12.9 ^a	1.66	109A	219.45	<13.3	<7.8	1.12

**Table 4.12. Total Uranium Content in Vadose Zone Sediments Determined by Three Methods.
(3 Pages)**

ID	Depth (ft bgs) ⁽¹⁾	GEA (µg/g)	XRF (µg/g)	Acid (µg/g)	ID	Depth (ft bgs) ⁽¹⁾	GEA (µg/g)	XRF (µg/g)	Acid (µg/g)
27	62.1	NA	NA	1.04	110A	222.05	<14.9	27.3 ^b	NA
29	66.05	NA	NA	1.03	113	225.9	NA	<9	0.41
31D	68.95	<38.6	NA	1.87	<i>Plio-plistocene Gravel Unit</i>				
31C	69.45	<34.6	NA	2.12	115A	230.75	<13.5	NA	0.34
31B	69.95	<46.3	13.5 ^a	1.63	120A	241.45	<10.9	<7.7	0.33
31A	70.45	<39.0	NA	0.94	123A	245.75	<09.8	NA	2.48
33	73.5	NA	NA	0.99	127A	253.15	<14.9	NA	NA

⁽¹⁾ to convert to meters multiply by 0.3048

^a Values may be higher than background values for comparable uncontaminated Hanford formation sediments

^b Values may signify tank related contamination.

NA = sample was not analyzed by the designated technique; GEA = gamma energy analyses XRF = x-ray fluorescence and Acid = 8 M nitric acid extraction.

299-E33-46 (near Tank 241-B-110)

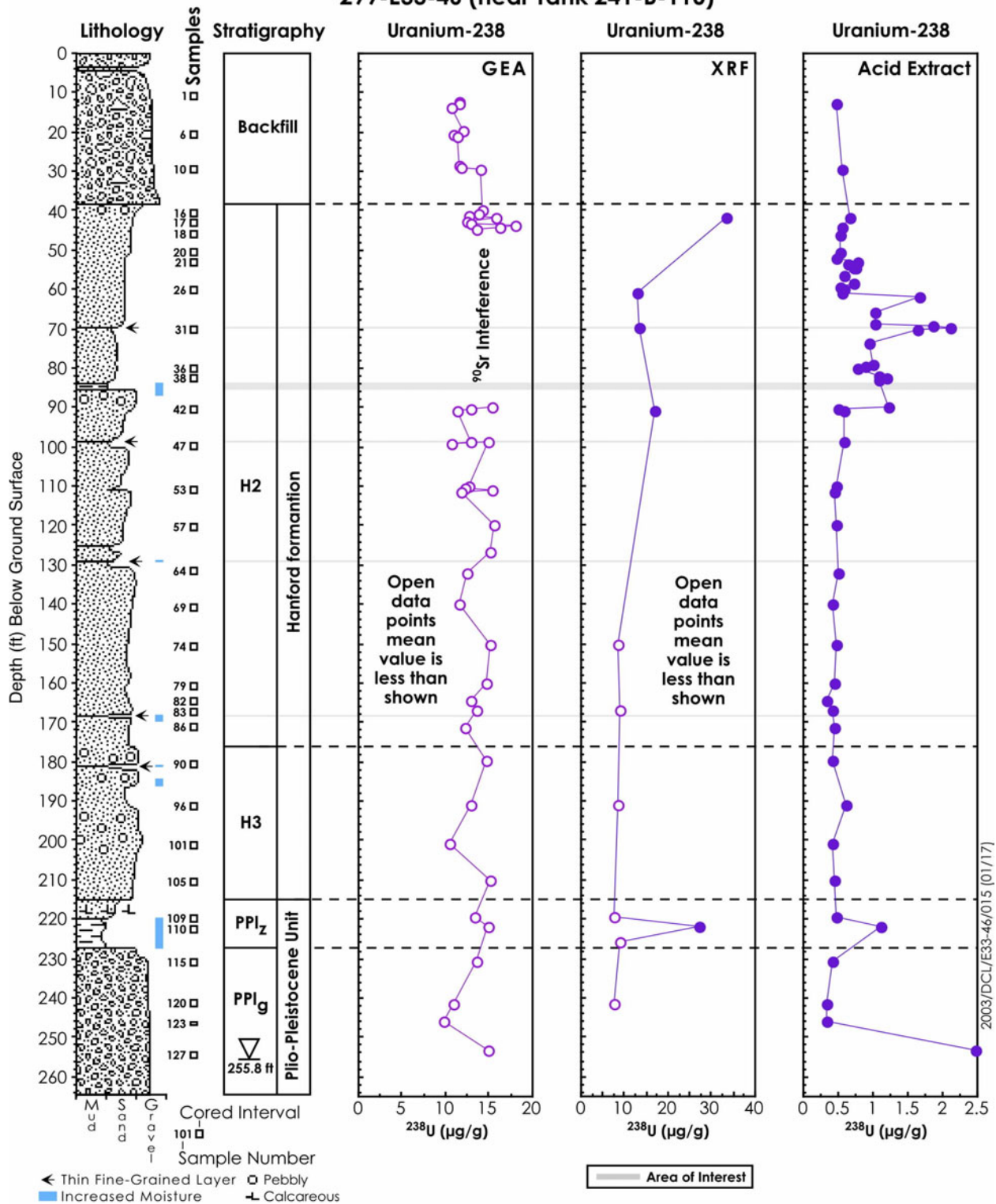


Figure 4.13. Total Uranium in Sediment Based on Three Techniques

The values in Table 4.13 that are denoted with ^(b) show low K_d values that indicate some uranium mobility or alternatively a significant fraction of the uranium is in the porewater. The calculated in situ desorption K_d values for the samples between the depths of 60.7 and approximately 30 m (99 ft) bgs (shown in Table 4.13 in red type) are low (range 1.4 to 107 mL/g; average 23 mL/g). In the narrow zone between 20 and 23 m (66 and 74 ft) bgs the in-situ desorption K_d for uranium averages 3.2 mL/g but is not as low as for the uranium at borehole 299-E33-45 near the BX-102 overfill of uranium metals waste from the bismuth phosphate reprocessing campaigns (see Serne et al. 2002e).

Table 4.13. Calculated In Situ Desorption K_d Values for Uranium in Vadose Sediments at 299-E33-46

ID	Depth (ft bgs) ⁽¹⁾	U sol'n ($\mu\text{g/L}$)	U solid ($\mu\text{g/g}$)	K_d (mL/g)
<i>Backfill</i>				
02B-UFA	12.94	32.2	<11.60	>360
02A	13.7	27	<10.8	>400
06B-UFA	20.62	25.4	<11	>433
06A	21.12	24	<11.4	>475
10A	29.42	15	<14.1	>940
<i>Hanford H2 Sand (upper sequence) Unit</i>				
16A	41.72	22	<15.9	>723
17A	44.02	21	<16.2	>771
18A	46.42	35		
20A	50.62	70 ^a		
21C	52.02	63 ^a		
21A	53.02	69 ^a		
22	54.6	597 ^a		
24	56.7	632 ^a		
26-A	60.72	560 ^a	12.9	23^{ab}
27	62.1	842 ^a		
29	66.05	2056 ^a		
31C	69.45	9714 ^a	<34.6	3.56^{ab}
31B	69.95	9731 ^a	13.5	1.39^{ab}
31A	70.45	8510 ^a	<39	4.58^{ab}
33	73.5	2703 ^a		
35	77.35	1351 ^a		
36C	79.45	1847 ^a	<48.7	26^{ab}
36A	79.95	2161 ^a	<48.5	22^{ab}

Table 4.13. Calculated In Situ Desorption K_d Values for Uranium in Vadose Sediments at 299-E33-46

ID	Depth (ft bgs)⁽¹⁾	U sol'n ($\mu\text{g/L}$)	U solid ($\mu\text{g/g}$)	K_d (mL/g)
38C	82.05	3547 ^a	<33.5	9 ^{ab}
38A	83.05	3425 ^a	<34.7	10 ^{ab}
Background Upper H2 Sand		6 to 9		
<i>Thin Fine Grained Lens</i>				
39	84.55	312		
39-dup	84.55	270		
<i>Hanford H2 Sand (middle sequence) Unit</i>				
41	87.85	40		
42A	90.62	160 ^a	17.1	107
46	96.8	836 ^a		
47A	98.62	580 ^a	<14.8	>26 ^{ab}
53A	111.42	150 ^a	<11.8	>79
57A	119.92	141 ^a	<15.6	>111
64A	131.85	31	<12.5	>403
69A	140.05	33	<11.6	>352
74A	150.15	32	<8.5	>266
79A	160.15	26	<14.8	>569
82A	164.55	43	<12.9	>300
83A	166.85	34	<8.8	>259
Background Middle H2 Sand		7 to 24		
<i>Fine Grained Lens</i>				
84-UFA	168.45	32.3		
84	168.45	18		
Background Fine Grained Lens		7 to 10		
<i>Hanford H2 Sand Unit</i>				
86A	171.15	33	<12.3	>373
<i>Hanford H3 Sand Unit</i>				
90A	179.85	27	<14.8	>548
96A	190.8	24	<12.8	>533
101A	200.95	19	<10.5	>553
105A	209.95	17	<15.2	>894
Background H3 Sand		8 to 13		

Table 4.13. Calculated In Situ Desorption K_d Values for Uranium in Vadose Sediments at 299-E33-46

ID	Depth (ft bgs) ⁽¹⁾	U sol'n (µg/L)	U solid (µg/g)	K_d (mL/g)
<i>Plio-pliestocene Mud Unit</i>				
109A	219.45	17	<7.8	>459
110A	222.05	5	27.3	5460
113	225.9	5	<9	>1800
Background PPlz		2 to 10		
<i>Plio-pliestocene Gravel Unit</i>				
115A	230.75	12	<13.5	>1125
120A	241.45	20	<10.9	>545
123A	245.75	10	<9.8	>980
127A	253.15	12	<14.9	>1242
Background PPlg		15		

⁽¹⁾ to convert to meters multiply by 0.3048

^a Zones with elevated concentrations in comparison with the nearby uncontaminated sediment (background sediment ranges shown in **BOLD**)

^b K_d values are low reflecting presence of U(VI) from liquid waste when compared to K_d values for natural U that leaches from sediments

Empty cells indicate no analyses were performed. Background ranges are from clean sediment at borehole 299-E33-338 east of B Tank Farm fence line.

4.3.4 Technetium-99 Content in the Vadose Zone Sediments

Technetium-99 was measured unequivocally at low concentrations only in the PPlz unit between 68 and 69 m (222 and 226 ft) bgs at concentrations between 40 and 50 pCi/g in the sediment (Table 4.10). Above in the Hanford sediments, there may be very trace concentrations of technetium between 20 to 25, 15 to 20, and 7 to 10 pCi/g at 21, 24 to 25, and 58 to 67 m (70, 79 to 83, and 190 to 220 ft) bgs, respectively. Depending on acid matrix, the detection limit for total technetium-99 in the sediments was between 3 to 6 pCi/g therefore most of the observed values in the Hanford formation are close to the detection limit. The water leachable technetium-99 data are shown in Table 4.5 and Figure 4.5 after conversion to porewater concentrations. The water versus acid extractable technetium data are shown in Figure 4.14 in units of pCi per gram of sediment. The data are not of sufficient quality to calculate or discuss technetium in situ desorption K_d values. We do not believe that there is any indication that technetium is being sorbed/bound to the vadose zone sediments.

299-E33-46 (near Tank 241-B-110)

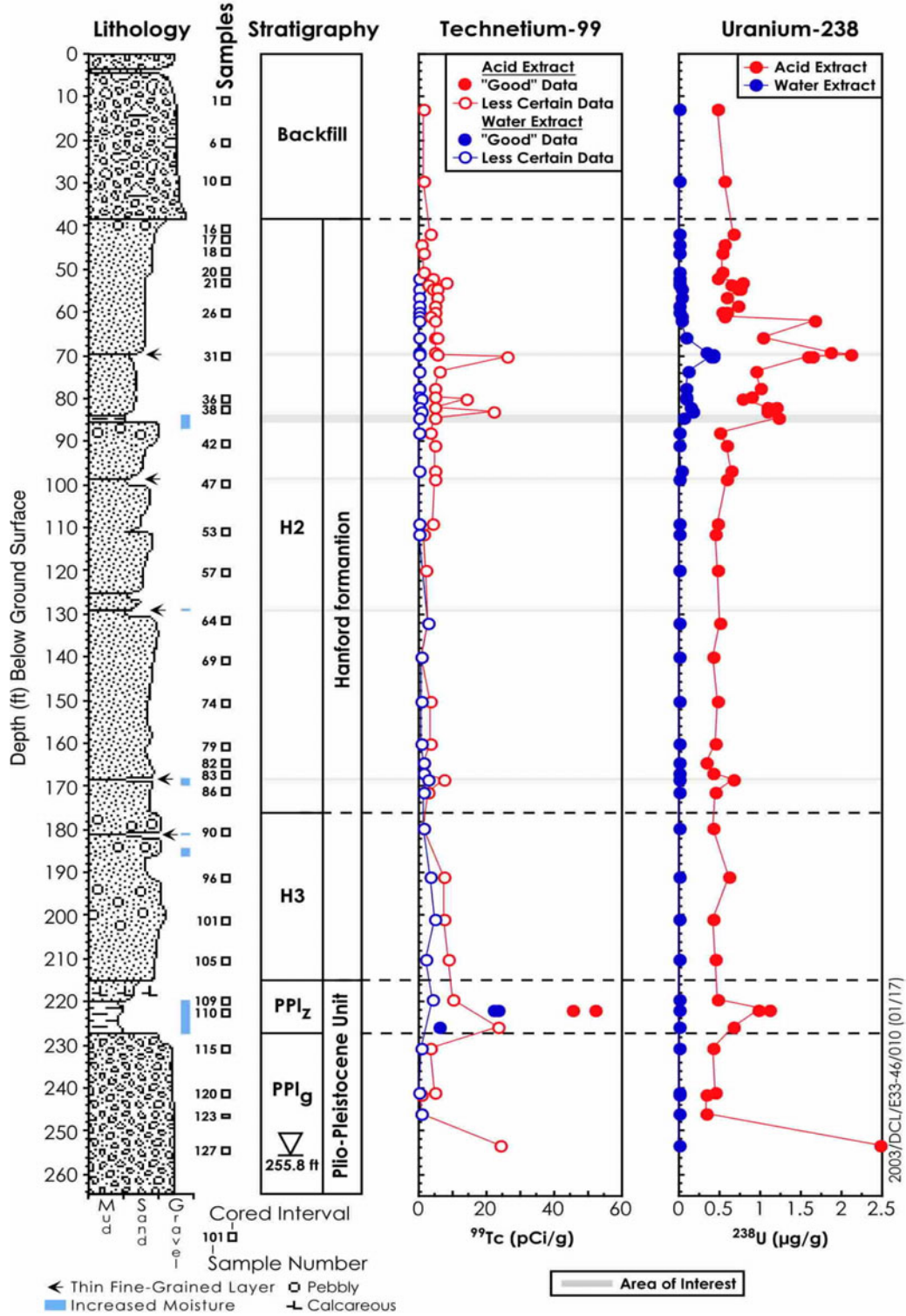


Figure 4.14. Technetium-99 and Uranium Concentrations in Acid and Water Extracts

4.3.5 Recharge Estimates Based on Technetium-99 Distribution in Sediments from Borehole 299-E33-46

If our conclusion that the water and acid extract data discussed in Section 4.3.4 shows that technetium is a non-reacting constituent, then it is possible to generate an estimate of the recharge rate in the vicinity of borehole 299-E33-46. If we assume that the transfer line loss, which occurred in 1972, has been pushed deeper into the vadose zone profile solely by natural recharge, we can estimate the recharge rate from the position of the peak in technetium-99 in the borehole. There are three depths at which there are small peaks of technetium-99 observed in the borehole sediments. Using a simple steady-state model, equation shown below, with all of the “facts” known about the tank farm construction (depth of the transfer line) and geology (depth to groundwater, depth of penetration of non-reacting technetium-99, water content of sediments), and estimates for other parameters, we calculated a range of recharge values (shown in Table 4.14).

$$R = \theta(\Delta L / T)$$

where:

R = recharge rate in mm/yr

θ = volumetric water content (vol/vol)

ΔL = travel distance in mm

T = travel time in years.

Known “facts” for borehole 299-E33-46 and tank B-110 include:

- Transfer Line Leak depth from bgs 7.6 m (25 feet).
- Year elapsed between leak and sampling (1972 to 2001)= approximately 30 years
- Travel Length of technetium-99 minor peak in Hanford H2 unit (Dlmin)= 32.61 m (132-25 ft bgs)
- Travel Length of technetium-99 peak in Hanford H3 unit (Dlmid)= 53.64 m (201 –25 ft bgs)
- Travel Length of technetium peak in PPlz unit (Dlmax)= 61.26 m (226-25 ft bgs)
- Average gravimetric water content (based on Table 4.1 from 20 to 201 ft bgs) is =0.043 g/g or 4.3 wt. %.

To convert to volumetric moisture content one multiplies by sediment bulk density, but we have no direct measurements of bulk density. Thus assuming a range of bulk densities from 1.6 to 1.8 g/cm³ for the sediments underneath tank B-110, we calculate the recharge rates found in Table 4.14.

Table 4.14. Estimated recharge rates based on Tc-99 plume depth beneath B-110

Water Content (vol/vol)	Estimated Bulk Density (g/cm ³)	Time (yrs)	Depth (m)	Depth (mm)	Recharge (mm/yr)
0.0688	1.6	30	32.61	32614	74.7
0.0730	1.7	30	32.61	32614	79.4
0.0773	1.8	30	32.61	32614	84.1
0.0688	1.6	30	53.64	53645	122.9
0.0730	1.7	30	53.64	53645	130.6
0.0773	1.8	30	53.64	53645	138.3
0.0688	1.6	30	61.26	61265	140.4
0.0730	1.7	30	61.26	61265	149.2
0.0773	1.8	30	61.26	61265	158.0

If the distance traveled since the leak occurred is assumed to be represented by the minor peak (shown in Figure 4.5 in the Hanford H2 sand unit at approximately 40 m (132 ft) bgs DLmin (32.61 m) and the average volumetric water content is in the range from 0.069 to 0.077, the range of recharge is from 74.7 to 84.1 mm/yr. If the distance that the technetium-99 traveled from the transfer line leak is assumed to be measured by the larger peak in Figure 4.5 in the Hanford H3 sand unit at approximately 61 m (201 ft) bgs DLmid (53.64 m), then the recharge rate is considerably higher (range from 122.9 to 138.3 mm/yr). If we assume that the technetium-99 in the PPlz mud unit is from the B-110 transfer line leak, then the recharge estimate is between 140 and 158 mm/yr. Based on the fact that the average annual precipitation at Hanford is approximately 162 mm/yr and lysimeter studies for un-vegetated Hanford sediments have yielded recharge estimates between 40 and 111 mm/yr (see Gee et al. 1992), we feel that the latter two estimates based on the technetium-99 distributions in the Hanford H3 sand unit and the PPlz mud unit are unrealistically high. This indicates that either another source of contamination likely placed these two deeper zones of technetium-99 in the vadose zone profile or that other sources of water besides natural recharge have moved the technetium-99 deeper into the profile. The data for the small technetium-99 plume at approximately 38 m (126 ft) bgs in the Hanford H2 sand unit seems more reasonable as the extent of migration since the transfer line leak in 1972 at tank B-110.

Another very recent analysis of natural recharge rates is being created by S. M. Narbutovskih at PNNL for inclusion in the Hanford Site Wide Groundwater Monitoring annual report for fiscal year 2002 (PNNL-14187, draft). She has observed most of the wells in the B-BX-BY WMA that are monitored for Tc-99 exhibited simultaneous Tc-99 peaks in November 2000 that have since started to diminish. Narbutovskih concludes that Tc-99 from the vadose zone has drained into the groundwater throughout the WMA in response to meteoric water inputs (e.g., winter rains and snowmelt events) or some wide-spread source of water from Hanford activities. Narbutovskih's recharge estimate is approximately 115 mm/yr. Note that such a calculation does not preclude individual tank leaks, such as that from B110 to arrive later than November 2000. Based on this analysis we suggest that the minor peak, detected in sediment

samples taken from borehole 299-E33-46, is associated with the transfer line leak from B110 and the deeper technetium-99 peak is related to other sources.

4.3.6 Tritium Content in Vadose Zone Sediments

Table 4.15 lists the tritium content of the 1:1 sediment to water extracts reported per gram of dry sediment. For most of the samples two to four replicates were analyzed and the table shows the average and standard deviation of the measurements. Only one water extract appears to contain measurable tritium above the detection limit. The sample was measured only once so it may not be as reliable as the other data from sediment extracts that were measured several times. The one apparent tritium containing sample was from a depth of 17 m (56.7 ft) bgs, which is a sample with definite high sodium, nitrate, strontium-90 and other contaminants. The groundwater at 78 m (255.8 ft) bgs contains 2810 pCi/L of tritium but it is not likely that the tritium comes from the borehole 299-E33-46 sediments.

4.4 Total Carbon, Calcium Carbonate, and Organic Carbon Content of Vadose Zone Sediment

Table 4.16 shows the total carbon, inorganic carbon, and organic carbon contents of the vadose zone sediment at selected depths. The inorganic carbon was also converted to the equivalent calcium carbonate content. The sediment in the backfill, upper sand sequence and middle sand sequence of the H2 unit are relatively low in carbonate and organic carbon with the calcium carbonate equivalent content ranging from 1.14 to 1.33 % by weight. The two thin lenses in the Hanford H2 unit have slightly higher calcium carbonate contents (1.5 to 2.1 % by weight). The Hanford H3 unit has only 1.1% by weight calcium carbonate equivalent content. The fine- grained PPlz mud shows slightly higher calcium carbonate, averaging 1.7 % by weight. The coarse grained PPlg contains the least calcium carbonate, averaging 0.475% and low organic carbon content. There is no evidence of rich calcareous zones in the entire profile such is found underlying the PPlz unit in 200 West Area. The calcium carbonate equivalent carbon in the contaminated sediments is very similar to the ranges of carbonate measured in the clean borehole (average and standard deviation by lithology is shown in Table 4.16 and total data set is found in Lindenmeier et al. 2002).

Table 4.15. Tritium Content in Vadose Zone Sediments Based on Water Extracts (pCi/g). (2 Pages)

ID	Depth (ft bgs) ⁽¹⁾	Tritium pCi/g	±σ pCi/g
<i>Backfill</i>			
02A	13.7	-1.85 ^a	2.95
06A	21.12	-5.05 ^a	0.81
10A	29.42	-1.06 ^a	0.53
<i>Hanford H2 Sand (upper sequence) Unit</i>			
16A	41.72	-1.19 ^a	4.69
17A	44.02	2.11	
18A	46.42	2.04	2.55
20A	50.62	1.64	2.2
21A	53.02	2.77	3.79
24	56.7	32.64 ^b	
26C	59.72	0.58	1.8
31C	69.45	-1.02 ^a	2.07
31A	70.45	-1.79 ^a	2.24
36A	79.95	-2.88 ^a	
38A	83.05	0.27	
<i>Thin Fine Grained Lens</i>			
39	84.55	-0.9 ^a	1.05
<i>Hanford H2 Sand (middle sequence) Unit</i>			
42A	90.62	-1.51 ^a	0.03
47A	98.62	-2.56 ^a	
53A	111.42	-3.14 ^a	1.19
57A	119.92	-0.5 ^a	
64A	131.85	-0.93 ^a	0.29
69A	140.05	-1.35 ^a	
74A	150.15	1.08	
79A	160.15	-2.58 ^a	
82A	164.55	-0.52 ^a	
83A	166.85	4.65	
<i>Fine Grained Lens</i>			
84	168.45	-3.5	2.59

Table 4.15. Tritium Content in Vadose Zone Sediments Based on Water Extracts (pCi/g). (2 Pages)

ID	Depth (ft bgs) ⁽¹⁾	Tritium pCi/g	±σ pCi/g
<i>Hanford H2 Sand Unit</i>			
86A	171.15	-0.4	
<i>Hanford H3 Sand Unit</i>			
90A	179.85	0.24	
96A	190.8	-2.91	
101A	200.95	7.76	1.17
105A	209.95	-0.02	0.09
<i>Plio-pliestocene Mud Unit</i>			
109A	219.45	-1.06	1.93
110A	222.05	-0.82	2.7
113	225.9	1.21	5.91
<i>Plio-pliestocene Gravel Unit</i>			
115A	230.75	-1.13	0.34
120A	241.45	1.43	0.03
123A	245.75	-2.38	0.09
127A	253.15	-1.83	2.05

⁽¹⁾ to convert to meters multiply by 0.3048

^a Negative values indicate that result was less than the counter background.

^b Value may indicate presence of tritium.

Empty cells indicate that no analyses were performed.

σ represents standard deviation of duplicate analyses.

Table 4.16. Carbon Content in Vadose Sediment from 299-E33-46

ID	Depth (ft bgs) ⁽¹⁾	Total Carbon (% wt)	Inorganic Carbon (% wt)	Organic Carbon (% wt)	IC as CaCO ₃ (% wt)
<i>Backfill</i>					
02A	13.7	0.22	0.17	0.05	1.42
06A	21.12	0.18	0.13	0.05	1.08
10A	29.42	0.18	0.11	0.07	0.92
<i>Hanford H2 Sand (upper sequence) Unit</i>					
16A	41.72	0.25	0.18	0.06	1.50
17A	44.02	0.29	0.24	0.05	2.00

Table 4.16. Carbon Content in Vadose Sediment from 299-E33-46

ID	Depth (ft bgs)⁽¹⁾	Total Carbon (% wt)	Inorganic Carbon (% wt)	Organic Carbon (% wt)	IC as CaCO₃ (% wt)
18A	46.42	0.3	0.23	0.07	1.92
20A	50.62	0.28	0.22	0.06	1.83
21A	53.02	0.236	0.184	0.050	1.53
22	54.6	0.08	0.07	0.01	0.58
24	56.7	0.02	0.16	0.04	1.33
25	58.4	0.19	0.14	0.05	1.17
26C	59.72	0.18	0.13	0.05	1.08
26-A	60.72	0.17	0.08	0.09	0.67
27	62.1	0.17	0.13	0.04	1.08
29	66.05	0.14	0.09	0.05	0.75
31B	69.95	0.19	0.15	0.04	1.25
31A	70.45	0.23	0.19	0.05	1.58
33	73.5	0.23	0.17	0.06	1.42
35	77.35	0.2	0.2	0	1.67
36A	79.95	0.18	0.14	0.04	1.17
38A	83.05	0.21	0.17	0.04	1.42
Background Upper H2 Sand					1.23±0.23
<i>Thin Fine Grained Lens</i>					
39	84.55	0.25	0.18	0.07	1.50
<i>Hanford H2 Sand (middle sequence) Unit</i>					
41	87.85	0.16	0.1	0.06	0.83
42A	90.62	0.19	0.14	0.04	1.17
46	96.8	0.19	0.15	0.04	1.25
47A	98.62	0.15	0.12	0.03	1.00
53A	111.42	0.22	0.18	0.04	1.50
57A	119.92	0.18	0.14	0.04	1.17
64A	131.85	0.14	0.1	0.04	0.83
69A	140.05	0.38	0.31	0.07	2.58
74A	150.15	0.165	0.13	0.035	1.08
79A	160.15	0.14	0.09	0.05	0.75
82A	164.55	0.18	0.12	0.06	1.00
83A	166.85	0.18	0.14	0.04	1.17

Table 4.16. Carbon Content in Vadose Sediment from 299-E33-46

ID	Depth (ft bgs)⁽¹⁾	Total Carbon (% wt)	Inorganic Carbon (% wt)	Organic Carbon (% wt)	IC as CaCO₃ (% wt)
Background Middle H2 Sand					1.23±0.23
<i>Fine Grained Lens</i>					
84	168.45	0.19	0.13	0.06	1.08
Background Fine Grained Lens					NA
<i>Hanford H2 Sand Unit</i>					
86A	171.15	0.33	0.25	0.08	2.08
<i>Hanford H3 Sand Unit</i>					
90A	179.85	0.19	0.16	0.03	1.33
96A	190.8	0.13	0.11	0.02	0.92
101A	200.95	0.19	0.15	0.04	1.25
105A	209.95	0.14	0.1	0.04	0.83
Background H3 Sand					0.67±0.01
<i>Plio-pliestocene Mud Unit</i>					
109A	219.45	0.175	0.125	0.05	1.04
110A	222.05	0.34	0.27	0.09	2.25
113	225.9	0.22	0.22	0.00	1.83
Background PPlz					1.69±0.28
<i>Plio-pliestocene Gravel Unit</i>					
115A	230.75	0.13	0.09	0.04	0.75
120B	240.95	0.09	0.08	0.01	0.67
120A	241.45	0.1	0.06	0.04	0.50
123A	245.75	0.03	0	0.03	0.00
127A	253.15	0.08	0.02	0.06	0.17
Background PPlg					0.72

⁽¹⁾ to convert to meters multiply by 0.3048

BOLD denotes values for background sediments from same lithology from clean borehole 299-E33-338.

4.5 8 M Nitric Acid Extractable Amounts of Selected Elements

The amount of material that was extractable from the vadose zone sediment into 8 M nitric acid is shown in Tables 4.17 and 4.18. Prior to gaining access to an x-ray fluorescence unit that can determine the total composition of contaminated sediment directly, we had no accurate method to determine directly the total elemental composition of the contaminated sediment. As described in Serne et al. (2002a), we tried total fusion digestion of sediment as well as 8 M nitric acid. Neither technique works well for

Hanford vadose zone sediment. The total fusion dilutes the acid-extract solution too much to get useful data for most trace metals and based on the x-ray fluorescence analyses, the 8 M nitric acid extraction dissolves only a few percent to at best 50% of various major constituents.

The 8 M nitric acid extraction is a protocol used by the U.S. Environmental Protection Agency to estimate the maximum concentrations of regulated metals in contaminated sediment that would be biologically available. We subjected aliquots of contaminated sediment from the 299-E33-46 borehole to the acid extraction to search for obvious signs of elevated concentrations of elements from leaked tank fluids.

Both tables include the range for acid extractable sediments from the background or clean borehole (299-E33-338) just east of the B tank farm fence line for the same lithologies. It would appear that the major cation data in Table 4.17 shows that borehole 299-E33-46 contains elevated concentrations of acid extractable sodium between 16 and 21 m (53 and 69.5 ft) bgs. Aside from sodium there does not appear to be elevated concentrations of acid extractable major or RCRA metals although the arsenic data in Table 4.18 does appear to show elevated levels in the 299-E33-46 borehole. However, the measurement of arsenic by ICP-MS in difficult matrices such as 8 M nitric acid is fraught with difficulty. We do not believe that the differences in the clean and contaminated boreholes' acid extractable arsenic is meaningful because often the mass spectrometer shows sporadic mass interferences for arsenic isotopes that we have not resolved.

In general, the percentages of the common cations and RCRA metals that was water extractable versus acid extractable are quite low, similar to natural sediments that do not contain large amounts of waste. For the slant borehole sediments under SX-108 tank, greater than 80% of the sodium that was acid extractable was also water extractable showing the large mass of sodium that leaked from the SX-108 tank (see Serne et al. 2002c for more details). No dramatic water leachable versus acid extractable percentages were observed for the sediments from 299-E33-46 because the composition of the fluids that leaked into the sediments was not as highly concentrated as the solutions that leaked at the SX tank farm.

Table 4.17. Acid-Extractable Major Element Content of the Vadose Sediment from 299-E33-46 Borehole. (4 Pages)

ID	Depth (ft bgs)⁽¹⁾	Calcium (µg/g)	Magnesium (µg/g)	Sodium (µg/g)	Potassium (µg/g)	Strontium (µg/g)	Barium (µg/g)	Aluminum (µg/g)	Silicon (µg/g)	Iron (µg/g)
<i>Backfill</i>										
02A	12.94	7981	4509	509	1125	32	74.4	8.24E+03	16.3	1.86E+04
10A	29.42	7164	4429	672	1041	37	120.5	8.78E+03	12.8	2.11E+04
<i>Hanford H2 Sand (upper sequence) Unit</i>										
16A	41.72	9346	5329	397	1292	35	88.2	8.68E+03	10.4	1.83E+04
17A	44.02	8981	4939	335	1165	34	64.8	7.82E+03	27.4	1.69E+04
18A	46.42	8964	5212	264	1113	30	60.4	7.50E+03	16.0	1.68E+04
20A	50.62	9133	5218	411	1199	28	54.9	7.62E+03	19.1	1.63E+04
21C	52.02	7639	4149	504	1169	28	55.1	5.84E+03	79.1	1.31E+04
21A	53.02	8123	4778	691 ^a	1241	28	70.8	7.33E+03	33.8	1.58E+04
21A Dup	53.44	8421	4803	767 ^a	1451	30	75.6	7.83E+03	31.5	1.69E+04
22	54.60	7737	4532	895 ^a	1311	27	70.1	6.48E+03	56.5	1.45E+04
22 Dup	54.60	8328	4647	1002 ^a	1381	29	54.1	7.04E+03	53.5	1.52E+04
24	56.70	6680	4087	1147 ^a	1335	25	54.7	5.97E+03	108.2	1.38E+04
25	58.40	8949	4143	848 ^a	1188	31	64.8	6.16E+03	59.1	1.35E+04
26C	59.72	7184	4432	901 ^a	1288	24	51.7	6.43E+03	40.3	1.40E+04
26C Dup	59.72	7621	4696	827 ^a	1232	25	59.4	6.56E+03	43.8	1.43E+04
26A	60.72	6789	3997	791 ^a	1043	20	55.2	6.41E+03	50.4	1.43E+04
27	62.10	8256	5063	961 ^a	1126	24	56.0	6.45E+03	34.1	1.42E+04
29	66.05	8168	4736	777 ^a	1148	28	62.3	6.86E+03	29.3	1.65E+04
29 Dup	66.05	8466	4973	751 ^a	1247	29	62.7	7.19E+03	27.6	1.66E+04

Table 4.17. Acid-Extractable Major Element Content of the Vadose Sediment from 299-E33-46 Borehole. (4 Pages)

ID	Depth (ft bgs) ⁽¹⁾	Calcium (µg/g)	Magnesium (µg/g)	Sodium (µg/g)	Potassium (µg/g)	Strontium (µg/g)	Barium (µg/g)	Aluminum (µg/g)	Silicon (µg/g)	Iron (µg/g)
31C	69.45	8652	4910	600 ^a	1336	32	66.1	7.45E+03	43.3	1.55E+04
31B	69.95	8031	5244	533	1551	33	59.4	7.96E+03	56.4	1.47E+04
31A	70.45	8048	5258	494	1437	30	63.8	8.37E+03	26.2	1.58E+04
31A Dup	70.45	8322	5461	531	1517	33	58.8	8.35E+03	20.8	1.56E+04
33	73.50	8584	5551	543	1414	33	58.9	7.79E+03	56.5	1.59E+04
35	77.35	8270	5441	573	1743	38	76.3	8.66E+03	37.2	1.52E+04
36C	79.45	7581	4962	488	1529	33	65.8	7.56E+03	92.8	1.39E+04
36A	79.95	7737	5437	516	1628	36	76.1	8.89E+03	13.6	1.58E+04
38C	82.05	7140	4956	488	1516	33	70.6	7.46E+03	94.3	1.43E+04
38C Dup	82.05	7968	5394	582	1684	38	76.6	8.57E+03	43.8	1.54E+04
38A	83.05	7981	5429	558	1709	35	84.8	9.05E+03	20.4	1.61E+04
Background	low	7700 to	4600	270	1100	30	62.0	7.10E+03	88.0	1.40E+04
	high	8200	4700	290	1300	34	71.0	7.70E+03	89.0	1.60E+04
<i>Thin Fine Grained Lens</i>										
39	84.55	9121	6070	457	2323	40	105.7	1.02E+04	62.8	1.86E+04
<i>Hanford H2 Sand (middle sequence) Unit</i>										
41	87.85	7351	4507	386	1073	31	66.3	6.97E+03	93.6	1.47E+04
42A	90.62	7772	5000	351	1186	32	71.3	8.13E+03	27.5	1.61E+04
46	96.80	7295	5173	460	1049	29	60.9	6.78E+03	67.6	1.44E+04
47A	98.62	8013	5120	473	1107	29	66.0	7.62E+03	42.1	1.66E+04
52	109.00	7310	4857	448	1134	30	60.7	6.47E+03	107.3	1.39E+04
53A	111.42	7496	5324	637 ^a	1204	36	67.2	8.38E+03	50.9	1.54E+04

Table 4.17. Acid-Extractable Major Element Content of the Vadose Sediment from 299-E33-46 Borehole. (4 Pages)

ID	Depth (ft bgs) ⁽¹⁾	Calcium (µg/g)	Magnesium (µg/g)	Sodium (µg/g)	Potassium (µg/g)	Strontium (µg/g)	Barium (µg/g)	Aluminum (µg/g)	Silicon (µg/g)	Iron (µg/g)
57A	119.92	6460	4464	296	965	27	58.5	6.54E+03	106.8	1.30E+04
64A	131.85	7935	5014	321	1188	38	63.1	8.19E+03	32.2	1.60E+04
69A	140.05	6526	4241	235	1011	30	61.0	6.74E+03	106.6	1.34E+04
74A	150.15	7048	5234	281	1165	35	59.5	7.85E+03	43.8	1.43E+04
79A	160.15	6178	4714	238	1036	27	62.1	6.85E+03	40.2	1.33E+04
82A	164.55	6325	4877	222	1033	30	62.6	6.93E+03	42.3	1.30E+04
83A	166.85	6281	4898	233	1075	30	53.9	7.22E+03	31.0	1.33E+04
Background	low	6800	4660	250	1040	26	55.0	6.60E+03	46.0	1.30E+04
	high	7600	4800	340	1290	36	73.0	7.90E+03	126.0	1.70E+04
<i>Fine Grained Lens</i>										
84	168.45	9174	5860	395	1488	41	77.5	9.13E+03	31.8	1.69E+04
<i>Hanford H2 Sand Unit</i>										
86A	171.15	7486	4822	257	1215	33	75.9	7.65E+03	34.2	1.59E+04
Background	low	9200	5400	310	1400	42	67	9.00E+03	18	1.60E+04
	high	15600	9400	440	2800	65	162.0	1.70E+04	108.0	2.70E+04
<i>Hanford H3 Sand Unit</i>										
90A	179.85	6772	4325	317	1235	33	73.4	7.54E+03	26.2	1.63E+04
96A	190.80	6262	4595	255	995	32	62.3	7.10E+03	27.2	1.48E+04
101A	200.95	6503	4468	242	973	29	58.2	7.06E+03	35.2	1.48E+04
105A	209.95	6490	4304	318	936	32	66.0	7.54E+03	16.7	1.71E+04
Background	low	6200	4000	320	930	29	67.0	6.50E+03	18.0	1.60E+04
	high	6400	4400	340	980	31	162.0	6.70E+03	108.0	2.70E+04

Table 4.17. Acid-Extractable Major Element Content of the Vadose Sediment from 299-E33-46 Borehole. (4 Pages)

ID	Depth (ft bgs)⁽¹⁾	Calcium (µg/g)	Magnesium (µg/g)	Sodium (µg/g)	Potassium (µg/g)	Strontium (µg/g)	Barium (µg/g)	Aluminum (µg/g)	Silicon (µg/g)	Iron (µg/g)
<i>Plio-pliestocene Mud Unit</i>										
109A	219.45	7628	5509	245	1441	39	74.6	8.93E+03	14.6	1.48E+04
110A	222.05	11434	8035	298	2934	52	140.5	2.17E+04	8.6	2.87E+04
110A Dup	222.05	10619	7660	289	2832	51	139.0	2.07E+04	8.9	2.67E+04
113	225.90	10535	6291	420	1799	48	99.7	1.10E+04	15.5	1.90E+04
Background	low	6900	4900	270	1200	34	60.0	7.60E+03	77.0	1.30E+04
	high	13600	9300	410	2600	64	132.0	2.25E+04	290.0	3.90E+04
<i>Plio-pliestocene Gravel Unit</i>										
115A	230.75	5991	3852	327	1007	29	71.2	6.92E+03	18.9	1.67E+04
120B	240.95	6166	4125	516	893	32	70.5	7.17E+03	13.6	1.71E+04
120A	241.45	4251	2766	347	725	22	64.6	5.03E+03	25.3	1.20E+04
123A	245.75	2485	1700	230	471	16	55.1	3.56E+03	17.4	7.65E+03
127A	253.15	3773	2654	321	737	20	74.2	4.94E+03	18.8	1.21E+04
Background	low	5600	3600	370	980	39	77	6.00E+03	105	1.30E+04
	high									

⁽¹⁾ to convert to meters multiply by 0.3048

^a Values indicate contamination

Background low and high range values are for samples from same lithologies from clean borehole 299-E33-338.

Table 4.18. Acid-Extractable RCRA Metal Content of the Vadose Sediment from 299-E33-46 Borehole. (3 Pages)

ID	Depth ft bgs	Arsenic (µg/g)	Selenium (µg/g)	Silver (µg/g)	Cadium (µg/g)	Lead (µg/g)	Chromium (µg/g)
<i>Backfill</i>							
02A	12.94	2.22	(7.03E-02)	0.03	0.07	3.38	8.6
10A	29.42	1.24	(4.88E-02)	0.02	0.05	2.64	13.2
<i>Hanford H2 Sand (upper sequence) Unit</i>							
16A	41.72	2.96	(3.57E-02)	0.03	0.06	3.91	11.6
17A	44.02	2.21	<2.20E-01	0.03	0.05	3.64	8.9
18A	46.42	3.82	(3.27E-02)	0.04	0.07	4.66	11.2
20A	50.62	3.00	(4.20E-02)	0.04	0.06	3.51	10.7
21C	52.02						7.9
21A	53.02	2.24	(3.93E-02)	0.03	0.05	3.71	9.5
21A Dup	53.44	2.72	(3.15E-02)	0.03	0.07	3.10	10.3
22	54.60						9.6
22 Dup	54.60						9.6
24	56.70						7.6
25	58.40						8.7
26C	59.72						9.5
26C Dup	59.72						11.8
26A	60.72	2.70	(5.11E-02)	0.04	0.06	3.91	7.6
27	62.10						9.4
29	66.05						9.9
29 Dup	66.05						11.4
31C	69.45						11.5
31B	69.95						15.5
31A	70.45	4.62 ^a	(5.91E-02)	0.04	0.08	4.82	14.7
31A Dup	70.45	3.69 ^a	(1.26E-02)	0.04	0.07	4.08	14.1
33	73.50						15.3
35	77.35						16.2
36C	79.45						13.2
36A	79.95	3.71 ^a	(2.49E-02)	0.04	0.07	3.69	15.4
38C	82.05						14.1

Table 4.18. Acid-Extractable RCRA Metal Content of the Vadose Sediment from 299-E33-46 Borehole. (3 Pages)

ID	Depth ft bgs	Arsenic (µg/g)	Selenium (µg/g)	Silver (µg/g)	Cadium (µg/g)	Lead (µg/g)	Chromium (µg/g)
38C Dup	82.05						16.7
38A	83.05	3.93 ^a	(9.61E-03)	0.04	0.08	4.20	15.9
Background	low	0.80	0.05	0.025	0.06	2.30	6.40
	high	1.00	0.06	0.028	0.07	2.90	7.70
<i>Thin Fine Grained Lens</i>							
39	84.55						18.2
<i>Hanford H2 Sand (middle sequence) Unit</i>							
41	87.85						11.3
42A	90.62	2.67	(1.47E-02)	0.03	0.06	3.23	11.1
46	96.80						14.0
47A	98.62	3.03	(1.30E-02)	0.04	0.06	3.43	11.1
52	109.00						11.2
53A	111.42	2.57	<2.00E-01	0.03	0.05	3.58	11.4
57A	119.92	2.35	(5.38E-03)	0.03	0.05	2.59	10.9
64A	131.85	2.47	(6.26E-03)	0.03	0.06	2.61	13.6
69A	140.05	2.07	<2.24E-01	0.03	0.06	2.92	10.2
74A	150.15	2.73	(1.35E-03)	0.03	0.07	3.02	14.1
79A	160.15	2.35	(9.19E-03)	0.04	0.06	2.67	12.1
82A	164.55	2.55	<2.30E-01	0.08	0.06	2.94	12.4
83A	166.85	2.43	<2.25E-01	0.04	0.06	2.81	13.2
Background	low	0.90	0.04	0.03	0.06	2.50	12.00
	high	1.26	0.08	0.04	0.10	4.00	14.50
<i>Fine Grained Lens</i>							
84	168.45						18.0
<i>Hanford H2 Sand Unit</i>							
86A	171.15	2.81	(4.73E-02)	0.04	0.06	3.61	11.0
Background	low	1.20	0.05	0.04	0.09	3.60	17.0
	high	2.70	0.06	0.08	0.23	7.00	36.0
<i>Hanford H3 Sand Unit</i>							
90A	179.85	2.40	(2.54E-02)	0.03	0.07	2.91	8.5

Table 4.18. Acid-Extractable RCRA Metal Content of the Vadose Sediment from 299-E33-46 Borehole. (3 Pages)

ID	Depth ft bgs	Arsenic (µg/g)	Selenium (µg/g)	Silver (µg/g)	Cadium (µg/g)	Lead (µg/g)	Chromium (µg/g)
96A	190.80	2.21	<2.13E-01	0.03	0.06	2.99	10.9
101A	200.95	2.12	(4.02E-02)	0.03	0.05	2.91	10.7
105A	209.95	2.25	(2.19E-02)	0.03	0.07	12.32	10.7
Background	low	0.70	0.05	0.02	0.07	2.10	9.0
	high	0.80	0.08	0.03	0.08	2.50	11.0
<i>Plio-pliestocene Mud Unit</i>							
109A	219.45	2.93	(1.34E-02)	0.03	0.07	3.08	18.2
110A	222.05	6.08	<2.09E-01	0.10	0.24	13.38	28.4
110A Dup	222.05	5.40	<2.06E-01	0.09	0.22	12.59	26.5
113	225.90						20.9
Background	low	1.30	0.05	0.03	0.08	2.80	9.0
	high	5.90	0.10	0.12	0.27	21.00	11.0
<i>Plio-pliestocene Gravel Unit</i>							
115A	230.75	1.97	(1.86E-02)	0.03	0.05	4.88	8.6
120B	240.95						11.5
120A	241.45	1.10	(1.52E-02)	0.03	0.05	21.40	5.6
123A	245.75	0.66	(2.53E-02)	0.02	0.03	2.34	2.4
127A	253.15	1.09	(1.36E-02)	0.03	0.05	20.42	6.3
Background	low	0.496	0.066	0.032	0.058	2.325	7.29
	high						

⁽¹⁾ to convert to meters multiply by 0.3048

^a Zones with elevated concentrations in comparison with the nearby uncontaminated sediment (uncontaminated ranges shown for same lithologies in samples from borehole 299-E33-338.

() Values in parentheses are below quantification limit but above the detection limit and thus considered useful.

Blank spaces denote no analyses performed for these samples

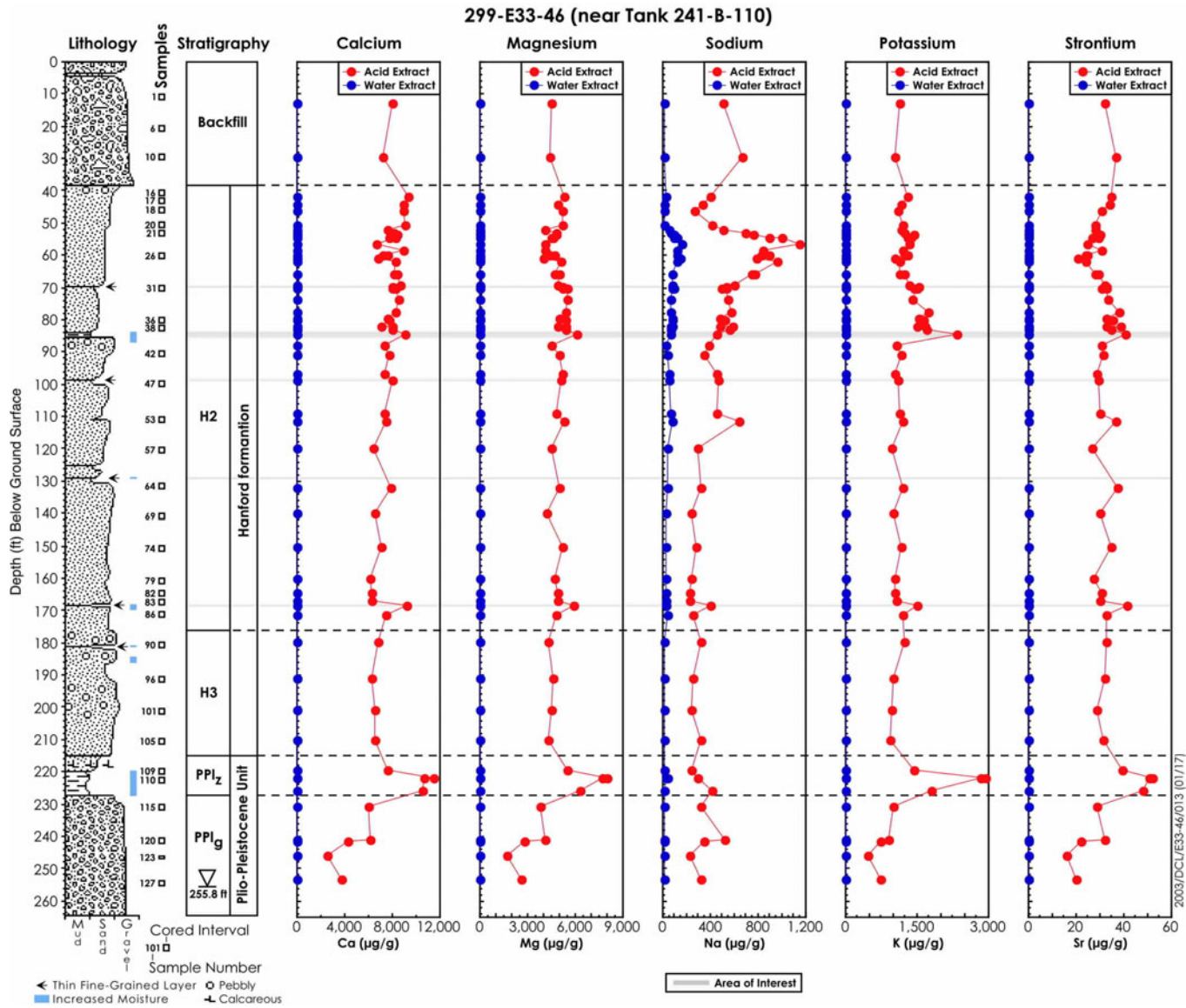


Figure 4.15. Comparison Between Acid and Water Extractable Concentrations of Major Cations

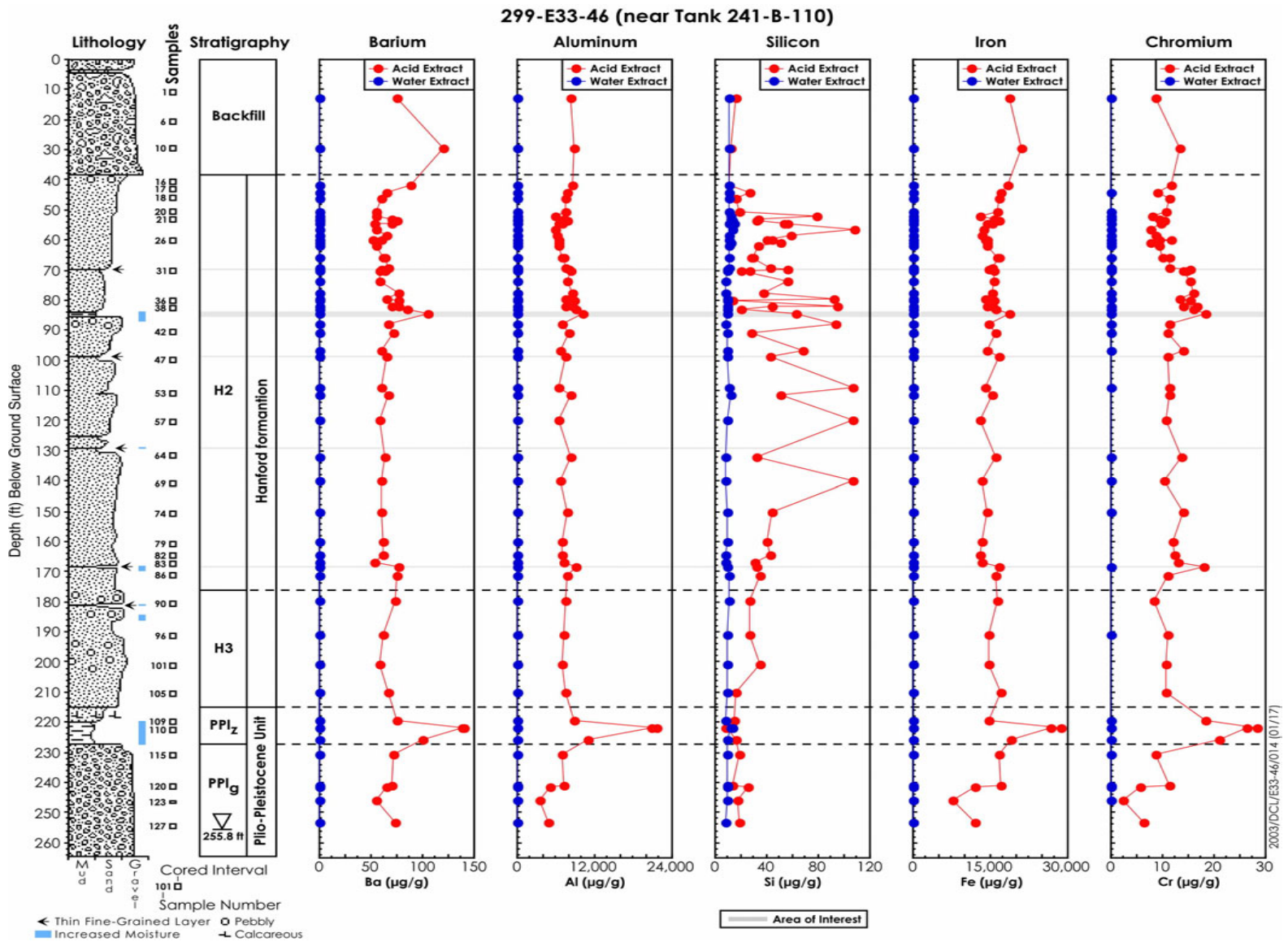


Figure 4.16. Comparison Between Acid and Water Extractable Concentrations of Ba, Al, Si, and Fe

4.6 Sediment Total Oxide Composition

Eleven samples of the bulk vadose zone sediment from the 299-E33-46 borehole were crushed and analyzed with x-ray fluorescence to obtain the complete composition of the sediment. Additional aliquots of the same eleven samples were subjected to particle size analysis and the clay separates were retained. The total oxide composition of the bulk sediments was used to aid in the quantification of mineralogy that will be discussed later.

The total elemental oxide composition for the bulk sediment is shown in Table 4.19. Using two types of x-ray fluorescence instruments, we were able to analyze for all natural elements from sodium through uranium. We lack the capability for measuring the concentrations of only carbon, beryllium, boron, fluorine, lithium, and nitrogen. However, the carbon content of the bulk sediment was analyzed, as discussed in Section 4.4, so data for that component is available. The beryllium, boron, fluorine, and lithium content of the sediment likely is small; therefore, the oxide mass of the sediment should be able to be calculated and come close to 100% mass balance. We have assumed that the iron present in the sediment is all iron (III) oxide though there may be some reduced (ferrous oxides) iron also present.

The mass balances for the bulk sediment vary from 90.3 to 99.3 % by weight. The low mass balances for samples in the PPlz mud unit appear to be caused by low silica values and perhaps low alumina values. The same low mass balances were found in the analyses of the sediments from the PPlz unit at the contaminated borehole (299-E33-45) east of tank BX-102. We suspect that there is a matrix correction that has not been optimized for the mineralogy in this lithology that is causing us to under predict the silica content. As found for uncontaminated sediment from outside other tank farms, the Hanford formation sediment is dominated by silica and alumina. Calcium, carbonate, iron, magnesium, potassium, sodium, and titanium make up most of the rest of the oxides. We do not have a large database of total elemental compositions but when compared to the two clean RCRA boreholes near SX Tank Farm (see Serne et al. 2002a), and the clean borehole east of the B Tank Farm (see Lindenmeier et al. 2002), the contaminated sediment at 299-E33-46 does not show significantly higher contents of any element. The total elemental composition of uncontaminated sediments from the clean borehole east of the B Tank Farm, 299-E33-338 and presented in Lindenmeier et al. (2002), was determined using total fusion and ICP and ICP-MS by an outside analytical vendor as compared to the XRF analyses performed on the contaminated sediments such that direct comparison is not easy. For the major constituents, the XRF data for silica in the PPlz unit presented in Table 4.19 does appear to be low by approximately 5 wt % based on data from the clean borehole.

For some trace constituents such as tin, antimony, and cesium the XRF results shown in Table 4.20 are higher by a factor of ten than values for comparable samples from the clean borehole (see Lindenmeier et al. 2002). We do not believe that the higher values for some trace metals in the contaminated sediments from borehole 299-E33-46 reflect contamination. It is much more probable that the observed differences reflect the two totally independent analytical methods used to obtain the data.

Table 4.19. Total Composition of the Vadose Zone Sediment from 299-E33-46 Percent Weight as Oxides

ID	16A	26A	31B	42A	74A	84	96A	109A	110A	113	120B
Depth (ft)⁽¹⁾	41.72	60.72	69.95	90.62	150.15	168.45	190.8	219.45	222.05	225.9	240.95
Unit	H2 upper	H2 upper	H2 upper	H2 middle	H2 middle	thin silt	H3	PPlz	PPlz	PPlz	PPlg
CO ₂	0.66	0.29	0.55	0.51	0.48	0.48	0.40	0.46	0.99	0.81	0.29
Na ₂ O	2.23	2.37	1.98	2.53	2.65	2.73	2.52	2.15	1.06	1.67	2.20
MgO	1.00	1.15	1.16	1.25	1.43	1.27	1.05	1.72	1.32	1.96	1.19
Al ₂ O ₃	11.80	12.28	11.76	12.00	12.61	12.98	11.67	12.79	13.91	12.06	10.94
SiO ₂	69.96	70.38	65.68	68.67	71.03	70.38	66.96	66.32	60.54	60.97	64.61
P ₂ O ₅	<0.275	<0.275	<0.275	<0.275	<0.275	<0.275	<0.298	<0.298	<0.275	<0.451	<0.298
SO ₃	<0.062	<0.070	<0.080	<0.085	<0.085	<0.080	<0.085	<0.087	<0.080	<0.082	<0.090
Cl	<0.012	<0.013	<0.013	<0.012	<0.013	<0.012	<0.012	<0.013	<0.013	<0.012	<0.013
K ₂ O	2.25	2.36	2.42	2.19	2.25	2.17	1.92	2.09	2.28	1.86	1.61
CaO	3.68	3.53	3.12	3.54	3.51	3.50	3.96	3.47	2.88	3.97	4.11
TiO ₂	0.70	0.66	0.60	0.69	0.63	0.64	0.80	0.63	0.87	0.80	0.98
V ₂ O ₅	0.011	0.006	0.006	<0.006	<0.006	0.006	0.012	0.009	0.011	0.011	0.018
Cr ₂ O ₃	0.004	0.005	0.006	0.006	0.008	0.009	0.006	0.010	0.010	0.008	0.006
MnO	0.063	0.058	0.058	0.069	0.072	0.067	0.073	0.067	0.070	0.099	0.095
Fe ₂ O ₃	4.09	3.92	3.39	4.39	4.12	4.03	4.89	3.85	5.89	5.35	6.21
CoO	<0.006	0.009	<0.005	<0.006	0.006	<0.006	0.009	0.006	<0.006	<0.006	0.010
NiO	0.001	0.002	0.003	0.003	0.003	0.003	0.003	0.004	0.005	0.004	0.002
CuO	0.002	0.002	0.002	0.002	0.002	0.002	0.002	0.002	0.004	0.003	0.002

Table 4.19. Total Composition of the Vadose Zone Sediment from 299-E33-46 Percent Weight as Oxides

ID	16A	26A	31B	42A	74A	84	96A	109A	110A	113	120B
Depth (ft)⁽¹⁾	41.72	60.72	69.95	90.62	150.15	168.45	190.8	219.45	222.05	225.9	240.95
Unit	H2 upper	H2 upper	H2 upper	H2 middle	H2 middle	thin silt	H3	PPlz	PPlz	PPlz	PPlg
ZnO	0.007	0.006	0.005	0.006	0.006	0.006	0.006	0.006	0.011	0.008	0.008
Rb ₂ O	0.009	0.009	0.009	0.008	0.007	0.008	0.007	0.007	0.011	0.007	0.005
SrO	0.049	0.042	0.047	0.049	0.053	0.054	0.055	0.057	0.037	0.049	0.045
YO ₂	0.003	0.002	0.002	0.002	0.002	0.003	0.002	0.002	0.004	0.003	0.003
ZrO ₂	0.019	0.015	0.014	0.015	0.011	0.015	0.012	0.014	0.029	0.022	0.015
BaO	0.093	0.086	0.090	0.094	0.088	0.088	0.096	0.087	0.084	0.090	0.080
ThO ₂	<0.001	<0.001	<0.001	0.001	0.001	0.001	0.001	<0.001	0.001	0.001	0.001
UO ₃	0.004	0.002	0.002	0.002	0.001	0.001	0.001	<0.001	0.003	<0.001	<0.001
Total	96.99	97.54	91.28	96.41	99.34	98.82	94.85	94.14	90.40	90.31	92.83

⁽¹⁾ to convert to meters multiply by 0.3048

Table 4.20. Total Trace Constituents in Vadose Zone Sediment from 299-E33-46 in µg/g (ppm)

ID	16A	26A	31B	42A	74A	84	96A	109A	110A	113	120B
Depth (ft)⁽¹⁾	41.72	60.72	69.95	90.62	150.15	168.45	190.8	219.45	222.05	225.9	240.95
Unit	H2 upper	H2 upper	H2 upper	H2 middle	H2 middle	thin silt	H3	PPlz	PPlz	PPlz	PPlg
Ga	14.5	15.2	12.9	15.9	13	15.1	13.2	16	19	16.5	14.7
As	5.4	5.1	4.6	<2.5	4.8	5.8	<2.3	4.6	9.6	7.4	3.8
Se	1.7	<1.6	<1.6	<1.6	1.7	<1.7	<1.6	<1.6	<1.7	<1.7	<1.7
Br	<1.3	<1.3	<1.2	<1.3	<1.3	<1.3	<1.1	<1.1	<1.3	<1.3	<1.3
Nb	7.3	6.9	6.3	7.5	6.6	6.3	5.8	6.8	14.4	12.03	6.08
Mo	<1.9	<1.5	<1.5	1.7	1.5	1.7	1.5	<1.4	2.34	<1.8	<1.4
Ru	14	<9.9	<10	10	9.1	12	10	<8.4	<9.7	<11	<7.9
Rh	<14	<11	<11	11	10	13	11	<8.6	<10	<12	<8.1
Pd	<15	<11	<12	12	11	13	11	<9.9	<11	<12	<8.9
Ag	17	<13	<13	13	12	15	12	<10	<12	<13	<10
Cd	<19	<14	<15	14	13	17	14	<11	<14	<15	<11
In	<21	<16	<16	17	14	19	16	<13	<16	<17	<13
Sn	<23	<18	<18	18	16	21	17	<15	<17	<18	<14
Sb	<25	<19	<19	20	19	23	20	<17	<19	<20	<16
Te	<30	<22	<23	21	19	26	20	<17	<23	<22	<16
I	<37	<24	<27	29	23	33	27	<20	<27	<30	<20
Cs	<42	<35	<34	36	33	42	35	<28	35	<37	<27
La	<51	<38	<38	38	37	46	40	<33	<39	<39	<33
Ce	<67	<57	<60	62	60	75	57	<48	81	<66	<47

Table 4.20. Total Trace Constituents in Vadose Zone Sediment from 299-E33-46 in µg/g (ppm)

ID	16A	26A	31B	42A	74A	84	96A	109A	110A	113	120B
Depth (ft)⁽¹⁾	41.72	60.72	69.95	90.62	150.15	168.45	190.8	219.45	222.05	225.9	240.95
Unit	H2 upper	H2 upper	H2 upper	H2 middle	H2 middle	thin silt	H3	PPlz	PPlz	PPlz	PPlg
Hg	<3.7	<3.6	<3.5	<3.7	<3.8	4.9	<3.8	<3.6	<3.7	<3.8	<3.9
Pb	8.9	9.7	14.7	12.5	9.5	7.9	13.7	9	22.1	11.4	12.2

⁽¹⁾ to convert to meters multiply by 0.3048

4.7 Particle Size Measurements on Vadose Zone Sediment

The hydrometer method was used to determine the particle size distributions of several samples from 299-E33-46 as shown in Table 4.21. No wet sieving was done to separate the gravel and sand fractions from each other so the particle size data shows only combined gravel + sand, silt, and clay fractions. The thin fine-grained lenses and Plio-Pleistocene silts are highlighted in yellow shading in the table. One sample at the very top of the Plio-Pleistocene silt (sample 109A) does not contain very much silt and clay even though it is assigned to the silt layer. The same situation was found at borehole 299-E33-45 such that we conclude that the uppermost portion of the PPlz unit is in fact coarser grained than the middle and deepest portions.

Besides the hydrometer estimate of clay-size particles, we physically separated the clay material from the silt by performing numerous re-suspensions of the slurry and decanting off the clays after the silts had settled. The mineralogical characterization of this clay fraction is described below in section 4.9.

4.8 Particle Density of Bulk Sediment

The particle density for each of the 299-E33-46 borehole samples that were used in the hydrometer procedure is shown in Table 4.22. The values are similar to those for uncontaminated sediment from the same lithologic facies found in 200W (see Serne et al. 2002a) and in general are about 0.05 to 0.10 g/cm³ higher than values measured for the uncontaminated sediments from borehole 299-E33-338 located east of the B Tank Farm. The differences in particle density between the sediment samples from this contaminated and the uncontaminated borehole are likely caused by analyst's artifacts. Differences on the order of 0.1 g/cm³ have been found on identical samples that were analyzed by three different lab staff during the characterization of the SX Tank Farm vadose zone sediments. There does not appear to be any statistically significant differences in the particle densities for the 299-E33-46 or for that matter 299-E33-338 clean or background sediments versus lithologic unit. The average value for all the Hanford formation sediments for boreholes 299-E33-46 and 299-E33-338 is 2.76 ± 0.14 g/cm³ similar to the value 2.78 g/cm³ often used for generic Hanford formation sediments. The average particle density for the Plio-pleistocene sediments from the two boreholes is 2.78 ± 0.07 g/cm³.

4.9 Mineralogy

XRD analysis of the 11-bulk sediment samples from borehole 299-E33-46 shows the samples to all have a similar mineralogical signature. XRD analysis the sediment shows the samples collected from the Hanford formation (16A, 26A, 31B, 42A, 74A, and 84A) appear to be mineralogically similar. The sediments are mostly quartz and feldspar (both plagioclase and alkali-feldspar), with trace amounts of mica, chlorite, and an amphibole. Samples examined from the lower Hanford unit (H3) along with samples from the PPlz and PPlg unit all contain quartz and feldspars, along with significant amounts of clay material, predominantly mica and chlorite. For example, the XRD tracing of a typical sediment sample (110A) from the PPlz unit is provided in Figure 4.17, along with a quartz reference pattern. The main reflection for quartz is $26.63^\circ 2\theta$, followed by less intense reflections at 20.86 , 36.53 , 39.46 , 42.43 , 50.12 , $59.92^\circ 2\theta$. The main reflections associated with feldspar minerals are found between $27.34^\circ 2\theta$ and $27.92^\circ 2\theta$, with the higher 2θ values belonging to the plagioclase series. Chlorite and mica minerals were identified on the x-ray tracings by the reflections at $6.3^\circ 2\theta$ and $8.8^\circ 2\theta$, respectively. The presence

of an amphibole was established by the characteristic 100% reflection at $10.5^\circ 2\theta$. Additionally, trace amounts of the zeolite, laumontite, were identified in most of the samples by a diffraction peak positioned at $9.36^\circ 2\theta$.

One interesting observation was noted on samples 96A and 109A. The XRD tracings from these two samples indicate an unusually high concentration of the amphibole mineral (hornblende) compared to all the other samples. Hornblende is typically found in most Hanford sediments, but only as trace amounts.

Table 4.21. Particle Size Distribution Percent Weight

ID	Depth (ft bgs) ⁽¹⁾	% Gravel plus %Sand	%Silt	%Clay
<i>Backfill</i>				
No Sample Analyzed				
<i>Hanford H2 Sand (upper sequence) Unit</i>				
16A	41.72	95.90	2.60	1.50
26A	60.72	96.16	1.92	1.92
31B	69.95	96.10	2.96	0.94
<i>Thin Fine Grained Lens</i>				
No Sample Analyzed				
<i>Hanford H2 Sand (middle sequence) Unit</i>				
42A	90.62	91.31	2.79	5.91
74A	150.15	91.43	5.83	2.74
<i>Fine Grained Lens</i>				
84	168.45	68.06 ^a	28.85 ^a	3.08 ^a
<i>Hanford H3 Sand Unit</i>				
96A	190.8	96.54	2.21	1.25
<i>Plio-pliestocene Mud Unit</i>				
109A	219.45	89.48	8.97	1.55
110A	222.05	7.00 ^a	85.73 ^a	7.27 ^a
113	225.9	53.74 ^a	39.82 ^a	6.44 ^a
<i>Plio-pliestocene Gravel Unit</i>				
120B	240.95	87.44	9.81	2.76

⁽¹⁾ to convert to meters multiply by 0.3048

^a Fine grained samples

Table 4.22. Particle Density of Bulk Sediment from 299-E33-46

ID	Depth (ft bgs)⁽¹⁾	Ave. Particle Density (g/cm³)	σ (g/cm³)
<i>Backfill</i>			
No Sample Analyzed			
<i>Hanford H2 Sand (upper sequence) Unit</i>			
16A	41.72	2.81	0.097
26A	60.72	2.65	0.028
31B	69.95	2.90	0.238
<i>Thin Fine Grained Lens</i>			
No Sample Analyzed			
<i>Hanford H2 Sand (middle sequence) Unit</i>			
42A	90.62	2.89	0.017
74A	150.15	2.91	0.047
<i>Fine Grained Lens</i>			
84	168.45	2.79	0.019
<i>Hanford H3 Sand Unit</i>			
96A	190.8	2.91	0.018
<i>Plio-pliestocene Mud Unit</i>			
109A	219.45	2.91	0.020
110A	222.05	2.82	0.024
113	225.9	2.71	0.061
<i>Plio-pliestocene Gravel Unit</i>			
120B	240.95	2.78	0.024

⁽¹⁾ to convert to meters multiply by 0.3048

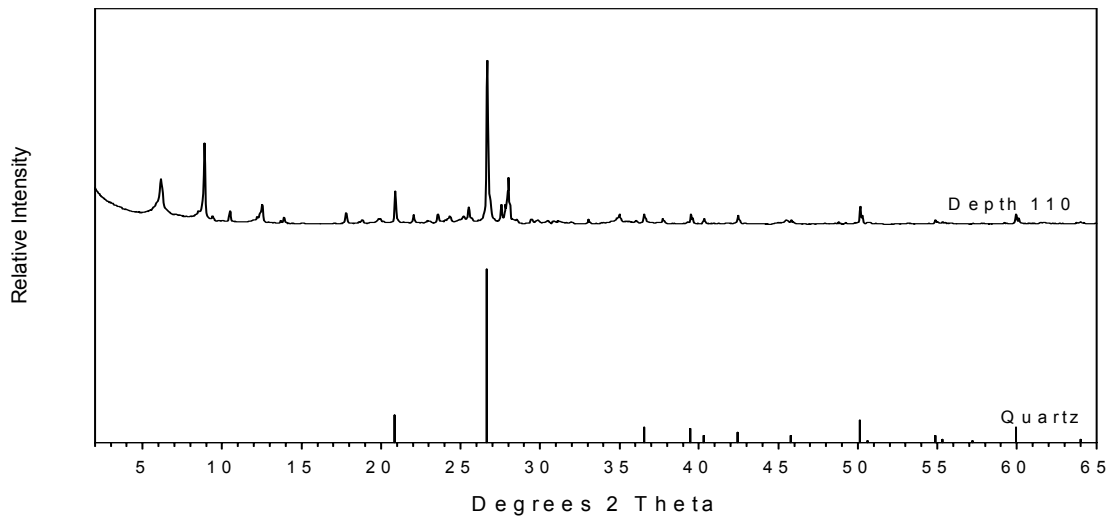


Figure 4.17. XRD Tracing of sample 110A along with the standard reference pattern for quartz.

Results from the semi quantification of the minerals in the bulk samples are provided in Table 4.23. Quartz concentrations ranged from 22.4 wt % (96A) to 43.5 wt % (31B), with an average concentration of 33 ± 6 wt %. The borehole sediment contained plagioclase feldspar concentrations from 10 to 34 wt % and potassium feldspar content measured between 8 to 37 wt-%. Plagioclase feldspar was more abundant than potassium feldspar in all but three samples (16A, 26A, and 84A). Over all, the feldspar content (both plagioclase and alkali feldspars) averaged about 43 ± 6 wt-%. The amphibole phase comprised <9 wt % at most, with the majority of samples having concentrations in the 2 to 4 wt % range.

Clay minerals identified in the whole rock sediment included mica and chlorite. Mica concentrations ranged from a low of 6.5 wt % (120B) to a high of 32 wt % (113A), with most of the intervals having concentrations between 7 and 15 wt %. Chlorite concentrations were <7 wt% in all sediments analyzed with the exception of two samples in the Plio-Pleistocene Mud Unit. Samples 109A and 110A contained 11.7 and 21.2 wt % chlorite, respectively. Smectite and kaolinite minerals were not identified in the whole rock sediment samples due in part to the sample preparation technique and the low overall concentration.

X-ray diffraction analysis was performed on the <2 micron fraction of each sample and the results are presented below. The clay fraction is dominated by four clay minerals: smectite, chlorite, illite, and kaolinite with minor amounts of quartz and feldspar. Figure 4.18 provides XRD-tracings of a typical clay fraction (from sample 110A) following four different treatments. Smectites are considered the fraction of the magnesium-saturated sub-sample that gives a basal reflection at $5.85^\circ 2\theta$ and expands to $5.28^\circ 2\theta$

upon solvation with ethylene glycol. Saturation with a potassium cation shifts the reflection down to $7.3^{\circ} 2\theta$ followed by the irreversible collapse to $8.88^{\circ} 2\theta$ after heating for one hour at 575°C .

Illite is the simplest of the four clay mineral phases to identify in this sediment. The basal reflections are located at 8.88 , 17.8 , and $26.7^{\circ} 2\theta$. The various treatments including cation saturation, solvation with ethylene glycol, and heating do not affect the structure of the illite. This is shown in Figure 4.18 by examination of the illite basal reflection at $8.88^{\circ} 2\theta$. The increase in intensity of the $8.88^{\circ} 2\theta$ reflection between the heated and the unheated potassium-saturated sample is due to the incorporation of the smectite reflection resulting from the smectite structure collapsing.

Table 4.23. Semi-quantitative XRD Results of Minerals from the S01052 Borehole.

Sample ID	Mineral Phase (wt-%)						Goodness of fit ¹
	Quartz	Amphibole	Plagioclase	K-Spar	Mica	Chlorite	
<i>Hanford H2 Sand (upper sequence) Unit</i>							
16A	34.8	1.0	12.7	36.6	10.4	4.5	0.57
26A	33.3	0.5	9.6	37.2	14.2	5.2	0.78
31B	43.5	2.8	27.4	13.2	9.1	4.0	0.46
<i>Hanford H2 Sand (middle sequence) Unit</i>							
42A	38.5	3.1	28.5	16.5	9.4	4.0	0.41
74A	39.6	2.0	23.0	20.2	11.8	3.5	0.71
<i>Fine Grained Lens</i>							
84A	34.5	2.9	19.5	29.1	8.5	5.6	0.81
<i>Hanford H3 Sand Unit</i>							
96A	22.4	4.0	29.1	12.3	27.0	5.2	0.22
<i>Plio-Pleistocene Mud Unit</i>							
109A	31.1	7.6	27.9	14.3	7.5	11.7	0.22
110A	26.5	4.7	14.1	18.8	14.6	21.2	0.30
113A	25.3	3.5	24.8	7.8	31.7	6.9	0.17
<i>Plio-Pleistocene Gravel Unit</i>							
120B	32.6	8.7	34.1	13.4	6.5	4.6	0.20

¹ Values closest to 1.0 represent an ideal refinement.

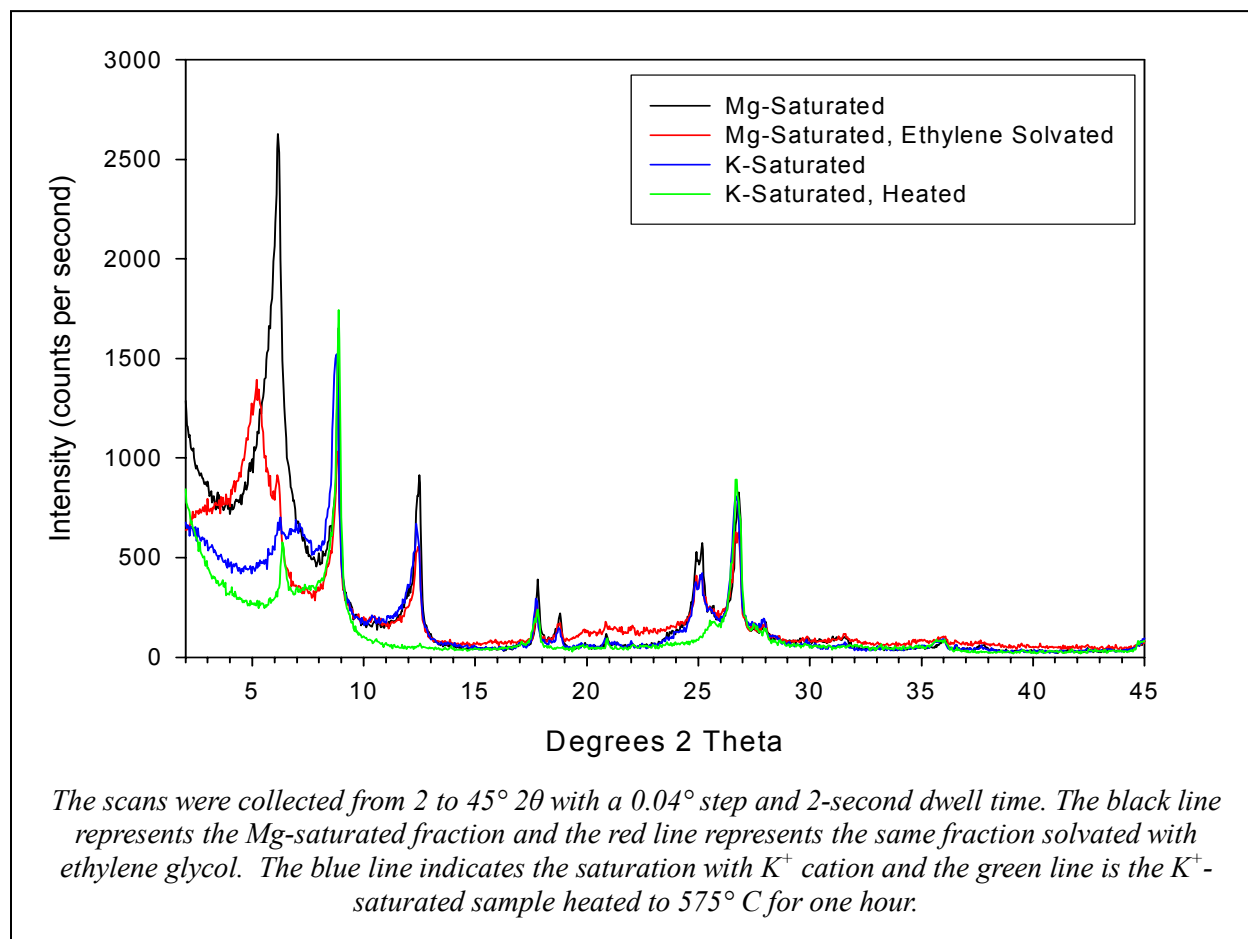


Figure 4.18. XRD tracings of preferentially oriented clay slides taken from Borehole 299-E33-46 sample 110A

Chlorites are identified by their basal series of diffraction peaks at 6.24, 12.5, 18.8, and 25.2° 2θ, which are unaffected by cation saturation or ethylene glycol solvation. Heating to 575°C shifts the first order reflection to 6.37° 2θ and also tends to diminish or eliminate the higher order reflections (12.5, 18.8, and 25.2° 2θ) as shown in Figure 4.18. Kaolinite is difficult to identify in the presence of a chlorite mineral. Basal reflections characteristic to kaolinite are positioned at 12.5 and 24.9° 2θ, which are superimposed on the even-order chlorite peaks. These kaolinite reflections are unaffected by cation saturation and ethylene glycol solvation. When heated the kaolinite structure becomes amorphous and the reflections are eliminated. Positive identification of kaolinite in the presence of chlorite can be determined by examination of the 24.9 to 25.2° 2θ region of the XRD tracing. The kaolinite basal reflection at 24.9° 2θ can be distinguished from the chlorite 25.2° 2θ reflection (Figure 4.18). Furthermore, published reports characterizing similar clay fractions of Hanford sediment identify kaolinite by electron microscopy.

Trace amounts of quartz are evident by the diffraction peak located at $20.85^\circ 2\theta$. The 100% reflection for quartz ($26.6^\circ 2\theta$) is hidden by the third basal reflection of illite located at $26.6^\circ 2\theta$. Plagioclase feldspar is also identified in the clay fraction by the minor diffraction peak at $27.8^\circ 2\theta$.

Semi-quantification results of the clay minerals in the < 2 micron fraction are presented in Table 4.24. Total recoveries were normalized to 100% and the normalization factor used for each sample is provided in the last column. Smectites ranged in concentrations from a low of 22 wt % (74A) to a high of 50 wt % (110A). Illite amounts varied from 30 to 56 wt % with the majority of samples having concentrations in the 40 to 50 wt % range. Chlorite and kaolinite were the least abundant of the clay minerals identified in the samples with concentrations equal to or less than 20 wt % and 9 wt %, respectively. Quartz and feldspar minerals were present as trace amounts in the clay fraction and therefore were not included in totals presented in Table 4.24.

Total clay recoveries were within $\pm 25\%$ of the “ideal” 100% for eight of the 11 samples analyzed. Factors affecting the semi-quantification procedure (preparation and condition of the clay filter cake) were generally controlled and not thought to be a significant factor. Quantitative analysis is considered good if errors amount to $\pm 10\%$ of the amounts present for major constituents and $\pm 20\%$ for minerals whose concentrations are less than 20% (Moore and Reynolds, 1997). Other x-ray diffractograms of the bulk sediment and clay fractions are presented in Appendix D.

Table 4.24. Semi-quantitative XRD Results of Clay Minerals Separated from the Sediment Collected from Borehole 299-E33-46

Sample ID	Mineral Phase (wt-%)				Normalization Factor
	Smectite	Illite	Chlorite	Kaolinite	
16A	30	48	12	9	0.87
26A	27	52	13	8	0.86
31B	23	56	12	9	0.67
42A	35	44	13	8	0.66
74A	22	53	18	8	1.01
84A	46	30	20	5	1.25
96A	32	44	16	9	1.10
109A	28	49	17	6	0.88
110A	50	38	6	6	0.75
113A	32	46	13	9	0.84
120B	39	40	15	6	2.26

4.10 Matric Suction Potential Measurements

Water-potential measurements have been included in the Hanford Tank Farm Vadose Zone Characterization Program to document the energy state of pore waters in the tank farm sediments. At the tank farms, vegetation is absent, surface soils are coarse-textured, and the potential for drainage (recharge) is high (Gee 1987; Gee et al. 1992). However, actual drainage rates are generally unknown. Attempts are currently being made to determine the soil water matrix potential and use the analysis to confirm the occurrence of recharge within the Hanford Site Tank Farms.

The status of soil water can be defined by either the amount of water in the soil (water content) or by the force that holds water in the soil matrix (i.e., the matric potential or suction) (Or and Wraith, 2002). In recent studies, Serne et al. (2002e) measured both gravimetric water content and matric water potential (filter paper method) on core samples obtained from borehole 299-E33-45 in the BX environs. The same filter paper technique was used at 299-E33-46 and 299-E33-338, within the B-BX-BY WMA. All core samples from 299-E33-46 from the surface to the water table were analyzed. A sandwich of three Whatman #42 filter papers was placed in the sediment, sealed, and equilibrated for at least 21 days. The water content of the middle filter paper (not allowed to collect sediment particles) was subsequently measured and the water potential obtained from a predetermined water-retention characteristic curve. The filter-paper method provides a good estimate of water potentials over the range from -0.01 to -2 MPa (1 to 200 m (3.3 to 656 ft) suction head) (Deka et al. 1995).

Table 4.25 and Figure 4.19 show the matric potentials as a function of depth for the 299-E33-46 samples. Also plotted in Figure 4.19 is the gravity head expressed in pressure units (MPa). The gravity head is zero at the water table and increases linearly with height to the soil surface. For 299-E33-46, the water potential, as measured from the core samples, is much less than the gravity potential from the surface down to 70 m (230 ft) excepting one data point at about 44 m (145 ft) bgs, which appears to be a bad data point. The general trend is that the water potentials are consistent with a draining profile (water potentials wetter than -0.01 MPa). Below 71 m (233 ft) to the water table at approximately 78 m (approximately 255.8 ft), there appears to be a drier condition than above these depths. Note that the lower depths contain coarse materials, so sample handling (e.g. drying) may be responsible for the apparent drier matric potentials. In any case, it appears that borehole 299-E33-46 has a matric potential profile that strongly suggests drainage is occurring. The green line in Figure 4.19 is the theoretical line that represents the steady state unit gradient condition, which represents a matric potential in a sediment profile that is neither draining or drier than (actively evapotranspiring) than equilibrium conditions. Matric potential values to the left of the unit gradient line suggest a draining profile.

For borehole 299-E33-338 (C3391), located outside the southeast corner of the B tank farm in relatively undisturbed terrain, the matric potential data are considerably drier than at 299-E33-46 borehole, particularly near the surface. These matric potential data (see Figure 4.20) are consistent with the hypothesis that non-vegetated areas, with coarse-textured surfaces, drain more than areas with similar soil, but with vegetation present. It appears that the wetting from meteoric sources has not reached to the water table at the 299-E33-338 site.

Table 4.25. Matric Potential Measurements on Core and Grab Samples from Borehole 299-E33-46

Depth (ft bgs) (¹)	Measured Core (Mpa)	Theoretical Matric Potential (Mpa)	Depth (ft bgs) (¹)	Measured Core (Mpa)	Theoretical Matric Potential (Mpa)	Depth (ft bgs) (¹)	Measured Core (Mpa)	Theoretical Matric Potential (Mpa)
<i>Backfill</i>			<i>Thin Fine-grained Lens</i>			<i>H2-lower sand</i>		
12.94	0.0031	0.7402	No sample			170.9	0.0191	0.2588
14.07	0.0292	0.7368	<i>H2-middle sand</i>			171.4	0.0090	0.2573
20.87	0.0606	0.7161	90.37	0.0181	0.5042	<i>H3 sand</i>		
21.37	0.0124	0.7145	90.87	0.0420	0.5027	179.6	0.0101	0.2323
29.17	0.0041	0.6908	99.37	0.1044	0.4768	180.1	0.0067	0.2307
29.67	0.1435	0.6892	98.87	0.0954	0.4783	190.6	0.0175	0.1987
<i>H2-upper sand</i>			111.17	0.0140	0.4408	191	0.0166	0.1975
41.47	0.0036	0.6533	111.67	0.0199	0.4393	200.7	0.0109	0.1679
41.97	0.0033	0.6518	119.67	0.0091	0.4149	201.2	0.0197	0.1664
43.77	0.0043	0.6463	120.17	0.0105	0.4134	209.7	0.0089	0.1405
44.27	0.0031	0.6447	131.6	0.0128	0.3786	210.2	0.0069	0.1390
46.17	0.0037	0.6390	132.1	0.0057	0.3770	<i>PPlz mud</i>		
46.67	0.0038	0.6374	139.8	0.0133	0.3536	219.2	0.0356	0.1116
50.37	0.0021	0.6262	140.3	1.0656	0.3520	219.7	0.0251	0.1100
50.87	0.0026	0.6246	149.9	0.0097	0.3228	221.9	0.0303	0.1033
52.77	0.0030	0.6188	150.4	0.0135	0.3213	<i>PPlg gravelly sand</i>		
53.27	0.0029	0.6173	159.9	0.0048	0.2923	230.5	0.0014	0.0771
60.47	0.0026	0.5954	160.4	0.0093	0.2908	241.2	0.1963	0.0445
60.97	0.0030	0.5938	164.3	0.0094	0.2789	253.9	0.0916	0.0058
70.2	0.0057	0.5657	164.8	0.0077	0.2774	253.4	0.0295	0.0073
70.7	0.0036	0.5642	166.6	0.0103	0.2719			
79.2	0.0068	0.5383	167.1	0.0117	0.2704			
79.7	0.0087	0.5368	<i>Thin Fine-grained Lens</i>					
82.8	0.0059	0.5273	No sample					
83.3	0.0097	0.5258						

(¹) to convert to meters multiply by 0.3048

299-E33-46 (near Tank 241-B-110)

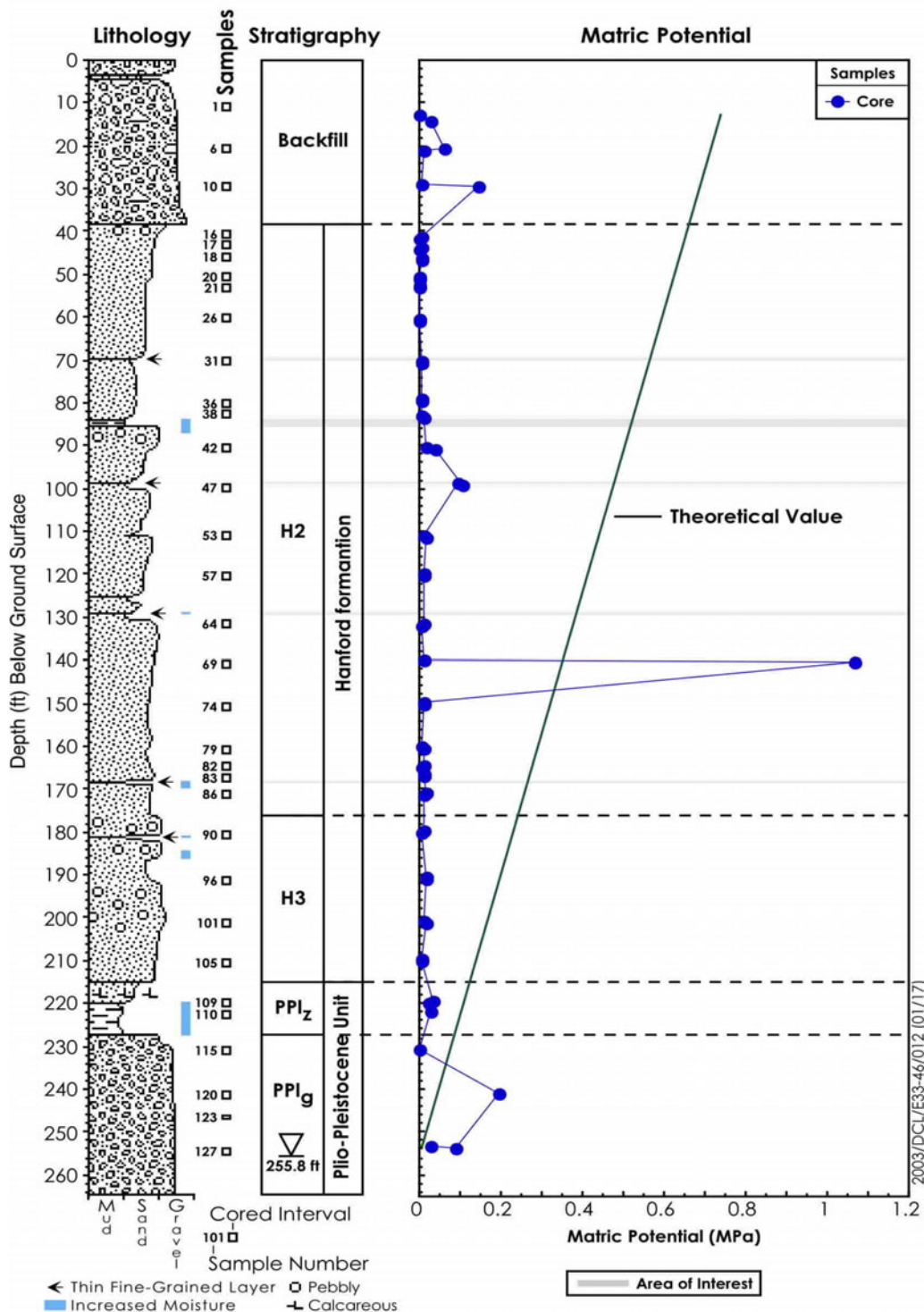


Figure 4.19. Matric Water Potential Measured by Filter Paper Technique on Core Samples from Borehole 299-E33-46

299-E33-338

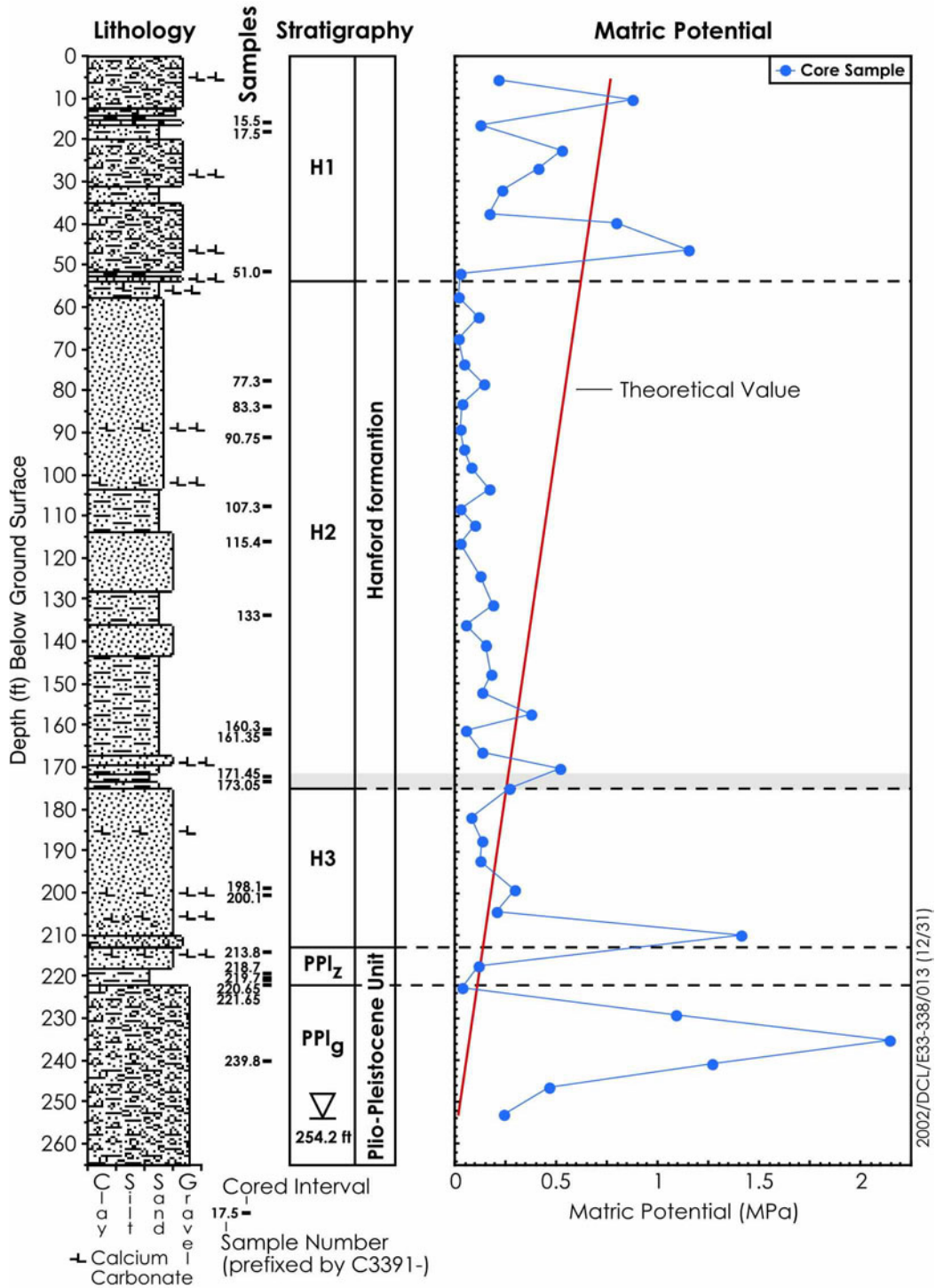


Figure 4.20. Matric Water Potential Measured by Filter Paper Technique on Core Samples from Borehole 299-E33-338 Located Outside the SE Perimeter of the B Tank Farm.

4.11 Vadose Zone Monitoring System

A series of instruments was placed in the vadose zone sediments at borehole 299-E33-46 as the casing was being pulled out of the ground in July and August 2001. The Vadose Zone Monitoring System (VZMS) consists of eight sets of sensors placed at depths ranging from 0.9 m (3 ft) to 68.9 m (226 ft) bgs. The sensors are used for continuous monitoring of vadose-zone hydraulic properties at and beneath the surface of the tank farm. The VZMS sensor arrays consisted of advanced tensiometers, water contents sensors, heat-dissipation units, solution samplers (also called suction candles), temperature sensors, and a water-flux meter. Figure 4.21 shows the configuration of the sensor nest before insertion into the borehole. Gee et al. (2001, 2003) provide details on the installation and a description of each instrument. Table 4.26 shows the depths below ground surface at which the instruments are deployed. The instruments are surrounded by silica flour (SCS-90, U. S. Silica, Ottawa, IL) that was wetted with potable water (Columbia River source) during the installation as the casing was being removed. The silica flour was poured as a slurry such that it made good contact between the formation and the sensors. The slurry was allowed to settle and then a 0.3 m layer of sand (30 mesh) was added above the slurry. The rest of the borehole up to the next instrument nest was filled with bentonite granules as the casing was withdrawn.

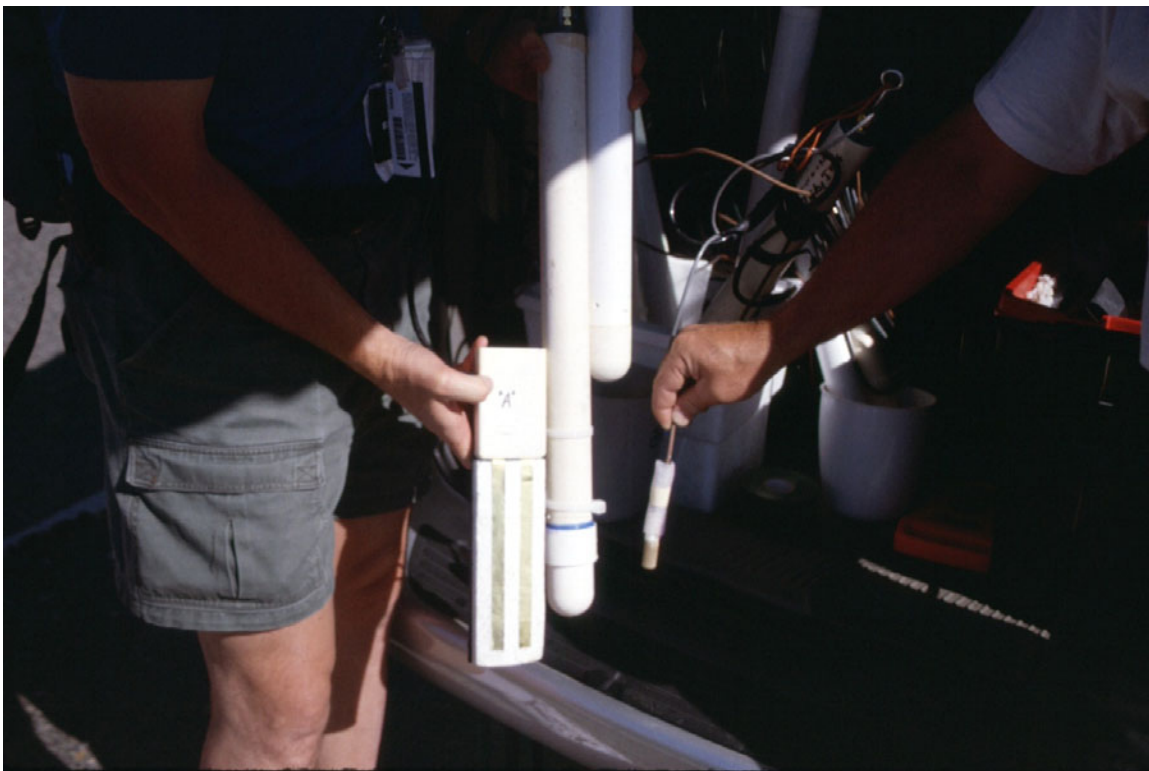


Figure 4.21. Vadose-Zone Monitoring System (without water-flux meter and temperature sensor) Before Deployment in B Tank Farm. Sensors from left to right are the Modified CSI Water Content Sensor, Advanced Tensiometer, Suction Candle, and Heat-Dissipation Unit.

Table 4.26. VZMS Sensor Placement in Borehole 299-E33-46 near Tank B110 in B Tank Farm

Depth (bgs)	WFM ^(a)	AT	HDU ^(b)	WC ^(c)	Temp	SC ^(d)
3		X		X	X	
6	X	X	X	X	X	
9		X		X	X	
15		X	X	X	X	X
53		X		X	X	X
82		X	X	X	X	X
218		X		X	X	X
226		X	X	X	X	X

^(a) WFM =Water Flux Meter;

^(b) HDU =Heat Dissipation Unit;

^(c) WC =Water Content Sensor

^(d) SC =Suction Candle (solution sampler)

The instruments were deployed at each depth from the deepest to the shallowest depth through the casing as it was withdrawn. The casing was raised to just above the depth of interest and the instrument cluster, silica flour, sand introduced down the casing into the open hole at the desired depth. The casing was cut off at the surface as lengths were withdrawn. The uppermost 3 depths were not instrumented with solution samplers (suction candles).

Data have been collected from each instrument since February 2002 and vadose zone porewater has been extracted from all the suction candles on the following dates: 02/12/2002, 05/17/2002, 07/02/2002, 07/30/2002, and 9/24/2002. The chemical composition of the waters removed from the suction candles are reported in Tables 4.27 to 4.29. The chemical composition of the porewaters obtained through the suction candle devices shows that the first sampling after installation has rather dilute concentrations more reflective of the potable water (from the Columbia River) that was used to wet the solids that were packed around the instrument sensors. Subsequent samples of porewater extracted approximately three to seven months after sensor installation show that the waters are gaining dissolved salts. The chemical composition of the porewaters obtained through the suction candles for some constituents appears to be reaching a steady state value most similar to the porewaters obtained out of the core materials using the ultra centrifuge (UFA) but for other constituents the concentrations versus time are either still rising (especially at and below 82 ft bgs) or in a few instances fluctuating or even dropping. Further, the trends versus time for the chemical evolution of any given constituent shows variation with depth; that is the chemical evolution is not the same for each constituent at all depths. Most of the variation in composition versus time is not analytical vagaries but must reflect actual variation because the duplicate measurements on field duplicate samples are showing excellent reproducibility. It will be interesting to follow the evolution of the chemical composition of the porewater with time and to attempt to correlate the variations with other data being collected from the other sensors deployed at the same depths.

Table 4.27. pH, Electrical Conductivity and Anion Composition of Suction Candle Derived Porewaters vs. Time

Sample Date	Depth (bgs-ft) ⁽¹⁾	pH	EC (mS/cm)	Fluoride (mg/L)	Chloride (mg/L)	Nitrite (mg/L)	Bromide (mg/L)	Nitrate (mg/L)	Carbonate (mg/L)	Sulfate (mg/L)	Phosphate (mg/L)
2/12/2002	15	7.55	0.831	0.43	19.38	<0.080	0.26	80.72	276.10	112.82	<0.240
	53	7.19	0.192	0.19	4.33	<0.080	<0.137	0.56	97.17	19.68	<0.240
	82	7.15	0.176	0.12	4.20	0.09	<0.137	0.58	94.86	11.64	<0.240
	82 dup	7.13	0.175	0.09	4.18	0.11	<0.137	0.48	98.17	11.54	<0.240
	218	7.16	0.172	0.06	4.20	0.18	<0.137	<0.292	97.25	11.63	<0.240
	226	7.14	0.172	0.17	4.35	0.10	<0.137	0.53	92.09	11.88	<0.240
5/17/2002	15	7.89	0.811	0.29	14.66	<0.080	0.26	92.10	251.62	84.71	0.81
	53	8.19	4.42	8.32	23.26	0.33	0.61	143.38	737.91	1588.71	1.07
	82	8.52	2.049	39.61	11.42	0.11	1.14	85.45	1258.20	439.77	1.28
	82 dup	8.47	2.598	NA	NA	NA	NA	NA	NA	NA	NA
	218	7.97	1.254	0.57	17.15	0.43	0.35	171.62	210.80	287.13	0.77
	226	7.74	0.706	0.24	11.92	0.19	0.25	122.61	164.47	89.43	<0.240
7/02/2002	15	7.93	0.766	<0.028	14.24	<0.080	0.26	93.62	343.14	85.49	0.53
	53	8.07	4.300	8.38	21.49	0.86	0.60	145.99	592.83	1741.23	1.01
	82	8.34	2.845	44.44	12.92	0.14	1.37	105.46	1368.64	619.17	1.04
	218	7.87	1.358	0.55	18.04	0.23	0.36	190.07	260.66	317.81	<0.0240
	226	7.54	0.688	0.26	11.19	0.34	0.22	102.30	247.24	95.78	0.18
	226 dup	7.55	0.684	NA	NA	NA	NA	NA	NA	NA	NA
7/30/2002	15	8.23	0.766	0.32	13.64	<0.080	0.3	96.73	270.45	80.28	0.47
	53	8.54	4.419	7.5	19.3	0.35	0.54	145.13	491.26	1694.66	0.9
	82	8.78	3.363	40.67	16	0.17	1.5	137.38	711.93	843.85	0.82
	82 dup	8.68	3.368	NA	NA	NA	NA	NA	NA	NA	NA
	218	8.29	1.541	0.5	18.66	0.18	0.41	206.34	247.33	401.26	<.240
	226	8.23	0.799	0.19	14.03	0.15	0.42	177.66	157.54	97.53	<.240

4.100

Table 4.27. pH, Electrical Conductivity and Anion Composition of Suction Candle Derived Porewaters vs. Time

Sample Date	Depth (bgs-ft) ⁽¹⁾	pH	EC (mS/cm)	Fluoride (mg/L)	Chloride (mg/L)	Nitrite (mg/L)	Bromide (mg/L)	Nitrate (mg/L)	Carbonate (mg/L)	Sulfate (mg/L)	Phosphate (mg/L)
9/24/2002	15	8.05	0.744	0.28	11.92	0.22	<.137	100.16	N/A	84.31	<.240
	53	8.41	4.268	8.07	18.65	0.33	0.57	147.72	N/A	1781.7	<.240
	82	8.55	3.775	41.54	19.58	0.18	1.46	170.53	N/A	1234.53	<.240
	218	8.1	2.534	0.4	25.03	0.11	0.39	269.97	N/A	1068.27	<.240
	226	8.02	0.983	0.22	17.07	0.17	0.49	311.32	N/A	106.53	<.240

⁽¹⁾ to convert to meters multiply by 0.3048

N/A analyte was not determined in this sample

Table 4.28. Major Cations and Selected Trace Metals Composition of Suction Candle Derived Porewaters vs. Time

Sample Date	Depth (bgs-ft) ⁽¹⁾	Sodium (mg/L)	Magnesium (mg/L)	Potassium (mg/L)	Calcium (mg/L)	Strontium (ug/L)	Barium (ug/L)	Technetium-99 (pCi/L)	Uranium (ug/L)	Aluminum (ug/L)	Silicon (mg/L)	Sulfur (mg/L)
2/12/2002	15	96.8	14.4	17.6	68.6	362	181	30.5	15.5	(22)	39.8	39.7
	53	8.6	5.4	1.3	17.5	96	20	13.6	0.7	(16)	4.0	7.8
	82	4.3	4.8	1.4	17.3	97	15	17.0	0.4	(23)	3.3	4.9
	82 dup	4.5	4.7	1.4	17.3	96	14	20.4	0.4	(27)	3.2	4.8
	218	4.8	4.8	1.7	16.7	90	11	17.0	1.2	(22)	3.3	4.9
	226	4.6	4.7	2.0	16.7	91	19	20.4	0.6	(28)	3.2	4.8
5/17/2002	15	83.3	13.1	10.1	61.8	303	85	<170	11.8	ND	40.0	30.2
	53	939.0	17.7	29.9	65.2	546	106	<170	25.6	ND	41.4	584.4
	82	572.8	2.6	16.8	11.4	101	53	<1700	639.8	ND	42.3	158.1
	82 dup	579.5	2.6	16.8	11.7	101	56	<1700	647.2	ND	42.7	158.4
	218	162.2	15.7	13.5	72.2	388	138	1.15E+05	6.2	ND	38.2	94.6
	226	40.8	17.1	5.8	70.8	367	84	7.48E+04	4.5	ND	35.9	32.4

Table 4.28. Major Cations and Selected Trace Metals Composition of Suction Candle Derived Porewaters vs. Time

Sample Date	Depth (bgs-ft) ⁽¹⁾	Sodium (mg/L)	Magnesium (mg/L)	Potassium (mg/L)	Calcium (mg/L)	Strontium (ug/L)	Barium (ug/L)	Technetium-99 (pCi/L)	Uranium (ug/L)	Aluminum (ug/L)	Silicon (mg/L)	Sulfur (mg/L)
7/02/2002	15	86.6	13.2	9.2	59.7	323	124	<848	12.3	ND	39.6	31.5
	53	951.2	16.6	27.1	59.9	597	85	33.9	30.1	ND	39.5	598.3
	82	660.5	2.9	18.4	13.3	130	92	339.2	669.1	ND	41.0	216.5
	218	199.4	17.0	14.1	75.3	438	163	1.44E+05	6.6	ND	42.0	113.4
	226	40.5	15.5	4.5	64.0	360	138	6.02E+04	5.3	ND	35.1	32.0
	226 dup	42.1	16.6	4.9	67.0	377	99	6.17E+04	5.2	ND	36.8	33.9
7/30/2002	15	83.6	12.5	9.8	58.1	303	114	17.0	12.4	ND	40.5	26.8
	53	1023.9	16.2	21.9	57.9	646	75	101.8	33.6	ND	41.9	577.1
	82	833.1	3.5	17.9	16.5	161	92	3.73E+03	571.9	ND	44.1	297.2
	82 dup	826.8	3.5	17.8	16.3	161	94	1.19E+03	577.8	ND	44.2	297.5
	218	241.9	18.1	14.4	79.1	463	197	1.50E+05	7.4	ND	43.5	134.8
	226	49.0	19.9	6.5	82.9	453	129	1.28E+05	5.3	ND	38.7	31.9
9/24/2002	15	85.8	13.1	10.7	57.6	300	125	271.4	10.9	ND	42.1	27.2
	53	1010.1	16.6	30.3	55.8	653	80	322.2	35.5	ND	43.1	606.0
	82	946.2	4.3	25.9	19.6	207	109	831.0	521.7	(58)	42.1	388.8
	218	401.2	41.3	21.8	160.0	877	101	1.88E+05	8.3	ND	44.3	332.2
	226	58.4	25.8	7.0	100.4	545	182	2.62E+05	4.8	ND	37.8	33.9

⁽¹⁾ to convert to meters multiply by 0.3048

ND = not determined on this sample

Table 4.29. Selected Trace Metals Composition of Suction Candle Derived Porewaters vs. Time

Sample Date	Depth (bgs-ft) ⁽¹⁾	Chromium (µg/L)	Manganese (µg/L)	Iron (µg/L)	Zinc (µg/L)	Arsenic (µg/L)	Selenium (µg/L)	Molybdenum (µg/L)	Ruthenium (µg/L)	Silver (µg/L)	Cadmium (µg/L)	Lead (µg/L)
2/12/2002	15	NA	98	NA	NA	(3)	<50.0	27.4	NA	<0.1	(1.9)	(1)
	53	NA	59	NA	NA	<50.0	(0)	(24)	NA	<0.1	(1.1)	(0)
	82	NA	56	NA	NA	<50.0	<50.0	(13)	NA	<0.1	(1.3)	(4)
	82 dup	NA	56	NA	NA	<50.0	<50.0	(14)	NA	<0.1	(1.2)	(4)
	218	NA	54	NA	NA	<50.0	<50.0	(22)	NA	<0.1	(0.6)	(1)
	226	NA	42	NA	NA	<50.0	<50.0	(23)	NA	<0.1	(1.0)	(1)
5/17/2002	15	6.82	NA	NA	316	7.13	1.30	24.0	(0.01)	<0.100	0.811	3.89
	53	7.59	NA	NA	(136)	32.8	12.1	308	(0.01)	<0.100	(0.34)	(0.6)
	82	8.84	NA	NA	(147)	112	10.8	216	(0.20)	(0.00)	(0.33)	2.05
	82 dup	9.31	NA	NA	(173)	112	10.9	208	(0.23)	<0.100	(0.33)	2.01
	218	17.09	NA	NA	414	8.43	5.99	49.0	1.50	<0.100	(0.22)	1.40
	226	89.28	NA	NA	(304)	7.93	4.20	10.5	0.750	(0.00)	(0.38)	(0.8)
7/02/2002	15	7.12	ND	(79)	200	8.06	1.61	24.2	(0.01)	<0.100	(0.21)	(0.7)
	53	8.82	ND	(156)	156	42.5	18.2	325	(0.03)	<0.100	(0.31)	(0.4)
	82	9.58	ND	(165)	332	102	12.1	227	0.257	<0.100	(0.29)	2.59
	218	42.81	ND	(108)	549	9.61	7.94	54.7	1.75	<0.100	(0.16)	(0.8)
	226	75.23	ND	(320)	230	9.84	3.80	7.78	0.508	<0.100	(0.19)	(0.4)
	226 dup	74.44	ND	(239)	211	9.94	4.15	7.60	0.513	<0.100	(0.20)	(0.8)

Table 4.29. Selected Trace Metals Composition of Suction Candle Derived Porewaters vs. Time

Sample Date	Depth (bgs-ft) ⁽¹⁾	Chromium (µg/L)	Manganese (µg/L)	Iron (µg/L)	Zinc (µg/L)	Arsenic (µg/L)	Selenium (µg/L)	Molybdenum (µg/L)	Ruthenium (µg/L)	Silver (µg/L)	Cadmium (µg/L)	Lead (µg/L)
7/30/2002	15	7.17	ND	(6)	711	8.67	3.67	27.3	(0.14)	(0.05)	0.263	1.96
	53	10.02	ND	(10)	695	48.0	21.8	321	(0.07)	(0.01)	0.479	2.81
	82	11.36	ND	(34)	298	88.5	16.7	209	(0.37)	(0.04)	0.335	3.30
	82 dup	10.84	ND	(37)	217	88.1	17.3	208	(0.35)	(0.02)	0.322	3.13
	218	99.86	ND	(10)	212	9.14	10.7	53.9	2.00	(0.06)	0.289	1.02
	226	150.24	ND	(5)	138	9.15	8.02	6.39	1.57	(0.18)	0.293	0.770
9/24/2002	15	6.54	(28)	(35)	657	8.08	1.47	23.0	(0.11)	<0.250	0.147	0.979
	53	10.16	(25)	(37)	843	50.4	21.2	309	(0.09)	<0.250	0.478	1.82
	82	10.37	(26)	(53)	(269)	76.7	17.6	201	(0.41)	<0.250	0.324	3.45
	218	176.18	(52)	(28)	(276)	8.55	18.5	68.1	2.42	<0.250	0.262	(0.42)
	226	307.47	(13)	(27)	(134)	8.92	11.7	6.49	2.87	<0.250	0.102	0.609

⁽¹⁾ to convert to meters multiply by 0.3048

() Values in parentheses are below quantitation limit but above the detection limit and thus considered useful.

An average value for the last two to three suction candle samplings for the major cations, anions, and trace metals of interest (technetium-99 and uranium) are plotted along with the porewaters obtained from the cores using ultracentrifugation and the dilution corrected porewaters obtained from the 1:1 sediment to water extracts in Figures 4.1 through 4.5. In general, the suction candle generated porewaters show the same trends as discussed in Section 4.2 where the dilution corrected 1:1 sediment to water extracts and UFA porewater results are described. Namely the pH of the suction candle samples at 16 and 25 m (53 and 82 ft) bgs are higher than in the rest of the borehole profile suggesting the presence of caustic fluid from the tank. The electrical conductivity of the suction candle samples is highest for the 16 m (53 ft) bgs depth and at 25 m (82 ft) bgs is higher than the rest of other shallower and deeper profile values suggesting that the contamination plume is still located predominately between these two depths. There is high fluoride at 25 m (82 ft) bgs that is not increasing with time. The nitrate concentrations in the suction candle samples is increasing versus time below 25 m (82 ft) bgs and is highest at 66 m (218 ft) bgs. The sulfate concentration is also increasing versus time and is high between the depths of 16 and 66 m (53 and 218 ft) bgs. As shown in Figure 4.2, the suction candle sulfate values are much higher than the UFA squeezed porewaters and the dilution corrected water extract values. There may be sulfate in the materials used to pack around the sensors or in some of the sensors themselves (gypsum?).

The suction candle cation data show high sodium between the depths of 16 and 25 m (52 and 82 ft) bgs as would be expected based on other measurements shown in Figure 4.3. The sodium concentrations at most depths where suction candles are present appear to be increasing with time. The divalent cations (calcium, magnesium, and strontium) are all low in the suction candle-obtained porewater at 25 m (82 ft) bgs. The low concentrations reflect the effects of the high sodium in the leaked tank fluids causing ion exchange reactions that push the divalent cations deeper in the vadose zone sediment profile.

The technetium-99 and uranium concentrations in the suction candle porewater are similar to the values from the other two porewaters collected with the UFA or calculated from the water extracts. Namely, elevated uranium concentrations are found at 25 m (82 ft) bgs and to a lesser extent at 16 m (53 ft) bgs. The technetium-99 suction candle values are high at both 66 and 69 m (218 and 226 ft) bgs and much lower at shallower depths suggesting that either the entire technetium plume has been pushed into the Plio-Pleistocene mud unit from above or that the technetium has migrated into the sediments horizontally for other sources than the tank B-110 transfer line leak.

4.12 Groundwater Analyses

The chemical composition of the groundwater is reported in Table 4.30. The data are also plotted along with the calculated porewater (obtained from the dilution corrected 1:1 water extracts), ultracentrifuged porewaters taken from the core samples and in the in-situ suction candle samples obtained over time. All the data are plotted in Figures 4.1 through 4.5. In general, the vadose zone porewater obtained from the cores by ultracentrifugation and the suction candles still emplaced in the decommissioned borehole, obtained by drawing a vacuum periodically to extract fluid, contain more dissolved common cations and anions than the groundwater sample. The groundwater sample is influenced by inputs from uncontaminated recharge water, as well as fluids disposed to cribs, trenches and ponds that had lower concentrations of contaminants than tank fluids thus we would expect the groundwater to be more dilute.

The technetium-99 and nitrate concentrations in the groundwater are 1815 pCi/L and 16.4 mg/L, respectively. This yields a ratio of 111 pCi/mg. For the overlying Hanford H3 sand unit (UFA squeezed) and in the Plio-Pleistocene mud unit (both UFA squeezed and suction candle), the ratio ranges from 760 and 400 to 900 pCi/mg, respectively. This suggests that the technetium-99 in the groundwater at 299-E33-46 has been diluted with waters with another source of nitrate provided that the technetium-99 has entered the groundwater from vertically descending through the vadose zone sediments.

The tritium concentration in the groundwater does not appear to come from the vadose sediments at borehole 299-E33-46 that overly the water table because no tritium was found, excepting at depths from about 14 to 18 m (46 to 60 ft) bgs, in the vadose zone profile. At the value found in the groundwater (2810 pCi/L) we should have been able to measure tritium in the overlying sediments. It is thus not clear that the source of the contamination in the groundwater obtained from the water table at 299-E33-46 before the borehole was decommissioned is from the vadose zone near tank B-110.

For a few of the constituents the vadose zone water and groundwater have similar concentrations, such as alkalinity, fluoride, phosphate, aluminum, barium and silicon. These constituents are likely controlled by dissolution reactions with the sediments.

Table 4.30. Composition of Groundwater Taken from Borehole 299-E33-46 at 255.8 ft bgs.

Constituent	Units	Value	Constituent	Units	Value
pH Measurement		7.87±0.05	Chromium	ug/L	7
Specific Conductance	uS/cm	360	Cobalt	ug/L	<8.2
Dissolved organic carbon	ug/L	390±120	Copper	ug/L	<1.2
Alkalinity as CaCO ₃	mg/L	100	Iron	ug/L	38.1
Chloride	mg/L	7.8	Magnesium	mg/L	9.95
Cyanide	ug/L	<2.5	Manganese	ug/L	29.2
Fluoride	mg/L	0.31	Nickel	ug/L	3.4
Nitrate	mg/L	16.4	Potassium	mg/L	4.62
Nitrite	mg/L	<0.007	Sodium	mg/L	16.1
Sulfate	mg/L	33.7	Strontium	mg/L	0.185
Phosphate	mg/L	"--"	Silicon	mg/L	"--"
Aluminum	ug/L	<7	Zinc	ug/L	9.5
Barium	ug/L	35.9	Technetium-99	pCi/L	1815±118
Cadmium	ug/L	<0.15	Tritium	pCi/L	2810
Calcium	mg/L	34.8	Uranium	ug/L	2.76±0.09

“--“ constituent was not measured

5.0 Summary and Conclusions

In this section, we present summary information on what the 299-E33-46 sediment characterization data means. Conclusions are included to aid in making decisions on what interim actions and future studies are needed to make current and future tank farm operations less likely to unfavorably effect the environment.

5.1 Conceptual Model of the Geology at 299-E33-46

Borehole 299-E33-46 is located approximately 15 ft from the northeast edge of single-shell tank 241-B-110. The vertical borehole was installed by using the cable-tool technique between May 8 and June 26, 2001. Total depth of the borehole was 264.4 ft and groundwater was encountered at 255.8 ft bgs. Anticipated perched-water conditions were not encountered atop a fine-grained silt layer at 220 ft bgs. A total of 33 two-ft long, 4-inch diameter split-spoon core samples were obtained by pushing the sampler out ahead of the advancing casing. Grab samples were collected between these core sample intervals to yield near continuous samples to a depth of 78.3 m (257 ft). Eight vadose zone porewater sensor arrays were installed in the borehole at selected depths prior to removal of temporary casing and decommissioning the borehole.

Each of the 33 split spoon cores contained four 6-in long liners that were opened in the chemistry lab and geologically described during the sub-sampling process to obtain aliquots used in the various characterization activities. In addition 54 out of a total of 120 composite grab samples were also geologically described and characterized.

Three primary stratigraphic units were penetrated by this borehole: 1) backfill materials, 2) the Hanford formation, and 3) the Plio-Pleistocene unit. Backfill material consists of predominantly dark to olive gray, moderately sorted, silty sandy gravel to gravelly sand, which is unconsolidated and weakly to strongly calcareous. The backfill extends from the ground surface to a depth of 11.7 m (38.5 ft).

The Hanford formation is divided into three informal units (H1, H2, and H3). However, it appears that the H1 unit was completely removed during excavation in the vicinity of borehole 299-E33-46, and then later used as backfill. The Hanford formation beneath the backfill consists of mostly sand separated by several distinctly finer (fine sand to silt) strata. A total of three moisture spikes occur within the Hanford formation associated with these fine-grained intervals and/or other interfaces between strata with contrasting grain sizes.

The Hanford formation H2 unit is present between 38.5 to 176 ft bgs. The Hanford formation H2 unit consists of mostly olive gray, moderately to well sorted, fine- to coarse-grained sand beds. These beds show occasional weak horizontal laminations and are generally non-calcareous to weakly calcareous. The most common sediment type within the H2 unit, a medium-to coarse grained sand is often described as “salt and pepper” sands because of the

roughly equal amounts of dark- (basaltic) and light-colored (quartz and feldspar) grains. Dispersed within the Hanford formation H2 unit is four separate, relatively thin (≤ 2 ft), olive brown to grayish brown, compact, well-sorted fine sand to silt beds. These occur at depths of about 69.7, 98.5, 123, and 168 ft bgs.

Below the H2 unit lays the H3 unit, a predominantly coarser-grained gravelly sand sequence that extends to base of the Hanford formation at 65.5 m (215 ft) bgs. The top of the Hanford formation H3 unit is defined by a transition from predominantly sand to slightly gravelly sand at 53.6 m (176 ft) bgs. The Hanford formation H3 unit is about 11.9 m (39 ft) thick, the base of which is defined by the top of the Plio-Pleistocene unit silty facies (PPlz) at 65.5 m (215 ft) bgs. The H3 unit is unconsolidated and non-calcareous to weakly calcareous. The H3 unit in 299-E33-46 grades downward into medium to coarse sand with depth.

A fine-grained sediment that we designate as the PPlz unit underlies the basalt-rich sands of the Hanford formation in borehole 299-E33-46 between 65.5 m (215 ft) and 69.4 m (227.7 ft) bgs. This unit can be subdivided into two facies types in borehole 299-E33-46. The upper part of the PPlz unit consists of a pale olive, loose, laminated, very-well sorted, calcareous, fine- to medium-grained, quartzo-feldspathic sand. The lower part of the PPlz unit consists of a grayish brown, laminated to massive, compacted and very well sorted, moderately calcareous, silt to silty fine sand.

The defining characteristics of the sediment from the PPlz unit include its relatively high calcium carbonate content, uniform texture, and predominantly quartzo-feldspathic mineralogy. Relatively high neutron moisture and gamma activity on geophysical logs in addition to the core and grab samples that were visually inspected corroborate that the lower part of the PPlz unit in this borehole is fine-grained (mostly silt).

A sequence of sandy gravel to gravelly sand was encountered starting at a depth of 69.4 m (227.7 ft) bgs. This material, designated as the PPlg unit, consists of mostly olive gray, loose, clast-supported, moderately to poorly sorted mixtures of gravel and sand. This unit contains a moderate amount (~30-50%) of basalt and is non-calcareous. The PPlg unit extends beyond the bottom of the borehole, which was terminated at 264.4 ft bgs.

The most striking features in the field logs are several thin zones of increased moisture and a zone of high total gamma reading. Starting from the ground surface, a zone of increased moisture appears to conform with a 1.5 ft thick layer of fine sand sandwiched between layers of coarse sand at 84.0-85.5 ft bgs. A similar spike in neutron-moisture logs occurs in several nearby tank vadose zone dry wells (20-10-02, 20-07-11, and 20-08-07). Another high-moisture zone is associated with a thin (0.3 ft) silt layer at 168.1-168.4 ft bgs; a core sample obtained from this zone yielded almost 20 wt% water in the laboratory. A third increase in moisture lies near a sand-gravelly sand interface, perhaps associated with some fine and organic(?) -rich layers (between 185 to 190 ft bgs). A final sharp increase in neutron moisture occurs at a depth between 220-228 ft bgs associated with the silt-dominated facies (PPLz) of the Plio-Pleistocene

unit. These three thin lenses may cause significant horizontal spreading of liquid fluxes from the tank farms.

A few other fine-grained beds are present (i.e., 69.7, 98.5, and 129 ft depths), however these do not show up as increased-moisture zones on either the neutron-moisture log or in the laboratory analyses, probably because they are thin (0.5-1.0 cm [0.016-0.03 ft]). These thin fine-grained beds also probably escaped sub-sampling for moisture in the laboratory.

The total gamma log shows a significant zone, ~12 m (40 ft) thick, of radionuclide contamination that has been confirmed by laboratory analyses to be Sr-90 occurs at the top of the Hanford formation H2 unit starting just below the interface with the overlying coarse-grained backfill. The base of the Sr-90 contamination as defined by bremsstrahlung radiation in the spectral gamma log is well defined and occurs just above a 0.5 m (1.5 ft) thick very fine sand layer at 85 ft bgs, which may have acted as a localized perched zone or capillary boundary.

The discharge of large volumes of waste water in the early 1950s, raised the water table in the vicinity of the 241-B Tank Farm to over 4.9 m (16 ft) above pre-Hanford conditions. Based on historical well water level measurements, the groundwater reached a maximum elevation of approximate 124 m (407 ft) MSL in the 1967-68 time frame, with a secondary maximum, just below this in the 1986-89 time frame. Water levels have declined approximately 7-8 ft since 1989 at a rate of approximately 20 cm/yr (0.7 ft/yr). The maximum water table is estimated to have reached a depth of about 76.2 m (250 ft) bgs, well below the fine silt PPlz unit that could act as a perched water table. The geologists logs made during the drilling of 299-E33-46 indicate that the groundwater table was encountered at a depth of 77.9 m (255.8 ft) bgs. This suggests that the groundwater level has dropped almost 2 m (6 ft) in the vicinity of borehole 299-E33-46 since the late 1980s. There was no sign of perched water in the vicinity of 220 ft bgs as was found at the borehole drilled east of the BX tank farm, 299-E33-45.

In general, the near horizontal fine-grained thin lenses in the Hanford formation and the thick Plio-Pleistocene mud unit likely cause anisotropy in water flow. The vertical distribution of technetium-99, nitrate and tritium in the vadose zone does not readily lead to the observed concentrations in the groundwater.

5.2 Vertical Extent of Contamination

The following paragraphs describe measurements of various parameters that help us determine the extent of vertical migration of the tank leak plume. We used several parameters including electrical conductivity, nitrate, pH, sodium, and technetium-99 concentrations in water extracts for our main indicators to determine the leading edge of the tank leak plume. The concentrations of acid-extractable or directly measured constituents in the sediment were used to delineate the total inventory of constituents within the plume. For technetium-99, the water-extractable and acid/total concentrations were similar, signifying that this mobile constituent does remain in the vadose zone porewater and hardly interacts with the sediment.

Based on evaluating all these measurements, we cannot conclude that the borehole data establishes the vertical extent of tank contamination.

The moisture content is a direct measure of the mass of fluid in the vadose zone sediment. One would logically assume that wetter than normal conditions would represent the existence of leaked tank liquor but as found at most of the boreholes studied, the moisture content is indicative mainly of grain size. The first region with elevated moisture is the 1.5-ft thick mud lens at 84 to 85.5 ft bgs [22.86 m] within the Hanford H2 sand unit. Near the bottom of the Hanford H2 unit at 168 ft bgs is a moist ~0.3 ft thick lens of fine-grained material with moisture contents of 20.2% by weight. Within the Hanford H3 unit there is a slightly moist lens at 185 ft bgs with a moisture content of 12.3 wt. % compared to values of 3 to 4 wt % nearby. The PPlz lithology between 220 and 226 ft bgs is the wettest material in the borehole with moisture contents ranging from 15 to 29 wt %. The gravels below this PPlz silt are relatively dry down to the water table that currently is found at 255.8 ft bgs.

The second parameter measured was the pH of water extracts of the vadose zone sediment. The pH profile shows that between 52 and 83 feet (30.48 and 45.72 meters) bgs (in the Hanford formation H2 middle sand sequence), there are elevated values [8.5 to 9.5] suggesting the presence of caustic waste interaction. Below the fine-grained lens at ~84 to 85 ft bgs is another lobe of slightly elevated pH with values between 8.8 and 9.1. This deeper zone with elevated pH extends from 96 to 120 ft bgs and is also within the Hanford formation H2 unit. The thin fine-grained lens at ~85 ft bgs does not show elevated pH or elevated electrical conductivity and thus appears to be acting as a partial barrier to tank related fluid migration. The observed pH values are not nearly as high as would be expected for sediment completely saturated with tank liquor. One plausible explanation for the lower than expected pH is that the pH re-neutralizes with time from slow dissolution of alumino-silicates or with absorption of carbon dioxide that exists in the vadose zone air-filled porosity. Both processes would mute the initial pH excursion to high values over time.

The third parameter that was assessed to estimate the vertical extent of the leak plume was dilution-corrected electrical conductivity for water extracts. The electrical conductivity profile is similar to the elevated pH profile in that it shows two regions of high values. The shallower region of elevated EC starts a bit shallower [at 50.6 ft bgs] than the elevated pH region and extends down to the thin fine-grained lens at 84-85 ft bgs. The dilution corrected (calculated) porewater electrical conductivity ranges from 6.5 to 15 mS/cm in this region. The deeper elevated EC zone extends from 90.6 to 140 ft bgs with calculated porewater conductivities ranging from 5.7 to 12.75 mS/cm. This zone of elevated electrical conductivity is less concentrated than the shallow zone and resides within the lower portion of the Hanford formation H2 unit. The porewaters that were extracted from selected samples using the ultracentrifuge [UFA] show slightly lower pH values than the 1:1 sediment to water extracts and the actual porewater electrical conductivity values are often significantly lower than calculated porewater conductivities obtained by making dilution corrections on the 1:1 sediment to water extracts. This discrepancy was also found at borehole 299-E33-45 east of the BX-102 tank.

The fourth parameter that was measured to define the vertical extent of contamination was nitrate. There is shallow nitrate contamination starting at about 50.6 ft bgs that extends to 77.4 ft bgs, perhaps reaching the thin fine-grained lens at 84.5 ft bgs. Still within the Hanford formation H2 unit between the depths of 87.8 and 168 ft bgs is a more concentrated nitrate plume. At 134 ft bgs the highest nitrate calculated porewater concentration is found [~ 1500 mg/L]. The H2 sediment porewater between 164.5 and 168.5 ft bgs contains ~ 500 mg/L nitrate. The Hanford formation H3 sediment also contains elevated nitrate porewater concentrations that vary between 100 to 200 mg/L. The PPlz unit also appears to contain slightly elevated nitrate porewater concentrations at ~ 130 mg/L. The 299-E33-46 borehole sediments in the PPlg coarse-grained unit may also contain elevated nitrate porewater concentrations of ~ 50 mg/L. Thus the sediment water extracts from this borehole appear to show elevated nitrate is present all the way to the groundwater; however the bulk of the nitrate is found in the sediment between the depth of 110 to 168.5 ft bgs in the Hanford H2 sand sequence with values reaching as high as 6.15 g/L or ~ 0.1 M at 47.6 meters (156.2 feet) bgs.

The porewater fluoride concentrations are elevated above the uncontaminated sediment baseline range of 0.4 to 23 mg/L over a depth region from 50.6 to 111.4 ft bgs. The highest fluoride porewater concentrations are found between 61 and 83 ft bgs within the Hanford formation H2 unit at values that range from 110 to 210 mg/L.

The bicarbonate concentration in the porewaters also is elevated in the H2 middle sand sequence between 75 and 167 ft bgs; both above and within in the same zone with the largest nitrate concentrations. Interestingly, the bicarbonate distribution in the sediment water extracts mimics the elevated pH profile suggesting that either dissolution of natural carbonate minerals or capture of vadose zone carbon dioxide during tank waste fluid neutralization might be the cause. The porewater bicarbonate maximum concentration varies between 0.1 and 0.21 M between 110 to 130 ft bgs.

The porewater sulfate concentrations appear to be slightly elevated in the deeper depths of the borehole, rather than within the Hanford H2 unit where tank related fluids are generally found. The most significant concentrations of sulfate in the shallow vadose zone are found in a narrow zone within the middle sand sequence of the H2 unit between 140 and 166 ft bgs. No UFA squeezings were obtained from sediments from this narrow zone and the natural background sediments in the borehole to the east, 299-E33-338 are also elevated. More puzzling are the elevated sulfate concentrations in the PPlg lithology at the bottom of the borehole. The dilution corrected porewater concentrations reach values ~ 500 mg/L compared to natural background values of ~ 40 mg/L.

The porewater chloride concentrations do not appear to be significantly elevated compared to the nearby natural sediments from borehole 299-E33-338. Thus the observed chloride profile likely reflects natural conditions. The phosphate porewater distribution in the vadose zone sediment at borehole 299-E33-46 shows elevated concentrations between ~ 54.6 and 82 ft bgs

within the H2 upper sand sequence, the maximum concentrations are found in a thin zone at ~60 ft bgs with a dilution corrected value of 108 mg/L (0.0011 M).

The fifth indicator species used to define the vertical extent of contamination was sodium in the water extract. Sodium is the dominant cation in tank liquor. The maximum sodium porewater concentration is about 0.122 M in the zone from 54.6 to 62.1 ft bgs and 0.101 M between 98 and 120 ft bgs. The three highest porewaters based on electrical conductivity have a chemical composition that is essentially 0.15 M sodium and 0.13 M bicarbonate, 0.01 M fluoride, 0.007 M sulfate and 0.003 M nitrate. The actual porewater cation concentrations are in general always lower than the calculated porewater concentrations derived from dilution correcting the 1:1 sediment to water extracts.

The depth profiles for the divalent alkaline earth cations calcium, magnesium, and strontium and show remarkable similarities. All show depleted concentrations over the depth range from between 50.6 or 52 ft bgs down to 120 ft bgs where the concentrations return to values similar to those found in uncontaminated sediments. Conversely, the porewater sodium concentration is elevated from 50.6 ft bgs down to 201 ft bgs in the H3 sand sequence. The cation profiles for the divalent cations (Ca, Mg, and Sr) and the mono-valent cations (K and Na) are related through ion exchange reactions wherein the divalent cations that dominant the exchange sites in the natural sediments are stripped off and replaced by the sodium and potassium (perhaps an impurity in the sodium hydroxide used at Hanford to neutralize acidic waste streams).

Finally, there also appears to be elevated concentrations of soluble Al and Fe in the shallow profile between 52 and 70 and 52 and 80 ft bgs, respectively. Soluble Si also appears elevated in discontinuous zones between 52 and 120 ft bgs. These zones of high readily water soluble Al, Fe, and Si may represent amorphous reaction or weathering products from tank waste interactions with the vadose zone sediments.

Potassium-40 was the only gamma-emitting isotope quantitated in the profile, but the bremsstrahlung radiation was observed between the depths of 46 and 89 ft bgs. The uranium-238 activity was below the GEA detection limit for the entire vadose zone profile suggesting low concentrations are present. No detectable gamma emitting fission products such as ^{137}Cs , ^{152}Eu , ^{154}Eu , ^{125}Sb , or the activation product ^{60}Co , that are often observed in the field logging of the dry boreholes around Hanford's single shell tanks were observed in the sediments.

Strontium-90 is considered to be the primary radionuclide released from tank B-110 transfer line and is concentrated in the sediment between 19 and 28 m (62 and 83 ft) bgs at concentrations between 1,000 and 11,250 pCi/g. Strontium-90 in the sediments is not readily water leachable with distilled water and several hours contact. In general the water leach and total acid leachable Sr in the vadose zone sediments suggest that the in-situ desorption Kd value is >100 ml/g for the diluted 1:1 sediment to water extract solution.

All the technetium-99 data in the shallow depths is suspect thus it is difficult to determine if the technetium profile at 299-E33-46 from the tank B-110 transfer line leak can be traced from below the tank all the way to the groundwater and whether B-110 is the source of technetium-99 in the deep sediments and groundwater. Other sources could be nearby crib discharges. If we put credence in the technetium-99 depth profile, then simple steady-state recharge analyses suggest that the slight technetium-99 peak in the H2 unit at ~132 ft bgs is where the transfer line leak has migrated to over the last 30 years. The two apparent more concentrated peaks of technetium-99 found in the deep H3 unit and the PPlz unit would require unrealistically high recharge rates to have been occurring in the last 30 years to drive the technetium to these depths. It is more likely that the technetium found at the deeper depths is from some horizontal migration of fluids containing technetium-99 from other sources that was carried to depth by active disposal of large quantities of contaminated water or some other driving force such as domestic water line leaks, recharge from topographic lows for snow melt etc.

There are elevated concentrations of uranium in the vadose zone pore water between 50.6 and 120 ft bgs (within the upper sand sequence of H2). There is no indication of elevated uranium in the H3 unit, PPlz or PPlg units.

In summary, the moisture content, pH, electrical conductivity, fluoride, sulfate, phosphate, sodium, strontium-90 and uranium profiles do not identify the leading edge of the plume. The profiles of only nitrate, suggests that the leading edge of the plume could have reached the water table at borehole 299-E33-46; however horizontal migration of nitrate rich waters in the PPlz unit might be the cause of the higher than background nitrate concentrations in the deep vadose zone profile. The majority of the tank fluids still resides in the shallow Hanford H2 sand unit.

5.3 Detailed Characterization to Elucidate Controlling Geochemical Processes

The more detailed characterization activities of the cores from 299-E33-46 borehole added some insight on the processes that control the observed vertical distribution of contaminants and on their migration potential into the future. The first key finding was that the 1:1 sediment to water extracts are a reasonable estimate of the porewater chemistry in the vadose zone sediment. We extracted porewater from eleven sediment samples using high-speed centrifugation. The chemical composition of the actual porewater was found to be adequately estimated by dilution correcting the 1:1 water extracts. Because it is much easier to obtain a water extract of the vadose zone sediment this finding is important to understanding the porewater chemistry throughout the vadose zone plumes under disposal facilities and leaking tanks. Constituents that showed the best agreement include electrical conductivity, nitrate, sodium, and technetium.

The porewaters in the sediment from the cores in the Hanford formation unit (H2) were dominated by sodium and bicarbonate. The three most concentrated porewaters based on electrical conductivity have a chemical composition that is essentially 0.15 M sodium and 0.13 M bicarbonate, 0.01 M fluoride, 0.007 M sulfate and 0.003 M nitrate. The actual porewater

cation concentrations are in general always lower than the calculated porewater concentrations derived from dilution correcting the 1:1 sediment to water extracts. These concentrations are more dilute than porewaters found at 299-E33-45 east of the BX-102 tank and much more dilute than porewaters under the self boiling REDOX waste tanks in SX tank farm that reached 16 to 17 M sodium nitrate with one molar concentrations of calcium, 0.5 M chromate, and several tenths molar chloride, magnesium, potassium, and sulfate. There is also a faint indication that water extractable uranium is elevated in the vadose zone pore water between 50.6 and 120 ft bgs (within the upper sand sequence of H2). There is no indication of elevated uranium in the H3 unit, PPlz or PPlg units.

There is no indication that there are elevated concentrations of RCRA metals in acid or water extracts from 299-E33-46 borehole sediment.

The water-extractable major cations suggest that an ion-exchange process dominates the porewater/sediment interactions where tank fluid passed by or currently exists. The depth profiles for the divalent alkaline earth cations calcium, magnesium, and strontium and show remarkable similarities. All show depleted concentrations over the depth range from between 50.6 or 52 ft bgs down to 120 ft bgs where the concentrations return to values similar to those found in uncontaminated sediments. Conversely, the porewater sodium concentration is elevated from 50.6 ft bgs down to 201 ft bgs in the H3 sand sequence. The cation profiles for the divalent cations (Ca, Mg, and Sr) and the mono-valent cations (K and Na) are related through ion exchange reactions wherein the divalent cations that dominant the exchange sites in the natural sediments are stripped off and replaced by the sodium and potassium (perhaps an impurity in the sodium hydroxide used at Hanford to neutralize acidic waste streams).

5.4 Estimates of Sorption-Desorption Values

In this section, we discuss our measurement and data synthesis used to quantify the adsorption-desorption values for the major contaminants found in the sediment at 299-E33-46 borehole. We estimated the K_d for various contaminants using one method. By combining the data from the dilution corrected 1:1 water extracts, which represent the porewater, with the activities measured on the sediment, we can get a semi-quantitative sense of what the desorption K_d is. For a contaminant that has very little water-soluble mass, such as cesium-137, the K_d can be approximated as the amount of mass in the total sample per gram of dry sediment divided by the amount of mass in the porewater per milliliter. For a contaminant that is quite soluble in the water extract (~equivalent to saying that the contaminant resides mainly in the porewater within the sediment), one needs to subtract the amount that was water extractable from the total amount present in the moist sediment sample to obtain a value for the amount that would remain on the solid at equilibrium with the pore fluid.

Using these measured distributions, the in-situ desorption K_d for strontium-90 was consistently > 100 ml/g. The technetium-99 desorption data were not of sufficient quality to determine quantitative values because of the low concentrations present but we do not believe

that the technetium-99 is adsorbing to the sediments. Therefore a desorption K_d of zero, meaning that the technetium-99 is not interacting with the sediment, should be assumed. The technetium in-situ desorption K_d data are consistent with a wealth of literature that finds essentially no technetium adsorption onto Hanford Site sediment ([Kaplan and Serne 1995](#); [Kaplan and Serne 2000](#)).

A second method of determining K_d values would be laboratory batch tests. Batch desorption tests were performed for strontium-90 for several time periods using numerous solutions by the Science and Technology Program (see Appendix D in the B-BX-BY FIR ([Knepp 2002](#))).

5.5 Other Characterization Observations

The ratio of one ostensibly mobile species to others in the porewaters can be used to determine relative mobilities. If the absolute concentrations of co-migrating species are changed solely by dilution with existing porewater, then the ratio of the two should remain constant. Unlike similar ratio discussions for other contaminated boreholes (SX-41-09-39 and 299-W23-19; see [Serne et al. 2002b and 2002d](#)), the ratios for the porewaters from borehole 299-E33-46 are not constant. It is likely that the low absolute concentrations of constituents such as technetium-99 and relatively low concentrations of nitrate and uranium cause the ratio approach to be compromised by analytical error.

Further, the dilution corrected porewaters in general do not appear to be of the same composition as this estimate for Sr recovery waste. The technetium-99 concentrations found in the porewaters are generally much lower than those that should be found in Sr recovery waste. Compared to the fluoride found in the porewater both the technetium-99 and nitrate are too low based on Larson's estimates of the chemical composition of Sr recovery waste.

The percentage of the total sediment metal concentrations that is acid extractable from the contaminated sediment is slightly higher than for uncontaminated sediment for only sodium. The anthropomorphic sodium does show a higher percentage of the total concentrations are acid extractable from the sediment between 53 and 69.5 ft bgs compared to uncontaminated sediment. Except for the sodium results, we expected there to be a larger increase than was observed for the contaminated sediment suggesting that the comparison of percentages of the total composition of any element that is acid extractable is not a very sensitive indicator of the presence of tank liquors or its reaction products with vadose zone sediment. More discussions on looking for alteration products is found in the mineralogy section.

As part of our characterization of the contaminated sediment, parameters that can control contaminant migration were measured. Key parameters that were measured on the borehole sediment include the calcium carbonate content, particle size distribution, and bulk and clay size mineralogy.

Particle size measurements showed that the fine grained thin lens at 84 ft bgs within the H2 unit has at least 6.5% silts and sands compared to most of the Hanford formation that is ~ 90 to 95 % sand. The middle and lower portion of the PPlz unit also contains a high percentage of fines.

There is no evidence of rich calcareous zones in the entire profile such is found underlying the PPlz unit in 200 West Area. The calcium carbonate content of the Hanford formation sediments vary between 0.6 to 2.6 % by weight with an average of 1.3 ± 0.4 wt %. The fine grained PPlz mud shows slightly higher calcium carbonate, averaging 1.7 % by weight. The coarse grained PPlg contains the least calcium carbonate (average 0.475% by weight).

As found for uncontaminated sediment from outside other tank farms, the Hanford formation sediment is dominated by silica and alumina. Calcium, carbonate, iron, magnesium, potassium, sodium, and titanium make up most of the rest of the oxides.

XRD analysis of the 11-bulk sediment samples from borehole 299-E33-46 shows the samples to all have a similar mineralogical signature. Quartz concentrations in the bulk sediments ranged from 22.4 wt-% to 43.5 wt-%, with an average concentration of 33 ± 6 wt-%. The bulk sediments contained plagioclase feldspar concentrations from 10 to 34 wt-% and potassium feldspar content measured between 8 to 37 wt-%. The borehole sediment contained plagioclase feldspar concentrations from 10 to 34 wt-% and potassium feldspar content measured between 8 to 37 wt-%. Plagioclase feldspar was more abundant than potassium feldspar in all but three samples. Over all, the feldspar content (both plagioclase and alkali feldspars) averaged about 43 ± 6 wt-%. The amphibole phase comprised < 9 wt-% at most, with the majority of samples having concentrations in the 2 to 4 wt-% range. Clay minerals identified in the whole rock sediment included mica and chlorite. Mica concentrations ranged from a low of 6.5 wt-% to a high of 32 wt-%, with most of the intervals having concentrations between 7 and 15 wt-%. Chlorite concentrations were < 7 -wt% in all sediments analyzed with the exception of two samples in the Plio-Pleistocene Mud Unit that contained 11.7 and 21.2 wt-% chlorite, respectively.

The clay fraction is dominated by four clay minerals: smectite, chlorite, illite, and kaolinite with minor amounts of quartz and feldspar. Semi-quantification results of the clay minerals in the < 2 micron fraction showed that smectites ranged in concentrations from a low of 22 wt-% to a high of 50 wt-%. Illite amounts varied from 30 to 56 wt-% with the majority of samples having concentrations in the 40 to 50 wt-% range. Chlorite and kaolinite were the least abundant of the clay minerals identified in the samples with concentrations equal to or less than 20 wt-% and 9 wt-%, respectively. Quartz and feldspar minerals were present as trace amounts in the clay fraction.

No evidence of mineral alteration or precipitation resulting from the interaction of the tank liquor with the sediment was observed based on the x-ray diffraction measurements. However, SEM scans, which are much more sensitive and more appropriate for finding subtle indications of caustic attack were not performed.

The matric potential of all cores samples from 299-E33-46 from the surface to the water table was determined by the filter paper method. For 299-E33-46, the water potential is much less than the gravity potential from the surface down to 70 m (230 ft) excepting one data point at about 145 ft bgs, which appears to be a bad data point. The general trend is that the water potentials are consistent with a draining profile (water potentials wetter than -0.01 MPa). Below 71 m (233 ft) and to the water table at ~78 m (~255.8 ft), there appears to be a drier condition than above that depth. But these lower depths contain coarse materials, so sample handling (e.g. drying) may be responsible for the apparent drier matric potentials. In any case, it appears that borehole 299-E33-46 has a matric potential profile that strongly suggests drainage is occurring.

A series of instruments was placed in the vadose zone sediments at borehole 299-E33-46 as the casing was being pulled out of the ground in July and August 2001. The sensors are used for continuous monitoring of vadose-zone hydraulic properties and porewater at and beneath the surface of the tank farm. Vadose zone porewater has been extracted from suction candles periodically. Porewater extracted ~three to seven months after sensor installation shows that the waters are gaining dissolved salts. The chemical composition of the porewaters obtained through the suction candles for some constituents appears to be reaching a steady state value most similar to the porewaters obtained out of the core materials using the ultra centrifuge. Further, the trends versus time for the chemical evolution of any given constituent shows variation with depth; that is the chemical evolution is not the same for a constituent at all depths. Most of the variation in composition versus time is not analytical vagaries but must reflect actual variation because duplicate samples are showing excellent reproducibility. It will be interesting to follow the evolution of the chemical composition of the porewater with time and to attempt to correlate the variations with other data being collected from the other sensors deployed at the same depths. In general, the suction candle generated porewaters show pH values at 53 and 82 ft bgs that are higher than in the rest of the borehole profile suggesting the presence of caustic fluid from the tank. The electrical conductivity of the suction candle samples is highest for the 53 ft bgs depth and at 82 ft bgs is higher than the rest of the shallower and deeper profile suggesting that the contamination plume is still located between these depths. There is high fluoride at 82 ft bgs that is not increasing with time. The nitrate concentrations in the suction candle samples is increasing versus time below 82 ft bgs and is highest at 218 ft bgs. The sulfate concentration is also increasing versus time and is high between the depths of 53 and 218 ft bgs. The suction candle sulfate values are much higher than the UFA squeezed porewaters and the dilution corrected water extract values. There may be sulfate in the materials used to pack around the sensors or in some of the sensors themselves. The technetium-99 suction candle values are high at both 218 and 226 ft bgs and much lower above suggesting that either the technetium plume has been pushed into the Plio-Pleistocene mud unit from above or horizontally for other sources than the B-110 tank transfer line leak.

The technetium-99 to nitrate ratio in the groundwater at 299-E33-46 is much lower than in the overlying vadose zone porewaters suggesting that the groundwater has been diluted with waters with another source of nitrate if the technetium-99 has entered the groundwater from vertically descending through the vadose zone sediments.

It is thus not clear that the source of the contamination for any constituent in the groundwater obtained before borehole 299-E33-46 was decommissioned is from the vadose zone sediments near tank B-110.

6.0 References

- American Society of Agronomy (ASA). 1986a. "Hydrometer Method." Chapter 15-5 in *Methods of Soil Analysis-Part 1, 2nd edition of Physical and Mineralogical Methods*, SSSA Book Series No. 5, ed. A Klute, pp. 404-408. Soil Science Society of America, Madison, Wisconsin.
- American Society of Agronomy (ASA). 1986b. "Pynchnometer Method." Chapter 14-3 in *Methods of Soil Analysis-Part 1, 2nd Edition of Physical and Mineralogical Methods*, SSSA Book Series No. 5, ed .A Klute, pp. 378-379. Soil Science Society of America, Madison, Wisconsin.
- American Society of Agronomy (ASA). 1996. "Elemental Analysis by XRF Spectroscopy." Chapter 7 in *Methods of Soil Analysis-Part 3, Chemical Methods*, SSSA Book Series 5, ed. DL Sparks, pp. 161-223. Soil Science Society of America, Madison, Wisconsin.
- American Society for Testing and Materials (ASTM) D4129-88. 1988. "Standard Test Method for Total and Organic Carbon in Water by High Temperature Oxidation and by Coulometric Detection." American Society for Testing and Materials, West Conshohocken, Pennsylvania.
- American Society for Testing and Materials (ASTM) D2488-93. 1993. "Standard Practice for Description and Identification of Soils (Visual-Manual Procedure)." American Society for Testing and Materials, West Conshohocken, Pennsylvania.
- American Society for Testing and Materials (ASTM) D2216-98. 1998. "Test Method for Laboratory Determination of Water (Moisture) Content of Soil and Rock." American Society for Testing and Materials, West Conshohocken, Pennsylvania.
- American Society for Testing and Materials (ASTM) D-5298-94. 2002. "Test Method for Measurement of Soil Potential (Suction) Using Filter Paper." American Society for Testing and Materials, West Conshohocken, Pennsylvania.
- Baker VR, BN Bjornstad, AJ Busacca, KR Fecht, EP Kiver, UL Moody, JG Rigby, DF Stradling, and AM Tallman. 1991. "Quaternary Geology of the Columbia Plateau." In *Quaternary Nonglacial Geology*, ed. RB Morisson, Geol. Soc. Am. K-2:215-250. Conterminous U.S. Geology of North America, Boulder, Colorado.
- Bjornstad BN, KR Fecht, and CJ Pluhar. 2001. "Long History of Pre-Wisconsin, Ice-Age, Cataclysmic Floods: Evidence from Southeastern Washington State", *J. of Geology*. Volume 109, p. 695-713.
- Brindley G.W, and G. Brown (eds.). 1980. "Crystal Structures of Clay Minerals and Their X-Ray Identification." *Monograph No. 5*, Mineralogical Society, London, England.

- Caggiano JA. 1996. *Assessment Groundwater Monitoring Plan for Single Shell Tank Waste Management Area B-BX-BY*. WHC-SD-ENV-AP-002. Westinghouse Hanford Company, Richland, Washington.
- Caggiano, J.A., and S.M. Goodwin. 1991. *Interim Status Groundwater Monitoring Plan for the Single-Shell Tanks*. WHC-SD-EN-AP-012, Westinghouse Hanford Company, Richland, Washington.
- CH2M HILL. 2000. *Site Specific SST Phase 1 RFI/CMS Work Plan Addendum for WMA-B-BX-BY*. RPP-6072, Rev. 1. CH2M HILL Hanford Group, Inc. Richland, Washington.
- Connelly, M.P., B.H. Ford, J.W. Lindberg, S.J. Trent, C.D. Delaney, and J.V. Borghese. 1992. *Hydrogeologic Model for the 200 East Groundwater Aggregate Area*. WHC-SD-EN-TI-019, Westinghouse Hanford Company, Richland, Washington.
- Deka RN, M Wairiu, PW Mtakwa, CE Mullins, EM Veenendaal, and J Towend. 1995. "Use and Accuracy of the Filter Paper Method for Measuring Soil Matric Potential," *European J. of Soil Sci.* 46:233-238.
- DOE. 1988. *Consultation Draft Site Characterization Plan*. DOE/RL-0164, 9 volumes, U.S. Department of Energy, Richland Operations Office, Richland, Washington.
- DOE. 1999. *Phase 1 RCRA Facility Investigation/Corrective Measures Study Work Plan for the SST Waste Management Areas*. DOE/RL-99-36, Rev. 0, U.S. Department of Energy, Richland Operations Office, Richland, Washington.
- DOE-GJPO. 1999a. *Vadose Zone Characterization Project at the Hanford Tank Farms: B Tank Farm Report*. GJO-HAN-28, prepared by U.S. Department of Energy Grand Junction Office for U.S. Department of Energy, Richland Operations Office, Richland Washington.
- DOE-GJPO. 1999b. *Vadose Zone Characterization Project at the Hanford Tank Farms: Tank summary data report for Tank B-110*. GJO-HAN-131, prepared by U.S. Department of Energy Grand Junction Office for U.S. Department of Energy Office of River Protection, Richland Washington.
- Drever JI. 1973. "The Preparation of Oriented Clay Mineral Specimens for X-Ray Diffraction Analysis by a Filter-Membrane Peel Technique." *Amer. Minerl.* 58:553-554.
- EPA Method 300.0A. 1984. *Test Method for the Determination of Inorganic Anions in Water by Ion Chromatography*. EPA-600/4-84-017, U.S. Environmental Protection Agency, Washington, D.C.
- EPA Method 3050B. 2000a. "Acid Digestion of Sediments, Sludges, and Soils." *Test Methods for Evaluating Solid Waste, Physical/Chemical Methods*. EPA Publication SW-846, available online <http://www.epa.gov/epaoswer/hazwaste/test/sw846.htm>

EPA Method 6010B. 2000b. “Inductively Coupled Plasma-Atomic Emission Spectrometry.” *Test Methods for Evaluating Solid Waste, Physical/Chemical Methods*. EPA Publication SW-846, available online <http://www.epa.gov/epaoswer/hazwaste/test/sw846.htm>

EPA Method 6020. 2000c. “Inductively Coupled Plasma-Mass Spectrometry.” *Test Methods for Evaluating Solid Waste, Physical/Chemical Methods*. EPA Publication SW-846, available online <http://www.epa.gov/epaoswer/hazwaste/test/sw846.htm>

Folk RL. 1968. *Petrology of Sedimentary Rocks*. Hemphill, Austin, Texas.

Gee G.W. 1987. *Recharge at the Hanford Site. Status Report*. PNL-6403. Pacific Northwest Laboratory, Richland, Washington.

Gee GW, MJ Fayer, ML Rockhold, and MD Campbell. 1992. “Variations in Recharge at the Hanford Site,” *NW Sci.* 66:237-250.

Gee GW, AL Ward, JB Sisson, JM Hubbell, and HA Sydnor. 2001. *Installation of a Hydrologic Characterization Network for Vadose Zone Monitoring of a Single-Shell Tank Farm at the U. S. Department of Energy Hanford Site*. PNNL-13172, Pacific Northwest National Laboratory, Richland, WA (see <http://vadose.pnl.gov>).

Gee, G. W., A. L. Ward, J. B. Sisson, J. M. Hubbell, D. A. Myers, and H. A. Sydnor. 2003. *Hydrologic Characterization Using Vadose Zone Monitoring Tools: Status Report*. PNNL-14115, Pacific Northwest National Laboratory, Richland, WA (see <http://vadose.pnl.gov>).

Jackson ML. 1969. *Soil Chemical Analysis – Advanced Course – 2nd Edition*. Department of Soil Science, University of Wisconsin, Madison.

Jones TE, BC Simpson, MI Wood, and RA Corbin. 2001. *Preliminary Inventory Estimates for Single-Shell Leaks in B, BX, and BY Tank Farms*. RPP-7389, Rev. 0, CH2M-HILL Hanford Group, Inc., Richland, Washington.

Kaplan DI, and RJ Serne. 1995. *Distribution Coefficient Values Describing Iodine, Neptunium, Selenium, Technetium, and Uranium Sorption to Hanford Sediment*. PNL-10379, Supplement 1, Pacific Northwest Laboratory, Richland, Washington.

Kaplan DI, and RJ Serne. 2000. *Geochemical Data Package for the Hanford Immobilized Low-Activity Tank Waste Performance Assessment (ILAW-PA)*. PNNL-13037, Rev.1, Pacific Northwest National Laboratory, Richland, Washington.

Knepp AJ. 2002a. *Field Investigation Report for Waste Management Area B-BX-BY*. RPP-10098, CH2M HILL Hanford Group, Inc., Richland, Washington.

Knepp AJ. 2002b. *Field Investigation Report for Waste Management Area S-SX*. RPP-7884, Rev. 0, CH2M HILL Hanford Group, Inc., Richland, Washington.

- Larson, D. E. 1967. *B-Plant Phase III Flowsheets*. ISO-986, Isochem, Inc, Richland, Washington.
- Last GV, BN Bjornstad, MP Bergeron, DW Wallace, DR Newcomer, JA Schramke, MA Chamness, CS Cline, SP Airhart, and JS Wilbur. 1989. *Hydrogeology of the 200 Areas Low-Level Burial Grounds - An Interim Report*. PNL-6820, 2 volumes, Pacific Northwest Laboratory, Richland, Washington.
- Lindenmeier CW, RJ Serne, BN Bjornstad, GW Gee, HT Schaef, DC Lanigan, MJ Lindberg, RE Clayton, VL LeGore, IV Kutnyakov, SR Baum, KN Geiszler, KMM Valenta, TS Vickerman, and LJ Royack. 2002, *Characterization of Vadose Zone Sediment: RCRA Borehole 299-E33-338 Located Near the B-BX-BY Waste Management Area*, PNNL-14121, Pacific Northwest National Laboratory, Richland, Washington.
- Lindsey KA, BN Bjornstad, JW Lindberg, and KM Hoffman. 1992. *Geologic Setting of the 200 East Area: An Update*. WHC-SD-EN-TI-012, Westinghouse Hanford Company, Richland, Washington.
- Lindsey KA, SP Reidel, KR Fecht, JL Slate, AG Law, and AM Tallman. 1994. "Geohydrologic Setting of the Hanford Site, South-Central Washington." *In Geologic Field Trips in the Pacific Northwest*. eds. DA Swanson and RA Hagerud, pp. 1C-1 to 1C-16. Geological Society of America Meeting, Geological Society of America, Boulder, Colorado.
- Lindsey, K. A., S. E. Kos, and K. D. Reynolds. 2000. *Vadose Zone Geology of Boreholes 299-W22-50 and 299-W23-19 S-SX Waste Management Area, Hanford Site, South-Central Washington*. RPP-6149, Rev. 0. Waste Management Technical Services, Richland, Washington.
- Lindsey KA, SE Kos, and KD Reynolds. September 2001. *Vadose Zone Geology of Boreholes 299-E33-45 and 299-E33-46 B-BX-BY Waste Management Area, Hanford Site, South-Central Washington*. RPP-8681, Rev. 0. Prepared for the Office of River Protection, CH2M HILL Hanford Group, Inc., Richland, Washington.
- Moore DM, and RC Reynolds, Jr. 1997. *X-Ray Diffraction and the Identification and Analysis of Clay Minerals*. Oxford University Press, New York.
- Narbutovskih SM. 1998. *Results of Phase I Groundwater Quality Assessment for Single Shell Tank Waste Management Areas B-BX-BY at the Hanford Site*. PNNL-11826, Pacific Northwest National Laboratory, Richland, Washington.
- Or D, and JM Wraith. 2002. "Soil Water Content and Water Potential Relationships," pp. 49-84. In: *Soil Physics Companion*, ed. AW Warrick, CRC Press, Boca Raton, Florida.
- Pacific Northwest Laboratory (PNL). 1990a. *Procedures for Groundwater Investigations*. PNL-MA-567-DO-1, Pacific Northwest Laboratory, Richland, Washington.

- Pacific Northwest Laboratory (PNL). 1990b. *Procedures for Groundwater Investigations*. PNL-MA-567-SFA-2, Pacific Northwest Laboratory, Richland, Washington.
- Pacific Northwest National Laboratory (PNNL). 1997. *Gamma Energy Analysis Operation and Instrument Verification Using the Genie2000™ Support Software*. PNNL-RRL-01, Pacific Northwest National Laboratory, Richland, Washington.
- Pacific Northwest National Laboratory (PNNL). 1998. *Inductively Coupled Plasma Mass Spectrometric (ICP-MS) Analysis*. PNNL-AGG-415, Pacific Northwest National Laboratory, Richland, Washington.
- Pacific Northwest National Laboratory (PNNL). 1999. *Visual Description and Classification of Potentially Contaminated Borehole Samples*. PNL Procedure D9T81-99-GVL-1, Pacific Northwest National Laboratory, Richland, Washington.
- Pacific Northwest National Laboratory (PNNL). 2000. *Liquid Scintillation Counting and Instrument Verification Using the 1400 DSM™ Support Software*. PNNL-AGG-002 Pacific Northwest National Laboratory, Richland, Washington.
- Puget Sound Power and Light (PSPL). 1982. *Skagit/Hanford Nuclear Project, Preliminary Safety Analysis Report*. v. 4. *Appendix 20*. Amendment 23, Puget Sound Power and Light Company. Bellevue, Washington.
- Price, WH and KR Fecht. 1976. *Geology of the 241-B Tank Farm*. ARH-LD-129, Atlantic Richfield Hanford Company, Richland, Washington.
- Reidel SP, and KR Fecht. 1994. *Geologic Map of the Priest Rapids 1:100,000 Quadrangle, Washington*. Washington Division of Geology and Earth Resources Open-File Report 94-13, 22 p.
- Reynolds KD. 2001. *Summary Report: 241-B-110 Well (C3360) 299-E33-46*. RPP-8633, Rev. 0, Prepared for CH2M Hill Hanford Group, Inc., by Duratek Federal Services, Inc., Northwest Operations, Richland, Washington.
- Rhoades JD. 1996. "Salinity: Electrical Conductivity and Total Dissolved Solids." In *Methods of Soil Analysis Part 3*. ed. JM Bigham, pp. 417-435. American Society of Agronomy, Madison, Wisconsin.
- Serne RJ, HT Schaefer, BN Bjornstad, BA Williams, DC Lanigan, DG Horton, RE Clayton, VL LeGore, MJ O'Hara, CF Brown, KE Parker, IV Kutnyakov, JN Serne, AV Mitroshkov, GV Last, SC Smith, CW Lindenmeier, JM Zachara, and DS Burke. 2002a. *Characterization of Vadose Zone Sediment: Uncontaminated RCRA Borehole Core Samples and Composite Samples*. PNNL-13757-1, Pacific Northwest National Laboratory, Richland, Washington.

Serne RJ, HT Schaef, BN Bjornstad, DC Lanigan, GW Gee, CW Lindenmeier, RE Clayton, VL LeGore, MJ O'Hara, CF Brown, RD Orr, G.V Last, IV Kutnyakov, DS Burke, TC Wilson, and BA Williams. 2002b. *Characterization of Vadose Zone Sediment: Borehole 299-W23-19 [SX-115] in the S-SX Waste Management Area*. PNNL-13757-2, Pacific Northwest National Laboratory, Richland, Washington.

Serne RJ, GV Last, HT Schaef, DC Lanigan, CW Lindenmeier, CC Ainsworth, RE Clayton, VL LeGore, MJ O'Hara, CF Brown, RD Orr, IV Kutnyakov, TC Wilson, KB Wagnon, BA Williams, and DB Burke. 2002c. *Characterization of Vadose Zone Sediment, Part 4: Slant Borehole SX-108 in the S-SX Waste Management Area*. PNNL-13757-4, Pacific Northwest National Laboratory, Richland, Washington.

Serne RJ, GV Last, GW Gee, HT Schaef, DC Lanigan, CW Lindenmeier, RE Clayton, VL LeGore, RD Orr, MJ O'Hara, CF Brown, DS Burke, AT Owen, IV Kutnyakov, and TC Wilson. 2002d. *Characterization of Vadose Zone Sediment: Borehole 41-09-39 in the S-SX Waste Management Area*. PNNL-13757-3, Pacific Northwest National Laboratory, Richland, Washington.

Serne, RJ, GV Last, GW Gee, HT Schaef, DC Lanigan, CW Lindenmeier, MJ Lindberg, RE Clayton, VL LeGore, RD Orr, IV Kutnyakov, SR Baum, KN Geiszler, CF Brown, MM. Valenta, and TS Vickerman. 2002e. *Characterization of Vadose Zone Sediment: Borehole 299-E33-45 Near BX-102 in the B-BX-BY Waste Management Area*. PNNL-14083, Pacific Northwest National Laboratory, Richland, Washington.

Slate JL. 2000. *Nature and Variability of the Plio-Pleistocene Unit in the 200 West Area of the Hanford Site*. BHI-01203, Rev. 0, Bechtel Hanford, Inc., Richland, Washington.

Tallman AM, KR Fecht, MC Marratt, and GV Last. 1979. *Geology of the Separations Areas, Hanford Site, South-Central Washington*. RHO-ST-23, Rockwell Hanford Operations, Richland, Washington.

United States Geological Survey (USGS). 2001. "Alkalinity and Acid Neutralizing Capacity." *National Field Manual for the Collection of Water-Quality Data*. Available online at <http://water.usgs.gov/owq/FieldManual/Chapter6/6.6-contents.html>

Wentworth CK. 1922. "A grade scale and class terms for clastic sediments." *Journal of Geology*, Vol. 30, p. 377-392.

Williams, B.A., B.N. Bjornstad, R. Schalla, and W.D. Webber. 2000. *Revised Hydrogeology for the Suprabasalt Aquifer System, 200-East Area and Vicinity, Hanford Site, Washington*. PNNL-12261, Pacific Northwest National Laboratory, Richland, Washington.

Wood MI, TE Jones, R Schalla, BN Bjornstad, and SM Narbutovskih. 2000. *Subsurface Conditions Description of the B-BX-BY Waste Management Area*. HNF-5507, Rev. 0A. CH2M HILL Hanford Group, Inc., Richland, Washington.

Appendix A

299-E33-46

**Geologic Descriptions of Split-Spoon and Grab Samples Performed
During Core/Sample Opening In PNNL Laboratory**

Grab Samples

Pacific Northwest National Laboratory		DAILY BOREHOLE LOG			Boring/Well No <u>299-E33-46</u>		Depth <u>74.3-83.6</u>		Date <u>5-8-02</u>		Sheet 1 of 13	
					Location <u>241-B-110</u>		Project <u>Tank Farm Vadose</u>					
Logged by <u>BN Bjornstad</u>						Drilling Contractor _____						
Reviewed by _____						Date _____						
Lithologic Class. Scheme _____						Procedure _____ Rev _____						
Steel Tape/E-Tape _____ / _____						Field Indicator Equip. 1) _____ 2) _____						
						Depth Control Point _____						

DEPTH ()	TIME	SAMPLES		CONTAMINATION		MOIS- TURE	GRAPHIC LOG				LITHOLOGIC DESCRIPTION (particle size distribution, sorting, mineralogy, roundness, color, reaction to HCl, etc.)	HO ADDED	CASING	DRILLING COMMENTS (drilling rate, down time, blow counts, water level, drill fluid, etc.)
		TYPE	ID NUMBER	INSTR.	READING		C	Z	S	G				
74.3-			# 34			SM								Samples orig. collected: 4-3-01 Have been in cold storage w/o tape around lids for over a year
76.5			S01052											
80.5-			# 39			SM								Moisture samples collected from wettest portions of sample
81.3														
83.3-			# 38			SM								Same as immed. above
83.6														

A.1

W=WT, M=MOI, D=DY

1996/DG/FF/DC/DB/001

Grab Samples

Pacific Northwest National Laboratory	DAILY BOREHOLE LOG	Boring/Well No <u>299-E33-46</u>	Depth <u>90.9-102.9</u>	Date <u>5-8-02</u>	Sheet <u>2 of 13</u>
		Location <u>241-B-110</u>	Project <u>Tank Farm Vadose</u>		
Logged by <u>BN Bjornstad</u>			Drilling Contractor _____		
Reviewed by _____			Date _____		
Lithologic Class. Scheme _____		Procedure _____		Rey _____	
Steel Tape/E-Tape <u>1</u>		Field Indicator Equip. 1) _____		2) _____	
			Driller _____		
			Rig/Method _____		
			Depth Control Point _____		

DEPTH ()	TIME	SAMPLES		CONTAMINATION		MOIS- TURE	GRAPHIC LOG				LITHOLOGIC DESCRIPTION (particle size, distribution, sorting, mineralogy, roundness, color, reaction to HCl, etc)	HD ADDED	CASING	DRILLING COMMENTS (drilling rate, down time, blow counts, water level, drill fluid, etc)	
		TYPE	ID NUMBER	INSTR.	READING		C	Z	S	G					
90.9- 92.0			#43			SM	0	1	1	1					(g) S, slightly pebbly fn- crs sand, mod sorted, 2.5Y4/2 (dk grayish brn) loose, mostly crs sand 5-10% granules - v fn pebbles, WK rxn w/ HCl.
92.0- 94.3			#44			SM	0	1	1	1					Sand, fn-crs, mostly med- grayish brn, wk rxn w/ HCl 30-40% basalt, loose, mod sorted
94.3- 96.0			#45			SM	0	1	1	1					Same as immed. above.
99.87- 100.2			#47			SM	0	1	1	1					Sand, fn-crs, mostly med- crs, grayish brn, wk rxn w/ HCl, loose, mod. sorted, 30-40% basalt
100.2- 102.9			#48			SM	0	1	1	1					Sand, mostly crs sand, few v. fn pebbles, dk grayish brn, v wk rxn w/ HCl, mod sorted, 40-50% basalt, <5% pebbles

A2

W = Wet, M = Moist, D = Dry

1990/DJ/11/DCDBLOG

Grab Samples

Pacific Northwest National Laboratory		DAILY BOREHOLE LOG			Boring/Well No <u>299-E33-46</u>			Depth <u>102.9-115.8</u> Date <u>5-8-02</u>		Sheet <u>3</u> of <u>13</u>	
Location <u>271-B-110</u>					Project <u>TANK Farm Vadose</u>						
Logged by <u>BN Bjornstad</u>					Drilling Contractor _____						
Reviewed by _____ Date _____					Driller _____						
Lithologic Class. Scheme _____ Procedure _____ Rev _____					Rig/Method _____						
Steel Tape/E-Tape <u>1</u> Field Indicator Equip. 1) _____ 2) _____					Depth Control Point _____						

DEPTH ()	TIME	SAMPLES		CONTAMINATION		MOIS- TURE	GRAPHIC LOG				LITHOLOGIC DESCRIPTION (particle size distribution, sorting, mineralogy, roundness, color, reaction to HCl, etc)	HD ADDED	CASING	DRILLING COMMENTS (drilling rate, downtime & low counts, water level, drill fluid, etc)	
		TYPE	ID NUMBER	INSTR.	READING		C	Z	S	G					
102.9- 104.8			#49			SM	•	•	•	•					
104.8- 106.6			#50			SM	•	•	•	•					
106.6- 108.3			#51			SM	•	•	•	•					
112- 114			#54			SM	•	•	•	•					
114- 115.8			#55			SM	•	•	•	•					

A.3

W=Wet, M=Moist, U=Dry

1997/DG/PHD/CDB/001

Grab Samples

Pacific Northwest National Laboratory		DAILY BOREHOLE LOG			Boring/Well No <u>299-E33-46</u>		Depth <u>115.8-124.3</u>		Date <u>5-8-02</u>		Sheet <u>4 of 13</u>	
					Location <u>241-B-110</u>		Project <u>Tank Farm Vadose</u>					
Logged by <u>BN Bjornstad</u>							Drilling Contractor _____					
Reviewed by _____							Date _____					
Lithologic Class. Scheme _____							Procedure _____					
Steel Tape/E-Tape <u>1</u>							Field Indicator Equip. 1) _____ 2) _____					
							Driller _____					
							Rig/Method _____					
							Depth Control Point _____					

DEPTH ()	TIME	SAMPLES		CONTAMINATION		MOIS- TURE	GRAPHIC LOG				LITHOLOGIC DESCRIPTION (particle size distribution, sorting, mineralogy, roundness, color, reaction to HCl, etc.)	HD ADDED	CASING	DRILLING COMMENTS (drilling rate, downtime, blow counts, water level, drill fluid, etc.)	
		TYPE	ID NUMBER	INSTR.	READING		C	Z	S	G					
115.8 - 118.2			#56			SM	•	•	•	•					
120.7 - 122.3			#58			SM	•	•	•	•					
122.7 - 124.3			#59			SM	•	•	•	•					
122.7 - 124.3			#60			SM	•	•	•	•					Same as #59?

A.4

W = Wet, M = Moist, U = Dry

1899/DQ/PPDQDBI/001

Grab Samples

Pacific Northwest National Laboratory		DAILY BOREHOLE LOG			Boring/Well No <u>299-E33-46</u>		Depth <u>124.3-133.3</u> Date <u>5-8-02</u>		Sheet <u>5 of 13</u>	
Logged by <u>BN Bjornstad</u>					Drilling Contractor _____					
Reviewed by _____ Date _____					Driller _____					
Lithologic Class. Scheme _____ Procedure _____ Rev _____					Rig/Method _____					
Steel Tape/E-Tape _____ / _____					Field Indicator Equip. 1) _____ 2) _____					
Depth Control Point _____										

DEPTH ()	TIME	SAMPLES		CONTAMINATION		MOIS- TURE	GRAPHIC LOG				LITHOLOGIC DESCRIPTION (particle size distribution, sorting, mineralogy, roundness, color, reaction to HCl, etc.)	NO ADDED	CASING	DRILLING COMMENTS (drilling rate, down time, blow counts, water level, drill fluid, etc.)	
		TYPE	ID NUMBER	INSTR.	READING		C	Z	S	G					
124.3- 125.8			#61			SM									
125.8- 127.7			#62			SM									
127.7- 130.1			#63			SM									
132.4- 133.3			#65			SM									

A.5

W = Wet, M = Moist, D = Dry

1596/DCL/P/DOC/BLK00

Grab Samples

Pacific Northwest National Laboratory	DAILY BOREHOLE LOG	Boring/Well No <u>299-E33-46</u>	Depth <u>133.3-140.6</u> Date <u>5-8-02</u>	Sheet <u>6 of 13</u>
Location <u>241-B-110</u>		Project <u>Tank Farm Vadose</u>		
Logged by <u>BN Bjornstad</u>		Drilling Contractor _____		
Reviewed by _____		Date _____		
Lithologic Class. Scheme _____		Procedure _____		
Steel Tape/E-Tape _____		Field Indicator Equip. 1) _____ 2) _____		
Rig/Method _____		Depth Control Point _____		

DEPTH ()	TIME	SAMPLES		CONTAMINATION		MOIS- TURE	GRAPHIC LOG				LITHOLOGIC DESCRIPTION (particle size distribution, sorting, mineralogy, roundness, color, reaction to HCl, etc.)	HD ADDED	CASING	DRILLING COMMENTS (drilling rate, down time, flow counts, water level, drill fluid, etc.)	
		TYPE	ID NUMBER	INSTR.	READING		C	Z	S	G					
133.3-			#66			SM									
135.1															
135.1-			#67			SM									
136.9															
136.9-			#68			SM									
138.3															
140.6-			#70												
?															

A.6

Grab Samples

Pacific Northwest National Laboratory		DAILY BOREHOLE LOG			Boring/Well No <u>299-E33-46</u>		Depth <u>152.4-162.8</u>		Date <u>5-8-02</u>		Sheet <u>8</u> of <u>13</u>	
Location <u>241-B-110</u>					Project <u>Tank Farm Vadose</u>							
Logged by <u>B N Bjornstad</u>						Drilling Contractor _____						
Reviewed by _____						Date _____						
Lithologic Class. Scheme _____						Procedure _____						
Steel Tape/E-Tape _____						Field Indicator Equip. 1) _____ 2) _____						
						Driller _____						
						Rig/Method _____						
						Depth Control Point _____						

DEPTH ()	TIME	SAMPLES		CONTAMINATION		MOIS- TURE	GRAPHIC LOG				LITHOLOGIC DESCRIPTION (particle size distribution, sorting, mineralogy, roundness, color, reaction to HCl, etc)	HD ADDED	CASING	DRILLING COMMENTS (drilling rate, down time, blow counts, water level, drill fluid, etc.)	
		TYPE	ID NUMBER	INSTR.	READING		C	Z	S	G					
152.4-			#76			SM									
154.4															
154.4-			#77			SM									
156.6															
156.6+			#78			SM									
158.6															
160.4-			#79			SM									
160.7															
160.7-			#80			SM									
162.8															

W=Wet, M=Moist, D=Dry

1998/01/PROC09/000

Grab Samples

Pacific Northwest National Laboratory	DAILY BOREHOLE LOG	Boring/Well No <u>299-E33-46</u>	Depth <u>160.7-171.7</u>	Date <u>5-8-02</u>	Sheet <u>9 of 13</u>
		Location <u>241-B-110</u>	Project <u>Tank Farm Vadose</u>		
Logged by <u>BN Bjornstad</u>			Drilling Contractor _____		
Reviewed by _____			Date _____		
Lithologic Class. Scheme _____			Procedure _____		
Steel Tape/E-Tape <u>1</u>			Field Indicator Equip. 1) _____ 2) _____		
			Rig/Method _____		
			Depth Control Point _____		

DEPTH ()	TIME	SAMPLES		CONTAMINATION		MOISTURE	GRAPHIC LOG				LITHOLOGIC DESCRIPTION (particle size distribution, sorting, mineralogy, roundness, color, reaction to HCl, etc.)	HO ADDED	CASING	DRILLING COMMENTS (drilling rate, down time, low counts, water level, drill fluid, etc.)			
		TYPE	ID NUMBER	INSTR.	READING		C	Z	S	G							
160.7- 162.8			#01			SM											
164.8- 165.1			#02			SM											
165.1- 167.4			#03			SM											
168.1- 168.4			#05			M											
171.4- 171.7			#06			SM											

A9

W = wet, M = moist, D = dry

1996/01/PFDC/DB/001

Grab Samples

Pacific Northwest National Laboratory	DAILY BOREHOLE LOG	Boring/Well No <u>299-E33-46</u>	Depth <u>171.7-183.1</u>	Date <u>5-8-02</u>	Sheet <u>10 of 13</u>
Logged by <u>BN Bjornstad</u>		Location <u>241-B-110</u>		Project <u>Tank Farm Vadose</u>	
Reviewed by _____			Date _____		
Lithologic Class. Scheme _____		Procedure _____		Rev _____	
Steel Tape/E-Tape _____		Field Indicator Equip. 1) _____		2) _____	
Drilling Contractor _____			Driller _____		
Rig/Method _____			Depth Control Point _____		

DEPTH ()	TIME	SAMPLES		CONTAMINATION		MOIS- TURE	GRAPHIC LOG				LITHOLOGIC DESCRIPTION (particle size distribution, sorting, mineralogy, roundness, color, reaction to HCl, etc.)	HD ACC'D	CASING	DRILLING COMMENTS (drilling rate, down time, blow counts, water level, drill fluid, etc.)	
		TYPE	ID NUMBER	INSTR.	READING		C	Z	S	G					
171.7- 174.1			#87			SM	•	•	•	•					Sand, fn-crs, 50% crs 40% med sand, med. sorted, dk grayish brn, 25-30% % basalt, loose, wk rxn w/ HCl
174.1- 176.1			#88			SM	•	•	•	•					Same as immed. above w/ few wkly cemented aggregates
176.1- 178.1			#89			SM	•	•	•	•					(g) S, pebbly sand, 5-10% fn pebble, 30% crs sand, 60% med sand, med sorted, dk grayish brn, 30-40% basalt, wk rxn w/ HCl
180.1- 180.4			#90			SM	•	•	•	•					Same as immed. above
180.4- 183.1			#91			SM	•	•	•	•					Fn-med sand with silty layer (silty fn sand - calcareous) silty layer firm and compact dk grayish brn, poorly sorted,

A10

W = Wet, M = Moist, D = Dry

1590/DG/1/1000/BL001

Grab Samples

Pacific Northwest National Laboratory	DAILY BOREHOLE LOG	Boring/Well No <u>299-E33-46</u>	Depth <u>183.1-217.7</u> Date <u>5-8-02</u>	Sheet <u>11</u> of <u>13</u>
Location <u>241-B-110</u>		Project <u>Tank Farm Vadose</u>		
Logged by <u>B N Bjornstad</u>		Drilling Contractor _____		Driller _____
Reviewed by _____		Date _____		Rig/Method _____
Lithologic Class. Scheme _____		Procedure _____		Depth Control Point _____
Steel Tape/E-Tape <u>1</u>		Field Indicator Equip. 1) _____ 2) _____		

DEPTH ()	TIME	SAMPLES		CONTAMINATION		MOIS-TURE	GRAPHIC LOG				LITHOLOGIC DESCRIPTION (particle size distribution, sorting, mineralogy, roundness, color, reaction to HCl, etc.)	HD ADDED	CASING	DRILLING COMMENTS (drilling rate, down time, low counts, water level, drill fluid, etc.)		
		TYPE	ID NUMBER	INSTR.	READING		C	Z	S	G						
183.1- 184.3			#92			SM	0	0	0	0					qs, 15% pebbles, 30% crs sand, 30% fin sand, dk crn.ish brn, poorly sorted, wk rxn w/ HCl 40-50% basalt	
184.3- 185.9			#93			M	0	0	0	0					Same as immed. above w/ a little more weathered w/ clay rinds around some pebbles - more moisture	
185.9- 187.8			#94			SM	0	0	0	0					Sand, 70% md, 20% crs, mod. sorted, wk rxn w/ HCl, dk crn.ish brn, 25-30% basalt, trace pebbles to 0.5 cm	
187.8- 189.1			#95			SM	0	0	0	0					Same as immed. above	
215.7- 217.7			#100			SM	0	0	0	0					Sand, 100% fin sand, well sorted, felsic, lots of cemented aggregates, mod-stony rxn w/ HCl, 2.5V/2 crn.ish brn	Top Plid - Pleistocene silty layer

A11

Grab Samples

Pacific Northwest National Laboratory	DAILY BOREHOLE LOG	Boring/Well No <u>299-E33-46</u>	Depth <u>219.9-224.3</u> Date <u>5-8-02</u>	Sheet <u>12 of 13</u>
Logged by <u>BN Bjorustad</u>		Location <u>241-B-110</u>		Project <u>Tank Farm Vadose</u>
Reviewed by _____ Date _____		Drilling Contractor _____		Driller _____
Lithologic Class. Scheme _____ Procedure _____ Rev _____		Rig/Method _____		Depth Control Point _____
Steel Tape/E-Tape _____ / _____		Field Indicator Equip. 1) _____ 2) _____		

DEPTH ()	TIME	SAMPLES		CONTAMINATION		MOISTURE	GRAPHIC LOG				LITHOLOGIC DESCRIPTION (particle size distribution, sorting, mineralogy, roundness, color, reaction to HCl, etc.)	HD ADDED	CASING	DRILLING COMMENTS (drilling rate, down time, blow counts, water level, drill fluid, etc.)	
		TYPE	ID NUMBER	INSTR.	READING		C	Z	S	G					
219.7-			#109			SM									Top PPA silt layer
220.0						M									just above 220' 0"
222.4-			#110			M									
222.7															
222.7-			#111			M									
224.3															
222.7-			#112			M									
224.3															

A.12

W = Wet, M = Moist, U = Dry

1998/DG/P/DOC08/001

Core Samples

Pacific Northwest National Laboratory		DAILY BOREHOLE LOG			Boring/Well No <u>299-E33-46</u>		Depth <u>10-11.5</u>	Date <u>7-10-01</u>	Sheet <u>1</u> of <u>32</u>	
					Location <u>241-B-110</u>		Project <u>Tank Farm Vadose Zone</u>			
Logged by <u>BN Bjornstad</u>									Drilling Contractor _____	
Reviewed by _____						Date _____			Driller _____	
Lithologic Class. Scheme <u>Folk/Wentworth</u>						Procedure <u>D9TB1-99-GVL-01 Rev 0</u>			Rig/Method _____	
Steel Tape/E-Tape <u>1</u>						Field Indicator Equip. 1) _____ 2) _____			Depth Control Point _____	

DEPTH ()	TIME	SAMPLES		CONTAMINATION		MOIS- TURE	GRAPHIC LOG				LITHOLOGIC DESCRIPTION (particle size distribution, sorting, mineralogy, roundness, color, reaction to HCl, etc.)	H ₂ O ADDED	CASING	DRILLING COMMENTS (drilling rate, down time, blow counts, water level, drill fluid, etc.)
		TYPE	ID NUMBER	INSTR.	READING		C	Z	S	G				
10.0- 10.5		S.S.	SO1052- 2C			M	X							Liner only 1/2 full
							O							
							O							
							O							
							O							
10.5- 11.0		S.S.	SO1052-2B			M	O							
							O							
							O							
							O							
							O							
11.0- 11.5		S.S.	SO1052-2A			M	X							Liner ~ 3/4 full
							O							
							O							
							O							
							O							

A14

W = Wet, M = Moist, D = Dry

Core Samples

Pacific Northwest National Laboratory		DAILY BOREHOLE LOG			Boring/Well No <u>299-E33-46</u>			Depth <u>19.37-21.37</u> Date <u>7-10-01</u>		Sheet <u>2</u> of <u>32</u>	
Location <u>241-B-110</u>					Project <u>Tank Farm Vadose Zone</u>						
Logged by <u>BN Bjornstad</u>					Drilling Contractor _____						
Reviewed by _____					Date _____						
Lithologic Class. Scheme <u>Folk/Wentworth</u>					Procedure <u>D9791-99-6VL-01 Rev 0</u>						
Steel Tape/E-Tape <u>1</u>					Field Indicator Equip. 1) _____ 2) _____						
					Depth Control Point _____						

DEPTH ()	TIME	SAMPLES		CONTAMINATION		MOIS- TURE	GRAPHIC LOG				LITHOLOGIC DESCRIPTION (particle size distribution, sorting, mineralogy, roundness, color, reaction to HCl, etc.)	H ₂ O ADDED	CASING	DRILLING COMMENTS (drilling rate, down time, blow counts, water level, drill fluid, etc.)
		TYPE	ID NUMBER	INSTR.	READING		C	Z	S	G				
19.37-		S.S.	S01052-6D			M								Liner only ~1/3 full
19.87														
19.87-		S.S.	-6C			M								100% full
20.37														
20.37-		S.S.	-6B			M								100% full
20.87														
20.87-		S.S.	-6A			M								90% full
21.37														

A15

W = Wet, M = Moist, D = Dry

Core Samples

Pacific Northwest National Laboratory		DAILY BOREHOLE LOG			Boring/Well No <u>299-E33-46</u>		Depth <u>42.27-44.27</u>		Date <u>7-10-01</u>		Sheet <u>5 of 32</u>	
		Location <u>241-B-110</u>			Project <u>Tank Farm Vadose Zone</u>							
Logged by <u>B.N. Bjornstad</u>							Drilling Contractor _____					
Reviewed by _____							Date _____					
Lithologic Class. Scheme <u>Folk/Wentworth</u>							Procedure <u>D9701-99-GVL-01 Rev 0</u>					
Steel Tape/E-Tape <u>1</u>							Field Indicator Equip. 1) _____ 2) _____					
Depth Control Point _____												

DEPTH ()	TIME	SAMPLES		CONTAMINATION		MOIS- TURE	GRAPHIC LOG				LITHOLOGIC DESCRIPTION (particle size distribution, sorting, mineralogy, roundness, color, reaction to HCl, etc.)	H ₂ O ADDED	CASING	DRILLING COMMENTS (drilling rate, down time, blow counts, water level, drill fluid, etc.)
		TYPE	ID NUMBER	INSTR.	READING		C	Z	S	G				
42.27		S.S.	SO1052-17D	D		M	0	0	0	0			100% Full	slough?
42.77							0	0	0	0				
42.77		S.S.	-17C			M	0	0	0	0			100% Full	
43.27														
43.27		S.S.	-17B			M							100% Full	
43.77														
43.77		S.S.	-17A			M							80% Full	
44.27														

818

W = Wet, M = Moist, D = Dry

1998/DCU/PROC/DBL001

Core Samples

Pacific Northwest National Laboratory		DAILY BOREHOLE LOG			Boring/Well No <u>299-E33-46</u> Location <u>241-B-110</u>				Depth <u>44.67-46.67</u> Date <u>7-12-01</u>		Sheet <u>6 of 32</u>			
Logged by <u>BN Bjornstad</u>								Drilling Contractor _____		Date _____				
Reviewed by _____								Driller _____		Rig/Method _____				
Lithologic Class. Scheme <u>Folk/Wentworth</u>								Procedure <u>D9TB1-99-6VL-01 Rev 0</u>		Depth Control Point _____				
Steel Tape/E-Tape <u>1</u>								Field Indicator Equip. 1) _____ 2) _____						
DEPTH ()	TIME	SAMPLES		CONTAMINATION		MOIS- TURE	GRAPHIC LOG				LITHOLOGIC DESCRIPTION (particle size distribution, sorting, mineralogy, roundness, color, reaction to HCl, etc.)	H ₂ O ADDED	CASING	DRILLING COMMENTS (drilling rate, down time, blow counts, water level, drill fluid, etc.)
		TYPE	ID NUMBER	INSTR.	READING		C	Z	S	G				
44.67	1330	S.S.	S010 S2-18D			M	[Vertical Column with Dotted Pattern]				Sand, md-cr, SY 5/2 (olive gray), 100% sand - mostly coarse, well sorted, loose, max part size = cr sand, no rxn w/ HCl			100% Full
45.17														
45.17		S.S.	-18L			M					Same as above			100% Full
45.67														
45.67		S.S.	-18B			M					Same as above			100% Full
46.17														
46.17		S.S.	-18A			M					Same as above			75% Full
46.67														

619

W = Wet, M = Moist, D = Dry

1999/DCL/PROC/DBL001

Core Samples

Pacific Northwest National Laboratory		DAILY BOREHOLE LOG			Boring/Well No <u>299-F33-46</u>		Depth <u>48.87-50.87</u> Date <u>7-12-01</u>		Sheet <u>7</u> of <u>32</u>							
					Location <u>241-B-110</u>		Project <u>Tank Farm Vadose Zone</u>									
Logged by <u>BN Bjornstad</u>						Drilling Contractor _____										
Reviewed by _____						Date _____			Driller _____							
Lithologic Class. Scheme <u>Folk / Wentworth</u>						Procedure <u>DAT81-99-GVK-01 Rev 0</u>			Rig/Method _____							
Steel Tape/E-Tape <u>1</u>						Field Indicator Equip. 1) _____ 2) _____			Depth Control Point _____							
DEPTH ()	TIME	SAMPLES		CONTAMINATION		MOIS- TURE	GRAPHIC LOG				LITHOLOGIC DESCRIPTION (particle size distribution, sorting, mineralogy, roundness, color, reaction to HCl, etc.)	H ₂ O ADDED	CASING	DRILLING COMMENTS (drilling rate, down time, blow counts, water level, drill fluid, etc.)		
		TYPE	ID NUMBER	INSTR.	READING		C	Z	S	G						
48.87	1400	S.S.	S01052-20	D		M							100% Full			
49.37																
49.37																
49.37		SS	-20C			M							90% Full			
49.87																
49.87																
49.87		SS	-20B			M							100% Full			
50.37																
50.37																
50.37		S.S.	-20A			M							90% Full			
50.87																

W = Wet, M = Moist, D = Dry

1999/DCL/PROC/D8L001

A.20

Core Samples

Pacific Northwest National Laboratory		DAILY BOREHOLE LOG			Boring/Well No <u>299-E33-46</u>		Depth <u>51.27-63.27</u> Date <u>7-12-01</u>		Sheet <u>8</u> of <u>32</u>		
Location <u>241-B-110</u>					Project <u>Tank Farm Vadose Zone</u>						
Logged by <u>BN Bjornstad</u>							Drilling Contractor _____				
Reviewed by _____							Date _____				
Lithologic Class. Scheme <u>Folk/Wentworth</u>							Procedure <u>D9T81-99-64-01 Rev 0</u>				
Steel Tap/E-Tape _____							Field Indicator Equip. 1) _____ 2) _____				
Depth Control Point _____											

DEPTH ()	TIME	SAMPLES		CONTAMINATION		MOIS- TURE	GRAPHIC LOG				LITHOLOGIC DESCRIPTION (particle size distribution, sorting, mineralogy, roundness, color, reaction to HCl, etc.)	H ₂ O ADDED	CASING	DRILLING COMMENTS (drilling rate, down time, blow counts, water level, drill fluid, etc.)
		TYPE	ID NUMBER	INSTR.	READING		C	Z	S	G				
51.27- 51.77	1430	S.S.	S01052-21D			D	[Hand-drawn lithologic log showing sand with pebbles]						90% Full	
51.77- 52.27						M	[Hand-drawn lithologic log showing finer sand]						80% Full	
52.27- 52.77		S.S.	-21B			M	[Hand-drawn lithologic log showing well-sorted sand]						100% Full	
52.77- 53.27		S.S.	-21A			M	[Hand-drawn lithologic log showing similar sand]						90% Full	

A.21

W = Wet, M = Moist, D = Dry

1998/OCL/PROC/D8L001

Core Samples

Pacific Northwest National Laboratory		DAILY BOREHOLE LOG			Boring/Well No <u>299-E33-46</u>		Depth <u>58.97-60.97</u>		Date <u>7-12-01</u>		Sheet <u>9</u> of <u>32</u>			
					Location <u>241-B-110</u>		Project <u>Tank Farm Vadose Zone</u>							
Logged by <u>BN Bjornstad</u>						Drilling Contractor _____								
Reviewed by _____						Date _____								
Lithologic Class. Scheme <u>Fulk/Wentworth</u>						Procedure <u>D9T81-99-6VL-01 Rev 0</u>								
Steel Tape/E-Tape <u>1</u>						Field Indicator Equip. 1) _____ 2) _____								
Depth Control Point _____														
DEPTH ()	TIME	SAMPLES		CONTAMINATION		MOIS- TURE	GRAPHIC LOG				LITHOLOGIC DESCRIPTION (particle size distribution, sorting, mineralogy, roundness, color, reaction to HCl, etc.)	H ₂ O ADDED	CASING	DRILLING COMMENTS (drilling rate, down time, blow counts, water level, drill fluid, etc.)
		TYPE	ID NUMBER	INSTR.	READING		C	Z	S	G				
58.97	1510	S.S.	S01052-26D	D		M	[Hand-drawn lithologic log showing a vertical column of sand with some internal texture]				Sand, md-crs, 100% sand		100% Full	
59.47											max part. size = CRS sand, 5Y5/2 (olive gray) moist color, loose, well sorted, WK rxn w/ HCl, sl. finer lens in middle			
59.47		S.S.	-26C			M	[Hand-drawn lithologic log showing a vertical column of sand with some internal texture]				"Salt and pepper"		100% Full	
59.97											Same as above - md-crs sand			
59.97			-26B			M	[Hand-drawn lithologic log showing a vertical column of sand with some internal texture]				Same as above except more md sand at top		100% Full	
60.47														
60.47			-26A			M	[Hand-drawn lithologic log showing a vertical column of sand with some internal texture]				Sand, md-crs, 100% S, max part size = CRS sand, 5Y5/2 (moist), loose, well sorted, WK rxn w/ HCl, "Salt and pepper"		100% Full	
60.97														

A.22

W = Wet, M = Moist, D = Dry

1892/DCL/PROC/08/001

Core Samples

Pacific Northwest National Laboratory		DAILY BOREHOLE LOG			Boring/Well No <u>299-E33-46</u>		Depth <u>68.7-70.7</u>		Date <u>7-12-01</u>		Sheet <u>10 of 32</u>			
		Location <u>241-B-110</u>			Project <u>Tank Farm Vadose Zone</u>									
Logged by <u>B N Bjornstad</u>						Drilling Contractor _____								
Reviewed by _____						Date _____								
Lithologic Class. Scheme <u>Folk/Wentworth</u>						Procedure <u>D9T91-99-6VL-01 Rev 0</u>								
Steel Tape/E-Tape <u>1</u>						Field Indicator Equip. 1) _____ 2) _____								
						Depth Control Point _____								
DEPTH ()	TIME	SAMPLES		CONTAMINATION		MOIS- TURE	GRAPHIC LOG				LITHOLOGIC DESCRIPTION (particle size distribution, sorting, mineralogy, roundness, color, reaction to HCl, etc.)	H ₂ O ADDED	CASING	DRILLING COMMENTS (drilling rate, down time, blow counts, water level, drill fluid, etc.)
		TYPE	ID NUMBER	INSTR.	READING		C	Z	S	G				
68.70-	15:30	S.S.	S01052-31D			M	0	0	0	0				100% Full
69.20														
69.20-		SS.	-31C			M								100% Full
69.70														
69.70-		S.S.	-31B			SM								100% Full
70.20														
70.20-		S.S.	-31A			SM								75% Full
70.70														

A.23

W = Wet, M = Moist, D = Dry

1996/0CL/PROC/DBLOG1

Core Samples

Pacific Northwest National Laboratory		DAILY BOREHOLE LOG			Boring/Well No <u>299-E33-46</u>		Depth <u>78.2-80.2</u>		Date <u>7-17-01</u>		Sheet <u>11</u> of <u>32</u>	
					Location <u>241-B-110</u>		Project <u>Tank Farm Vadose Zone</u>					
Logged by <u>B.N. Bjornstad</u>							Drilling Contractor _____					
Reviewed by _____							Date _____					
Lithologic Class. Scheme <u>Folk/Wentworth</u>							Procedure <u>D9T81-99-GVL-01 Rev 0</u>					
Steel Tape/E-Tape <u>1</u>							Field Indicator Equip. 1) _____ 2) _____					
							Depth Control Point _____					

DEPTH ()	TIME	SAMPLES		CONTAMINATION		MOIS- TURE	GRAPHIC LOG				LITHOLOGIC DESCRIPTION (particle size distribution, sorting, mineralogy, roundness, color, reaction to HCl, etc.)	NO ADDED	CASING	DRILLING COMMENTS (drilling rate, down time, blow counts, water level, drill fluid, etc.)
		TYPE	ID NUMBER	INTR.	READING		C	Z	S	G				
78.2- 78.7	945	S.S.	S01052-36D			M								frozen sample 100% fall
78.7- 79.2		S.S.	-36C			M								
79.2- 79.7		S.S.	-36B			M								
79.7- 80.2		S.S.	-36A			M								80% Fall

A.24

W = Wet, M = Moist, D = Dry

Core Samples

Pacific Northwest National Laboratory		DAILY BOREHOLE LOG				Boring/Well No <u>299-E33-46</u>				Depth <u>81.3-83.3</u>		Date <u>7-17-01</u>		Sheet <u>12 of 32</u>	
						Location <u>211-B-110</u>				Project <u>Tank Farm Vadose Zone</u>					
Logged by <u>BN Bjornstad</u>										Drilling Contractor _____					
Reviewed by _____										Date _____					
Lithologic Class. Scheme <u>Folk/Wentworth</u>										Procedure <u>09781-99-GVL-01 Rev 0</u>					
Steel Tape/E-Tape <u>1</u>										Field Indicator Equip. 1) _____ 2) _____					
Drilling Contractor _____										Driller _____					
Rig/Method _____										Depth Control Point _____					

DEPTH ()	TIME	SAMPLES		CONTAMINATION		MOIS- TURE	GRAPHIC LOG				LITHOLOGIC DESCRIPTION (particle size distribution, sorting, mineralogy, roundness, color, reaction to HCl, etc.)	H ₂ O ADDED	CASING	DRILLING COMMENTS (drilling rate, down time, blow counts, water level, drill fluid, etc.)
		TYPE	ID NUMBER	INSTR.	READING		C	Z	S	G				
81.3-		SS.	S01052-38P			M								100% Full
81.8														
81.8-		SS.	-38C			M								100% Full
82.3														
82.3-		SS.	-38B			M								100% Full
82.8														
82.8-		SS.	-38A			M								80% Full
83.3														

A.25

W = Wet, M = Moist, D = Dry

1998/OCL/PROC/D8L/001

Core Samples

Pacific Northwest National Laboratory		DAILY BOREHOLE LOG			Boring/Well No <u>299-E33-46</u>		Depth <u>88.87-90.87</u> Date <u>7-17-01</u>		Sheet <u>13</u> of <u>32</u>	
					Location <u>241-B-110</u>		Project <u>Tank Farm Vadose Zone</u>			
Logged by <u>B.N. Bjornstad</u>					Drilling Contractor _____					
Reviewed by _____					Date _____					
Lithologic Class. Scheme <u>Fuk/Wentworth</u>					Procedure <u>D 9781-99-6VL-01 Rev 0</u>					
Steel Tape/E-Tape <u>1</u>					Field Indicator Equip. 1) _____ 2) _____					
Depth Control Point _____										

DEPTH ()	TIME	SAMPLES		CONTAMINATION		MOIS- TURE	GRAPHIC LOG				LITHOLOGIC DESCRIPTION (particle size distribution, sorting, mineralogy, roundness, color, (reaction to HCl, etc.)	H ₂ O ADDED	CASING	DRILLING COMMENTS (drilling rate, down time, blow counts, water level, drill fluid, etc.)
		TYPE	ID NUMBER	INSTR.	READING		C	Z	S	G				
88.87- 89.37		S.S.	SO1052-42	D		M	o	o	o	o	o			100% Full
							o	o	o	o	o			
							o	o	o	o	o			
89.37- 89.87		S.S.	-42C			M	o	o	o	o	o			100% Full
							o	o	o	o	o			
							o	o	o	o	o			
89.87- 90.37		S.S.	-42B			SM	o	o	o	o	o			100% Full
							o	o	o	o	o			
							o	o	o	o	o			
90.37- 90.87		S.S.	-42A			M	o	o	o	o	o			80% Full
							o	o	o	o	o			
							o	o	o	o	o			

A.26

W = Wet, M = Moist, D = Dry

1996/02/PROC/DBL/001

Core Samples

Pacific Northwest National Laboratory		DAILY BOREHOLE LOG			Boring/Well No <u>299-E33-46</u>		Depth <u>97.87-99.87</u> Date <u>7-17-01</u>		Sheet <u>19</u> of <u>32</u>		
Location <u>241-B-110</u>					Project <u>Tank Farm Vadose Zone</u>						
Logged by <u>BN Bjornstad</u>							Drilling Contractor _____				
Reviewed by _____							Date _____				
Lithologic Class. Scheme <u>Frik/Wentworth</u>							Procedure <u>D9T01-99-6VL-01</u> Rev <u>0</u>				
Steel Tape/E-Tape <u>1</u>							Field Indicator Equip. 1) _____ 2) _____				
Depth Control Point _____											

DEPTH ()	TIME	SAMPLES		CONTAMINATION		MOIS- TURE	GRAPHIC LOG				LITHOLOGIC DESCRIPTION (particle size distribution, sorting, mineralogy, roundness, color, reaction to HCl, etc.)	H ₂ O ADDED	CASING	DRILLING COMMENTS (drilling rate, down time, blow counts, water level, drill fluid, etc.)
		TYPE	ID NUMBER	INSTR.	READING		C	Z	S	G				
97.87- 98.37	1200	S.S.	So1052-47D			M-								100% Full
						SM								
98.37- 98.87			-47C			M								100% Full
98.87- 99.37			-47B			SM								100% Full
99.37- 99.87			-47A											80% Full

A.27

W = Wet, M = Moist, D = Dry

1996 DCL/PROC/D6L/001

Core Samples

Pacific Northwest National Laboratory		DAILY BOREHOLE LOG				Boring/Well No <u>299-E33-46</u>				Depth <u>118.17-120.17</u> Date <u>7-17-01</u>				Sheet <u>16</u> of <u>32</u>	
		Location <u>241-B-110</u>				Project <u>Tank Farm Vadose Zone</u>									
Logged by <u>BN Bjornstad</u>										Drilling Contractor _____					
Reviewed by _____										Date _____					
Lithologic Class. Scheme <u>Folk/Wentworth</u>										Procedure <u>D95B1-99-GVL-01 Rev 0</u>					
Steel Tape/E-Tape <u>1</u>										Field Indicator Equip. 1) _____ 2) _____					
Depth Control Point _____															

DEPTH ()	TIME	SAMPLES		CONTAMINATION		MOISTURE	GRAPHIC LOG				LITHOLOGIC DESCRIPTION (particle size distribution, sorting, mineralogy, roundness, color, reaction to HCl, etc.)	H ₂ O ADDED	CASING	DRILLING COMMENTS (drilling rate, down time, blow counts, water level, drill fluid, etc.)		
		TYPE	ID NUMBER	INSTR.	READING		C	Z	S	G						
118.17-		S.S.	S01052	-570		SM							60% Fall			
118.67																
118.67-		S.S.		-570		SM							100% Fall			
119.17																
119.17-		S.S.		-578		M							100% Fall			
119.67																
119.67-		S.S.		-57A		M							80% Fall			
120.17																

A.29

W = Wet, M = Moist, D = Dry

Core Samples

Pacific Northwest National Laboratory		DAILY BOREHOLE LOG			Boring/Well No <u>299-E33-46</u>		Depth <u>138.3-140.3</u>		Date <u>7-17-01</u>		Sheet <u>18</u> of <u>32</u>	
Location <u>241-B-110</u>					Project <u>Tank Farm Vadose Zone</u>							
Logged by <u>BN Bjornstad</u>					Drilling Contractor _____							
Reviewed by _____					Date _____							
Lithologic Class. Scheme <u>Folk/Wentworth</u>					Procedure <u>DAT81-59-GVL-01 Rev 0</u>							
Steel Tape/E-Tape <u>1</u>					Field Indicator Equip. 1) _____ 2) _____							
Depth Control Point _____												

DEPTH ()	TIME	SAMPLES		CONTAMINATION		MOIS- TURE	GRAPHIC LOG				LITHOLOGIC DESCRIPTION (particle size distribution, sorting, mineralogy, roundness, color, reaction to HCl, etc.)	H ₂ O ADDED	CASING	DRILLING COMMENTS (drilling rate, down time, blow counts, water level, drill fluid, etc.)
		TYPE	ID NUMBER	INSTR.	READING		C	Z	S	G				
138.3	1355	S.S.	S01052-69D			W								100% Fall
138.8														Sample noticeably more <u>wet</u>
														(dk gray - wet color), loose, mod sorted, max part size = 1cm, fine sand lens in middle. WK rxn w/HCl
138.8		S.S.	-69C			M								
139.3														
139.3		S.S.	-69B			SM								
139.8														
139.8	1405	S.S.	-69A			M								
140.3														Same w/ single pebble (1cm dia).

A.31

W = Wet, M = Moist, D = Dry

Core Samples

Pacific Northwest National Laboratory		DAILY BOREHOLE LOG			Boring/Well No <u>299-E33-46</u>			Depth <u>148.4-150.4</u> Date <u>7-17-01</u>		Sheet <u>19</u> of <u>32</u>	
Location <u>241-B-110</u>					Project <u>Tank Farm Vadose Zone</u>						
Logged by <u>BN Bjornstad</u>							Drilling Contractor _____				
Reviewed by _____ Date _____							Driller _____				
Lithologic Class. Scheme <u>Folk/Wentworth</u> Procedure <u>D9T81-99-6V6-01 Rev 0</u>							Rig/Method _____				
Steel Tape/E-Tape <u>1</u> Field Indicator Equip. 1) _____ 2) _____							Depth Control Point _____				

DEPTH ()	TIME	SAMPLES		CONTAMINATION		MOIS- TURE	GRAPHIC LOG				LITHOLOGIC DESCRIPTION (particle size distribution, sorting, mineralogy, roundness, color, reaction to HCl, etc.)	NO ADDED	CASING	DRILLING COMMENTS (drilling rate, down time, blow counts, water level, drill fluid, etc.)
		TYPE	ID NUMBER	INSTR.	READING		C	Z	S	G				
148.4-		SS.	S01052-74D			M								100% Full
148.9														
148.9-		SS.	-74C			M								100% Full
149.4														
149.4-		SS.	-74B			M								100% Full
149.9														
149.9-			-74A			M								100% Full
150.4														

A.32

W = Wet, M = Moist, D = Dry

Core Samples

Pacific Northwest National Laboratory		DAILY BOREHOLE LOG			Boring/Well No <u>299-E33-46</u>		Depth <u>162.8-164.8</u>		Date <u>7-17-01</u>		Sheet <u>21</u> of <u>32</u>	
Location <u>241-B-110</u>					Project <u>Tank Farm Vadose Zone</u>							
Logged by <u>BN Bjornstad</u>						Drilling Contractor _____						
Reviewed by _____						Date _____						
Lithologic Class. Scheme <u>Folk/Wentworth</u>						Procedure <u>D9T81-99-GYL-01 Rev 0</u>						
Steel Tape/E-Tape <u>1</u>						Field Indicator Equip. 1) _____ 2) _____						
Depth Control Point _____												

DEPTH ()	TIME	SAMPLES		CONTAMINATION		MOIS- TURE	GRAPHIC LOG				LITHOLOGIC DESCRIPTION (particle size distribution, sorting, mineralogy, roundness, color, reaction to HCl, etc.)	H ₂ O ADDED	CASING	DRILLING COMMENTS (drilling rate, down time, blow counts, water level, drill fluid, etc.)
		TYPE	ID NUMBER	INSTR.	READING		C	Z	S	G				
162.8-		s.s.	Solo 52-82D			M								100% Full
163.3														
163.3+		s.s.	-82C			M								100% Full
163.8														
163.8+		s.s.	-82B			M								100% Full
164.3														
164.3-		s.s.	-82A			M								90% Full
164.8														

A.34

W = Wet, M = Moist, D = Dry

Core Samples

Pacific Northwest National Laboratory	DAILY BOREHOLE LOG	Boring/Well No <u>299-E33-46</u>	Depth <u>169.4-171.4</u> Date <u>7-18-01</u>	Sheet <u>23</u> of <u>32</u>
		Location <u>241-B-110</u>	Project <u>Tank Farm/Vadose Zone</u>	

Logged by <u>BN Bjornstad</u>	Drilling Contractor _____
Reviewed by _____ Date _____	Driller _____
Lithologic Class. Scheme <u>Folk/Wentworth</u> Procedure <u>D9701-99-6VL-01 Rev 0</u>	Rig/Method _____
Steel Tape/E-Tape <u>1</u> Field Indicator Equip. 1) _____ 2) _____	Depth Control Point _____

DEPTH ()	TIME	SAMPLES		CONTAMINATION		MOIS- TURE	GRAPHIC LOG				LITHOLOGIC DESCRIPTION (particle size distribution, sorting, mineralogy, roundness, color, reaction to HCl, etc.)	H ₂ O ADDED	CASING	DRILLING COMMENTS (drilling rate, down time, blow counts, water level, drill fluid, etc.)
		TYPE	ID NUMBER	INSTR.	READING		C	Z	S	G				
169.4- 169.9	940	S.S.	501052-86D			M								100% Full
169.4- 170.4		S.S.	-86C			M								100% Full
170.4- 170.9		S.S.	-86B			M								100% Full
170.9- 171.4		S.S.	-86A			M								80% Full

W = Wet, M = Moist, D = Dry

A.36

Core Samples

Pacific Northwest National Laboratory	DAILY BOREHOLE LOG	Boring/Well No <u>299-E33-46</u>	Depth <u>178.1-180.1</u> Date <u>7-18-01</u>	Sheet <u>24</u> of <u>32</u>
		Location <u>241-B-110</u>	Project <u>Tank Farm Vadose Zone</u>	

Logged by <u>B.N. Bjornstad</u>	Drilling Contractor _____
Reviewed by _____ Date _____	Driller _____
Lithologic Class. Scheme <u>Folk/Wentworth</u> Procedure <u>D9781-99-GVL-01 Rev 0</u>	Rig/Method _____
Steel Tape/E-Tape <u>1</u> Field Indicator Equip. 1) _____ 2) _____	Depth Control Point _____

DEPTH ()	TIME	SAMPLES		CONTAMINATION		MOIS- TURE	GRAPHIC LOG				LITHOLOGIC DESCRIPTION (particle size distribution, sorting, mineralogy, roundness, color, reaction to HCl, etc.)	H ₂ O ADDED	CASING	DRILLING COMMENTS (drilling rate, down time, blow counts, water level, drill fluid, etc.)		
		TYPE	ID NUMBER	INSTR.	READING		C	Z	S	G						
178.1		S.S.	501052-900			M							90% Fall			
178.6																
178.6			-90C			SM							Same as above but max part. size = 0.5 cm (sm. pebble)	95% Fall		
179.1													slightly drier than above			
179.1			-90B			M							Sand, md-v.crs. sand, 90% crs-v.crs. sand, 10% md sand, 5/5/2, loose well sorted, max part size = granule, no rxn w/ HCl	100% Fall		
179.6													"salt and pepper", wk rxn w/ HCl			
179.6			-90A			M							Same as immed. above	70% Fall		
180.1																

A.37

W = Wet, M = Moist, D = Dry

Core Samples

Pacific Northwest National Laboratory		DAILY BOREHOLE LOG			Boring/Well No <u>299-E33-46</u>		Depth <u>199.2-201.2</u> Date <u>7-18-01</u>		Sheet <u>26 of 32</u>	
Logged by <u>BN Bjornstad</u>					Drilling Contractor _____					
Reviewed by _____ Date _____					Driller _____					
Lithologic Class. Scheme <u>Folk/Wentworth</u>					Procedure <u>D9T21-99-GVL-01 Rev 0</u>					
Steel Tape/E-Tape <u>1</u>					Field Indicator Equip. 1) _____ 2) _____					
					Depth Control Point _____					

DEPTH ()	TIME	SAMPLES		CONTAMINATION		MOIS- TURE	GRAPHIC LOG				LITHOLOGIC DESCRIPTION (particle size distribution, sorting, mineralogy, roundness, color, reaction to HCl, etc.)	H ₂ O ADDED	CASING	DRILLING COMMENTS (drilling rate, down time, blow counts, water level, drill fluid, etc.)		
		TYPE	ID NUMBER	INSTR.	READING		C	Z	S	G						
199.2		S.S.	S01052	101D		M							90% Full			
199.7																
199.7		S.S.	-101C			M							100% Full			
200.2																
200.2		S.S.	-101B			M							100% Full			
200.7																
200.7		S.S.	-101A			M							80% Full			
201.2																

A.39

W = Wet, M = Moist, D = Dry

Core Samples

Pacific Northwest National Laboratory		DAILY BOREHOLE LOG			Boring/Well No <u>299-E33-46</u>		Depth <u>208.7-210.7</u> Date <u>7-18-01</u>		Sheet <u>27 of 32</u>	
		Location <u>241-B-110</u>			Project <u>Tank Farm Vadose Zone</u>					
Logged by <u>BN Bjornstad</u>					Drilling Contractor _____					
Reviewed by _____					Date _____					
Lithologic Class. Scheme <u>Folk/Wentworth</u>					Procedure <u>D9781-77-GVL-01 Rev 0</u>					
Steel Tape/E-Tape <u>1</u>					Field Indicator Equip. 1) _____ 2) _____					
					Depth Control Point _____					

DEPTH ()	TIME	SAMPLES		CONTAMINATION		MOIS- TURE	GRAPHIC LOG				LITHOLOGIC DESCRIPTION (particle size distribution, sorting, mineralogy, roundness, color, reaction to HCl, etc.)	H ₂ O ADDED	CASING	DRILLING COMMENTS (drilling rate, down time, blow counts, water level, drill fluid, etc.)
		TYPE	ID NUMBER	INSTR.	READING		C	Z	S	G				
208.7			S01051-105D			M	[Hand-drawn lithologic log showing sand texture]						70% Full	
209.2														
209.2			-105C			M							85% Full	
209.7														
209.7			-105B			M							100% Full	
210.2														
210.2			-105A			M							70% Full	
210.7														

A.40

W = Wet, M = Moist, D = Dry

Core Samples

Pacific Northwest National Laboratory		DAILY BOREHOLE LOG			Boring/Well No <u>299-E33-46</u>		Depth <u>217.7-219.7</u>		Date <u>7-18-01</u>		Sheet <u>28 of 32</u>	
		Location <u>241-B-110</u>			Project <u>Tank Farm Vadose Zone</u>							
Logged by <u>BN Bjornstad</u>						Drilling Contractor _____						
Reviewed by _____						Date _____						
Lithologic Class. Scheme <u>Folk/Wentworth</u>						Procedure <u>D9781-99-GV-01 Rev 0</u>						
Steel Tape/E-Tape <u>1</u>						Field Indicator Equip. 1) _____ 2) _____						
						Rig/Method _____						
						Depth Control Point _____						

DEPTH ()	TIME	SAMPLES		CONTAMINATION		MOISTURE	GRAPHIC LOG				LITHOLOGIC DESCRIPTION (particle size distribution, sorting, mineralogy, roundness, color, reaction to HCl, etc.)	H ₂ O ADDED	CASING	DRILLING COMMENTS (drilling rate, down time, blow counts, water level, drill fluid, etc.)
		TYPE	ID NUMBER	INSTR.	READING		C	Z	S	G				
217.7-218.2		SS	S01052-1	29D		M	X							70% Full
218.2-218.7		SS	-109C			M	/							100% Full
218.7-219.2		SS	-109B			M	/							100% Full
219.2-219.7		SS	-109A			M	/							100% Full

A.41

W = Wet, M = Moist, D = Dry

Core Samples

Pacific Northwest National Laboratory		DAILY BOREHOLE LOG			Boring/Well No <u>299-E33-46</u>			Depth <u>220.4-222.4</u> Date <u>7-18-01</u>		Sheet <u>29 of 32</u>				
Location <u>241-B-110</u>					Project <u>Tank Farm Vadose Zone</u>									
Logged by <u>B.N. Bjornstad</u>					Drilling Contractor _____									
Reviewed by _____ Date _____					Driller _____									
Lithologic Class. Scheme <u>Folk/Wentworth</u> Procedure <u>D9T81-99-GVL-01 Rev 0</u>					Rig/Method _____									
Steel Tape/E-Tape <u>1</u> Field Indicator Equip. 1) _____ 2) _____					Depth Control Point _____									
DEPTH ()	TIME	SAMPLES		CONTAMINATION		MOIS- TURE	GRAPHIC LOG				LITHOLOGIC DESCRIPTION (particle size distribution, sorting, mineralogy, roundness, color, reaction to HCl, etc.)	H ₂ O ADDED	CASING	DRILLING COMMENTS (drilling rate, down time, blow counts, water level, drill fluid, etc.)
		TYPE	ID NUMBER	INSTR.	READING		C	Z	S	G				
220.4-		S.S.	501052-110 D			M	[Graphic Log: 220.4 to 220.9]						70% Full	Plio-Pleistocene Overbank-Eolian Deposit?
220.9							[Graphic Log: 220.9 to 220.9]							
220.9+		S.S.	-110C			W	[Graphic Log: 220.9 to 221.4]						Wet at bottom	
221.4						M	[Graphic Log: 221.4 to 221.4]						80% Full	
221.4-		S.S.	-110B			M	[Graphic Log: 221.4 to 221.9]						100% Full	
221.9							[Graphic Log: 221.9 to 221.9]							
221.9+		S.S.	-110A			M	[Graphic Log: 221.9 to 222.4]						100% Full	
222.4							[Graphic Log: 222.4 to 222.4]							

W = Wet, M = Moist, D = Dry

A.42

Core Samples

Pacific Northwest National Laboratory		DAILY BOREHOLE LOG			Boring/Well No <u>299-E33-46</u>		Depth <u>245.5 - 254.4</u> Date <u>7-18-01</u>		Sheet <u>32 of 32</u>		
Location <u>241-B-110</u>					Project <u>Tank Farm Vadose Zone</u>						
Logged by <u>BN Bjornstad</u>							Drilling Contractor _____				
Reviewed by _____							Date _____				
Lithologic Class. Scheme <u>Folk / Wentworth</u>							Procedure <u>D9781-99-GVL-01 Rev 0</u>				
Steel Tape/E-Tape _____							Field Indicator Equip. 1) _____ 2) _____				
Depth Control Point _____											

DEPTH ()	TIME	SAMPLES		CONTAMINATION		MOIS- TURE	GRAPHIC LOG				LITHOLOGIC DESCRIPTION (particle size distribution, sorting, mineralogy, roundness, color, reaction to HCl, etc.)	H ₂ O ADDED	CASING	DRILLING COMMENTS (drilling rate, down time, blow counts, water level, drill fluid, etc.)
		TYPE	ID NUMBER	INSTR.	READING		C	Z	S	G				
245.5 246.0		S.S.	S01052-123A			SM	X	X	X	X			50% Full	
							v.u.	0.0.0	0.0.0	0.0.0				
							6.9'	6.00'						
252.9 253.4		S.S.	-126C			SM	X	X	X	X			50% Full	
							0.0.0	0.0.0	0.0.0					
							5.4/2	v. poorly sorted, max						
							part size = 1/4 cm	loose, no rxn w/ HCl						
253.4 253.9		S.S.	-126B			M	0.0.0	0.0.0	0.0.0				100% Full	
							0.0.0	0.0.0	0.0.0					
							0.0.0	0.0.0	0.0.0					
253.9 254.4		S.S.	-126A			SM	0.0.0	0.0.0	0.0.0				50% Full	
							0.0.0	0.0.0	0.0.0					
							X	X	X					

A.45

W = Wet, M = Moist, D = Dry

1995.DL/PROC/BL/001

Appendix B-1

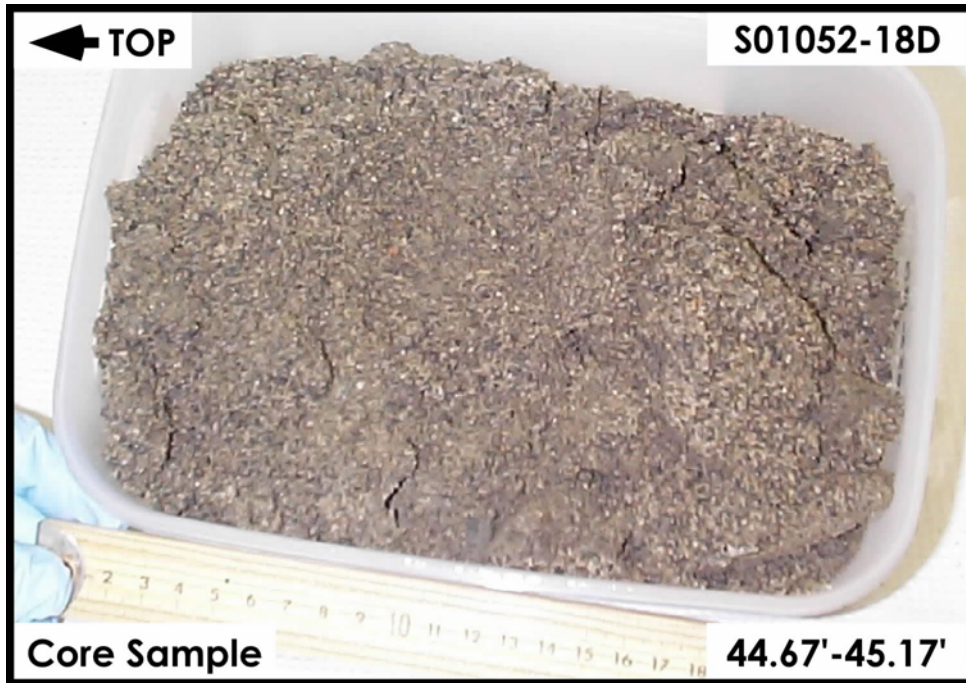
299-E33-46 Splitspoon Core Sample Photographs

Appendix B-1

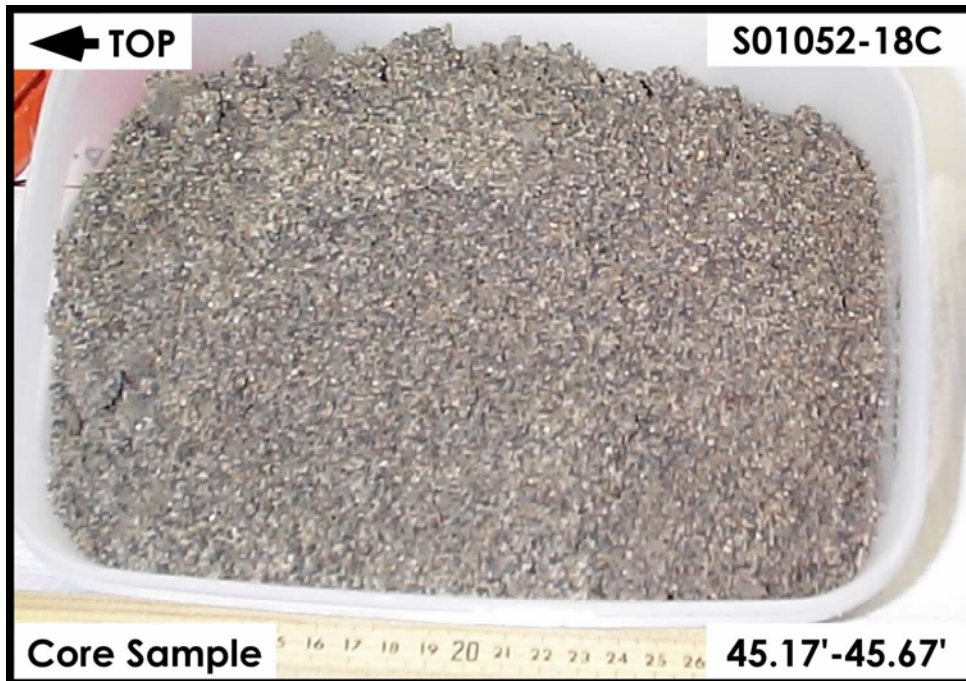
299-E33-46

Splitspoon Core Sample Photographs

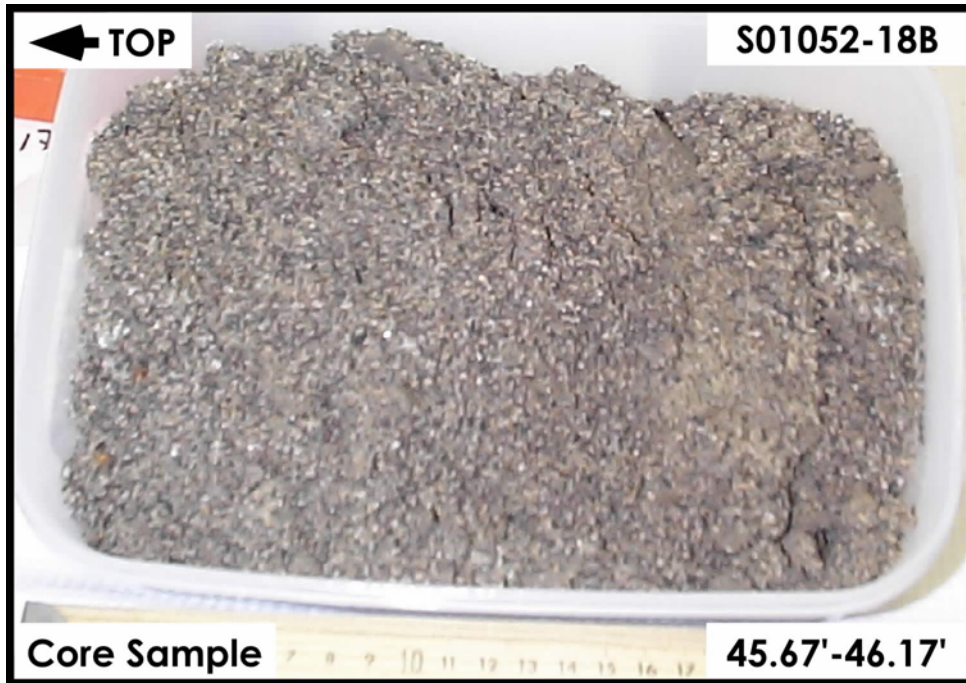
The following photographs were taken during the opening of the samples for performing the geologic descriptions and for aliquoting for chemical analyses. The photographs are sequenced from shallow depths to deeper depths. On the figure and in the captions we show the sample number designation, the orientation of the picture/core sample, the depth interval below ground surface that the sample represents and the lithology name assigned to the sample.



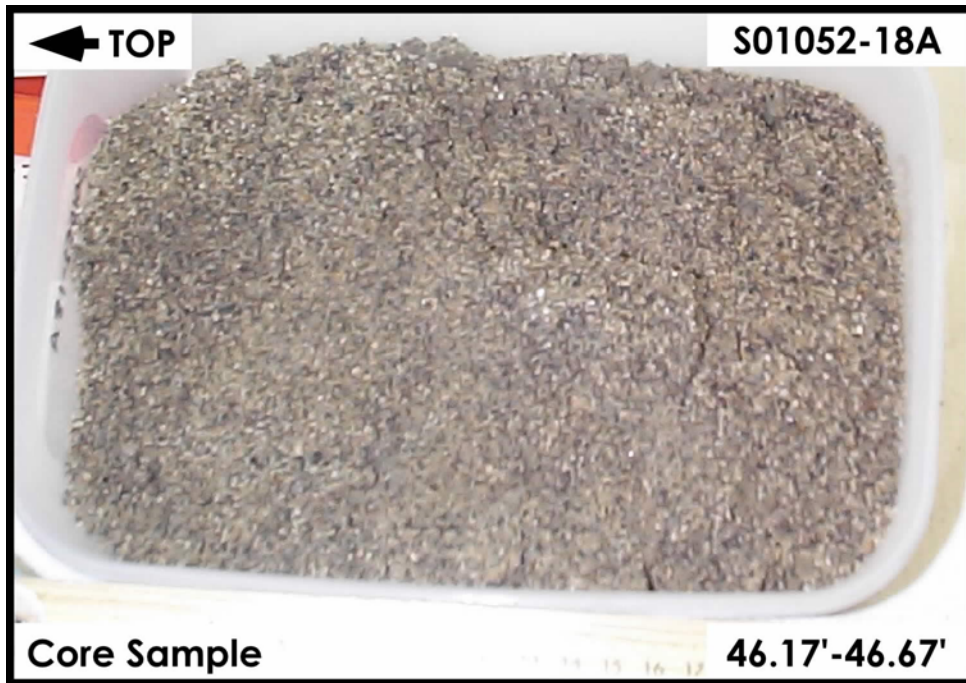
H2-Upper Sand and Gravel Sequence



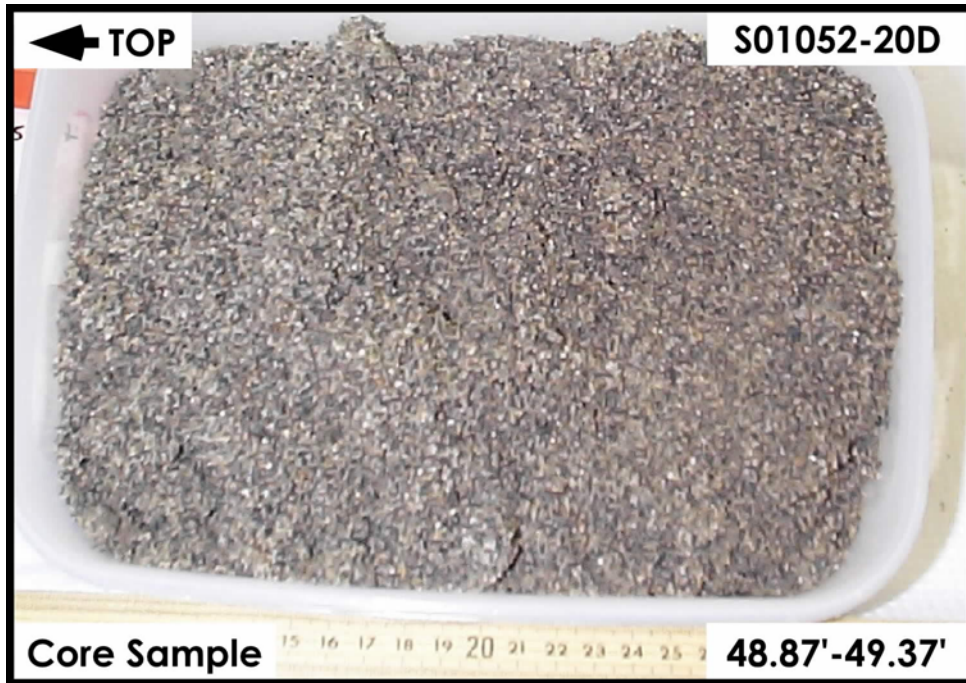
H2-Upper Sand and Gravel Sequence



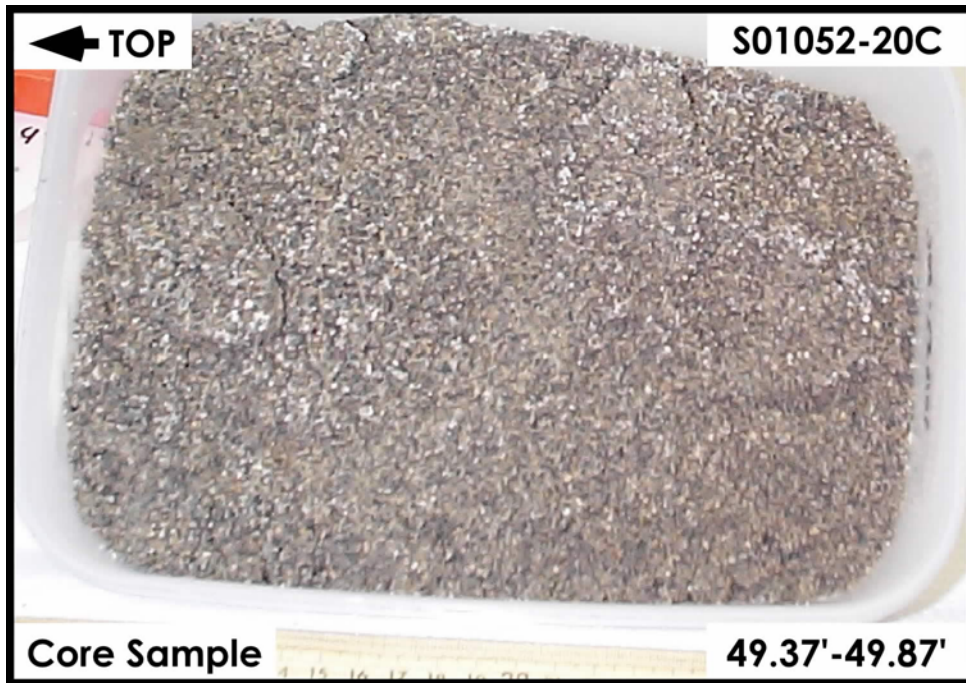
H2-Upper Sand and Gravel Sequence



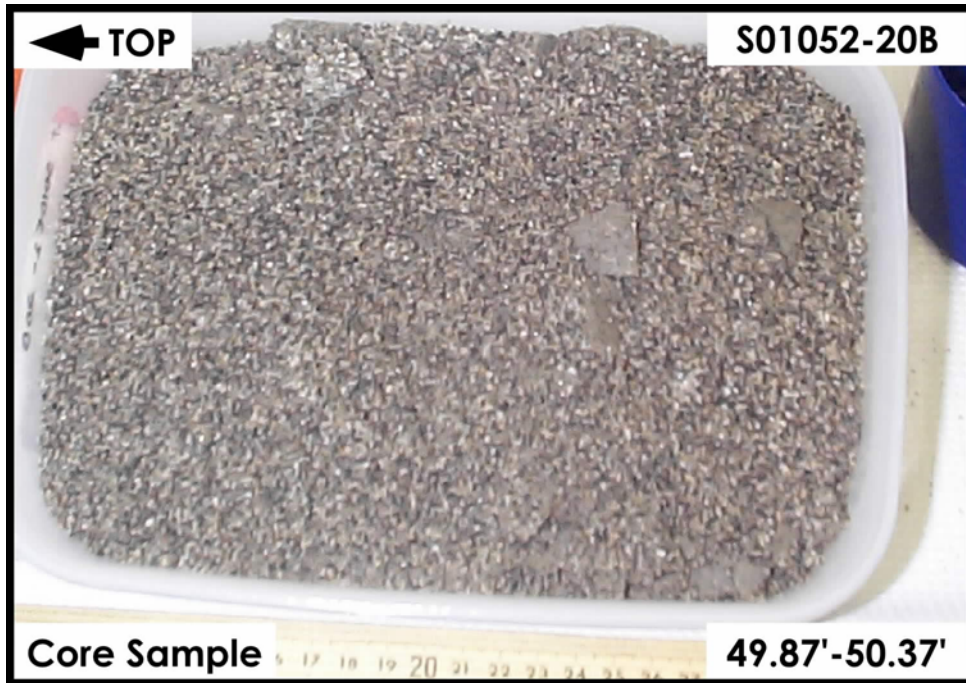
H2-Upper Sand and Gravel Sequence



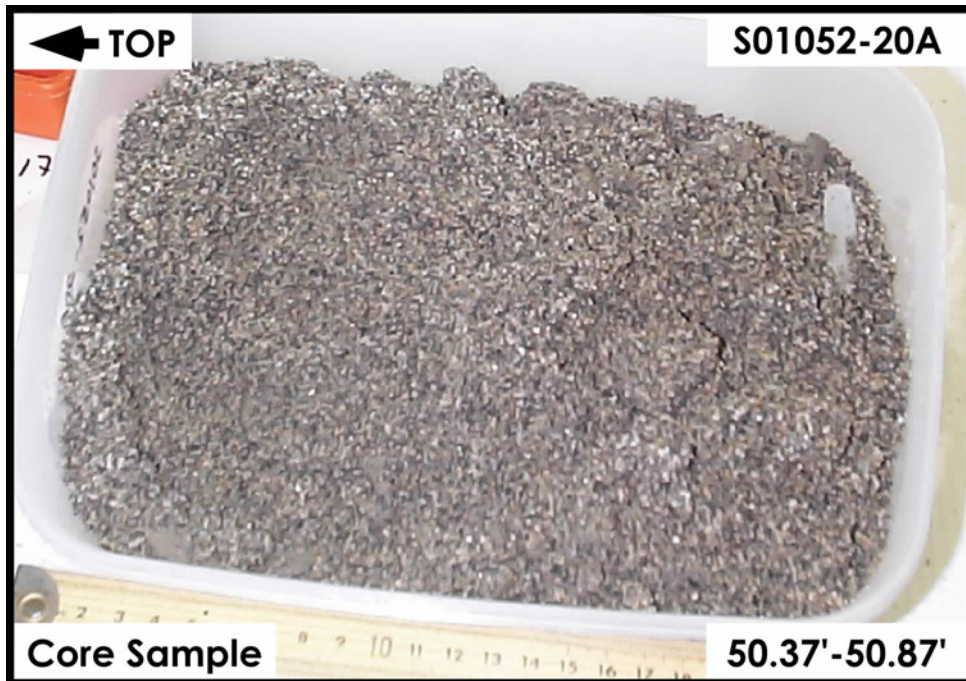
H2-Upper Sand and Gravel Sequence



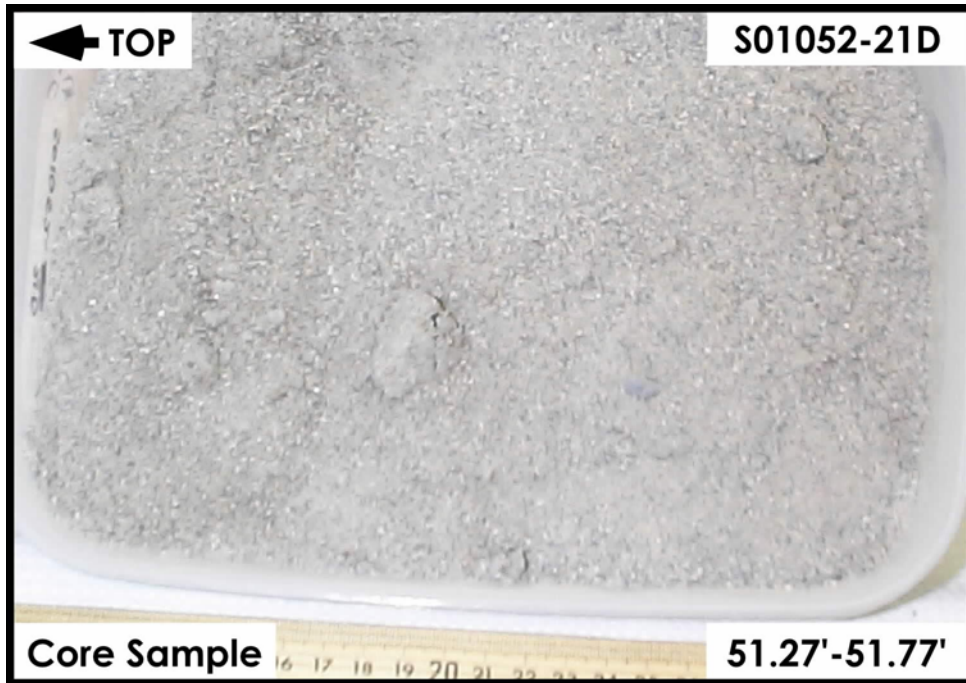
H2-Upper Sand and Gravel Sequence



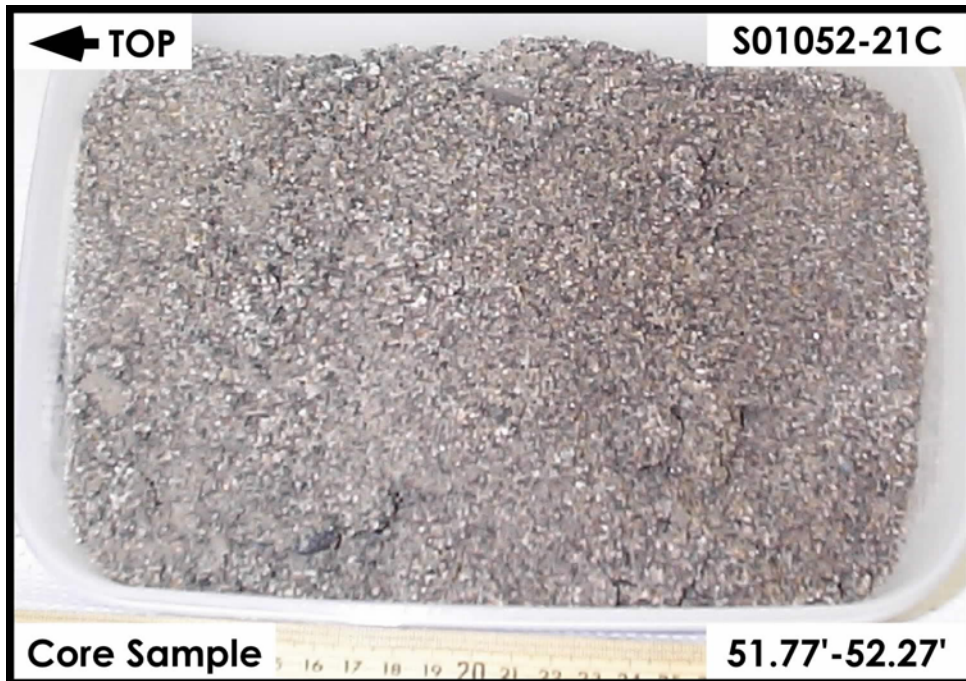
H2-Upper Sand and Gravel Sequence



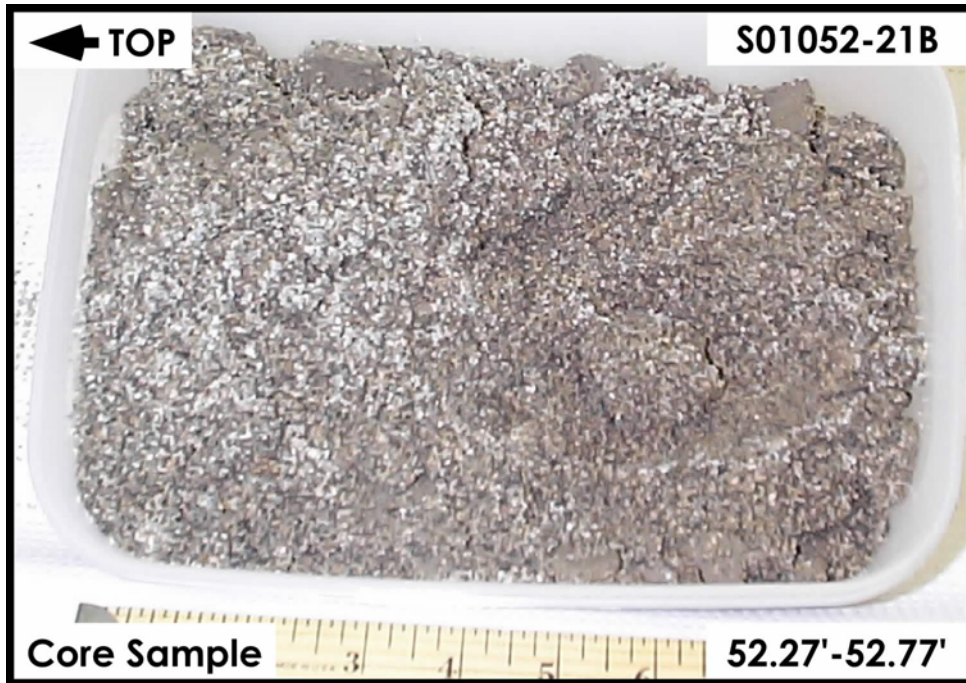
H2-Upper Sand and Gravel Sequence



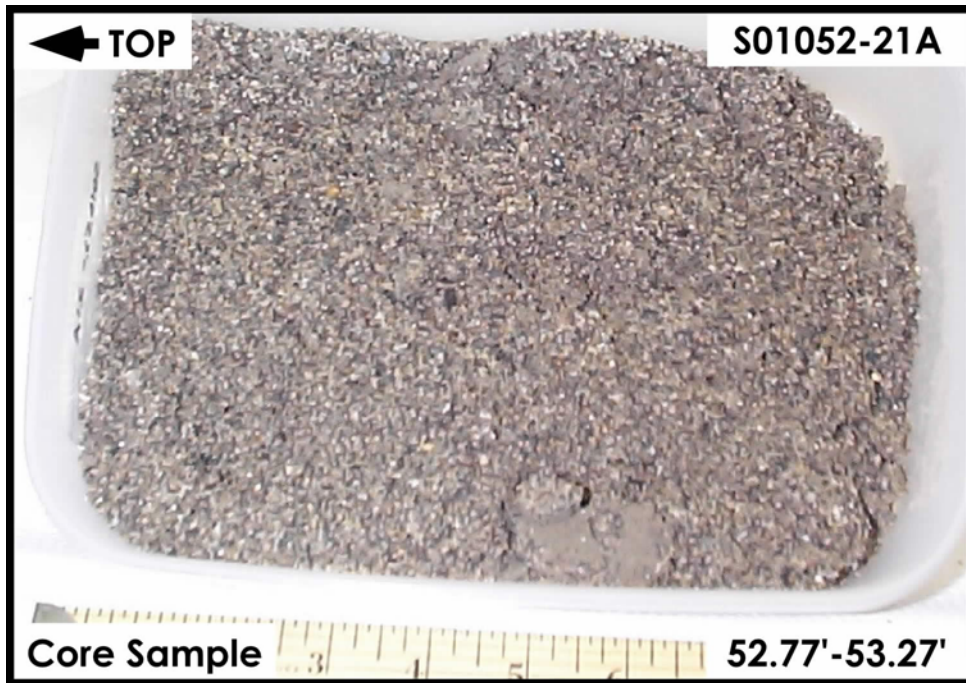
H2-Upper Sand and Gravel Sequence



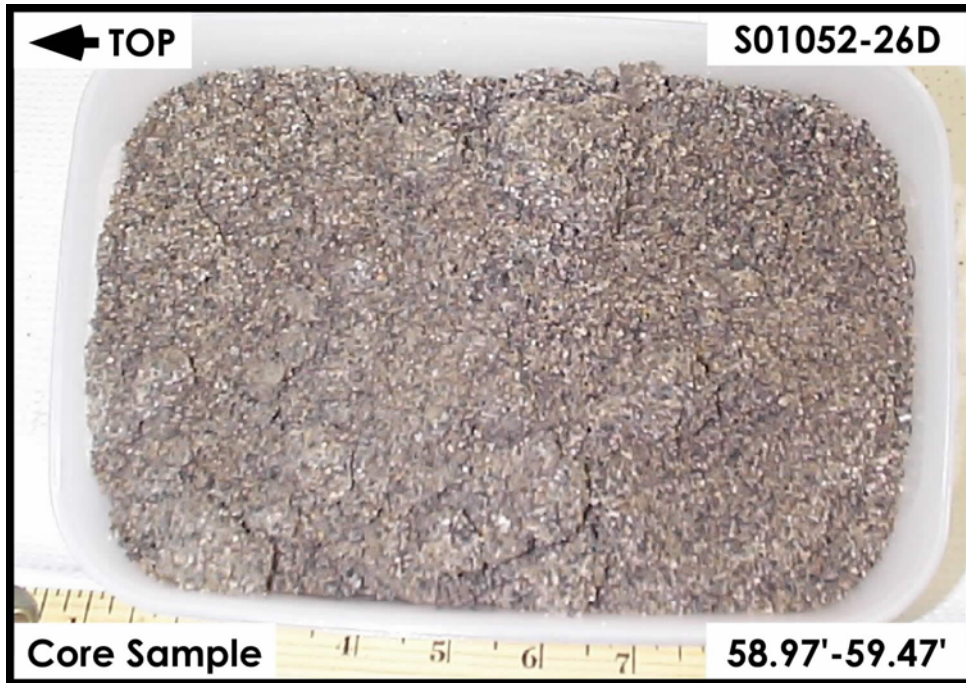
H2-Upper Sand and Gravel Sequence



H2-Upper Sand and Gravel Sequence



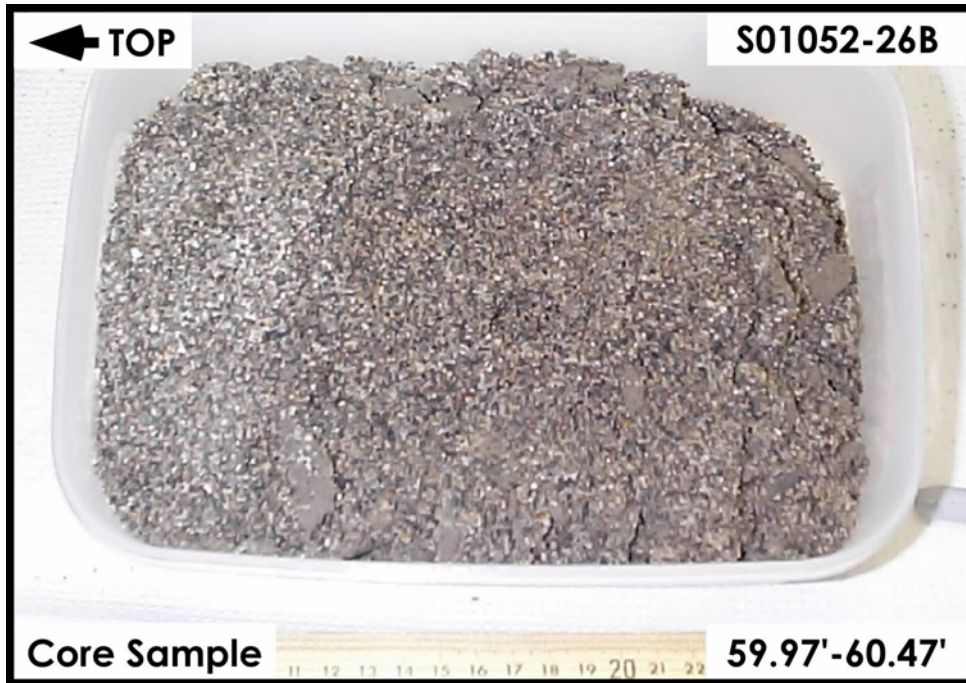
H2-Upper Sand and Gravel Sequence



H2-Upper Sand and Gravel Sequence



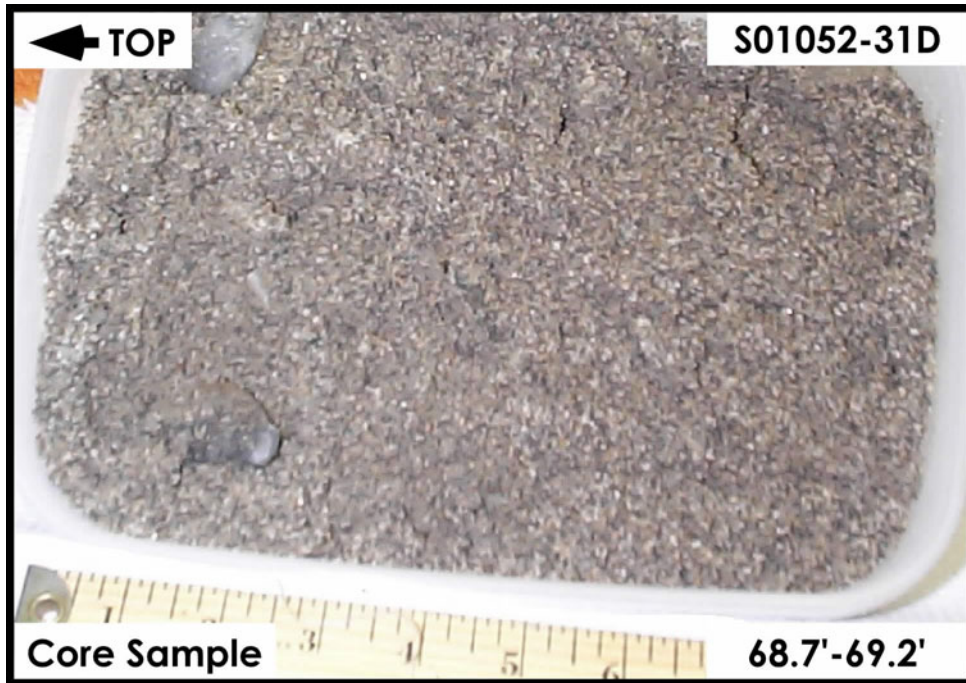
H2-Upper Sand and Gravel Sequence



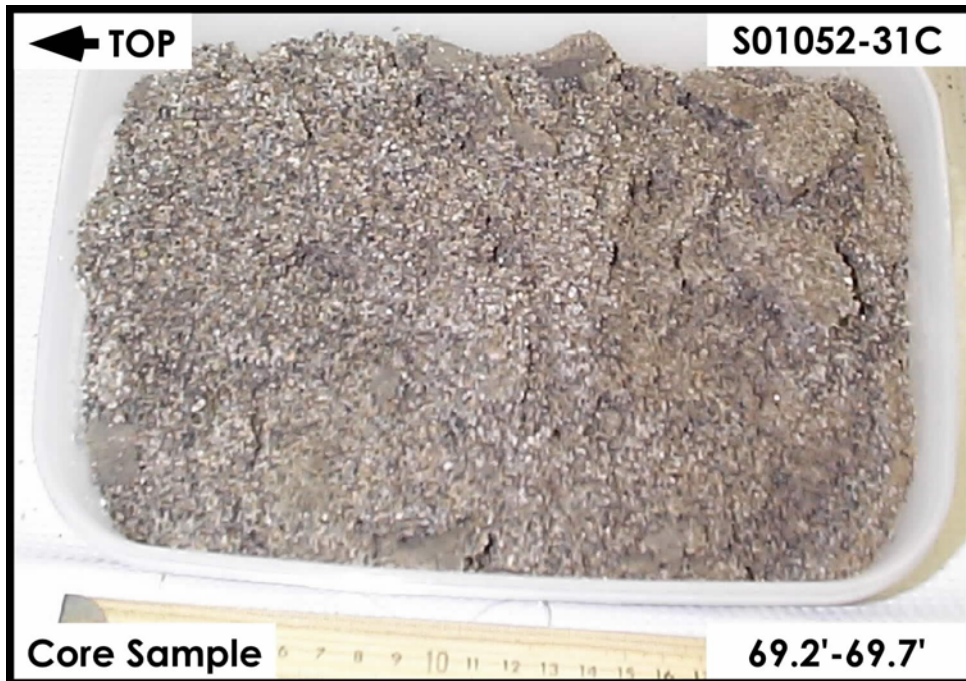
H2-Upper Sand and Gravel Sequence



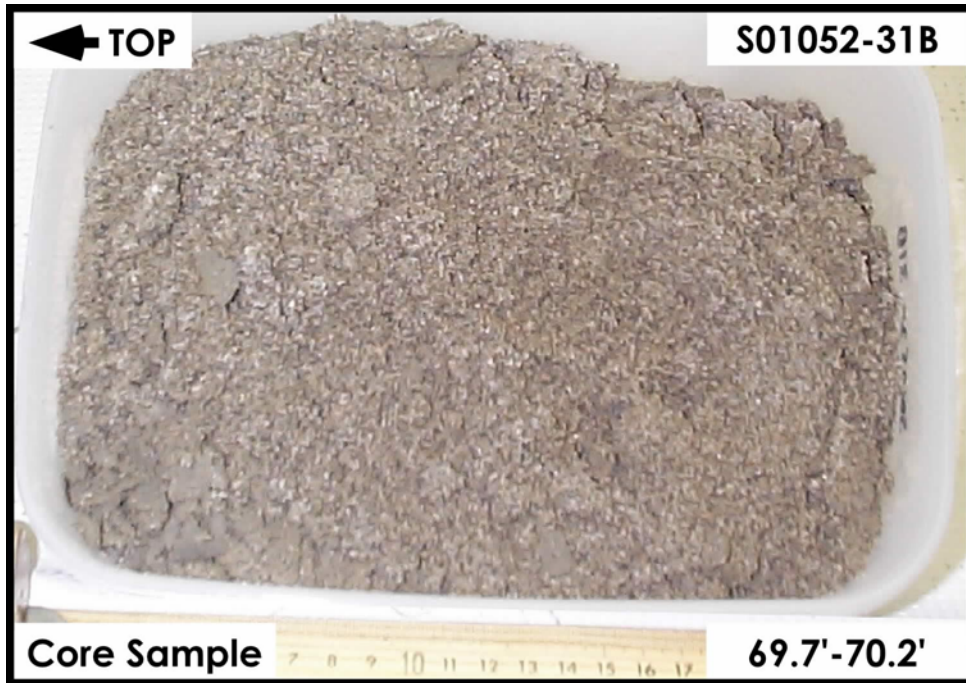
H2-Upper Sand and Gravel Sequence



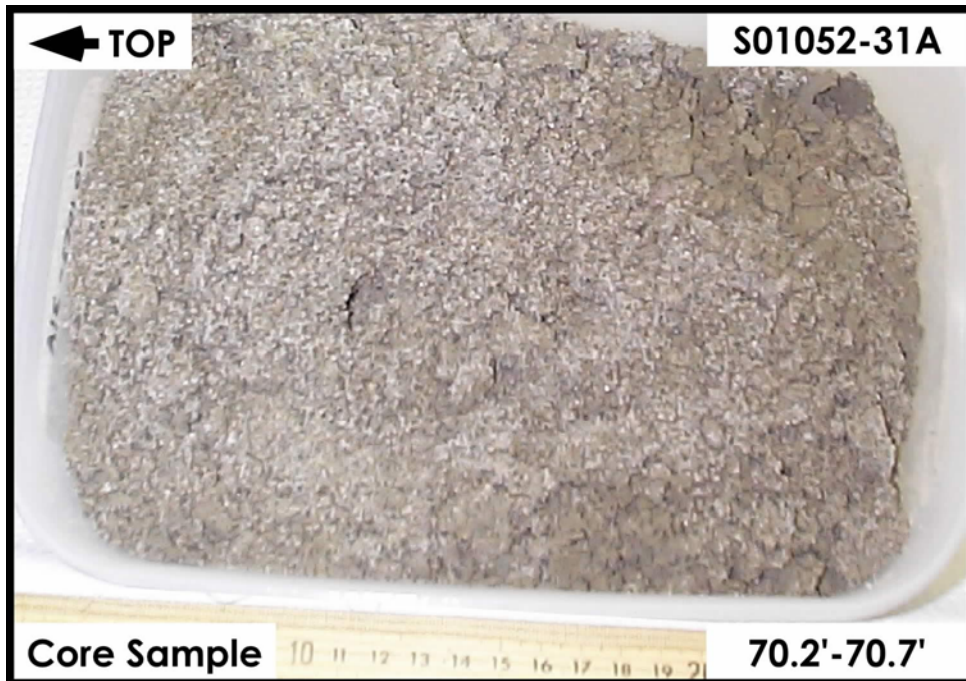
H2-Upper Sand and Gravel Sequence



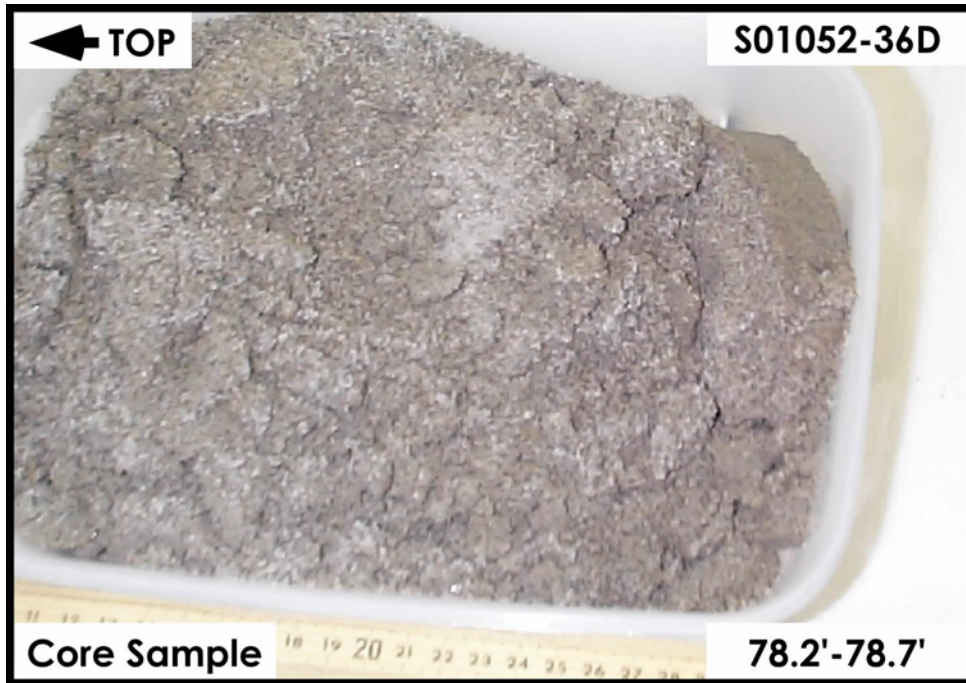
H2-Upper Sand and Gravel Sequence



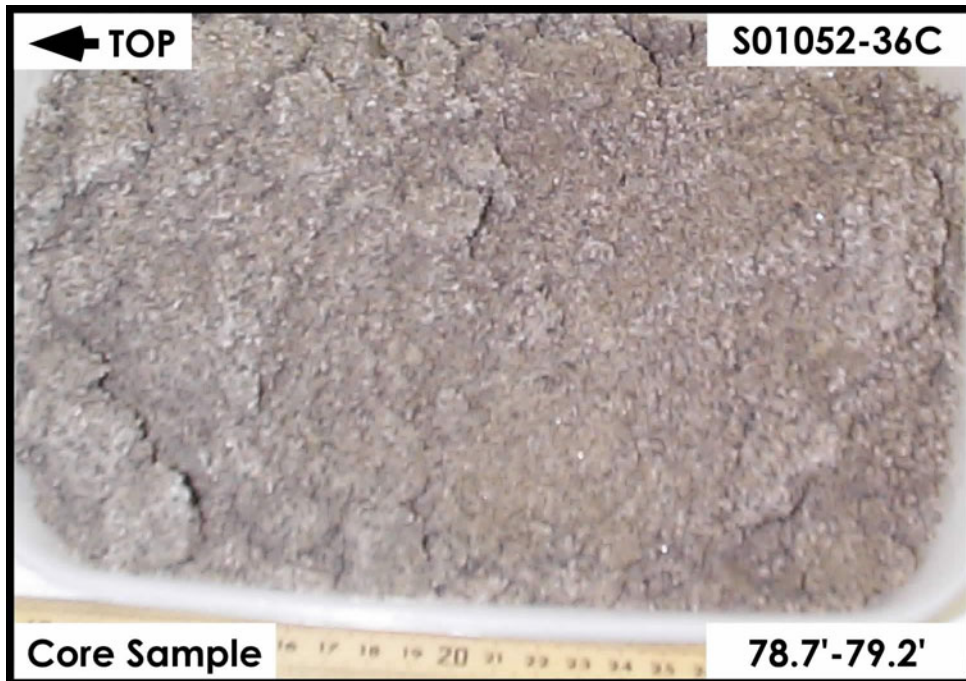
H2-Upper Sand and Gravel Sequence



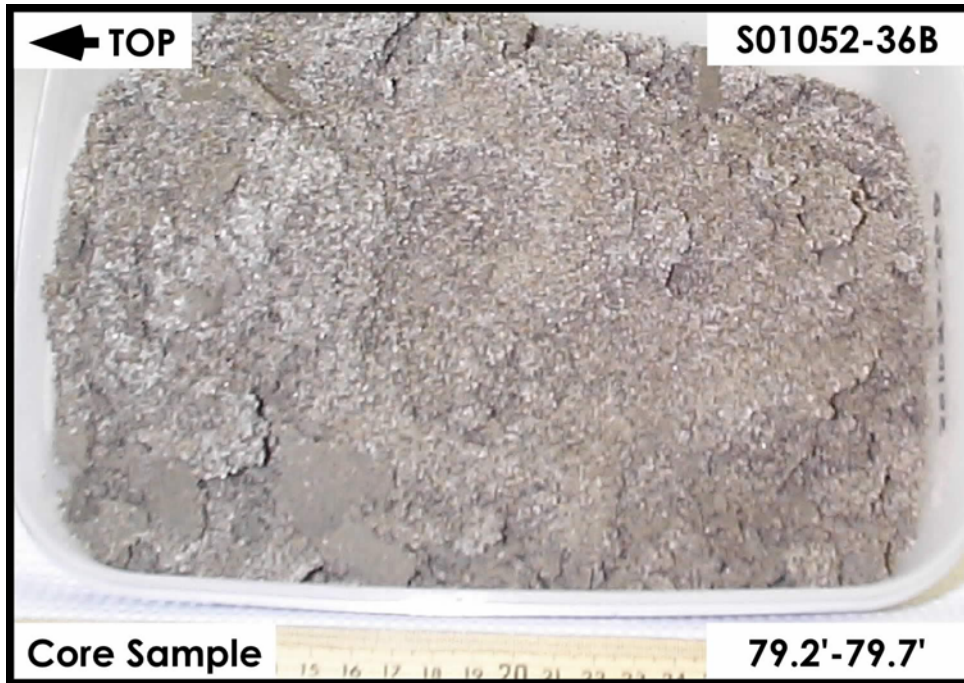
H2-Upper Sand and Gravel Sequence



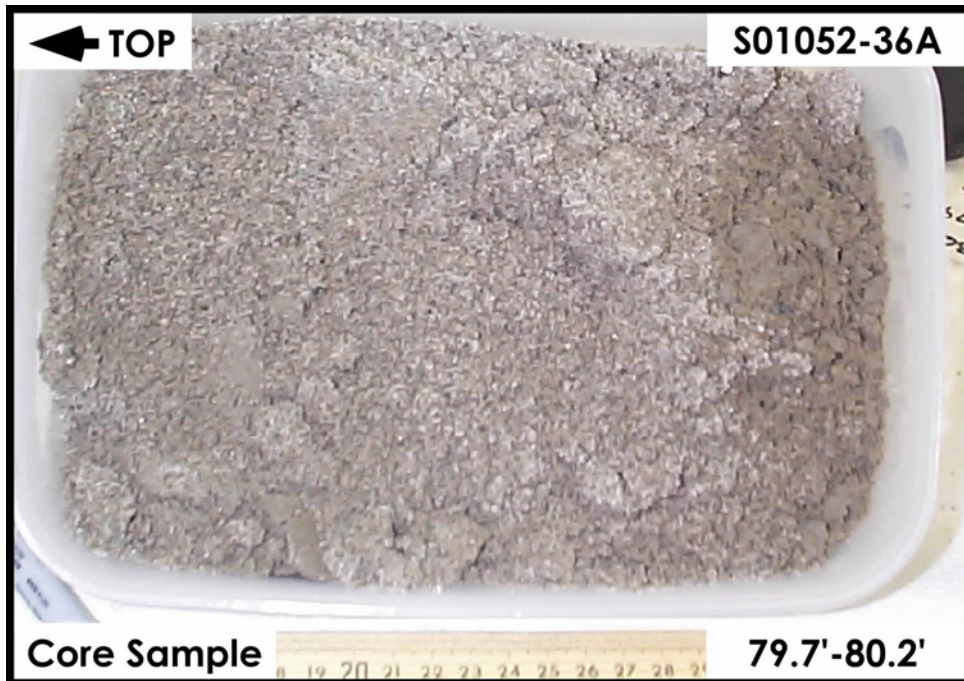
H2-Upper Sand and Gravel Sequence



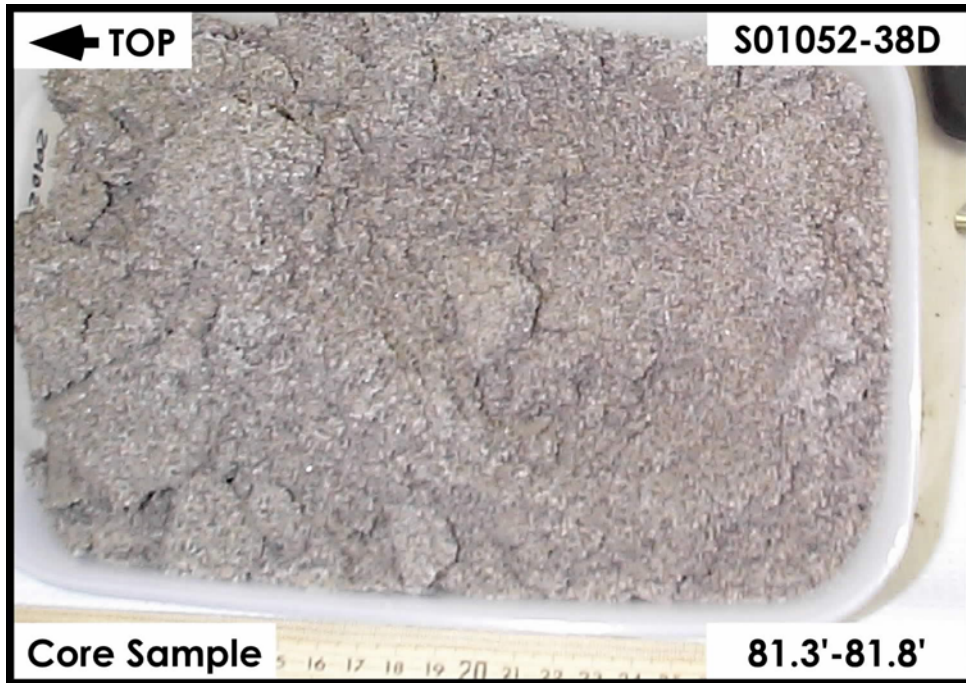
H2-Upper Sand and Gravel Sequence



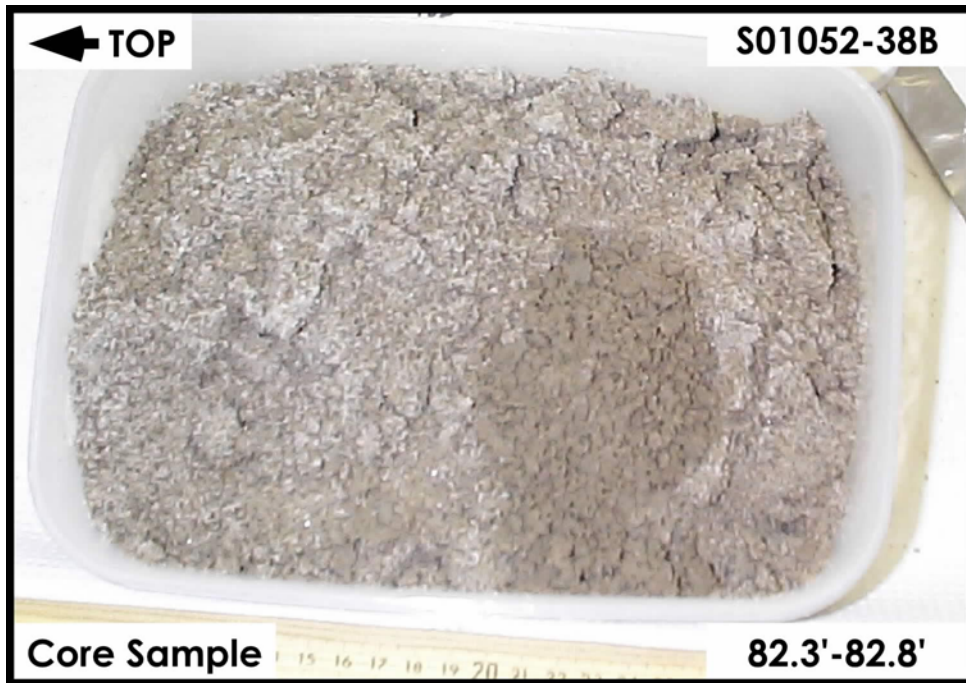
H2-Upper Sand and Gravel Sequence



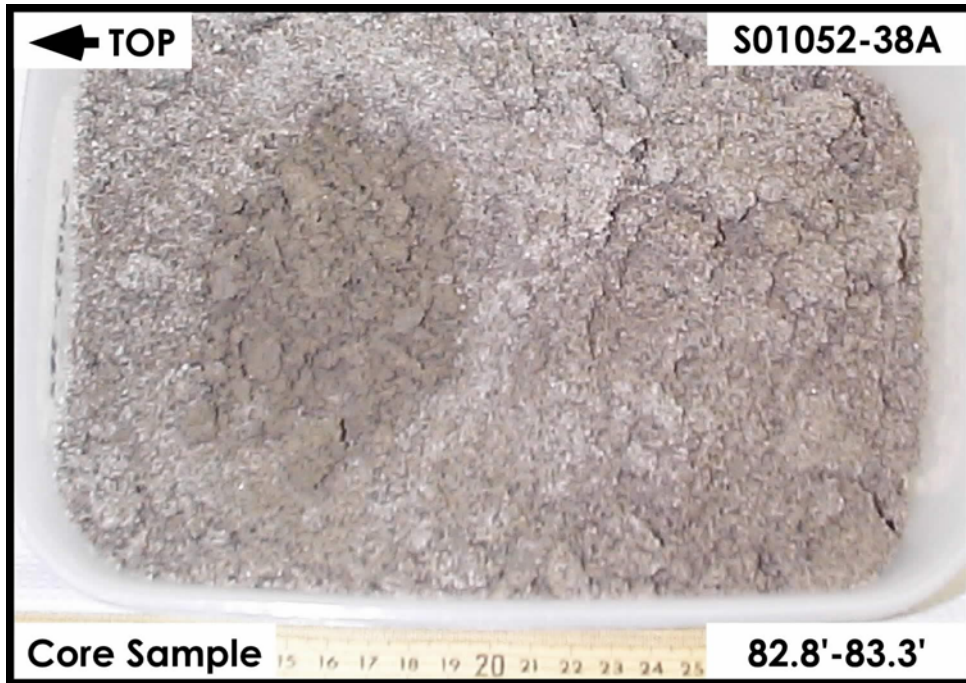
H2-Upper Sand and Gravel Sequence



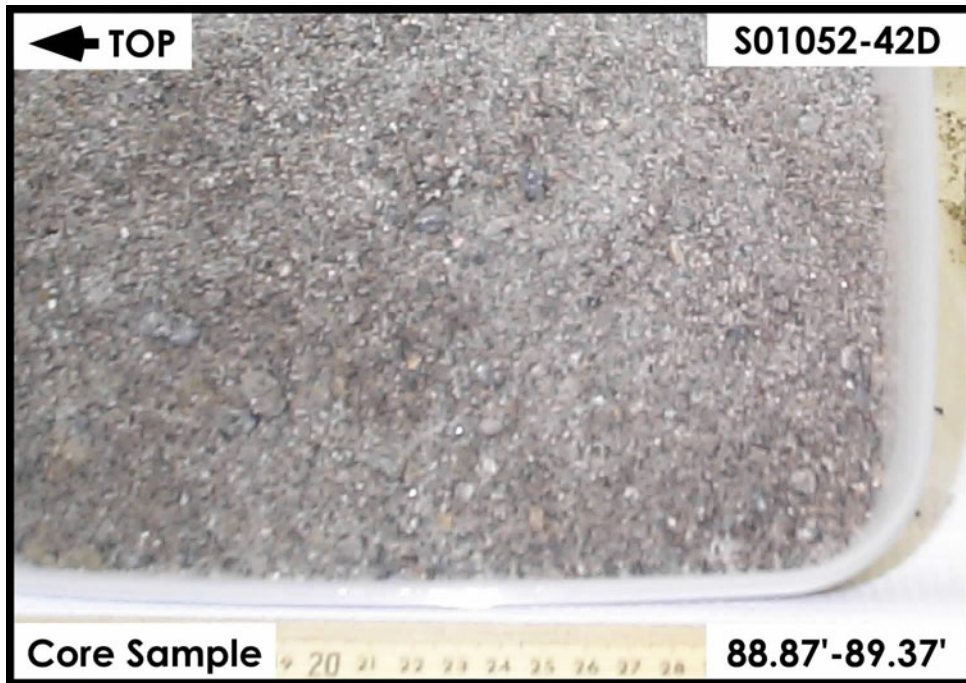
H2-Upper Sand and Gravel Sequence



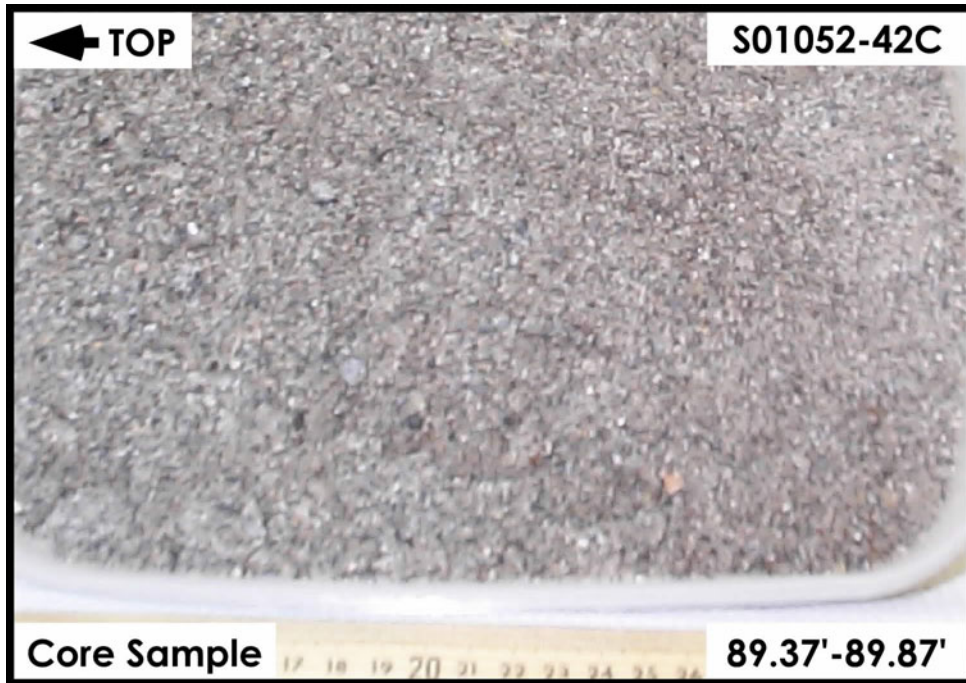
H2-Upper Sand and Gravel Sequence



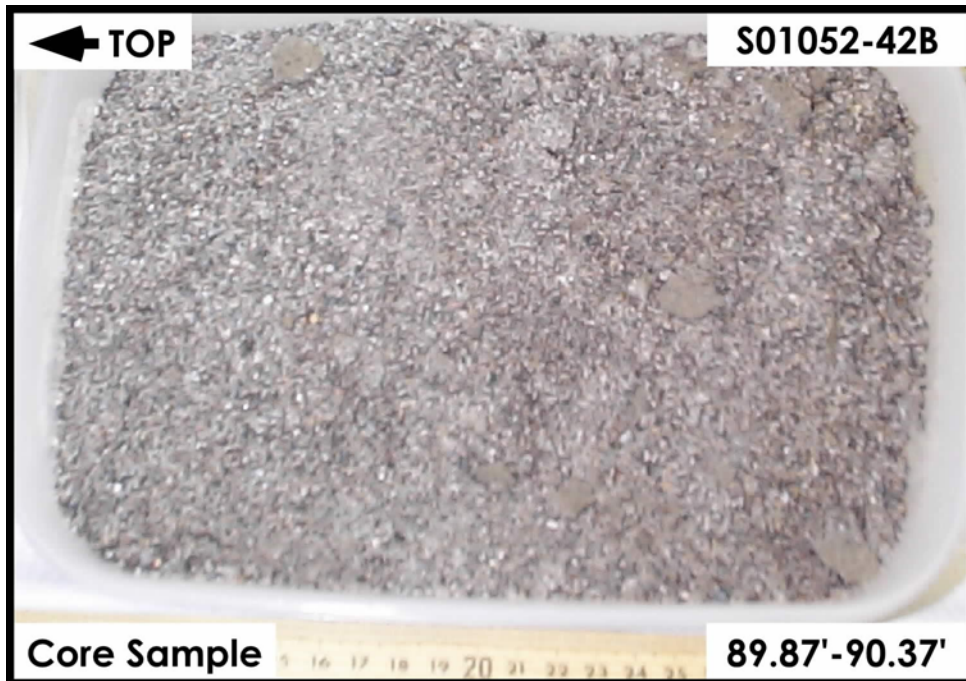
H2-Upper Sand and Gravel Sequence



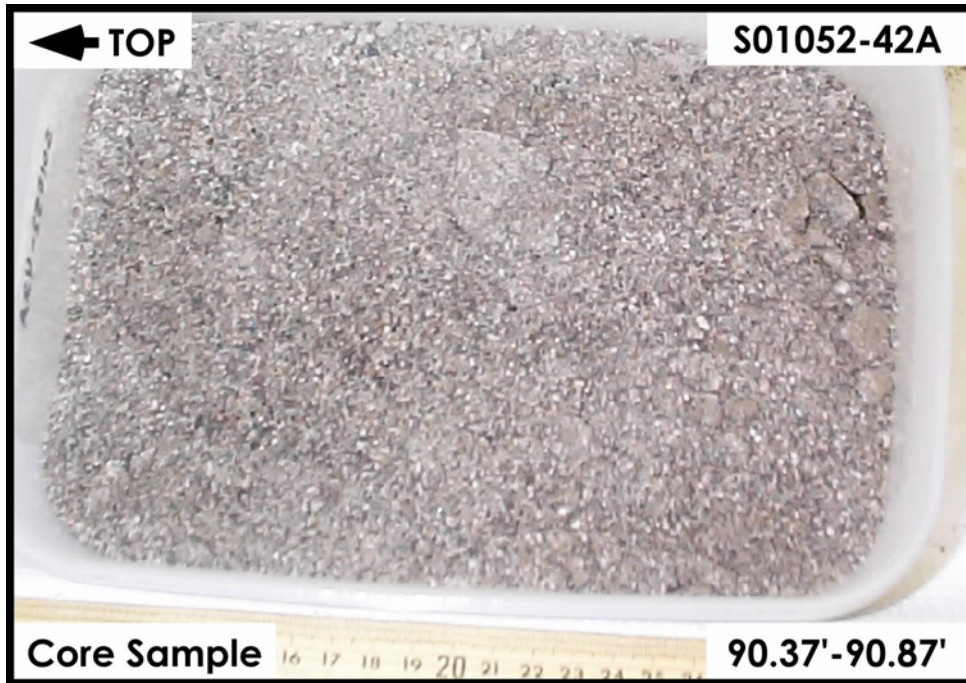
H2-Upper Sand and Gravel Sequence



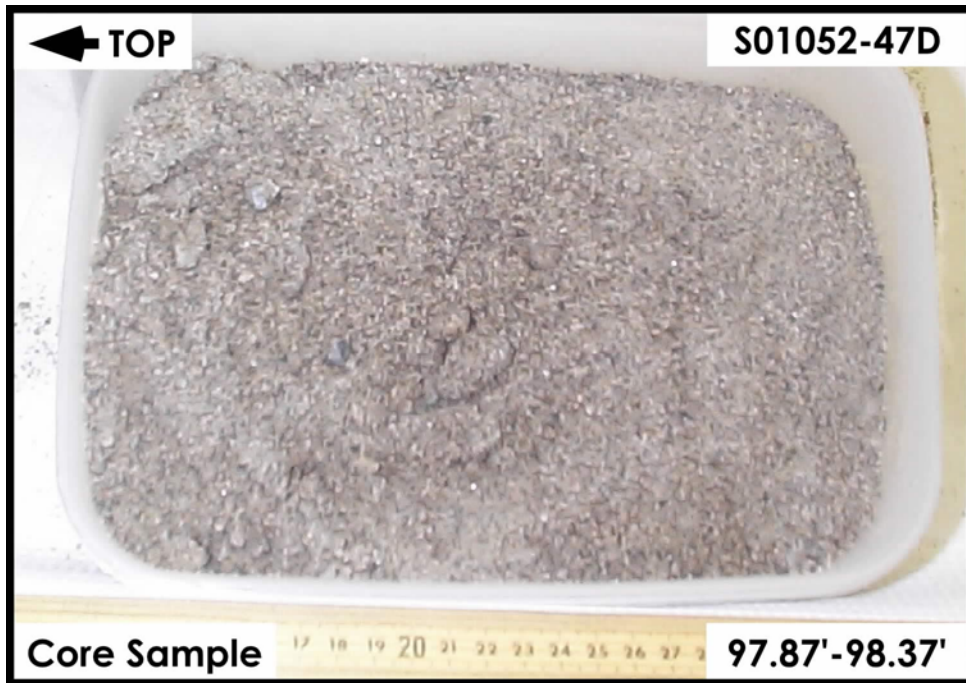
H2-Upper Sand and Gravel Sequence



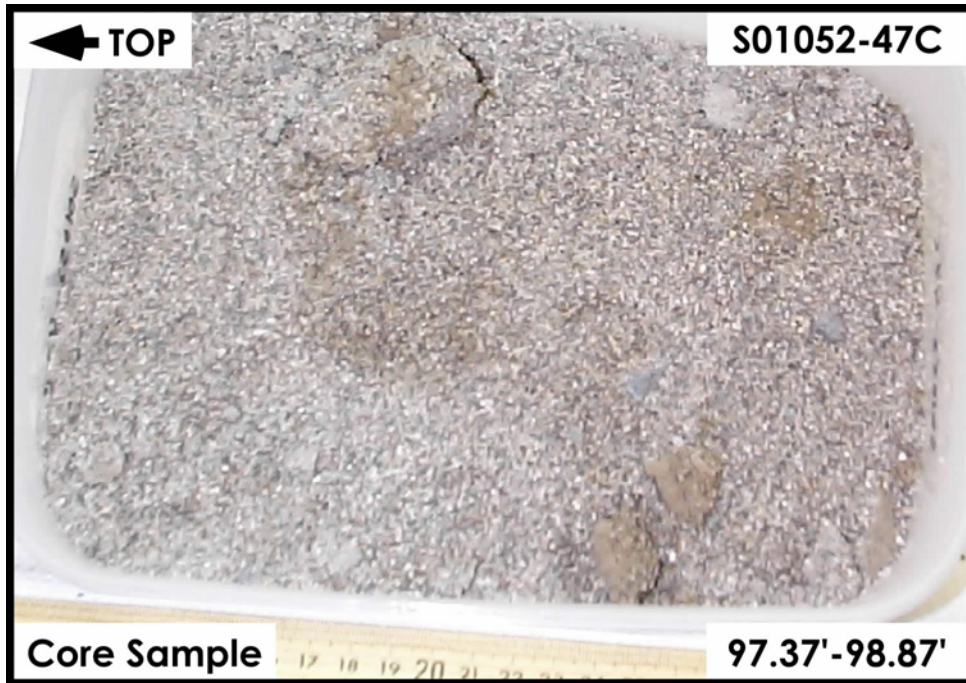
H2-Upper Sand and Gravel Sequence



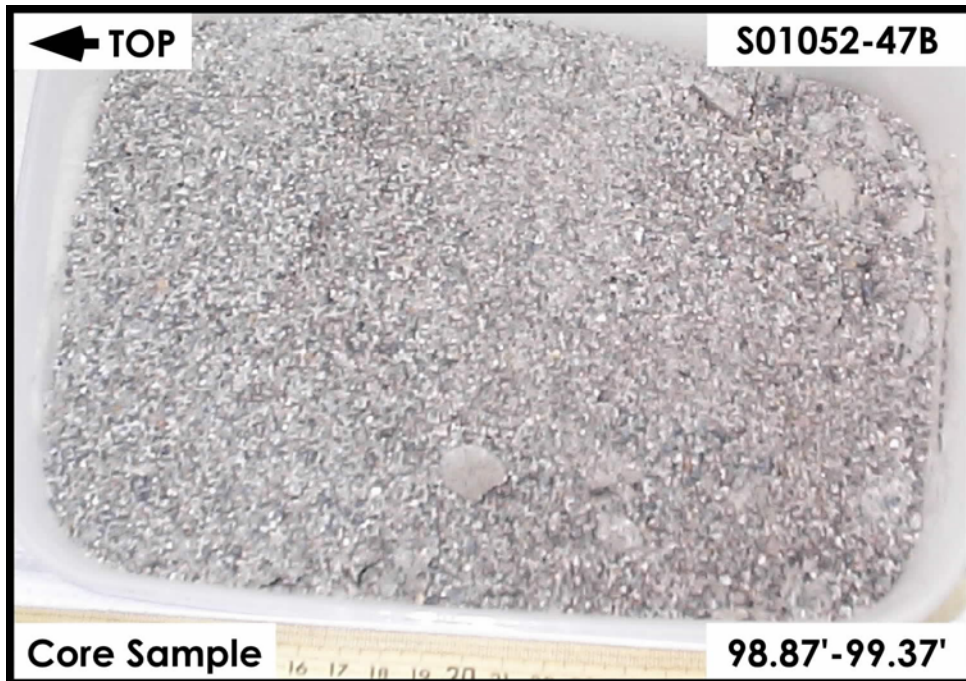
H2-Upper Sand and Gravel Sequence



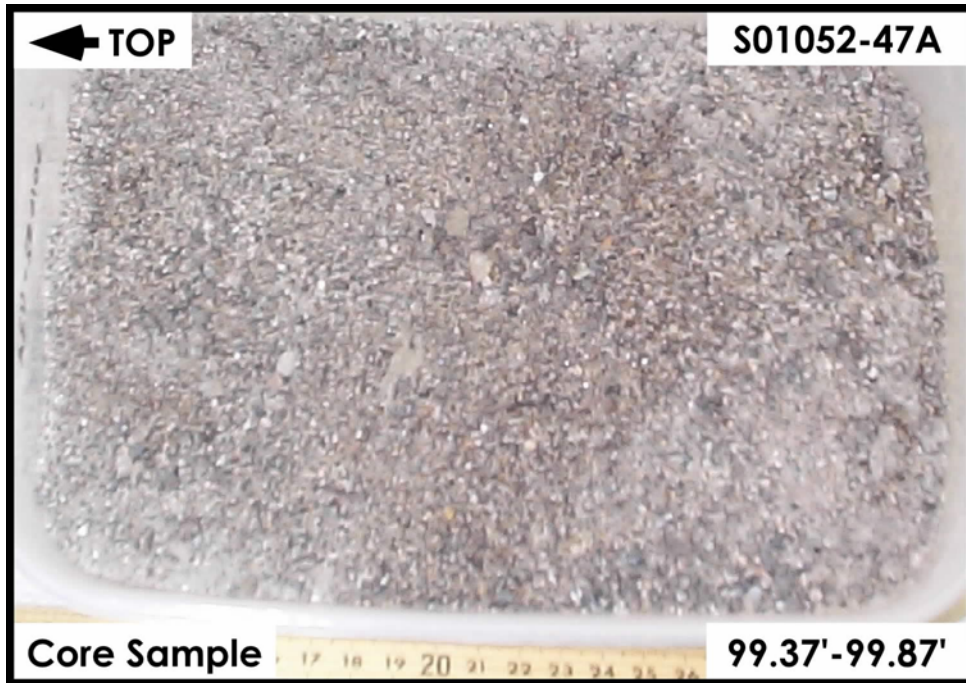
H2-Upper Sand and Gravel Sequence



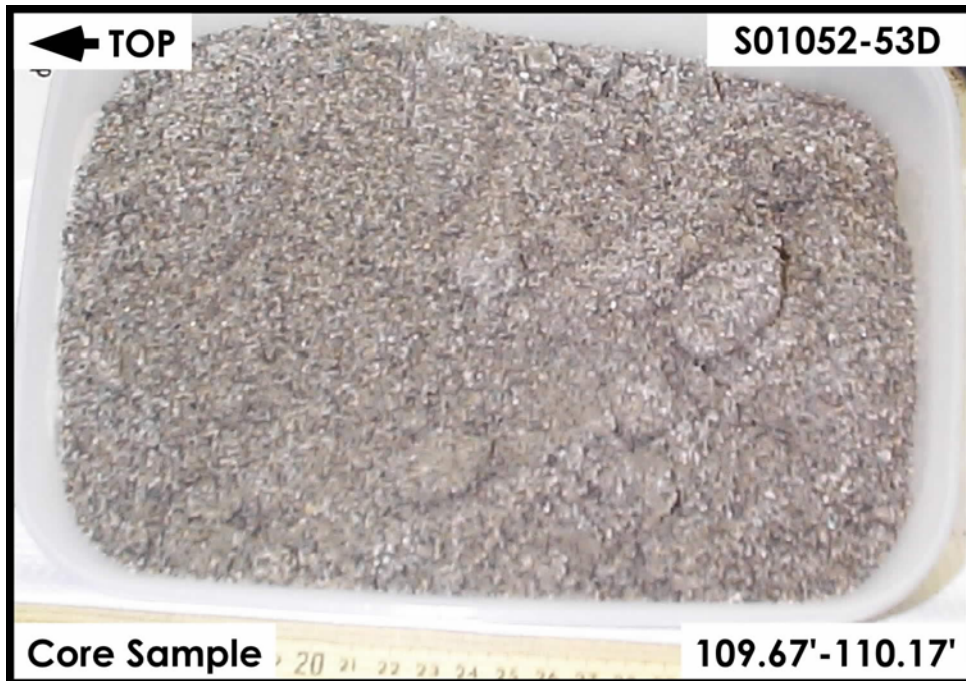
H2-Upper Sand and Gravel Sequence



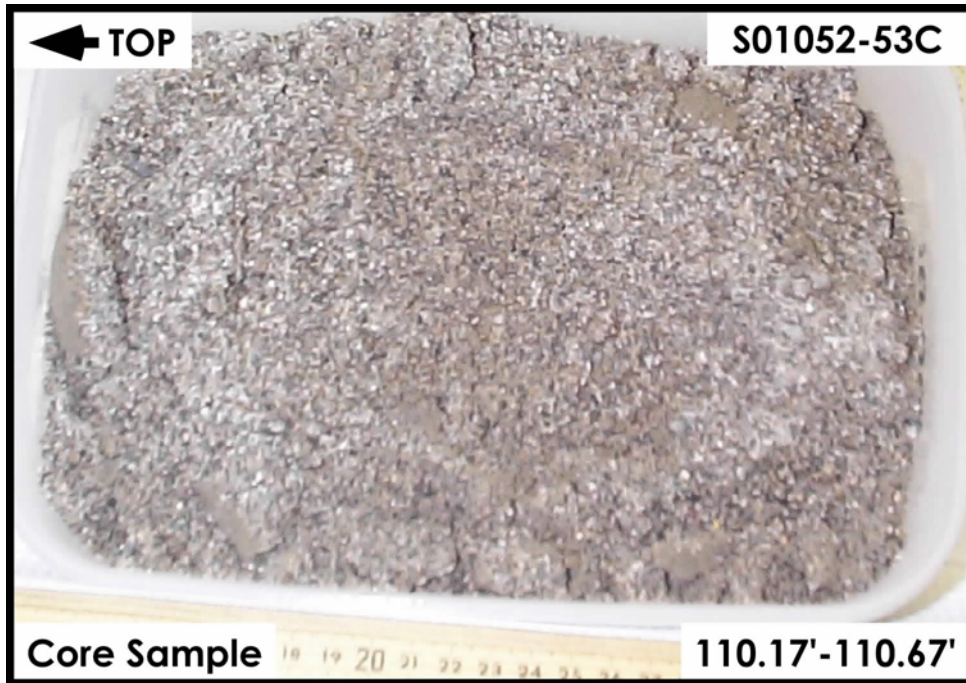
H2-Upper Sand and Gravel Sequence



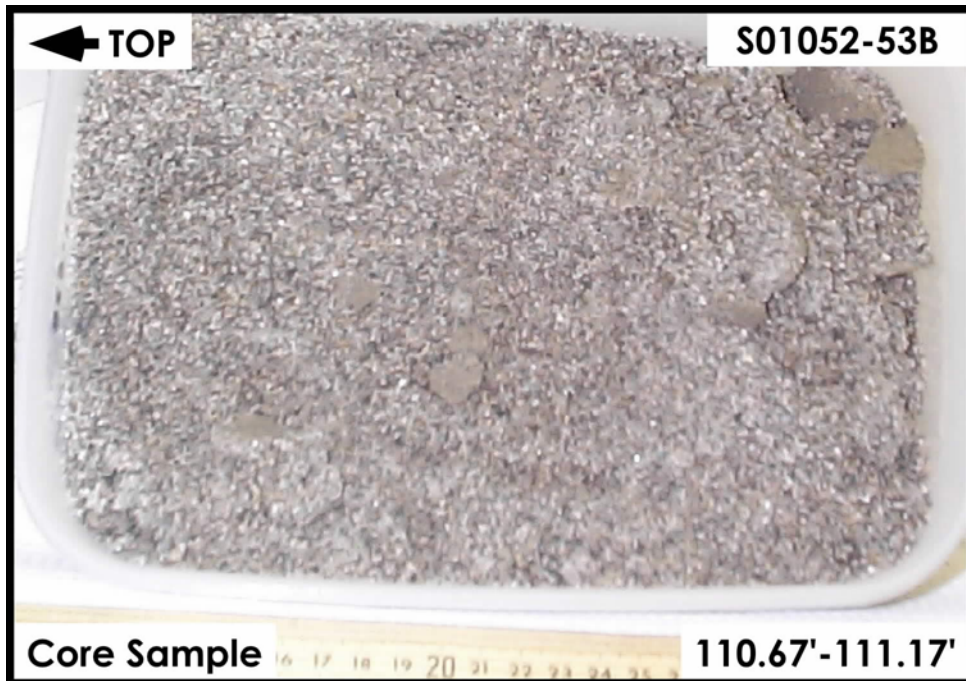
H2-Upper Sand and Gravel Sequence



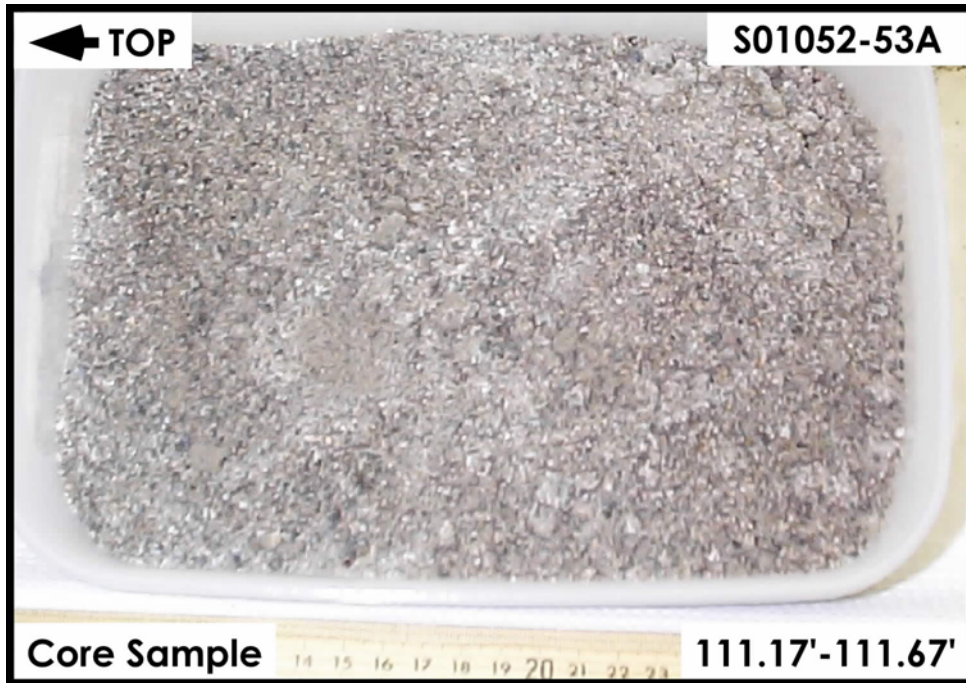
H2-Upper Sand and Gravel Sequence



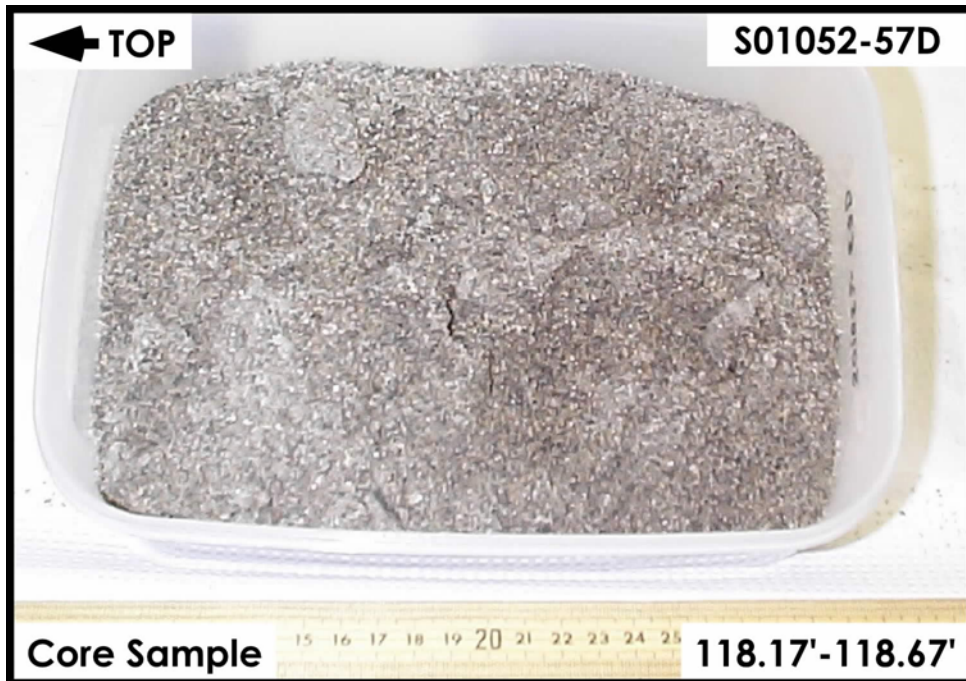
H2-Upper Sand and Gravel Sequence



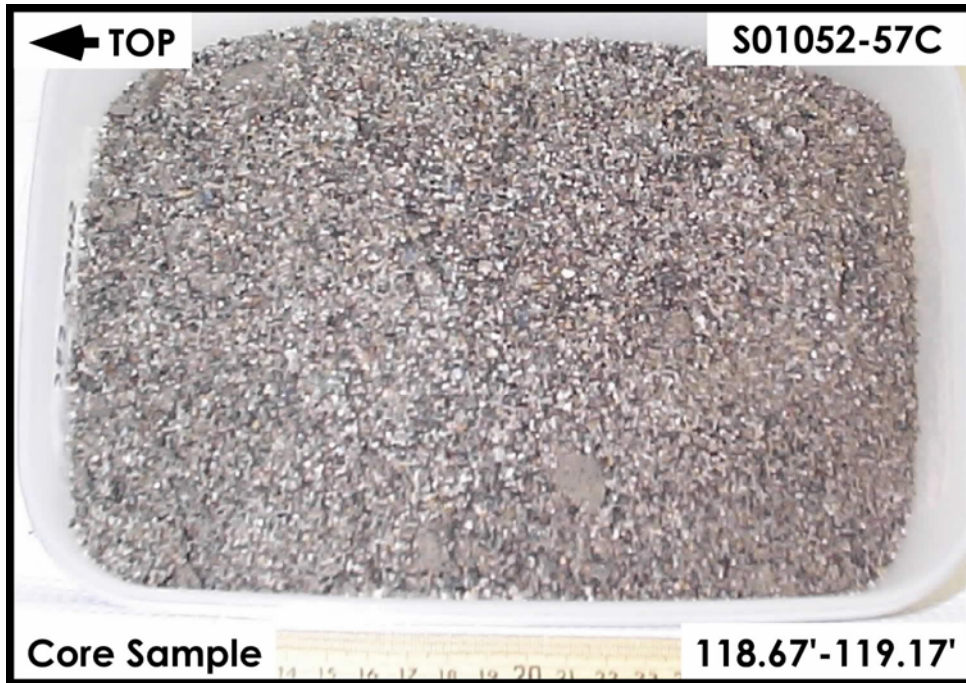
H2-Upper Sand and Gravel Sequence



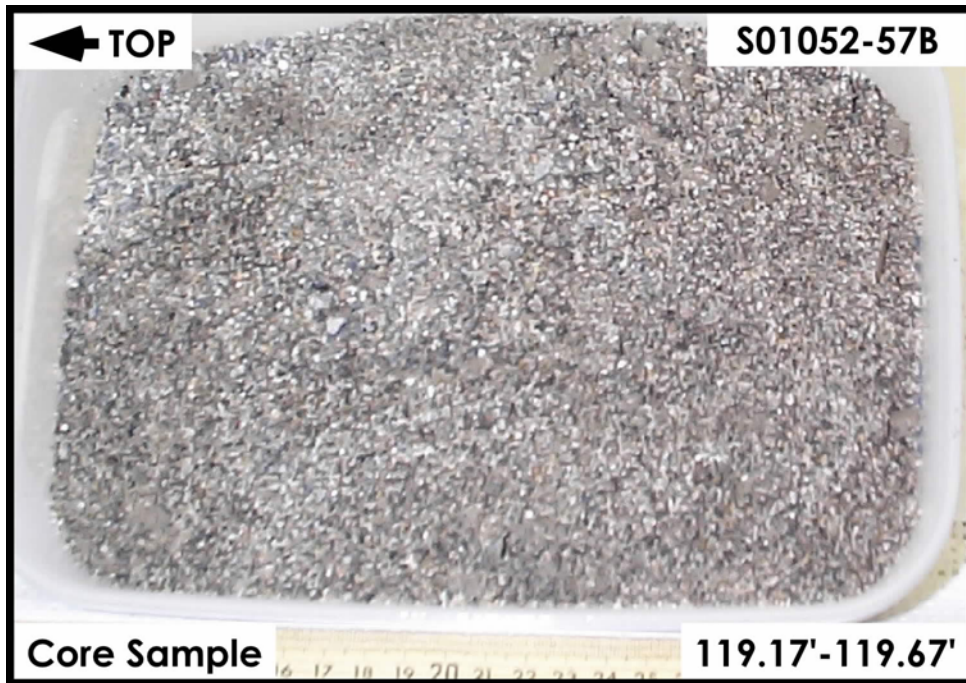
H2-Upper Sand and Gravel Sequence



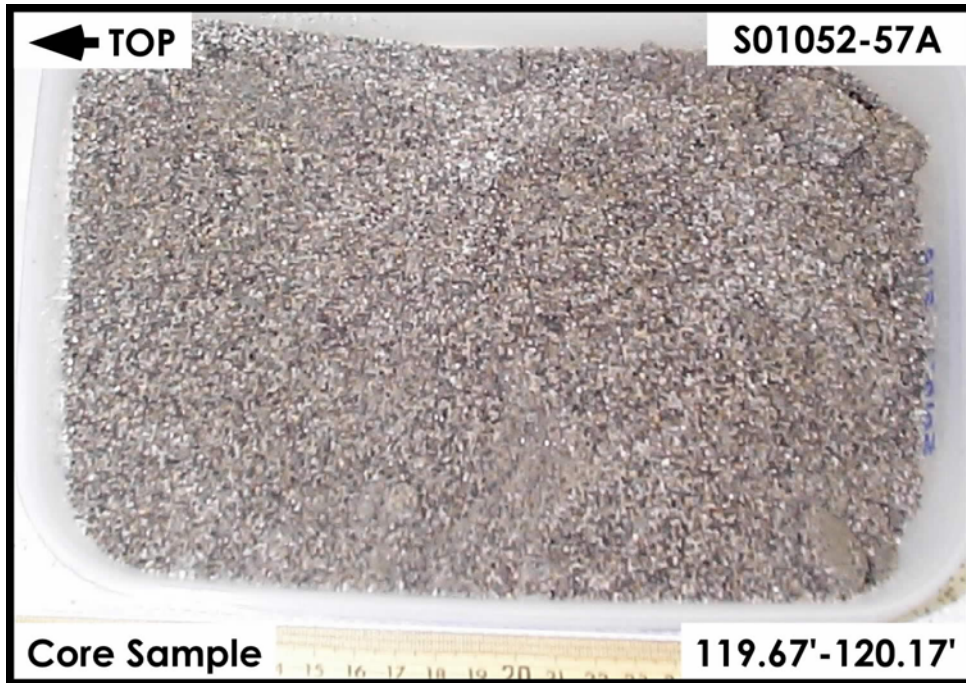
H2-Upper Sand and Gravel Sequence



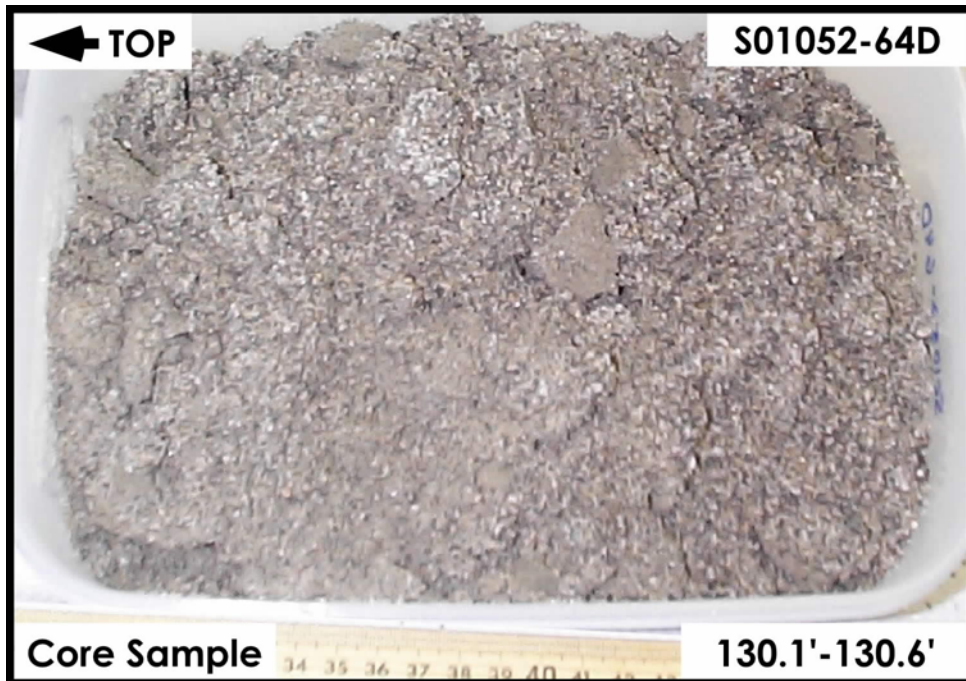
H2-Upper Sand and Gravel Sequence



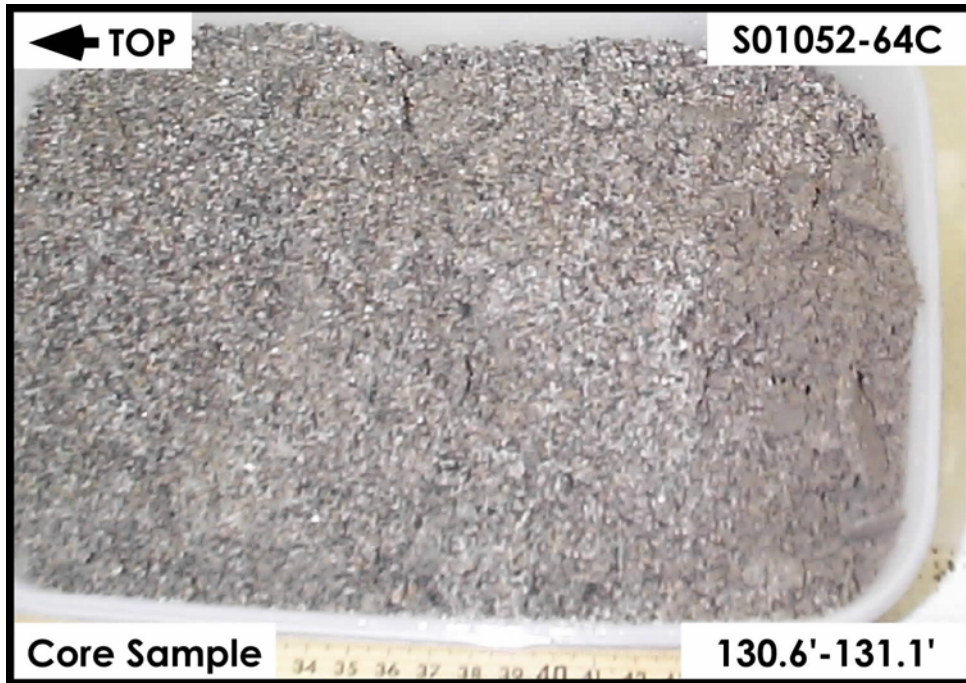
H2-Upper Sand and Gravel Sequence



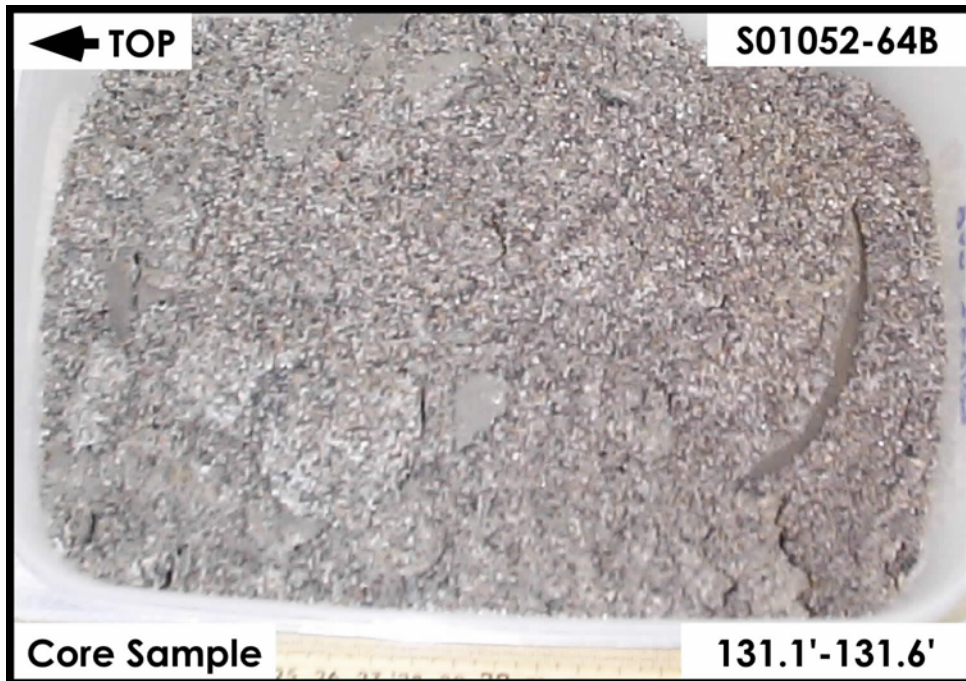
H2-Upper Sand and Gravel Sequence



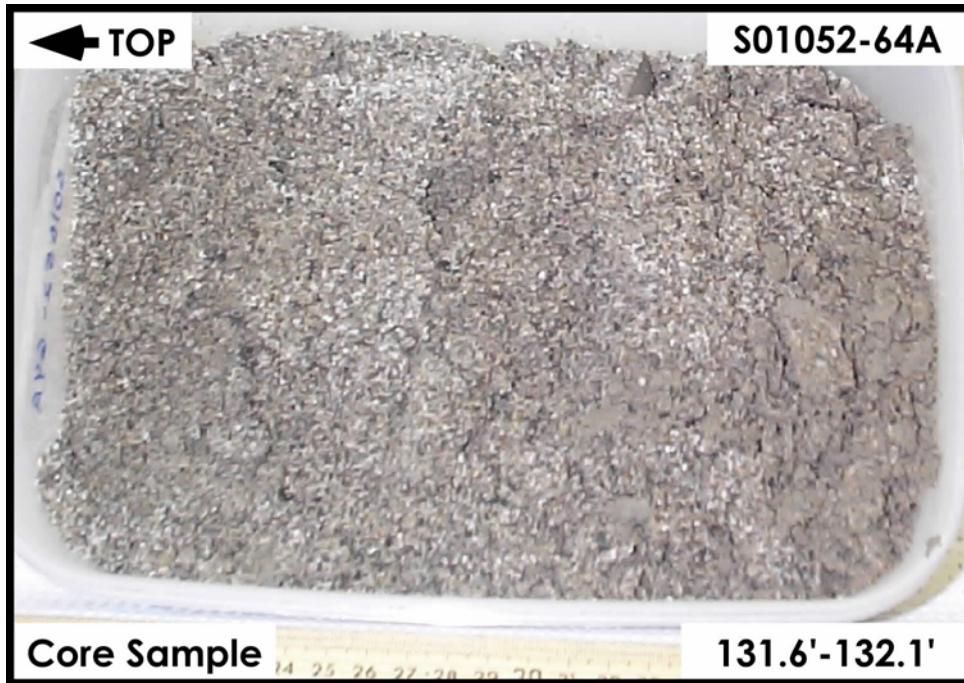
H2-Upper Sand and Gravel Sequence



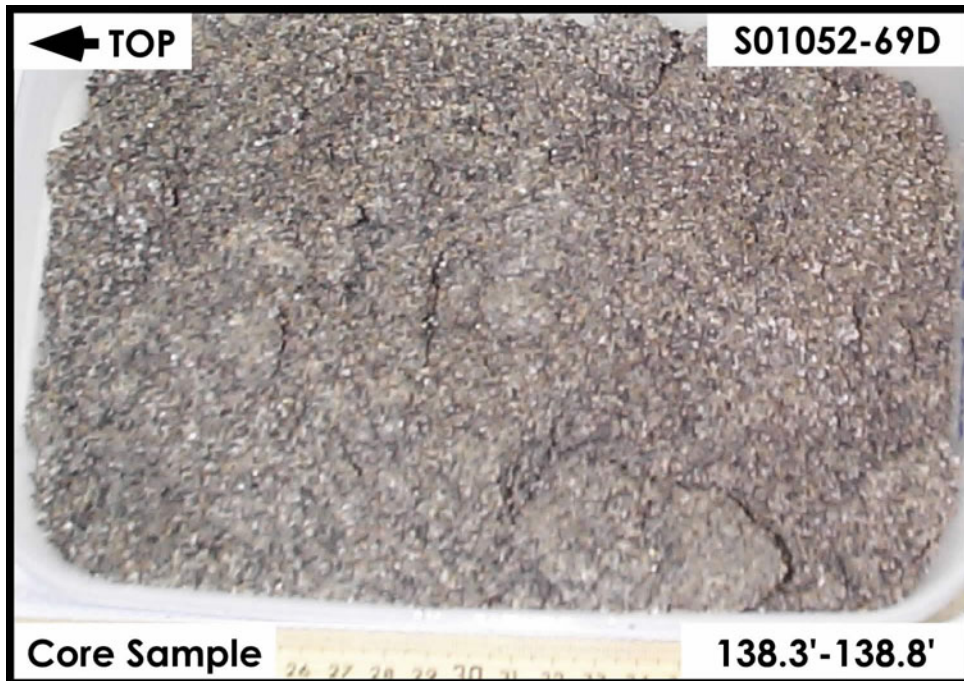
H2-Upper Sand and Gravel Sequence



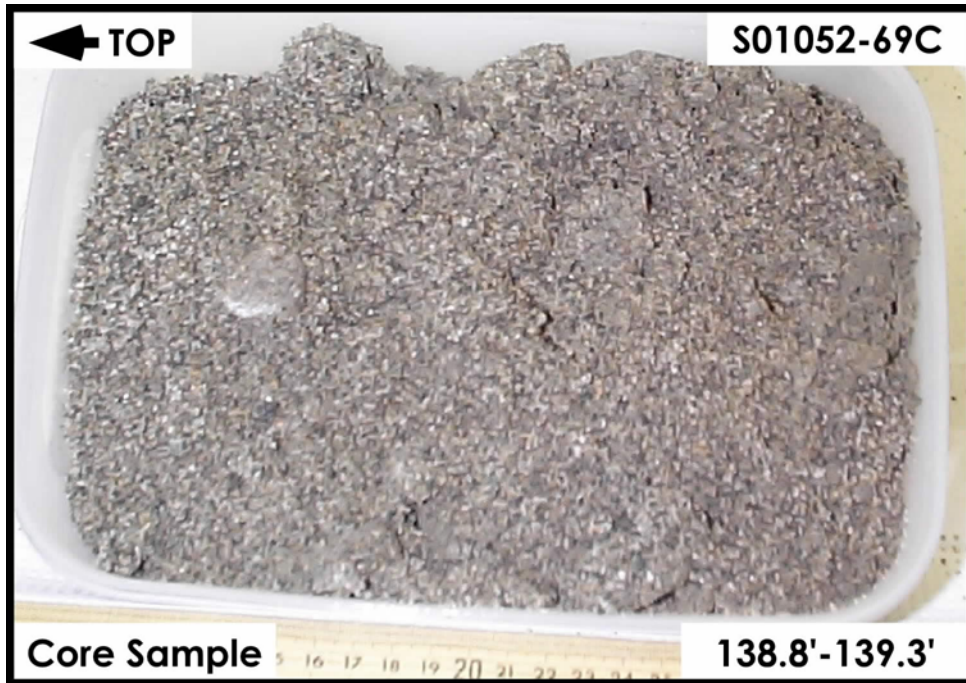
H2-Upper Sand and Gravel Sequence



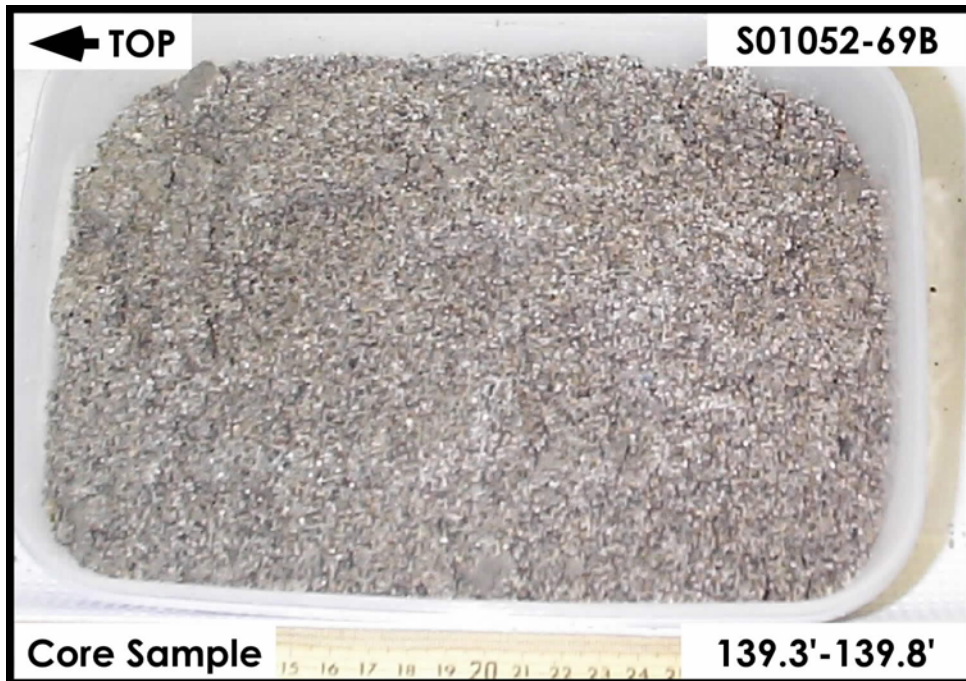
H2-Upper Sand and Gravel Sequence



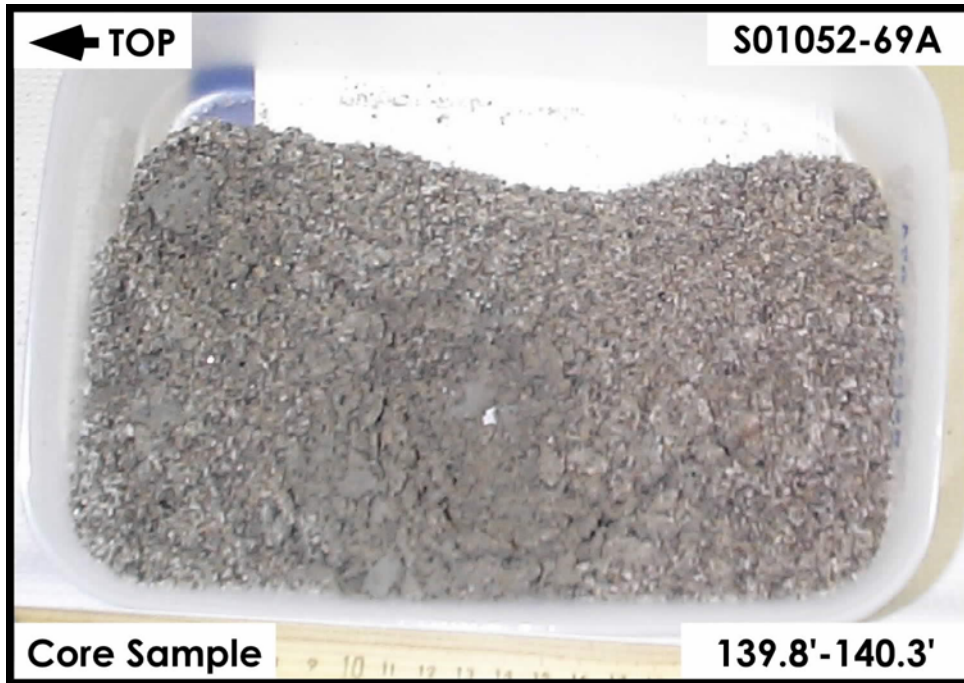
H2-Upper Sand and Gravel Sequence



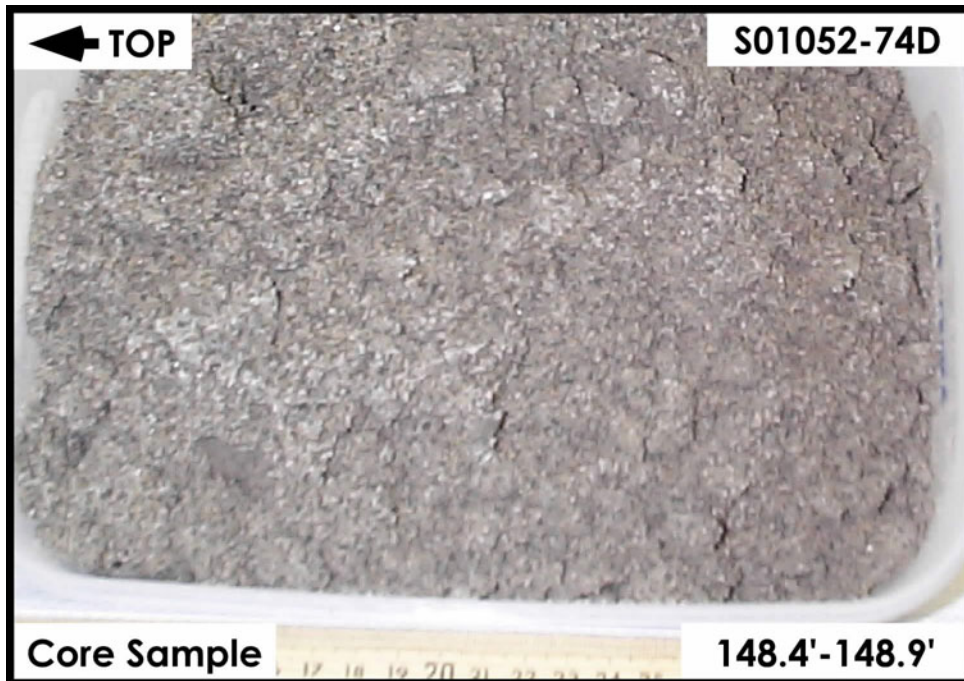
H2-Upper Sand and Gravel Sequence



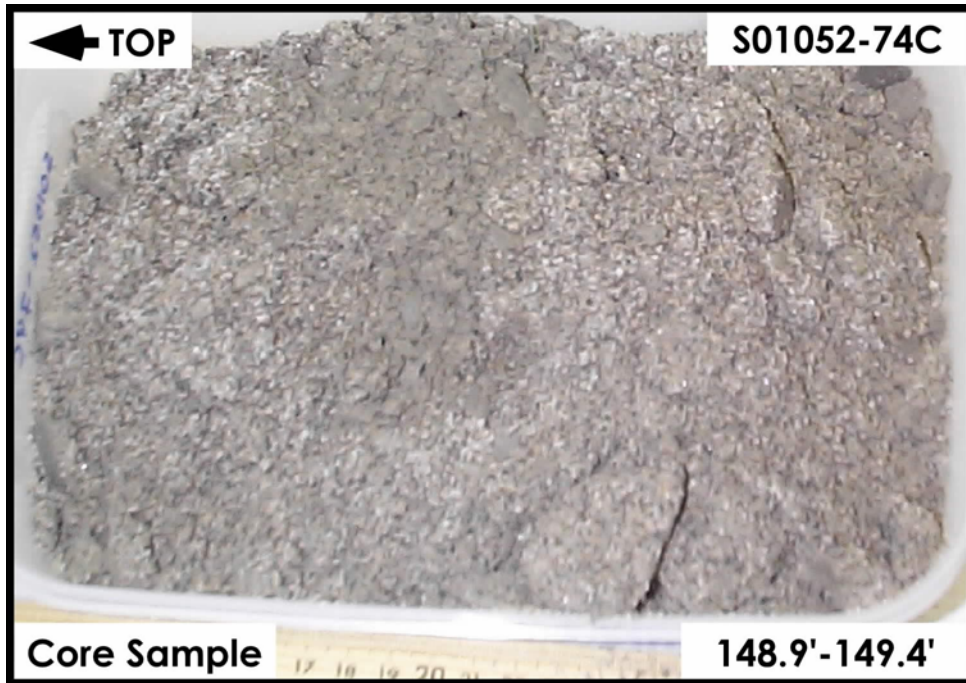
H2-Upper Sand and Gravel Sequence



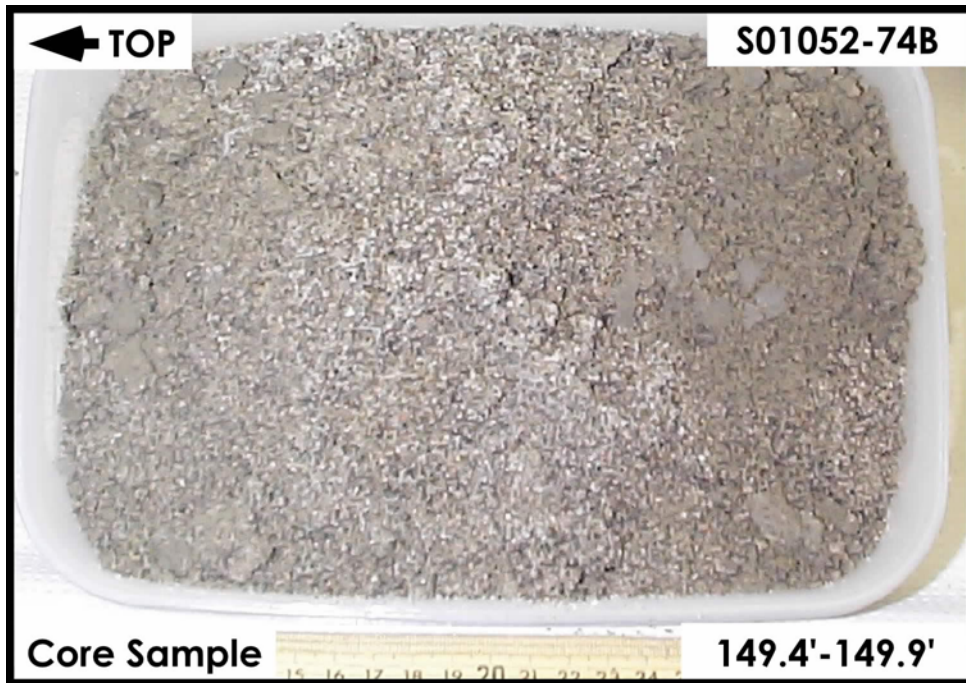
H2-Upper Sand and Gravel Sequence



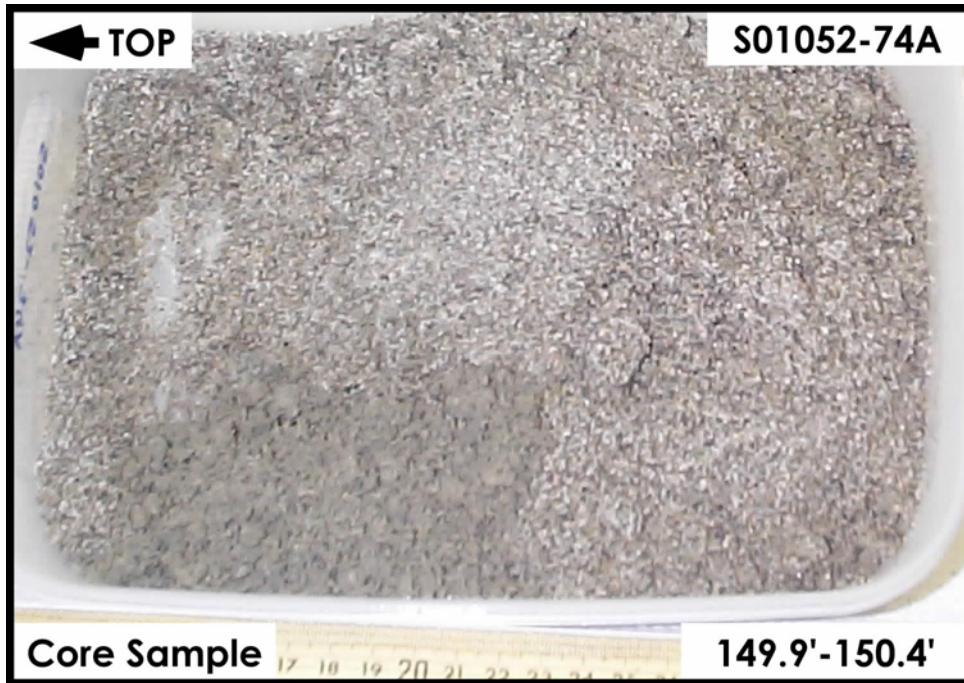
H2-Upper Sand and Gravel Sequence



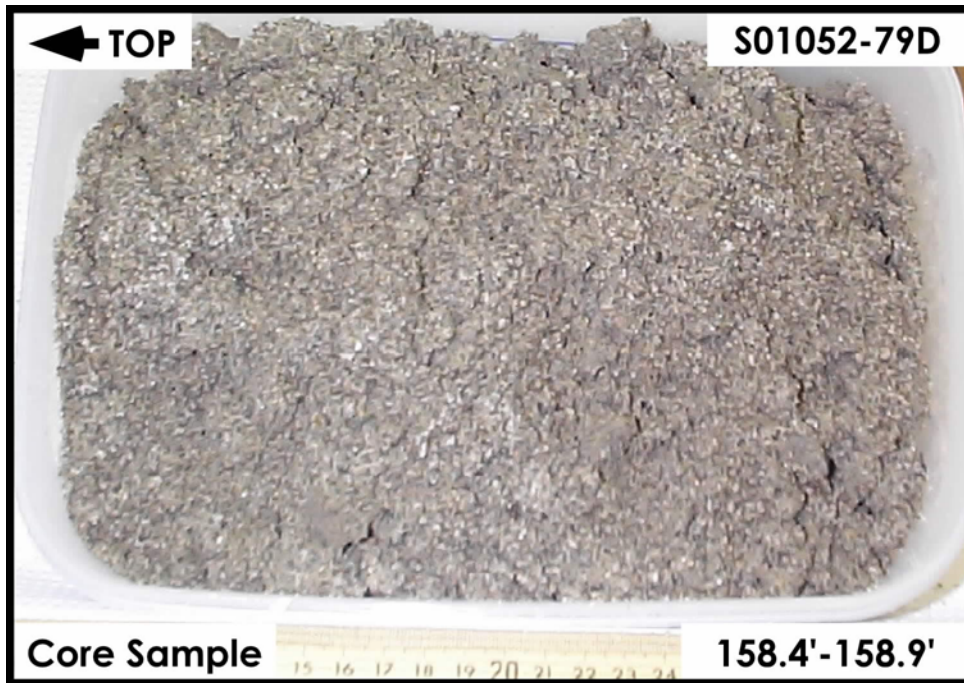
H2-Upper Sand and Gravel Sequence



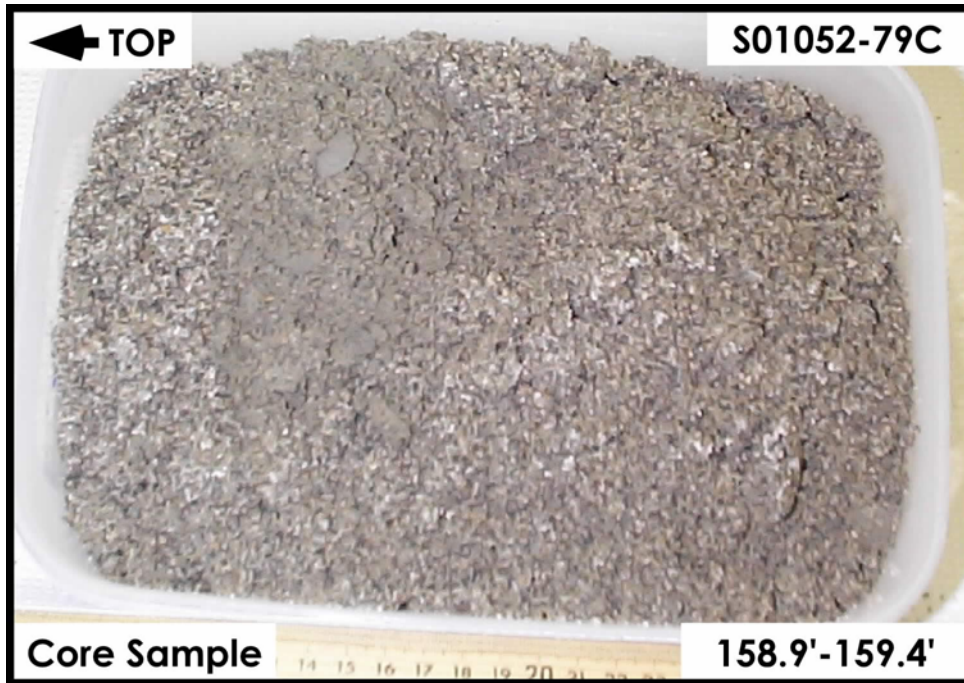
H2-Upper Sand and Gravel Sequence



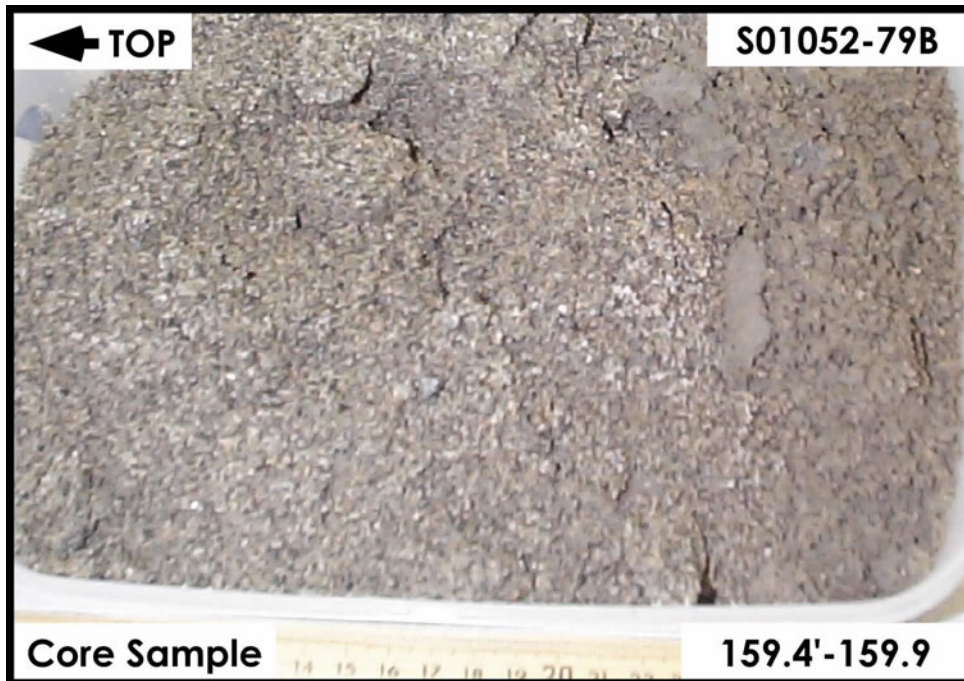
H2-Upper Sand and Gravel Sequence



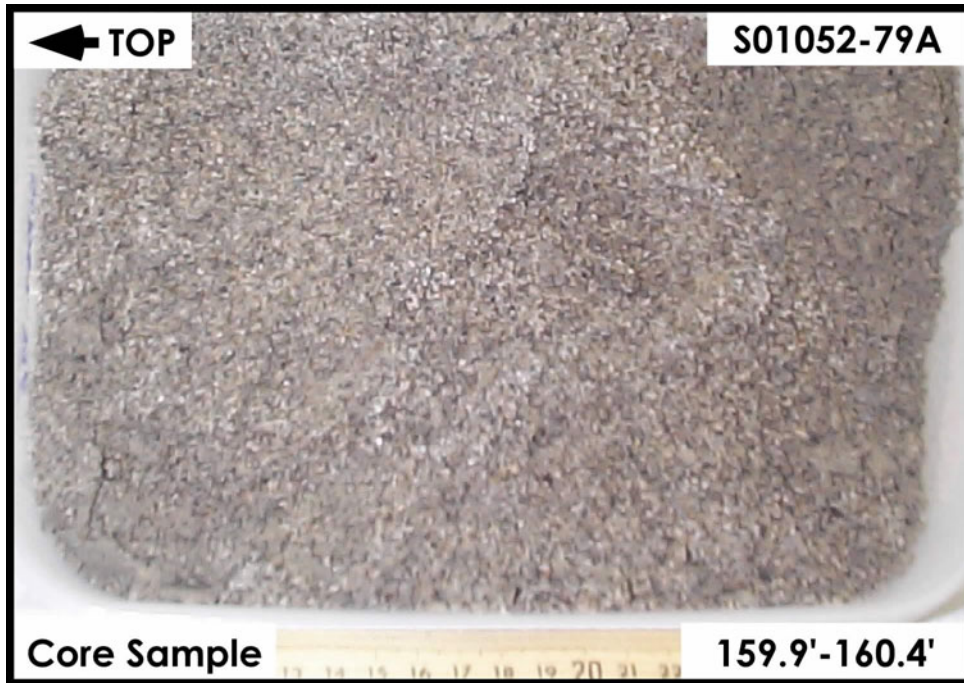
H2-Upper Sand and Gravel Sequence



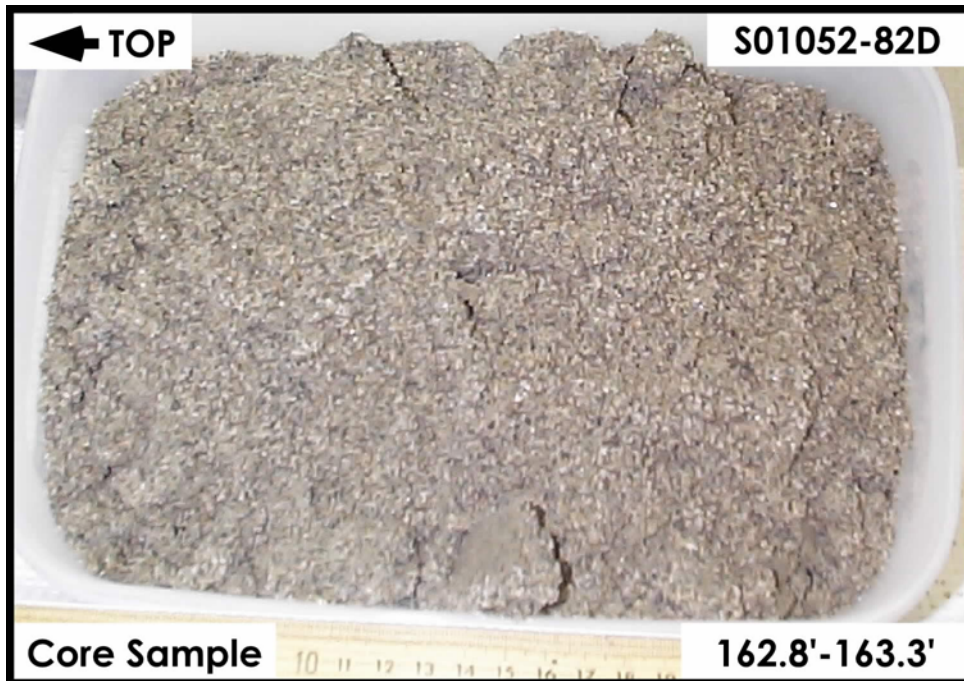
H2-Upper Sand and Gravel Sequence



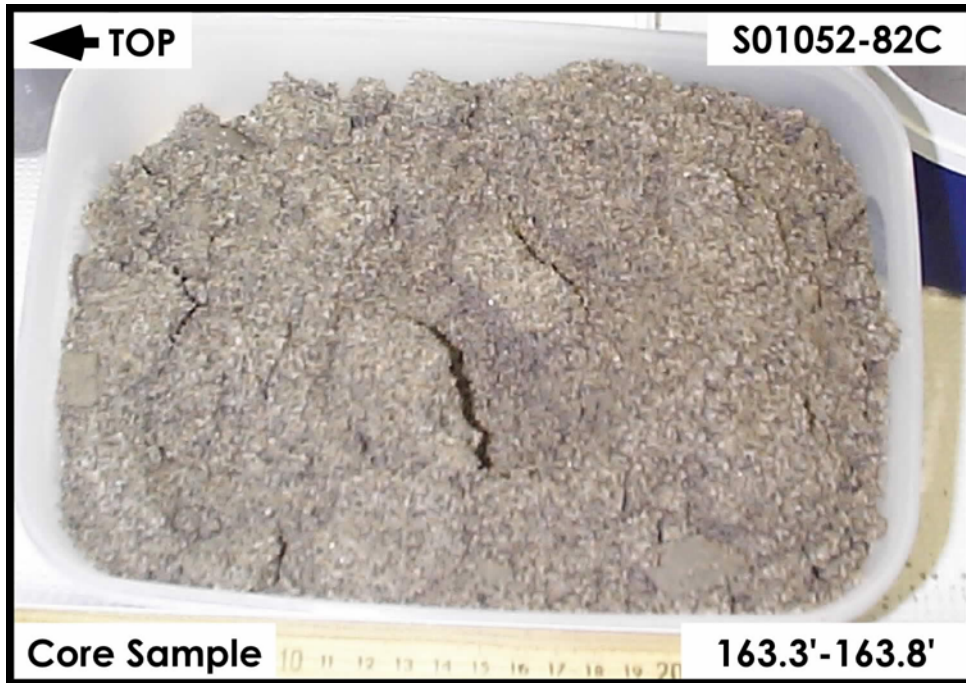
H2-Upper Sand and Gravel Sequence



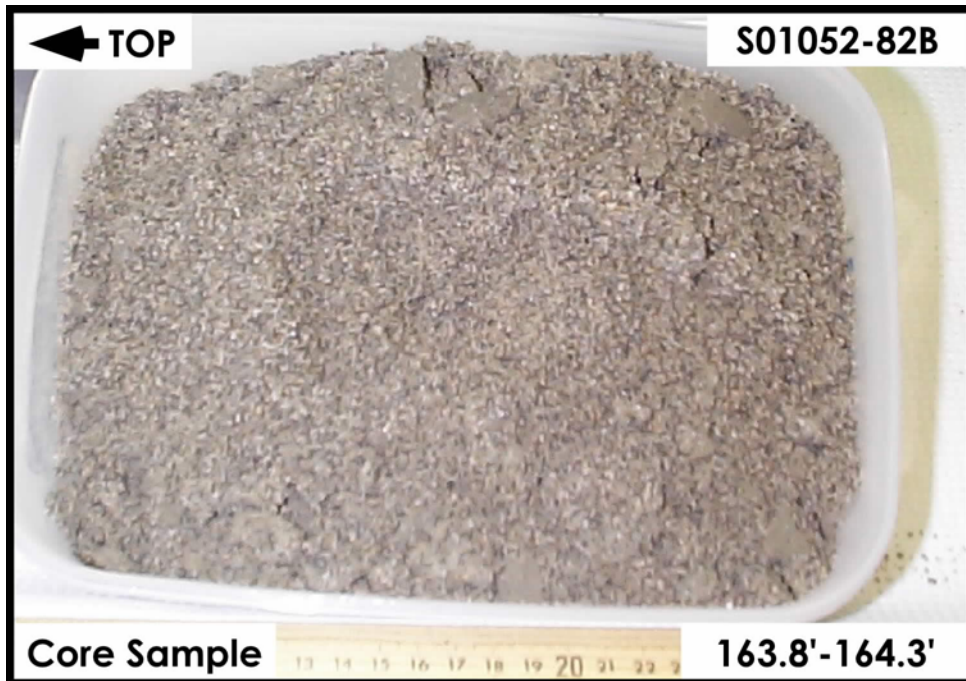
H2-Upper Sand and Gravel Sequence



H2-Upper Sand and Gravel Sequence



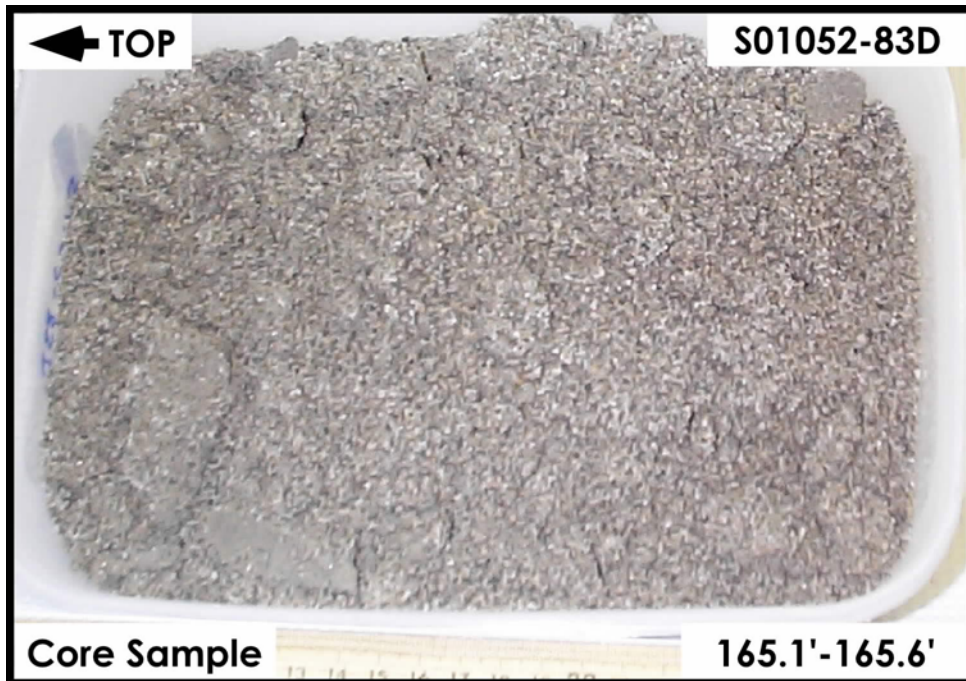
H2-Upper Sand and Gravel Sequence



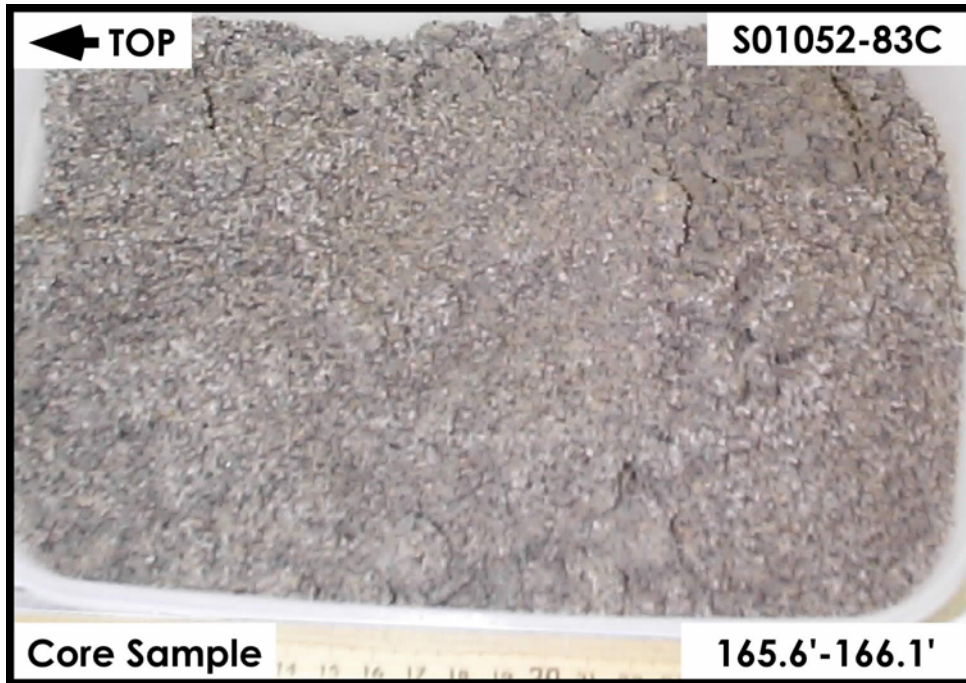
H2-Upper Sand and Gravel Sequence



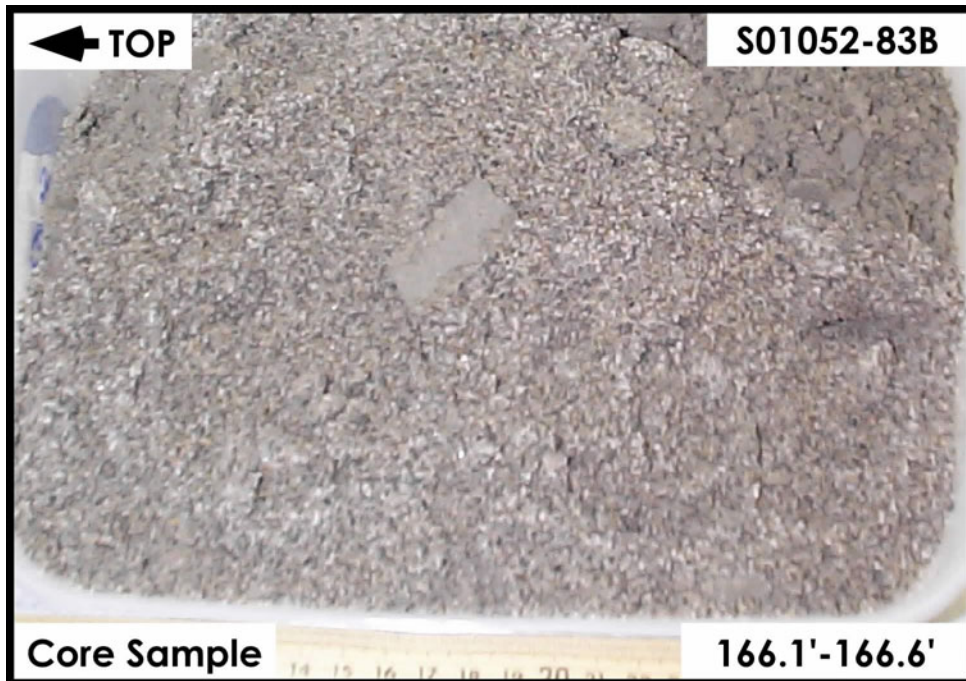
H2-Upper Sand and Gravel Sequence



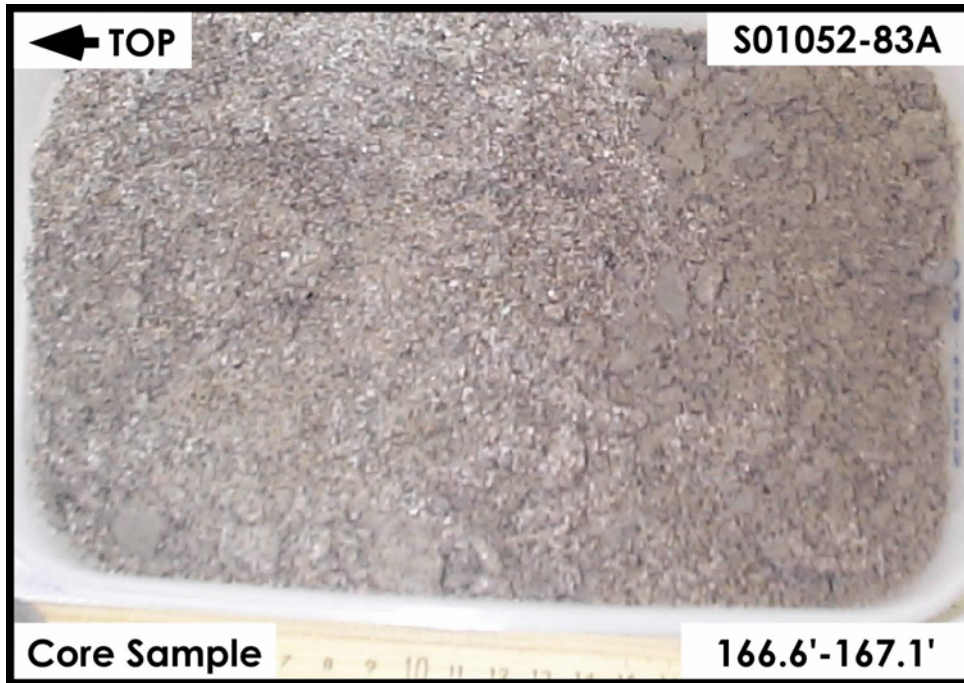
H2-Upper Sand and Gravel Sequence



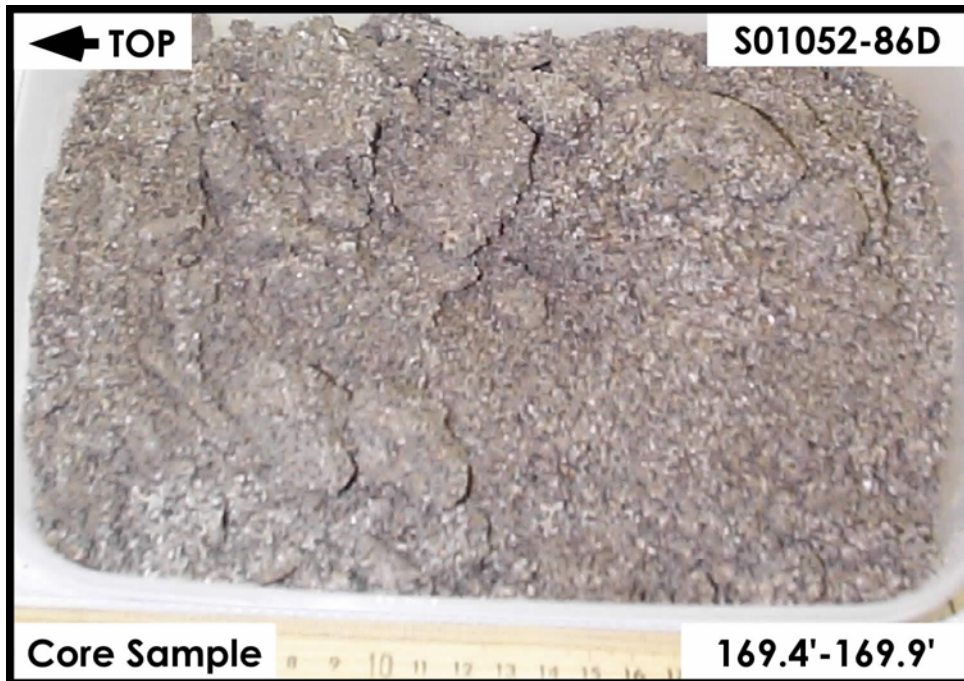
H2-Upper Sand and Gravel Sequence



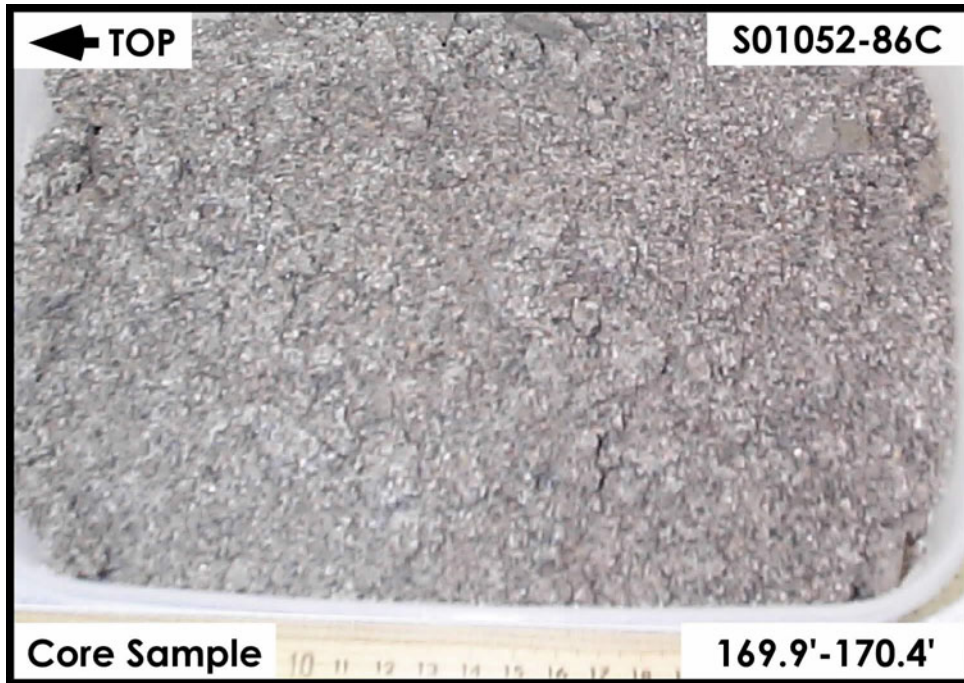
H2-Upper Sand and Gravel Sequence



H2-Upper Sand and Gravel Sequence



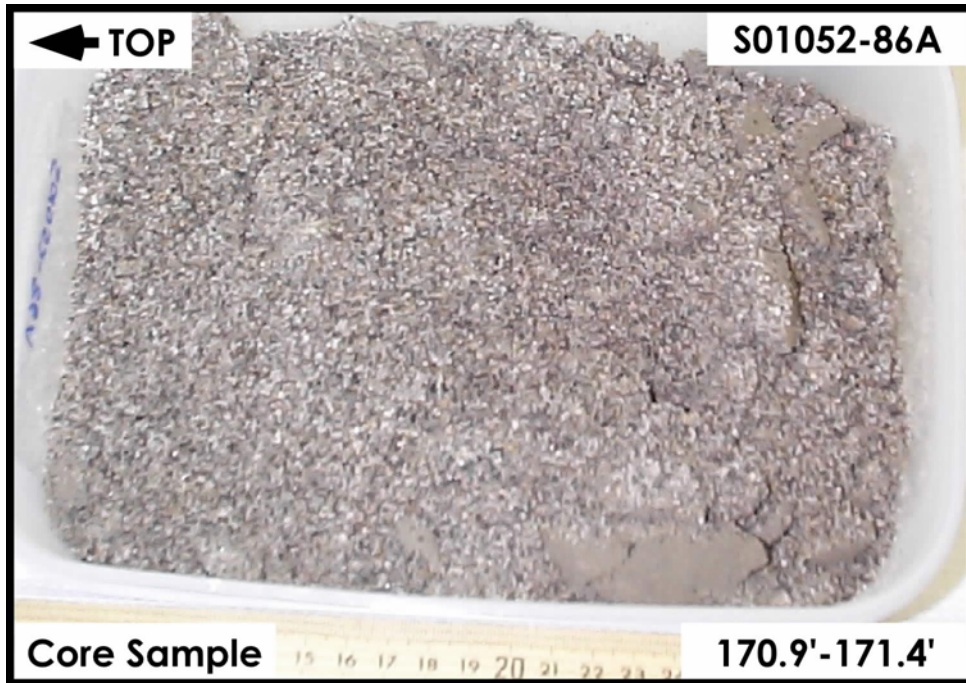
H2-Upper Sand and Gravel Sequence



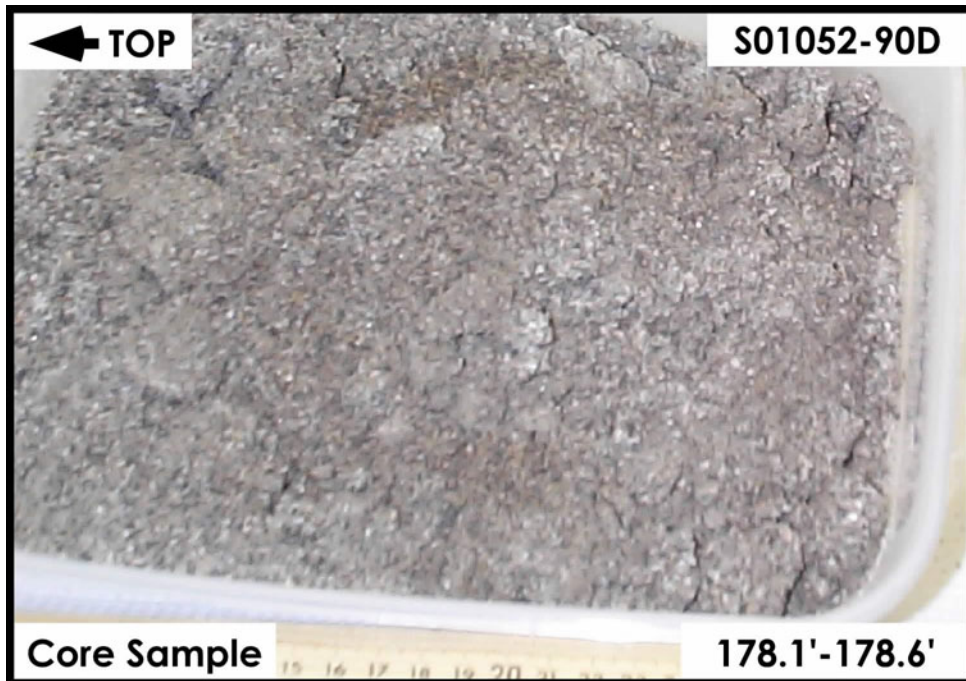
H2-Upper Sand and Gravel Sequence



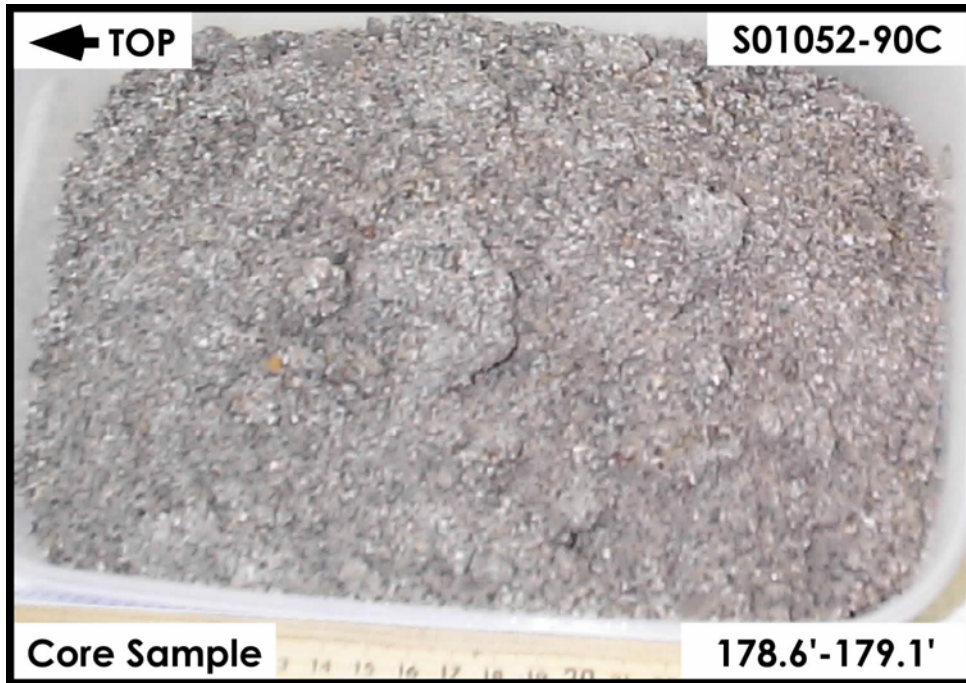
H2-Upper Sand and Gravel Sequence



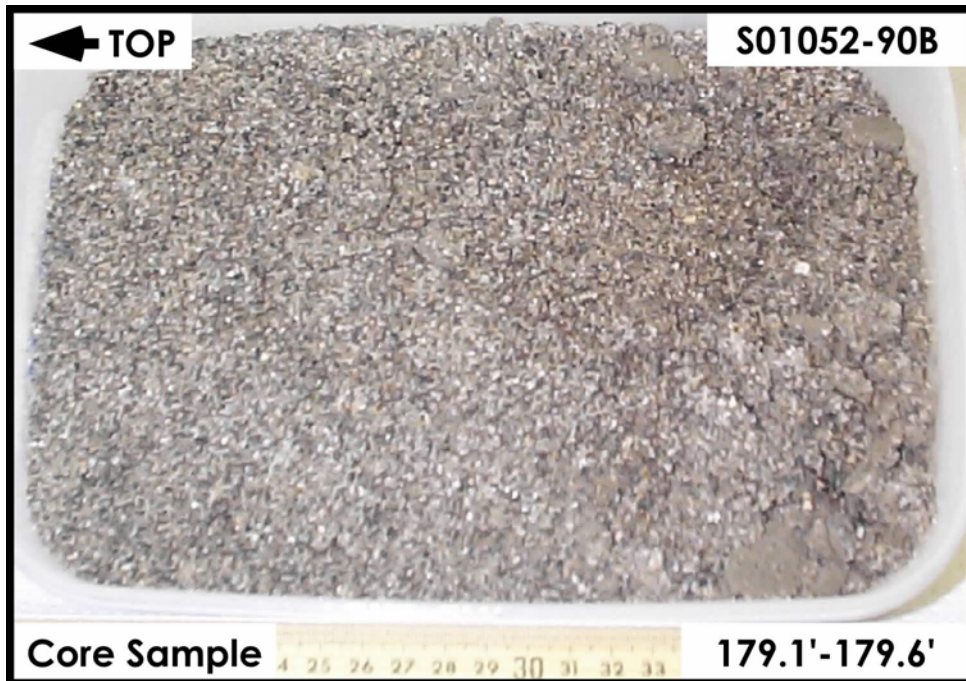
H2-Upper Sand and Gravel Sequence



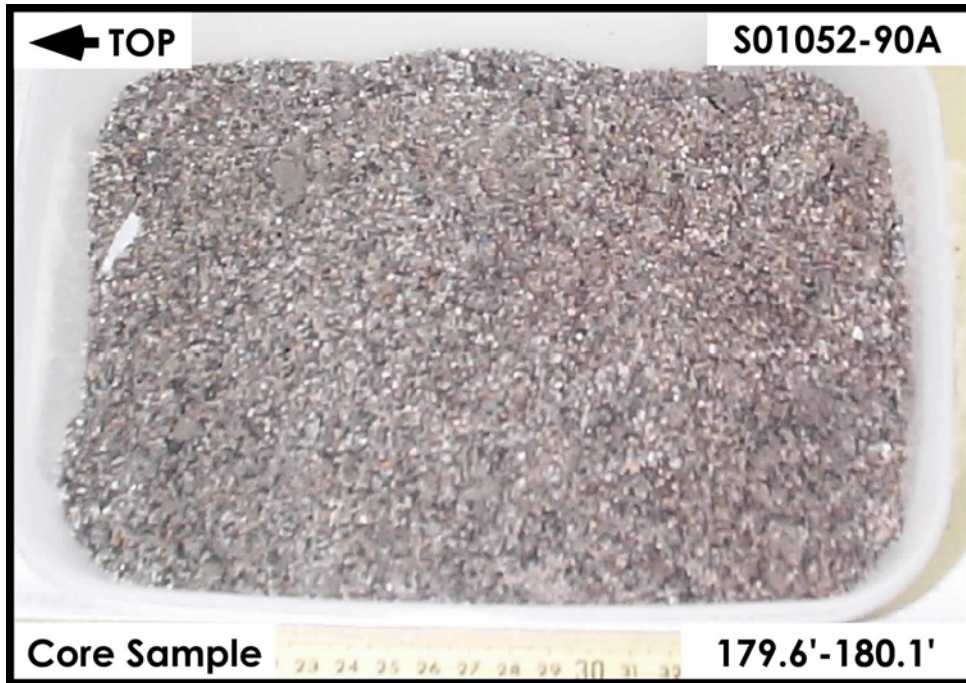
H3-Lower Sand and Gravel Sequence



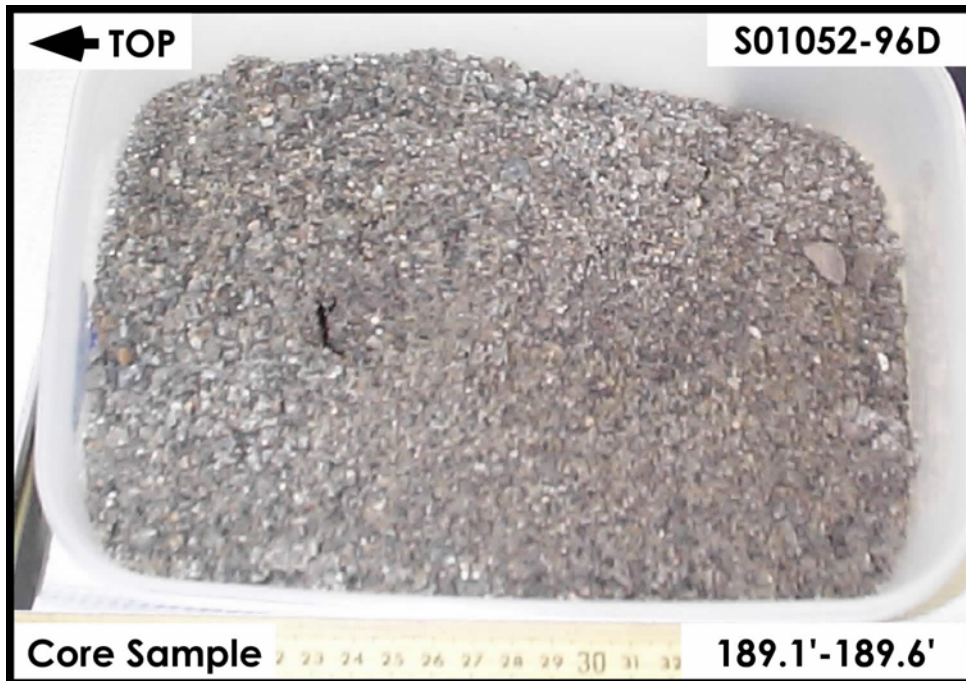
H3-Lower Sand and Gravel Sequence



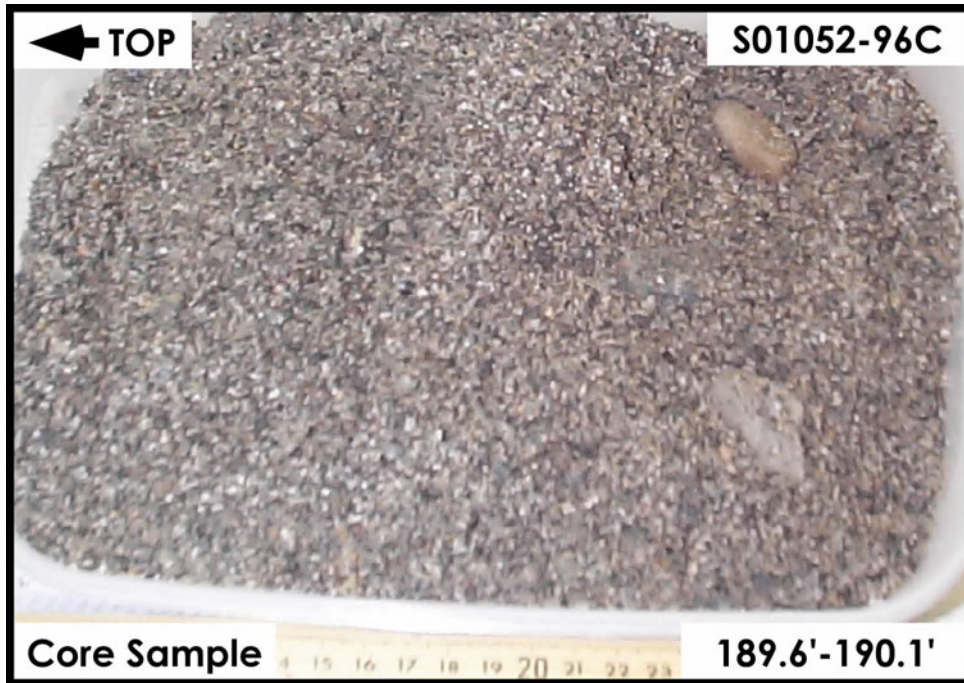
H3-Lower Sand and Gravel Sequence



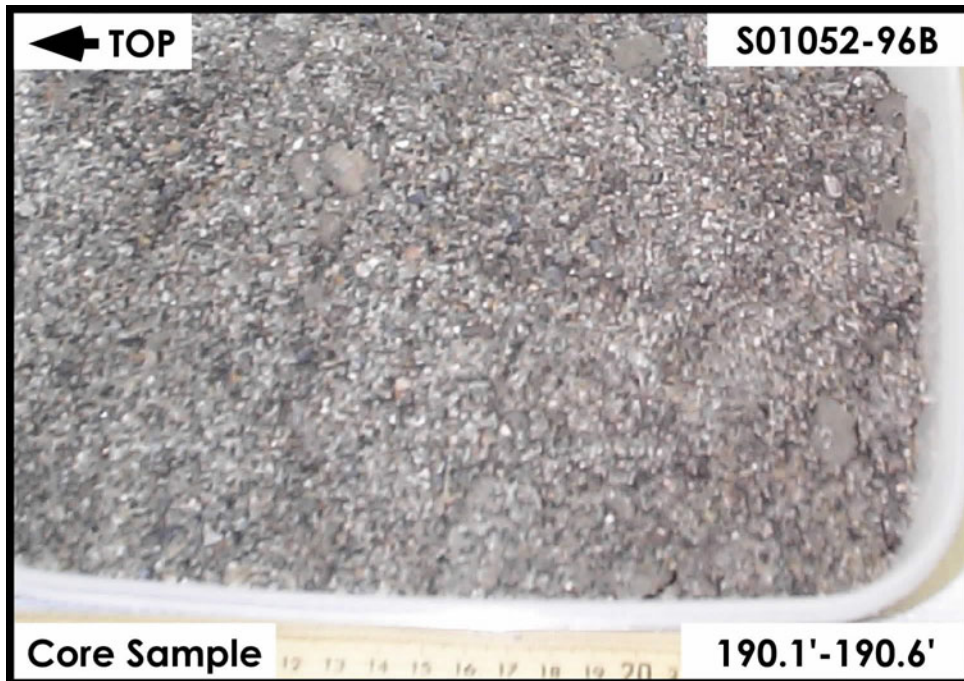
H3-Lower Sand and Gravel Sequence



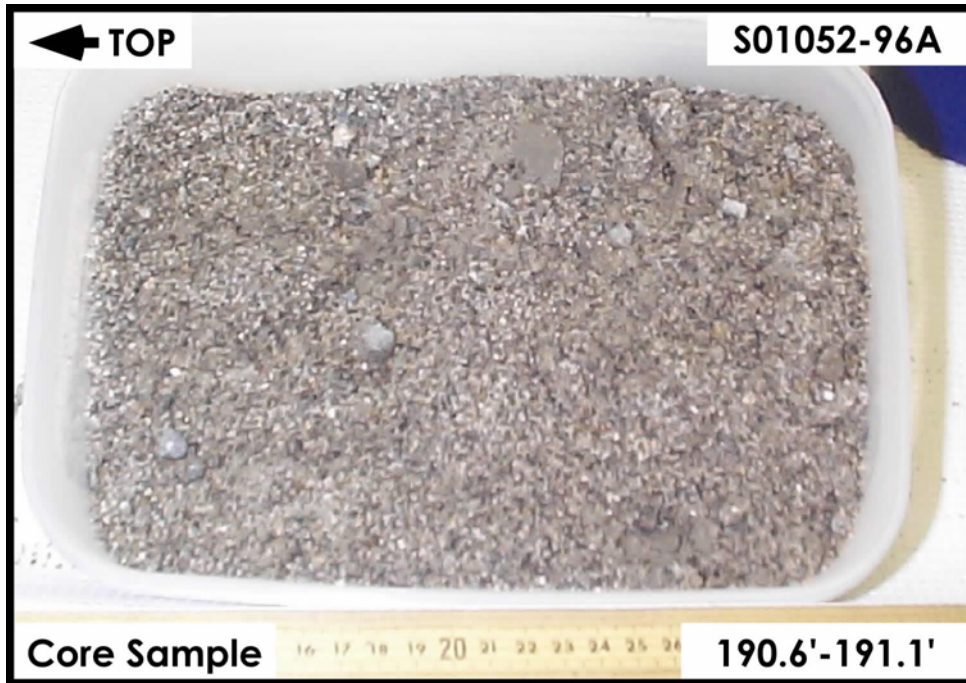
H3-Lower Sand and Gravel Sequence



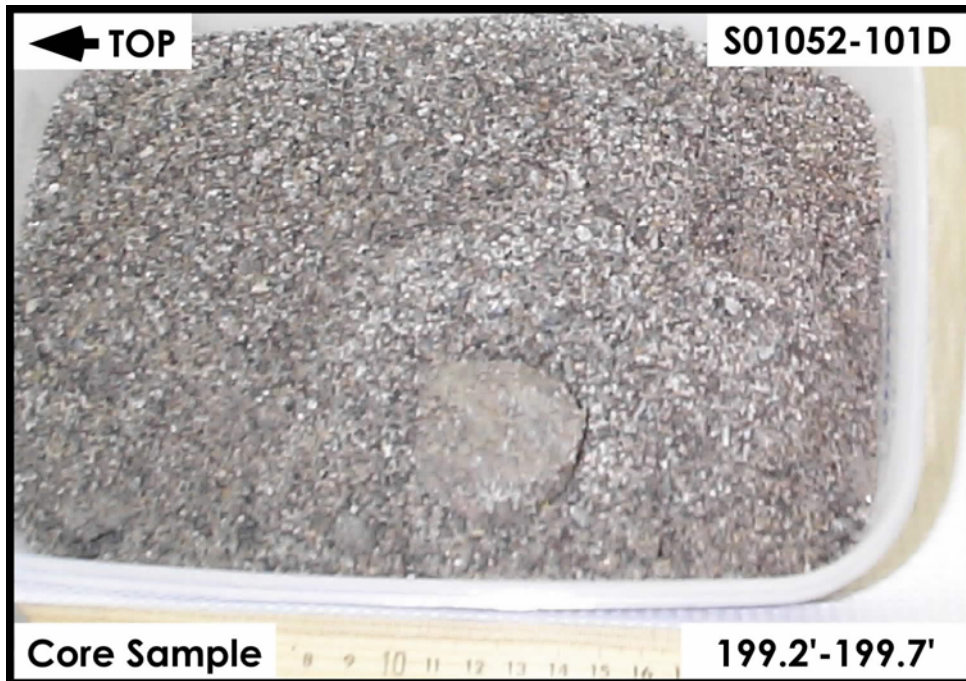
H3-Lower Sand and Gravel Sequence



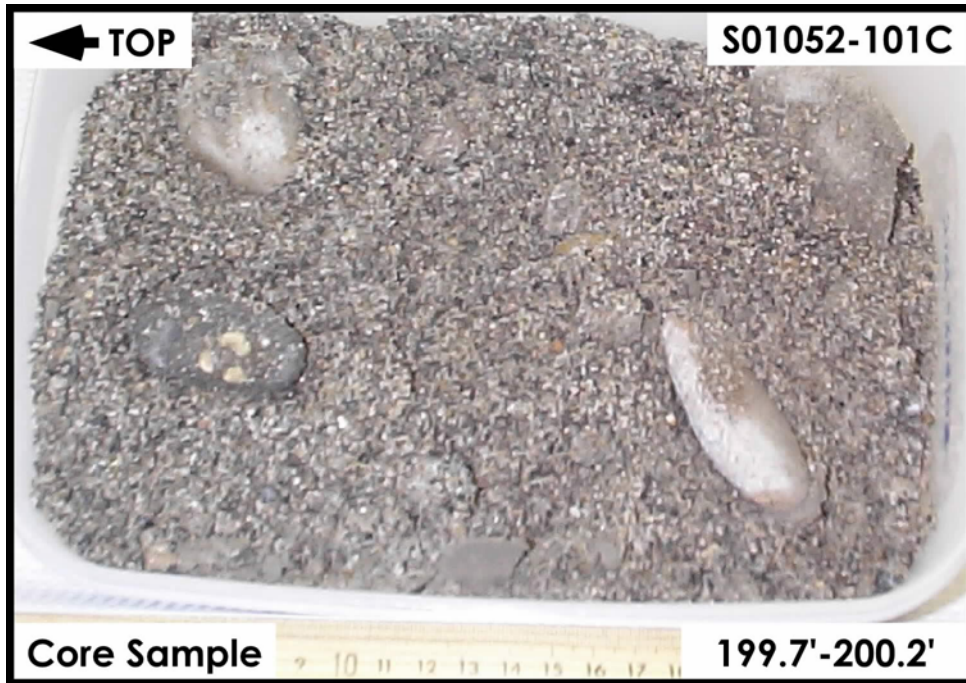
H3-Lower Sand and Gravel Sequence



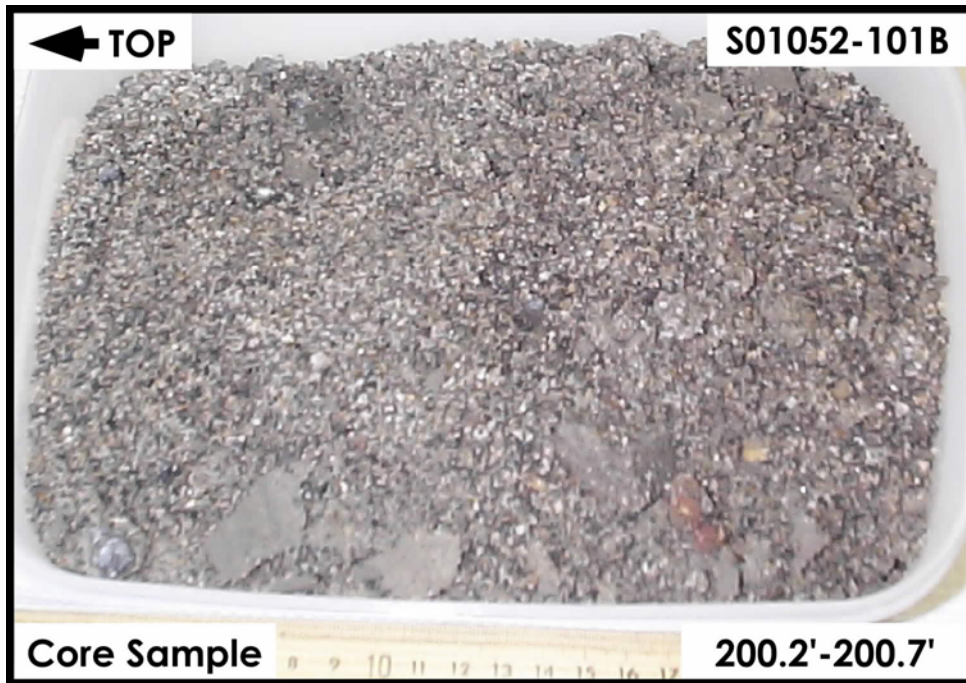
H3-Lower Sand and Gravel Sequence



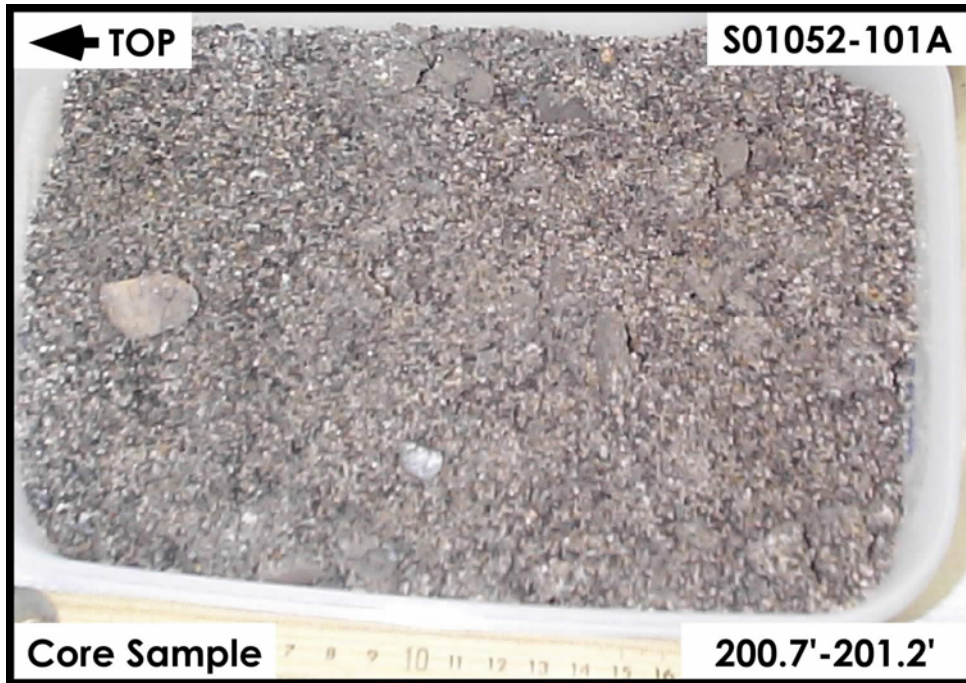
H3-Lower Sand and Gravel Sequence



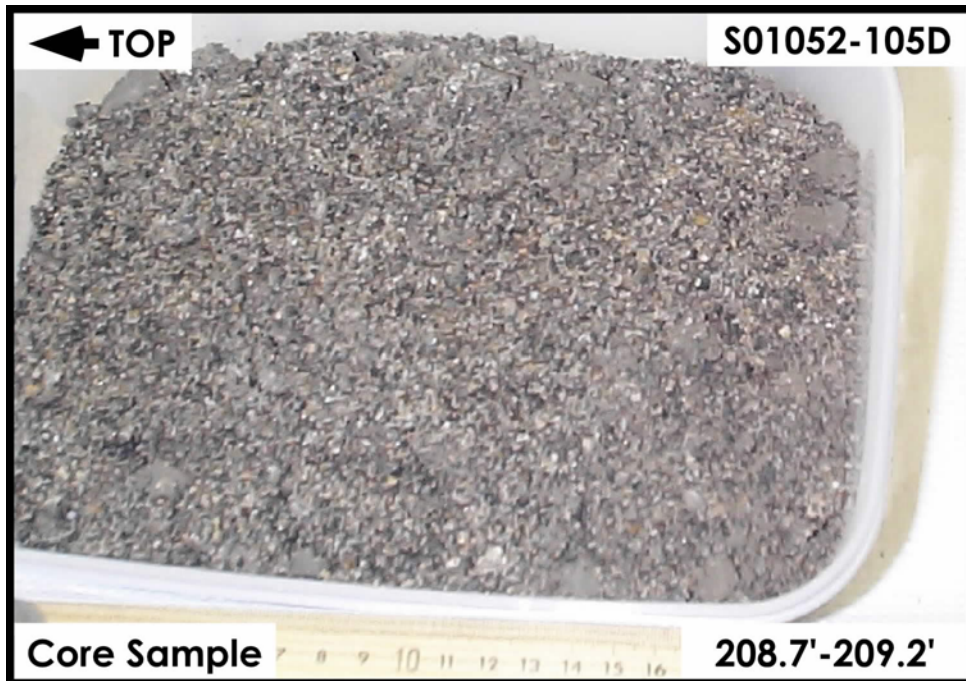
H3-Lower Sand and Gravel Sequence



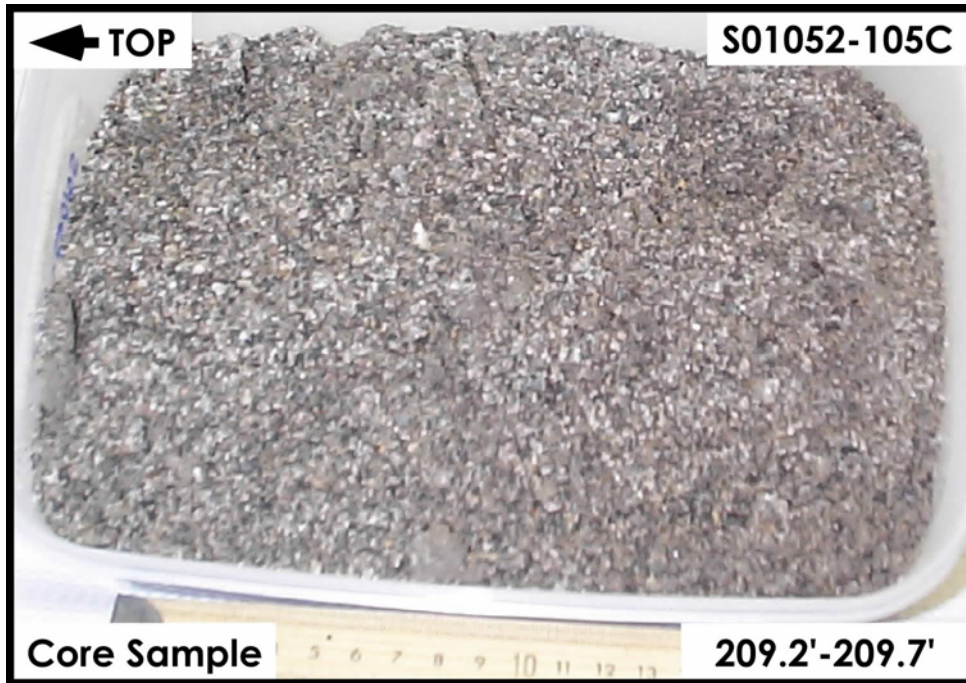
H3-Lower Sand and Gravel Sequence



H3-Lower Sand and Gravel Sequence



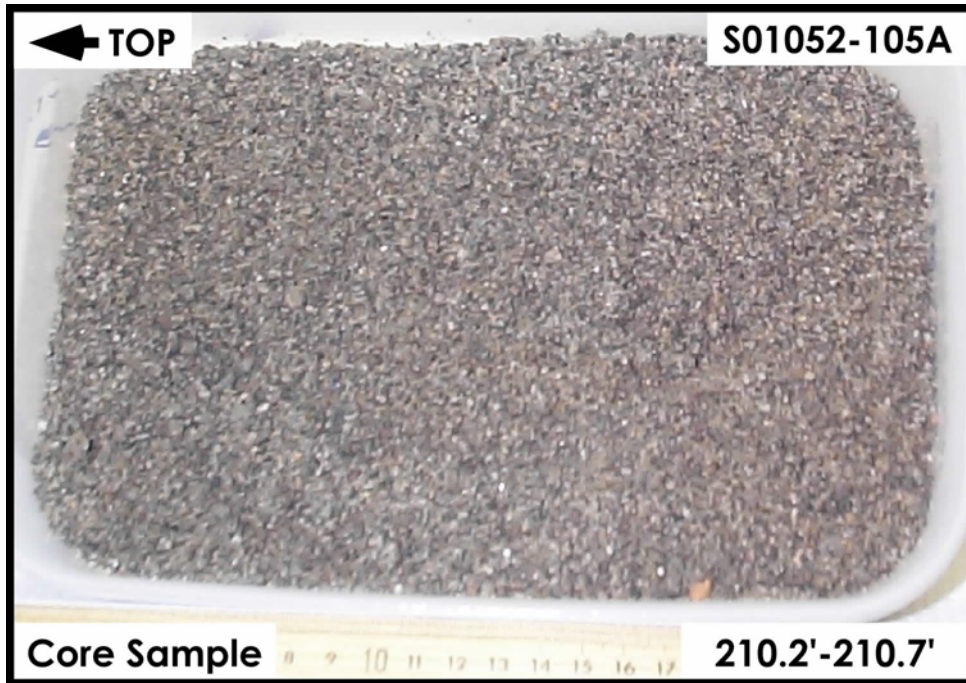
H3-Lower Sand and Gravel Sequence



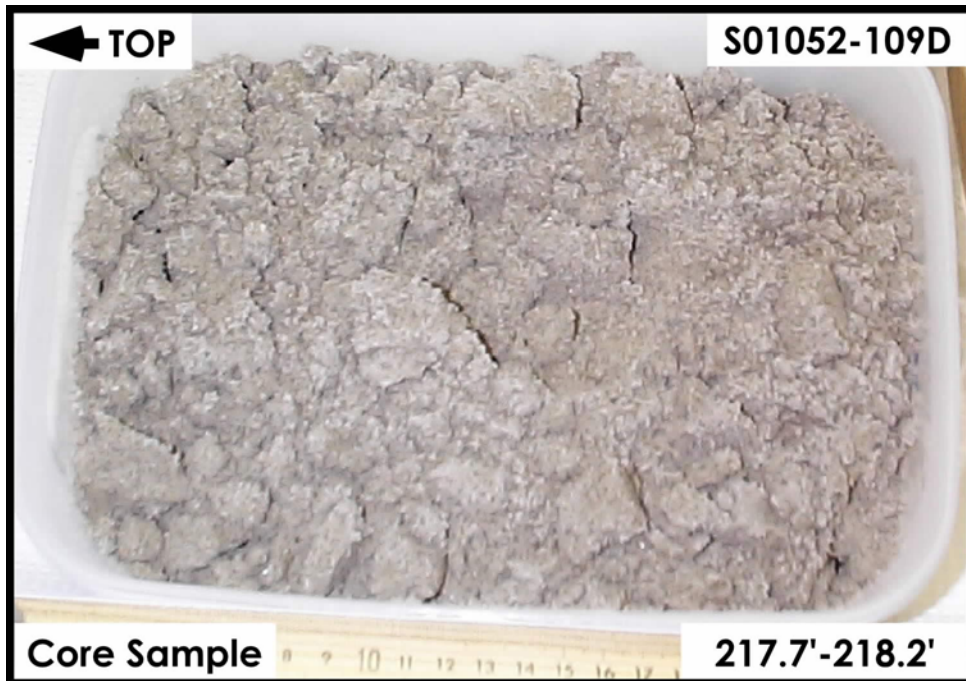
H3-Lower Sand and Gravel Sequence



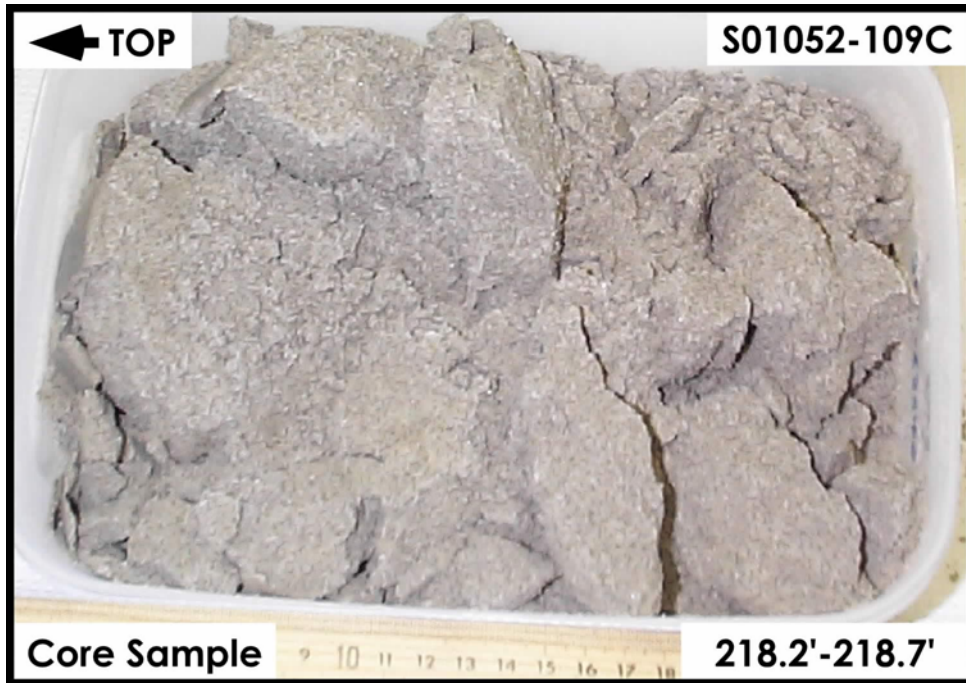
H3-Lower Sand and Gravel Sequence



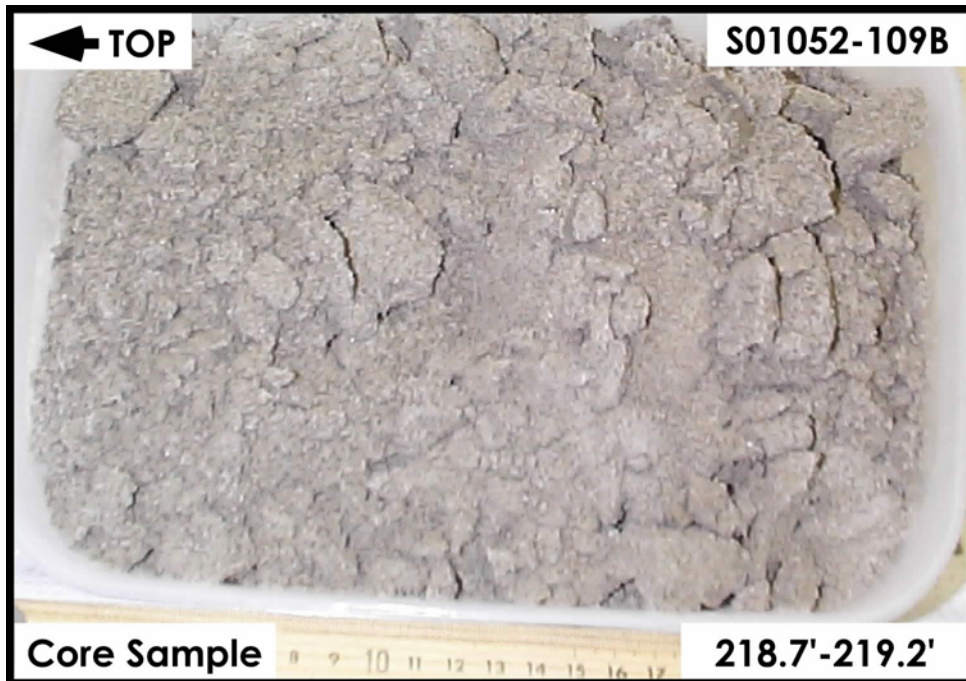
H3-Lower Sand and Gravel Sequence



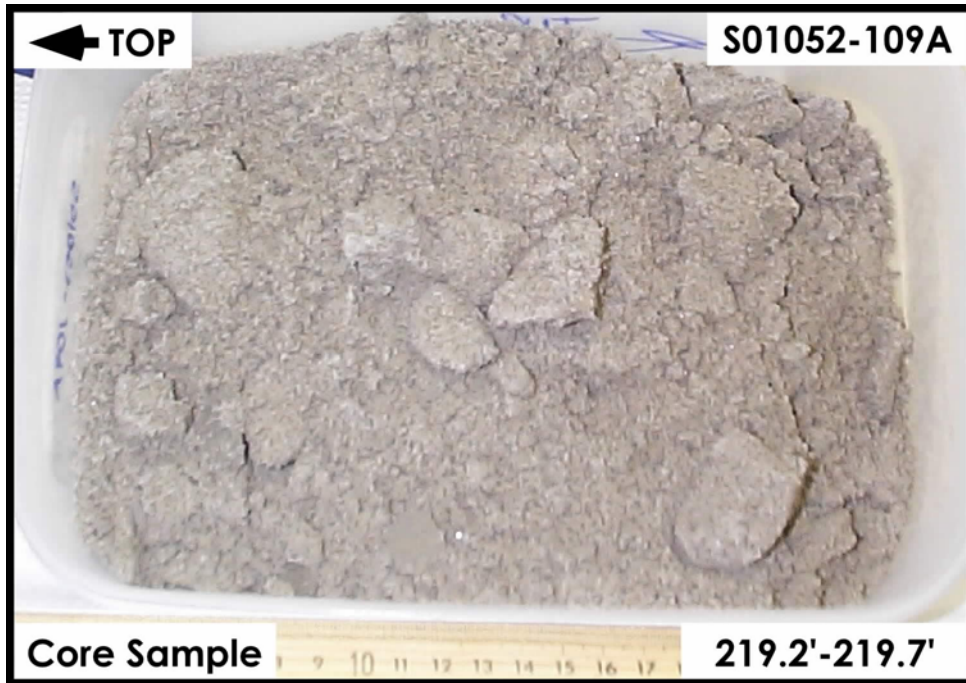
Plio-Pleistocene Silt Unit (PPlz)



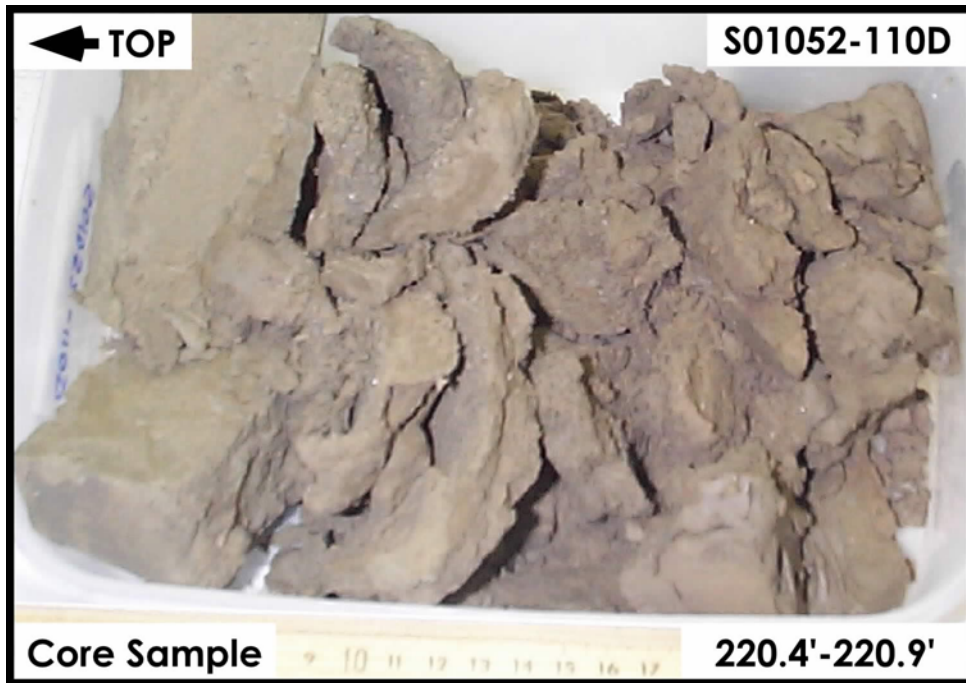
Plio-Pleistocene Silt Unit (PPlz)



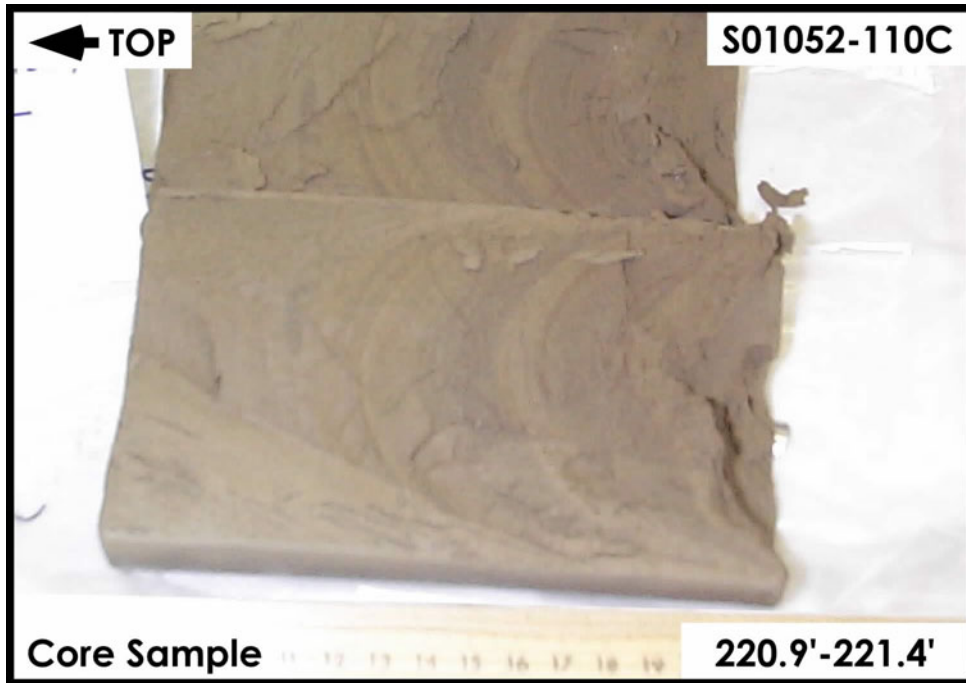
Plio-Pleistocene Silt Unit (PPlz)



Plio-Pleistocene Silt Unit (PPlz)



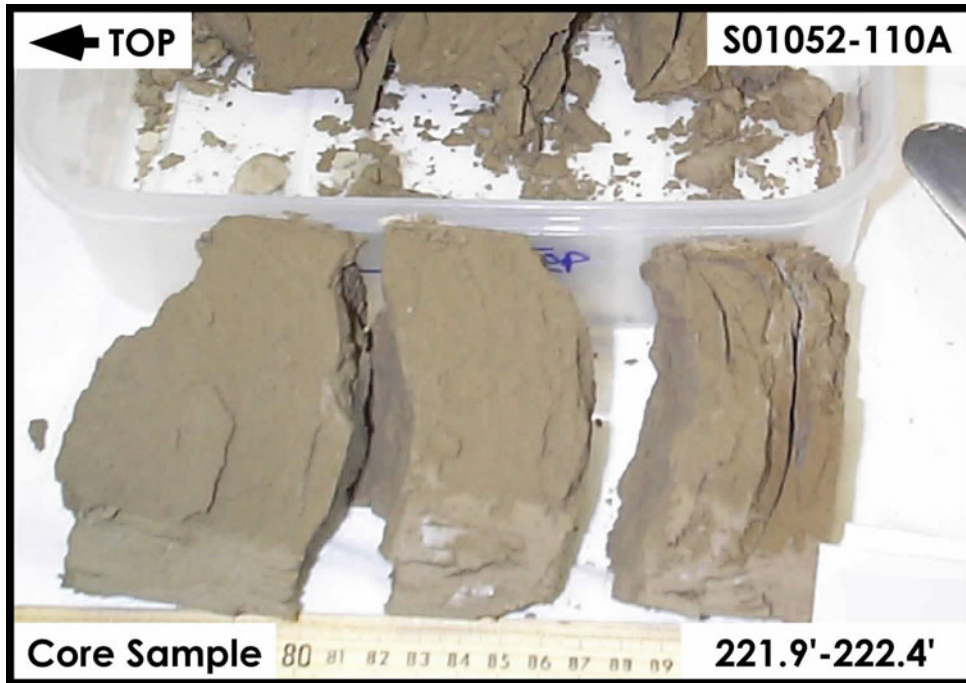
Plio-Pleistocene Silt Unit (PPlz)



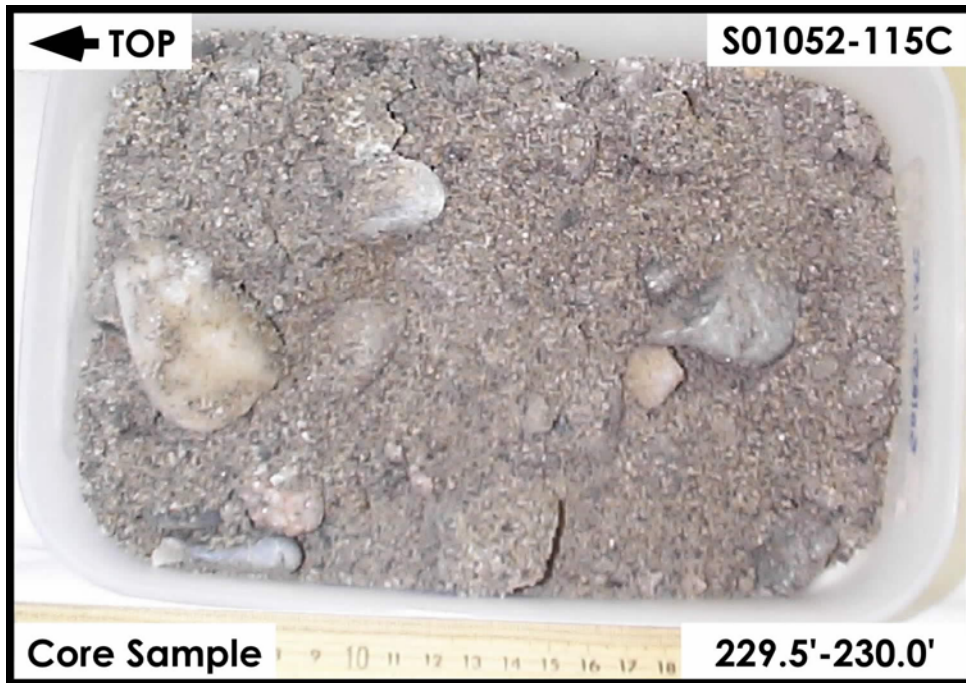
Plio-Pleistocene Silt Unit (PPlz)



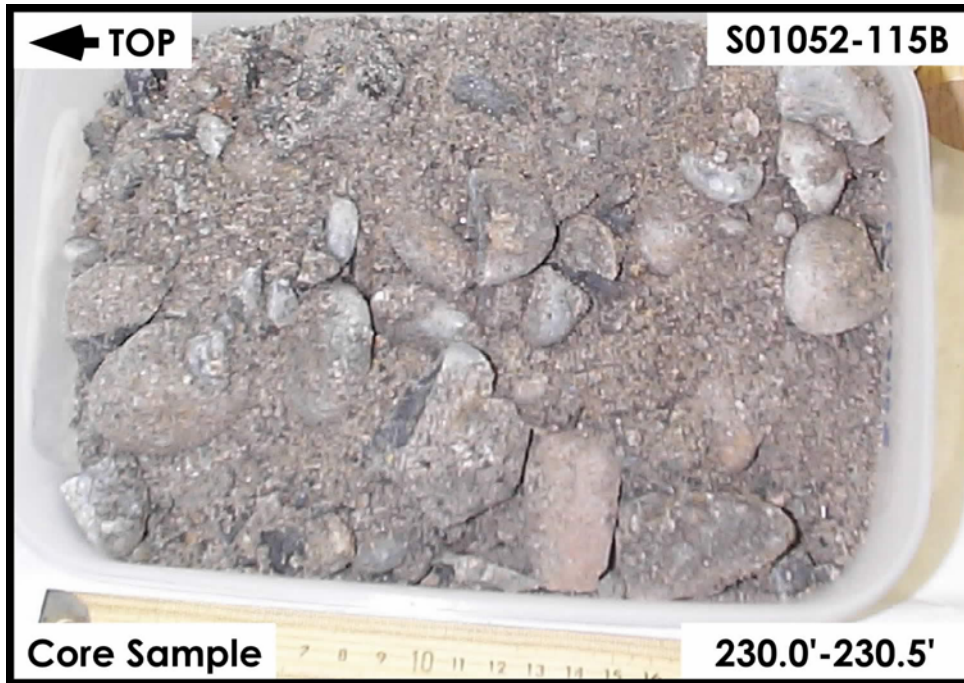
Plio-Pleistocene Silt Unit (PPlz)



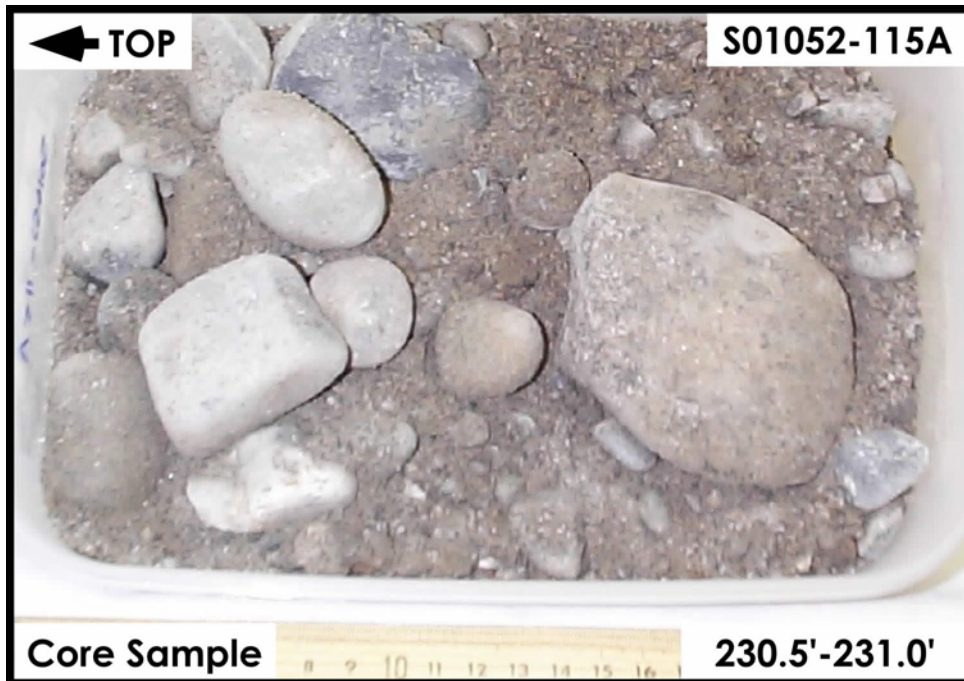
Plio-Pleistocene Silt Unit (PPlz)



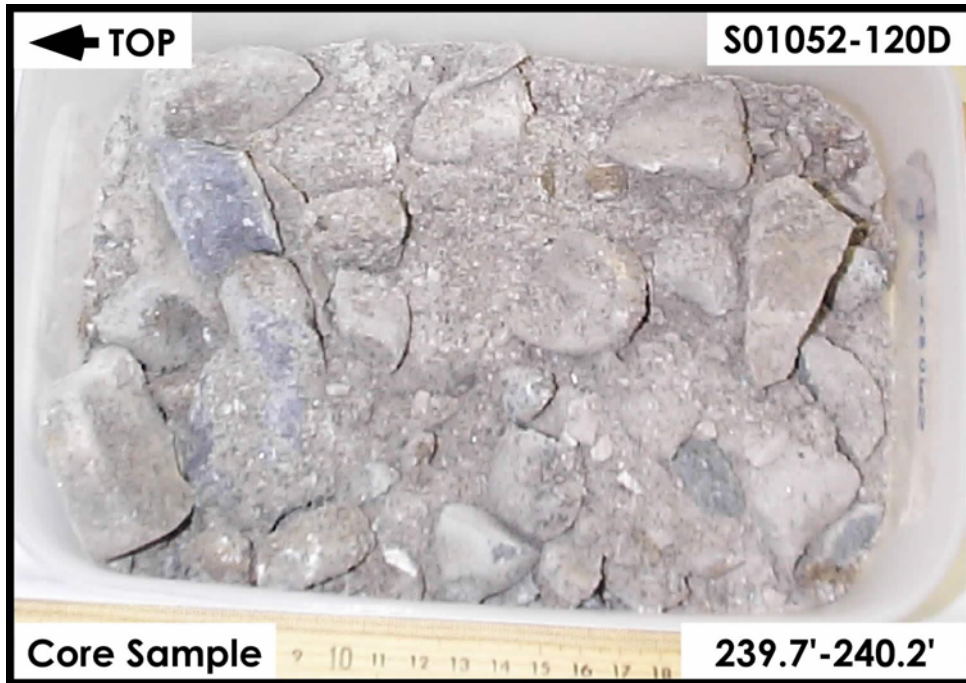
Plio-Pleistocene Gravel Unit (PPlg)



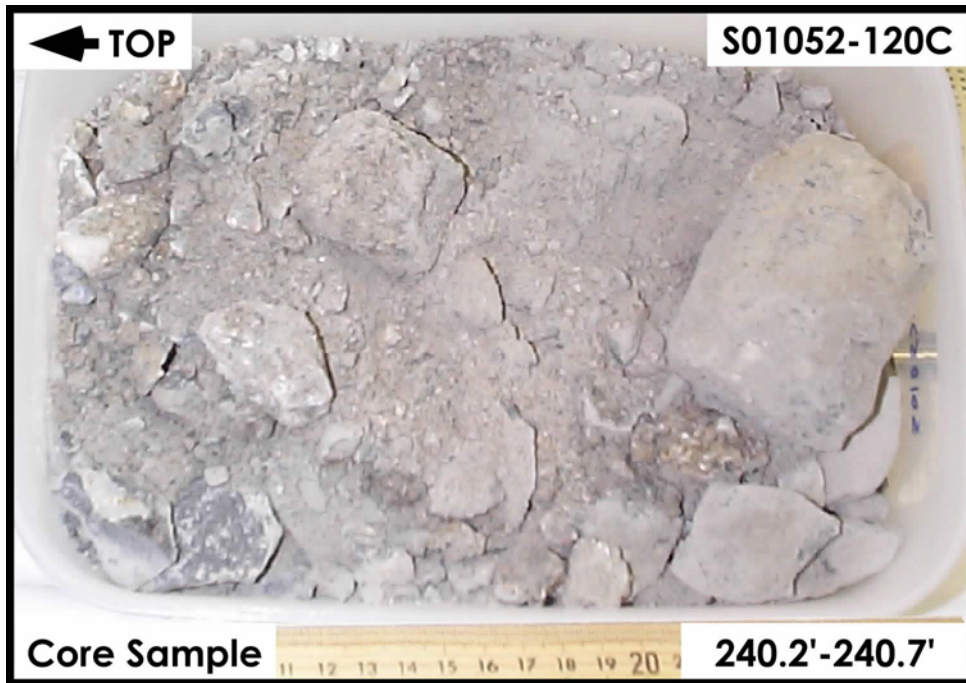
Plio-Pleistocene Gravel Unit (PPlg)



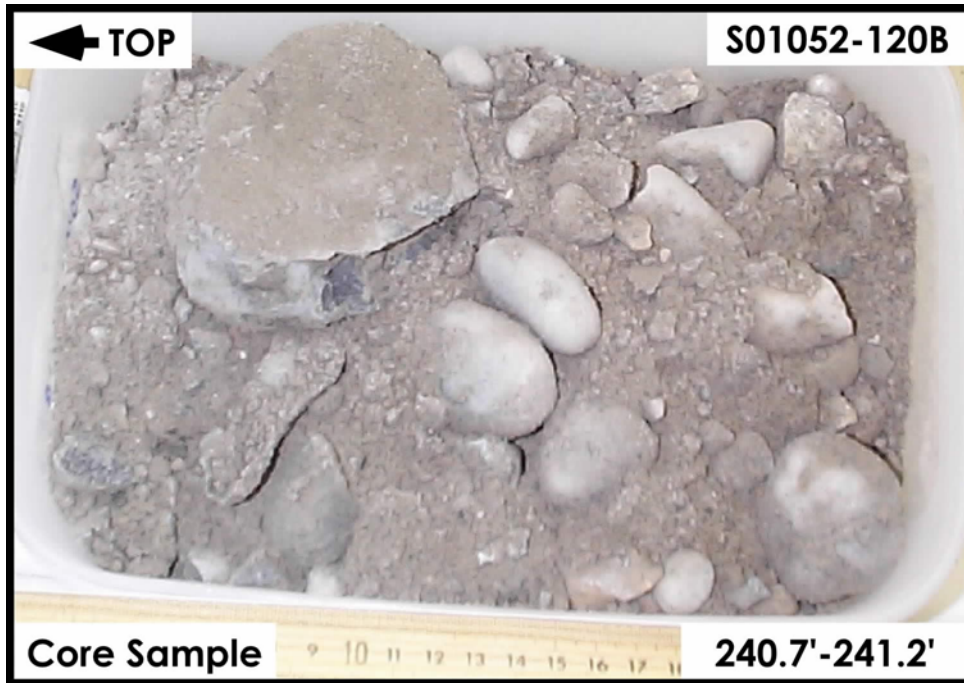
Plio-Pleistocene Gravel Unit (PPlg)



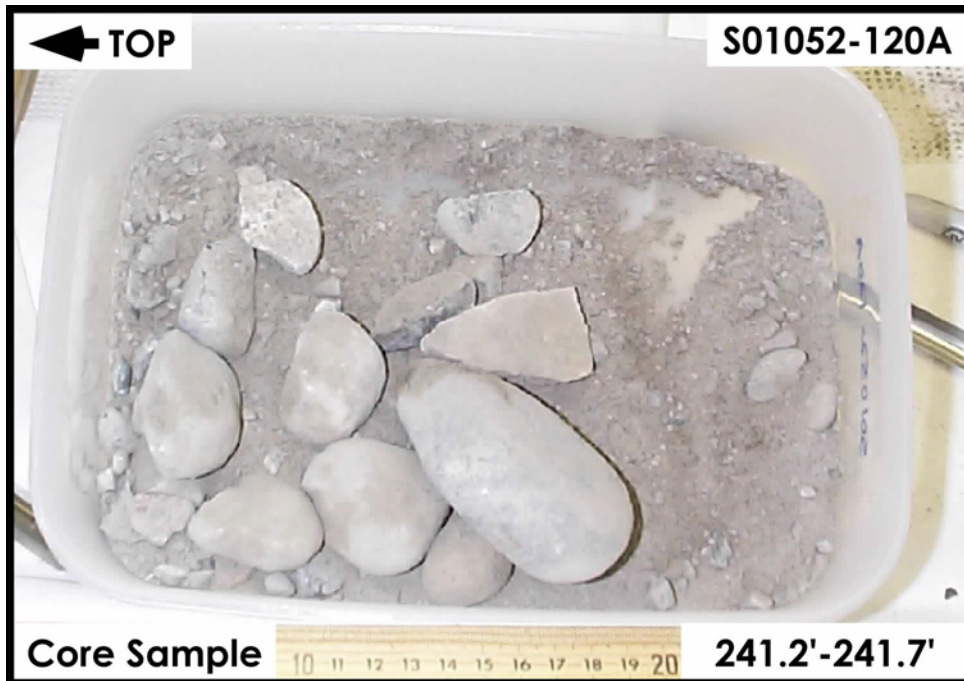
Plio-Pleistocene Gravel Unit (PPlg)



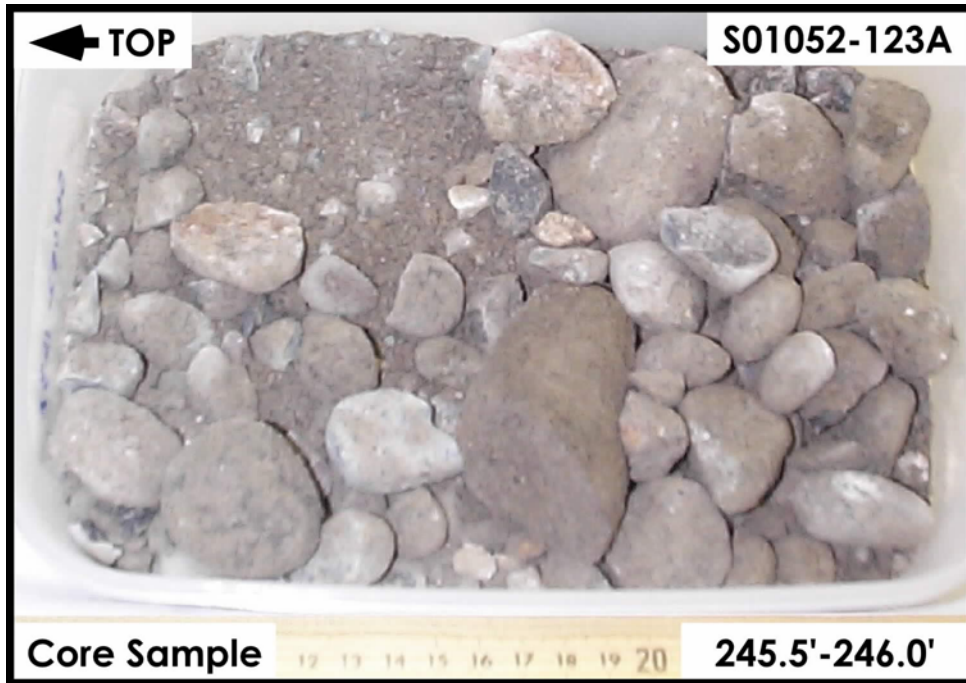
Plio-Pleistocene Gravel Unit (PPlg)



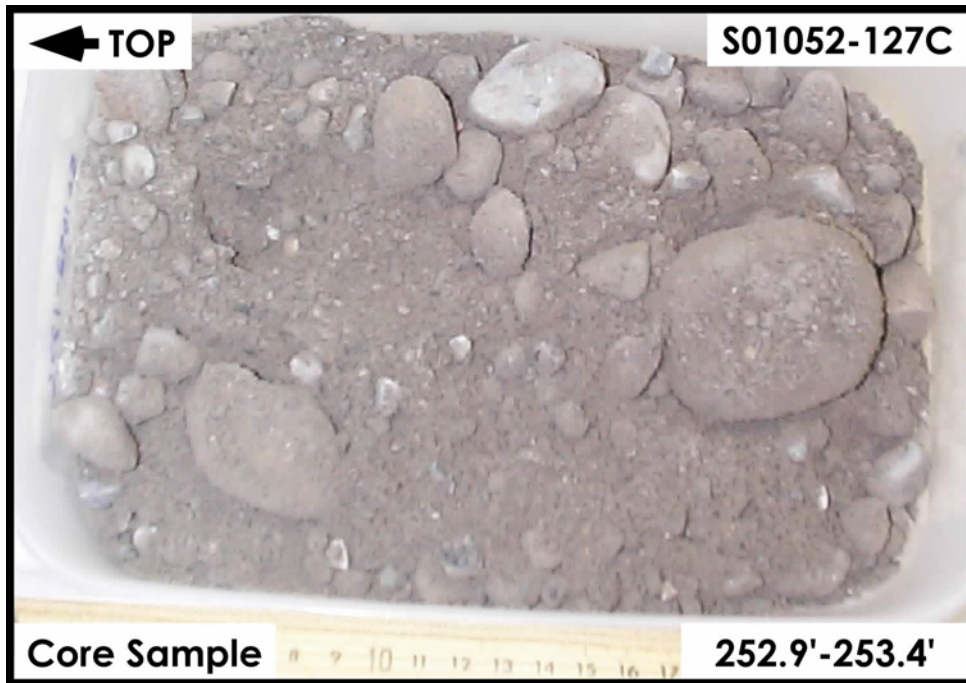
Plio-Pleistocene Gravel Unit (PPlg)



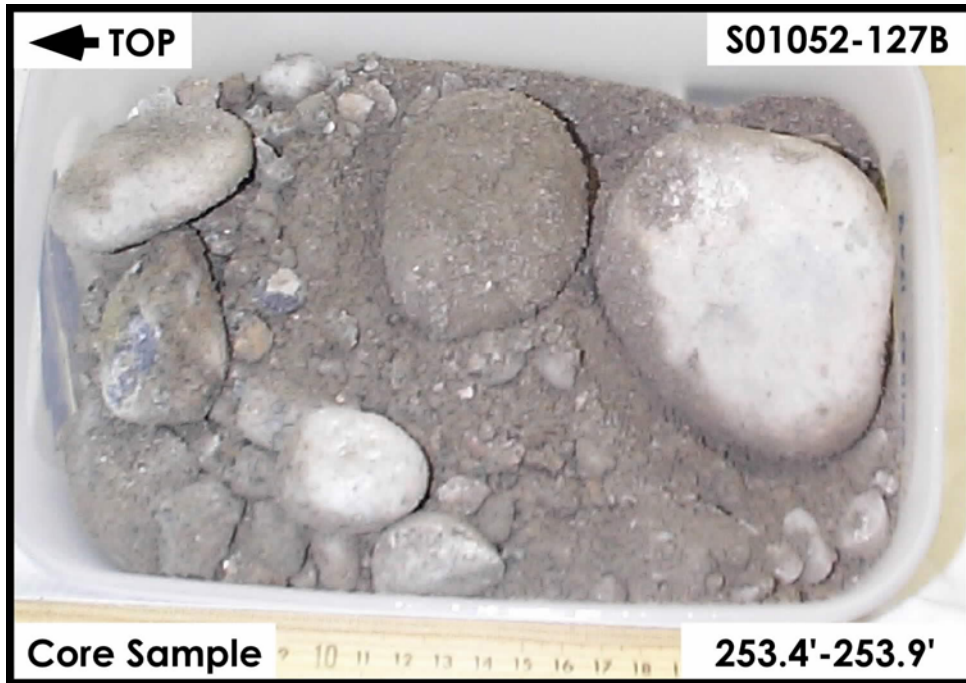
Plio-Pleistocene Gravel Unit (PPlg)



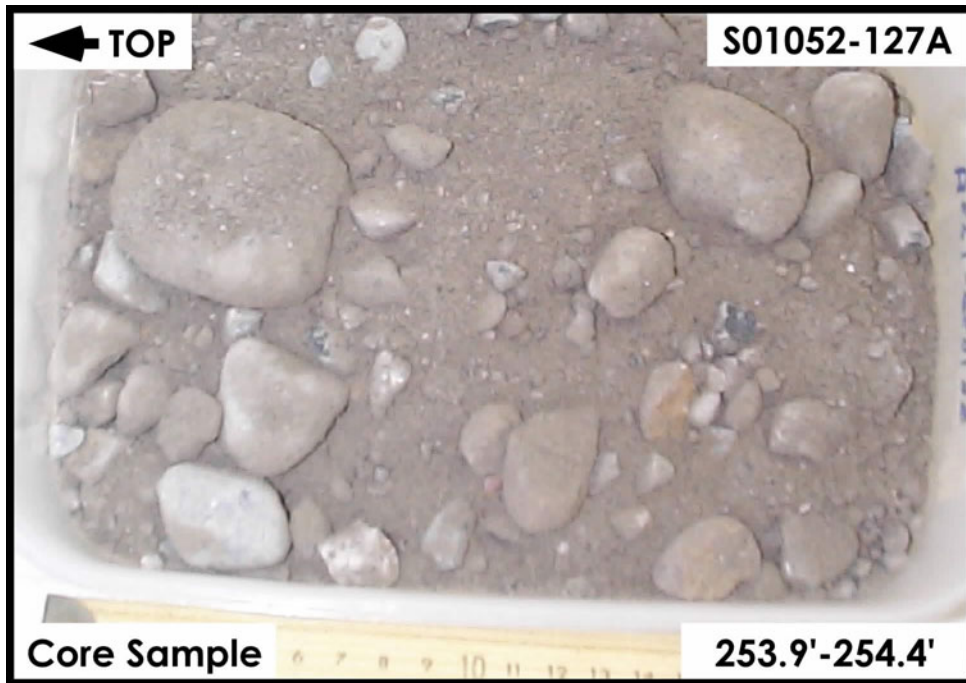
Plio-Pleistocene Gravel Unit (PPlg)



Plio-Pleistocene Gravel Unit (PPlg)



Plio-Pleistocene Gravel Unit (PPlg)



Plio-Pleistocene Gravel Unit (PPlg)

Appendix B-2

299-E33-46

Composite Grab

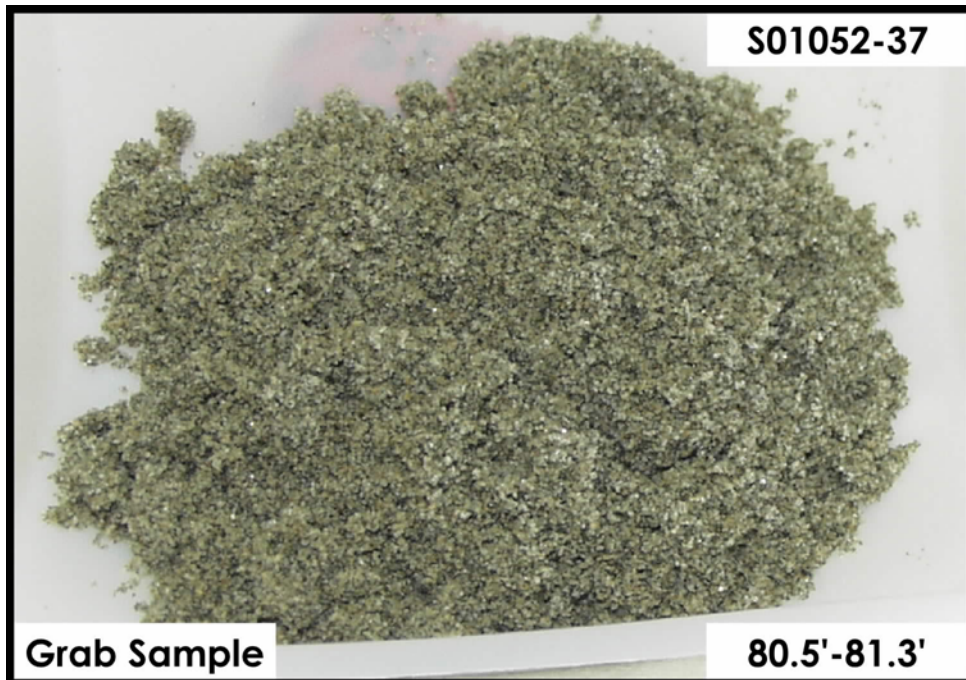
and

Splitspoon Shoe

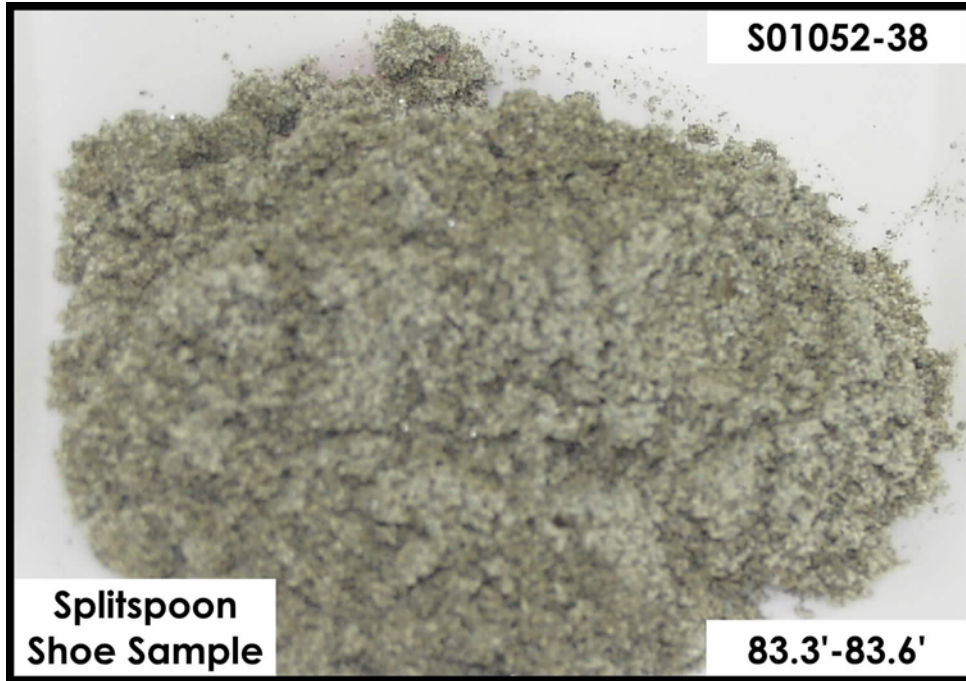
Sample Photographs



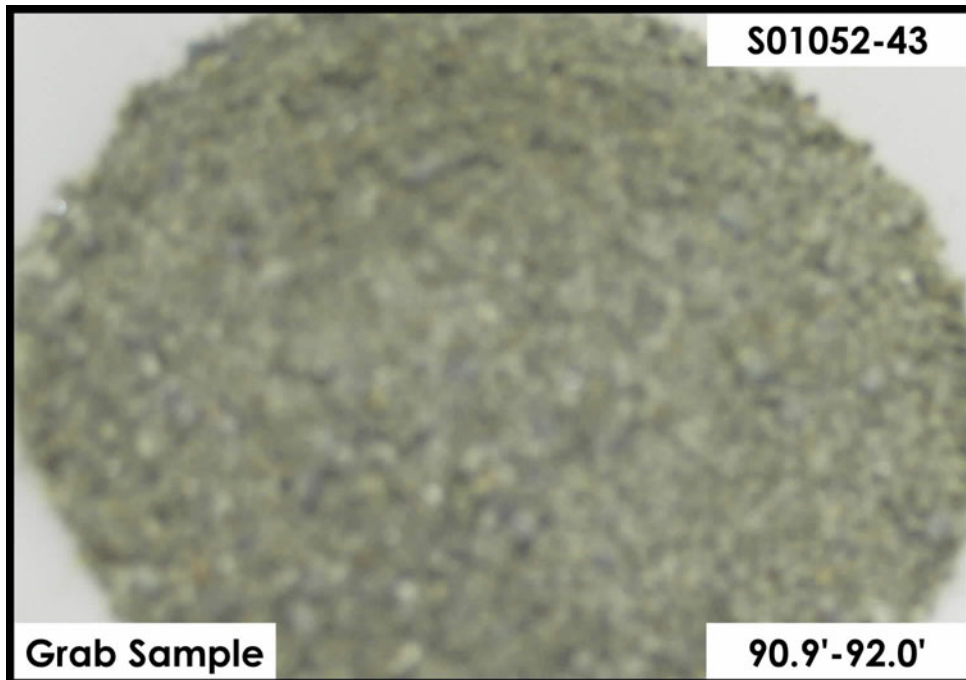
H2-Upper Sand and Gravel Sequence



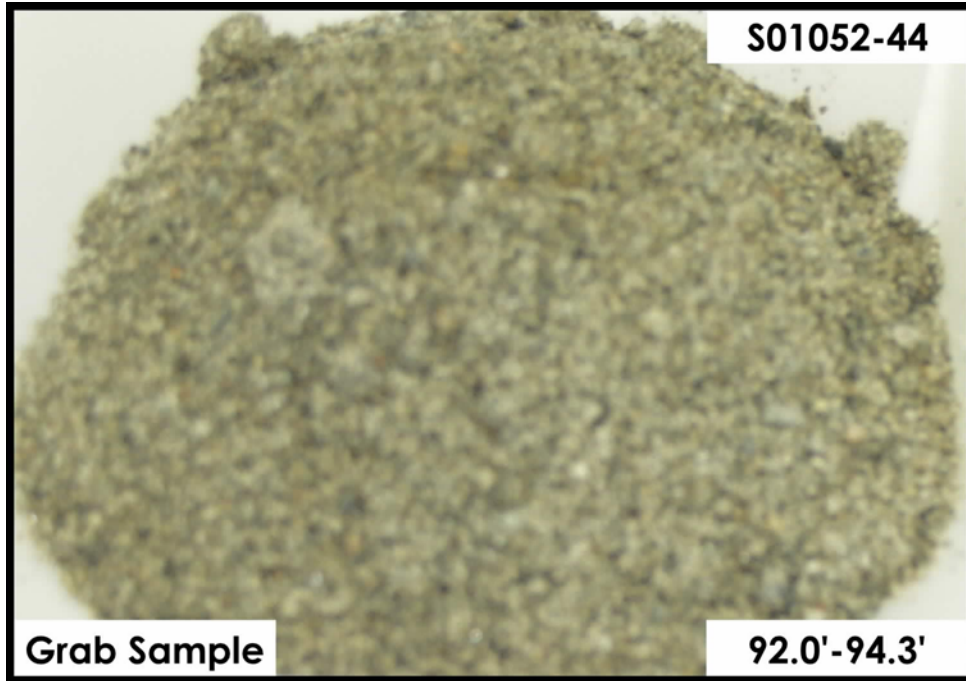
H2-Upper Sand and Gravel Sequence



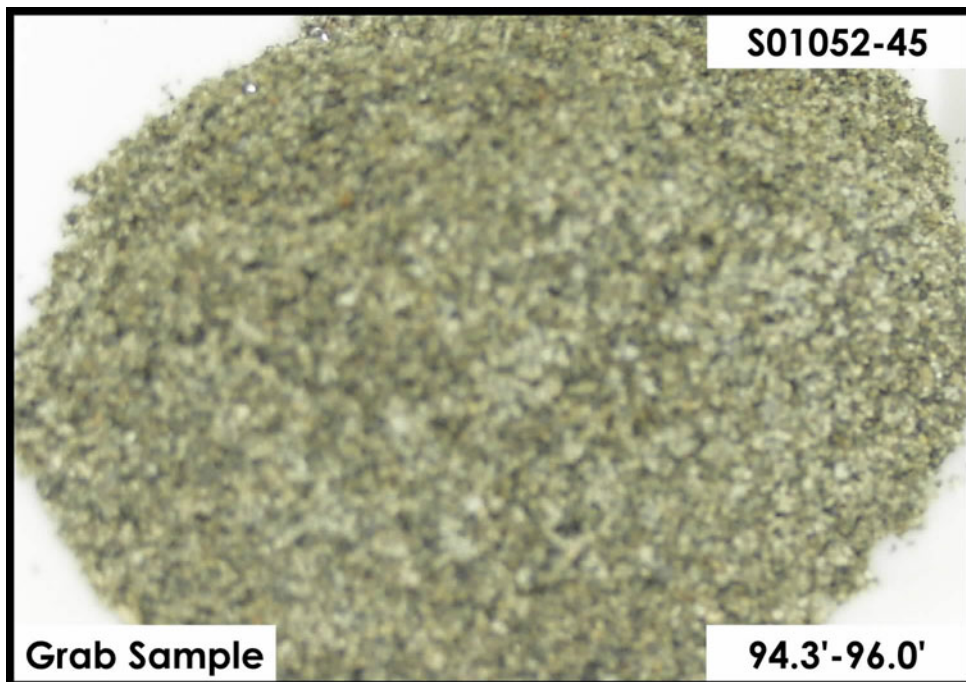
H2-Upper Sand and Gravel Sequence



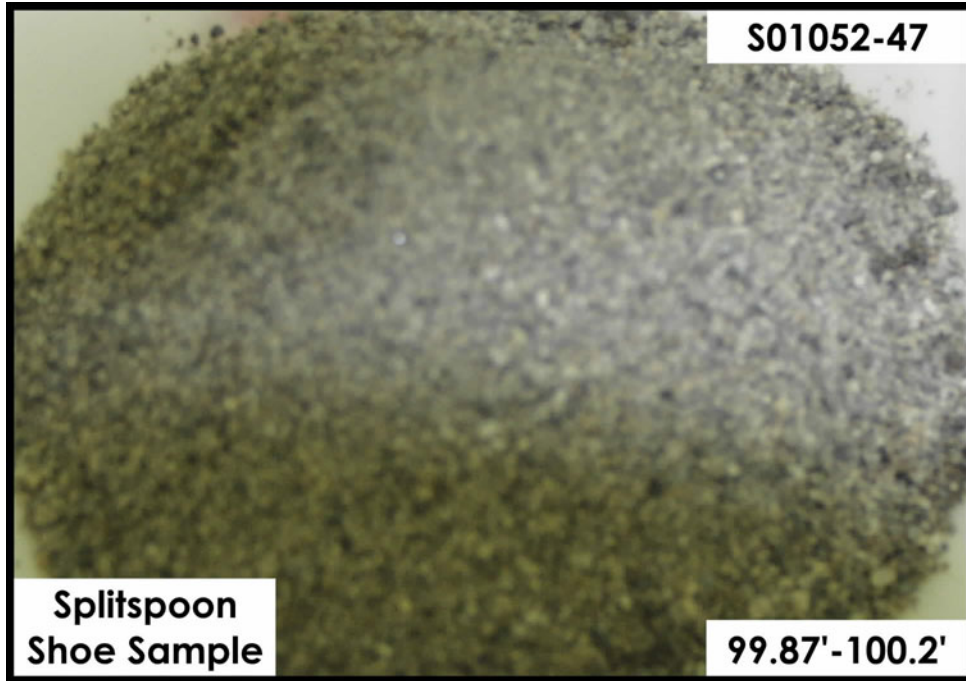
H2-Upper Sand and Gravel Sequence



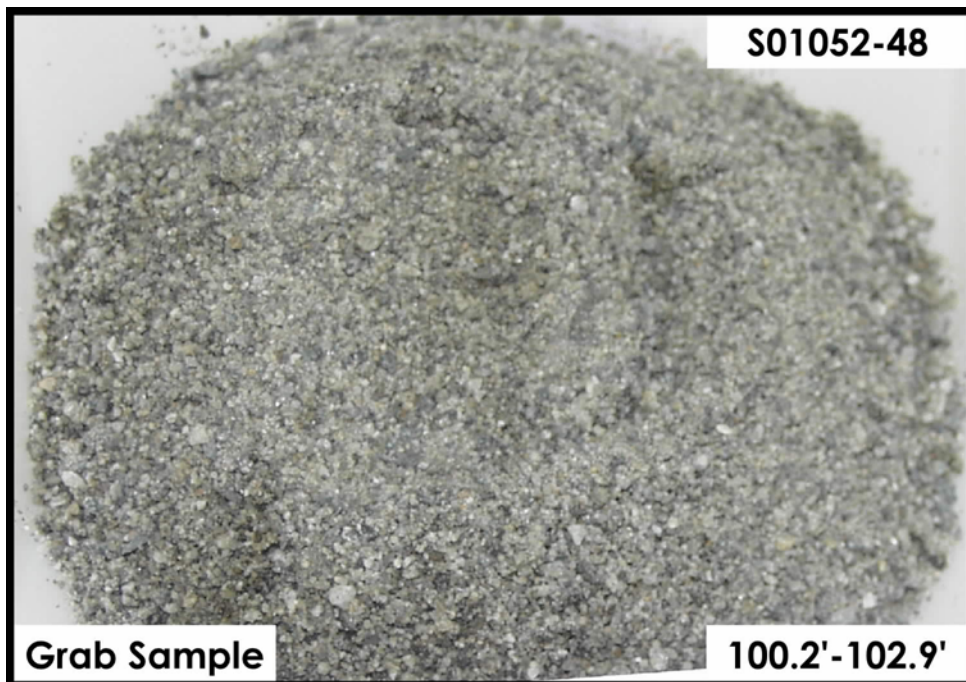
H2-Upper Sand and Gravel Sequence



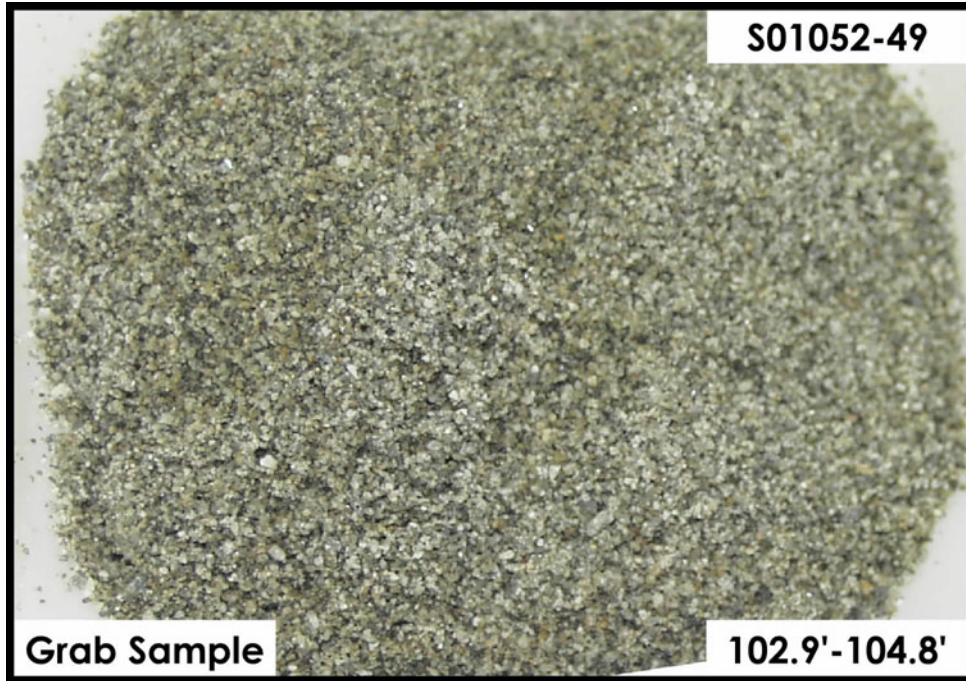
H2-Upper Sand and Gravel Sequence



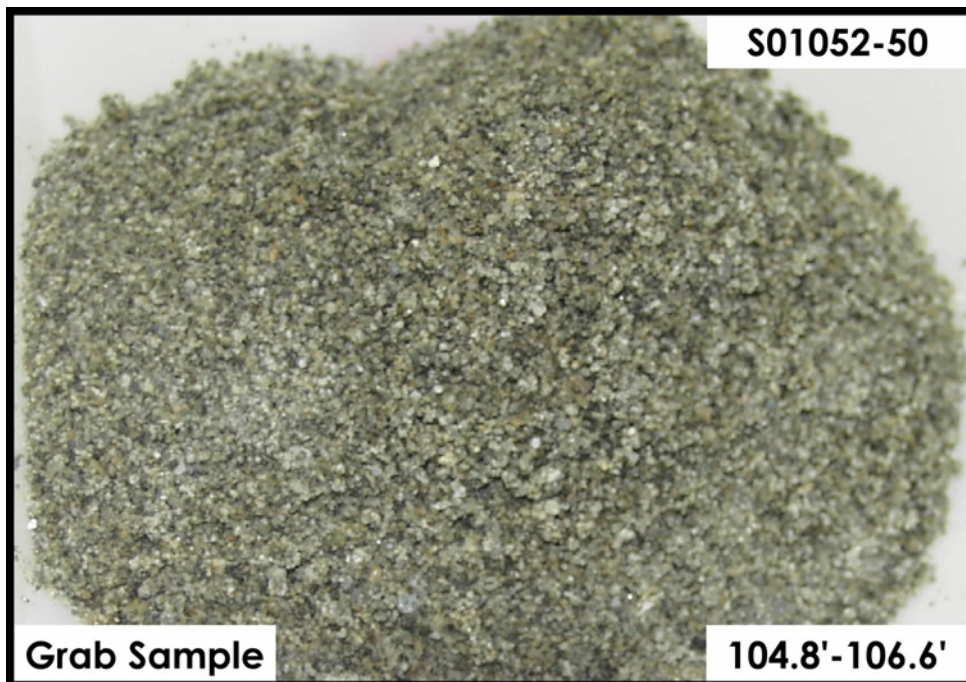
H2-Upper Sand and Gravel Sequence



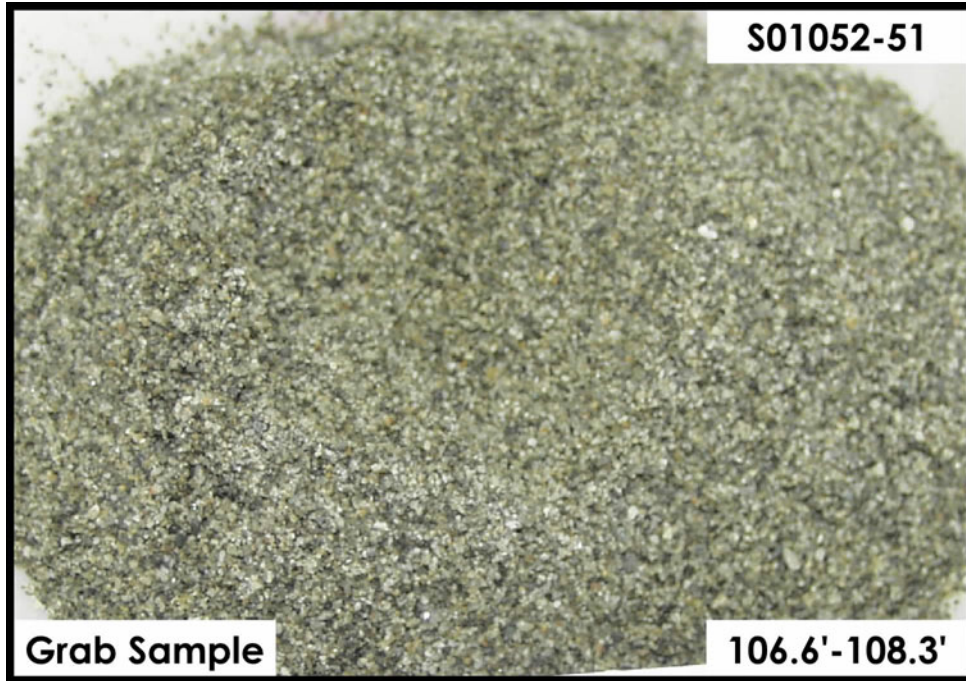
H2-Upper Sand and Gravel Sequence



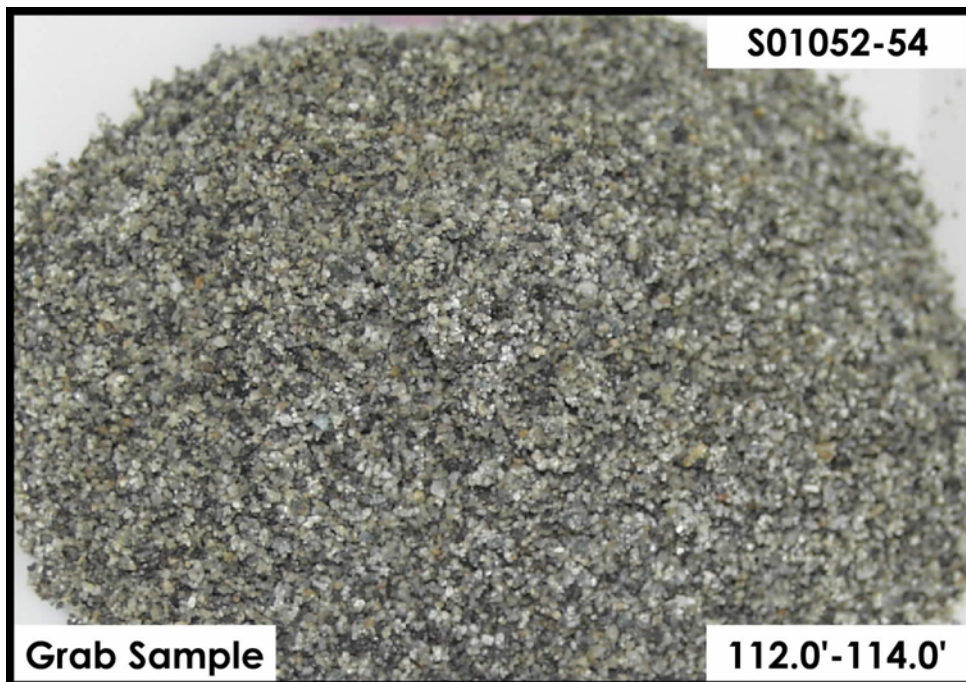
H2-Upper Sand and Gravel Sequence



H2-Upper Sand and Gravel Sequence



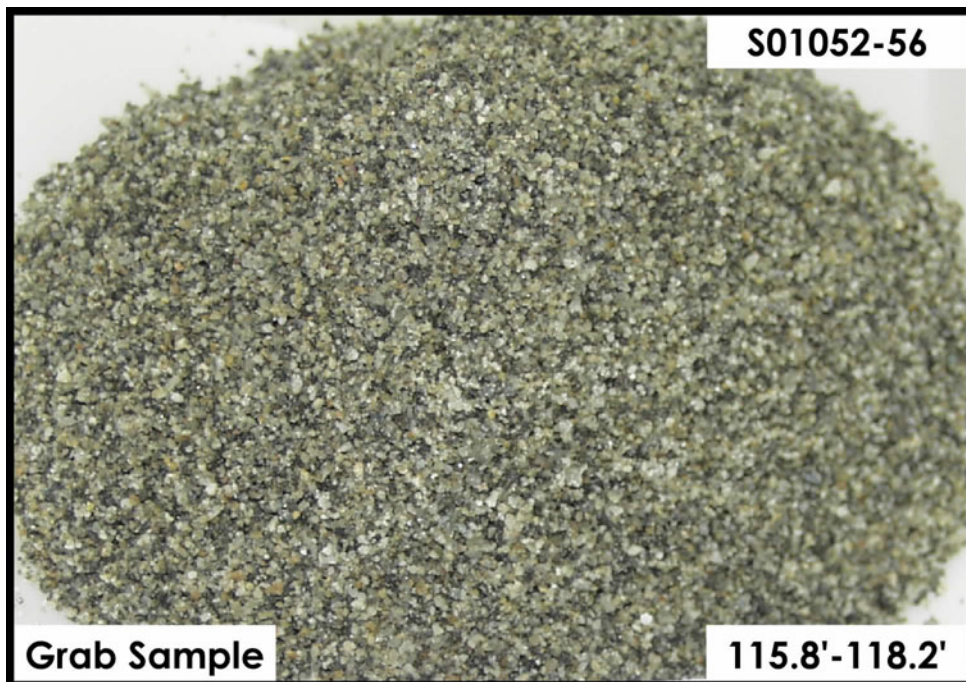
H2-Upper Sand and Gravel Sequence



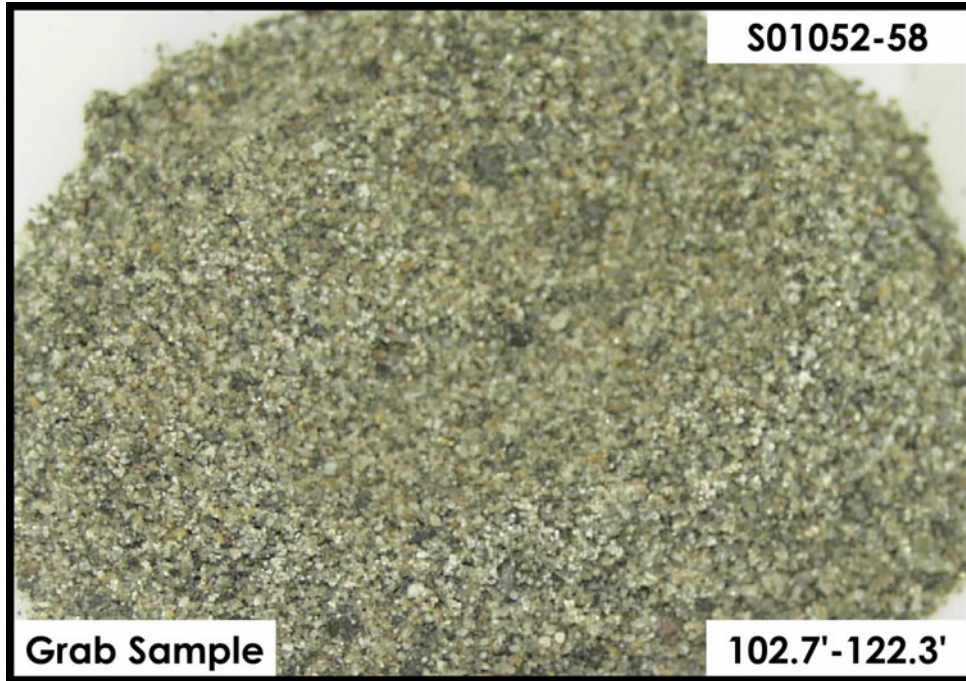
H2-Upper Sand and Gravel Sequence



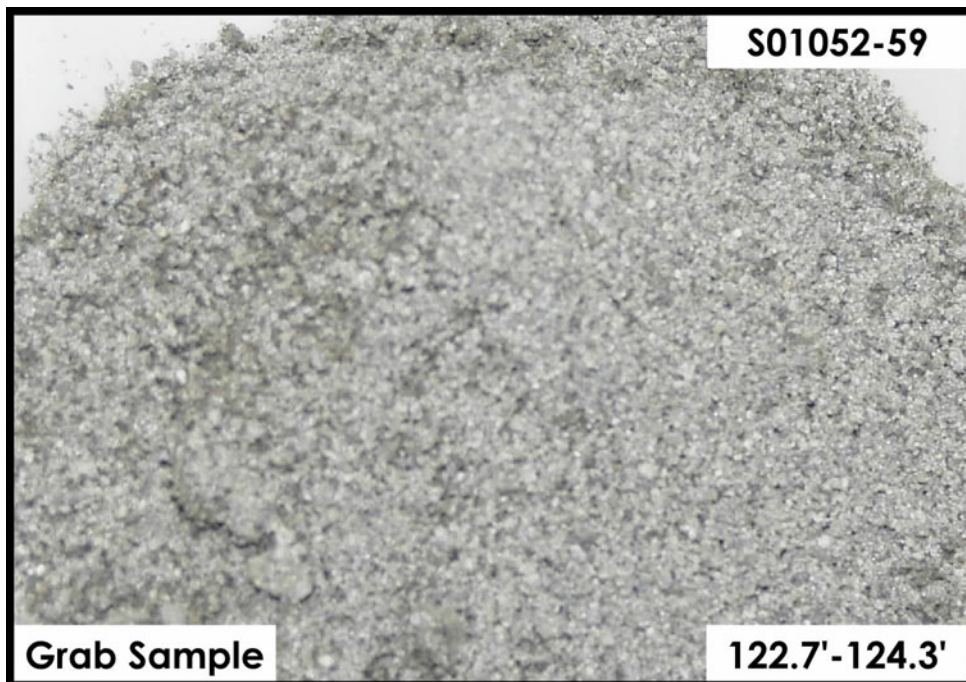
H2-Upper Sand and Gravel Sequence



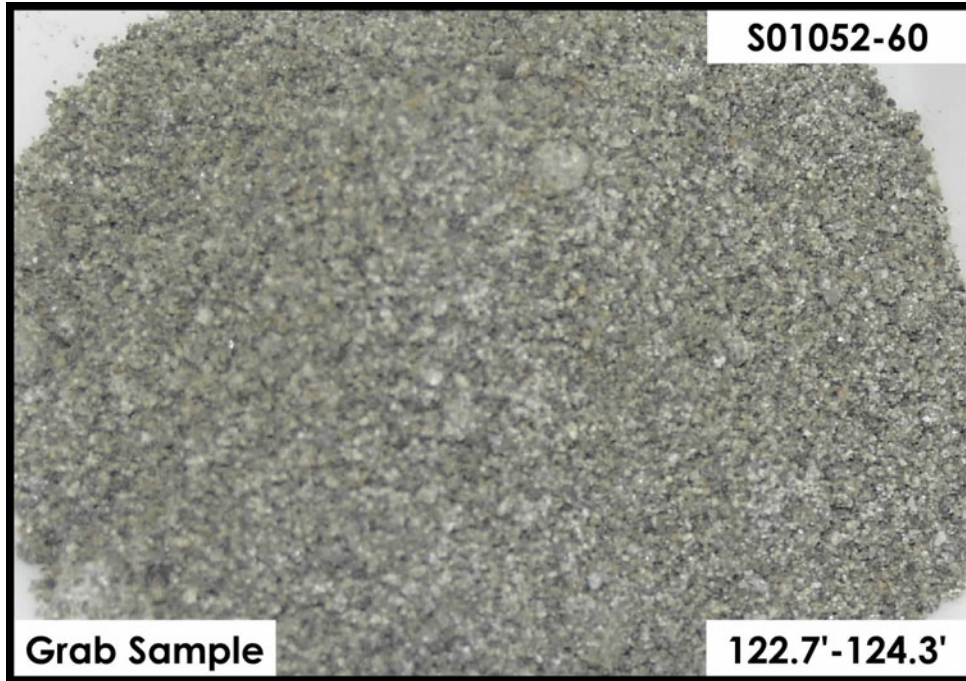
H2-Upper Sand and Gravel Sequence



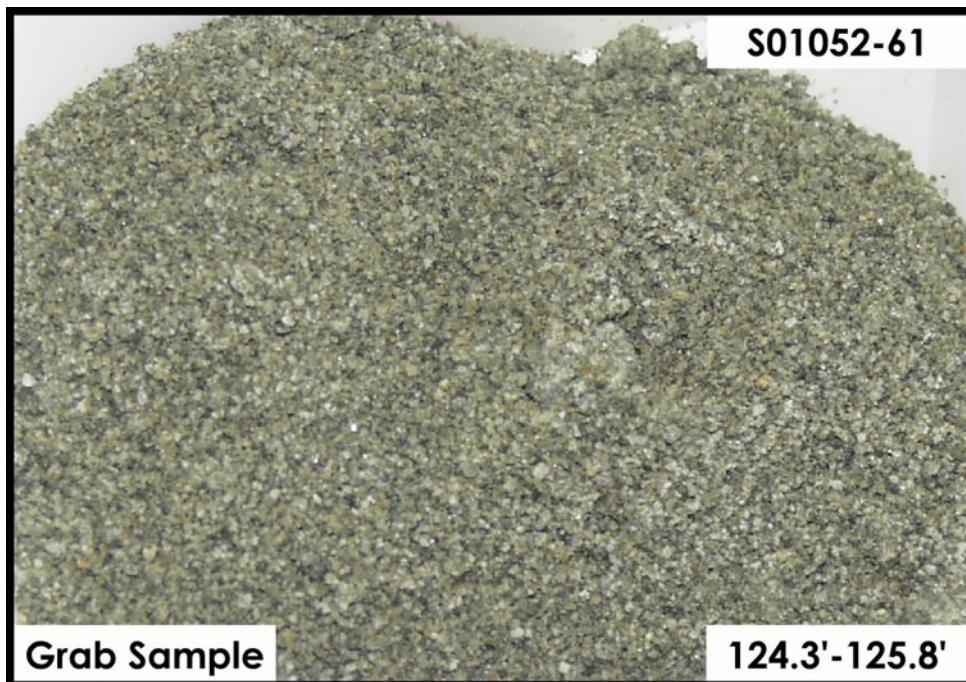
H2-Upper Sand and Gravel Sequence



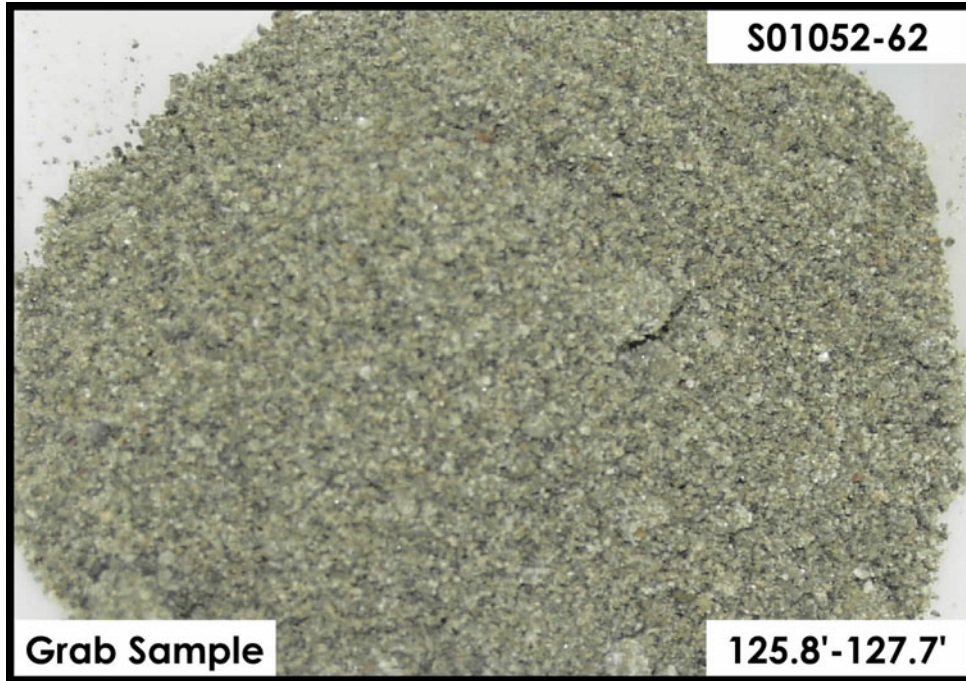
H2-Upper Sand and Gravel Sequence



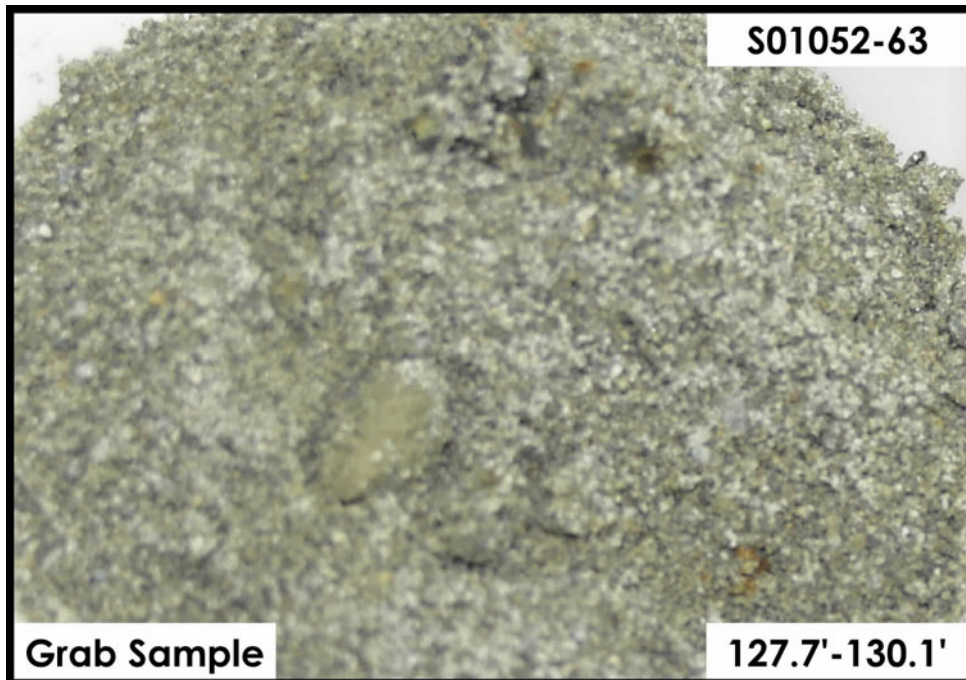
H2-Upper Sand and Gravel Sequence



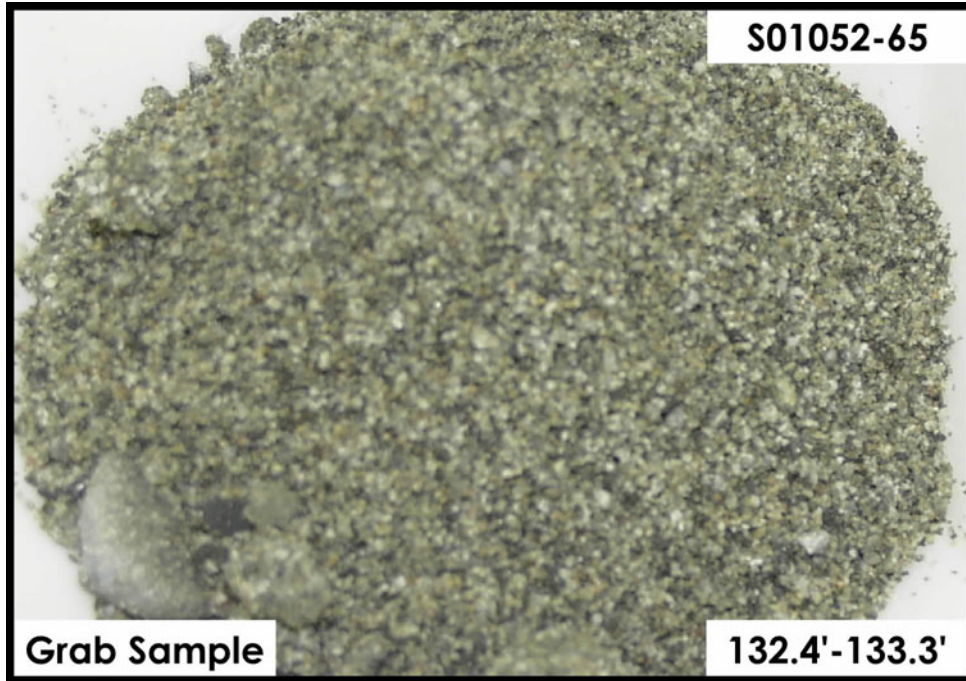
H2-Upper Sand and Gravel Sequence



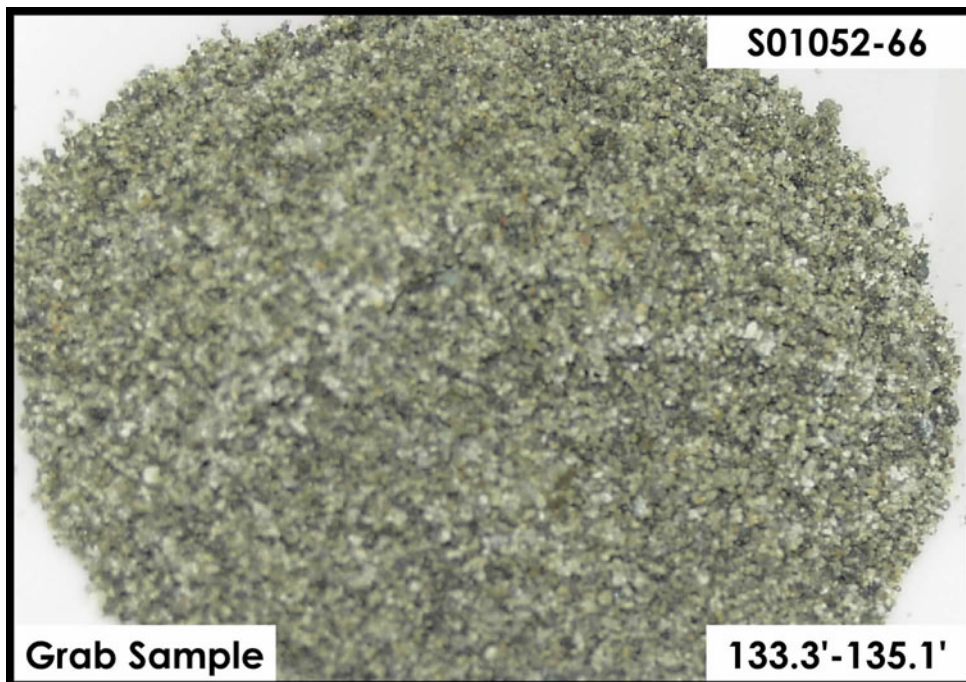
H2-Upper Sand and Gravel Sequence



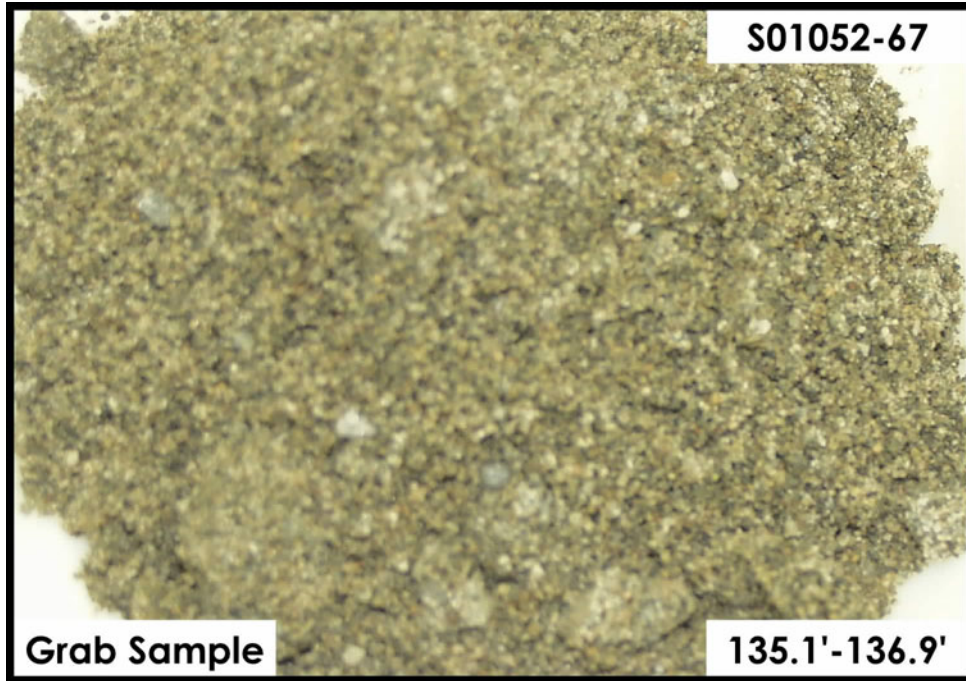
H2-Upper Sand and Gravel Sequence



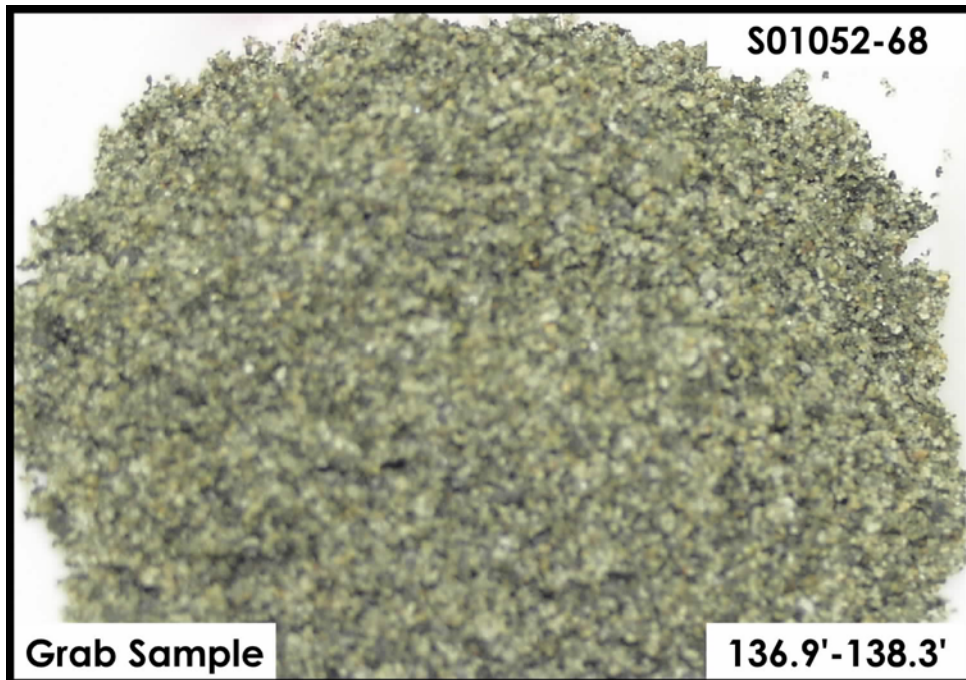
H2-Upper Sand and Gravel Sequence



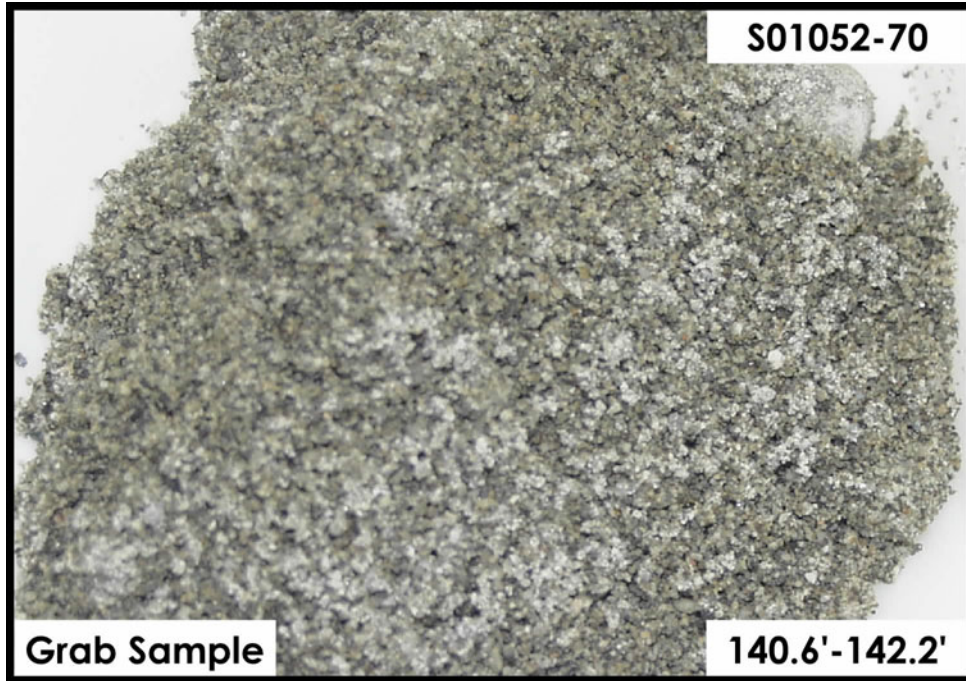
H2-Upper Sand and Gravel Sequence



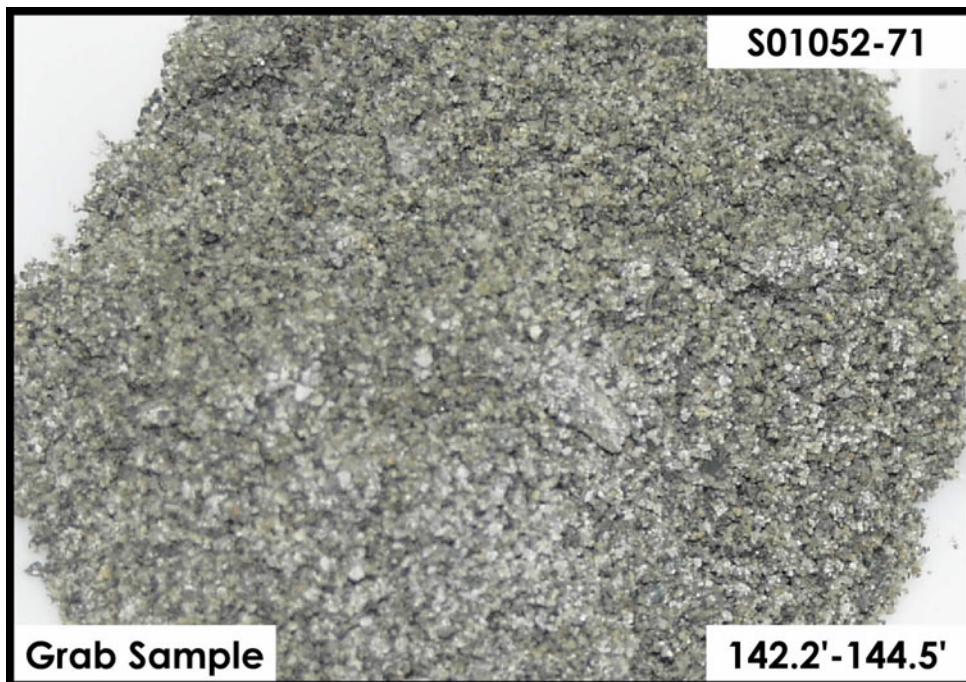
H2-Upper Sand and Gravel Sequence



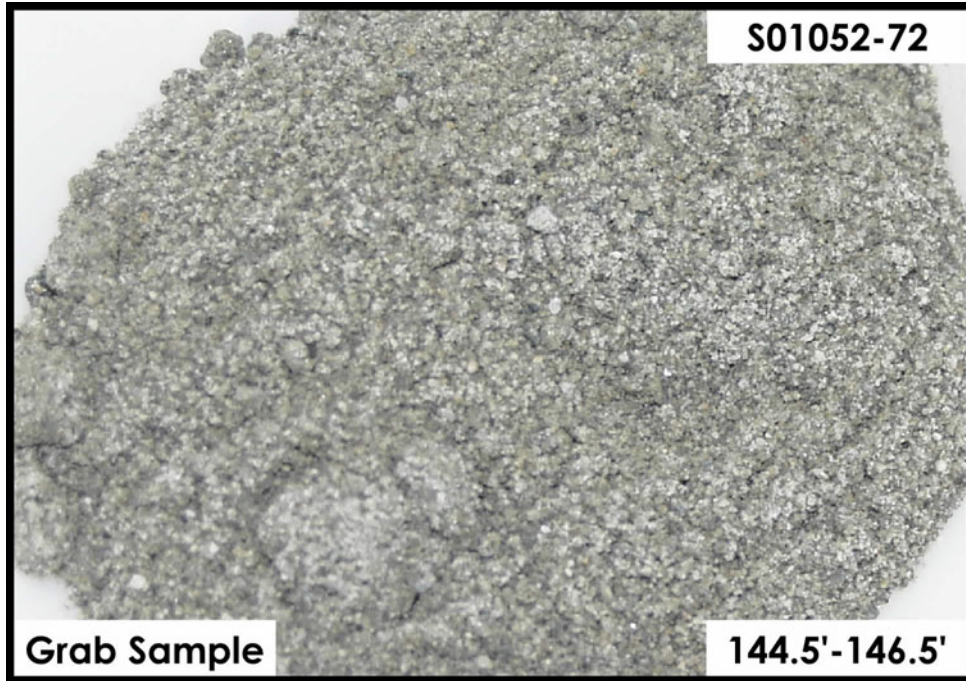
H2-Upper Sand and Gravel Sequence



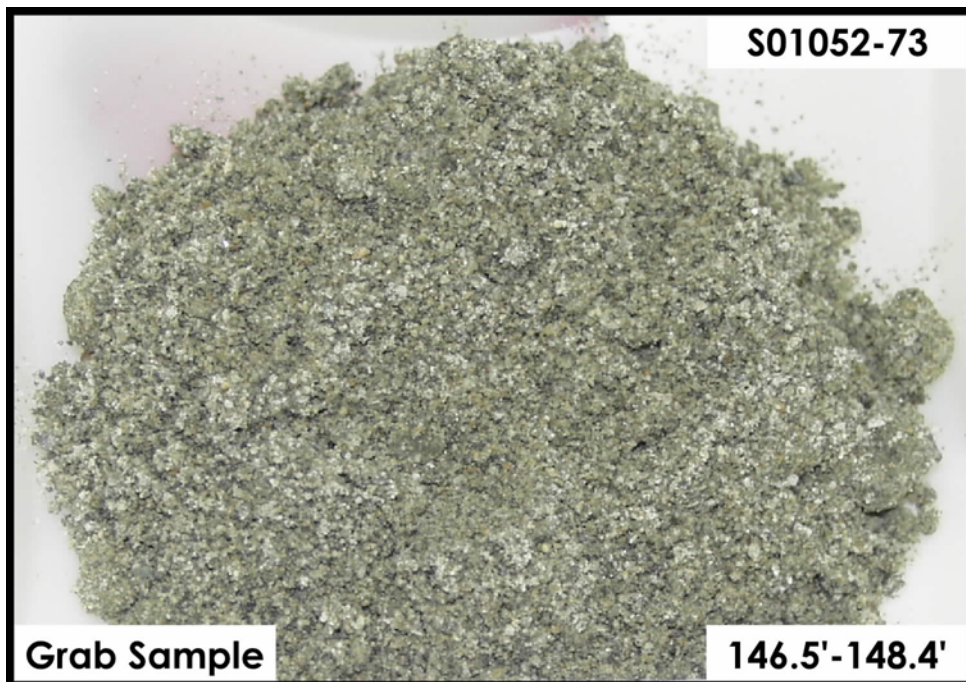
H2-Upper Sand and Gravel Sequence



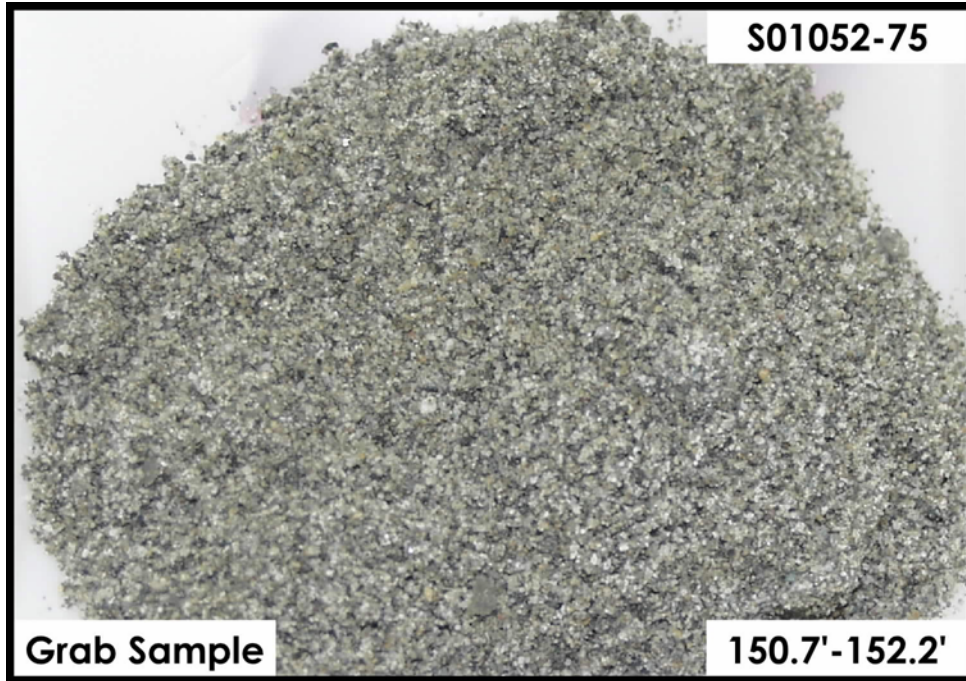
H2-Upper Sand and Gravel Sequence



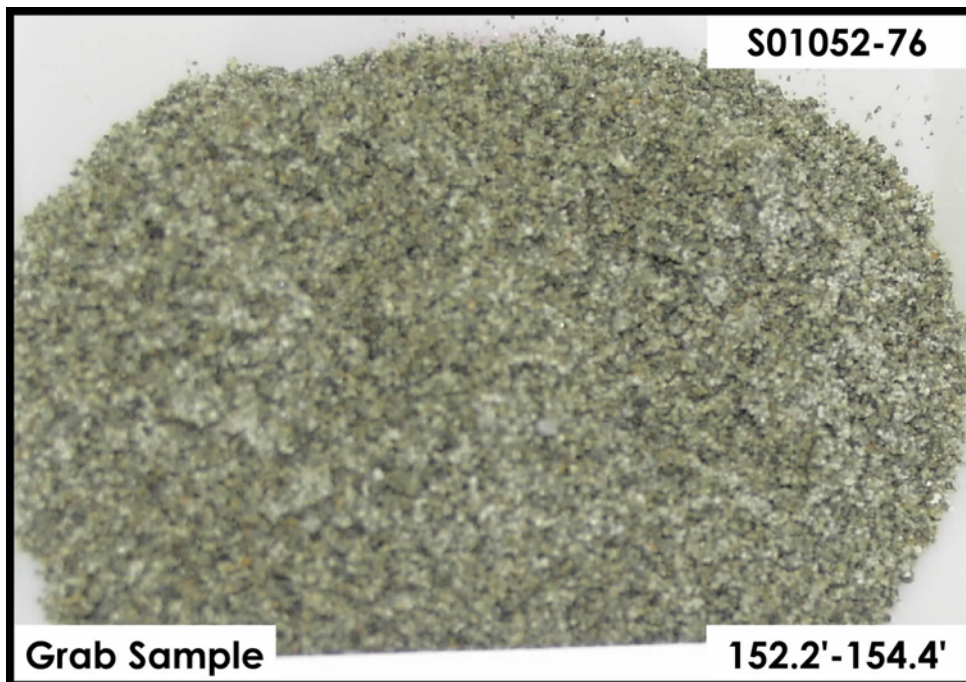
H2-Upper Sand and Gravel Sequence



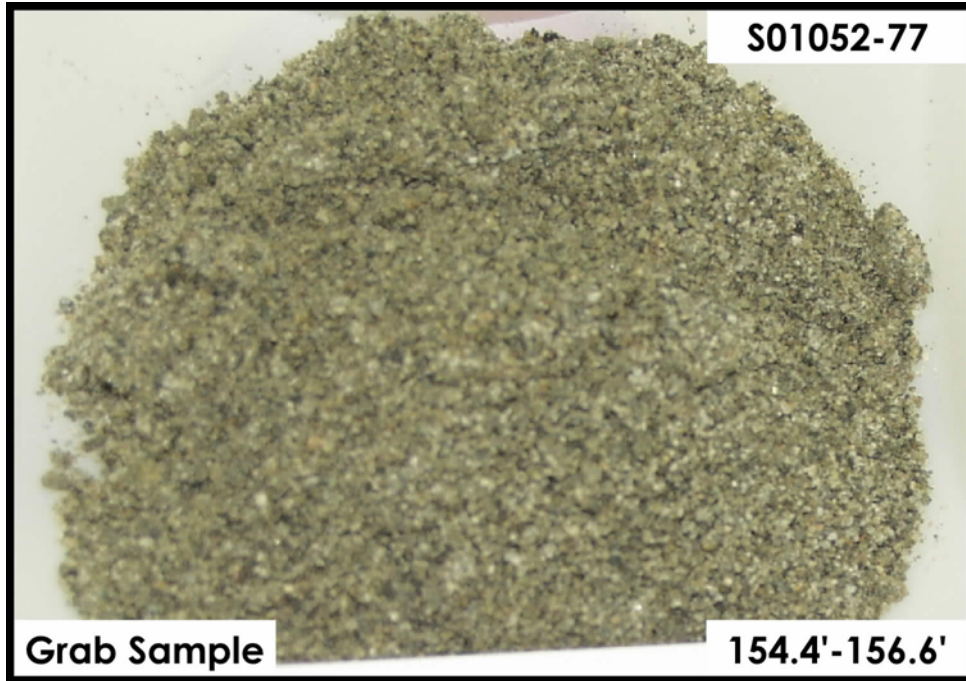
H2-Upper Sand and Gravel Sequence



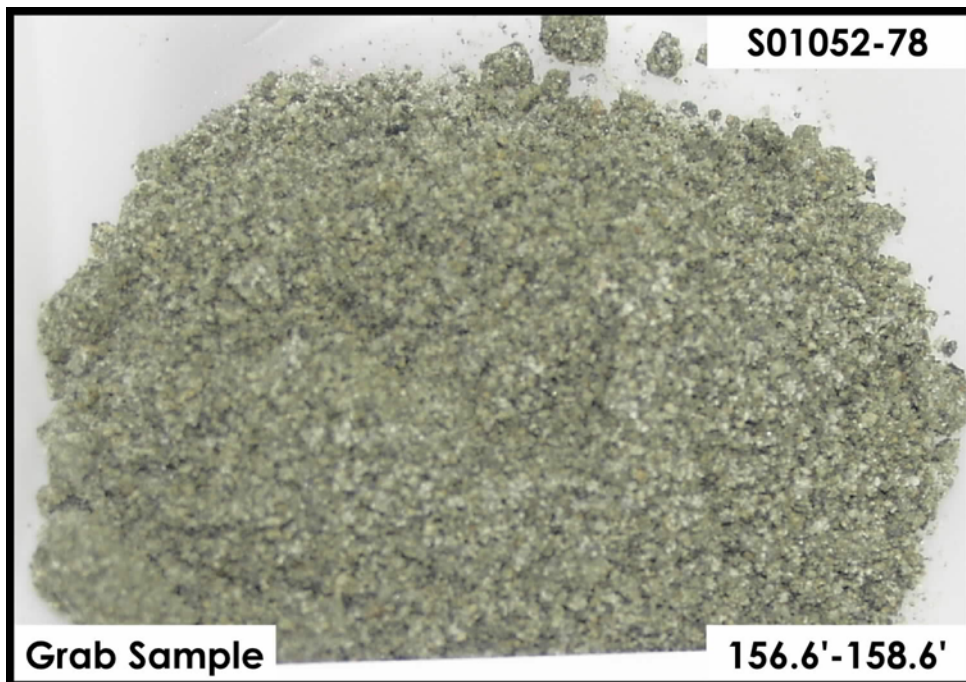
H2-Upper Sand and Gravel Sequence



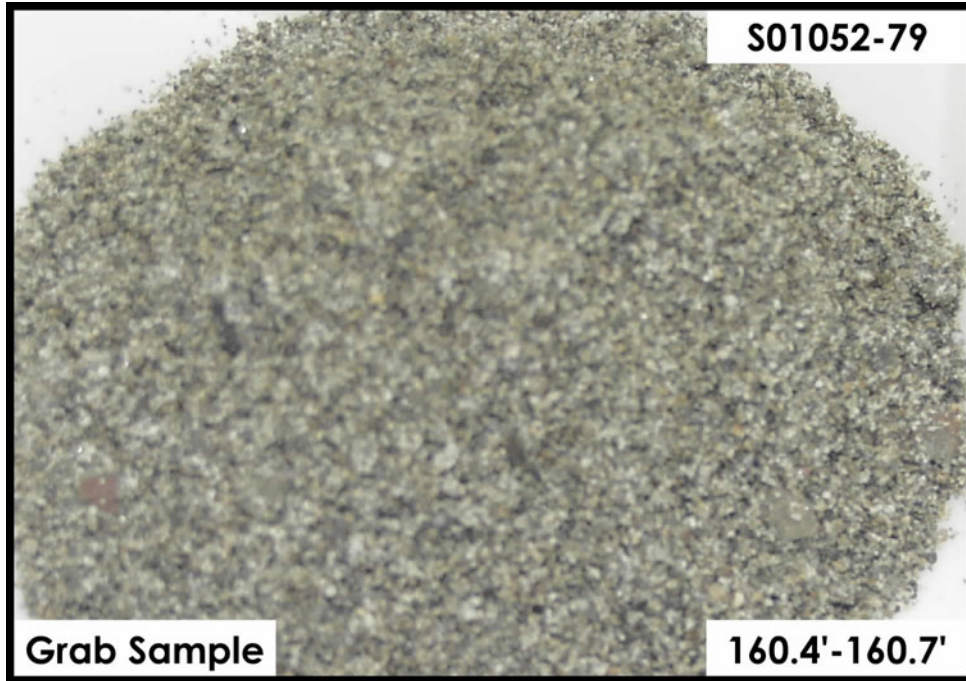
H2-Upper Sand and Gravel Sequence



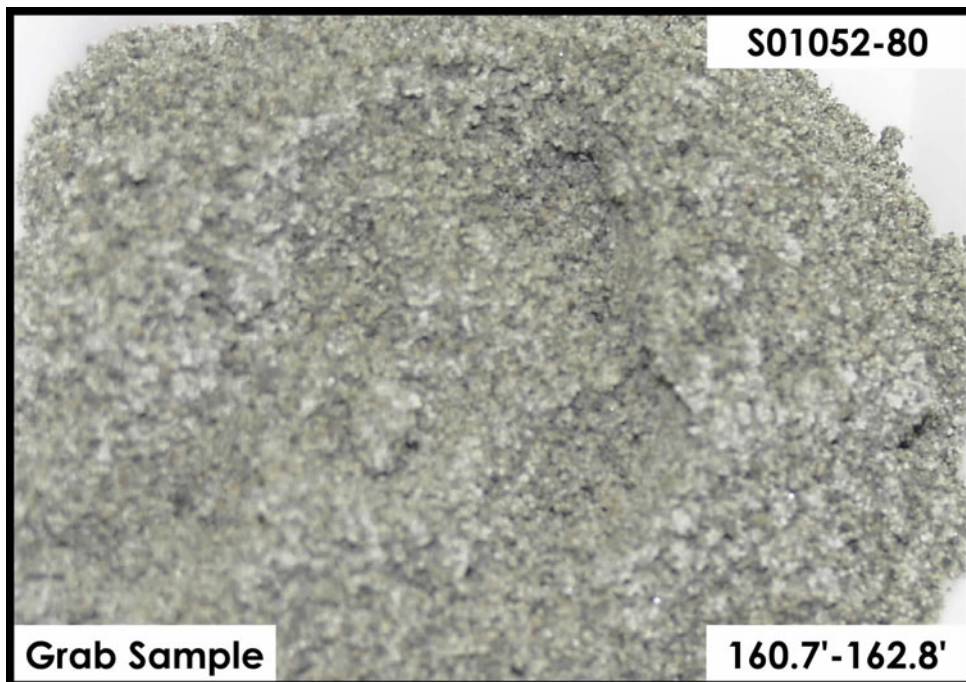
H2-Upper Sand and Gravel Sequence



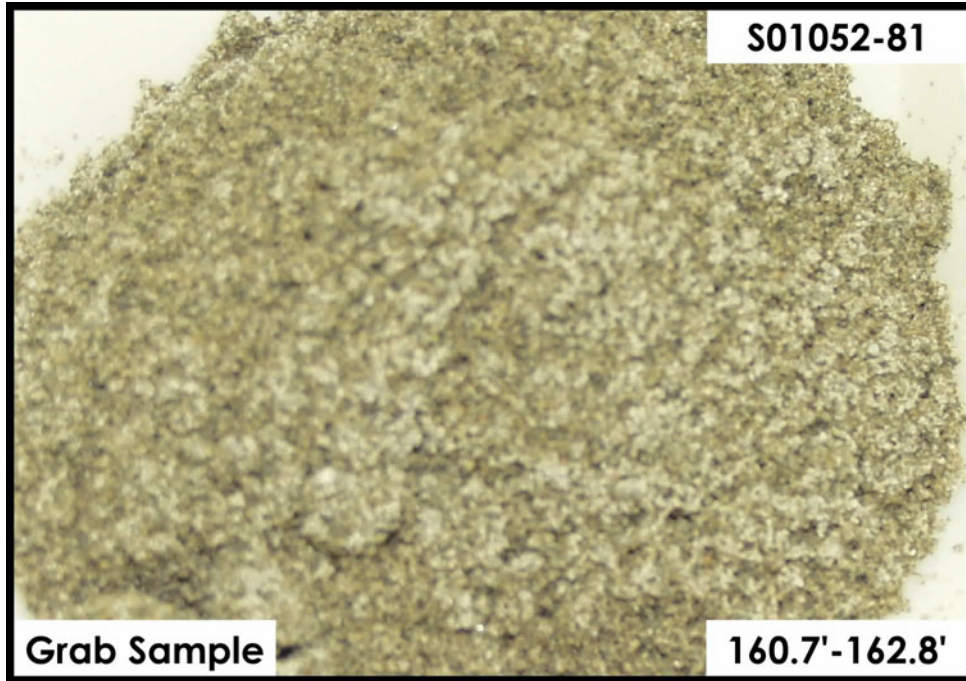
H2-Upper Sand and Gravel Sequence



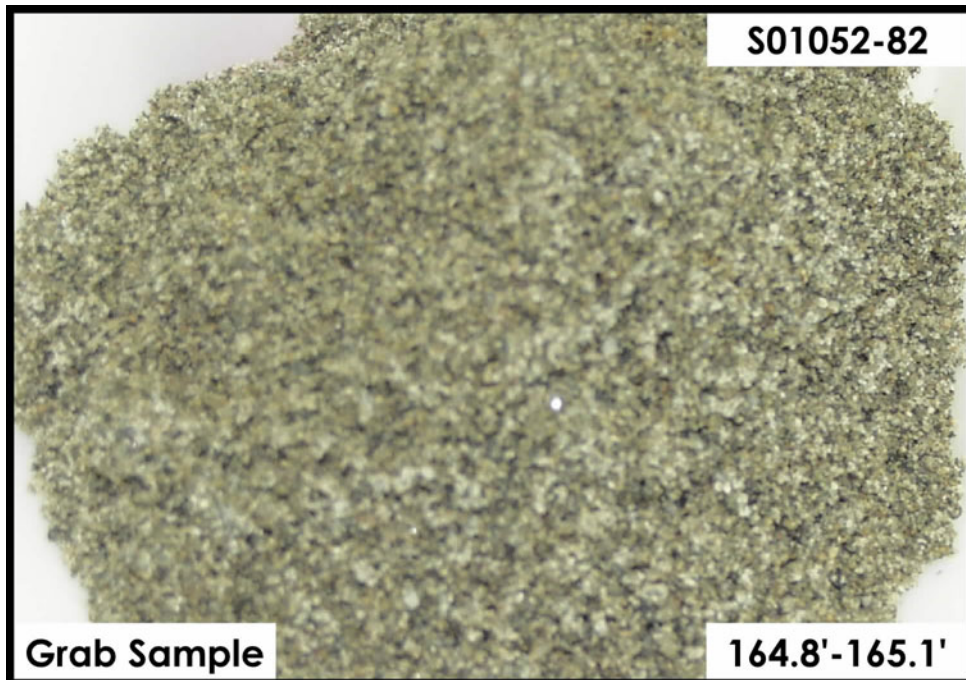
H2-Upper Sand and Gravel Sequence



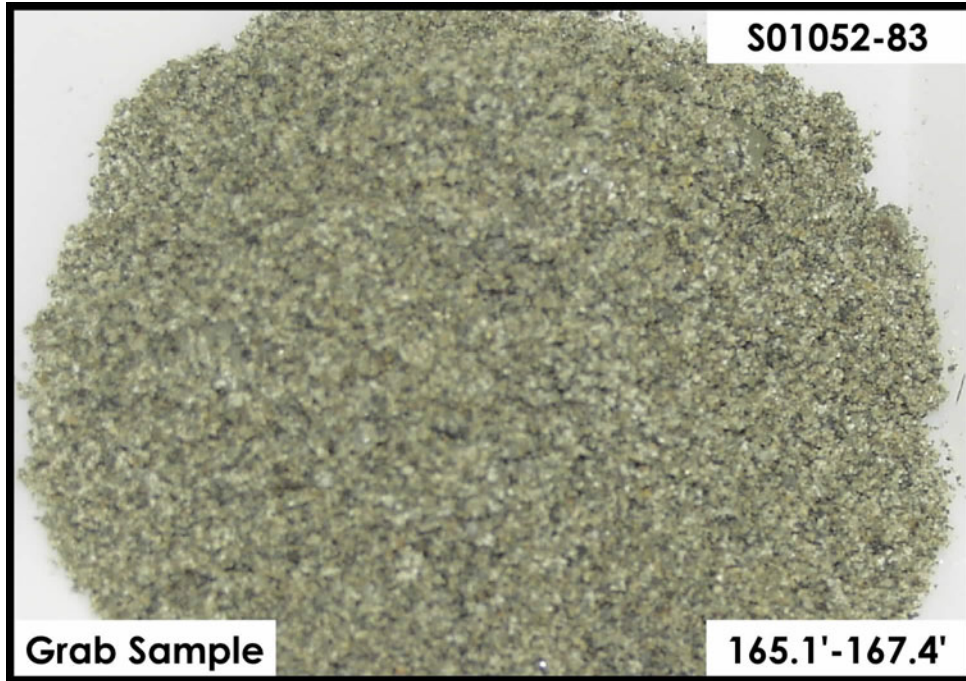
H2-Upper Sand and Gravel Sequence



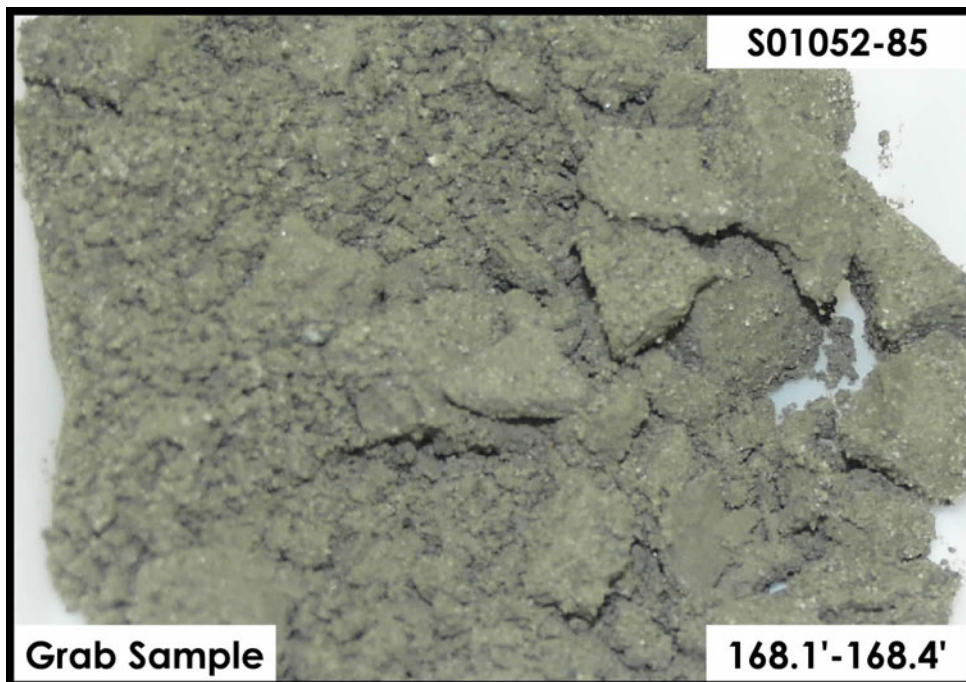
H2-Upper Sand and Gravel Sequence



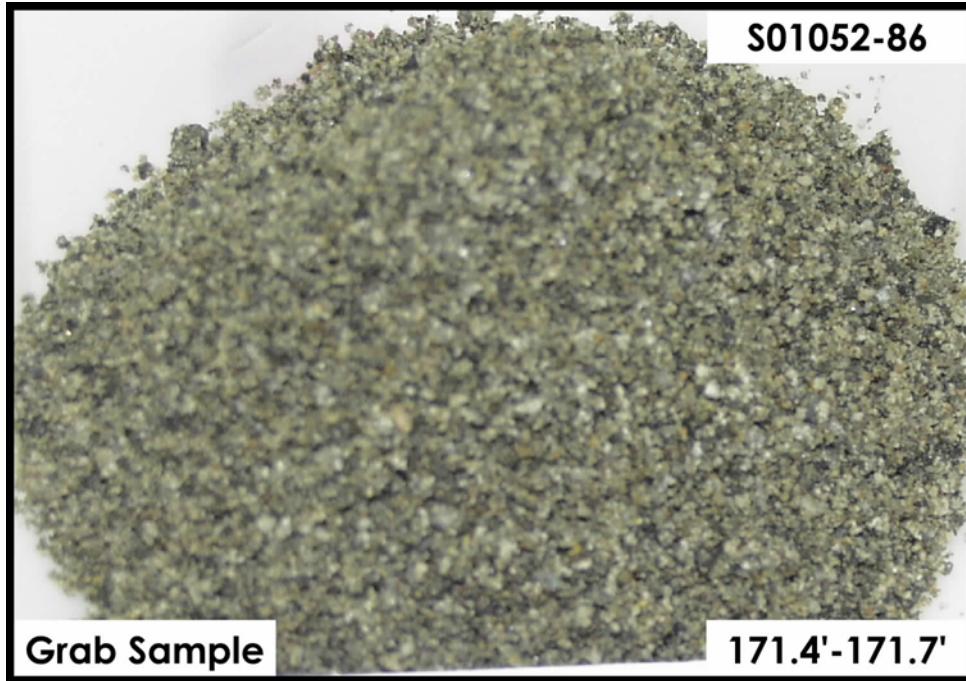
H2-Upper Sand and Gravel Sequence



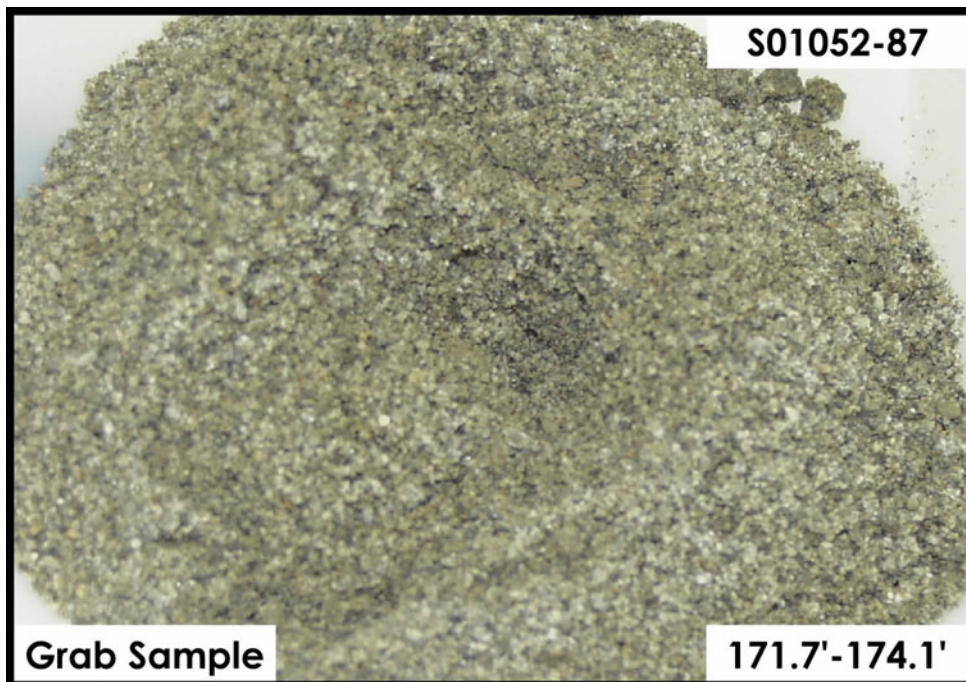
H2-Upper Sand and Gravel Sequence



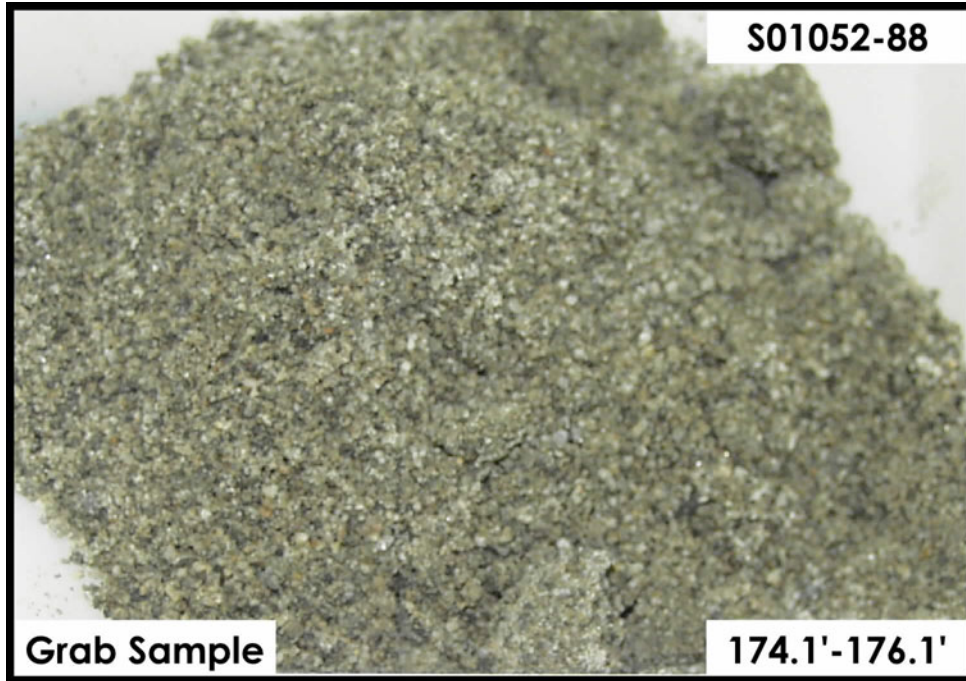
H2-Upper Sand and Gravel Sequence



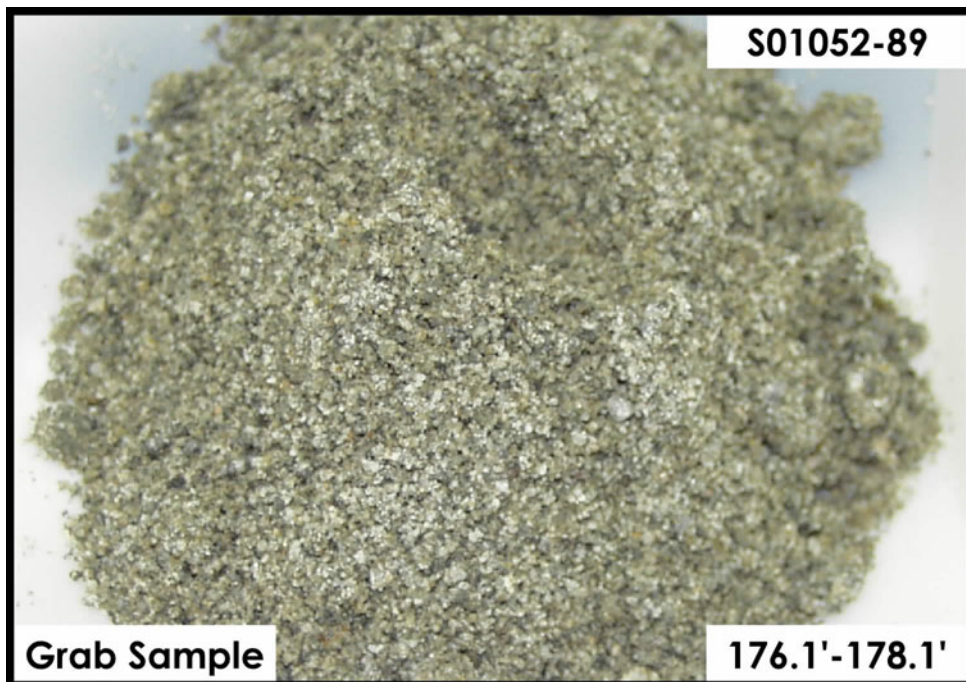
H2-Upper Sand and Gravel Sequence



H2-Upper Sand and Gravel Sequence



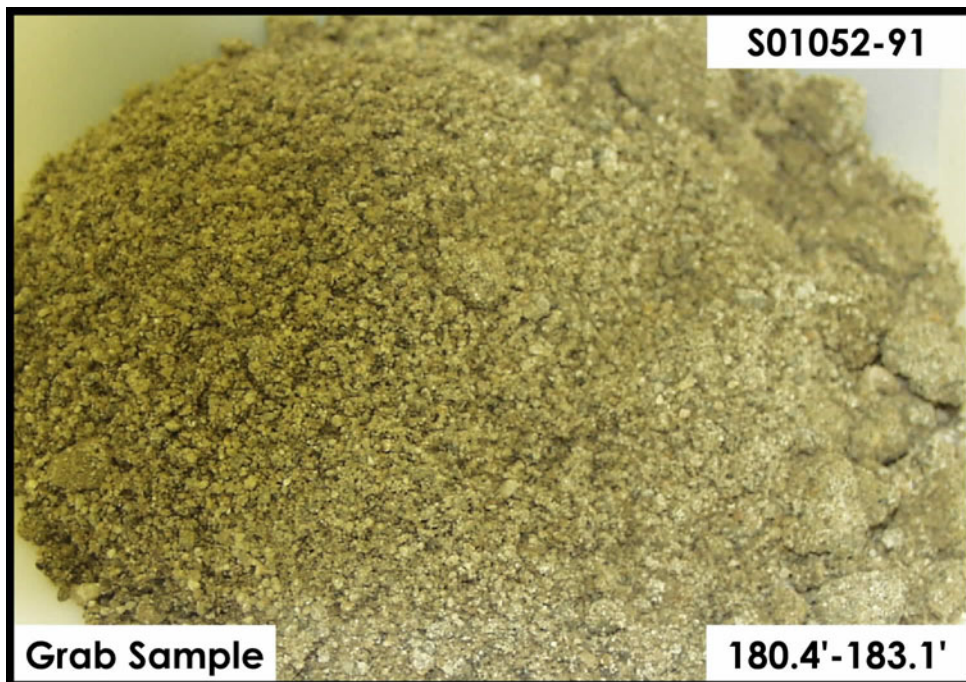
H2-Upper Sand and Gravel Sequence



H3-Lower Sand and Gravel Sequence



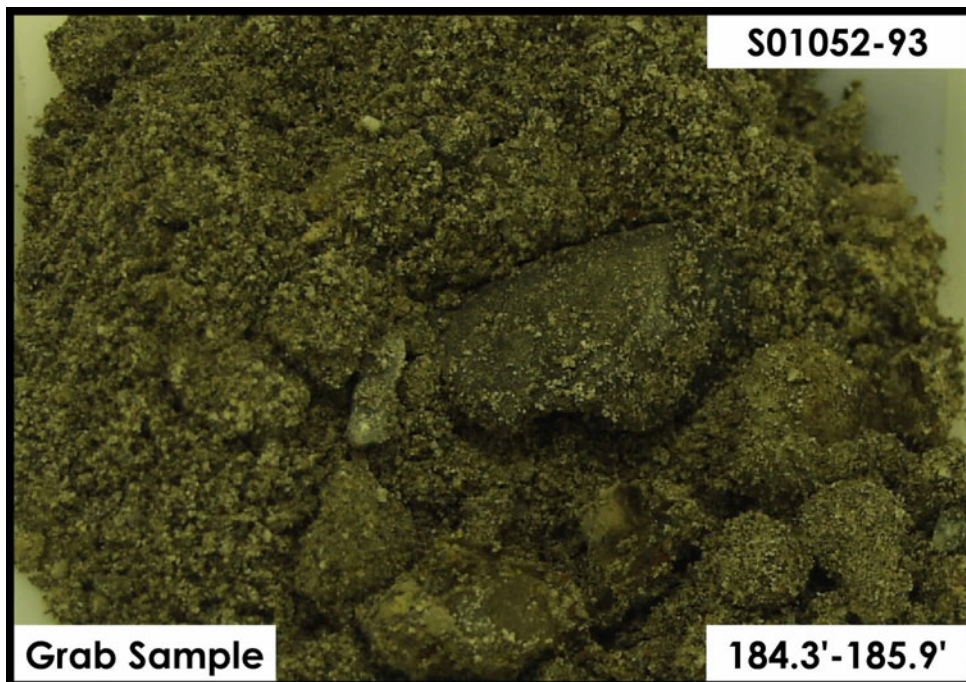
H3-Lower Sand and Gravel Sequence



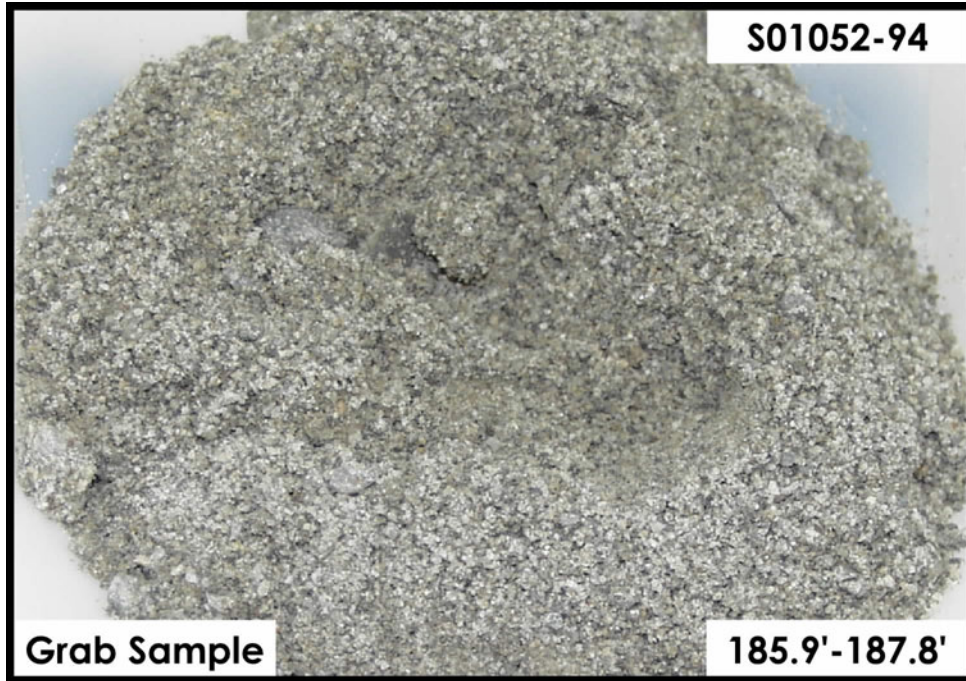
H3-Lower Sand and Gravel Sequence



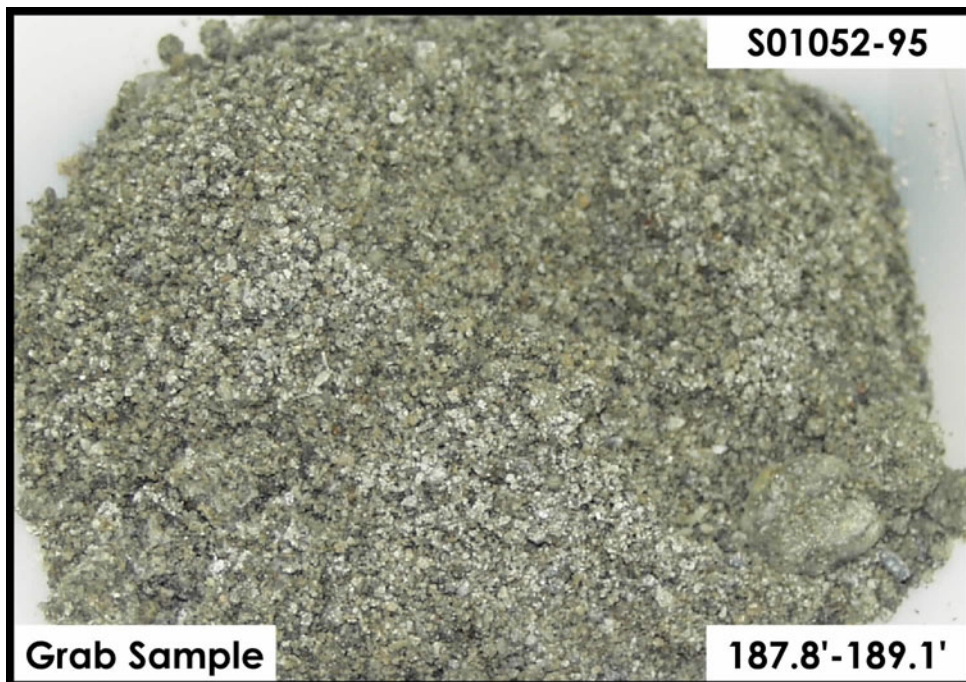
H3-Lower Sand and Gravel Sequence



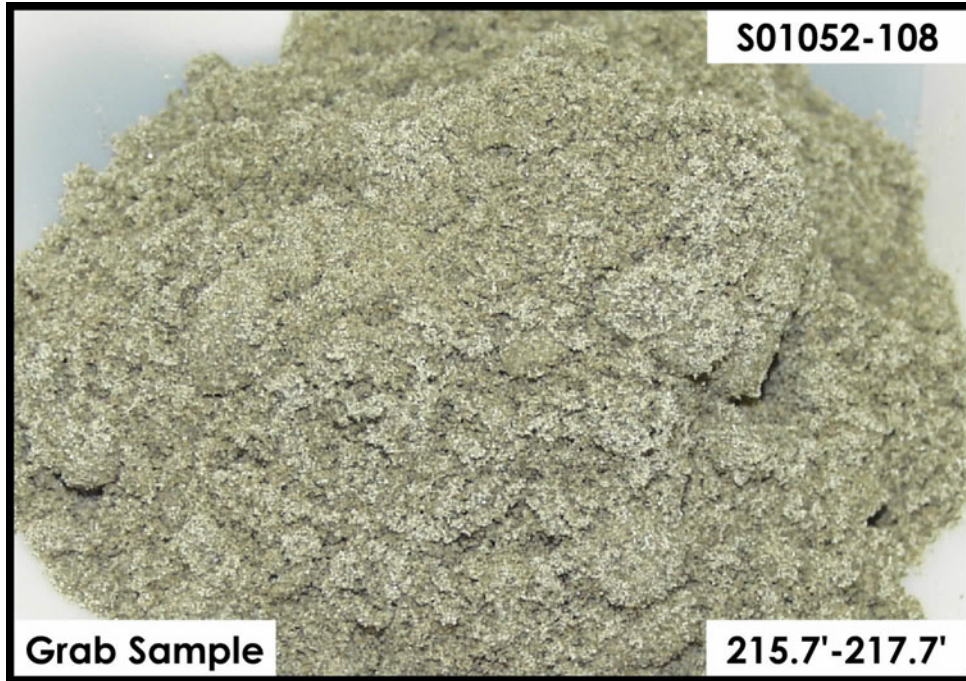
H3-Lower Sand and Gravel Sequence



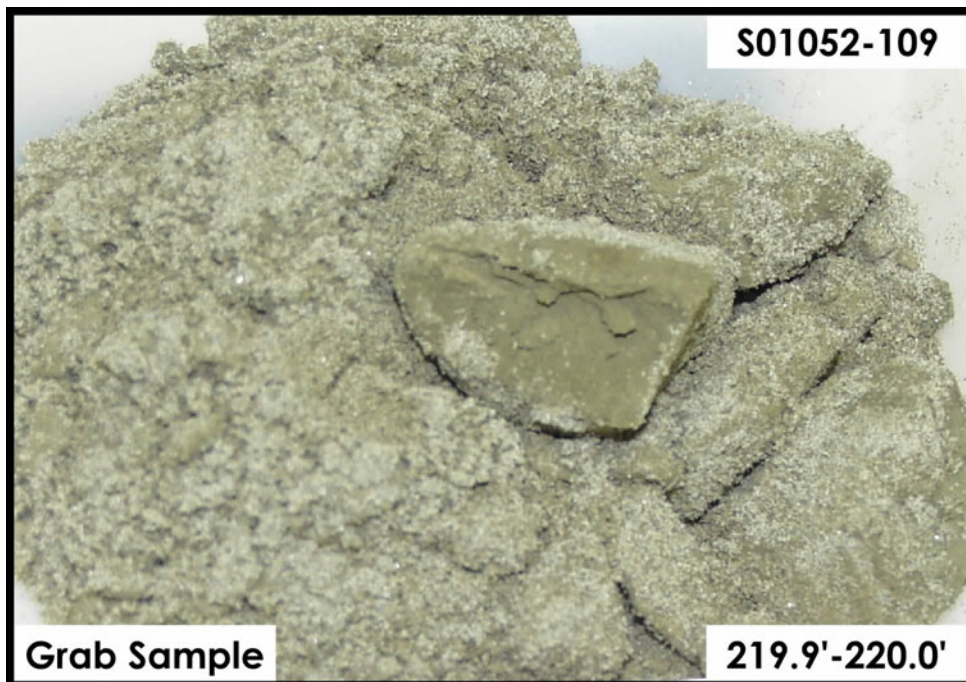
H3-Lower Sand and Gravel Sequence



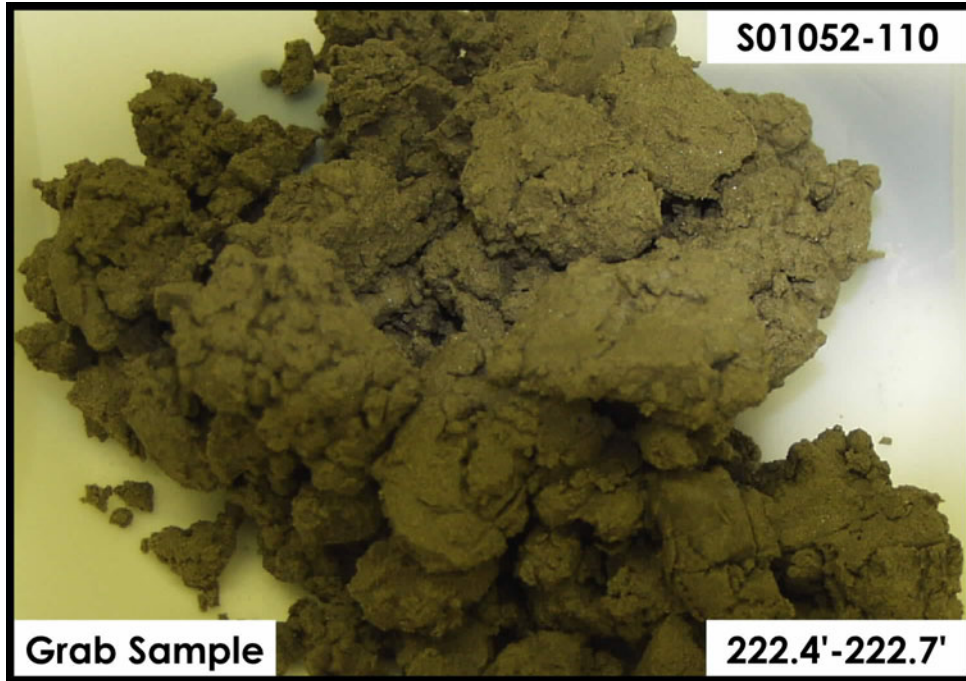
H3-Lower Sand and Gravel Sequence



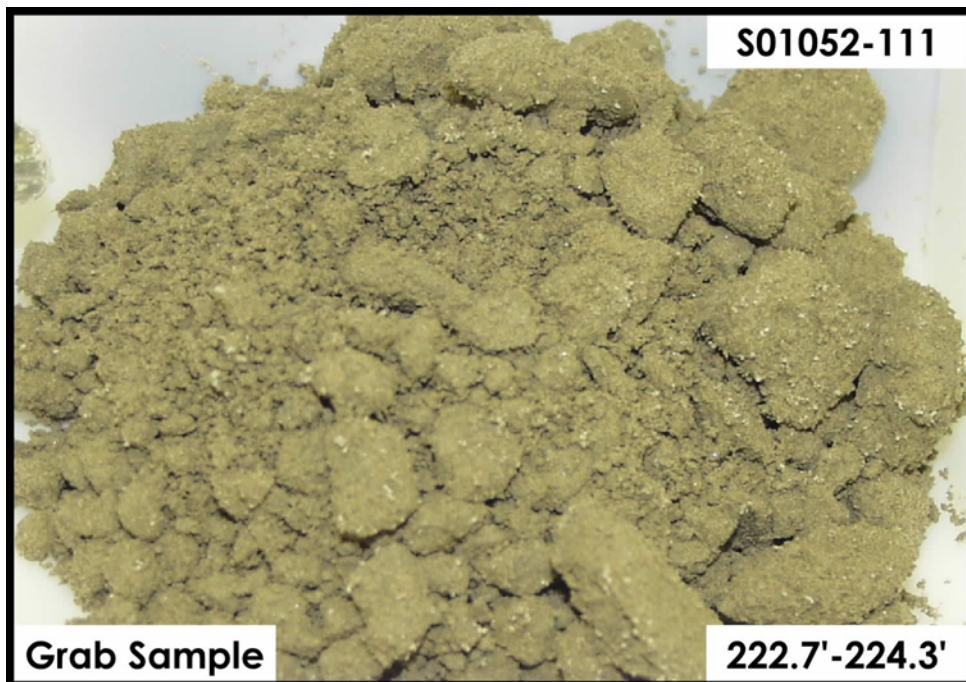
Plio-Pleistocene Silt Unit (PPlz)



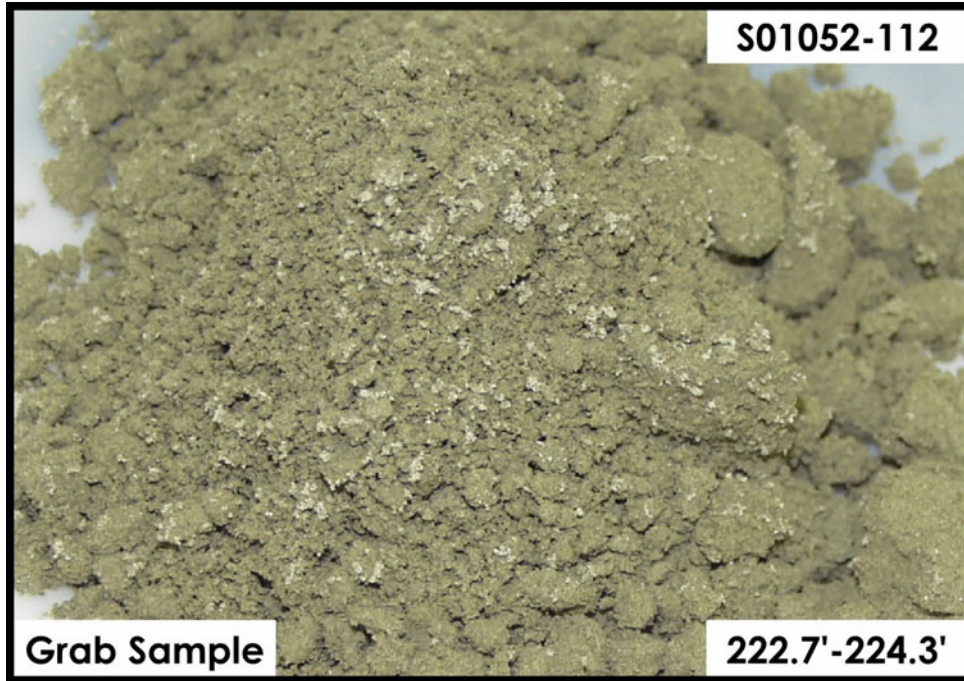
Plio-Pleistocene Silt Unit (PPlz)



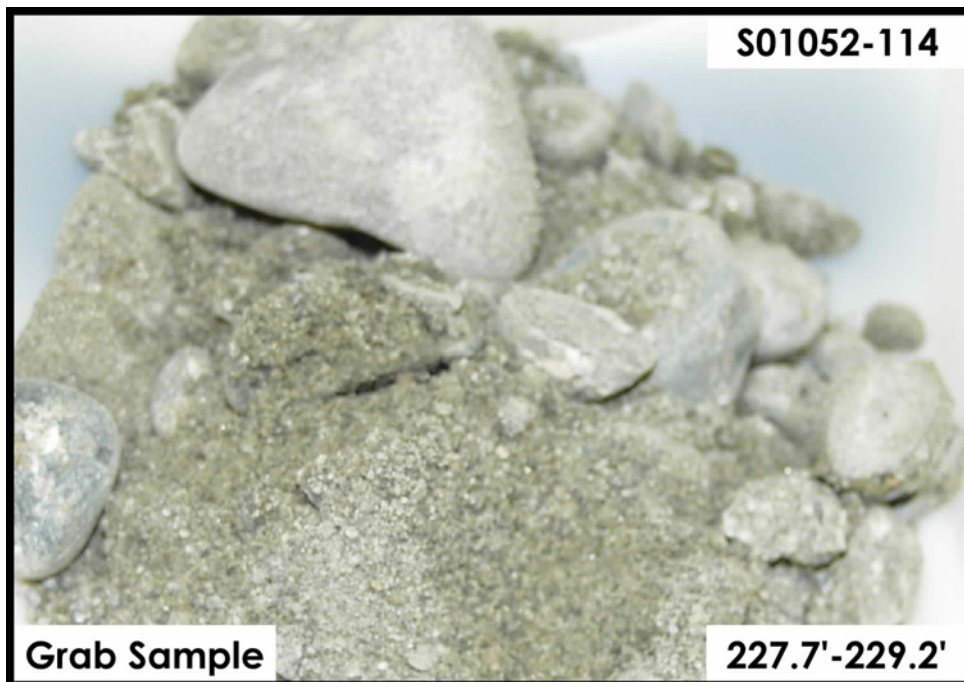
Plio-Pleistocene Silt Unit (PPlz)



Plio-Pleistocene Silt Unit (PPlz)



Plio-Pleistocene Silt Unit (PPlz)



Plio-Pleistocene Gravel Unit (PPlg)

Appendix C

Correlation Of Spectral Gamma Log Response Through Borehole Casing With ⁹⁰sr Concentration In Sediments

Appendix C

Correlation Of Spectral Gamma Log Response and ⁹⁰Sr Concentration for a Steel – Cased Borehole

RG McCain & CJ Koizumi

MACTEC-ERS

May 31, 2002

Executive Summary

In passive gamma-ray logging, the presence of anomalous gamma activity without detectable spectral lines associated with specific radionuclides may indicate the presence of a high-energy beta-emitting radionuclide such as ⁹⁰Sr. Brodzinski and Nielson (1980) described a means of estimating ⁹⁰Sr concentrations by measurement of bremsstrahlung radiation in the 60-236 KeV range. Baseline spectral gamma logging in the 241-B tank farm detected anomalous incoherent gamma activity with no identifiable gamma lines in several boreholes north and east of tank B-110. It was suggested in the B Tank Farm Report that this activity represented a probable subsurface plume of ⁹⁰Sr. Subsequently, laboratory analysis of soil samples from a new borehole (299-E33-46 / C3360) drilled in this region confirmed the presence of ⁹⁰Sr. Concentrations as high as 11,000 pCi/g of dry sediment were reported. Spectral gamma log data from this borehole are compared to sediment ⁹⁰Sr values measured by acid extraction and liquid scintillation counting. Shape factor analysis (Wilson, 1997, 1998) is shown to be useful in identifying zones of probable ⁹⁰Sr and a correlation between net counts in the 60 – 350 KeV range and ⁹⁰Sr concentration is established for the specific casing configuration. Recommendations are made for additional investigations to more fully investigate the nature of the bremsstrahlung phenomena with respect to cased boreholes, and to determine the effect of casing thickness on bremsstrahlung radiation inside the casing.

Background

During characterization logging in the 241-B Tank Farm, the SGLS detected anomalous incoherent gamma activity in boreholes northeast of tank B-110. Specifically, boreholes 20-10-02, 20-08-07 and 20-07-11 exhibited intervals of anomalous gamma activity with no evidence of well-defined energy peaks that would be diagnostic of specific radionuclides. Figure C.1 shows a combination plot for borehole 20-10-02. Note the anomalous total gamma activity between approximately 69 and 85 ft bgs in both the SGLS total gamma log (the fifth plot) and the Tank Farms gross gamma log (the sixth plot). This anomaly does not appear to be related to either man-made radionuclides or variations in natural radionuclides. Figure C.2 illustrates two typical spectra from borehole 20-10-02. Spectrum 3A2A1076 (60 ft) is typical of an uncontaminated portion of the borehole. Spectrum 3A2A1036 (80 ft) is an example of anomalous gamma activity. Note that there are no clearly defined gamma energy peaks other than those associated with natural radionuclides. Both represent approximately the same concentrations of natural radionuclides, and yet 3A2A1036 has a gross count rate approximately 3 times that of 3A2A1076.

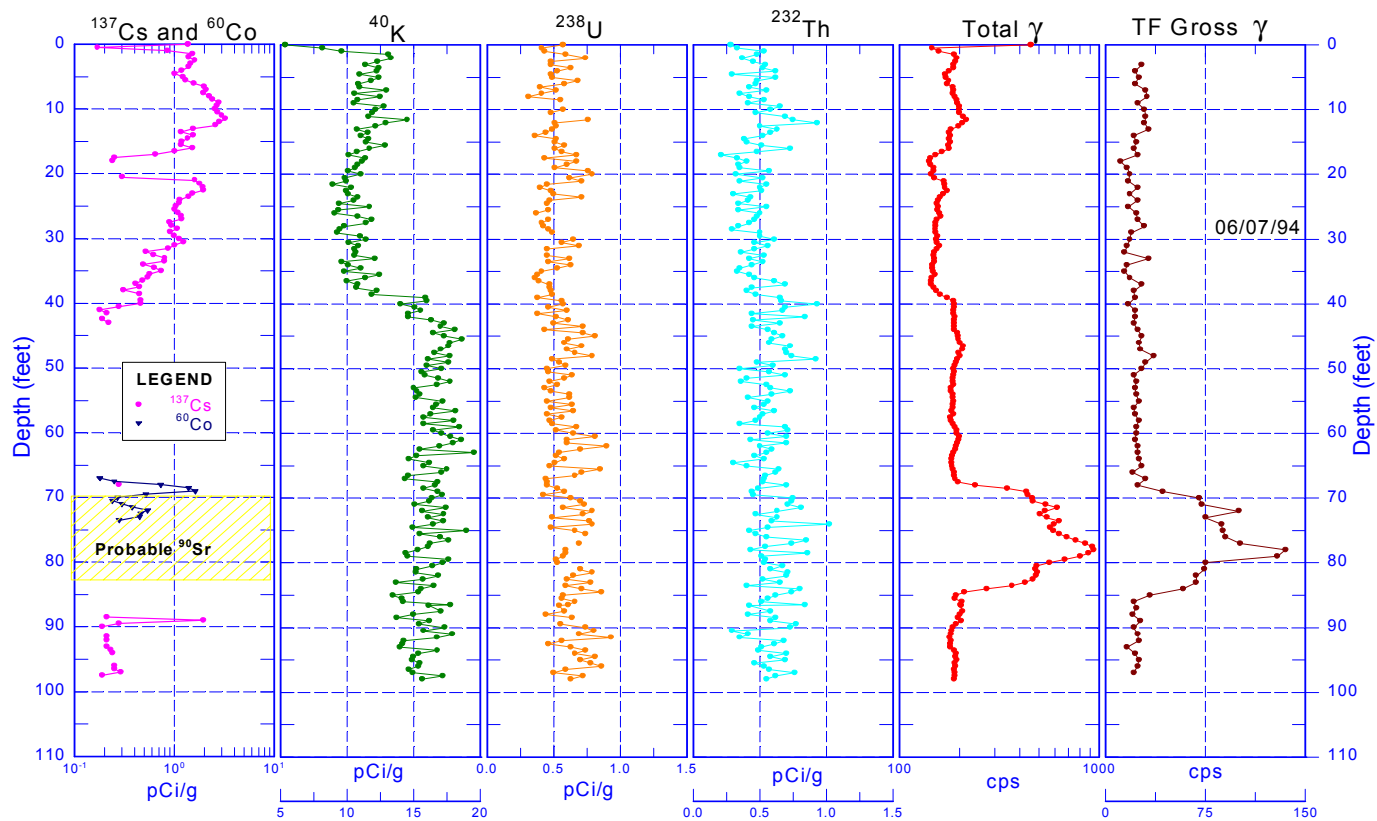
Note that the bulk of the difference in counts occurs as incoherent gamma counts below approximately 600 KeV. Brodzinski and Nielson (1980) and Wilson (1997) suggest that these incoherent counts may result from bremsstrahlung associated with the interaction between high-energy beta particles from $^{90}\text{Sr}/^{90}\text{Y}$ decay and the steel casing. In the B tank farm report (DOE, 2000) it was postulated that a subsurface zone of ^{90}Sr contamination had been encountered in this borehole and others in the vicinity.

Borehole (C3360 or 299-E33-46) was drilled in May 2001 to investigate this region and collect samples for laboratory analysis. ^{90}Sr concentrations in samples at selected depths have been determined (see Table 4.10 in the main text). The depth interval from 50 to 120 ft in borehole 299-E33-46 was logged with the SGLS, and man-made gamma-ray-emitting nuclides were determined to be absent, or present in negligible concentrations. Thus, emissions from such nuclides did not introduce significant extraneous spectral background. The photons in the borehole that were not due to natural radioactive sources were bremsstrahlung created by collisions and accelerations of the beta emissions from $^{90}\text{Sr}/^{90}\text{Y}$ decay. The borehole logging data was used test theories about the bremsstrahlung contributions to passive gamma-ray spectra, and the correlations of such bremsstrahlung signals to the ^{90}Sr concentrations.

The guide to the investigation was work by R.D. Wilson on spectral shape factor analysis, most of which is reported in Wilson (1997) that presents results of model studies using the MCNP radiation transport code and model experiments. Unfortunately, in relation to Wilson's work, borehole 299-E33-46 is an imperfect for this investigation, for at least two reasons:

- The borehole casing in Wilson's MCNP model was 0.313-inch-thick steel, whereas the steel casing in borehole 299-E33-46 is 0.514 inches thick. The effect of casing thickness on generation and transmission of bremsstrahlung gamma rays is unknown.
- The beta source in Wilson's MCNP model was "distributed uniformly 2 cm radially into the formation and extended ± 15.24 cm (± 6 in.) axially" (with respect to the center of the gamma-ray detector), whereas the ^{90}Sr distribution outside borehole 299-E33-46 appears to be somewhat non-uniform.

20-10-02 Combination Plot



C.3

FIGURE C.1 Combination Plot of Gamma Spectra for Man-made, Natural, and Total Gamma for Dry Well 20-02-10 Near Tank B-110.

C.4

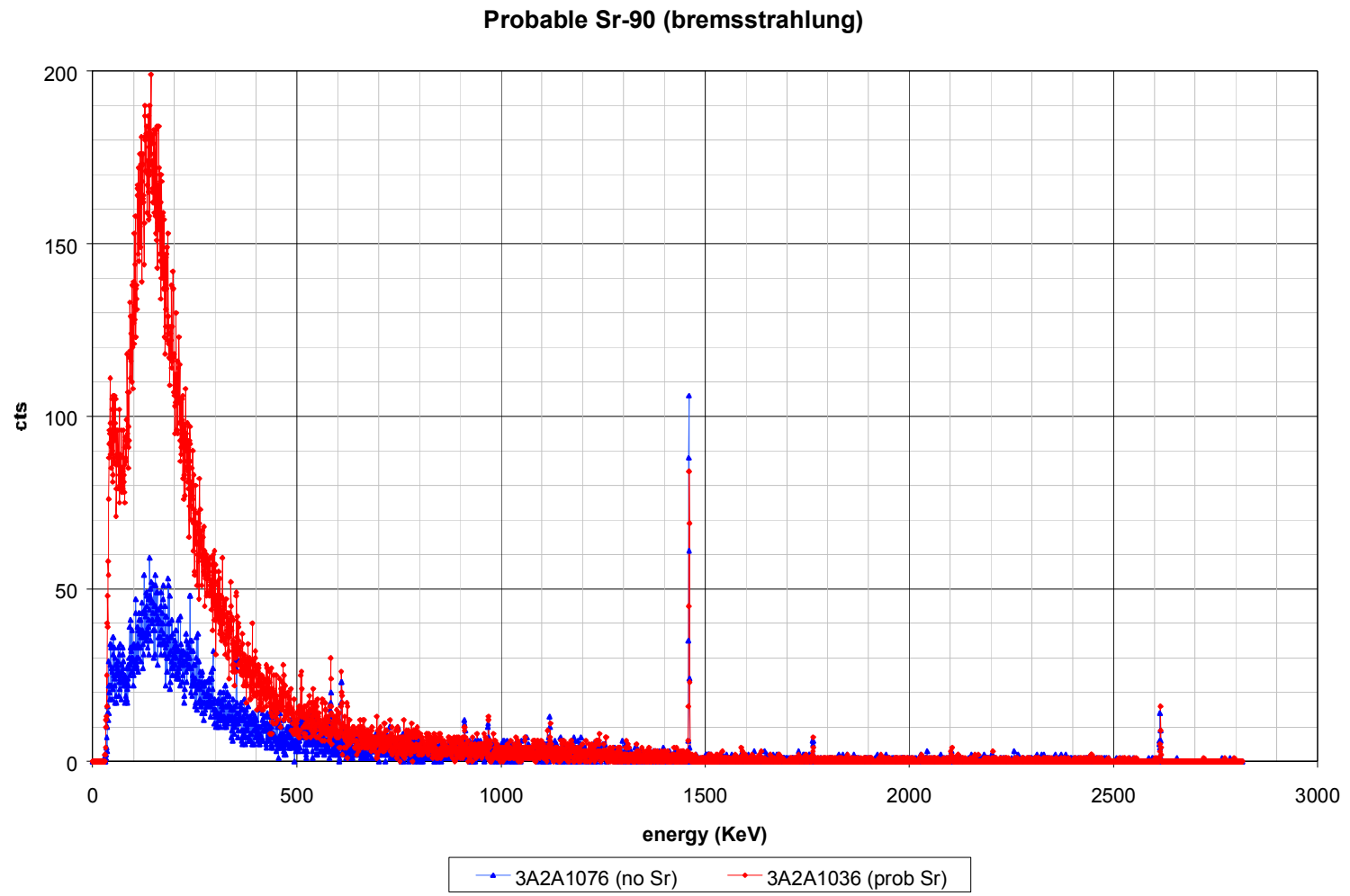


FIGURE C.2 Count Rate vs. Energy Level for Portions of Log where Sr-90 is present (Red) versus depth where Sr-90 is absent in Dry Well 20-02-10 Near Tank B-110

Shape Factor Analysis

The technique of shape factor analysis is described in Wilson (1997 & 1999). This technique was developed as a means to assess the distribution of ^{137}Cs and ^{60}Co with respect to the borehole axis. For both ^{137}Cs and ^{60}Co , a shape factor, SF1 was defined as the ratio between the energy peaks and the increased spectral noise due to Compton scattering. SF1 is sensitive to spectral differences for a borehole-confined source, a source uniformly distributed in the formation, and a remote source. However, it is only valid when the respective contaminant is present and has no bearing on identification of ^{90}Sr . It will not be discussed further in this document. Another shape factor was defined to assess the distribution of counts in the low-energy continuum:

$$SF2 = \frac{\text{counts}(60-350\text{KeV})}{\text{counts}(350-650\text{KeV})} \quad (\text{Wilson, 1997})$$

This factor is sensitive to differences in the scattered portions of the spectrum from gamma emitters and from bremsstrahlung sources. In particular, SF2 is capable of identifying the presence of low-energy bremsstrahlung radiation from the decay of $^{90}\text{Sr}/^{90}\text{Y}$ and is able to distinguish this spectral effect from the enhanced low-energy response obtained from remotely located ^{137}Cs and ^{60}Co . Wilson's model studies indicated that "*for virtually all gamma-emitting contaminants and for all possible source distributions, SF2 never exceeds a value of about 5. An SF2 value greater than 5 is evidence for the presence of a bremsstrahlung-producing energetic beta emitter, such as $^{90}\text{Sr}/^{90}\text{Y}$.*" (Wilson et al, 1997). Other reports (Wilson, 1997 and Wilson, 1999) have suggested that SF2 values may be as high as 20 in zones with significant ^{90}Sr concentration.

Figure C.3 shows the shape factor log for borehole 20-10-02. Note that within the region of anomalous total gamma activity between 69 and 85 ft bgs, SF2 attains a value of approximately 8. In this log, SF2 is calculated from counts in the two spectral windows after the contribution from naturally occurring radionuclides has been removed. This leads to the erratic behavior of SF2 in uncontaminated intervals.

RESULTS FROM BOREHOLE 299-E33-46

Figure C.4A shows a plot of total gamma count rate and count rate in the 60-350 KeV range for the 50 to 120 ft depth interval in borehole 299-E33-46. Figure C.4B shows laboratory measured ^{90}Sr concentrations plotted at the same depth scale. Figure C.4C shows SF2 and SF2* calculated as the ratio between counts in the 60-350 KeV range and counts in the 350-650 KeV range. SF2 is calculated using count rates corrected for natural radionuclides, while SF2* is calculated using gross (uncorrected) counts in the two energy windows. There appears to be a correlation between laboratory ^{90}Sr concentrations and either total gamma count rate or count rate for 60-350 KeV. Furthermore, SF2* has a value of about 3.3 to 3.6 in uncontaminated areas, rising to greater than 6 in intervals of high ^{90}Sr .

Figures C.5a and 5b display two HPGE spectra from borehole 299-E33-46. Both figures show the same two spectra; counts (vertical axis) are plotted on a log scale in Figure C.5a, and on a linear scale in Figure C.5b. The upper spectrum (named FOCA1024.S0) was recorded at a depth of 62.0 feet bgs, where the ^{90}Sr concentration was 11245 ± 363 pCi/g. The lower spectrum (named FOCA1100.S0) was recorded at a depth of 100.0 ft bgs, where the ^{90}Sr concentration was

zero, or close to zero. The full energy peaks are all associated with natural background; the peak for the 1460.8-keV gamma ray of ^{40}K , and the peak for the 2614.5-keV gamma ray of ^{208}Tl are labeled. Because spectrum FOCA1024.S0 contains no evidence of man-made gamma-ray emitters, the offset relative to spectrum FOCA1100.S0 is presumably due to bremsstrahlung associated with ^{90}Sr beta emissions.

Spectrum FOCA1024.S0 seems generally consistent with Wilson's MCNP simulation, which indicated that most of the bremsstrahlung contribution would appear in the part of the spectrum below 500 keV (see Figure 8 in Wilson's report).

Although the shape of spectrum FOCA1024.S0 more or less agrees with Wilson's model, the gross count rate apparently does not. Spectrum FOCA1024.S0 has a gross count rate equal to 2713.12 c/s, and spectrum FOCA1100.S0 has a gross count rate of 162.82 c/s. Since FOCA1024.S0 has a ^{90}Sr contribution, but FOCA1100.S0 does not, the difference of 2550.3 c/s would seem to be attributable to the ^{90}Sr contribution (assuming the potassium-uranium-thorium background is more or less uniform). The ^{90}Sr concentration corresponding to FOCA1024.S0 was 11245 pCi/g, meaning that the measurement sensitivity to ^{90}Sr was about 0.23 c/s per pCi/g. This is almost an order of magnitude higher than the value of 0.028 c/s per pCi/g that Wilson estimated.

Because the sensitivity was in substantial disagreement with Wilson's estimate, the sensitivity was recalculated using 22 spectra from ^{90}Sr -contaminated depths. A background gross count rate of 159.3 ± 13.4 c/s (uncertainty = $\pm 2\sigma$) was determined by calculating the average gross count rate of the spectra from depths below 90 feet, where the ^{90}Sr concentrations were zero, or close to zero. The background was subtracted from each of the 22 spectra, then each gross count rate was divided by the associated ^{90}Sr concentration. The average of the sensitivity values was 0.26 ± 0.18 c/s per pCi/g, which agreed with the initial finding.

SF2 for FOCA1024.S0 was calculated by subtracting counts from FOCA1100.S0 in each channel, computing the sums of the remainder over 60-350 KeV and 350-650 KeV, and dividing the two numbers. SF2* was calculated by dividing the total counts in the same channel ranges. SF2 was found to be 6.61 and SF2* was found to be 6.34. These values are somewhat lower than those encountered in dry well 20-10-02, and considerably lower than the value of 20 suggested by Wilson's model studies. This discrepancy may be due at least in part to the greater casing thickness. The maximum range of a 2.28 MeV beta particle from the daughter product ^{90}Y in iron is estimated to be on the order of 0.06 inches. This suggests that incident beta radiation only interacts with a relatively thin outer layer of the casing, and that the remaining casing material simply attenuates the bremsstrahlung gamma activity. Since lower-energy gamma rays are attenuated to a greater degree, this would result in a lower value of the SF2 ratio in thicker casing.

In spite of the sensitivity discrepancy, and differences between Wilson's MCNP model and the casing thickness and ^{90}Sr distribution presented by borehole 299-E33-46, values for several parameters were calculated from the SGLS spectra, and correlations between these parameter values and the ^{90}Sr concentrations were investigated.

20-10-02 Shape Factor Analysis Logs

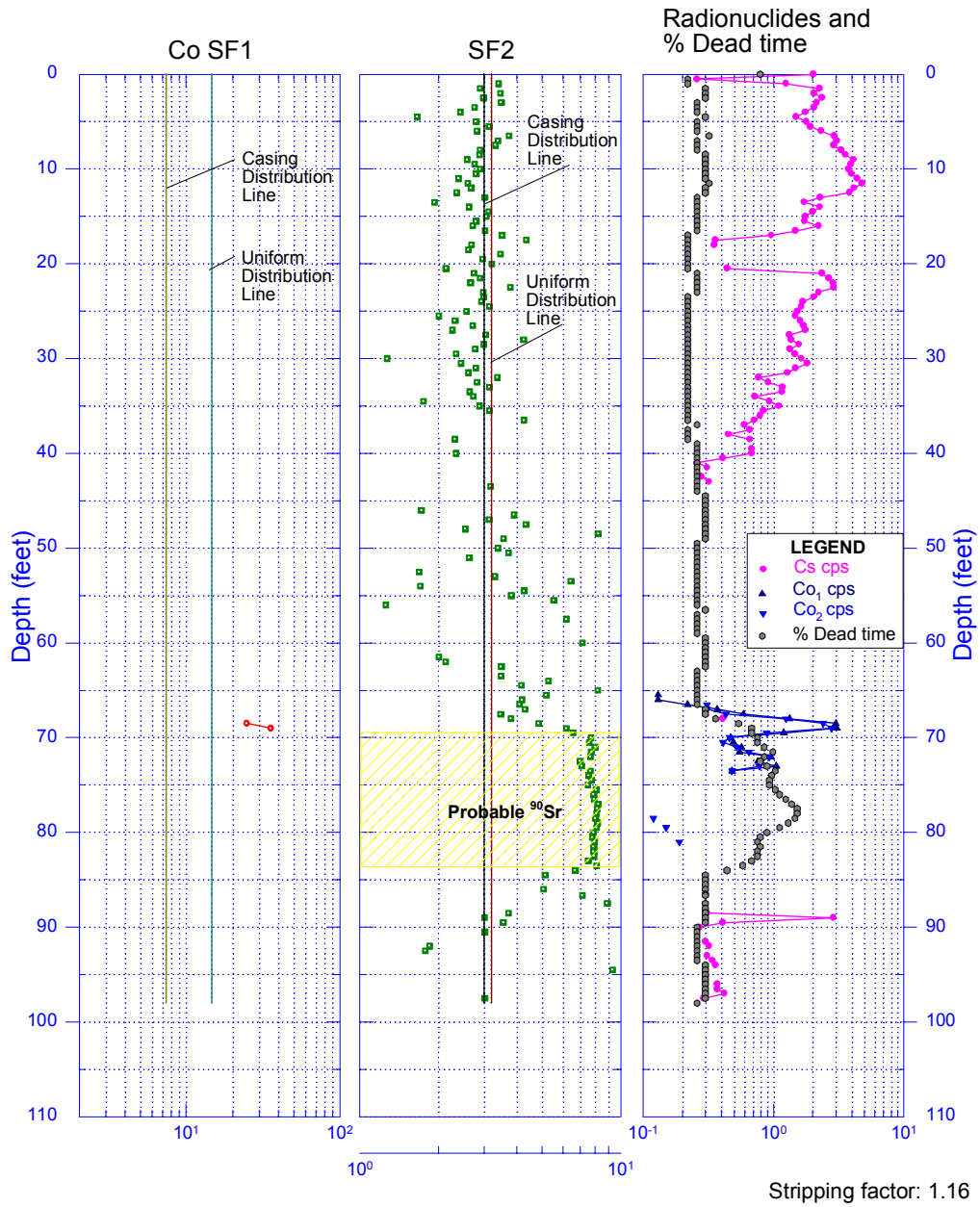
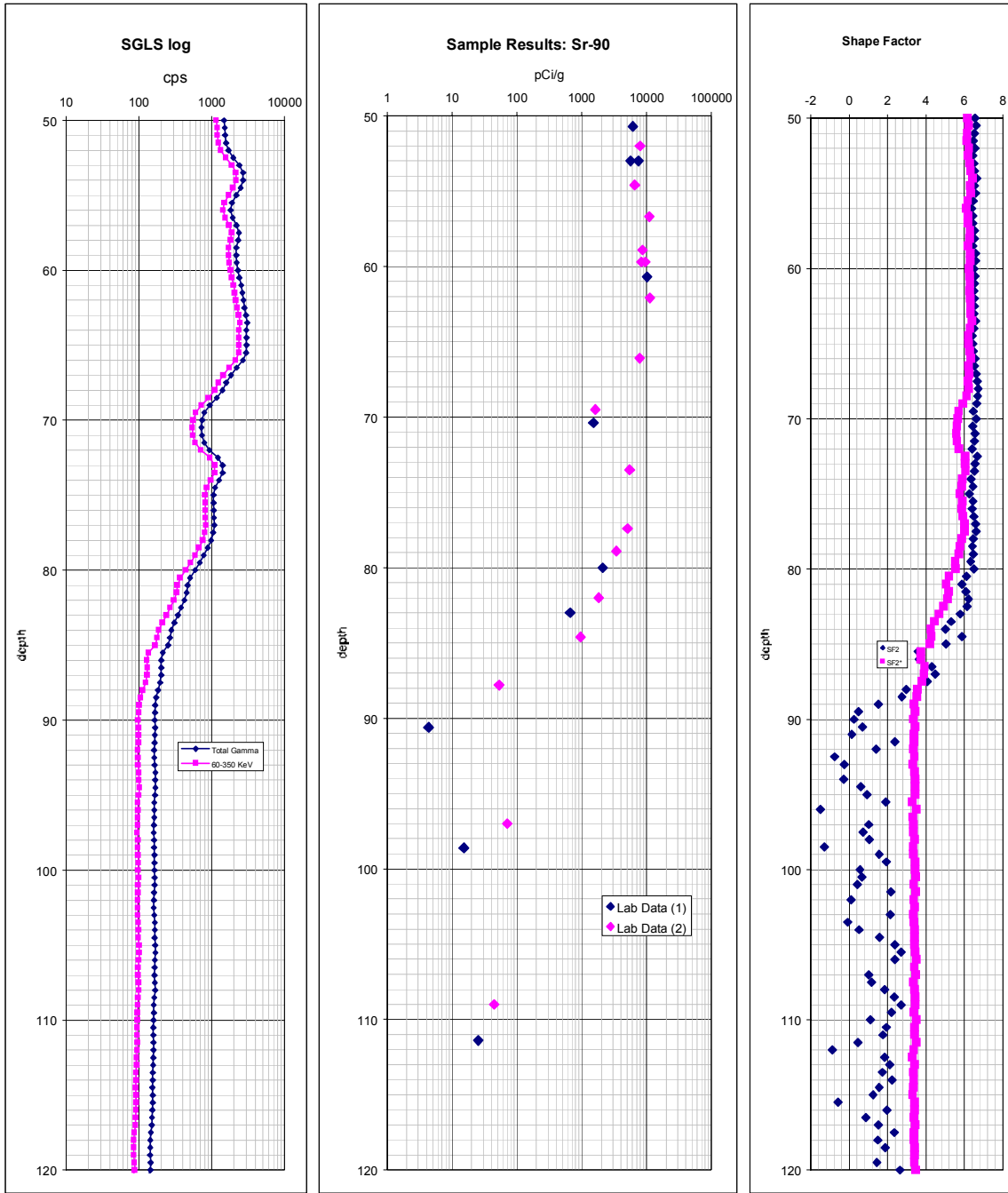


FIGURE C.3 Shape Factor Parameters versus Depth for Logging Spectra through Dry Well 20-02-10 Near Tank B-110

299-E33-46 (C3360)



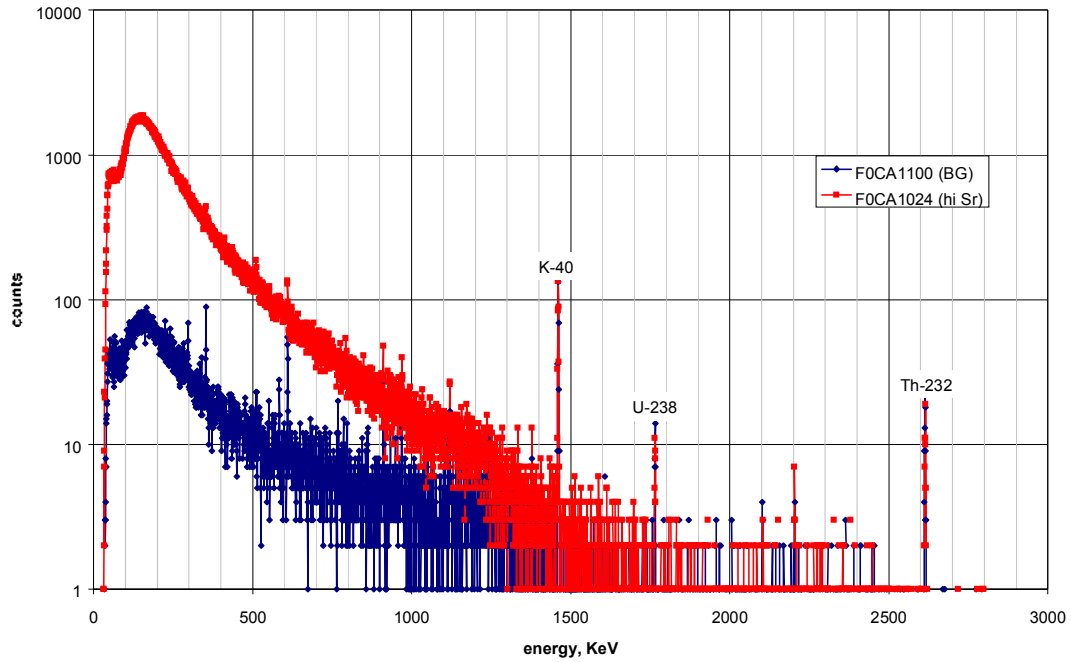
A

B

C

FIGURE C.4 Logging Data for Borehole 299-E33-46 versus Depth. (A.) Total Gamma; (B.) 60 to 350 Kev Window vs. Lab Measured Sr-90; (C.) Shape Factor Parameters

299-E33-46 Example Spectra



299-E33-46 Example Spectra

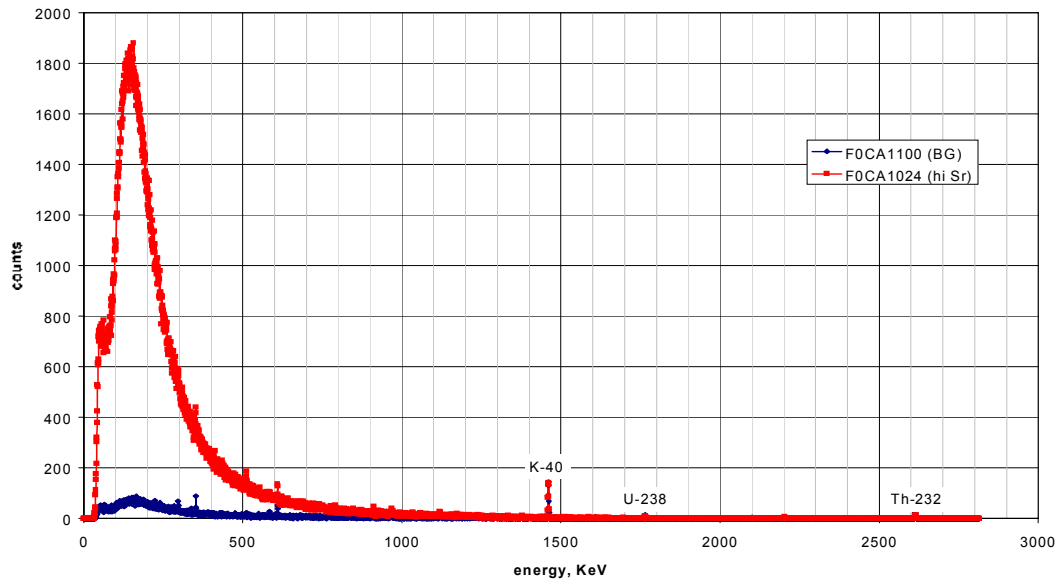


FIGURE C.5 Logging Spectra for Two Detectors vs. Energy for a Particular Depth at Borehole 299-E33-46. Top has counts on log scale and bottom has counts on linear scale.

Spectra from various depths, mostly where ^{90}Sr was present, were analyzed as follows. Count rates for two spectral windows were calculated, 60 keV to 350 keV (window 1) and 350 keV to 650 keV (window 2). Both windows are corrected for background using stripping factors based on the K-40, U-238 and Th-232 peaks. The ratio of the corrected rate for window 1 to the corrected rate for window 2 is Wilson's shape factor 2 (SF2). SF2 is plotted in relation to ^{90}Sr concentration in Figure C.6. Also plotted in Figure C.6 is a "modified" SF2, designated SF2*, which is the ratio of total counts in window 1 to total counts in window 2. Note that both SF2 and SF2* increase with increasing ^{90}Sr . Both are greater than 5 when ^{90}Sr concentrations are greater than 1000 pCi/g, and both seem to reach a maximum value between 6 and 7. At low ^{90}Sr concentrations, however, SF2 varies widely, while SF2* seems to have a relatively stable value between 3.3 and 3.6. From a mathematical perspective, this behavior should be expected: in intervals with no contamination, the corrected values for windows 1 and 2 should be close to zero, or even slightly negative. Division of two numbers close to zero can result in unpredictable results. At high ^{90}Sr concentrations, the counts due to bremsstrahlung dominate the spectra, and subtraction of background has little effect. In borehole 299-E33-46, one could infer that values of SF2 (or SF2*) greater than 5 indicate the presence of ^{90}Sr , while values less than 4 indicate that ^{90}Sr concentrations are less than 500 to 1000 pCi/g. For spectra where no ^{90}Sr is present, SF2* appears to be preferable, since it approaches a relatively stable value. Figure C.4C shows both SF2 and SF2* plotted as a function of depth. Note that SF2 is only stable where ^{90}Sr is present, while SF2* achieves stable values in both the contaminated interval and the uncontaminated interval.

Examination of Figure C.6 indicates that neither SF2 or SF2* appears to be useful as a quantitative indicator of ^{90}Sr concentration. Over the range of about 500 to 5000 pCi/g, it appears that both shape factors do increase with increasing ^{90}Sr content, but above about 5000 pCi/g, SF2 and SF2* values remain relatively constant. This behavior can be explained by the fact that both numbers are ratios. Below about 500 pCi/g, the contribution to the gamma spectrum from bremsstrahlung associated with $^{90}\text{Sr}/^{90}\text{Y}$ decay is relatively minor. The behavior of SF2 is erratic, because counts due to background have been removed and only "noise" is left to calculate the ratio. SF2* assumes a stable value, which represents the ratio based on typical levels of natural radionuclides. Between about 500 and 5000 pCi/g, the bremsstrahlung contribution becomes increasingly more important and the ratio changes. Above about 5000 pCi/g, the bremsstrahlung contribution dominates the spectra; counts in both windows increase proportionately, and both SF2 and SF2* exhibit little or no change with increasing concentration.

Count rates are more likely to exhibit a correlation with ^{90}Sr concentration over a wider range. Figures C.7 and C.8 show total gamma count rate and count rate in the 60 to 350 KeV energy range plotted as a function of ^{90}Sr concentration. Each figure shows both the total or gross count rate, as well as the net count rate after subtraction of background. The values plotted against ^{90}Sr concentration are based on a 3-point average of the SGLS data, centered on the midpoint depth of the sediment sample analyzed in the lab. Also shown on Figure C.7 is a line corresponding to the sensitivity of 0.26 cps/(pCi/g) determined above. This shows reasonable agreement with the net count values.

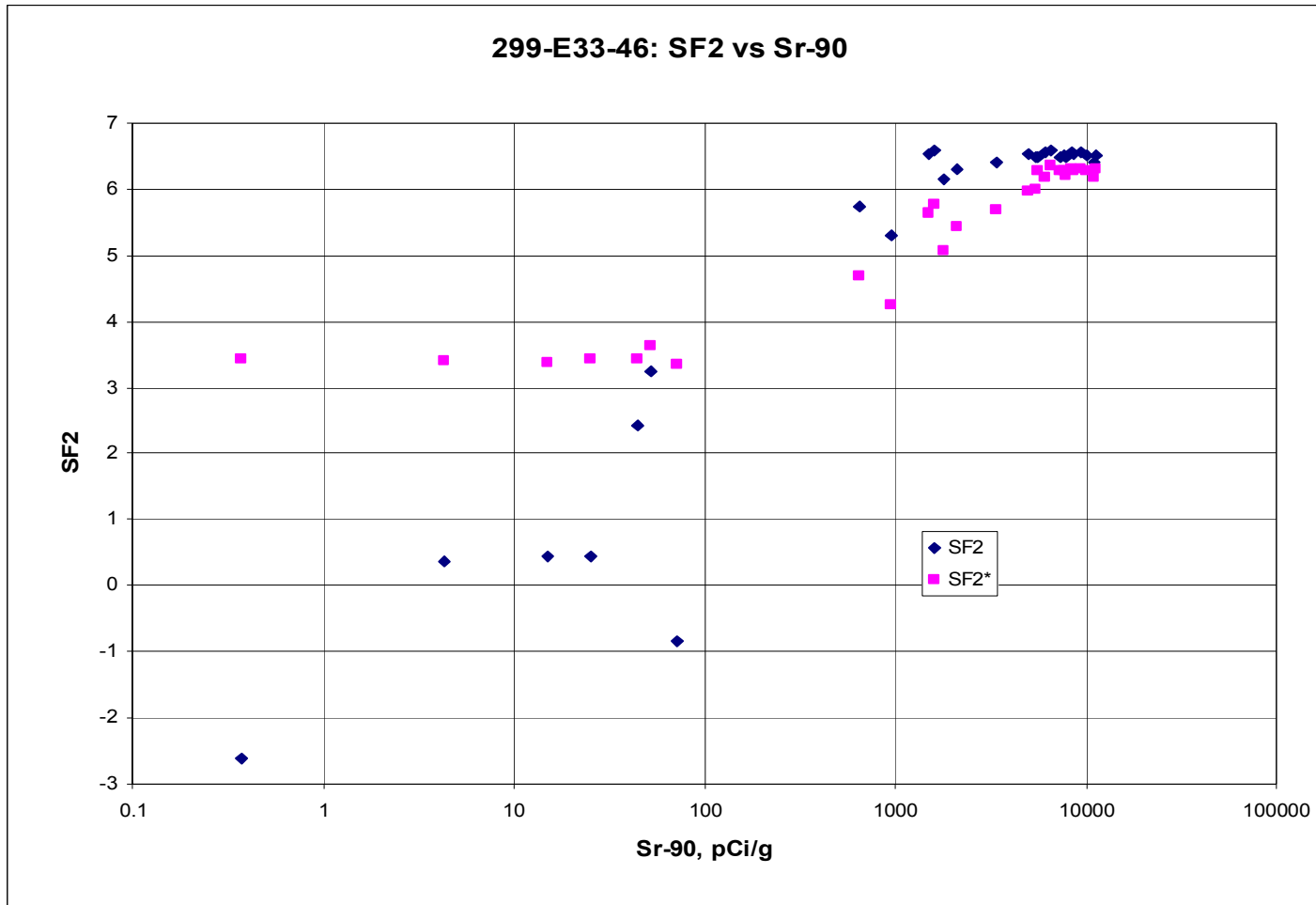


Figure C.6 Shape Factor Values for Gamma Log at Borehole 299-E33-46 versus Lab Measured Sr-90 Concentrations in Sediments from Same Depths

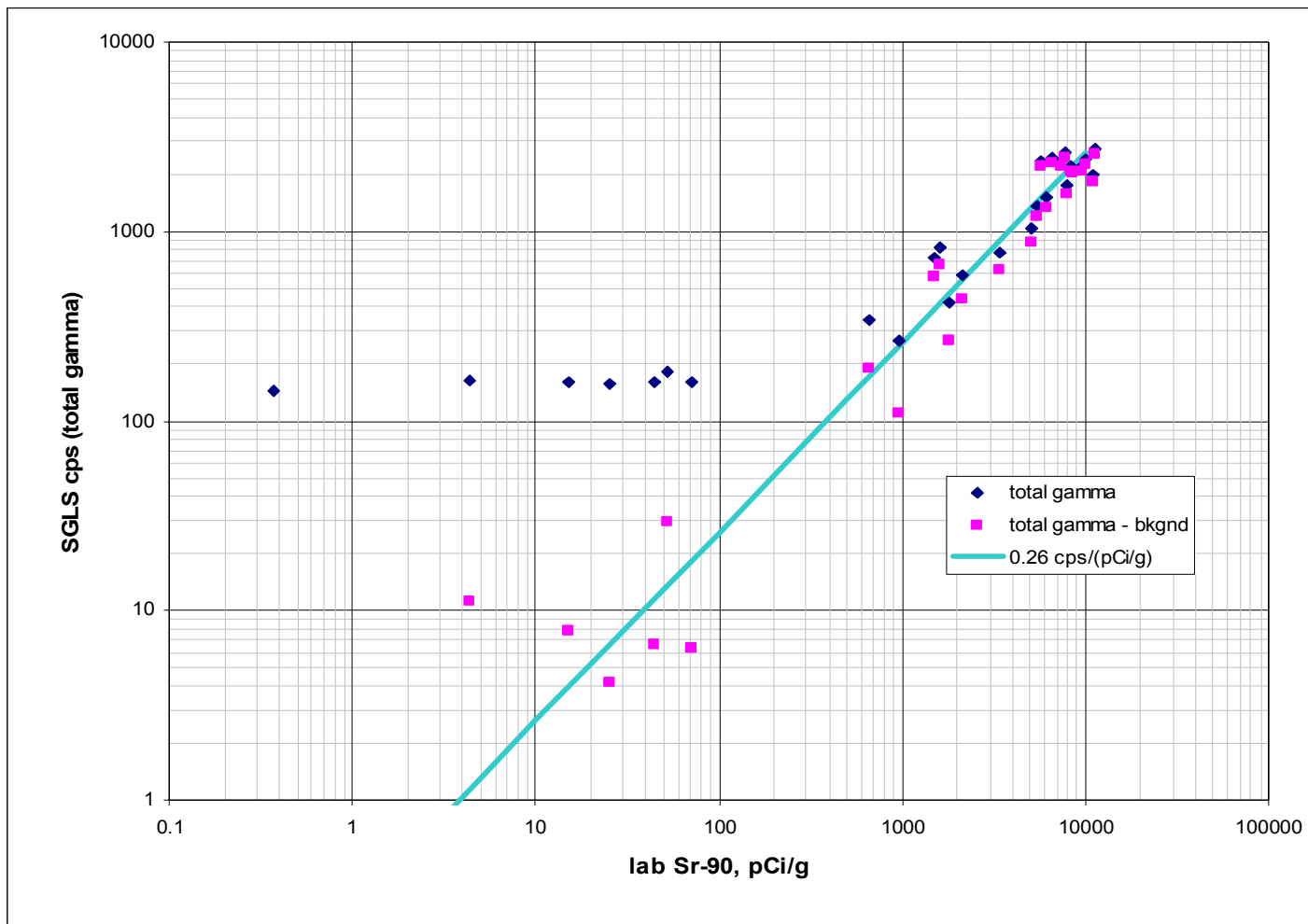


FIGURE C.7 Total Gamma Counts and Background Corrected Counts versus Lab Measured Sr-90 Contents for Sediments from Borehole 299-E33-46

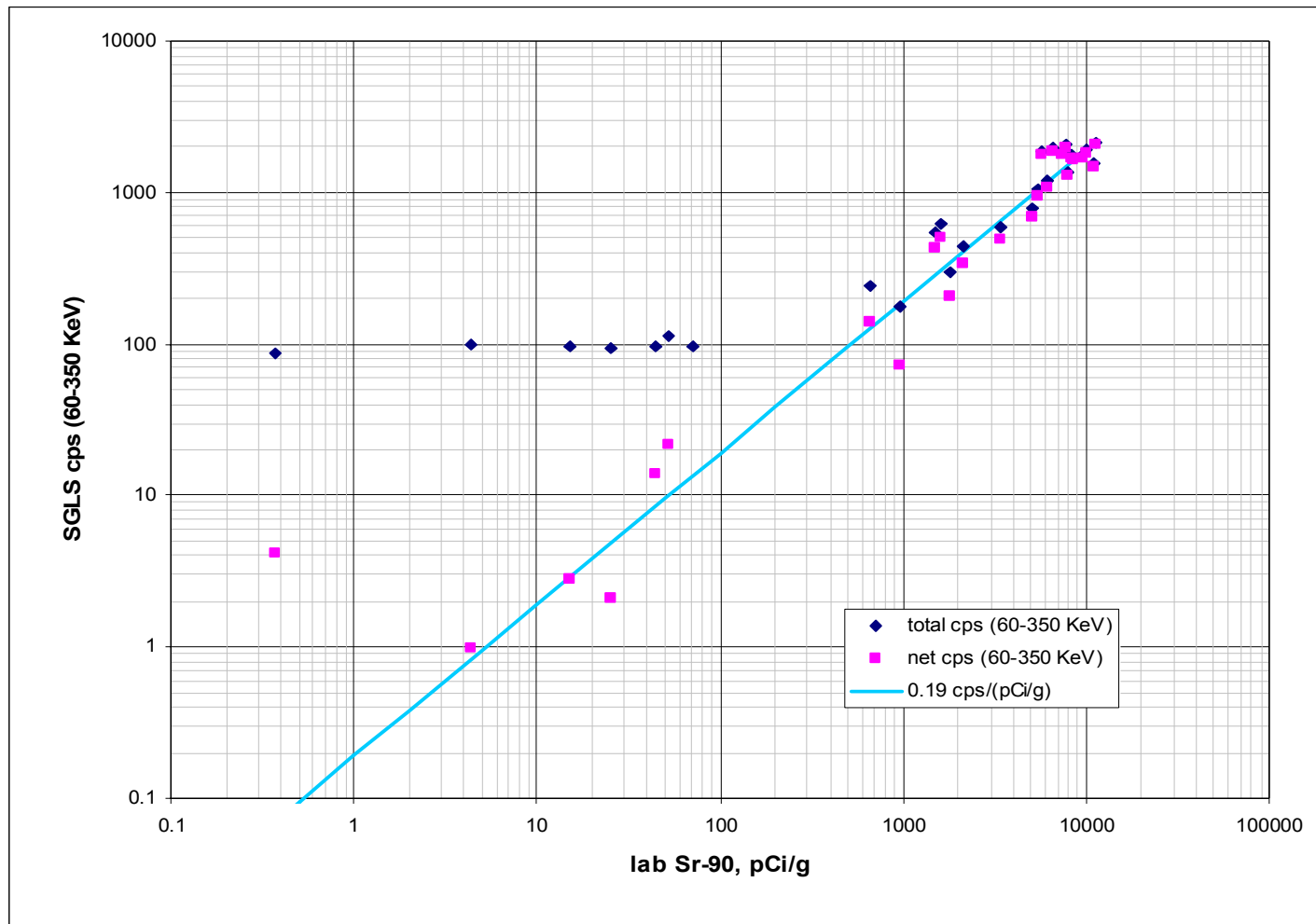


FIGURE C.8 Total and Net Count Rates for Log Spectra versus Lab Measured Sr-90 Contents for Sediments from Borehole 299-E33-46

However, the total count rate is subject to variation associated with the presence of any man-made radionuclides or with variations in natural radionuclide concentrations.

The results of model studies (Wilson, 1977) indicated that the bulk of the gamma activity associated with bremsstrahlung occurs in the 60 to 350 KeV window. Following Wilson's method, the net counts in this window can be determined by subtracting the background associated with the natural radionuclides ^{40}K , ^{238}U , and ^{232}Th , using stripping ratios developed by Koizumi and reported by Wilson (1997). The "net cps (60-350 KeV)" plotted in Figure C.8 are determined in this manner. With one exception, this plot shows a strong linear trend. A least-squares regression was used to estimate the sensitivity of SGLS net counts in the 60-350 KeV energy window to ^{90}Sr concentration. It was determined that:

$$N_{(60-350\text{KeV})} = 0.19 \times C_{^{90}\text{Sr}} \quad (R^2 = 0.874)$$

Where N is the net count rate and C is the ^{90}Sr concentration in pCi/g. This relationship is plotted as a line on Figure C.8. It can be re-arranged to:

$$C_{^{90}\text{Sr}} = 5.24 \times N_{(60-350\text{KeV})}$$

This relationship was developed for a borehole casing thickness of 0.514 in. Since the nature of bremsstrahlung generation associated with the interaction between high energy beta particles and steel casing is poorly understood, the equation above should not be used where the casing thickness is significantly different from 0.514 in.

Conclusions

Analysis of borehole spectral gamma measurements and laboratory determination of ^{90}Sr concentration in vadose zone sediment samples from borehole 299-E33-46 (C3360) has shown that relationships exist between SF2 and sediment ^{90}Sr concentration and between net counts in the 60 to 350 KeV energy window and sediment ^{90}Sr concentration. Comparison of the borehole logging data and laboratory measured sediment ^{90}Sr data resulted in the following findings and observations:

- The borehole casing in Wilson's MCNP model was 0.313-inch-thick steel, whereas the steel casing in borehole 299-E33-46 is 0.514 inches thick. The effect of casing thickness on generation and transmission of bremsstrahlung gamma rays is unknown.
- The beta source in Wilson's MCNP model was "distributed uniformly 2 cm radially into the formation and extending ± 15.24 cm (± 6 in.) axially" (with respect to the center of the gamma-ray detector), whereas the ^{90}Sr distribution in the sediment in the formation outside of the borehole 299-E33-46 casing appears to be non-uniform axially and of undetermined radial distribution, but most certainly larger than 2 cm.
- Only the borehole interval from 50 to 120 ft bgs was used for the comparison studies. The entire borehole was logged, but other intervals were logged with slightly different equipment and procedures. Variations in logging system response would complicate the comparison of log data and laboratory derived sediment values.
- Comparison of gamma spectra from intervals of high ^{90}Sr concentration with spectra from low concentration intervals indicated that bremsstrahlung associated with ^{90}Sr decay

resulted in greatly increased low energy counts, with the bulk of the activity below 350 KeV.

- After subtracting background, total gamma counts from the logging detector were compared to ^{90}Sr concentrations in sediment from the same depths. The average sensitivity was found to be approximately 0.26 cps per pCi/g. This is almost an order of magnitude higher than the value of 0.028 c/s per pCi/g predicted by Wilson, 1997.
- SF2 values on the order of 6 to 8 indicate the presence ^{90}Sr concentrations greater than 1000 pCi/g in the sediments interrogated by the logging tool. Wilson (1997) predicted the existence of a correlation between ^{90}Sr concentration and SF2, but the observed correlation does not fully conform to Wilson's expectations. Wilson's MCNP model predicted SF2 values greater than 20 in the presence of ^{90}Sr in the sediments outside the casing in model configurations.
- A modified shape factor, SF2*, is defined as the ratio between total counts in the 60-350 KeV and 350-650 KeV windows. Because background is not subtracted, SF2* tends to remain stable in the absence of contamination. SF2* assumes a value between 3.3 and 3.7 in uncontaminated intervals and increases to greater than 6 in intervals with high ^{90}Sr concentration. For ^{90}Sr concentrations on the order of 500 to 1000 pCi/g, SF2* values are transitional between 3.7 and 6.
- Cross-plots of SGLS total gamma vs ^{90}Sr concentration in the sediment show a linear trend, particularly when total counts are corrected for background. However, total counts are affected by the presence of man-made radionuclides, as well as by variations in natural radionuclides.
- Cross-plots of SGLS total counts and net counts in the 60 to 350 KeV energy range vs ^{90}Sr concentration in the sediments also show a strong linear trend. For this energy window, background counts can be estimated from the 1461, 1764 and 2615 KeV peaks, using stripping ratios developed by Koizumi. The net counts show a good correlation with ^{90}Sr concentration. The sensitivity is about 0.19 cps per pCi/g. It is possible that similar corrections could be made for limited amounts of ^{137}Cs and ^{60}Co , using stripping ratios estimated from modeling and shape factor experiments. This would allow ^{90}Sr concentrations to be estimated in the presence of other gamma emitting contaminants.

Recommendations

The results of this study and previous experience in B tank farm and elsewhere indicate that, at least in the absence of other gamma emitting contaminants, ^{90}Sr can be detected by spectral gamma logging in steel-cased boreholes. It also appears that quantitative ^{90}Sr concentrations can be estimated, at least to an order of magnitude accuracy. Unfortunately, there are a number of unknown factors that must be investigated before a widely applicable gamma spectra-to- ^{90}Sr in sediments relationship can be established. Specific recommendations for future work include the following:

- Conduct experiments to investigate the nature of gamma ray generation and transmission associated with bremsstrahlung.

Discrepancies exist in the relationship between ^{90}Sr concentrations and gross gamma count rate, and in the behavior of SF2 in the presence of ^{90}Sr . In both cases, the relationship observed in the field differs significantly from predictions based on radiation transport modeling. These discrepancies may be due to the difference in casing thickness, or to errors in the way bremsstrahlung is addressed in the model. A relatively simple experiment could be set up to investigate the effects of casing thickness on gamma activity from bremsstrahlung. Gamma spectra would be recorded from a detector placed a short distance from a ^{90}Sr source. Steel plates with various thicknesses between about 0.25 and 1.0 inches would be placed between the source and the detector, and the data would be evaluated to determine the effect of casing thickness on gamma detector response. This experiment would also be modeled with the radiation transport code and model results compared to measurement data.

- Perform additional modeling to investigate the effects of casing thickness, ^{90}Sr concentrations, and the presence of other radionuclides on spectral gamma response.

The borehole geometry with a distributed source is much more difficult to construct in a physical model, but numerical modeling can be performed to estimate response.

- Collect additional sample data where possible and log all boreholes in which samples containing elevated ^{90}Sr concentrations are encountered.

Comparison of borehole log data and laboratory measured sediment ^{90}Sr data in multiple boreholes will help validate the model predictions.

References

- Brodzinski, R.L. and H.L. Nielson. 1980. "A Well-Logging Technique for the In-Situ Determination of ^{90}Sr ," Nuclear Instruments and Methods, 173: 299-301.
- DOE. 2000. *Hanford Tank Farms Vadose Zone: B Tank Farm Report*, GJO-99-113-TAR, GJO-HAN-28, U.S. Department of Energy, Grand Junction Project Office, Grand Junction, Colorado.
- Wilson, R. D., C. J. Koizumi, J. E. Meisner, and D. C. Stromswald. 1997. "Spectral Shape Analysis for Contaminant Logging at the Hanford Site," 1997 IEEE Nuclear Science Symposium, Albuquerque, November, 1997.
- Wilson, R. D. 1997. *Spectrum Shape-Analysis Techniques Applied to the Hanford Tank Farms Spectra Gamma Logs*. GJO-96-13-TAR, GJO-HAN-7, prepared by MACTEC-ERS for the Grand Junction Office, Grand Junction, Colorado.
- Wilson, R. D. 1998. *Enhancements, Validations and Applications of Spectrum Shape-Analysis Techniques Applied to Hanford Tank Farms Spectral Gamma Logs*. GJO-97-25-TAR, GJO-HAN-15, prepared by MACTEC-ERS for the Grand Junction Office, Grand Junction, Colorado.

Appendix D

X-Ray Diffractograms for Bulk and Clay Sized Sediments From Borehole 299-E33-46

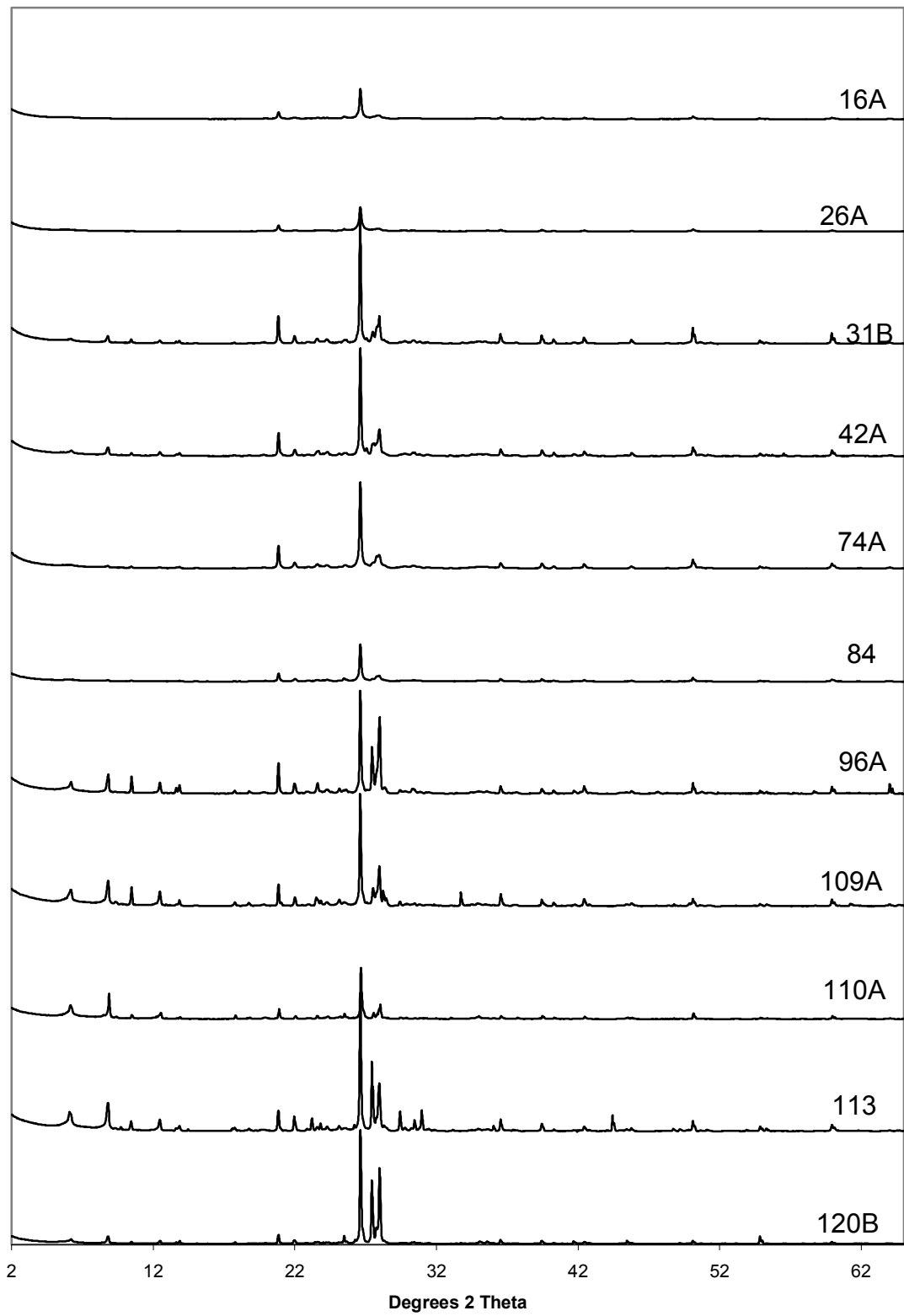


Figure D-1. Bulk Powder XRD Tracings for Sediments from Borehole 299-E33-46.

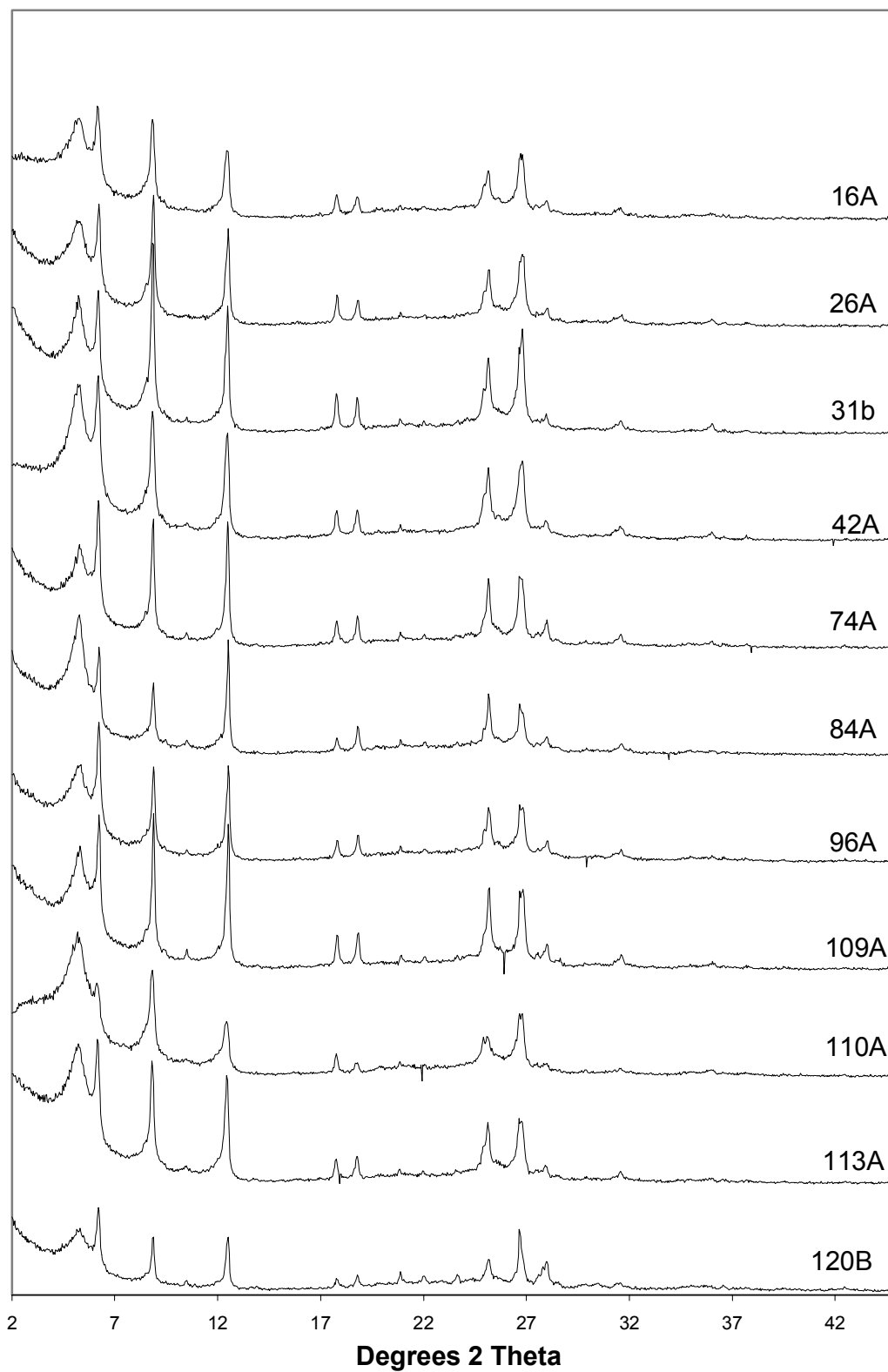


Figure D-2. Clay XRD Tracings from Sediments from 299-E33-46.

Distribution

**No. of
Copies**

**No. of
Copies**

OFFSITE

Dr. Harry Babad
2540 Cordoba Court
Richland, WA 99352-1609

Pat Brady
Geochemistry Department, 6118
Sandia National Laboratories
P.O. Box 5800
Albuquerque, New Mexico 87185-0750

Charles R. Bryan
Sandia National Laboratories
4100 National Parks Highway
Carlsbad, N.M. 88220

Susan Carroll
Lawrence Livermore National Laboratory
Mail Stop L-219
Livermore, CA 94550

Jon Chorover
Associate Professor - Environmental
Chemistry
Department of Soil, Water and
Environmental Science
Shantz 429, Building #38
University of Arizona
Tucson, AZ 85721-0038

Dave G. Coles
Coles Environmental Consulting
750 South Rosemont Rd
West Linn, OR 97068

Mark Conrad
Department of Earth and Planetary Sciences
University of California Berkeley
Berkeley, CA 94720

Dr. James A. Davis
U.S. Geological Survey
MS-465
345 Middlefield Rd.
Menlo Park, CA 94025

Donald J. DePaolo
Geology & Geophysics Dept., MC4767
University of California
Berkeley, CA 94720-4767

Dirk A. Dunning
Oregon Office of Energy
625 Mariona St. N. E.
Salem, OR 97301-3742

Mark Ewanic
MSE Technology Applications, Inc.
200 Technology Way
Butte, MT 59701

Markus Flury
Department of Crop and Soil Sciences
Washington State University
Pullman, WA 99164

Amy P. Gamerdinger
2122 E. Hawthorne
Tucson, AZ 85719

**No. of
Copies**

Jim Harsh
Department of Crop & Soil Sciences
Washington State University
Johnson Hall – Room 249
Pullman WA 99164-6420

Dr. Cliff Johnston
Soil Chemistry and Mineralogy
1150 Lily Hall
Purdue University
West Lafayette, IN 47907-1150

Dr. Daniel I. Kaplan
Westinghouse Savannah River Company
Bldg. 774-43A, Rm 215
Aiken, SC 29808

Dr. Peter C. Lichtner
Los Alamos National Laboratory
P.O. Box 1663
Los Alamos, NM 87545

Patrick Longmire
Los Alamos National Laboratory
Mail Stop J534
P.O. Box 1663
Los Alamos, NM 87545

Kate Maher
The Center for Isotope Geochemistry
301 McCone Hall
University of California, Berkeley
Berkeley, CA 94702-4746

Melanie A. Mayes
Environmental Sciences Division
Oak Ridge National Laboratory
P.O. Box 2008
Oak Ridge, TN 37831-6038

**No. of
Copies**

Dr. Kathryn L. Nagy
Department of Earth and Environmental
Sciences
University of Illinois at Chicago (MC-186)
845 West Taylor Street
Chicago, IL 60607-7059

Heino Nitsche
Director, Center for Advanced Environmental
and Nuclear Studies
Lawrence Berkeley National Laboratory
1 Cyclotron Road
MS 70A-1150
Berkeley, CA 94720

Phil Reed
U.S. Nuclear Regulatory Commission
Office of Nuclear Regulatory Research
Division of Systems Analysis and Regulatory
Effectiveness
Radiation Protection, Env. Risk and Waste
Management Branch
Mail Stop: T9-F31
Washington, DC 20555-0001

Richard J. Reeder
Dept. of Geosciences
State University of New York at Stony Brook
Stony Brook, NY 11794-2100

Al Robinson
68705, E 715 PRNE
Richland WA 99352

Phil Rogers
13 Mountain Oak
Littleton, CO 80127

**No. of
Copies**

David Shafer
Desert Research Institute
University of Nevada
P.O. Box 19040
Las Vegas, NV 89132-0040

Dawn A. Shaughnessy
Glenn T. Seaborg Center
Lawrence Berkeley National Laboratory
1 Cyclotron Road
MS 70A-1150
Berkeley, CA 94720

Doug Sherwood
Rivers Edge Environmental
1616 Riverside Drive
West Richland, WA 99353

David K. Shuh
Lawrence Berkeley National Lab
1 Cyclotron Road
Mail Stop 70A-1150
Berkeley, CA 94720

James "Buck" Sisson
Idaho National Engineering and
Environmental Laboratory
PO Box 1625, MS-2107
Idaho Falls, ID 83415-2107

Carl I. Steefel
Lawrence Livermore National Laboratory
Earth & Environmental Sciences Directorate
Mail Stop L-204
PO Box 808
Livermore, CA 94551-9900

Dr. Samuel J. Traina, Director
Sierra Nevada Research Institute
University of California, Merced
P.O. Box 2039
Merced, CA 95344

**No. of
Copies**

Dr. T. T. Chuck Vandergraaf
Atomic Energy Of Canada, Limited
Whiteshell Nuclear Research Establishment
Pinawa, Manitoba ROE 1LO
Canada

Dr. Jiamin Wan
Lawrence Berkeley National Laboratory
1 Cyclotron Rd. MS 70-0127A
Berkeley, CA 94720

Mr. Ronald G. Wilhelm
Office of Radiation and Indoor Air
401 M Street, S.W.
Mail Code 6603J
Washington, D.C. 20460

W. Alexander Williams
US Department of Energy
Office of Environmental Restoration
EM-33
19901 Germantown Road
Germantown, MD 20874-1290

ONSITE

- 4 **DOE Office of River Protection**
- | | |
|--------------|-------|
| C. A. Babel | H6-60 |
| P. E. LaMont | H6-60 |
| R. W. Lober | H6-60 |
| R. B. Yasek | H6-60 |
- 8 **DOE Richland Operations Office**
- | | |
|-----------------------------|-------|
| B. L. Foley | A6-38 |
| J. P. Hanson | A5-13 |
| R. D. Hildebrand | A6-38 |
| K. A. Kapsi | A5-13 |
| J. G. Morse | A6-38 |
| K. M. Thompson | A6-38 |
| DOE Public Reading Room (2) | H2-53 |

<u>No. of Copies</u>			<u>No. of Copies</u>		
	Bechtel Hanford, Inc.			R. W. Bryce	E6-35
	K. R. Fecht	H0-02		R. E. Clayton	P7-22
				W. J. Deutsch	K6-81
18	CH2M Hill Hanford Group, Inc.			P. E. Dresel	K6-96
	J. E. Auten	E6-35		K. M. Geisler	P7-22
	K. C. Burgard	L6-57		M. J. Fayer	K9-33
	M. P. Connelly	E6-35		A. R. Felmy	K8-96
	E. A. Fredenburg	H9-03		M. D. Freshley	K9-33
	T. E. Jones (2)	E6-35		J. S. Fruchter	K6-96
	A. J. Knepp (2)	H6-60		D. G. Horton	K6-81
	F. M. Mann (5)	E6-35		J. P. Icenhower	K6-81
	W. J. McMahon	E6-35		C. T. Kincaid	E6-35
	C. W. Miller	H9-03		K. M. Krupka	K6-81
	D. A. Myers (3)	E6-35		I. V. Kutnyakov	P7-22
				G. V. Last (3)	K6-81
3	Duratek Federal Services, Inc., Northwest Operations			V. L. LeGore	P7-22
	M. G. Gardner	H1-11		M. J. Lindberg	P7-22
	K. D. Reynolds	H1-11		C. W. Lindenmeier (2)	P7-22
	D. E. Skoglie	H1-11		W. J. Martin	K6-81
				S. V. Mattigod	K6-81
				B. P. McGrail	K6-81
3	Environmental Protection Agency			P. D. Meyer BPO	
	Nick Ceto	B5-01		C. J. Murray	K6-81
	D. A. Faulk	B5-01		S. M. Narbutovskih	K6-96
	M. L. Goldstein	B5-01		R. D. Orr	K6-81
				E. M. Pierce	K6-81
2	Flour Federal Services			S. P. Reidel	K6-81
	R. Khaleel	E6-17		R. J. Serne (20)	P7-22
	R. J. Puigh	E6-17		H. T. Schaef	K6-81
				W. Um	P7-22
5	Flour Hanford, Inc.			M. Valenta	P7-22
	T. W. Fogwell	E6-35		T. S. Vickerman	P7-22
	B. H. Ford	E6-35		B. A. Williams	K6-81
	J. G. Hogan	H1-11		S. B. Yabusaki	K9-36
	V. G. Johnson	E6-35		J. M. Zachara	K8-96
	M. I. Wood	H8-44		Hanford Technical Library (2)	P8-55
64	Pacific Northwest National Laboratory				
	S. R. Baum	P7-22			
	B. N. Bjornstad (3)	K6-81			
	C. F. Brown	P7-22			